Summary of Activities

2014

CANADA-NUNAVUT GEOSCIENCE OFFICE

ᑲᓇᑕᐅᔪᒻ-ᓄᓇᕗᑦᓗ ᐅᖃᖅᑲᓂᖅ ᖁᑎᐅᓵᖅᑎᓐᓂᒃᑐᓂᒃ

BUREAU GÉOSCIENTIFIQUE CANADA-NUNAVUT

KANATAMI-NUNAVUMI GEOSCIENCE TITIGAKVIIT

CANADA-NUNAVUT
GEOSCIENCE OFFICE

BUREAU GÉOSCIENTIFIQUE
CANADA-NUNAVUT

ᑲᓇᑕᒥ-ᓄᓇᕗᑦ
ᑕᓪᓕᖅᑲᓂᖅ ᖃᐅᔨᓴᖃᑎᖓᓕᒃ

KANATAMI-NUNAVUMI
GEOSCIENCE TITIGAKVIIT

SUMMARY OF ACTIVITIES 2014

This publication is also available, free of charge, as colour digital files in Adobe Acrobat® PDF format from the Canada-Nunavut Geoscience Office website: www.cngo.ca/

Every reasonable effort is made to ensure the accuracy of the information contained in this report, but Natural Resources Canada does not assume any liability for errors that may occur. Source references are included in the report and users should verify critical information.

When using information from this publication in other publications or presentations, due acknowledgment should be given to Canada-Nunavut Geoscience Office. The recommended reference is included on the title page of each paper. The complete volume should be referenced as follows:

Canada-Nunavut Geoscience Office (2015): Canada-Nunavut Geoscience Office Summary of Activities 2014; Canada-Nunavut Geoscience Office, 190 p.

ISSN 2291-1235 Canada-Nunavut Geoscience Office Summary of Activities (Print)
ISSN 2291-1243 Canada-Nunavut Geoscience Office Summary of Activities (Online)

Front cover photo: Wilder Greenman examining fluvial cross-beds of the 1.9 Ga Burnside River Formation, along the western shore of Elu Inlet. Photo by Alessandro Ielpi, Geological Survey of Canada, Canada-Nunavut Geoscience Office.

Back cover photo: Upper Ordovician limestone exposed on the western side of Akpatok Island. Photo by Shunxin Zhang, Canada-Nunavut Geoscience Office.

Foreword

I am pleased to be releasing the Canada-Nunavut Geoscience Office (CNGO) Summary of Activities 2014 volume. This is the third annual edition of a publication that summarizes preliminary or final results from projects supported by the CNGO, as well as key invited research. The rapid release of observations and data through this publication provides valuable information to government and industry stakeholders across Nunavut.

Its release is always a special moment for me as Chief Geologist, but this year it is bittersweet because it will be the last release of which I will be a part. I am extremely proud of, and grateful to, all staff and external collaborators for their contributions to this publication during my tenure at the Canada-Nunavut Geoscience Office. Each contribution has demonstrated the breadth and quality of research being conducted by the office and its collaborators. This quality geoscience information is important for helping support land-use management in Nunavut.

The Canada-Nunavut Geoscience Office (CNGO) was established in 1999 to help foster the development of Nunavut's mineral and energy resources and infrastructure. It is a partnership between the Government of Nunavut (GN), Natural Resources Canada (NRCan) and Aboriginal Affairs and Northern Development Canada (AANDC). Nunavut Tunngavik Incorporated (NTI) is an ex-officio member of the office. Fully staffed, the office consists of six employees with expertise in Precambrian, Paleozoic and Quaternary geology; GIS; and online data dissemination. In October 2014, the CNGO welcomed its first visiting Post-Doctoral Fellow, thus adding considerably to its geoscience capacity.

The mandate of the CNGO is to provide accessible geoscience information and expertise in Nunavut that supports 1) responsible resource exploration and development, 2) responsible infrastructure development, and 3) geoscience capacity building and outreach. In 2014, the CNGO received approval for a new two-year geoscience program focused on delivering activities that support responsible natural resource development, protect investments in infrastructure and disseminate geoscience information.

The CNGO Summary of Activities 2014 volume presents preliminary results from this new geoscience program. This year's volume continues to take advantage of the CNGO Geoscience Data Series as the means for disseminating several new digital datasets (e.g., analytical datasets, polygon files, point data) that support papers in the volume. Where appropriate, this series will be referenced in Summary of Activities papers, with links provided to the online repository.

This year's volume is divided into five sections and consists of 17 papers. The sections include 'Mineral deposit studies', 'Regional geoscience', 'Geoscience for infrastructure', 'Carving stone' and 'Outreach and capacity building'. All papers will be available for download at www.cngo.ca.

The 'Mineral deposit studies' section consists of two papers. The first focuses on the distribution, composition and petrogenesis of a selected number of granitic pegmatites on Hall Peninsula, in order to evaluate their metallogenic potential, with an emphasis on Sn, Li, Cs and Ta, and also gem potential. The second provides observations on a suite of mafic, ultramafic and layered mafic-ultramafic sills that occur on Meta Incognita Peninsula. Their presence, along with that of similar bodies across southern Baffin Island, potentially indicate a major large igneous province event that warrants further study.

The papers in the 'Regional geoscience' section continue to focus on observations and results from the Hall Peninsula Integrated Geoscience Program (HPIGP), as well as new work conducted in collaboration with the Geo-Mapping for Energy and Minerals (GEM) program. The focus of these activities is on bedrock and surficial mapping and a range of thematic studies from Hall Peninsula, Meta Incognita Peninsula, Akpatok Island and the Elu Basin. New results include geochronology, till geochemistry, geochemistry and other analytical data, along with new regional geological overviews of Meta Incognita Peninsula and Akpatok Island, and a new aeromagnetic survey being flown north of Iqaluit.

This year's 'Geoscience for infrastructure' section highlights exciting new collaborative research conducted in Frobisher Bay by the CNGO, NRCan, the Government of Nunavut Department of Environment and partners from Canadian universities. The purpose of this work is to improve the understanding of the geology of Frobisher Bay, in order to support decision-making with respect to the use of its seabed. An invited paper provides an informative overview of the range of applications that the seabed mapping conducted from the RV Nuliajuk can have in Nunavut. Finally, results from permafrost research at the Iqaluit International Airport, conducted in collaboration with Natural Resources Canada, is also provided. New geophysical data are being used to better characterize permafrost conditions and processes in this area.

The 'Carving stone' section consists of a paper focused on the geology and resource assessment at the Opingivik quarry on Cumberland Sound. This quarry has the potential to be a new source of supply for Inuit carvers in the south Baffin area. This work involves a collaboration between the CNGO, the Government of Nunavut and the community of Pangnirtung. A second paper provides an update on results generated by the Nunavut Carving Stone Deposit Evaluation Program in the Kitikmeot region, on Hall Peninsula and on the Belcher Islands.

Finally, a summary of a geoscience workshop in Nuuk, Greenland, co-ordinated by the Geological Survey of Denmark and Greenland (GEUS) and the Canada-Nunavut Geoscience Office (CNGO), is provided in the 'Outreach and capacity building' section. This workshop focused on exchanging information about mineral and petroleum resources, and discussing geoscience questions of interest to Nunavut, Greenland, Canada and Denmark.

Acknowledgments

The CNGO thanks all authors of papers in this third Summary of Activities. Your dedication has been greatly appreciated and is critical in helping the CNGO deliver such a quality product. RnD Technical is also thanked for their technical editing and assembling of the volume. In addition, special thanks are extended to reviewers of papers:

Alfredo Camacho, University of Manitoba
Calvin Campbell, Geological Survey of Canada
Caroline Duchesne, Geological Survey of Canada
Richard Ernst, Ernst Geoscience
Linda Ham, Government of Nunavut
Karen Hanghøj, Geological Survey of Denmark and Greenland
Jeff Harris, Geological Survey of Canada
Donald James, Government of Nova Scotia
Charlie Jefferson, Geological Survey of Canada
Denis Lavoie, Geological Survey of Canada
Anne-Marie LeBlanc, Geological Survey of Canada
Vicki McNicoll, Geological Survey of Canada
Roger Paulen, Geological Survey of Canada
David Schneider, University of Ottawa
David Scott, Canadian Polar Commission
Holly Steenkamp, Canada-Nunavut Geoscience Office
Mike Thomas, Geological Survey of Canada
Brian Todd, Geological Survey of Canada
Natasha Wodicka, Geological Survey of Canada

David Mate
Chief Geologist
Canada-Nunavut Geoscience Office
www.cngo.ca/

Préface

C'est avec un réel plaisir que je lance cette plus récente édition du *Sommaire des activités* du Bureau géoscientifique Canada-Nunavut (BGCN). Il s'agit de la troisième édition de cette publication qui brosse un tableau général des résultats préliminaires ou finaux de projets ayant reçus l'aval du Bureau, ainsi que ceux ayant été menés par d'importants chercheurs invités. La mise en circulation rapide d'observations et de données par le biais de cette publication permet de partager des renseignements importants avec les intervenants gouvernementaux et industriels de l'ensemble du Nunavut.

La mise en circulation de ce volume représente un moment qui revêt pour moi, en tant que géologue en chef, une importance particulière, moment qui m'est d'autant plus doux-amer cette année qu'il s'agit de ma dernière prestation à ce titre. Je suis extrêmement fier de toutes les contributions faites à cette série au cours de mon mandat, aussi bien par les employés du Bureau que par nos collaborateurs externes, et je les en remercie. Chaque contribution a su démontrer l'ampleur et la qualité des recherches qui se poursuivent par le biais de nos chercheurs et de nos collaborateurs. De l'information géoscientifique d'une telle qualité s'impose si l'on veut assurer le soutien de projets de gestion des terres à l'échelle du Nunavut.

Le Bureau géoscientifique Canada-Nunavut (BGCN) a été créé en 1999 en vue de promouvoir le développement des ressources ainsi que de l'infrastructure minière et énergétique du Nunavut. Il s'agit d'un partenariat entre le gouvernement du Nunavut, Ressources naturelles Canada (RNCan) et le ministère des Affaires autochtones et Développement du Nord Canada (AANDC). La société Nunavut Tunngavik Incorporated (NTI) est membre d'office du Bureau. Lorsque tous les postes y sont occupés, celui-ci regroupe six employés spécialisés dans la géologie du Précambrien, du Paléozoïque et du Quaternaire, le système d'information géographique et la diffusion de données en ligne. En octobre 2014, le BGCN accueillait son premier boursier de recherches postdoctorales invité dont les talents viennent s'ajouter au capital géoscientifique du Bureau.

Le mandat du BGCN est de fournir des données et un savoir-faire géoscientifique à la portée de tous en vue d'appuyer 1) l'exploration et l'exploitation responsables des ressources, 2) l'aménagement responsable de l'infrastructure, et 3) le renforcement des capacités géoscientifiques et la sensibilisation du public. En 2014, le Bureau s'est vu octroyer la direction d'un nouveau programme de deux ans qui porte sur l'élaboration de travaux visant la mise en valeur responsable des ressources naturelles, la protection des mises de fonds dans des projets d'infrastructure et la diffusion de renseignements de nature géoscientifique.

La publication *Sommaire des activités 2014* présente des résultats préliminaires découlant de ce nouveau programme. Le volume exploite également l'information disponible grâce à la *Série des données géoscientifiques*, qui permet la diffusion de nouveaux ensembles de données numériques (par ex., des ensembles de données analytiques, polygonales ou ponctuelles) à l'appui des rapports publiés dans le volume. Le cas échéant, la série est citée en référence dans les rapports paraissant dans le *Sommaire des activités* et un lien permet l'accès au dépôt de données électroniques.

La présente édition du volume comprend cinq sections et regroupe un total de 17 articles. Les sections sont les suivantes : « Études sur les gisements minéraux », « Études géoscientifiques régionales », « Études géoscientifiques liées à l'infrastructure », « Pierre à sculpter » et « Sensibilisation du public et renforcement des capacités ». Tous les articles seront publiés (en anglais seulement, accompagnés de résumés en français) sur Internet et pourront être téléchargés depuis le www.cngo.ca.

La section « Études sur les gisements minéraux » présente deux articles. Le premier porte sur des travaux se penchant sur l'étude de la répartition, de la composition et de la pétrogénèse d'un nombre désigné de pegmatites granitiques de la péninsule Hall en vue d'établir leur potentiel métallogénique, surtout en ce qui a trait à la présence de plomb, de lithium, de césium et de tantale, de même que leur potentiel de receler des gemmes. Le second met l'accent sur l'étude d'une suite de filons-couches mafiques, ultramafiques et mafiques-ultramafiques stratifiés découverts dans la péninsule Meta Incognita. Leur présence, ainsi que celle de corps minéralisés semblables dans l'ensemble de la partie méridionale de l'île de Baffin, peut être liée à celle d'une importante province ignée dont l'existence pourrait justifier la poursuite d'études plus approfondies.

Les rapports réunis dans la section « Études géoscientifiques régionales » continuent de faire le point sur les observations et les résultats découlant du Projet géoscientifique intégré de la péninsule Hall et sur de nouveaux travaux entrepris dans le cadre du programme de géocartographie de l'énergie et des minéraux (GEM). Ces travaux portent sur la cartographie de surface et du substratum rocheux, et couvrent toute une gamme d'études thématiques entreprises dans la péninsule Hall, la péninsule Meta Incognita, l'île Akpatok et le bassin d'Elu. De nouveaux résultats et données analytiques provenant d'analyses géochronologiques, géochimiques et de la géochimie du till sont disponibles, ainsi que de nouvelles interprétations de la géologie régionale de la péninsule Meta Incognita et de l'île Akpatok, en plus de données provenant d'un nouveau levé aéromagnétique effectué au-dessus de la région s'étendant au nord d'Iqaluit.

La section « Études géoscientifiques liées à l'infrastructure » met en évidence les nouveaux projets de recherche de nature collaborative entrepris dans la baie Frobisher par le BGCN, Ressources naturelles Canada, le ministère de l'Environnement du gouvernement du Nunavut, ainsi qu'en collaboration avec des partenaires issus d'universités canadiennes. Ces recherches ont pour objet d'améliorer l'état des connaissances au niveau de la géologie de la région de la baie Frobisher en vue d'appuyer la prise de décisions en matière d'utilisation du fond marin à cet endroit. Une communication sollicitée fournit un aperçu instructif au sujet de l'utilité que peut représenter pour le Nunavut les travaux de cartographie du fond marin menés à partir du navire de recherche océanographique *Nuliajuk*. Enfin, les résultats provenant de travaux sur le pergélisol entrepris à l'aéroport international d'Iqaluit en collaboration avec Ressources naturelles Canada sont également présentés. De nouvelles données géophysiques servent à mieux caractériser les conditions propres au pergélisol et les processus associés dans la région.

La première contribution de la section « Pierre à sculpter » comporte un rapport axé sur la géologie et le potentiel en pierre à sculpter que recèle la carrière Opingivik dans la région du détroit de Cumberland. Cette carrière pourrait constituer une nouvelle source d'approvisionnement pour les sculpteurs inuits de la région méridionale de l'île de Baffin. Ces travaux mettent en jeu le BGCN, en collaboration avec le gouvernement du Nunavut et la collectivité de Pangnirtung. Un deuxième article offre une mise à jour des résultats obtenus dans la région de Kitikmeot, dans la péninsule Hall et dans les îles Belcher, dans le cadre du programme d'évaluation des gisements de pierre à sculpter du Nunavut.

Enfin, un résumé d'un atelier tenu à Nuuk, au Groenland, portant sur les géosciences et dont la coordination était assurée par le Service géologique du Danemark et du Groenland et le Bureau géoscientifique Canada-Nunavut, constitue la contribution de la section de la « Sensibilisation du public et renforcement des capacités ». Cet atelier a porté sur l'échange d'information au niveau des ressources minérales et pétrolières et a permis de discuter d'enjeux géoscientifiques d'intérêt commun au Nunavut, au Groenland, au Canada et au Danemark

Remerciements

Le Bureau tient à remercier les auteurs des articles publiés dans cette troisième édition du *Sommaire des activités*. Votre dévouement est extrêmement apprécié et c'est grâce à vous que nous pouvons publier un document d'une telle qualité. Merci à RnD Technical d'avoir vu à l'édition technique et à l'assemblage de ce numéro. Nos remerciements s'adressent également aux personnes suivantes, lecteurs critiques des articles :

Alfredo Camacho, Université du Manitoba
Calvin Campbell, Commission géologique du Canada
Caroline Duchesne, Commission géologique du Canada
Richard Ernst, Ernst Geosience
Linda Ham, Gouvernement du Nunavut
Karen Hanghøj, Service géologique du Danemark et du Groenland
Jeff Harris, Commission géologique du Canada
Donald James, Gouvernement de la Nouvelle-Écosse
Charlie Jefferson, Commission géologique du Canada
Denis Lavoie, Commission géologique du Canada
Anne-Marie LeBlanc, Commission géologique du Canada
Vicki McNicoll, Commission géologique du Canada
Roger Paulen, Commission géologique du Canada
David Schneider, Université d'Ottawa
David Scott, Commission canadienne des affaires polaires
Holly Steenkamp, Bureau géoscientifique Canada-Nunavut
Mike Thomas, Commission géologique du Canada
Brian Todd, Commission géologique du Canada
Natasha Wodicka, Commission géologique du Canada

David Mate
Géologue en chef
Bureau géoscientifique Canada-Nunavut
www.cngo.ca/

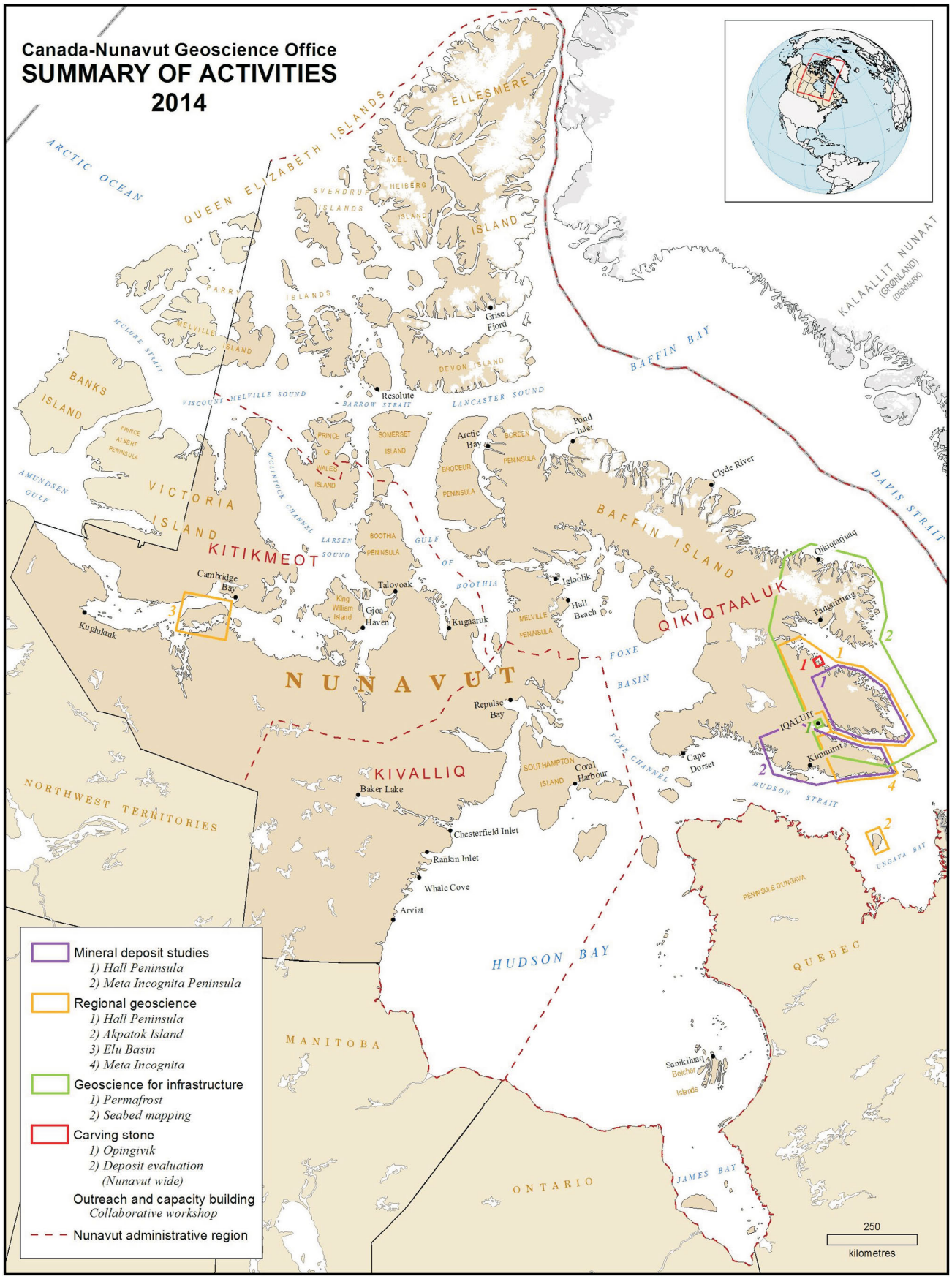
Canada-Nunavut Geoscience Office
SUMMARY OF ACTIVITIES
2014
ARCTIC OCEAN
QUEEN ELIZABETH ISLANDS
ELLESMERE ISLAND
AXEL HEIBERG ISLAND
SVERDRUP ISLANDS
PARRY ISLANDS
MELVILLE ISLAND
M'CLURE STRAIT
BANKS ISLAND
PRINCE ALBERT PENINSULA
VICTORIA ISLAND
AMUNDSEN GULF
KITIKMEOT
VISCOUNT MELVILLE SOUND
BARROW STRAIT
LANCASTER SOUND
BAFFIN BAY
KALAALLIT NUNAAT (GRØNLAND) (DENMARK)
DAVIS STRAIT
DEVON ISLAND
Grise Fiord
Resolute
PRINCE OF WALES ISLAND
SOMERSET ISLAND
M'CLINTOCK CHANNEL
LARSEN SOUND
BOOTHIA PENINSULA
GULF OF BOOTHIA
BRODEUR PENINSULA
BORDEN PENINSULA
Arctic Bay
Pond Inlet
Clyde River
BAFFIN ISLAND
QIKIQTAALUK
Qikiqtarjuaq
Pangnirtung
Iqaluit
Kimmirut
Cape Dorset
Igloolik
Hall Beach
MELVILLE PENINSULA
Cambridge Bay
Kugluktuk
Taloyoak
King William Island
Gjoa Haven
Kugaaruk
NUNAVUT
FOXE BASIN
FOXE CHANNEL
Repulse Bay
HUDSON STRAIT
KIVALLIQ
Baker Lake
SOUTHAMPTON ISLAND
Coral Harbour
Chesterfield Inlet
Rankin Inlet
Whale Cove
Arviat
NORTHWEST TERRITORIES
HUDSON BAY
PENINSULE D'UNGAVA
UNGAVA BAY
QUEBEC
MANITOBA
ONTARIO
JAMES BAY
Sanikiluaq
Belcher Islands
Mineral deposit studies
1) Hall Peninsula
2) Meta Incognita Peninsula
Regional geoscience
1) Hall Peninsula
2) Akpatok Island
3) Elu Basin
4) Meta Incognita
Geoscience for infrastructure
1) Permafrost
2) Seabed mapping
Carving stone
1) Opingivik
2) Deposit evaluation
(Nunavut wide)
Outreach and capacity building
Collaborative workshop
Nunavut administrative region
250
kilometres

Contents

Location and characterization of pegmatites in the southern Baffin Island region, Nunavut: field and satellite observations

A. Bigio[1,3], P. Budkewitsch[2] and D. Lentz[3]

[1]*Mineral Resources Division, Nunavut Regional Office, Aboriginal Affairs and Northern Development Canada, Iqaluit, Nunavut, alia.bigio@aandc.gc.ca*

[2]*Mineral Resources Division, Nunavut Regional Office, Aboriginal Affairs and Northern Development Canada, Iqaluit, Nunavut*

[3]*Department of Earth Sciences, University of New Brunswick, Fredericton, New Brunswick*

This work was part of the 2012–2014 Hall Peninsula Integrated Geoscience Program (HPIGP), led by the Canada-Nunavut Geoscience Office (CNGO) in collaboration with the Government of Nunavut, Aboriginal Affairs and Northern Development Canada, and the Geological Survey of Canada. It involved strong contributions from the Universities of Alberta, Dalhousie, Laval, Manitoba, Ottawa, Saskatchewan and New Brunswick, and the Nunavut Arctic College. It has benefitted from support by local and Inuit-owned businesses and the Polar Continental Shelf Program. The focus is on bedrock and surficial geology mapping (1:100 000 scale). In addition, a range of thematic studies is being conducted, including Archean and Paleoproterozoic tectonics, geochronology, landscape uplift and exhumation, microdiamonds, sedimentary-rock xenoliths and permafrost. The goal is to increase the level of geological knowledge and better evaluate the natural-resource potential in this frontier area.

Bigio, A., Budkewitsch, P. and Lentz, D. 2015: Location and characterization of pegmatites in the southern Baffin Island region, Nunavut: field and satellite observations; *in* Summary of Activities 2014, Canada-Nunavut Geoscience Office, p. 1–10.

Abstract

A number of granitic pegmatite dykes intrude the country rock on Hall Peninsula, southern Baffin Island, Nunavut. The aim of this project is to study the distribution, composition and petrogenesis of a select number of these pegmatites and evaluate their metallogenic potential. It is anticipated that this research will highlight any rare metal, rare-earth element, and/or gem potential in pegmatites on Hall Peninsula, to companies that are interested in those commodities, with an emphasis on Sn, Li, Cs and Ta in particular. This project will also include an examination of the source of parent melts, relative paragenesis, timing with respect to late orogenic evolution, and absolute ages of emplacement. Lithogeochemical and mineral-chemical analysis of the pegmatites is being done using whole-rock geochemistry and laser-ablation, multiple-collector, inductively coupled plasma–mass spectrometry.

A broader regional context has been added to this project through the use of pegmatite samples obtained from both the Cumberland and Meta Incognita peninsulas. As pegmatites are not generally large targets, and can be easily overlooked in larger scale mapping projects, an attempt is being made to develop an approach that can identify them using various remote sensing methods.

Résumé

Des dykes de pegmatite granitique ont été mis en place par intrusion dans les roches environnantes de la péninsule Hall, dans l'île de Baffin, au Nunavut. Le présent projet a pour objet d'étudier la répartition, la composition et la pétrogenèse d'un nombre déterminé de ces roches pegmatitiques et de procéder à une évaluation de leur potentiel sur le plan métallogénique. On prévoit que ces recherches mettront en évidence, à l'intention des sociétés qui portent un intérêt à ces marchandises, le potentiel des pegmatites de la péninsule Hall de receler des métaux rares, des éléments des terres rares et, le cas échéant, des gemmes, ainsi que, plus particulièrement, la présence d'étain, de lithium, de césium et de tantale. On procèdera également, dans le cadre de ce projet, à l'étude de la source des bains magmatiques de même origine, de la paragenèse relative, du moment de leur formation en fonction de l'évolution orogénique tardive et de l'âge absolu correspondant à leur mise en place. Des analyses lithogéochimiques et chimico-minérales des pegmatites au moyen de la géochimie sur roche totale et l'ablation laser couplée à un spectromètre de masse à source à plasma inductif sont en cours.

This publication is also available, free of charge, as colour digital files in Adobe Acrobat® PDF format from the Canada-Nunavut Geoscience Office website: http://cngo.ca/summary-of-activities/2014/.

Un volet régional plus étendu a été ajouté à ce projet grâce au recours à des échantillons de pegmatite provenant des péninsules Cumberland et Meta Incognita. En raison du fait que les pegmatites ne constituent pas habituellement des cibles de taille et qu'elles peuvent facilement être omises au cours de projets de cartographie à grande échelle, on tente de mettre au point une approche susceptible de permettre leur repérage à l'aide de diverses méthodes de télédétection.

Introduction

The geology of Hall Peninsula can be divided into two main lithological assemblages: in the west, Paleoproterozoic metasedimentary rocks, containing leucogranite dykes and granitic intrusions, and supracrustal rocks—primarily pelite, semipelite and psammite—which locally show evidence of partial melting (Machado et al., 2013; Dyck and St-Onge, 2014; Skipton and St-Onge, 2014). In the east, an Archean orthogneiss complex consists of tonalite and monzogranite units with enclaves of mafic and ultramafic rocks, all of which are crosscut by syenogranite dykes. Supracrustal rocks are present in the east as well and are found structurally above and below the Archean basement (From et al., 2013, 2014; Dyck and St-Onge 2014; Skipton and St-Onge, 2014). Figure 1 shows selected pegmatite locations that were identified during the 2012–2014 field seasons.

The pegmatites are found primarily in the eastern half of the peninsula and appeared late in its Paleoproterozoic deformational history, during the Trans-Hudson Orogen (Skipton and St-Onge, 2014). They occur primarily as dykes that crosscut the regional metamorphic fabric, although foliation-parallel pegmatites are also present. They have mineral assemblages typical of S-type granitic compositions, suggesting a metasedimentary source (Dyck and St-Onge, 2014). Their mineralogy varies between K-feldspar and plagioclase feldspar, with quartz, biotite, muscovite, magnetite, graphite, tourmaline and rare apatite and beryl. The pegmatites usually display very coarse grained textures including blocky feldspar crystals, graphic feldspar-quartz intergrowths, and biotite occurring as books or sheets. Figure 2 shows an example of graphic texture in one of the pegmatites on Hall Peninsula; this texture is common to many of the localities.

Selected field observations of southern Hall Peninsula pegmatite dykes

The pegmatites discovered and sampled during the 2012–2014 field seasons on Hall Peninsula will be analyzed for major- and trace-element geochemistry in selected minerals (specifically, biotite and feldspar) through laser-ablation, multiple-collector, inductively coupled plasma–mass spectrometry (LA-MC-ICP-MS) procedures; used with pegmatites, this mineral-chemical analysis methodology helps to determine the degree of fractionation and potential for hosting mineralization, specifically Li, Sn, Cs, Ta or gems (Selway et al., 2005; Van Lichtervelde et al., 2007). Below is a description of selected pegmatites that were visited during fieldwork in 2014. The spatial locations of the stations discussed in this paper are identified in Figure 3; the stations are distributed both along-strike and across-strike in transects that cover a broad range of pegmatite occurrences on Hall Peninsula.

Crenulation basin pegmatite dykes (stations 14SUB-A063 to A068)

This location, including stations from 14SUB-A063 to A068 (Figure 3), was first visited in 2013, and revisited in 2014 specifically to examine the pegmatites. The site consists of large bodies of amphibolite and metasedimentary semipelite that have been intruded by pegmatite dykes and pods. Faserkiesel texture is common in the metasedimentary rocks, as are alternating leucosome-melanosome layers; the sillimanite knots are strongly flattened, showing a high degree of strain, and average from 1 to 3 cm in diameter. Large radiating clusters of black tourmaline are present in many of the pegmatite dykes, with most crystals subhedral to euhedral in form (Figure 4a). Coarse-grained blocky feldspar is also present in most of the pegmatite dykes. One large (6 by 3 m) pegmatite outcrop contains the usual quartz, feldspar and biotite, but also garnet and between approximately 5 and 10% blue-green apatite. Many of the apatite crystals are also euhedral and range from 5 to 30 mm in length along their longest axis. Extremely large, between 10 and 20 cm in length, euhedral black tourmaline crystals were discovered in one 0.5 m wide, 15 m long pegmatite dyke, along with large euhedral albite and tourmaline crystals and books of biotite several centimetres thick.

The contacts between the pegmatite dykes and the amphibolite vary from diffuse with reaction rims (Figure 4b) to sharp and distinct; the diffuse contacts are more common parallel to the foliation of the amphibolite.

Tourmaline valley pegmatite dykes (stations 14SUB-A057 to A062)

This location includes stations 14SUB-A057 to A062. There are several large pegmatite dykes in the area, mainly trending from approximately north to 025° and exposed over about 100 m on a gently sloping hillside. They range between 6 and 10 m wide, and contain quartz, K-feldspar, biotite (often in books), black tourmaline, dark brown tourmaline, muscovite, garnet and trace apatite. The dykes are locally somewhat discordant to the metasedimentary rocks, showing a 'ripped-up' texture of hostrock slivers and xenoliths at the contacts, but in general are concordant to the main fabric elements with regard to emplacement.

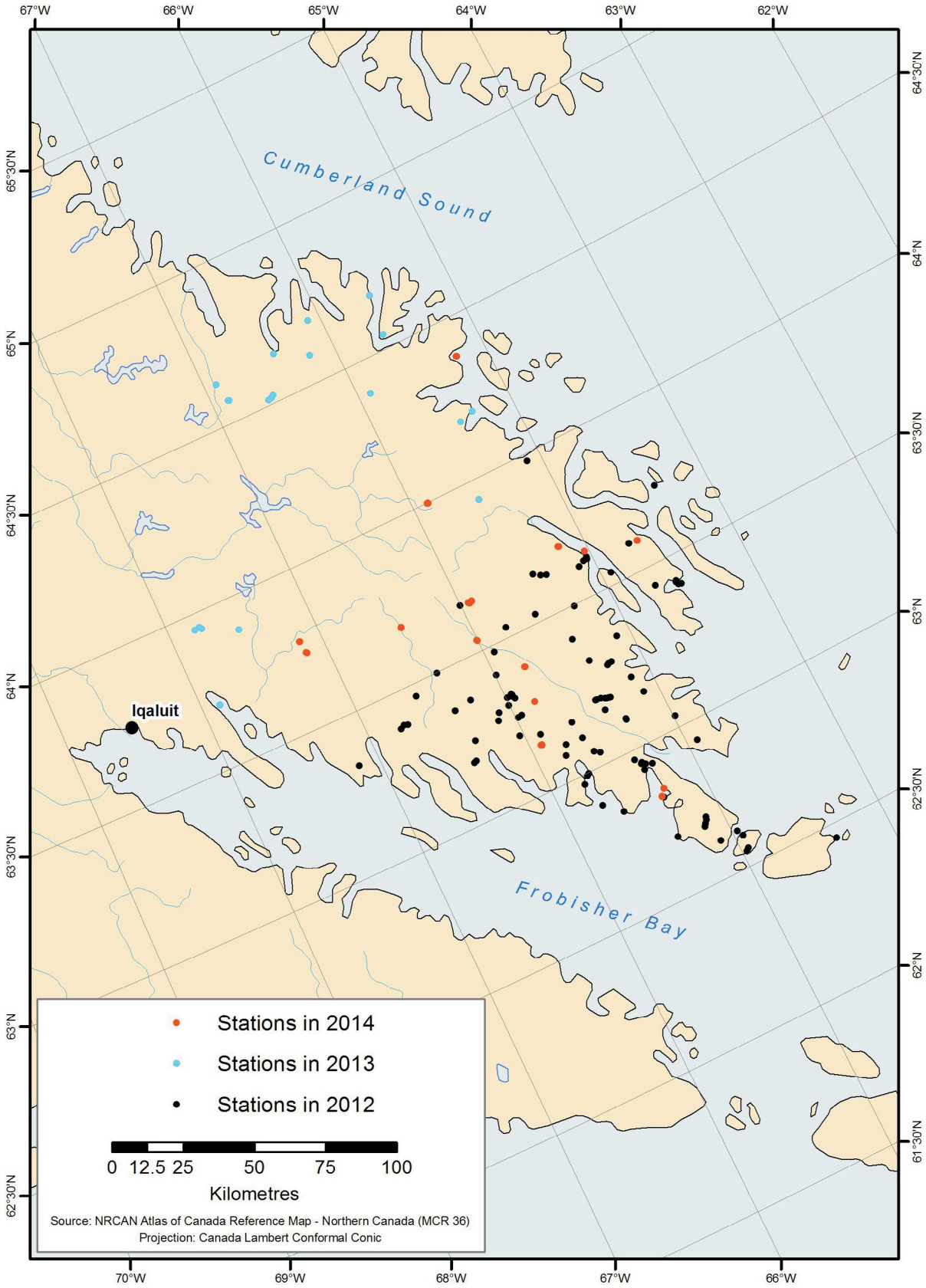

Figure 1: Pegmatite locations on Hall Peninsula identified during the 2012–2014 field seasons. Black markers indicate 2012 stations, blue markers indicate 2013 stations and orange markers indicate 2014 stations.

Figure 2: Graphic intergrowth texture between quartz and feldspar, a characteristic common to many pegmatite dykes in the southern Baffin region.

The dykes are extremely tourmaline rich (Figure 5a), especially at the contacts with the metasedimentary country rock; in some places the tourmaline content approaches 40%. Some of the tourmaline material is translucent to transparent and a deep brown colour, and may be dravite, but opaque black schorl tourmaline is more common. Many of the tourmaline crystals are club shaped and are generally larger toward the central parts of the dykes.

A single beryl crystal, 5 cm in length along its longest axis, was collected from this location at station 14SUB-A059 (Figure 5b). It occurred in a small (~10 cm across) pod of muscovite at the contact between the pegmatite and the metasedimentary rocks, and is subhedral, with a pale yellowish-green colour. An attempt was made to locate other muscovite pods, which might also contain beryl, but no further occurrences were found. None of the pegmatites at this location (or at any others visited during the program) appeared to have miarolitic cavities (Èerný et al., 2012)—void spaces in granitic pegmatites in which crystals are able to grow, and which often produce gem-quality or museum-quality specimens.

White ridge pegmatite dyke (stations 14SUB-A073 and A074)

This location includes stations 14SUB-A073 and A074. The site consists of a massive pegmatite dyke, trending east and outcropping as a ridge that averages 20 m wide and is over 100 m long, and intrudes amphibolitic country rock. The mineralogy is mainly feldspars, quartz and biotite, all of which are extremely coarse grained (Figure 6a), as well as occasional pods of rose quartz and rare apatite and black tourmaline. Rose quartz with graphic intergrowth texture is also present. Sheets of biotite over 50 cm in length are common (Figure 6b), as are smaller biotite crystals with a 'window' texture, where the crystals have an open centre surrounding quartz and feldspar material (Figure 6c).

Remote predictive mapping of pegmatite dykes using RapidEye satellite images

Remote sensing techniques can be used to find and assess granitic pegmatites for their rare-element mineralization potential (Peng et al., 2011; Sinergeo, 2013). In the Arctic the potential for application of these methods is considerable.

Vegetation cover in the southern Baffin region ranges from non-existent to moderate, making optical remote sensing a suitable method for remote predictive mapping in general (Harris et al., 2008; Budkewitsch et al., 2013) and for locating pegmatites in particular. The difficulty is in differentiating pegmatites from similarly reflective pale tonalite or granodiorite bodies that are found throughout Hall Peninsula. However, this identification should be possible where the pegmatites are sufficiently wide with respect to the resolution of the remote sensing data (i.e., if they are wider than twice the resolution of the image).

RapidEye satellite data consists of five spectral bands in the visible and near-infrared part of the spectrum (RapidEye AG, 2011). Granitic pegmatites do not contain any unique spectral absorption features in this spectral range. The pale colours of feldspar and high albedo of quartz, however, tend to be expressed with a high reflectance across all bands, which may facilitate their identification in single bands or in various false colour images created from the data (Figure 7). The resolution of RapidEye data is approximately 6.5 m and sampled to 5 m pixels (Naughton et al., 2011; RapidEye AG, 2011). Therefore the minimum dimensions of pegmatite exposures that can be readily identified are approximately 10 m wide and 50 to 100 m long (Figure 8). Many pegmatite dykes of these dimensions are not recorded on published geological maps, but their presence may be identified in these satellite images providing researchers with the information they need to locate these small dykes. A number of pegmatite dykes of this size were discovered during the 2014 program.

Where pegmatite bodies are large enough to be imaged in satellite data, they are visible provided certain characteristics are present. Pegmatite exposures expressed as resistant ridges are locally visible in satellite images due to the relative durability of coarse-grained quartz- and feldspar-rich mineralogy compared to the adjacent country rock. A second factor that assists with their identification is the paler colour of the granitic pegmatite in contrast with the often more mafic country rock found in the region, such as amphibolite. As both of these features can occur in rocks that are not pegmatites but that are found adjacent to gneissic rocks of southern Baffin Island, they are not conclusive for the identification of pegmatites. When pegmatite dykes are discordant in strike to gneissosity, however, they are easier to distinguish.

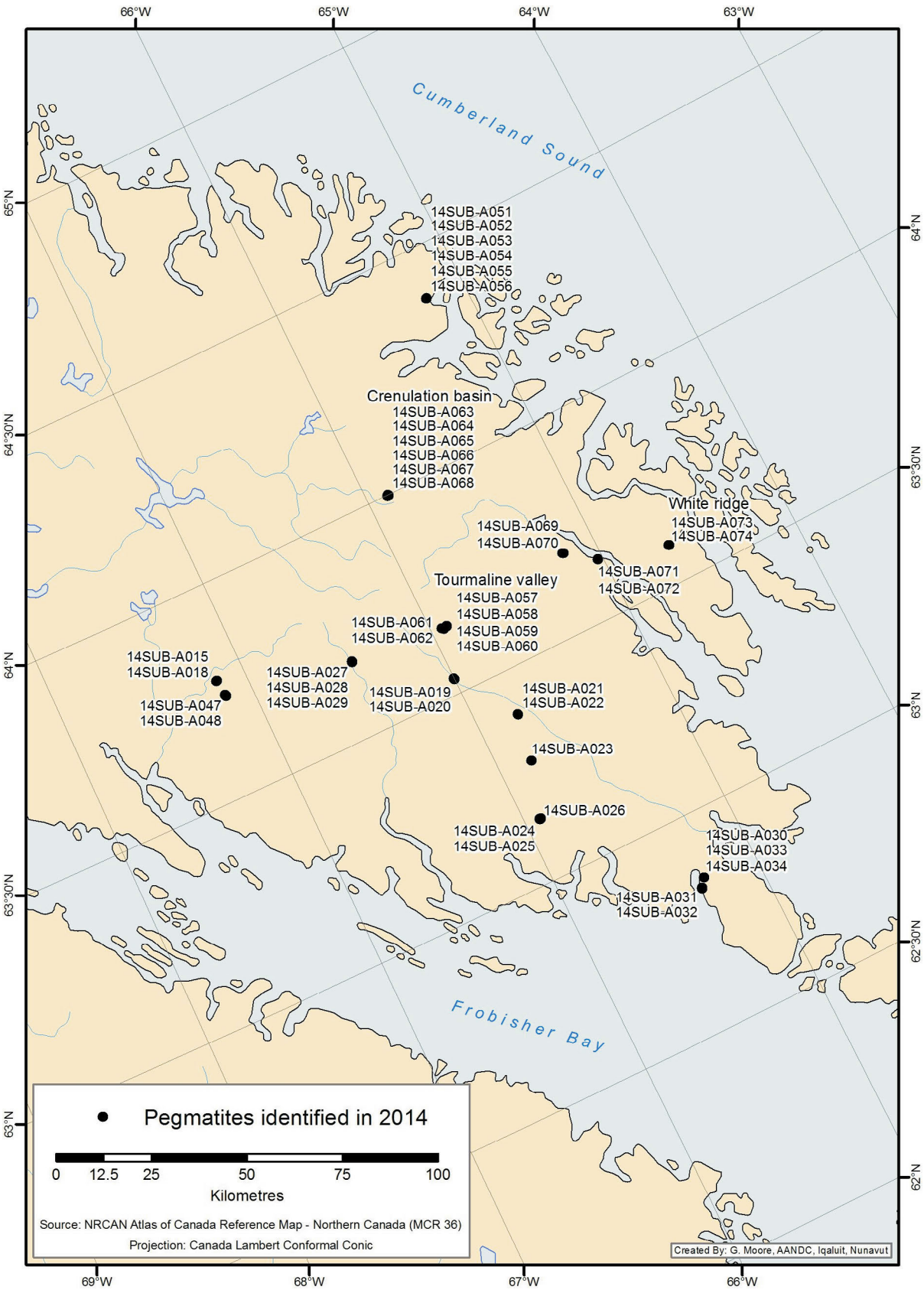

Figure 3: Pegmatite dykes sampled in the 2014 field season on Hall Peninsula, labelled with station numbers. Abbreviation: AANDC, Aboriginal Affairs and Northern Development Canada.

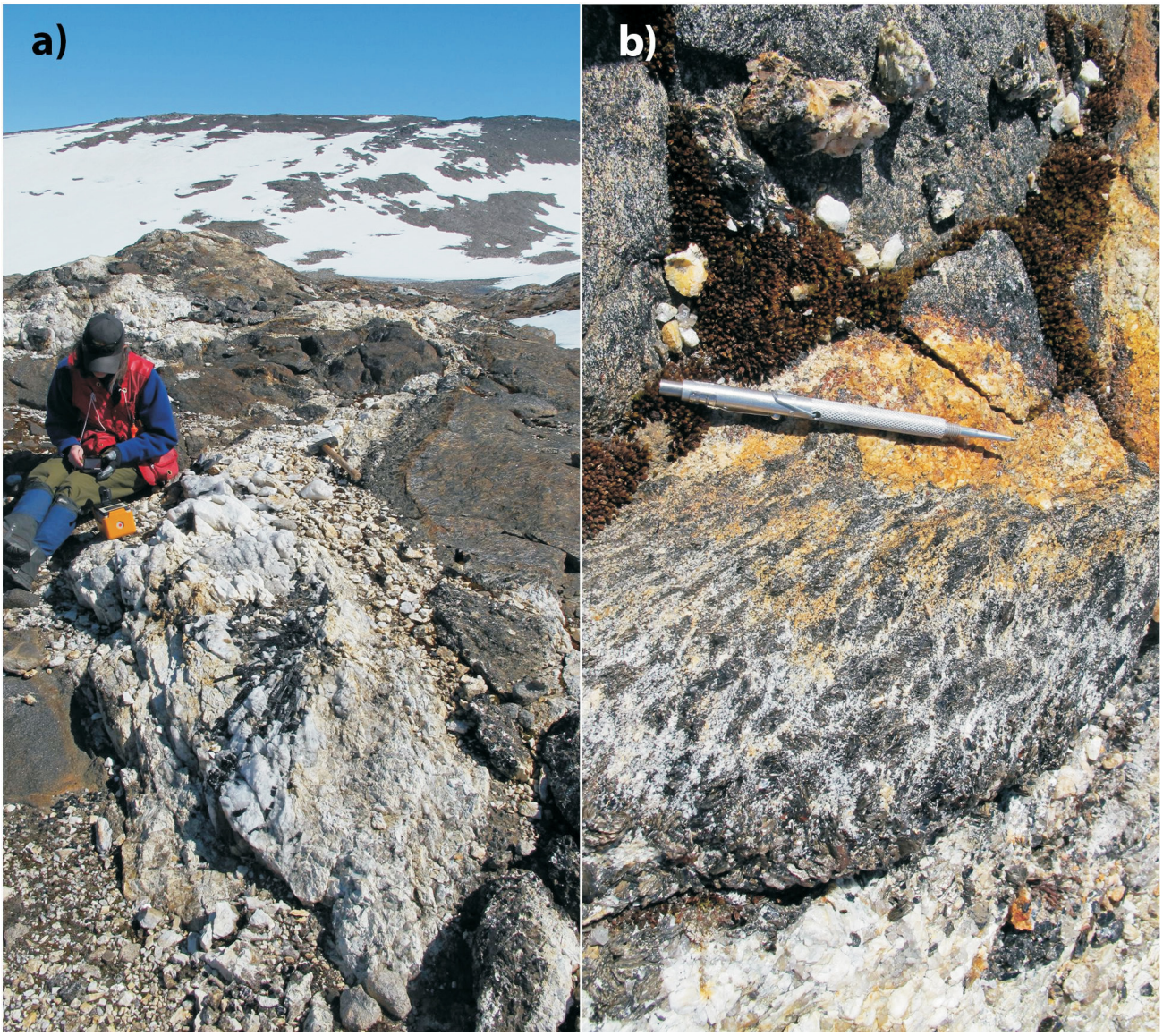

Figure 4: Pegmatite textures at Crenulation basin (see Figure 3 for location, southern Hall Peninsula): **a)** metre-scale tourmaline cluster in pegmatite at Crenulation basin, intruding amphibolite country rock; **b)** 'leopard-spot' reaction texture at the contact between a pegmatite intrusion and the amphibolite country rock.

As an example of this type of study, Peng et al. (2011) attempted to identify metallogenic pegmatites using remote sensing in the Azubai area of Xinjiang province, China, a region known for its high number of economically valuable pegmatite deposits. Existing geological maps and field observations were used to 'train' detection algorithms. Field observations consisted of measuring rock samples with a portable spectrometer to obtain average rock type spectral reflectance data. This data was used to build a library of rock reflectance spectra with which classifications derived from the RapidEye satellite imagery were compared. Pegmatite samples were determined to have the highest reflectance, from 0.36 to 0.76, whereas granite was slightly lower at 0.29 to 0.46. The authors were successful in using this method of classification to identify three new exploration targets in their field area (Peng et al., 2011). The process described by Sinergeo (2013) begins with a study of the geology of the pegmatite fields to be evaluated, followed by satellite image classification for possible targets, drilling on those targets, and then developing 3D models to further characterize the pegmatites located. Analysis of the structure and mineralogy of the pegmatites determines their potential for economic extraction.

Several suspected exposures of pegmatites identified in RapidEye data were validated in the field (including stations 14SUB-A069, A070, A071, A072 and A074). Although a predictive approach using RapidEye data was helpful, several identified targets were false positives and did not turn out to be pegmatite, and several known pegma-

Figure 5: Mineralization present in pegmatite dykes at station 14SUB-A059, Hall Peninsula: **a)** rich tourmaline crystallization in pegmatite vein; **b)** beryl crystal in situ, surrounded by a small 'pod' of muscovite.

tites were also not identified according to the criteria described above. Nonetheless, as a complementary tool, the satellite data served a useful purpose to assist with the fieldwork.

Pegmatite evaluation with EXPLORANIUM® GR-135 Plus radioisotope detector

The EXPLORANIUM® GR-135 Plus radioisotope detector was used to evaluate pegmatites in the field for gamma-ray activity, which could indicate minerals suitable for radiometric dating, or potential uranium mineralization. Several pegmatites with radioactivity higher than the background average were located during the 2014 fieldwork, including 14SUB-A020, at which an outcrop with a maximum total counts per second (cps) value of 4952 was identified, and 14SUB-A074, at which an outcrop with a maximum total cps of 5278 was identified. Several other pegmatites returned high readings on the GR-135 detector. Samples from these pegmatites will be prioritized for future geochronology work.

Economic considerations

Pegmatites are major sources of economically significant elements, such as Li, Cs, Ta and Sn, and rare-earth elements (REEs), as well as ceramic-grade feldspar and electronics-grade quartz and gems such as beryl or gem-quality tourmaline (Èerný and Ercit, 2005). As the economic potential of Baffin Island pegmatites has not been previously evaluated, publishing information about the geochemistry and mineralogy of pegmatites in the southern Baffin region can provide industry with possible targets for exploration and evaluation. Fieldwork in Nunavut is often more expensive and more logistically difficult than in other Canadian regions, so narrowing down target areas can be helpful in allowing companies to focus their exploration plans on the most prospective areas before they put boots on the ground.

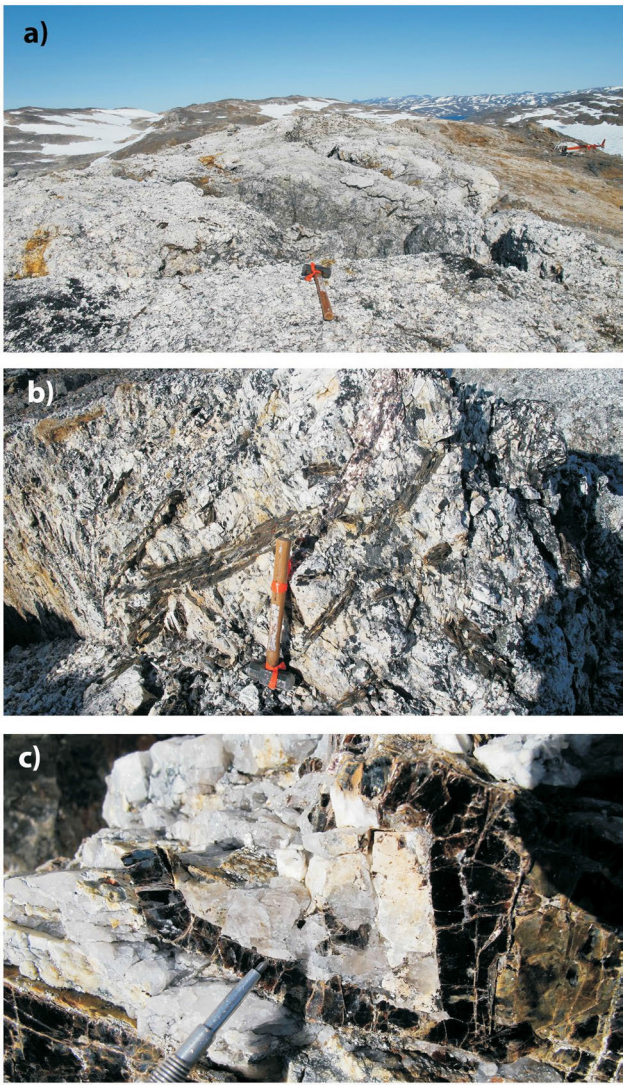

Figure 6: White ridge pegmatite outcrop, stations 14SUB-A073 and A074, located on the large peninsula between Allen and Brevoort islands: **a)** looking east along the main pegmatite outcrop at station 14SUB-A074, which consists almost entirely of extremely coarse-grained pegmatite material and is approximately 20 m wide; note the bright reflections on the surfaces of feldspar crystals; hammer in foreground is 50 cm long; **b)** metre-scale sheets and books of biotite in pegmatite boulder at station 14SUB-A074; hammer is 50 cm long; **c)** 'window'-texture biotite surrounding quartz and feldspar at station 14SUB-A074; tip of scratch tool is 2 mm across.

Figure 7: RapidEye image taken August 31, 2012, showing the location of stations 14SUB-A073 and A074, Hall Peninsula (north up, 2 by 1.5 km), and a large pegmatite dyke exposed over a strike length of approximately 100 m. The image uses bands 3, 2 and 1 as red, green and blue (RGB) values, giving a near-true colour image (RapidEye AG, 2011).

The global markets for lithium and REEs are currently supplied primarily by Australia, Chile and China. However, the potential for economic deposits of rare earths and rare metals exists in several places in Canada. Although no REE production or refining is currently taking place in Canada, the investment and political climates are stable and the mining industry has the necessary expertise (House of Commons, Standing Committee on Natural Resources, 2014). Lithium is currently being mined in Quebec, where Canada Lithium Corp., has been producing lithium carbonate since 2013. Demand for REEs and other rare metals and elements is expected to increase worldwide due to increasing demand for advanced electronics products and clean energy applications (CREEN, 2013). Therefore, increased supply of these commodities would be beneficial to the Canadian economy (House of Commons, Standing Committee on Natural Resources, 2014).

Conclusions

Over 30 pegmatites were visited and sampled during fieldwork on Hall Peninsula. Whole-rock lithogeochemistry and LA-MC-ICP-MS mineral-chemical work is planned for the majority of the samples to determine their rare metal and gem potential, and age. To date, the gem potential for pegmatites in the southern Baffin region appears to be low, as no pegmatite containing miarolitic cavities has been discovered. The source of these pegmatites (i.e., anatectic melting versus later emplacement from a parent melt source at depth) and their place in the tectonometamorphic settings of Hall, Cumberland and Meta Incognita peninsulas will require further work in order to be determined.

In the limited visual examination of RapidEye satellite data, several larger pegmatites were detected, and later confirmed when compared to sites visited during the fieldwork, which indicates a potential use for satellite image

Figure 8: Pegmatite dyke at stations 14SUB-A073 and A074, Hall Peninsula, looking north. Station 14SUB-A074 is located on the white outcrop below the dark amphibolite unit, and is approximately 20 m wide. A small feeder vein of pegmatite material is visible in the centre of the photo.

data in mapping pegmatite in the Arctic and in other arid, sparsely-vegetated settings where exposures are prominent. As the geological terrane of the region appears to be suited to this type of analysis, next steps for the project include development of a pegmatite classification scheme and the processing of available RapidEye satellite data to identify potential targets.

Acknowledgments

The authors would like to thank H. Steenkamp and D.J. Mate and the Canada-Nunavut Geoscience Office for their financial and logistical support of this project; the Canadian Northern Economic Development Agency's Strategic Investments in Northern Economic Development (SINED) program, which also provided funding for the HPIGP; D. Lentz in his capacity as M.Sc. advisor to the corresponding author; J. Harris and D.J. Mate for their reviews; T. Sifrer with RnD Technical for the technical editing; G. Moore at Aboriginal Affairs and Northern Development Canada (AANDC) for cartography assistance; and the Nunavut Regional Office of AANDC.

References

Budkewitsch, P., Bilodeau, C. and Senkow, M.D. 2013: Identification of iron-rich components in bedrock and till from multispectral satellite imaging in support of geoscience mapping of Hall Peninsula, Baffin Island, Nunavut; *in* Summary of Activities 2012, Canada-Nunavut Geoscience Office, p. 85–92.

House of Commons, Standing Committee on Natural Resources 2014: The rare earth elements industry in Canada: summary of evidence, 41st Parliament, Second Session, June 2014; House of Commons, Canada, URL <http://www.parl.gc.ca/Content/HOC/Committee/412/RNNR/WebDoc/WD-6669744/412_RNNR_reldoc_PDF/RareEarthElements-Summary-e.pdf> [September 25, 2014].

Canadian Rare Earth Elements Network (CREEN) 2013: Global REE production; Canadian Institute of Mining, Metallurgy and Petroleum, website, URL <http://www.cim.org/en/RareEarth/Home/GlobalReeProduction.aspx> [September 22, 2014].

Èerný, P. and Ercit, T.S. 2005: The classification of granitic pegmatites revisited; The Canadian Mineralogist, v. 43, p. 2005-2026, doi: 10.2113/gscanmin.43.6.2005, [November, 2014].

Èerný, P., London, D. and Novàk, M. 2012: Granitic pegmatites as reflections of their sources; Elements, v. 8, p. 289–294, doi:10.2113/gselements.8.4.289, [November, 2014].

Dyck, B.D. and St-Onge, M.R. 2014. Dehydration-melting reactions, leucogranite emplacement and the Paleoproterozoic structural evolution of Hall Peninsula, Baffin Island, Nunavut; *in* Summary of Activities 2013, Canada-Nunavut Geoscience Office, p. 73–84.

From, R.E., Camacho, A.L. and St-Onge, M.R. 2013: Preliminary observations on the nature and origin of the eastern orthogneiss complex of southern Hall Peninsula, Baffin Island, Nunavut; *in* Summary of Activities 2012, Canada-Nunavut Geoscience Office, p. 43–54.

From, R.E., St-Onge, M.R. and Camacho, A.L. 2014: Preliminary characterization of the Archean orthogneiss complex of Hall Peninsula, Baffin Island, Nunavut; *in* Summary of Activities 2013, Canada-Nunavut Geoscience Office, p. 53–62.

Harris, J. R., ed. 2008: Remote predictive mapping: an aid for northern mapping; Geological Survey of Canada, Open File 5643, 306 p.

Machado, G., Bilodeau, C., Takpanie, R., St-Onge, M.R., Rayner, N.M., Skipton, D.R., From, R.E., MacKay, C.B., Creason, C.G. and Braden, Z.M. 2013: Hall Peninsula regional bedrock mapping, Baffin Island, Nunavut: summary of fieldwork; *in* Summary of Activities 2012, Canada-Nunavut Geoscience Office, p. 13–22.

Naughton, D., Brunn, A., Czapla-Myers, J., Douglass, S., Thiele, M., Weichelt, H. and Oxfort, M. 2011: Absolute radiometric calibration of the RapidEye multispectral imager using the reflectance-based vicarious calibration method; Journal of Applied Remote Sensing, v. 5, 23 p.

Peng, G.-X., Ye, Z.-C., Gao, G.-M., Feng, D.-S. and Xiong, Y. 2011: Pegmatite remote sensing extraction and metallogenic prediction in Azubai area, Xinjiang; Transactions of Nonferrous Metals Society of China, v. 21, p. 543–548.

RapidEye AG. 2011: RapidEye satellite imagery product specifications, version 3.2.; RapidEye AG, product manual, 47 p., URL <http://www.rapideye.de/upload/RE_Product_Specifications_ENG.pdf> [November 2014].

Selway, J., Breaks, F.W. and Tindle, A.G. 2005: A review of rare-element (Li-Cs-Ta) pegmatite exploration techniques for the Superior Province, Canada, and large worldwide tantalum deposits; Exploration and Mining Geology, v. 14, p. 130.

Sinergeo Lda. 2013: Prospeg project - pegmatite remote sensing and mapping final report; Universidade de Minho, 138 p., URL <http://www.prospeg.org/en/resultados?article=8> [November 2014].

Skipton, D.R. and St-Onge, M.R. 2014: Paleoproterozoic deformation and metamorphism in metasedimentary rocks west of Okalik Bay: a field template for the evolution of eastern Hall Peninsula, Baffin Island, Nunavut; *in* Summary of Activities 2013, Canada-Nunavut Geoscience Office, p. 63–72.

Steenkamp, H.M. and St-Onge, M.R. 2014: Overview of the 2013 regional bedrock mapping program on northern Hall Peninsula, Baffin Island, Nunavut; *in* Summary of Activities 2013, Canada-Nunavut Geoscience Office, p. 27–38.

Van Lichtervelde, M., Grégoire, M., Linnen, R.L. and Béziat, D. 2007: Trace element geochemistry by laser ablation IAP-MS of micas associated with Ta mineralization in the Tanco pegmatite, Manitoba, Canada; Contributions to Mineralogy and Petrology, v. 155, p. 791–806.

Mafic, ultramafic and layered mafic-ultramafic sills, Meta Incognita Peninsula, southern Baffin Island, Nunavut

M.R. St-Onge[1], N.M. Rayner[2], D. Liikane[3] and T. Chadwick[3]

[1]*Natural Resources Canada, Geological Survey of Canada, Ottawa, Ontario, Marc.St-Onge@NRCan-RNCan.gc.ca*

[2]*Natural Resources Canada, Geological Survey of Canada, Ottawa, Ontario*

[3]*Department of Earth Sciences, Carleton University, Ottawa, Ontario*

This work was part of the Geo-mapping for Energy and Minerals (GEM) Program on Baffin Island and is being led by the Geological Survey of Canada (GSC) in collaboration with the Canada-Nunavut Geoscience Office, Aboriginal Affairs and Northern Development Canada, Nunavut Arctic College, the University of Ottawa and Carleton University. The study area comprises all or parts of six 1:250 000 scale National Topographic System map areas south and east of Iqaluit (NTS 025G, I, J, K, N, O). The objective of this work is to complete the regional bedrock mapping for the southern half of Baffin Island and develop a new, modern, geoscience compilation for the region.

St-Onge, M.R., Rayner, N.M., Liikane, D. and Chadwick, T. 2015: Mafic, ultramafic and layered mafic-ultramafic sills, Meta Incognita Peninsula, southern Baffin Island, Nunavut; *in* Summary of Activities 2014, Canada-Nunavut Geoscience Office, p. 11–16.

Abstract

This paper summarizes the 2014 field observations on a suite of mafic, ultramafic and layered mafic-ultramafic sills on Meta Incognita Peninsula, Baffin Island, Nunavut. The sills, several of which are up to hundreds of metres in thickness, are emplaced into the dominantly psammitic to pelitic sedimentary strata of the middle Paleoproterozoic Lake Harbour Group. Layering in both mafic and ultramafic bodies was observed on the centimetre to metre scale, with many intrusions containing disseminated sulphide, some associated with ferricrete. Within individual sills, compositional differentiation can range from pyroxenite/peridotite layers at the intrusive base to gabbro and leucogabbro units at the top. Similar bodies have previously been documented elsewhere on southern Baffin Island (Foxe, Hall and western Meta Incognita peninsulas), and a mantle-derived magmatic province of this size potentially represents a major large igneous province (LIP) event warranting further study. Forthcoming geochemical, petrological and geochronological analyses, part of an M.Sc. thesis on the petrology and geochemistry of the layered suite and associated mineralization, will be utilized to compare and improve on existing regional tectonic models of middle Paleoproterozoic extension in the eastern Trans-Hudson Orogen.

Résumé

Le présent document résume les observations de terrain faites en 2014 au sujet d'une suite de filons-couches mafiques, ultramafiques et mafiques-ultramafiques stratifiés de la péninsule Meta Incognita, dans l'île de Baffin, au Nunavut. Les filons-couches, dont plusieurs ont plusieurs centaines de mètres d'épaisseur, ont été mis en place dans les strates sédimentaires à composition prédominante psammitique-pélitique du groupe de Lac Harbour, datant du Paléoprotérozoïque moyen. On a noté la présence d'une stratification d'ordre centimétrique à métrique dans les intrusions mafiques et ultramafiques, dont plusieurs renferment des sulfures disséminés, parfois associés à des sédiments ferrugineux. Au sein des filons-couches individuels, la différenciation en terme de composition peut varier de la pyroxénite ou péridotite à l'endroit de la base intrusive, jusqu'au gabbro ou leucogabbro au sommet. La présence de filons-couches similaires a été remarquée ailleurs dans la partie sud de l'île de Baffin (péninsules Foxe et Hall et partie ouest de la péninsule Meta Incognita) et une province magmatique d'origine mantellique de cette taille peut constituer une importante province ignée faisant appel à une étude plus approfondie. Les analyses géochimiques, pétrologiques et géochronologiques à venir (thèse de maîtrise sur la pétrologie et la géochimie de la suite stratifiée et de la minéralisation associée) serviront à l'examen comparatif et à l'amélioration des modèles tectoniques actuels d'extension régionale ayant eu lieu au cours du Paléoprotérozoïque moyen dans la partie est de l'orogène trans-hudsonien.

This publication is also available, free of charge, as colour digital files in Adobe Acrobat® PDF format from the Canada-Nunavut Geoscience Office website: http://cngo.ca/summary-of-activities/2014/.

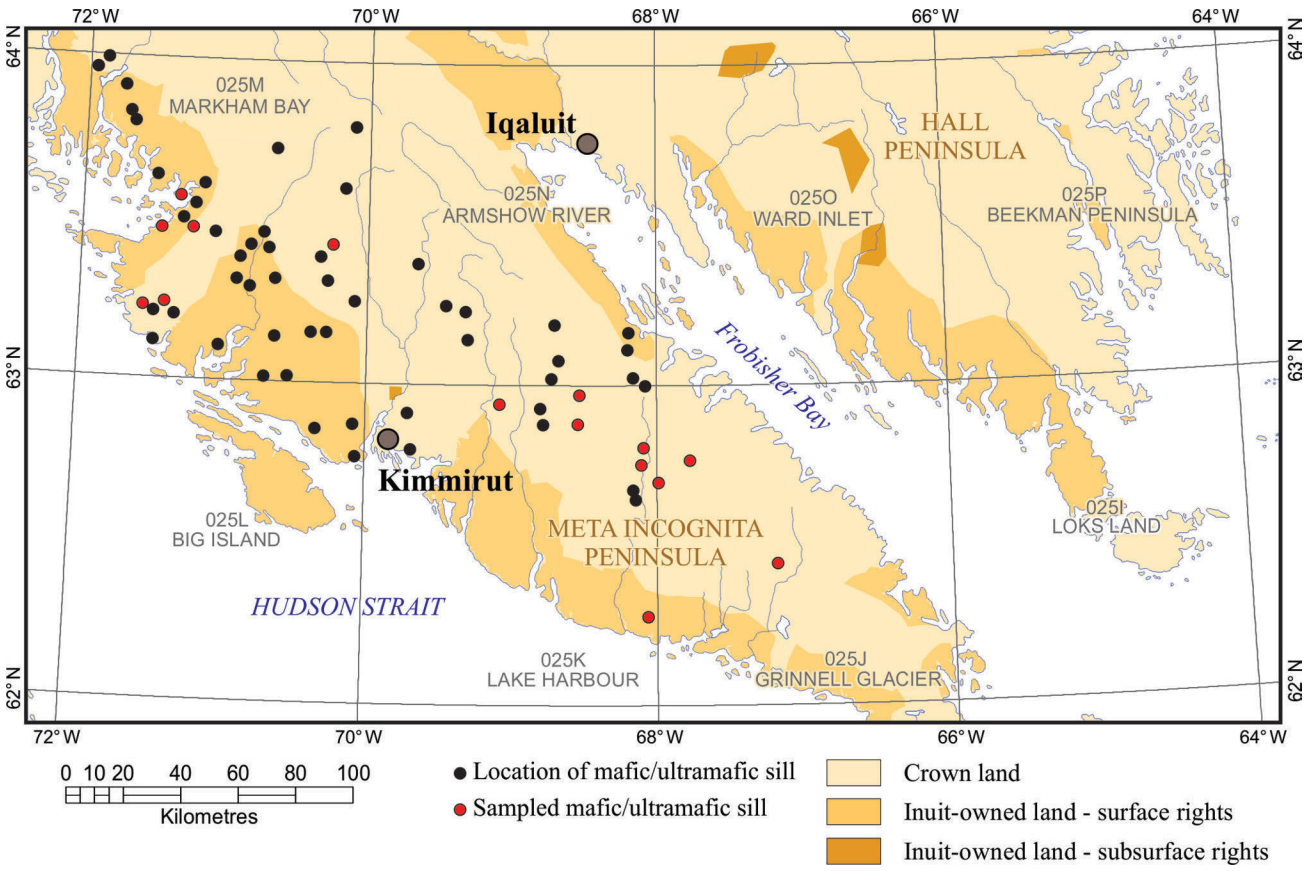

Figure 1: Location of the mafic, ultramafic and layered mafic-ultramafic sills on Meta Incognita Peninsula also showing proximity to the communities of Iqaluit and Kimmirut, as well as ownership of surface and subsurface mineral rights; intrusions sampled for geochemical and/or geochronological analysis are shown in red; the forthcoming lab work will form part of an M.Sc. thesis on the petrology and geochemistry of the layered suite and associated mineralization.

Introduction

The Geo-mapping for Energy and Minerals (GEM) program targeted Meta Incognita Peninsula in 2014 (St-Onge et al., 2015) to contribute to completing regional bedrock mapping coverage for the southern half of Baffin Island. Fieldwork was carried out between July 15 and August 15 (parts of NTS 25G, I, J, K, N, O) and was led by the Geological Survey of Canada (GSC) in collaboration with the Canada-Nunavut Geoscience Office (CNGO). Regional and targeted bedrock mapping also involved participants from Aboriginal Affairs and Northern Development Canada, Nunavut Arctic College, the University of Ottawa and Carleton University. The present report presents an overview of the main field characteristics and the economic potential identified for an extensive suite of mafic, ultramafic and layered mafic-ultramafic sills on Meta Incognita Peninsula (Figure 1).

Geological framework

The metasedimentary and metaplutonic units on Meta Incognita Peninsula are part of the northeastern (Quebec-Baffin) segment of the Trans-Hudson Orogen, a collisional orogenic belt that extends in a broad arcuate shape from northeastern to south-central North America (Hoffman 1988; Lewry and Collerson, 1990), and which comprises tectonostratigraphic assemblages accumulated on, or accreted to, the northern margin of the lower-plate Superior craton of Paleoarchean to Neoarchean age during the middle Paleoproterozoic (St-Onge et al., 2006, 2009). Southern Baffin Island is characterized by three orogen-scale stacked tectonic elements (St-Onge et al., 2002, 2015) that are separated by major deformation zones. The crustal architecture on the island includes the tectonostratigraphic units of the Lake Harbour Group (Jackson and Taylor, 1972) and a number of metaplutonic gneissic units interpreted by St-Onge et al. (2000) as the cover sequence and crystalline basement of a middle Paleoproterozoic accreted terrane termed the Meta Incognita microcontinent. Various phases of the Cumberland Batholith (Whalen et al., 2010) intrude the crystalline and cover units. The supracrustal, gneissic and plutonic rocks on the eastern Meta Incognita Peninsula were the main focus of fieldwork during the summer of 2014.

Lake Harbour Group

The quartzite, marble, psammite and semipelite sedimentary strata mapped on Meta Incognita Peninsula of southern

Baffin Island belong to the middle Paleoproterozoic Lake Harbour Group, with the well-exposed type locality situated north of the community of Kimmirut (St-Onge et al., 1996, 1998; Scott et al., 1997). Over much of the peninsula (St-Onge et al., 1999a-g, 2015), the Lake Harbour Group comprises units of quartzite, garnetiferous psammite, minor semipelite and pelite that are structurally overlain by laterally continuous to boudinaged bands of pale grey to white marble and calcsilicate rocks ('Kimmirut sequence' of Scott et al., 1997). At the eastern and western ends of the peninsula, including extensive exposures of supracrustal rocks on the eastern islands and bluffs (St-Onge et al., 2015) and around Markham Bay (Figure 1), the Lake Harbour Group is dominated by garnetiferous psammite interlayered with pelite/semipelite and is largely devoid of marble and calcsilicate rocks ('Markham Bay sequence' of Scott et al., 1997). Siliciclastic strata in both sequences are nevertheless locally sulphidic and intruded by an extensive suite of mafic to ultramafic rocks described below.

Mafic and ultramafic rocks

Generally concordant to slightly discordant sheets of coarse-grained metaperidotite, medium- to coarse-grained metaperidotite-metagabbro, and fine- to medium-grained metagabbro occur within both sequences of the Lake Harbour Group (St-Onge et al., 2015) on Meta Incognita Peninsula (Figure 1). Individual bodies are typically elongate to lensoid in map view, from 10 to 20 m thick—although some reach from 50 to a few hundred metres in thickness—and extend up to several kilometres along strike. The largest (folded) body observed is approximately 200 m thick and 5.6 km long by 1 km wide. Metamorphic mineral assemblages indicate prevailing amphibolite- to granulite-facies conditions during subsequent Trans-Hudson orogenesis (see St-Onge et al., 2015).

Metagabbro

Several of the mafic intrusions are homogeneous and preserve a well-developed subophitic texture. Others are characterized by a faint and discontinuous, to well-defined, compositional layering due to variations in the abundance of plagioclase and metamorphic clinopyroxene, orthopyroxene and/or hornblende (Figure 2). The centimetre- to metre-scale rhythmic layering is tentatively interpreted to principally result from variations in the modal abundance of plagioclase leading to cumulate stratification. The generally concordant nature, tabular shape, igneous textures and sharp contacts of both types of mafic intrusion suggest that they are sills (Figure 3).

Metaperidotite and metapyroxenite

Several ultramafic bodies, either clinopyroxene-orthopyroxene±hornblende metapyroxenite or olivine-clinopyroxene-orthopyroxene metaperidotite, were observed.

Figure 2: Layered metagabbro, Meta Incognita Peninsula, Baffin Island, Nunavut. Rhythmic layering is defined by variations in the modal amount of hornblende, clinopyroxene and plagioclase; hammer is 35 cm in length.

Figure 3: Mafic sill (dark) emplaced in Lake Harbour Group quartzite (white) and psammite (rusty brown) and subsequently folded, Meta Incognita Peninsula, Baffin Island, Nunavut; width of field of view is 800 m.

In numerous localities, the ultramafic rocks are lithologically layered at the centimetre to metre scale (Figure 4) with overall compositions grading from pyroxenite at the base overlain by peridotite and capped by gabbro to leucogabbro at the top (Figure 5), suggesting a way-up indicator if the layering is the result of magmatic differentiation. The transition from ultramafic to mafic rock types within a given body appears generally gradational and is tentatively interpreted as a primary igneous transition in a cumulate sequence. The contacts of all bodies with the host siliciclastic rocks of the Lake Harbour Group are conformable, and in rare instances chilled margins are preserved. Enclaves of host strata or evidence for partial melting (granophyric intrusive contacts) were not observed. As is the case for the mafic intrusions, overall the observations for the ultramafic bodies suggest they are best interpreted as sills. Many of the intrusions contain disseminated sulphide (pyrite and minor chalcopyrite); chromite and

Figure 4: Layered metaperidotite sill (chocolate brown) emplaced in Lake Harbour Group psammite (cream), Meta Incognita Peninsula, Baffin Island, Nunavut; hammer is 35 cm in length.

Figure 5: Layered and foliated leucogabbro at the top of a composite sill, Meta Incognita Peninsula, Baffin Island, Nunavut.

Figure 6: Gossan in Lake Harbour Group psammite adjacent to a layered mafic-ultramafic sill, Meta Incognita Peninsula, Baffin Island, Nunavut; hammer is 35 cm long.

pentlandite were not noted. Deep orange gossans (Figure 6) were observed in psammite adjacent to the mafic-ultramafic bodies with ferricrete (Figure 7) occurring at the base of some sills. The ferricrete comprises a medium to coarse clastic sediment cemented by an iron oxyhydroxide.

Regional considerations

Nickel–copper–platinum-group element magmatic sulphide deposits and showings have been documented in the Superior craton cover units of the Cape Smith belt of northern Quebec since the 1950s (see overviews in Green and Dupras, 1999; Lesher, 2007). A significant number of publications describe the petrogenesis, petrology and geochemistry of the middle Paleoproterozoic sulphide mineralization and related enrichment in platinum-group elements (PGE) in northern Quebec (e.g., Miller, 1977; Samis and Andersen, 1980; Naldrett, 1981; Barnes et al., 1982, 1992, 1997a, b; Dillon-Leitch et al., 1986; Giovenazzo et al., 1989; Barnes and Barnes, 1990; Barnes and Giovenazzo, 1990; Tremblay, 1990; Giovenazzo, 1991; Lesher and Ripley, 1992; Barnes and Picard, 1993; Lesher et al., 2001; Lesher, 2007) with a few considering the more regional (orogen scale) controls on the distribution and size of the deposits and showings (e.g., Giovenazzo et al., 1989; Giovenazzo, 1991; St-Onge and Lucas, 1994; Lesher, 2007).

In contrast, the layered mafic-ultramafic sills emplaced in the Lake Harbour Group siliciclastic rocks on southern Baffin Island have yet to be studied. Importantly, the mantle-derived intrusions define a new magmatic province that extends from Meta Incognita Peninsula in the east to Foxe Peninsula in the west, with potential extrusive equivalents preserved on the latter (Schooner Bay volcanic sequence; St-Onge et al., 2007), and thus the sills would appear to represent a major large igneous province (LIP) event (Ernst, 2014) and warrant further study. One of the co-authors on this field report, a senior undergraduate student and field assistant in 2014, is initiating an M.Sc. thesis on the petrology, geochemistry and geochronology of the layered mafic/ultramafic suite and associated mineralization. Whether this suite is coeval and has genetic similarities with layered intrusions in northern Quebec and the associated Raglan komatiite-hosted Ni-Cu-PGE deposits will be one of the questions tackled as part of the thesis.

Economic considerations

A number of lithological associations and occurrences with potential economic implications were identified during the 2014 systematic and targeted mapping campaign on Meta Incognita Peninsula. Most significantly, the layered mafic-ultramafic sills emplaced in sulphidic siliciclastic strata of the Lake Harbour Group have a lithological context similar to that hosting Ni–Cu–platinum-group element mineral-

Figure 7: Ferricrete below ultramafic sill, Meta Incognita Peninsula, Baffin Island, Nunavut; hammer is 35 cm long.

ization elsewhere in the Trans-Hudson Orogen (e.g., Raglan deposits in the eastern Cape Smith belt of northern Quebec; Lesher, 2007). Serpentinized ultramafic rocks, some of which still contain olivine, have been identified in a number of localities and may provide material suitable as carving stone.

Acknowledgments

Enthusiastic field assistance in the notably scenic yet physically demanding terrain of the eastern Meta Incognita Peninsula was provided by A. Bigio, R. Hinanik, H. Ireyak, A. Markey, D.J. Mate, D.R. Skipton and H.M. Steenkamp. In addition to contributions in the field, C. Gilbert's knowledge, care and organization of the project data management proved invaluable. Prowess in the kitchen exhibited by D. Guilfoyle fuelled the many and varied participants of the team and we are grateful for her contributions and flexibility. Universal Helicopters, and in particular pilots G. Nuttall and G. Hartery are thanked for safe and professional air support. Many thanks to the management and administrative support of S. Dehler, D.J. Mate, M. Francis, R. Khoun and T. Schroeder. The Polar Continental Shelf Program provided logistical support. Finally, A. Laviolette, G. Buller and R. Buenviaje are acknowledged for invaluable help with capturing the archival and new data for Meta Incognita Peninsula. The careful and insightful reviews of this paper provided by R. Ernst, B. Kjarsgaard and D.J. Mate were greatly appreciated.

Natural Resources Canada, Earth Sciences Sector contribution 20140285

References

Barnes, S.J. and Barnes, S.-J. 1990: A new interpretation of the Katinniq nickel deposit, Ungava, northern Quebec; Economic Geology, v. 85, p. 1269–1272.

Barnes, S.-J. and Giovenazzo, D. 1990: Platinum-group elements in the Bravo intrusion, Cape Smith fold belt, northern Quebec; Canadian Mineralogist, v. 28, p. 431–449.

Barnes, S.-J. and Picard, C.P. 1993: The behavior of platinum group elements during partial melting, crystal fractionation, and sulphide segregation: an example from the Cape Smith fold belt, northern Quebec; Geochimica et Cosmochimica Acta, v. 57, p. 79–87.

Barnes, S.-J., Coats, C.J.A. and Naldrett, A.J. 1982: Petrogenesis of a Proterozoic nickel sulfide-komatiite association: the Katiniq sill, Ungava, Quebec; Economic Geology, v. 77, p. 413–429.

Barnes, S.-J., Makovicky, E., Karup-Moller, S., Makovicky, M. and Rose-Hansen, J. 1997a: Partition coefficients for Ni, Cu, Pd, Pt, Rh and Ir between monosulphide solid solution and sulphide liquid and the implications for the formation of compositionally zoned Ni-Cu sulphide bodies by fractional crystallization of sulphide liquid; Canadian Journal of Earth Sciences, v. 34, p. 366–374.

Barnes, S.-J., Picard, C., Giovenazzo, D. and Tremblay, C. 1992: The composition of nickel-copper sulphide deposits and their host rocks from the Cape Smith fold belt, northern Quebec; Australian Journal of Earth Sciences, v. 39, p. 335–347.

Barnes, S.-J., Zientek, M. and Severson, M. 1997b: Ni, Cu, Au and platinum-group element contents of sulphides associated with intraplate magmatism: a synthesis; Canadian Journal of Earth Sciences, v. 34, p. 337–351.

Dillon-Leitch, H.C.H., Watkinson, D.H. and Coats, C.J.A. 1986: Distribution of platinum-group elements in the Donaldson West deposit, Cape Smith Belt, Quebec; Economic Geology, v. 81, p. 1147–1158.

Ernst, R.E. 2014: Large Igneous Provinces; Cambridge University Press, Cambridge, UK, 653 p.

Giovenazzo, D. 1991: Géologie et caractéristiques géochimiques des minéralisations Ni-Cu-EPG de la région de Delta, ceinture de Cape Smith, Nouveau Québec; Ph.D. thesis, Université du Québec à Chicoutimi.

Giovenazzo, D., Picard, C. and Guha, J. 1989: Tectonic setting of Ni-Cu-PGE deposits in the central part of the Cape Smith Belt; Geoscience Canada, v. 16, p. 134–136.

Green, A.H. and Dupras, N. 1999: Exploration model for komatiitic peridotite-hosted Ni-Cu-(PGE) mineralization in the Raglan Belt; *in* Komatiitic Peridotite-Hosted Fe-Ni-Cu-(PGE) Sulphide Deposits in the Raglan Area, Cape Smith Belt, New Quebec, C.M. Lesher (ed.), Laurentian University, Mineral Exploration Research Centre, Guidebook Series, v. 2, p. 191–199.

Hoffman, P.F. 1988: United Plates of America, the birth of a craton: Early Proterozoic assembly and growth of Laurentia; Annual Reviews of Earth and Planetary Sciences, v. 16, p. 543–603.

Jackson, G.D. and Taylor, F.C. 1972: Correlation of major Aphebian rock units in the northeastern Canadian Shield; Canadian Journal of Earth Sciences, v. 9, p. 1650–1669.

Lesher, C.M. 2007: Ni-Cu-(PGE) deposits in the Raglan area, Cape Smith Belt, New Quebec; *in* Mineral Deposits of Canada: a Synthesis of Major Deposit Types, District Metallogeny, the Evolution of Geological Provinces and Exploration Methods, W.D. Goodfellow (ed.), Geological Association of Canada, Special Publication, v. 5, p. 351–386.

Lesher, C.M. and Ripley, E.M. 1992: Sulfur isotope geochemistry of Proterozoic komatiitic peridotite-hosted Fe-Ni-Cu sul-

fide deposits, Cape Smith Belt, New Quebec; Geological Society of America, Abstracts with Programs, v. 24, p. A62.

Lesher, C.M., Burnham, O.M., Keays, R.R., Barnes, S.J. and Hulbert, L. 2001: Geochemical discrimination of barren and mineralized komatiites associated with magmatic Ni-Cu-(PGE) sulfide deposits; Canadian Mineralogist, v. 39, p. 673–696.

Lewry, J.F. and Collerson, K.D. 1990: The Trans-Hudson Orogen; extent, subdivisions, and problems; *in* The Early Proterozoic Trans-Hudson Orogen of North America, J.F. Lewry and M.R. Stauffer (ed.), Geological Association of Canada, Special Paper 37, p. 1–14.

Miller, A.R. 1977: Petrology and geochemistry of the 2-3 ultramafic sill and related rocks, Cape Smith–Wakeham Bay fold belt, Quebec; Ph.D. thesis, University of Western Ontario, London, Ontario.

Naldrett, A.J. 1981: Nickel sulfide deposits: classification, composition, and genesis; Economic Geology, v. 75, p. 628–685.

Samis, A.M. and Andersen, E.O. 1980: 1979 year-end report on the Kenty Project: summary of 1979 exploration programme on Ungava permits 567 and 568; Ministère de l'Énergie et des Ressources du Quebec, Document technique, GM 36257.

Scott, D.J., St-Onge, M.R., Wodicka, N. and Hanmer, S. 1997: Geology of the Markham Bay–Crooks Inlet area, southern Baffin Island, Northwest Territories; *in* Geological Survey of Canada, Current Research 1997-C, p. 157–166.

St-Onge, M.R. and Lucas, S.B. 1994: Controls on the regional distribution of iron-nickel-copper-platinum group element sulfide mineralization in the eastern Cape Smith Belt, Quebec; Canadian Journal of Earth Sciences, v. 31, p. 206–218.

St-Onge, M.R., Hanmer, S. and Scott, D.J. 1996: Geology of the Meta Incognita Peninsula, south Baffin Island: tectonostratigraphic units and regional correlations; *in* Geological Survey of Canada, Current Research 1996-C, p. 63–72.

St-Onge, M.R., Rayner, N.M., Steenkamp, H.M. and Skipton, D.R. 2015: Bedrock mapping of eastern Meta Incognita Peninsula, southern Baffin Island, Nunavut; *in* Summary of Activities 2014, Canada-Nunavut Geoscience Office, p. 105–118.

St-Onge, M.R., Sanborn-Barrie, M. and Young, M.D. 2007: Geology, Foxe Peninsula, Baffin Island, Nunavut; Geological Survey of Canada, Open File 5434, 1:200 000 scale, doi:10.4095/224222.

St-Onge, M.R., Scott, D.J. and Lucas, S.B. 2000: Early partitioning of Quebec: Microcontinent formation in the Paleoproterozoic; Geology, v. 28, p. 323–326.

St-Onge, M.R., Scott, D.J. and Wodicka, N. 1999a: Geology, Frobisher Bay, Nunavut; Geological Survey of Canada, "A" Series Map 1979A, 1:100 000 scale, doi:10.4095/210833.

St-Onge, M.R., Scott, D.J. and Wodicka, N. 1999b: Geology, Hidden Bay, Nunavut; Geological Survey of Canada, "A" Series Map 1980A, 1:100 000 scale, doi:10.4095/210835.

St-Onge, M.R., Scott, D.J. and Wodicka, N. 1999c: Geology, McKellar Bay, Nunavut; Geological Survey of Canada, "A" Series Map 1981A, 1:100 000 scale, doi:10.4095/210836.

St-Onge, M.R., Scott, D.J. and Wodicka, N. 1999d: Geology, Wright Inlet, Nunavut; Geological Survey of Canada, "A" Series Map 1982A, 1:100 000 scale, doi:10.4095/210840.

St-Onge, M.R., Scott, D.J. and Wodicka, N. 1999e: Geology, Blandford Bay, Nunavut; Geological Survey of Canada, "A" Series Map 1983A, 1:100 000 scale, doi:10.4095/210837.

St-Onge, M.R., Scott, D.J. and Wodicka, N. 1999f: Geology, Crooks Inlet, Nunavut; Geological Survey of Canada, "A" Series Map 1984A, 1:100 000 scale, doi:10.4095/210838.

St-Onge, M.R., Scott, D.J. and Wodicka, N. 1999g: Geology, White Strait, Nunavut; Geological Survey of Canada, "A" Series Map 1985A, 1:100 000 scale, doi:10.4095/210839.

St-Onge, M.R., Scott, D.J. and Wodicka, N. 2002: Review of crustal architecture and evolution in the Ungava Peninsula–Baffin Island area: connection to the Lithoprobe ECSOOT transect; Canadian Journal of Earth Sciences, v. 39, p. 589-610, doi:10.1139/E02-022.

St-Onge, M.R., Scott, D.J., Wodicka, N. and Lucas, S.B. 1998: Geology of the McKellar Bay–Wight Inlet–Frobisher Bay area, southern Baffin Island, Northwest Territories; *in* Geological Survey of Canada, Current Research 1998-C, p. 43–53.

St-Onge, M.R., Searle, M.P. and Wodicka, N. 2006: Trans-Hudson Orogen of North America and Himalaya-Karakoram-Tibetan Orogen of Asia: structural and thermal characteristics of the lower and upper plates; Tectonics, v. 25, TC4006, 22 p., doi:10.1029/2005TC001907.

St-Onge, M.R., Van Gool, J.A.M., Garde, A.A. and Scott, D.J. 2009: Correlation of Archaean and Palaeoproterozoic units between northeastern Canada and western Greenland: constraining the pre-collisional upper plate accretionary history of the Trans-Hudson orogen; *in* Earth Accretionary Systems in Space and Time, P.A. Cawood and A. Kroner (ed.), The Geological Society, London, Special Publications, v. 318, p. 193–235, doi:10.1144/SP318.7.

St-Onge, M.R., Wodicka, N. and Ijewliw, O. 2007: Polymetamorphic evolution of the Trans-Hudson Orogen, Baffin Island, Canada: integration of petrological, structural and geochronological data; Journal of Petrology, v. 48, p. 271–302, doi:10.1093/petrology/eg1060.

Tremblay, C. 1990: Les éléments du groupe du platine dans le dyke de Méquillon, ceinture du Cape Smith, Nouveau-Québec; M.Sc. thesis, Université du Québec à Chicoutimi.

Whalen, J.B., Wodicka, N., Taylor, B.E. and Jackson, G.D. 2010: Cumberland batholith, Trans-Hudson Orogen, Canada: petrogenesis and implications for Paleoproterozoic crustal and orogenic processes; Lithos, v. 117, p. 99–118, doi: 10.1016/j.lithos.2010.02.008.

New insights on the cooling history of Hall Peninsula, southern Baffin Island, Nunavut, using $^{40}Ar/^{39}Ar$ thermochronology on muscovite

D.R. Skipton[1], D.A. Schneider[2], D. Kellett[3] and N. Joyce[3]

[1]*Department of Earth Sciences, University of Ottawa, Ottawa, Ontario, dianeskipton@gmail.com*

[2]*Department of Earth Sciences, University of Ottawa, Ottawa, Ontario*

[3]*Natural Resources Canada, Geological Survey of Canada, Ottawa, Ontario*

This work was part of the 2012–2014 Hall Peninsula Integrated Geoscience Program (HPIGP), led by the Canada-Nunavut Geoscience Office (CNGO) in collaboration with the Government of Nunavut, Aboriginal Affairs and Northern Development Canada, and the Geological Survey of Canada. It involved strong contributions from the Universities of Alberta, Dalhousie, Laval, Manitoba, Ottawa, Saskatchewan and New Brunswick, and the Nunavut Arctic College. It has benefitted from support by local and Inuit-owned businesses and the Polar Continental Shelf Program. The focus is on bedrock and surficial geology mapping (1:100 000 scale). In addition, a range of thematic studies is being conducted, including Archean and Paleoproterozoic tectonics, geochronology, landscape uplift and exhumation, microdiamonds, sedimentary-rock xenoliths and permafrost. The goal is to increase the level of geological knowledge and better evaluate the natural-resource potential in this frontier area.

Skipton, D.R., Schneider, D.A., Kellett, D. and Joyce, N. 2015: New insights on the cooling history of Hall Peninsula, southern Baffin Island, Nunavut, using $^{40}Ar/^{39}Ar$ thermochronology on muscovite; *in* Summary of Activities 2014, Canada-Nunavut Geoscience Office, p. 17–30.

Abstract

This paper presents $^{40}Ar/^{39}Ar$ thermochronology on muscovite from three metapelite samples collected from eastern Hall Peninsula, Baffin Island, in the Paleoproterozoic Trans-Hudson Orogen. Muscovite from each sample was analyzed for mineral chemistry by electron microprobe. The highest-quality, unaltered and inclusion-free muscovite was selected from each sample and dated by the $^{40}Ar/^{39}Ar$ step-heating laser (CO_2) method. In addition, single spot analysis transects were performed on large muscovite grains using an ultraviolet (UV) laser to investigate within-grain $^{40}Ar/^{39}Ar$ age variations. The step-heating ages ranged from 1690 ±3 to 1657 ±3 Ma. For the three grains analyzed using the UV laser, spot ages range from ca. 1661–1640 Ma, ca. 1675–1645 Ma and ca. 1680–1652 Ma, with ages that decrease by 20–30 m.y. from core to rim. Available geochronology suggests that the age of peak metamorphism on Hall Peninsula is ca. 1850–1830 Ma, thus, the $^{40}Ar/^{39}Ar$ step-heating and UV laser data imply that eastern Hall Peninsula remained hotter than the nominal closure temperature of radiogenic Ar in muscovite (~420–450°C) for at least 140 m.y. after peak conditions. Hall Peninsula appears to represent a section of orogenic middle crust with an overall slow cooling rate similar to other large, hot Paleoproterozoic orogens.

Résumé

Le présent article fait état des résultats d'analyse thermochronologique ^{40}Ar-^{39}Ar sur la muscovite provenant de trois échantillons de métapélite recueillis dans la partie est de la péninsule Hall, dans l'île de Baffin, une région sise au sein de l'orogène trans-hudsonien d'âge paléoprotérozoïque. La chimie minérale de la muscovite provenant de chaque échantillon a été établie au moyen d'analyses effectuées par microsonde électronique. On a tiré de chacun de ces échantillons de la muscovite de la plus haute qualité, non altérée et libre de toute inclusion en vue de la soumettre à la méthode de datation ^{40}Ar-^{39}Ar (CO_2) réalisée par réchauffement au laser de l'échantillon par étapes successives. En outre, de gros grains de muscovite ont été soumis à des transects d'analyses sur grains uniques et une datation ponctuelle au moyen d'un laser ultraviolet (UV) en vue d'étudier les variations intragranulaires au niveau des âges ^{40}Ar-^{39}Ar. Les âges obtenus au moyen de la technique de réchauffement par étapes successives varient entre 1690 ± 3 et 1657 ±3 Ma. Dans le cas des trois grains analysés au moyen d'un laser UV, les âges varient entre 1661–1640 Ma, 1675–1645 Ma et 1680–1652 Ma, ces âges accusant une diminution de 20 à 30 millions d'années du centre vers l'extérieur des grains. Les données géochronologiques disponibles semblent indiquer que le métamorphisme a atteint son paroxysme il y a 1850–1830 Ma dans la péninsule Hall et, ainsi, les données provenant de la technique ^{40}Ar-^{39}Ar de réchauffement par étapes successives et celles obtenues au moyen du laser UV portent à croire que la température dans la partie est de la péninsule Hall a atteint un degré supérieur à la température nominale

This publication is also available, free of charge, as colour digital files in Adobe Acrobat® PDF format from the Canada-Nunavut Geoscience Office website: http://cngo.ca/summary-of-activities/2014/.

de fermeture propre à l'argon radiogénique de la muscovite (approximativement 420 à 450 °C) et s'est maintenue ainsi pendant au moins 140 millions d'années suivant le pic du métamorphisme. La péninsule Hall semble faire partie d'une section de croûte moyenne orogénique caractérisée par un taux de refroidissement lent, à l'instar d'autres zones orogéniques chaudes de grande taille d'âge paléoprotérozoïque.

Introduction

Hall Peninsula represents a lithologically diverse section of exhumed middle crust in the northeastern Paleoproterozoic Trans-Hudson Orogen. Metamorphic mineral assemblages indicate that Hall Peninsula experienced peak metamorphism at amphibolite- to granulite-facies conditions under pressures of about 5–7 kbar. Existing geochronology suggests that metamorphism began as early as 1886 Ma and peaked at ca. 1850–1830 Ma, with minor subsequent zircon and monazite growth at ca. 1780–1736 Ma and 1800–1770 Ma, respectively (Scott, 1999; Skipton et al., 2013; Rayner, 2014). Cooling ages (from the K-Ar method) have been determined on six samples, including biotite (ca. 1700–1507 Ma; Wanless et al., 1968, 1974), muscovite (ca. 1610 Ma; Lowdon, 1960) and hornblende (ca. 1670 Ma; Wanless et al., 1979). The cooling history is poorly understood, however, due to the wide range of K-Ar ages and the limited information provided by the K-Ar dating method relative to $^{40}Ar/^{39}Ar$ methods (cf. McDougall and Harrison, 1999). This cooling history is important for understanding the later stages of the Trans-Hudson orogeny and may shed light on late- to post-orogenic processes experienced by the middle crust in similar orogens.

In this study, muscovite from three metapelite rocks spanning an area of approximately 5000 km^2 on eastern Hall Peninsula (Figure 1) was selected for $^{40}Ar/^{39}Ar$ thermochronological analysis using both step-heating and ultraviolet (UV) laser probe methods. Based on Ar diffusion experiments, the nominal closure temperature of radiogenic Ar in a muscovite grain with a 500 µm radius at 5 kbar ranges from approximately 420 to 450°C for cooling rates of 1–10°C/Ma (Harrison et al., 2009). Even at a much faster cooling rate of 100°C/Ma, the closure temperature of Ar in the same sized muscovite grain at 5 kbar is approximately 490°C (Harrison et al., 2009), still well below the peak metamorphic temperature experienced on Hall Peninsula during the Trans-Hudson orogeny. Therefore, $^{40}Ar/^{39}Ar$ thermochronology on muscovite is an effective technique to evaluate the cooling history of this section of the Trans-Hudson Orogen during the later stages of orogenesis.

The step-heating technique is the conventional method for measuring Ar isotopes in K-bearing minerals. It involves incrementally heating a single muscovite grain and conducting isotopic measurements on each progressive volume of gas released. From these data, the apparent $^{40}Ar/^{39}Ar$ age of each heating step is calculated and plotted on an age spectrum diagram. Several consecutive steps yielding equivalent ages, within error, is referred to as the 'plateau age' and is considered to represent the time the mineral passed through its closure temperature. Conversely, an age spectrum may yield no discernible age plateau, or the ages of earlier and later steps may differ, requiring complex data interpretation with higher uncertainty on the cooling age, or even preventing an age from being calculated (cf. McDougall and Harrison, 1999). The step-heating method progressively releases Ar from the least to most retentive sites in a grain, but the consequent gas release spectrum does not yield spatially controlled age information. To determine whether the Ar isotopic pattern in a grain is indicative of temperature-controlled diffusion (i.e., younger apparent ages near the rim due to the diffusion of daughter ^{40}Ar out of the grain) and to relate that diffusion profile to a cooling rate, an $^{40}Ar/^{39}Ar$ laser spot age profile of the grain is required. For this reason, multiple spot analyses were conducted on an additional muscovite grain from each sample using the UV laser technique, permitting a thorough investigation of the within-grain distribution of Ar and, therefore, more confident interpretations of cooling histories.

Background geology

Hall Peninsula on southeastern Baffin Island, Nunavut, is part of the Paleoproterozoic Trans-Hudson Orogen (Figure 1), an accretionary/collisional zone that separates the lower-plate Superior craton from an upper-plate collage of Archean crustal blocks (Churchill Plate; Hoffman, 1988; Lewry and Collerson, 1990). The upper Churchill Plate collage in the Quebec–Baffin segment of the Trans-Hudson Orogen consists of the Rae craton and several microcontinents that were accreted to the southeastern Rae margin between ca. 1.88–1.84 Ga, prior to the terminal collision of the Churchill Plate with the Superior craton at 1.82–1.80 Ga (St-Onge et al., 2009). The Meta Incognita microcontinent, which includes much of southern Baffin Island, accreted to the southeastern Rae margin between ca. 1.883 and 1.865 Ga (St-Onge et al., 2006). The orthogneiss basement of the Meta Incognita microcontinent is overlain by a Paleoproterozoic clastic-carbonate-shelf succession (Lake Harbour Group), and both the crystalline basement and the Lake Harbour Group are intruded by ca. 1.865–1.848 Ga monzogranite to quartz-diorite plutons (Cumberland Batholith; Scott and Wodicka, 1998; St-Onge et al., 2000, 2007; Corrigan et al., 2009). The basement of the Meta Incognita microcontinent has been correlated with ca. 3.02–2.78 Ga orthogneiss in the lower-plate Superior mar-

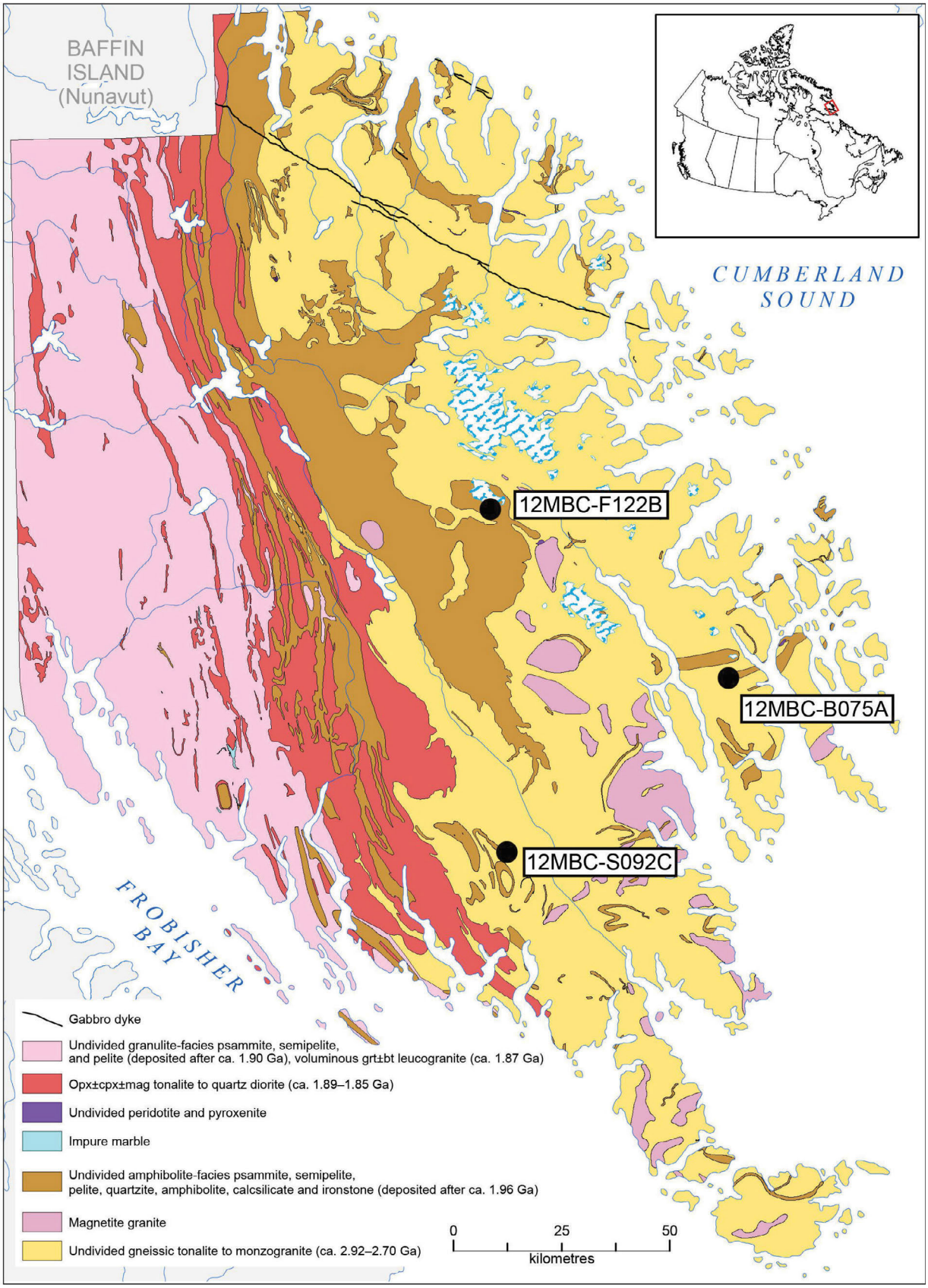

Figure 1: Simplified geology of southern Hall Peninsula, Baffin Island, Nunavut (modified after Machado et al., 2013; Steenkamp and St-Onge, 2014). Ages are from Scott (1999) and Rayner (2014). Locations are shown for the $^{40}Ar/^{39}Ar$ thermochronology samples described in this article. Abbreviations: bt, biotite; cpx, clinopyroxene; grt, garnet; mag, magnetite; opx, orthopyroxene.

gin in Northern Quebec (St-Onge et al., 2000), although it is uncertain whether the basement of the Meta Incognita microcontinent shares cratonic affinity with the Superior or Rae cratons, or whether it represents a separate cratonic block (St-Onge et al., 2009).

Geology of Hall Peninsula

Preliminary studies document that Hall Peninsula consists of ca. 1.89–1.85 Ga granitic plutons and ca. 1.93–1.89 Ga metasedimentary rocks, while the eastern portion of the peninsula comprises mostly Archean (ca. 2.92–2.80 Ga) orthogneiss basement (Blackadar, 1967; Scott, 1996, 1999). The plutonic rocks and supracrustal cover sequences on Hall Peninsula have been correlated with the Cumberland Batholith and Lake Harbour Group, respectively, on the Meta Incognita microcontinent (e.g., Scott, 1999). Several possibilities have been proposed for the cratonic origin of the Archean crystalline basement, including the Superior craton, the North Atlantic craton of southern Greenland, the Aasiaat domain in West Greenland, the Core Zone in northern Labrador or a separate Archean cratonic block of unique origin.

Recent 1:100 000 scale bedrock mapping (Machado et al., 2013; Steenkamp and St-Onge, 2014) and geochronology (e.g., Rayner, 2014) have enabled a more detailed understanding of Hall Peninsula's geological history. The western part of the peninsula comprises Paleoproterozoic metasedimentary rocks that host extensive orthopyroxene-bearing granitic intrusions (Figure 1). The supracrustal rocks include biotite–garnet–melt±cordierite±orthopyroxene±sillimanite pelite and semipelite, biotite±garnet psammite and minor biotite±garnet quartzite with localized occurrences of diopside-humite-phlogopite marble. Detrital zircon geochronology on quartzite indicates a maximum depositional age of 1906 ±9 Ma (Rayner, 2014). The supracrustal rocks have experienced granulite-facies metamorphism and muscovite and biotite dehydration melting produced leucogranite dykes and sills containing garnet±biotite or muscovite–sillimanite±garnet (Dyck and St-Onge, 2014). The crystallization age of one garnet-biotite leucogranite was determined to be 1867 ±8 Ma (Rayner, 2014). Crystallization ages of the suite of orthopyroxene-bearing granitic intrusions on western Hall Peninsula range from 1892 ±7 (Rayner, 2014) to 1857 +5/–3 Ma (Scott, 1999). These intrusions overlap in age with orthopyroxene-bearing granitoid plutons in both the Cumberland Batholith (ca. 1865–1848 Ga) on southern Baffin Island and the informally named Qikiqtarjuaq suite (ca. 1894–1889 Ga) on Cumberland Peninsula (Rayner et al., 2012).

The eastern portion of the peninsula is dominated by an Archean orthogneiss complex comprising mostly biotite±hornblende±magnetite tonalite and monzogranite that contain enclaves of diorite, amphibolite and pyroxenite (From et al., 2014). Paleoproterozoic supracrustal rocks in the eastern portion of Hall Peninsula form panels that are 10 m to 10 km thick and occur both structurally above and below the Archean orthogneiss (Steenkamp and St-Onge, 2014). The cover sequences are separated from the basement by sharp contacts that are parallel to the dominant regional foliation. The metasedimentary rocks of eastern Hall Peninsula include biotite–garnet±sillimanite±muscovite pelite and semipelite, biotite psammite and minor occurrences of garnet-biotite quartzite, diopside-humite-phlogopite marble and tremolite±tourmaline calcsilicate. In contrast to the supracrustal rocks to the west, those of the eastern assemblage almost always contain layers of amphibolite±ironstone, and are locally dominated by mafic rocks. Detrital zircon geochronology on psammite on eastern Hall Peninsula indicates a maximum depositional age of 1959 ±12 Ma (Rayner, 2014).

Metamorphic mineral assemblages in the eastern pelitic rocks indicate that peak metamorphic conditions reached amphibolite-facies metamorphism in this area. The low volumes of partial melt and widespread presence of muscovite suggest that the eastern portion of the peninsula underwent low degrees of muscovite dehydration melting and remained hydrous after the thermal peak (e.g., Dyck and St-Onge, 2014; Skipton and St-Onge, 2014). Thus, muscovite on eastern Hall Peninsula, including the muscovite dated in this study, is generally interpreted to have grown after the thermal peak but still at amphibolite-facies metamorphism. This interpretation is supported by textural relationships observed in thin section, such as intergrown muscovite and sillimanite together with quartz and muscovite symplectite textures, and muscovite grains that crosscut the dominant foliation, which are discussed in more detail below.

In some areas on eastern Hall Peninsula, the contact between Paleoproterozoic cover units and the underlying Archean basement is relatively undeformed and is locally marked by quartzite beds, suggesting that the contact may be depositional. Elsewhere, panels of supracrustal rocks and basement orthogneiss are repeated by eastward-directed, thick-skinned (D_2) thrusts (Steenkamp and St-Onge, 2014). Basement and supracrustal rocks are also deformed by outcrop-scale to map-scale, east-verging, thick-skinned (D_2) folds and south-verging, thick-skinned (D_3) crossfolds. Amphibolite- to granulite-facies metamorphism on Hall Peninsula is interpreted to have coincided with eastward-vergent shortening ($D_1 + D_2$). A summary of structural elements and associated deformation fabrics on Hall Peninsula is provided in Steenkamp and St-Onge (2014).

Recent U-Pb zircon analyses of high-U, low-U/Th zircon rims are interpreted to bracket the timing of metamorphic zircon growth on Hall Peninsula between ca. 1886 and 1828 Ma, with some evidence of a younger thermal event

during ca. 1780–1736 Ma (Scott, 1999; Rayner, 2014). In situ U-Pb monazite analyses indicate that major monazite growth occurred during regional metamorphism on Hall Peninsula during ca. 1850–1830 Ma, followed by subordinate but regionally extensive monazite growth between ca. 1800 and 1770 Ma (Skipton et al., 2013). Although additional work is needed for a more detailed understanding of the nature and timing of orogeny on Hall Peninsula, it is clear that it was part of a large, hot orogen with a protracted thermal history.

Sample descriptions

Biotite-muscovite-sillimanite-garnet pelite (sample 12MBC-F122B), central Hall Peninsula

Sample F122B was collected from a pelitic layer in a Paleoproterozoic succession of dominantly pelite and psammite that structurally overlies Archean tonalitic orthogneiss west of Okalik Bay (Figures 1, 2a–c). A 10 m thick quartzite bed occurs at the structural base of the metasedimentary section, directly on basement orthogneiss, and may represent a stratigraphic unconformity. Two dominant Paleoproterozoic deformation events are recognized in this area: east-directed shortening (D_1), which formed a west-dipping foliation, and younger south-directed shortening (D_3), which produced south-vergent folds (Figure 2c; Skipton and St-Onge, 2014). Evidence of east-verging, thick-skinned folding (D_2) is suggested by the overturned basement-cover contact (Skipton and St-Onge, 2014). These deformation events were accompanied by amphibolite-facies metamorphism.

Sample F122B contains biotite, muscovite, sillimanite (fibrolite), garnet, plagioclase, quartz, K-feldspar and tourmaline. Plagioclase and quartz account for only approximately 15% of the sample and are concentrated in 1 mm to 1 cm thick bands aligned parallel to foliation. Potassium feldspar is rare (<5%) and occurs in the bands of plagioclase and quartz. Garnet occurs as equant crystals up to 3 mm wide (Figure 3a). Muscovite occurs in three textural settings.

Figure 2: Field photographs of selected samples from the study area: **a)** partially melted layer of biotite-muscovite-sillimanite-garnet pelite (sample F122B) interbedded with psammite; **b)** interbedded pelite and psammite from near the location of sample F122B; **c)** detail of pelite from near sample F122B, showing S_1 fabric (yellow dashed line) folded by F_3 crenulations (green dashed line); **d)** a west-dipping, 3 m wide panel of biotite–muscovite–sillimanite–K-feldspar pelite (sample S92C) in tonalite orthogneiss; hammer is 40 cm long.

Muscovite and biotite occur in approximately equal proportions oriented parallel to D_1/D_2 foliation. These mica are dominantly coarse-grained and euhedral, suggesting coeval growth during D_1/D_2 (Figure 3a, b). In addition, post-D_1/D_2 muscovite overgrows syn-D_1/D_2 fibrolitic sillimanite (Figure 3a, c) and is axial planar to south-verging crenulations that formed during D_3 (Figure 3c). Muscovite also locally forms a symplectite texture with quartz.

Biotite–muscovite–garnet–sillimanite–K-feldspar pelite (sample 12MBC-B075A), Beekman Peninsula

Sample B075A is a pelitic rock that occurs in a south-dipping panel of Paleoproterozoic metasedimentary rocks surrounded by Archean tonalite orthogneiss on southeastern Hall Peninsula (Beekman Peninsula; Figure 1). In contrast to the west-dipping fabric that characterizes most of Hall Peninsula, this package of metasedimentary rocks dips to the south due to south-verging crossfolds that formed during the youngest regional deformation event (D_3). While the basal contact with Archean basement orthogneiss might represent a stratigraphic unconformity, basement rocks were likely thrust eastward over the metasedimentary rocks during D_2, prior to folding during D_3.

The major components of the pelite include biotite, quartz, sillimanite (fibrolite), plagioclase, K-feldspar, muscovite, garnet and tourmaline. Biotite defines a well-developed schistosity (S_1/S_2). Muscovite is less abundant than biotite, and generally occurs either parallel or subparallel to foliation (Figure 4a, b). Muscovite is also common at the edges of fibrolite+quartz aggregates, in which fibrolitic sillimanite forms elongate knots oriented parallel to foliation, which are surrounded by quartz (Figure 4b). Muscovite is sometimes found oriented at high angles to the foliation (Figure 4c) suggesting postkinematic (post-D_1/D_2) growth. Symplectic quartz intergrowths occur locally in both syn- and postkinematic muscovite grains (Figure 4c).

Biotite–muscovite–sillimanite–K-feldspar pelite (sample 12MBC-S092C), south-central Hall Peninsula

This sample was collected from a 3 m by 10 m block of pelite with tonalite orthogneiss occurring both structurally above and below the block (Figure 2d). It is likely that tonalite basement was thrust eastward over the pelite during D_2, similar to larger-scale thrust imbricates that occur elsewhere in eastern Hall Peninsula.

The principal minerals in the metapelite are biotite, muscovite, K-feldspar, plagioclase, quartz and sillimanite. A well-developed west-dipping gneissosity is defined by 0.5–2 mm thick bands of feldspar and quartz alternating with bands of biotite–muscovite±sillimanite (Figure 5a). Muscovite occurs as fine grains parallel or subparallel to foliation, although larger grains occur around aggregates of prismatic, foliation-parallel sillimanite crystals (Figure 5a–c). While some muscovite grains contain sillimanite inclusions or intergrowths of quartz or biotite, most are free of inclusions.

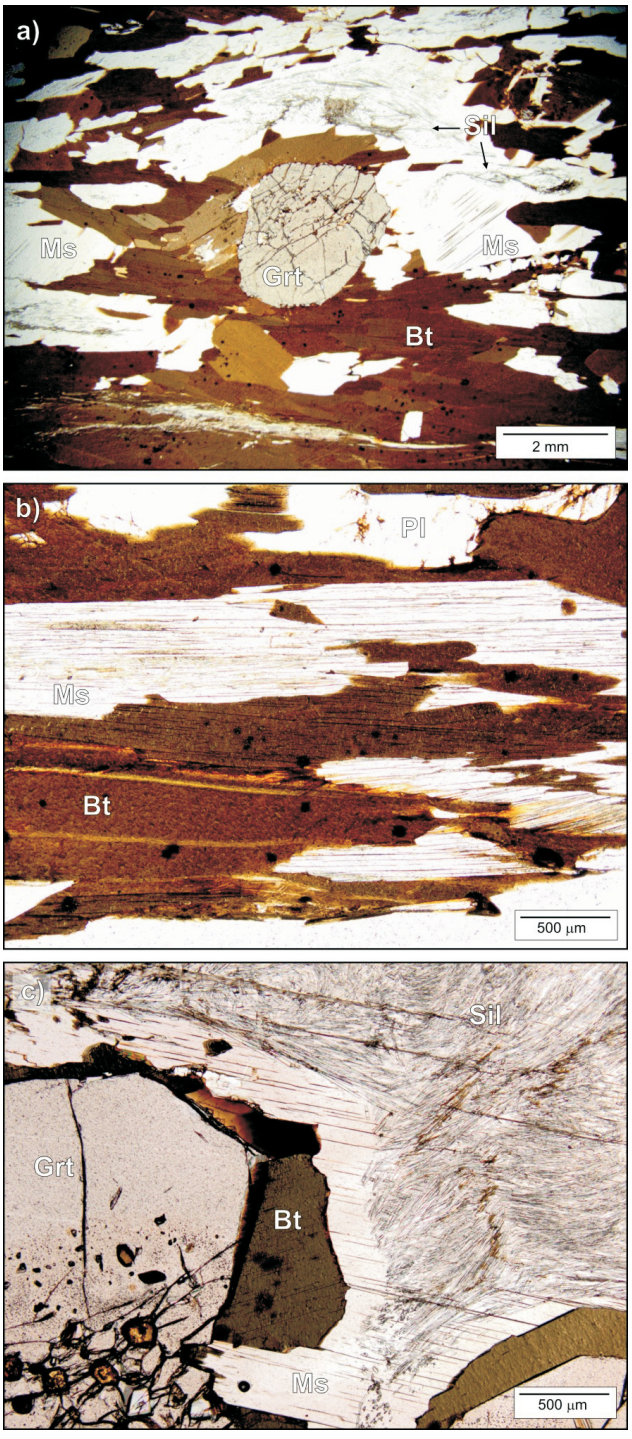

Figure 3: Photomicrographs of the sample F122B, with images in plane-polarized light: **a)** garnet (grt) surrounded by biotite (bt) and muscovite (ms), with sillimanite (sil; fibrolite) on muscovite cleavage planes; **b)** biotite, muscovite and plagioclase (pl) defining foliation; **c)** fibrolite knot surrounded by muscovite.

Methods

Electron microprobe analyses

Major element analyses of muscovite were conducted on polished thin sections of each sample using the JEOL JXA-8230 electron microprobe at the University of Ottawa–Canadian Museum of Nature MicroAnalysis Laboratory, Ottawa, Ontario. The microprobe was operated at 20 kV with a beam current of 20 nA and a 10 µm spot size. A total counting time of 40 s was used for unknowns, including

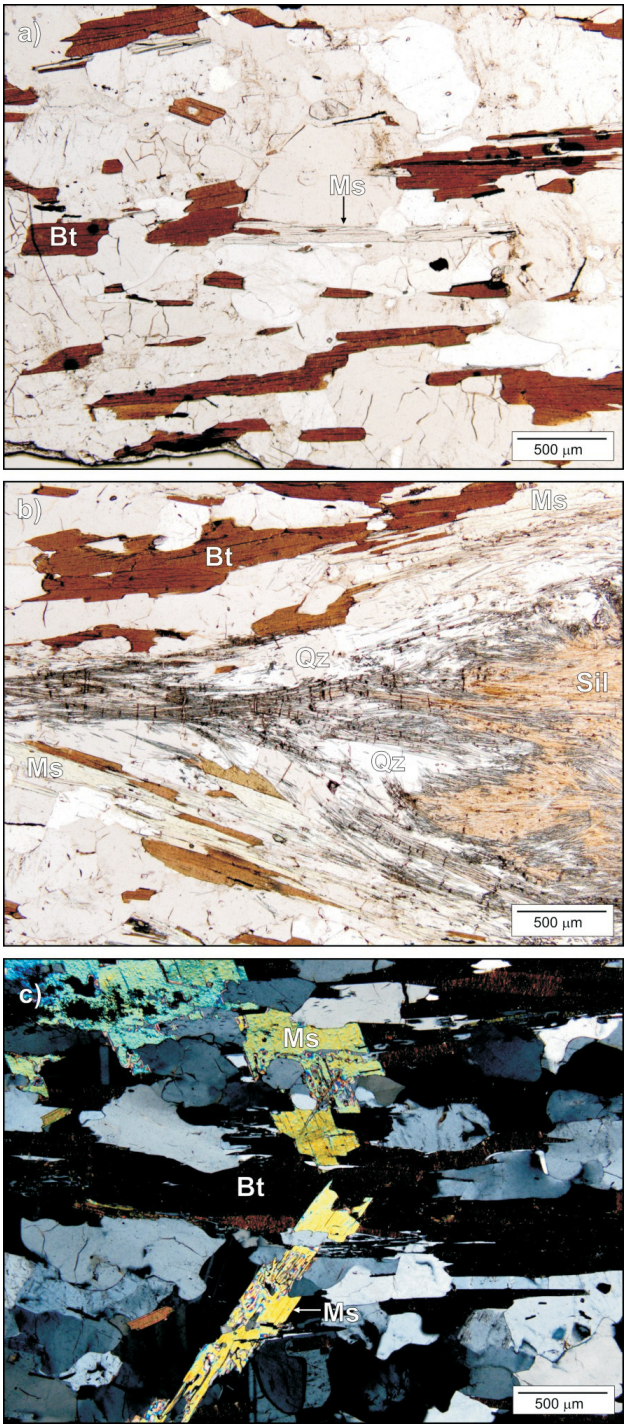

Figure 4: Photomicrographs of the sample B075A, with images in plane-polarized light unless otherwise indicated: **a)** muscovite (ms) and biotite (bt) defining foliation; **b)** fibrolite (sil) knot surrounded by quartz (qz) and muscovite; **c)** muscovite with symplectic quartz intergrowths crosscutting the main foliation (crosspolarized light).

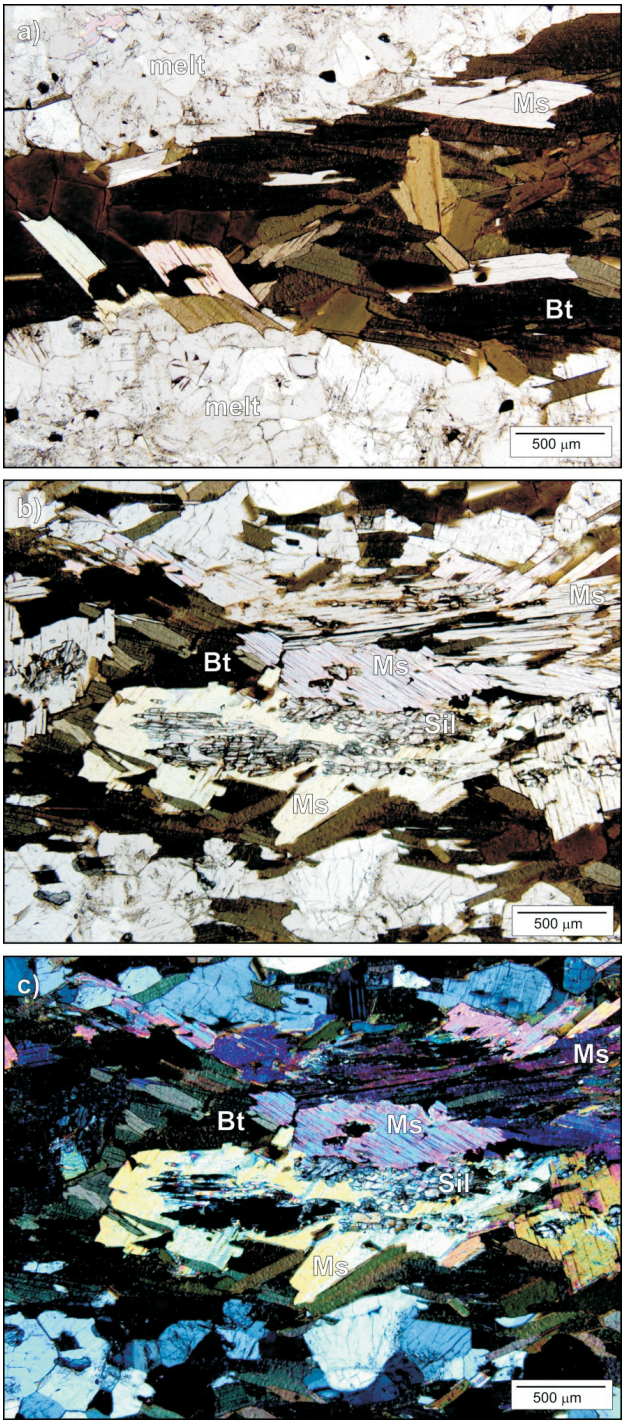

Figure 5: Photomicrographs of the sample S092C, with images in plane-polarized light unless otherwise indicated: **a)** band of biotite (bt) and muscovite (ms) between bands of feldspar and quartz (melt); **b)** sillimanite surrounded by large muscovite grains that crosscut the foliation; **c)** same image as in b) but in crosspolarized light.

20 s on the peak and 10 s on either side of the peak. A counting time of 10 s was used on background peaks, plus 10 s on each side of the peak, for a total counting time of 30 s. A combination of natural and synthetic standards were used for calibration and analyses were corrected using a ZAF matrix correction routine. Chemical formulas were calculated on the basis of 11 oxygen atoms. Three individual muscovite grains were analyzed in samples B75A and F122B and four grains were analyzed in sample S92C, with 1–10 microprobe analyses per grain. Grains were analyzed in a range of textural settings to ensure representative muscovite compositions.

$^{40}Ar/^{39}Ar$ thermochronological analyses

Each sample was crushed using a ceramic mortar and pestle. The crushed material was washed with water and acetone and then sieved to isolate the 250–500 µm fraction. The highest quality, most pristine grains were picked from each sample, so that grain fragments and grains with inclusions or signs of alteration were avoided. The grains were packed into aluminum foil packets and arranged in 35 mm long vertical tubes in an aluminum canister, and then irradiated in the research nuclear reactor at McMaster University in Hamilton, Ontario. The samples were irradiated for 320 h in position 8D in a medium total flux of approximately 1.3×10^{13} neutrons/cm^2/s operating at a 3 MW power level (cadmium shielded). Neutron flux was monitored using the PP-20 hornblende monitor (Hb3gr equivalent) with an apparent age of 1074 ±5 Ma (1σ; Jourdan et al., 2006). At least four PP-20 monitors were interspersed among the ten samples in each vertical tube of the irradiation can. The $^{40}Ar/^{39}Ar$ thermochronological analyses were conducted at the Noble Gas Laboratory at the Geological Survey of Canada in Ottawa, Ontario.

Individual muscovite grains were loaded into a sample holder and placed in a laser port under an ultrahigh vacuum. For step-heating analysis, the grains were loaded into 1.5 mm diameter holes in a copper sample holder, which was loaded into a CO_2 laser source chamber. A Photon Machines, Inc. Fusions 10.6 55 W CO_2 laser equipped with a beam-homogenizing lens was used to heat each muscovite grain for 30 s per step, and laser power was increased incrementally for each subsequent step. For the three samples analyzed, the heating schedules comprised 16–25 steps, ranging from 0.1 to 7 W. For the UV laser technique, each grain was loaded into a 5 mm diameter hole in an aluminum sample holder, which was then loaded into a UV laser source chamber. A pulsed wavelength-quadrupled New Wave Nd: YAG LUV266 (266 nm) UV laser was used to conduct single spot fusions forming two to three rim-core-rim transects on each grain, along with additional spots where necessary to ensure full coverage of potential discrete age domains. For each UV laser spot, the laser was rastered over a 50 µm by 50 µm area at 85% laser power, 10 µm beam diameter, 10 µm raster spacing and 20 Hz repetition rate, penetrating to an approximate vertical depth of 10 µm. Each rim-core-rim transect included between 10 and 20 raster spots. Flat grain surfaces were targeted to ensure good coupling between the laser and the muscovite grain in order to avoid potential altered zones on uneven surfaces and to consistently sample the same mica sheet within a grain.

The gas released during each incremental heating step or UV laser spot analysis was cleaned for 3–4 min using two SAES™ NP-10 getters held at ~400°C, and a room temperature getter containing HY-STOR® 201 calcium-nickel alloy pellets. The gas was then admitted to a Nu Instruments Limited Noblesse magnetic sector multicollector noble gas mass spectrometer. A Faraday cup was used to collect the ^{40}Ar signal while three ion-counting multipliers simultaneously collected ^{39}Ar, ^{37}Ar and ^{36}Ar using the MC-O multicollection method described in Kellett and Joyce (2014). Neutron flux gradients were evaluated by analyzing the PP-20 hornblende flux monitors and calculating J-factor values using linear interpolation between bracketing standards. Background values were measured in blank runs before and after each grain was analyzed and after every four incremental heating steps or UV laser spots. Background values are presented in the $^{40}Ar/^{36}Ar$ step-heating and UV laser data tables in Skipton et al. (2015)[4], together with the correction factors applied to account for reactor-induced interference reactions. Atmospheric $^{40}Ar/^{36}Ar$ measurements were conducted periodically during each analysis session using aliquots of air transferred to the extraction line. Using these air shot analyses, detector intercalibration corrections relative to a reference detector were applied to all sample gas analyses to correct for efficiency differences between detectors as well as for mass fractionation. Data collection, reduction, error propagation, age calculation and plotting were completed using the Mass Spec software (v. 7.93; Deino, 2001). Thorough descriptions of laboratory procedures, instrument specifications, data collection and correction factors are provided in Kellett and Joyce (2014).

In the discussion of step-heating results, a 'plateau' is defined as three or more consecutive heating steps yielding the same apparent age (within 1σ) that, together, comprise at least 30% of the total ^{39}Ar released. The plateau ages were calculated by weighting each included step by the inverse of the variance. Where no plateau was attained, the term 'pseudoplateau' refers to the age of selected nonconsecutive heating steps that yield the same apparent age and comprise at least 30% of the total ^{39}Ar released. In-

[4] *CNGO Geoscience Data Series GDS2015-001, containing the data sources used to compile this paper is available online to download free of charge at http://cngo.ca/summary-of-activities/2014/.*

tegrated ages were calculated by weighting all the individual steps by the fraction of ^{39}Ar released. Ages presented here are based on an assumed $^{40}Ar/^{36}Ar$ ratio of 298.56 for atmospheric Ar (Lee et al., 2006) and were calculated using the ^{40}K decay constant 5.543×10^{-10} a^{-1} from Steiger and Jäger (1977). All uncertainties on step-heating and UV laser ages presented in the text and figures are reported at the 1σ level. The error on J-factor values is included in the calculated ages (plateau, pseudoplateau and integrated) presented in the discussion of step-heating results to allow comparison between samples that occupied different positions in the irradiation can. The J-factor errors are not incorporated into age uncertainties when comparing relative ages of the individual heating increments plotted on the age spectra in Figure 6 because intragrain analyses have identical J-factor values. Similarly, the error on J-factor values is not included in the discussion of intragrain UV laser results.

Results

Muscovite composition

Electron microprobe data are presented in Skipton et al. (2015). The composition of muscovite in all three samples conforms to the chemical formula of muscovite ($K_2Al_4[Si_6Al_2O_{20}](OH, F)_4$). Muscovite in sample F122B

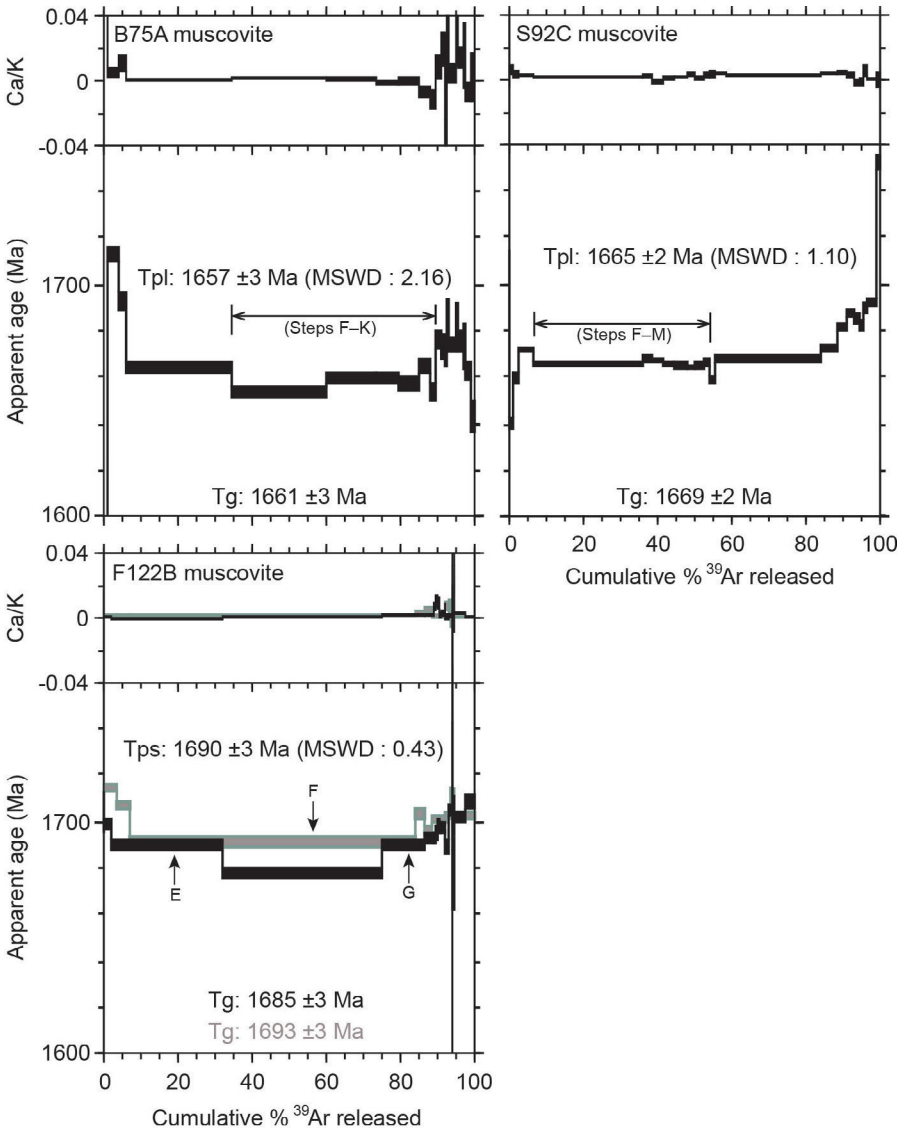

Figure 6: The $^{40}Ar/^{39}Ar$ age and Ca/K spectra for muscovite step-heating analyses. Refer to Figure 1 for sample locations and Skipton et al. (2015) for data. Errors on individual heating steps and on the calculated plateau (Tpl), pseudoplateau (Tps) and integrated (Tg) ages are quoted at the 1σ level. The Tpl was calculated using steps F–K for sample B75A, and steps F–M for sample S92C. The Tps for sample F122B was calculated using step F from the first aliquot (gray) and steps E and G from the second aliquot (black). Abbreviation: MSWD, mean square of weighted deviates.

is slightly richer in Na and poorer in K than in the other two samples. The composition of muscovite in each sample is relatively homogeneous regardless of grain size or structural position, and there are no identifiable within-grain compositional patterns.

$^{40}Ar/^{39}Ar$ step-heating results

The Ca/K and $^{40}Ar/^{39}Ar$ age spectra for step-heating analyses are shown in Figure 6, and the full corresponding dataset is provided in Skipton et al. (2015). The gas release spectrum for sample B75A yields a plateau age of 1657 ±3 Ma (mean square of weighted deviates, MSWD = 2.16; 55% of ^{39}Ar released), which was calculated from the midtemperature heating steps. Several low-volume gas release steps at the beginning and end of the heating schedule yield ages that are older than the plateau age, between ca. 1700 and 1665 Ma. For sample S92C, a plateau age of 1665 ±2 Ma (MSWD = 1.10; 47% of ^{39}Ar released) was calculated from the early to middle stages of gas release. The last nine gas-release steps yield older ages than the plateau age, mostly between 1690 and 1670 Ma. For sample F122B, most of the gas in the first aliquot was released in a single heating step (step F on Figure 6) and a plateau age cannot be calculated. After running a second aliquot of sample F122B, a pseudoplateau age of 1690 ±3 Ma (MSWD = 0.43) was calculated using step F from the first aliquot, in which the majority of ^{39}Ar was released (77%), and steps E and G from the second aliquot (41% of ^{39}Ar released). In both aliquots, low-volume gas releases at the start and end of the heating schedule yielded older ages, up to 1710 Ma.

$^{40}Ar/^{39}Ar$ UV laser analyses

The UV spot analysis locations are shown on grain maps in Figure 7, which are contoured by $^{40}Ar/^{39}Ar$ apparent age in 10 m.y. intervals. The data tables are presented in Skipton et al. (2015). In all three samples, the UV laser spot analyses show a decrease in $^{40}Ar/^{39}Ar$ age of 20–30 m.y. from core to rim (Figure 7). Sample B75A exhibits a core-to-rim decrease in cooling age from 1661 ±3 to 1640 ±4 Ma. There are, however, three young spot analyses in the grain interior (1645 ±3 Ma, 1645 ±3 Ma and 1643 ±3 Ma). In sample S92C, the ages of UV laser analyses decrease almost uniformly from 1675 ±3 Ma in the core to 1645 ±3 Ma in the rim. In sample F122B, the UV laser ages range from 1680 ±6 Ma near the grain interior to 1652 ±6 Ma at the grain edge. While the cooling ages are generally younger toward the grain edge, there is one anomalously young analysis in the core, yielding an age of 1655 ±6 Ma.

Discussion

Relative timing and conditions of muscovite growth

The metamorphic mineral assemblages in the three samples indicate that peak metamorphism occurred under amphibolite-facies conditions. Textural evidence implies that muscovite generally grew after the thermal peak, during the early stages of the retrograde path, but intergrown muscovite and fibrolite as well as muscovite-quartz symplectite suggest that growth still occurred under amphibolite-facies conditions.

In sample B75A, the abundance of fibrolitic sillimanite and K-feldspar and the scarcity of muscovite suggest that the second sillimanite isograd reaction was crossed (muscovite + plagioclase + quartz = K-feldspar + sillimanite + water). Thus, the muscovite in this sample is either the last remaining prograde muscovite, or represents minor retrograde muscovite growth, or perhaps a combination of both processes. The occurrence of symplectic quartz intergrowths in several muscovite grains implies that at least some muscovite was produced from the retrograde reversal of the second sillimanite isograd reaction (e.g., Peterman and Grove, 2010). Late muscovite growth is also suggested by the orientation of symplectic muscovite and quartz cross-cutting (overprinting) the higher-grade foliation (Figure 4c).

Sample S92C appears to have reached temperatures well above those required to cross the second sillimanite isograd reaction. This sample contains distinct bands of K-feldspar,

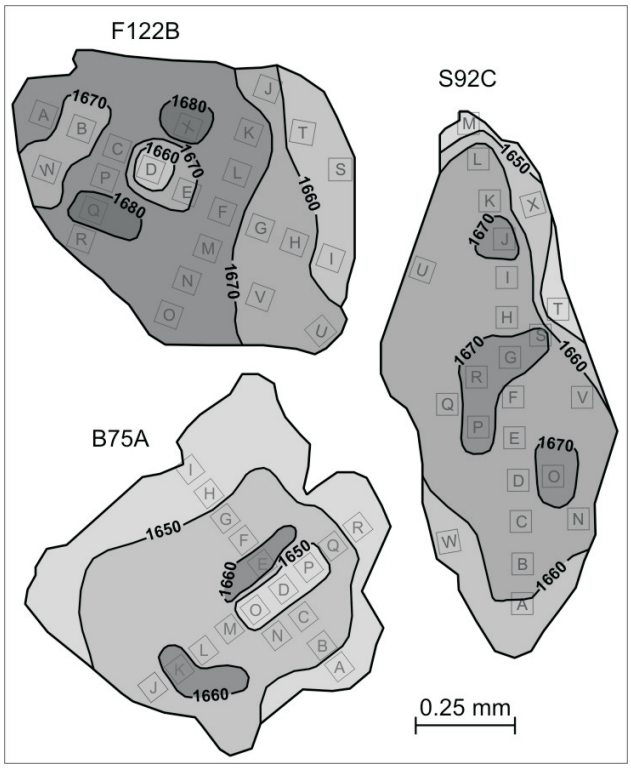

Figure 7: Each of the muscovite grains analyzed, contoured by $^{40}Ar/^{39}Ar$ age as determined by UV laser spot analyses. Each contour interval represents 10 m.y. and the oldest domains are shaded dark grey, grading to lighter grey with younger ages. The 50 µm by 50 µm laser spot analyses are represented by square boxes, each labelled with a letter that corresponds to an analysis step in the data table (Skipton et al., 2015).

plagioclase and quartz that likely represent melt produced during vapour-present muscovite dehydration melting (muscovite + plagioclase + quartz + water = sillimanite + melt) or, potentially, vapour-absent dehydration melting (muscovite + plagioclase + quartz = K-feldspar + sillimanite + melt). While prograde muscovite cannot be definitively ruled out, the abundance of K-feldspar and melt suggests that most prograde muscovite would have been consumed. Most muscovite in this sample probably formed after the thermal peak, during the reversal of muscovite breakdown reactions. This interpretation is supported by the existence of large muscovite grains overgrowing sillimanite (e.g., Peterman and Grove, 2010) and by numerous muscovite grains that crosscut the dominant foliation defined by biotite and gneissic banding (Figure 5).

In sample F122B, fibrolitic sillimanite probably grew when temperatures exceeded the second sillimanite isograd reaction and, potentially, muscovite dehydration-melting reactions. Bands of coarse-grained plagioclase, quartz and minor K-feldspar may represent melt that was produced during muscovite dehydration melting. Despite these reactions, muscovite is abundant, coarse grained and mostly appears to be in textural equilibrium with the other minerals, and K-feldspar is rare. This suggests that muscovite breakdown might have been minimal, or, potentially, that muscovite was produced on the retrograde path. Fibrolite is surrounded by large muscovite grains, many of which are nonparallel to the main foliation, and some muscovite grains contain symplectic quartz intergrowths. Together, these textures may represent the retrograde reversal of the second sillimanite isograd reaction, whereby postkinematic muscovite overgrows fibrolitic sillimanite while symplectic muscovite and quartz form at the expense of K-feldspar (e.g., Peterman and Grove, 2010).

In all three samples, the mineral assemblages and textures suggest that the latest period of muscovite growth or recrystallization was relatively early on the retrograde path (>500°C), following peak metamorphism at amphibolite-facies grade. Muscovite forms part of a regional post-peak amphibolite-facies assemblage that includes stable biotite, sillimanite and, locally, garnet. Under such conditions of muscovite growth (5 kbar and >500°C), it is unlikely that muscovite would retain any pre-peak radiogenic Ar history; it can therefore yield the timing of cooling (Warren et al., 2012). The possibility that some prograde muscovite survived muscovite-breakdown reactions cannot be ruled out; therefore, it is possible that such grains were analyzed in this study. However, since mineral assemblages suggest that regional metamorphic temperatures on eastern Hall Peninsula surpassed 500°C and reached about 700°C, it is unlikely that any prograde muscovite would have retained pre-peak radiogenic Ar (e.g., Warren et al., 2012). There is no evidence of lower-temperature retrograde minerals, such as chlorite, in these rocks, nor are there apparent signs of late hydrothermal activity such as veining or fluid alteration; therefore, the $^{40}Ar/^{39}Ar$ cooling age of muscovite is considered to record late-orogenic cooling from regional amphibolite-facies metamorphism.

Interpretation of cooling history

The closure temperature for thermal diffusion of radiogenic Ar in a muscovite grain with a 500 µm radius ranges from approximately 420 to 450°C with cooling rates of 1–10°C/Ma and a pressure of 5 kbar (Harrison et al., 2009). As discussed above, the muscovite in this study is inferred to have grown at >500°C and approximately 5 kbar, with only a slight decrease in pressure once temperatures cooled to 420–450°C. Cooling rates of 1–10°C/Ma are typical for large, hot, Paleoproterozoic orogens such as the Trans-Hudson Orogen (e.g., Dunlap, 2000). Thus, the $^{40}Ar/^{39}Ar$ ages in this study are interpreted to represent regional cooling of eastern Hall Peninsula below 450–420°C.

The $^{40}Ar/^{39}Ar$ step-heating data suggest that eastern Hall Peninsula cooled through 420–450°C by 1690 ±3 Ma at the earliest, and by 1657 ±3 Ma at the latest. The ca. 30 m.y. spread in $^{40}Ar/^{39}Ar$ step-heating ages among the three samples suggests that cooling was not concurrent across eastern Hall Peninsula. As discussed above, the estimated age of peak metamorphism on Hall Peninsula is ca. 1850 to 1830 Ma (Skipton et al., 2013); however, subsequent thermal and/or fluid activity is evinced by a suite of younger U-Pb ages, including ca. 1800–1770 Ma from monazite (Skipton et al., 2013), ca. 1780–1736 Ma from zircon rims (Scott, 1999; Rayner, 2014), and ca. 1740 Ma from titanite (Scott, 1999). Together, the U-Pb data and the $^{40}Ar/^{39}Ar$ step-heating ages suggest that Hall Peninsula remained at temperatures exceeding 420°C for at least 140 m.y. Considering metamorphism on eastern Hall Peninsula peaked at approximately 700°C, as suggested by mineral assemblages and the presence of partial melts, post-peak cooling probably occurred at a rate of 1–2°C/m.y. This cooling rate indicates that Hall Peninsula forms part of a hot, slow-cooling orogen, similar to several other Paleoproterozoic mountain belts (e.g., Dunlap, 2000).

For each sample, the $^{40}Ar/^{39}Ar$ UV laser results are generally consistent with the ages calculated from step-heating analyses. The plateau age of sample B75A (1657 ±3 Ma) is approximately equivalent to the average of the UV laser spot ages (ca. 1661–1640 Ma). The same is true of sample S92C, although the step-heating age of sample F122B (1690 ±3 Ma) is older than the oldest UV laser spot (ca. 1680 Ma).

Muscovite grains from all three samples exhibit 20–30 m.y. decreases in $^{40}Ar/^{39}Ar$ age from core to rim, which are interpreted to represent similar Ar thermal diffusion profiles. Young spot analyses in muscovite cores in samples B75A and F122B probably reflect the presence of crystal defects

that provided short diffusion pathways for Ar (e.g., Lee, 1995; Kramar et al., 2003). Possible cooling scenarios are currently being explored using thermal modeling software, such as slow cooling at a constant rate, or slow cooling followed by a period of rapid cooling. The 20–30 m.y. decreases in core-to-rim age appear to represent Ar thermal diffusion profiles that potentially required a faster cooling rate than 1–2°C/Ma. Nonetheless, it can be deduced from the ages of the muscovite cores that any possible periods of faster cooling occurred after ca. 1680 Ma, and that a cooling rate of approximately 1–2°C/Ma is appropriate for the high-temperature (700–450°C) portion of the cooling history.

Economic considerations

Diamond-bearing kimberlites are hosted by the Archean basement orthogneiss on eastern Hall Peninsula, and are currently the focus of exploration and development by Peregrine Diamonds Ltd. Since the $^{40}Ar/^{39}Ar$ thermochronology data presented here suggest that the middle crust on Hall Peninsula cooled through about 420–450°C by ca. 1640 Ma, it is likely that thermotectonic activity ceased before kimberlite emplacement during the Late Jurassic to Early Cretaceous. The Archean orthogneiss on eastern Hall Peninsula probably formed part of a thick, stable craton that was amenable to kimberlite intrusions. Ultramafic boudins within the Archean orthogneiss and the inlying Paleoproterozoic supracrustal rocks have been recognized as sources of carving stone (Steenkamp et al., 2014). The $^{40}Ar/^{39}Ar$ cooling ages indicate that Hall Peninsula cooled slowly after peak metamorphism and experienced sustained high temperatures (>420°C) for at least 140 m.y. The slow cooling through amphibolite-facies conditions might have contributed to the recrystallization of ultramafic protoliths, resulting in the development of strong, yet easily carvable stone.

Conclusions

- The muscovite cooling ages from three samples on Hall Peninsula of Baffin Island determined from $^{40}Ar/^{39}Ar$ step-heating analyses are 1690 ±3 Ma (sample F122B), 1665 ±3 Ma (sample S92C) and 1657 ±3 Ma (sample B75A).
- Ultraviolet laser spot analyses conducted on these same samples exhibit a 20–30 m.y. decrease in $^{40}Ar/^{39}Ar$ cooling ages from core to rim in all three samples. The UV laser spot ages range from 1661 ±3 to 1640 ±4 Ma (sample B75A), from 1675 ±3 to 1645 ±3 Ma (sample B75A) and from 1680 ±6 to 1652 ±6 Ma (sample F122B).
- Concomitant with available U-Pb data, the $^{40}Ar/^{39}Ar$ ages suggest that Hall Peninsula remained at temperatures above 420°C for at least 140 m.y., from ca. 1830 Ma or earlier, to ca. 1690 Ma, and locally as late as ca. 1640 Ma. The data imply that this portion of the Trans-Hudson Orogen cooled at a rate of about 1–2°C/Ma following peak metamorphism, forming a hot, slow-cooling terrane. The Ar diffusion profiles preserved in muscovite indicate that faster cooling may have followed as the Hall Peninsula middle crust cooled through 450–420°C.

Acknowledgments

This paper greatly benefitted from the geological observations and interpretations of H. Steenkamp, C. Bilodeau, G. Machado, M. St-Onge, M. Young and the CNGO-HPIGP bedrock mapping team. All members of HPIGP are thanked for their enthusiasm in the field and many invaluable discussions. This work was funded by the CNGO's HPIGP. The authors are grateful to G. Poirier for his help in the electron microprobe laboratory. A. Camacho and N. Rayner are thanked for thorough reviews that significantly improved the quality of this paper. The Canadian Northern Economic Development Agency's (CanNor) Strategic Investments in Northern Economic Development (SINED) program provided support for this work.

Natural Resources Canada, Earth Sciences Sector contribution 20140330

References

Blackadar, R.G. 1967: Geological reconnaissance, southern Baffin Island, District of Franklin; Geological Survey of Canada, Paper 66-47.

Corrigan, D., Pehrsson, S., Wodicka, N. and de Kemp, E. 2009: The Palaeoproterozoic Trans-Hudson Orogen: a prototype of modern accretionary processes; Geological Society, London, Special Publication 327, p. 457–479.

Deino, A.L. 2001: User's manual for Mass Spec v. 5.02; Berkeley Geochronology Center Special Publication 1a, Berkeley Geochronology Center, Berkeley California, 119 p.

Dunlap, W.J. 2000: Nature's diffusion experiment: the cooling rate cooling-age correlation; Geology, v. 28, no. 2, p. 139–142.

Dyck, B.J. and St-Onge, M.R. 2014: Dehydration-melting reactions, leucogranite emplacement and the Paleoproterozoic structural evolution of Hall Peninsula, Baffin Island, Nunavut; *in* Summary of Activities 2013, Canada-Nunavut Geoscience Office, p. 73–84.

From, R.E., St-Onge, M.R. and Camacho, A.L. 2014: Preliminary characterization of the Archean orthogneiss complex of Hall Peninsula, Baffin Island, Nunavut; *in* Summary of Activities 2013, Canada-Nunavut Geoscience Office, p. 53–62.

Harrison, M.T., Célérier, J., Aikman, A.B., Hermann, J. and Heizler, M.T. 2009: Diffusion of ^{40}Ar in muscovite; Geochimica et Cosmochimica Acta, v. 73, p. 1039–1051.

Hoffman, P.F. 1988: United Plates of America, the birth of a craton: Early Proterozoic assembly and growth of Laurentia; Annual Review of Earth and Planetary Sciences, v. 16, p. 543–603.

Jourdan, F., Verati, C. and Féraud, G. 2006: Intercalibration of the Hb3gr $^{40}Ar/^{39}Ar$ dating standard; Chemical Geology, v. 231, p. 177–189.

Kellett, D. and Joyce, N. 2014: Analytical details of the single- and multicollection $^{40}Ar/^{39}Ar$ measurements for conventional step-heating and total-fusion age calculation using the Nu Noblesse at the Geological Survey of Canada; Geological Survey of Canada, Technical Note 8, 27 p.

Kramar, N., Cosca, M.A., Buffat, P.-A. and Baumgartner, L.P. 2003: Stacking fault-enhanced argon diffusion in naturally deformed muscovite; *in* Geochronology: Linking the Isotopic Record with Petrology and Textures, D. Vance, W. Müller and I.M. Villa (ed.), Geological Society of London, Special Publication, v. 220, p. 249–260.

Lee, J.K.W. 1995: Multipath diffusion in geochronology; Contributions to Mineralogy and Petrology, v. 120, p. 60–82.

Lee, J.-Y., Marti, K., Severinghaus, J.P., Kawamura, K., Yoo, H.-S., Lee, J.B. and Kim, J.S. 2006: A redetermination of the isotopic abundances of atmospheric Ar; Geochimica et Cosmochimica Acta, v. 70, p. 4507–4512.

Lewry, J.F. and Collerson, K.D. 1990: The Trans-Hudson Orogen: extent, subdivisions and problems; *in* The Early Proterozoic Trans-Hudson Orogen of North America, J.F. Lewry and M.R. Stauffer (ed.), Geological Association of Canada, Special Paper 37, p. 1–14.

Lowdon, J.A.1960: Age determinations by the Geological Survey of Canada, Report 1 – isotopic ages; Geological Survey of Canada, Paper 60-17, p. 5–40.

Machado, G., Bilodeau, C., Takpanie, R., St-Onge, M.R, Rayner, N.M., Skipton, D.R., Young, M., From, R., MacKay, C., Creason, C.G. and Braden, Z.M. 2013: Hall Peninsula regional bedrock mapping, Baffin Island, Nunavut; *in* Summary of Activities 2012, Canada-Nunavut Geoscience Office, p. 13–22.

McDougall, I. and Harrison, T.M. 1999: Geochronology and Thermochronology by the $^{40}Ar/^{39}Ar$ Method (second edition); Oxford University Press, New York, New York, 269 p.

Peterman, E.M. and Grove, M. 2010: Growth conditions of symplectic muscovite + quartz: implications for quantifying retrograde metamorphism in exhumed magmatic arcs; Geology, v. 38, no. 12, p. 1071–1074.

Rayner, N.M. 2014: New U-Pb geochronological results from Hall Peninsula, Baffin Island, Nunavut; *in* Summary of Activities 2013, Canada-Nunavut Geoscience Office, p. 39–52.

Rayner, N.M., Sanborn-Barrie, M., Young, M.D. and Whalen, J.B. 2012: U-Pb ages of Archean basement and Paleoproterozoic plutonic rocks, southern Cumberland Peninsula, eastern Baffin Island, Nunavut; Geological Survey of Canada, Current Research, no. 2012-8, 28 p.

Scott, D.J. 1996: Geology of the Hall Peninsula east of Iqaluit, southern Baffin Island; Geological Survey of Canada, Current Research 1996-C, p. 83–91.

Scott, D.J. 1999: U-Pb geochronology of the eastern Hall Peninsula, southern Baffin Island, Canada: a northern link between the Archean of West Greenland and the Paleoproterozoic Torngat Orogen of northern Labrador; Precambrian Research, v. 93, p. 5–26.

Scott, D.J. and Wodicka, N. 1998: A second report on the U-Pb geochronology of southern Baffin Island; Geological Survey of Canada, Paper 1998-F, p. 47–57.

Skipton, D.R. and St-Onge, M.R. 2014: Paleoproterozoic deformation and metamorphism in metasedimentary rocks west of Okalik Bay: a field template for the evolution of eastern Hall Peninsula, Baffin Island, Nunavut; *in* Summary of Activities 2013, Canada-Nunavut Geoscience Office, p. 63–72.

Skipton, D.R., Schneider, D.A., St-Onge, M.R., Braden, Z.M. and Young, M.D. 2013: A wet affair: the middle orogenic crust of the Trans-Hudson Orogen, Baffin Island, Nunavut; Geological Society of America Abstracts with Programs, v. 45, no. 7, p. 885.

Skipton, D.R., Schneider, D.A., Kellett, D. and Joyce, N.J. 2015: Data tables accompanying "New insights on the cooling history of Hall Peninsula, southern Baffin Island, Nunavut using $^{40}Ar/^{39}Ar$ thermochronology on muscovite"; Canada-Nunavut Geoscience Office, Geoscience Data Series GDS2015-001, Microsoft® Excel® files, URL <http://cngo.ca/summary-of-activities/2014/> [January 2015].

St-Onge, M.R., Van Gool, J.A.M., Garde, A.A. and Scott, D.J. 2009: Correlation of Archaean and Palaeoproterozoic units between northeastern Canada and western Greenland: constraining the pre-collisional upper plate accretionary history of the Trans-Hudson orogen; Geological Society, London, Special Publication 318, p. 193–235.

St-Onge, M.R., Searle, M.P. and Wodicka, N. 2006: Trans-Hudson Orogen of North America and Himalaya–Karakorum–Tibetan Orogen of Asia: structural and thermal characteristics of the lower and upper plates; Tectonics, v. 25, p. 1–22, doi:10.1029/2005TC001907.

St-Onge, M.R., Scott, D.J. and Lucas, S.B. 2000: Early partitioning of Quebec: microcontinent formation in the Paleoproterozoic; Geology, v. 28, p. 323–326.

St-Onge, M.R., Wodicka, N. and Ijewliw, O. 2007: Polymetamorphic evolution of the Trans-Hudson Orogen, Baffin Island, Canada: integration of petrological, structural and geochronological data; Journal of Petrology, v. 48, p. 271–302.

Steenkamp, H.M. and St-Onge, M.R. 2014: Overview of the 2013 regional bedrock mapping program on northern Hall Peninsula, Baffin Island, Nunavut; *in* Summary of Activities 2013, Canada-Nunavut Geoscience Office, p. 27–38.

Steenkamp, H.M., Bros, E.R. and St-Onge, M.R. 2014: Altered ultramafic and layered mafic-ultramafic intrusions: new economic and carving stone potential on northern Hall Peninsula, Baffin Island, Nunavut; *in* Summary of Activities 2013, Canada-Nunavut Geoscience Office, p. 11–20.

Steiger, R.H. and Jäger, E. 1977: Subcommission on geochronology: convention on the use of decay constants in geo- and cosmochronology; Earth and Planetary Science Letters, v. 36, p. 359–362.

Warren, C.J., Hanke, F. and Kelley, S.P. 2012: When can muscovite $^{40}Ar/^{39}Ar$ dating constrain the timing of metamorphic exhumation?; Chemical Geology, v. 291, p. 79–86.

Wanless, R.K., Stevens, R.D., Lachance, G.R. and Edmonds, C.M. 1968: Age determinations and geological studies; *in* K-Ar isotopic ages, Report 8, Geological Survey of Canada, Paper 67-2A, p. 11–141.

Wanless, R.K., Stevens, R.D., Lachance, G.R. and DiLabio, R.N. 1974: Age determinations and geological studies; *in* K-Ar isotopic ages, Report 12, Geological Survey of Canada, Paper 74-2, p. 6–63.

Wanless, R.K., Stevens, R.D., Lachance, G.R. and DiLabio, R.N. 1979: Age determinations and geological studies; *in* K-Ar isotopic ages, Report 14, Geological Survey of Canada, Paper 79-2, p. 1–67.

New (2013–2014) U-Pb geochronological results from northern Hall Peninsula, southern Baffin Island, Nunavut

N.M. Rayner[1]

[1]*Natural Resources Canada, Geological Survey of Canada, Ottawa, Ontario, nicole.rayner@nrcan-rncan.gc.ca*

This work was part of the 2012–2014 Hall Peninsula Integrated Geoscience Program (HPIGP), led by the Canada-Nunavut Geoscience Office (CNGO) in collaboration with the Government of Nunavut, Aboriginal Affairs and Northern Development Canada, and the Geological Survey of Canada. It involved strong contributions from the Universities of Alberta, Dalhousie, Laval, Manitoba, Ottawa, Saskatchewan and New Brunswick, and the Nunavut Arctic College. It has benefitted from support by local and Inuit-owned businesses and the Polar Continental Shelf Program. The focus is on bedrock and surficial (1:100 000 scale) geological mapping. In addition, a range of thematic studies are being conducted that include Archean and Paleoproterozoic tectonics, geochronology, landscape uplift and exhumation, microdiamonds, sedimentary-rock xenoliths and permafrost. The goal is to increase the level of geological knowledge and better evaluate the natural-resource potential in this frontier area.

Rayner, N.M. 2015: New (2013–2014) U-Pb geochronological results from northern Hall Peninsula, southern Baffin Island, Nunavut; *in* Summary of Activities 2014, Canada-Nunavut Geoscience Office, p. 31–44.

Abstract

Ages for 11 bedrock samples from across Hall Peninsula, Baffin Island, Nunavut were determined by sensitive high-resolution ion microprobe zircon U-Pb geochronology. Ages for the basement complex include lineated tonalite dated at 2832 ±5 Ma. Tonalite gneiss occurs as depositional basement to quartzite exposed in the western limb of an early east-vergent overturned fold of basement and cover. The age of basement is 2792 ±9 Ma, and the overlying quartzite contains only Archean detritus of similar age. Deformed megacrystic monzogranite, dated at 2719 ±4 Ma, is exposed in a thrust panel overriding Paleoproterozoic sedimentary rocks with a maximum depositional age of 1967 ±8 Ma. Two other metasedimentary samples on western Hall Peninsula are demonstrably Paleoproterozoic, with a significant 1.9–2.3 Ga zircon. A fifth quartzite sample contains only Archean detritus and is interpreted to represent a locally sourced, basal clastic package. Metasedimentary rocks in the west are cut by extensive granulite-grade monzogranite dated at 1872 ±5 Ma and cut locally by quartz diorite with an age of 1852 ±7 Ma. Massive white-weathering monzogranite cutting foliated psammite yields an age of 1830 ±3 Ma. As this monzogranite is unaffected by the pervasive deformation episode, this is also a minimum age constraint on the timing of regional deformation.

Résumé

Les âges radiométriques de 11 échantillons de substratum rocheux recueillis à la grandeur de la péninsule Hall, dans l'île de Baffin, au Nunavut, ont été obtenus au moyen de la datation U-Pb sur zircon effectuée à l'aide d'une microsonde ionique à haute résolution et à haut niveau de sensibilité. Les âges associés au socle proviennent d'une tonalite à linéations d'étirement dont l'âge a été établi à 2832±5 Ma. Le gneiss tonalitique constitue le socle sédimentaire du quartzite affleurant dans le flanc occidental d'un ancien pli déversé à vergence est de socle et de couverture. L'âge du socle se situe à 2792 ±9 Ma et le quartzite sus-jacent ne renferme que des débris archéens du même âge. Du monzogranite mégacrystique déformé, dont l'âge a été établi à 2719 ±4 Ma, affleure dans un panneau de charriage qui chevauche des roches paléozoïques dont l'âge maximum de mise en place est de 1967 ±8 Ma. Deux autres échantillons de roches métasédimentaires provenant de la partie ouest de la péninsule Hall s'avèrent d'âge paléoprotérozoïque, ainsi qu'il en a été établi à l'aide d'un zircon substantiel âgé de 1,9 à 2,3 Ga. Un cinquième échantillon de quartzite ne renferme que des débris archéens et on estime qu'il provient d'un ensemble clastique basal d'origine locale. Des roches métasédimentaires à l'ouest sont recoupées par une grande unité de monzogranite au faciès des granulites, dont l'âge a été établi à 1872±5 Ma, ainsi qu'à certains endroits par de la diorite quartzique, dont l'âgé a été fixé à 1852±7 Ma. L'âge du monzogranite massif, auquel l'altération a conféré une teinte blanchâtre et qui recoupe de la psammite foliée, a été établi à 1830 ±3 Ma. Le monzogranite n'ayant pas été touché par la phase de déformation intense, fait que l'âge qui lui a été attribué représente également la limite d'âge pouvant correspondre à la phase de déformation régionale.

This publication is also available, free of charge, as colour digital files in Adobe Acrobat® PDF format from the Canada-Nunavut Geoscience Office website: http://cngo.ca/summary-of-activities/2014/.

Introduction

The Hall Peninsula Integrated Geoscience Project (2012–2014), led by the Canada-Nunavut Geoscience Office in collaboration with the Geological Survey of Canada (GSC) and a number of university and community partners, focuses on bedrock mapping and a range of thematic studies that includes Archean and Paleoproterozoic tectonics and geochronology. This contribution presents the second instalment of a comprehensive U-Pb geochronology research program carried out by the geochronology laboratories of the GSC in support of new 1:250 000 geological maps of Hall Peninsula, Baffin Island, Nunavut (Figure 1; Machado et al., 2013a; Steenkamp and St-Onge, 2014). Detailed descriptions of the geology of Hall Peninsula can be found in Machado et al. (2013b), MacKay et al. (2013), From et al. (2014), Skipton and St-Onge (2014) and Steenkamp and St-Onge (2014).

In this paper, zircon U-Pb results from 11 samples from across northern Hall Peninsula are presented. The samples were analyzed using the sensitive high-resolution ion microprobe (SHRIMP) at the Geological Survey of Canada in Ottawa, Ontario. A separate section for each sample contains lithological and zircon descriptions, as well as a discussion of the geochronological results and interpretation. Sample locations are plotted on Figure 1 and UTM locations presented in Rayner (2015)[2]. The objective of the geochronology research component of the Hall Peninsula Integrated Geoscience Project is to provide temporal pins for the geological observations. The suite of dated samples achieves this objective by characterizing the age range of the exposed tectonostratigraphic basement, constraining the maximum age of deposition of extensive metasedimentary assemblages and characterizing their provenance signature, and bracketing the timing of deformation through age determinations of Paleoproterozoic plutonic suites.

Analytical procedures

All samples were disaggregated using standard crushing and pulverizing techniques followed by density separation using a Wilfley table and through the use of heavy liquids (methylene iodide, MI). A magnetic separator was used to isolate a zircon separate. Details regarding the procedure, or any deviations from it, are noted in the sections relating to specific samples.

The SHRIMP analytical procedures followed those described by Stern (1997), with standards and U-Pb error propagation methods following Stern and Amelin (2003). Briefly, zircons were cast in 2.5 cm diameter epoxy mounts (GSC #677, 699, 727, 732, 735, 740) along with fragments of the GSC laboratory standard zircon (z6266, with $^{206}Pb/^{238}U$ age = 559 Ma). The midsections of the zircons were exposed using 9, 6 and 1 µm diamond compound, and the internal features of the zircons (such as zoning, structures and alteration) were characterized in backscattered electron mode (BSE) using a Zeiss EVO® 50 scanning electron microscope. The count rates of 11 masses including background were sequentially measured with a single electron multiplier. Offline data processing was accomplished using SQUID2 (version 2.22.08.04.30, rev. 30 Apr 2008). The 1σ external errors of $^{206}Pb/^{238}U$ ratios reported in Rayner (2015) incorporate the error in calibrating the standard. Common Pb correction used the Pb composition of the surface blank (Stern, 1997). Details of the analytical session, including spot size, number of scans, calibration error and the applications of any intra-element fractionation corrections are given in the footnotes of Rayner (2015). Isoplot v. 3.00 (Ludwig, 2003) was used to generate concordia plots and calculate weighted means. The error ellipses on the concordia diagrams and the weighted mean errors are reported at 2σ. Probability density diagrams were generated using AgeDisplay (Sircombe, 2004).

Results

Basement rocks

Tonalite (sample 13SUB-Y47B)

Sample description

A sample of biotite-clinopyroxene tonalite was collected south of Tawsig Fiord (Figure 1) as a thin 100 m panel between extensive metasedimentary rocks including psammite, quartzite and marble on the south side of an extensive synform. The tonalite exhibits a very weak foliation but a very strong lineation defined by biotite (Figure 2a). The metasedimentary rocks elsewhere are documented as Paleoproterozoic in age (see sample 13SUB-S139 in this report; Rayner, 2014a, b).

Zircon description

A magnetic separator was used to isolate a zircon separate and the grains were hand-picked from the nonmagnetic @ 3° side-slope fraction. The zircons recovered from the tonalite are typically prismatic and of relative high quality, ranging in colour from colourless to pale brown, and commonly contain colourless inclusions (Figure 3a). Oscillatory zoning is preserved in BSE images, and no complex structures, such as cores or rims, were recognized (Figure 3b).

Results and interpretation

A total of 26 analyses were carried out on 24 zircon grains (see Rayner, 2015). The weighted mean $^{207}Pb/^{206}Pb$ age of 24 analyses is 2832 ±5 Ma (mean square of the weighted deviates; MSWD = 1.4) and is interpreted as the age of

[2] *CNGO Geoscience Data Series GDS2015-002, containing the data or other information sources used to compile this paper, is available online to download free of charge at http://cngo.ca/summary-of-activities/2014/.*

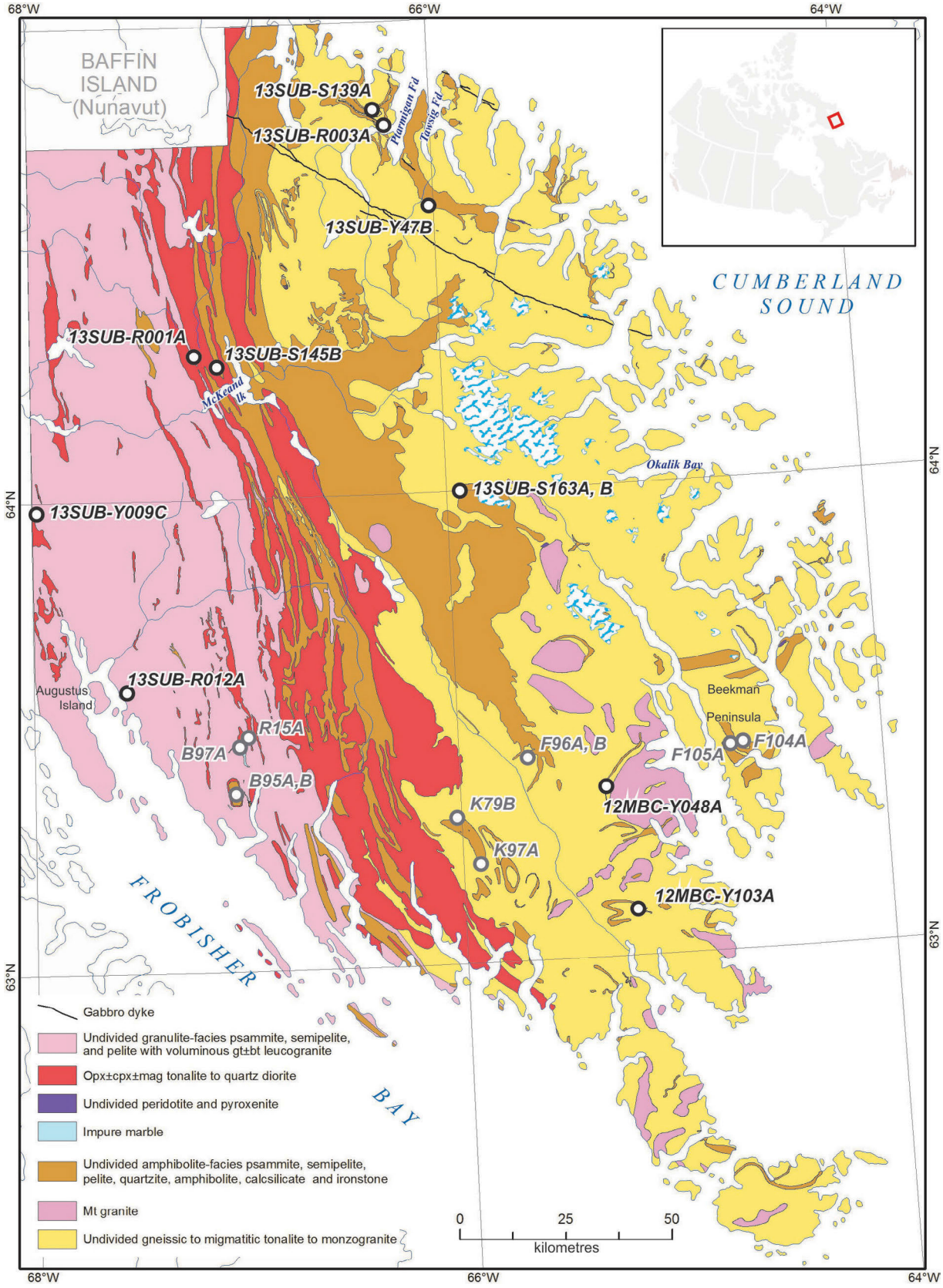

Figure 1: Preliminary, simplified geological map of Hall Peninsula, Baffin Island, Nunavut (modified from Machado et al, 2013a and Steenkamp and St-Onge, 2014) showing the locations of zircon geochronology samples described in the text (black circles and labels). The 2012–2013 sample locations are shown in grey. See Rayner (2014a, b) for 2012–2013 results. Mineral abbreviations: bi, biotite; cpx, clinopyroxene; gt, garnet; mt, magnetite; opx, orthopyroxene. The place name 'McKeand Lake' is unofficial.

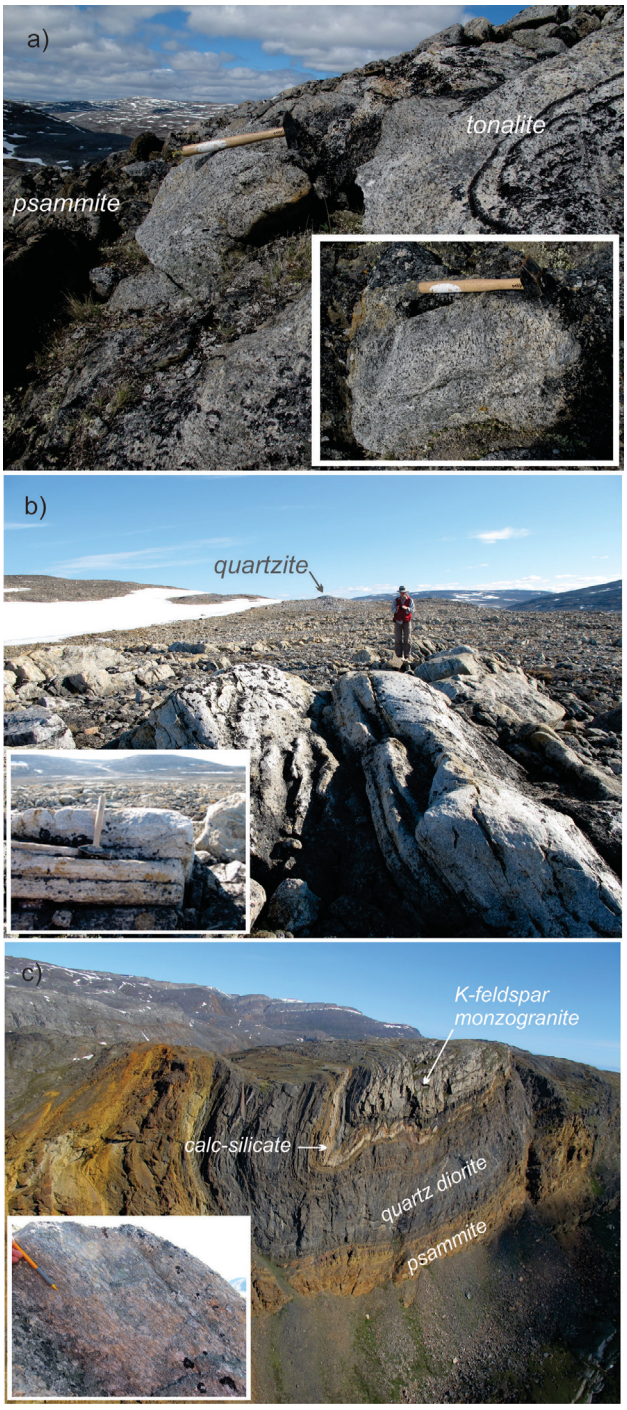

Figure 2: Field photographs of the basement samples and field relationships discussed in this paper: **a)** strongly lineated tonalite (sample 13SUB-Y47B) in contact with psammite, hammer is 40 cm long; inset detail of rod-like, lineated biotite in tonalite; **b)** tonalite gneiss with monzogranite injection, structurally above but stratigraphically below quartzite, geologist is 170 cm tall; inset: detail of tonalite (below hammer head) and monzogranite injection (behind hammer), hammer is 40 cm long; **c)** cliff exposure (300 m) of east-vergent fold of psammite, quartz diorite, calcsilicate and K-feldspar megacrystic monzogranite (sample 13SUB-R003A); inset: detail of strongly deformed sample collected for geochronology; pencil is 14 cm long.

crystallization of the tonalite. Two grains yield younger, nonreproducible ages, which are excluded from the calculation of the mean and interpreted as exhibiting minor Pb loss (analyses with dashed line ellipses; Figure 3c).

Tonalite (sample 13SUB-S163A)

Sample description

Interlayered biotite tonalite and biotite monzogranite gneiss is exposed stratigraphically below (but structurally above) a thick quartzite west of Okalik Bay (Figures 1, 2b). Structural observations suggest that the gneiss is depositional basement to a quartzite exposed in the western limb of a D_1 east-vergent overturned fold of basement and cover (Skipton and St-Onge, 2014). A sample of tonalite with minimal monzogranite injection was collected to characterize the age of the basement and for comparison with the detrital zircon provenance profile of the stratigraphically overlying quartzite (sample 13SUB-S163B, this paper).

Zircon description

Due to limited yield, zircon grains were hand-picked from heavy liquid MI 'sinks' separate. Elongate, prismatic, slightly turbid but highly fractured zircons were recovered from the biotite tonalite (Figure 3d). The BSE images reveal alteration of many of the grains, with spongy-textured interior regions, mimicking compositional zoning (Figure 3e). Core-rim relationships are observed in many grains, although in some cases it is difficult to establish whether the apparent break between core and rim is due to two generations of growth or a compositional/alteration change.

Results and interpretation

A total of 33 analyses of 24 grains yield ages ranging from 2934 to 1813 Ma (Figure 3f; Rayner, 2015). The three oldest analyses (11182-78.1 at 2840 Ma, 11182-25.1 at 2866 Ma and 11182-116.2 at 2934 Ma) are from obvious cores where zoning is truncated by overgrowths and are in-

Figure 3: Zircon images and concordia diagrams for Hall Peninsula, Nunavut, basement samples. Ellipses plotted and mean ages reported at the 2σ confidence level. Abbreviation: MSWD, mean square of weighted deviates: **a)** transmitted light image of zircon grains recovered from sample 13SUB-Y47B; **b**) backscattered electron (BSE) images of zircons from sample 13SUB-Y47B; white scale bar is 20 µm, white grain numbers and black ellipses correspond to analyses in Rayner (2015); **c)** concordia diagram of U-Pb results from sample 13SUB-Y47B; dashed line ellipses are excluded from the calculation of the weighted mean; **d)** transmitted light image of zircon grains recovered from sample 13SUB-S163A; **e**) BSE images of zircons from sample 13SUB-S163A; white scale bar is 20 µm, white grain numbers and black ellipses correspond to analyses in Rayner (2015); **f)** concordia diagram of U-Pb results from sample 13SUB-S163A; three analyses of inherited zircon are not shown but are given in data table (Rayner, 2015); **g)** transmitted light image of zircon grains recovered from sample 13SUB-R003A; **h**) BSE images of zircons from sample 13SUB-R003A; white scale bar is 20 µm, white grain numbers and black ellipses correspond to analyses in Rayner (2015); **i)** concordia diagram of U-Pb results from sample 13SUB-R003A.

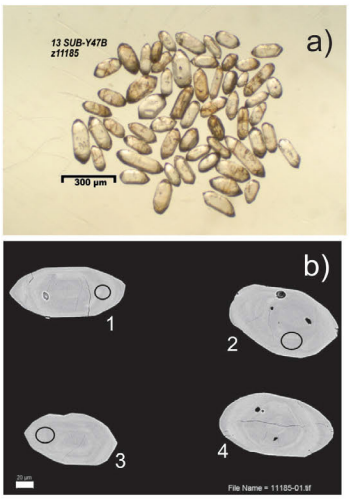
a)
13 SUB-Y47B
z11185
300 µm
b)
1
2
3
4
File Name = 11185-01.tif

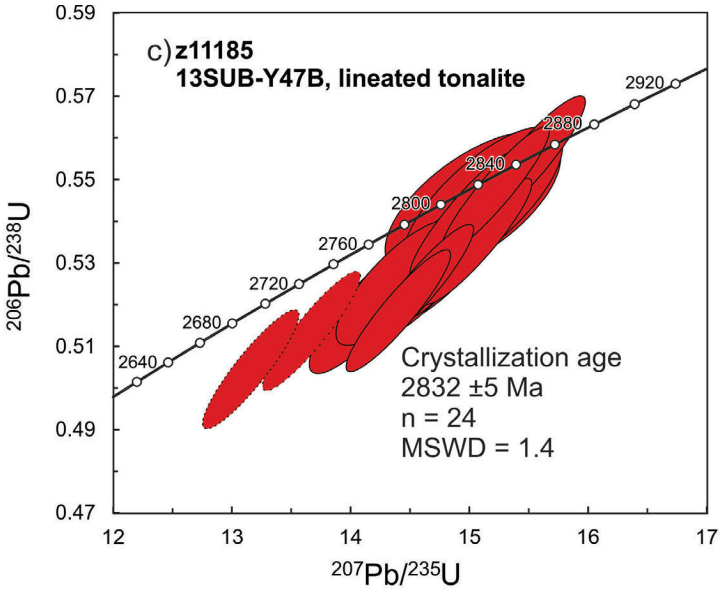
c) z11185
13SUB-Y47B, lineated tonalite
2920
2880
2840
2800
2760
2720
2680
2640
Crystallization age
2832 ±5 Ma
n = 24
MSWD = 1.4
0.59
0.57
0.55
0.53
0.51
0.49
0.47
12
13
14
15
16
17
206Pb/238U
207Pb/235U

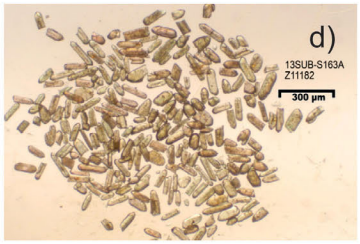
d)
13SUB-S163A
Z11182
300 µm

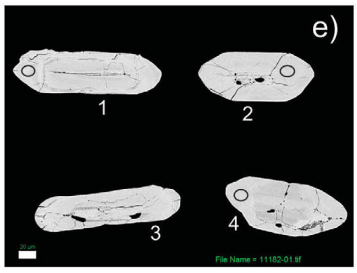
e)
1
2
3
4
File Name = 11182-01.tif

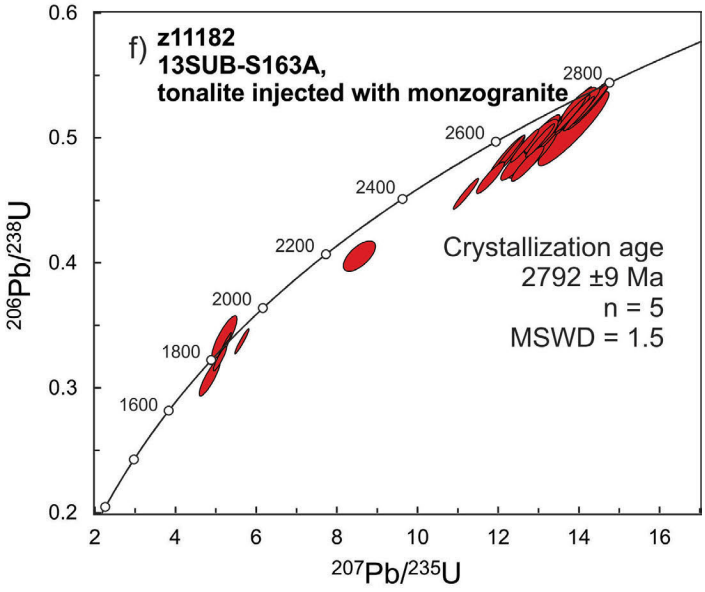
f) z11182
13SUB-S163A,
tonalite injected with monzogranite
2800
2600
2400
2200
2000
1800
1600
Crystallization age
2792 ±9 Ma
n = 5
MSWD = 1.5
0.6
0.5
0.4
0.3
0.2
2
4
6
8
10
12
14
16
206Pb/238U
207Pb/235U


g)
13SUB-R003A
z11140
nm@3*ss
picked for SHRIMP
300 µm

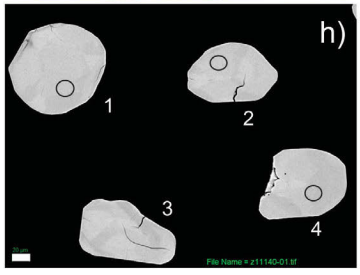
h)
1
2
3
4
File Name = z11140-01.tif

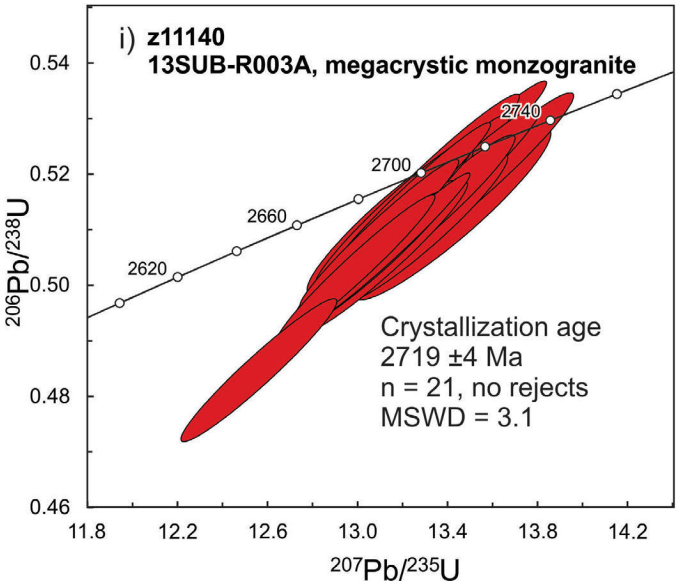
i) z11140
13SUB-R003A, megacrystic monzogranite
2740
2700
2660
2620
Crystallization age
2719 ±4 Ma
n = 21, no rejects
MSWD = 3.1
0.54
0.52
0.50
0.48
0.46
11.8
12.2
12.6
13.0
13.4
13.8
14.2
206Pb/238U
207Pb/235U

terpreted as inherited components in the tonalite. The majority of the analyses form a discordant array with $^{207}Pb/^{206}Pb$ ages between 2811 Ma and 2637 Ma. These results comprise analyses of single-phase zircon, as well as zircon rims around inherited cores. The upper limit of this array is defined by a cluster with a mean age of 2792 ±9 Ma (n = 5; MSWD = 1.5). A second subset of unzoned zircon rims yields a weighted mean $^{207}Pb/^{206}Pb$ age of 1855 ±13 Ma (n = 5, MSWD = 1.6), which roughly corresponds to the lower intercept of the discordant array described above. The 2.8 Ga age grouping is interpreted to represent the crystallization age of the tonalite gneiss. The 1855 Ma cluster may be a metamorphic overprint, or represent the age of monzogranite injection into the foliation of the gneiss. The author prefers the former, as similar injection should be observed in the adjacent sedimentary rocks in the case of the latter interpretation. A metamorphic overprint is interpreted to be responsible for Pb loss leading to discordance and drift to younger ages observed in the Archean, igneous zircon.

Monzogranite (sample 13SUB-R003A)

Sample description

A sample of a strongly foliated and lineated K-feldspar porphyritic monzogranite was collected from the core of a spectacularly exposed fold on the north side of Ptarmigan Fiord (Figures 1, 2c). The limbs of the fold comprise quartz-diorite, psammite, quartzite and calcsilicate units. The repetition of orthogneiss panels and metasedimentary rocks in cliff sides in the Ptarmigan Fiord area are interpreted as thrust imbricates composed of paired basement with its depositional cover (Steenkamp and St-Onge, 2014). This K-feldspar porphyritic monzogranite (sample 13SUB-R003A) and a psammite from an upper thrust imbricate (sample 13SUB-S139A) were collected to test this hypothesis.

Zircon description

A magnetic separator was used to isolate a zircon separate and the grains were hand-picked from the nonmagnetic @ 3° side-slope fraction. A relatively simple zircon population was recovered from the porphyritic monzogranite comprising clear, colourless to pale brown stubby prisms, with few inclusions and fractions (Figure 3g). Zoning is faint in BSE images and no cores/overgrowths are observed (Figure 3h).

Results and interpretation

A total of 21 analyses of 21 grains yield a weighted mean $^{207}Pb/^{206}Pb$ age of 2719 ±4 Ma (n = 21, MSWD = 3.1). The slight excess scatter indicated by the MSWD of 3.1 is attributed to geological complexity that could include Pb loss or inheritance of slightly older zircon. Minor Pb loss caused by the metamorphic and deformational overprint that affected this sample is the preferred explanation. Inheritance is a less likely cause due to the absence of cores in the BSE images.

Metasedimentary rocks

Quartzite (sample 13SUB-S163B)

Sample description

A sample of very clean, blue-grey quartzite was collected from a 24 m wide exposure in inferred stratigraphic contact with tonalite gneiss basement (see sample 13SUB-S163A, this paper, for more details). The quartzite is massive and thick-bedded, the basal unit of an extensive psammite-semipelite-pelite succession west of Okalik Bay (Figure 4a).

Zircon description

A magnetic separator was used to isolate a zircon separate and the grains were picked hand-picked from the nonmagnetic @ 10° side-slope fraction. Abundant zircon grains were recovered from the quartzite, many with a well-rounded morphology (Figure 5a inset). The BSE images reveal thin, unzoned, high-U (bright in BSE) overgrowths on many grains.

Results and interpretation

A total of 65 detrital zircon grains were analyzed to define the provenance profile of the quartzite. All grains yielded Archean ages between 3151 Ma and 2604 Ma with prominent modes at 2.70 Ga, 2.77 Ga, 2.81 Ga and 2.89 Ga (Figure 5a). These detrital modes are consistent with the known ages of basement (Figure 5a) including the underlying tonalite described earlier (sample 13SUB-S163A, crystallization at 2792 ±9 Ma, red star on Figure 5a).The youngest reproducible grain gave a mean $^{207}Pb/^{206}Pb$ age of 2707 ±9 Ma (grain 70, n = 3, MSWD = 0.55), which is considered the maximum age of deposition.

Psammite (sample 13SUB-S139A)

Sample description

In order to characterize the metasedimentary rocks that make up the multiple basement/cover thrust imbricates in the Ptarmigan Fiord area (Figures 1, 4b) a psammite was collected from sandy interbeds (Figure 4c) within a dominantly semipelite outcrop. The penetrative $D_1 + D_2$ deformation has been strongly crossfolded (D_3) with the crenulations preserved in semipelite horizons. This sample was collected from an upper basement/cover thrust package, not in immediate contact with the dated basement sample 13SUB-R003, but from an identical lithological and structural setting.

Zircon description

A magnetic separator was used to isolate a zircon separate and the grains were hand-picked from the nonmagnetic @ 10° side-slope fraction. The zircon grains are typically pale brown, rarely colourless, with extensive fracturing (Fig-

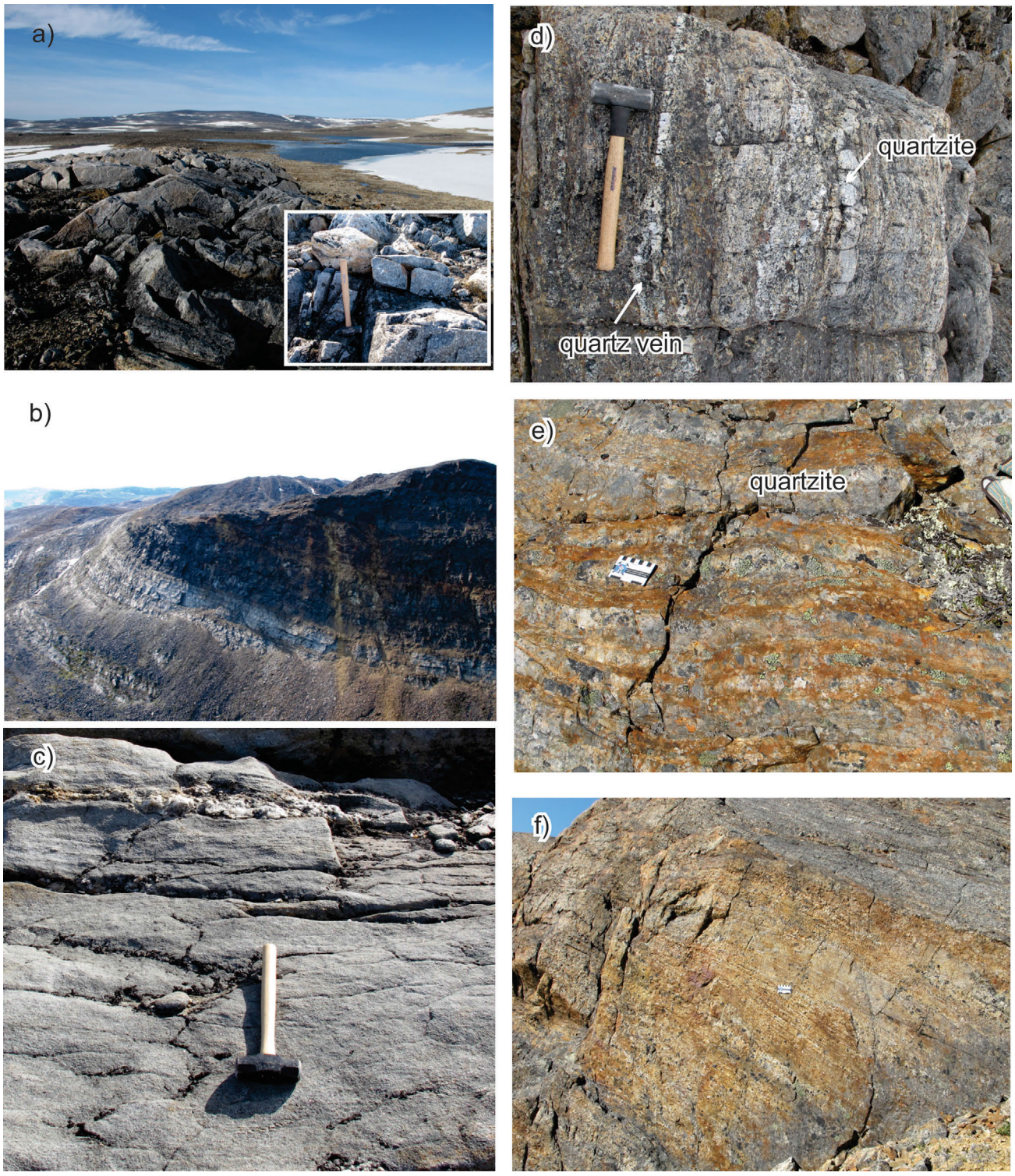

Figure 4: Sedimentary samples and field relationships, Hall Peninsula: **a)** 25 m thick, blue quartzite sample 13SUB-S163B sampled west of Okalik Bay that lies stratigraphically above Archean tonalite basement (sample 13SUB-S163A); inset: detail of block sampled for geochronology, hammer is 40 cm long; **b)** cliff face exposure (approximately 200 m tall) of rusty psammite in inferred stratigraphic contact with tonalite basement; sample 13SUB-S139A is a quartzite horizon within this upper basement/cover thrust panel; **c)** detail of quartzite horizon (sample 13SUB-S139A); hammer is 40 cm long; **d)** partially melted garnet-sillimanite-biotite semipelite with thin quartzite interbeds and quartz veining at station 13SUB-S145; the sampled unit (not shown) is dominated by quartzite, hammer is 40 cm long; **e)** alternating psammite and quartzite horizons sampled for geochronology to characterize metasedimentary rocks in western Hall Peninsula; sample 13SUB-Y009C is the thick quartzite layer in the upper right of photo, scale card is 9 cm long; **f)** well exposed cliff face1–2 m structurally up section from the location of sample 13SUB-R012 showing centimetre-scale alternating psammitic and semipelitic and partial melt layering, scale card (centre) is 9 cm long.

ure 5b inset). Grain edges and terminations are relatively sharp. Minor alteration is observed in the BSE images; rims are not evident.

Results and interpretation

A total of 63 analyses of detrital zircon grains yield nearly exclusively Paleoproterozoic ages (Figure 5b). There is a significant population of 1.96 Ga zircon grains. Replicate analyses of one young grain yields a mean age of 1967 ±8 Ma (grain 93, n = 2, MSWD = 0.77) that constrains the maximum age of deposition. The most prominent mode is at ca. 2.32 Ga, which is distinct from detrital samples from southern Hall Peninsula (Rayner, 2014a, b). The 2.6 Ga mode present in this sample is also rare in comparison to other samples documented in this and earlier studies (Rayner, 2014a, b). Notably, only one grain has an age comparable to the typical basement signature between 2.9 and 2.7 Ga. The provenance profile of this sample is most similar to a psammite from the east on Beekman Peninsula (see F104a, Figure 1; Rayner, 2014a, b), which also has a young population at 1.96 Ga, but contains only minor amounts of 2.3 Ga zircon and a larger component of 2.9–2.7 Ga detritus.

Quartzite (sample 13SUB-S145B)

Sample description

A grey weathered blocky outcrop of dominantly garnet sillimanite biotite semipelite (Figure 4d) includes a 3 m wide quartzite bed at its eastern end. This outcrop is part of an extensive panel of metasedimentary rocks in the western part of the map area, which is dominated by granulite-grade magmatic rocks (Figure 1).

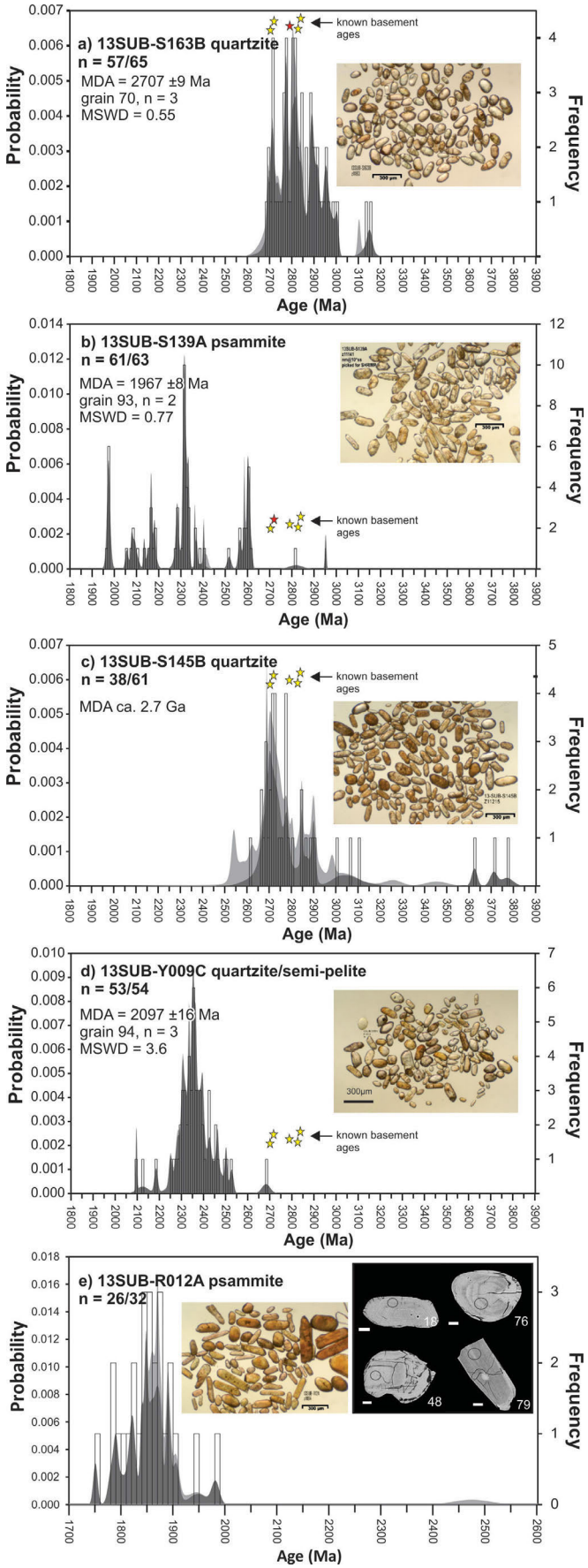

Figure 5: Probability density diagrams and histograms for detrital zircon samples from Hall Peninsula. Dark grey curves include only data that fall within the ±5% concordance threshold; light grey curves incorporate all data. Replicates and metamorphic overgrowths are not plotted, regardless of concordance. The bin width is 10 m.y. Maximum ages of deposition (MDA) are reported at the 2σ confidence level. Stars represent ages of known basement (this study; Rayner, 2014a, b). See text for discussion and Rayner (2015) for table of results: **a)** results from sample 13SUB-S163B; inset: transmitted light image of the recovered zircons, scale bar is 300 µm, red star corresponds to age of adjacent basement tonalite (sample 13SUB-S163A, this study); abbreviation: MSWD, mean square of the weighted deviates; **b)** results from sample 13SUB-S139A; inset: transmitted light image of the recovered zircons, scale bar is 300 µm, red star corresponds to the age of adjacent basement tonalite (13SUB-R003A, this study); **c)** results from sample 13SUB-S145B; inset: transmitted light image of the recovered zircons, scale bar is 300 µm; **d)** results from sample 13SUB-Y009C; inset: transmitted light image of the recovered zircons, scale bar is 300 µm; **e)** results from sample 13SUB-R012A; note change of x-axis scale; left inset: transmitted light image of the recovered zircons, scale bar is 300 µm; right inset: backscattered electron (BSE) images of zoned zircons from sample 13SUB- R012A; white scale bar is 20 µm, white grain numbers and black ellipses correspond to analyses in Rayner (2015). See text for discussion.

Zircon description

A magnetic separator was used to isolate a zircon separate and the grains were hand-picked from the nonmagnetic @ 5° side-slope fraction. The zircon grains are typically pale to medium brown, rarely colourless, with extensive fracturing (Figure 5c inset) and are moderately to well rounded.

Results and interpretation

Analyses of 61 analyses of detrital zircon grains (including replicates) yield dates between 3771 Ma and 2302 Ma (Rayner, 2015; replicates not plotted on Figure 5c). Most of the results fall in the range of typical basement ages between 2.9 Ga and 2.7 Ga. Nearly 50% of the analyses deviate from concordance by more than 5%, including all analyses younger than 2.6 Ga. The youngest concordant zircon yields an imprecise age of 2617 ±47 Ma (1σ), which is not reproduced in other grains. A more conservative estimate of the maximum age of deposition of the quartzite is constrained by the group of approximately 20 grains with dates clustering around 2.71 Ga.

Quartzite (sample 13SUB-Y009C)

Sample description

This sample was collected in the north-central part of the map area (Figure 1) from a thin enclave of metasedimentary rocks preserved in an area dominated by extensive granodiorite. The sedimentary enclave is strongly foliated and folded and is composed of alternating banks of rusty biotite-graphite semipelite and grey quartzite with minor biotite and garnet (Figure 4e). It was sampled for geochronology in order to characterize the sedimentary rocks in the western part of the map area, for provenance comparison with the lower-grade sedimentary rocks in the east.

Zircon description

A magnetic separator was used to isolate a zircon separate and the grains were hand-picked from the nonmagnetic @ 10° side-slope fraction. Abundant zircons were recovered, ranging in colour from pale pink, pale yellow, pale brown to colourless (Figure 5d, inset). The grains are high quality with few fractures or evidence of alteration. Grain edges and terminations are subrounded.

Results and interpretation

A total of 54 detrital zircon grains were analyzed yielding ages between 2683 Ma and 2094 Ma (Rayner, 2015). Replicate analyses on the youngest grain constrains the maximum age of deposition at 2097 ±16 Ma (grain 94, n = 3, MSWD = 3.6). As with sample 13SUB-S139A in the northeast, the detrital profile is dominated by 2.5–2.3 Ga zircon (Figure 5d) and there is very limited representation of detritus with a local basement age signature. In contrast with sample 13SUB-S139A and other samples from southwestern Hall Peninsula (samples 12MBC-B95 and 12MBC-R15; see Rayner, 2014a, b), ca. 1.96–1.90 Ga detritus is not identified.

Psammite (sample 13SUB-R012A)

Sample description

A psammite layer from an extensive semipelite/pelite+ calcsilicate package was collected on the Hall Peninsula mainland opposite Augustus Island (Figure 1). This area is characterized by granulite-facies metasedimentary rocks (psammite to pelite) and voluminous garnet-biotite leucogranite as well as extensive granulite-grade plutonic rocks. Most exposures of psammite-semipelite also include up to 15% garnet leucogranite injection along foliation, making it difficult to collect a 'clean' sample (Figure 4f).

Zircon description

A magnetic separator was used to isolate a zircon separate and the grains were hand-picked from the nonmagnetic @ 10° side-slope fraction. The zircon recovered was limited. Grains are pale to medium brown in colour, prismatic and typically subrounded to resorbed (Figure 5e, inset). In BSE images the zircon grains are commonly unzoned and highly altered.

Results and interpretation

A total of 31 zircons were analyzed yielding ages between 1981 and 1751 Ma (Figure 5e). Most of the zircons with ages between 1890 Ma and 1751 Ma are characterized by U concentrations in excess of 1000 ppm. These do not form a single statistical population with the scatter likely the result of Pb loss from radiation-damaged zircon. While a single age determination is not possible from this dataset, most of the analyses fall within the 1880–1840 Ma age range, which is a known period of magmatism in southern Baffin Island (Jackson et al., 1990; Wodicka and Scott, 1997; Scott and Wodicka, 1998; Scott, 1999, Whalen et al., 2010). Rocks of this age intrude the metasedimentary rocks on Hall Peninsula (Rayner, 2014a, b). Consequently, the author interprets these zircons as having crystallized during this extensive magmatic event and do not represent the detrital profile of the metasedimentary rock. While it is possible that some of the oldest zircons in this range that retain oscillatory zoning (grains 18, 48, 76, 79, 90; >1895 Ma; Figure 5e right inset) are detrital in origin, it is statistically impossible to distinguish these from a nearly coeval thermal/magmatic overprint. A single, discordant zircon falls outside this Paleoproterozoic cluster with a date of 2475 Ma.

Plutonic rocks

Orthopyroxene-monzogranite (sample 13SUB-R001A)

Sample description

The western part of the map area is characterized by an extensive granulite-grade plutonic suite that varies in compo-

sition from diorite to monzogranite (Figure 1). A sample of hornblende-biotite-magnetite-orthopyroxene monzogranite was collected northwest of McKeand lake in order to constrain the age of this relatively felsic component of the plutonic suite (Figure 6a).

Zircon description

A magnetic separator was used to isolate a zircon separate and the grains were hand-picked from the nonmagnetic @ 3° side-slope fraction. The zircons typically have an elongate prismatic crystal form with resorbed terminations (Figure 7a). In BSE images, the grains form two broad categories: zoned, fractured zircon and unzoned, unfractured zircon (Figure 7b). Each category forms discrete grains; one does not form rims around the other.

Results and interpretation

A total of 35 analyses were carried out on 33 zircon grains. The $^{207}Pb/^{206}Pb$ ages fall into two distinct groups. The younger group is a tight cluster with a weighted mean age of 1872 ±5 Ma (n = 22, MSWD = 1.6) derived from unzoned, unfractured zircon grains. These have U/Th ratios between 0.1 and 1.3 and are interpreted to represent the crystallization age of the monzogranite (Figure 7c inset). The remaining 14 older analyses are determined from zoned, fractured zircon and are interpreted as inherited. Most comprise a linear array with a cluster of concordant analyses near 2.72 Ga, whereas younger analyses (between 2.2 and 2.7 Ga) form an apparent discordia toward 1872 Ma (Figure 7c). Such a discordia would suggest Pb loss from a single inherited population (excluding the single concordant 3.5 Ga grain);

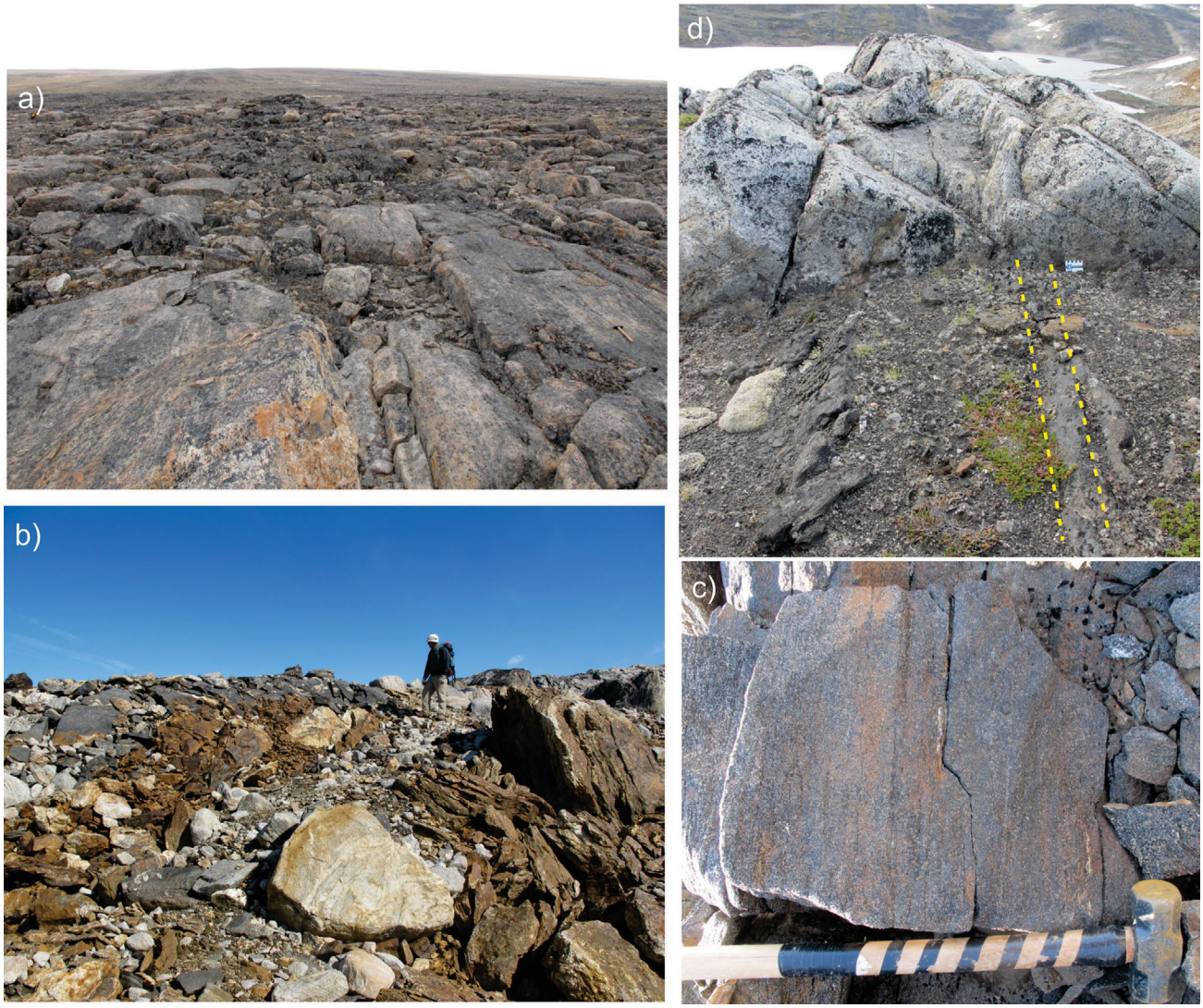

Figure 6: Paleoproterozoic plutonic samples and field relationships, Hall Peninsula. Counterclockwise from upper left: **a)** extensive exposure of strongly foliated hornblende-biotite-magnetite-orthopyroxene monzogranite (sample 13SUB-R001A); banding defined by alternating horizons of coarse- and fine-grained monzogranite, hammer (lower right of photo) is 40 cm long; **b)** quartz diorite (sample 12MBC-Y48A) intruding rusty pelite, geologist is 170 cm tall; **c)** detail of cumulate layering in geochronology sample of quartz diorite (sample 12MBC-Y48A), field of view is approximately 1 m; **d)** massive monzogranite (sample 12MBC-Y103A) cutting foliated (yellow dashed line) psammite, scale card (centre-right) is 9 cm across.

however, given the relatively large errors for each individual analysis it is not possible to assess whether this array represents principally a ca. 2.72 Ga inherited zircon population or one composed of variable (between 2.2 and 2.74 Ga) age zircon.

Quartz diorite (sample 12MBC-Y048A)

Sample description

A thin panel of quartz diorite is emplaced within a sedimentary-dominated package on southeastern Hall Peninsula (Figures 1, 6b). The associated pelite contains extensive partial melt with blebby K-feldspar and thick biotite schlieren. The quartz diorite contains heterogeneously distributed garnet and quartz. Compositional layering (2 mm scale) defined by enrichment in plagioclase and/or garnet relative to hornblende is consistent with an igneous cumulate texture (Figure 6c).

Zircon description

Most of the zircon from the quartz diorite are clear, colourless, equant prisms (Figure 7d). In BSE images the grains exhibit weak concentric zoning or are unzoned (Figure 7e).

Results and interpretation

A total of 24 analyses were carried out on 20 separate zircon grains yielding $^{207}Pb/^{206}Pb$ ages ranging from 1904 to 1776 Ma. Most of these analyses form a single statistical population with a weighted mean age of 1852 ±7 Ma (n = 20, MSWD = 2.0), which is tentatively interpreted as the crystallization age of the quartz diorite. The two youngest analyses (grains 49 and 42) and the two oldest analyses (grain 99 and 71) are excluded from the calculation of the mean. The young analyses are from distinctly zoned zircon (present as an overgrowth in the case of grain 49) and are interpreted to represent a metamorphic/fluid overprint related to the extensive infiltration of pegmatitic partial melt observed at this locality. The two older analyses are not reproducible, nor are they representative of a distinct zircon morphology. With the limited dataset available it is not possible to determine if these older ages are the results of geological variability (e.g., minor inheritance) or excess analytical scatter.

Biotite monzogranite (sample 12MBC-Y103A)

Sample description

A sample of massive, coarse-grained biotite monzogranite cuts a strongly foliated sedimentary panel at high-angle on southeastern Hall Peninsula (Figures 1, 6d). The age of the monzogranite will provide a constraint not only on the minimum age of deposition of the sedimentary sequence but also a minimum age for the penetrative deformation event recorded in the metasedimentary assemblage.

Zircon description

The zircon grains recovered from the monzogranite and uniformly medium brown and prismatic (Figure 7g). In BSE images, fracturing and alteration are evident in most grains (Figure 7h).

Results and interpretation

A total of 19 analyses were carried out on 19 zircon grains. The results cluster between 1847 and 1793 Ma. The weighted mean of sixteen analyses is 1830 ±3 Ma (MSWD = 2.6, excluding the three youngest analyses), which is interpreted as the crystallization age of the monzogranite and the minimum age of the pervasive, regional deformation event in the area. The excess scatter in the data indicated by the young excluded analyses and non-unity MSWD for the mean of the remaining analyses may be the result of Pb loss from these relatively high U (350–1600 ppm) and altered zircon grains.

Economic considerations

Precise, absolute age constraints are an essential component of modern mapping, as they provide temporal calibration of geological observations, strengthen regional correlations and place time brackets on tectonometamorphic events. The continued characterization of the detrital zircon provenance profile of Paleoproterozoic sedimentary rocks across Hall Peninsula advances the study of the origin and evolution of these base-metal prospective rocks. Further comparisons of the provenance profiles of sedimentary rocks across Hall Peninsula with similar datasets from Lake Harbour Group rocks on southern Baffin Island (host to coloured gemstones), Tasiuyak gneiss in Labrador (Scott and Gauthier, 1996; Scott, 1999) or possible equivalents in Greenland (Thrane and Connelly, 2006; Sanborn-Barrie et al., 2015) will contribute to the assessment of regional tectonostratigraphic correlations.

Conclusions

Hall Peninsula basement rocks

- The three new Archean basement ages presented in this report (2832 ±5 Ma, 2792 ±9 Ma and 2719 ±4 Ma) are consistent with those reported previously (samples F105a, F96B on Figure 1; Scott, 1999; Rayner, 2014a, b) defining a relatively uniform age range (dominantly 2.8–2.7 Ga) for the basement complex across eastern Hall Peninsula.

Hall Peninsula metasedimentary rocks

- Two quartzite samples (sample 13SUB-S163B, in contact with tonalite basement and sample 13SUB-S145B) yield provenance profiles with exclusively Archean results, dominated by known basement ages. As with a sample of quartzite from southeastern Hall Peninsula

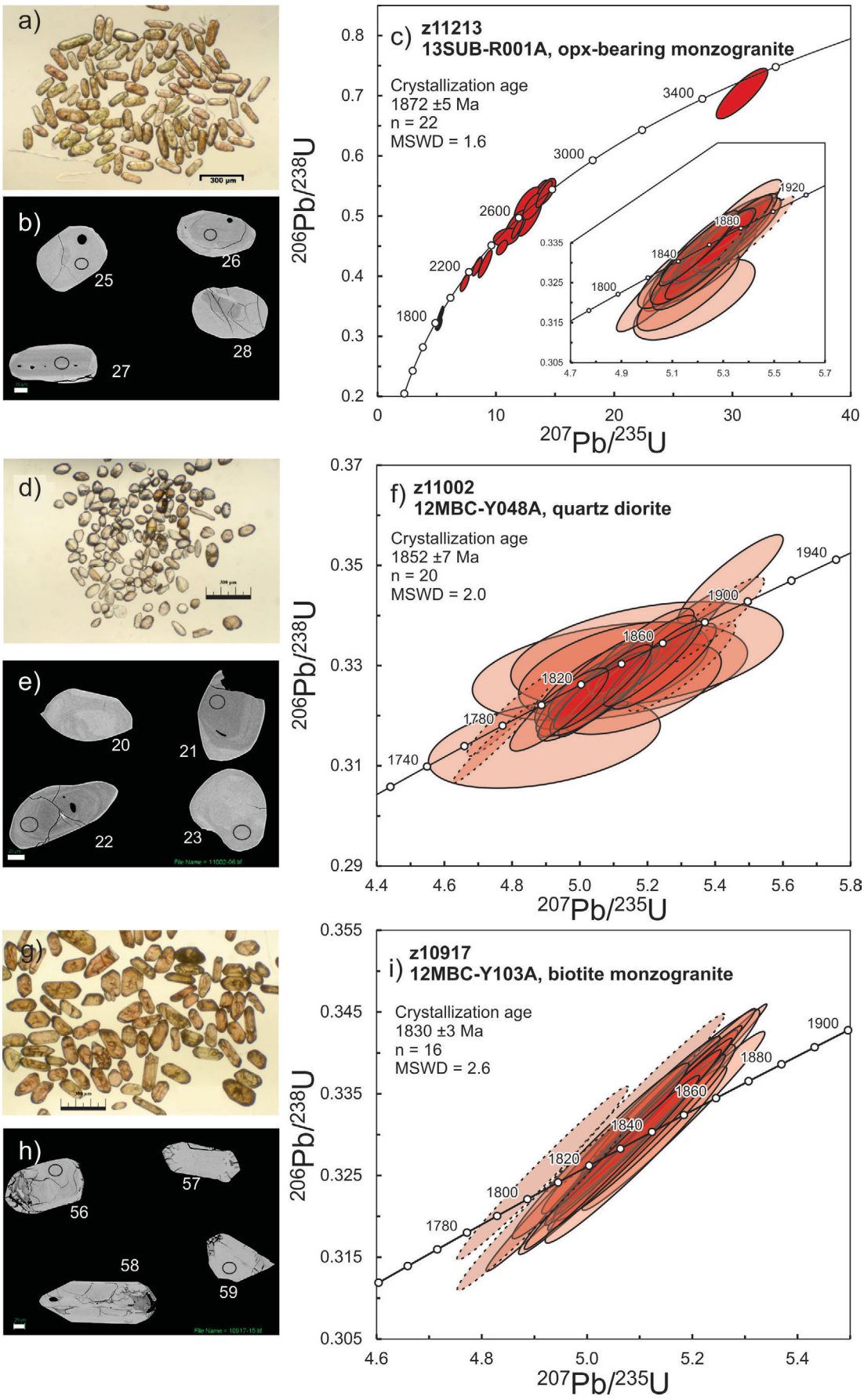
a)
300 µm
b)
25
26
27
28
c) z11213
13SUB-R001A, opx-bearing monzogranite
Crystallization age
1872 ±5 Ma
n = 22
MSWD = 1.6
3400
3000
2600
2200
1800
1920
1880
1840
1800
206Pb/238U
207Pb/235U
d)
e)
20
21
22
23
f) z11002
12MBC-Y048A, quartz diorite
Crystallization age
1852 ±7 Ma
n = 20
MSWD = 2.0
1940
1900
1860
1820
1780
1740
206Pb/238U
207Pb/235U
g)
h)
56
57
58
59
i) z10917
12MBC-Y103A, biotite monzogranite
Crystallization age
1830 ±3 Ma
n = 16
MSWD = 2.6
1900
1880
1860
1840
1820
1800
1780
206Pb/238U
207Pb/235U

(sample F96B on Figure 1, Rayner, 2014a, b) these likely represent a locally derived, basal sedimentary package.

- Although these quartzite samples only contain Archean detritus, they are inferred to be Paleoproterozoic in age because there is no evidence of unconformities or other temporal breaks between these samples and those with demonstrable Paleoproterozoic maximum depositional ages (sample 13SUB-S139A, 13SUB-Y009C, this study; samples F104A, K97A, R15A, B95A on Figure 1; see also Rayner 2014a, b).
- The age distribution of Paleoproterozoic detritus in these two samples exhibit significant differences. Psammite, sample 13SUB-S139A, contains a prominent but restricted mode at ca. 2.32 Ga and a young population at 1.96 Ga. The youngest detrital zircon from quartzite, sample 13SUB-Y009C, yields an age of 2.1 Ga and the provenance profile is dominated by a broad swath of results between 2.5 and 2.25 Ga. While there are some similarities, neither of these profiles strongly resembles those of previously dated metasedimentary rocks on Hall Peninsula (Rayner, 2014a, b).
- Detrital zircon sources at 1.96 Ga and 2.5–2.3 Ga are limited on Baffin Island.
- Further evaluation of these variations in provenance across Hall Peninsula and comparison with other units on Baffin Island and further afield is required to understand the evolution of this metasedimentary assemblage.

Hall Peninsula Paleoproterozoic plutonic rocks

- An orthopyroxene-bearing monzogranite is dated at 1872 ±5 Ma. This age is younger than the ca. 1890 Ma granulite-grade plutons previously dated (B97A on Figure 1; Scott, 1999; Rayner, 2014a, b) but identical in age to four other biotite- and/or garnet-bearing monzogranite samples in the region (samples B95B, K79B on Figure 1; Scott, 1999; Rayner, 2014a, b)
- A quartz diorite yields an age of 1852 ±7 Ma. Similar ages have been determined for more felsic compositions from western Hall Peninsula (Scott, 1999) and are ascribed to the southern continuation of the Cumberland Batholith (Jackson et al., 1990; Scott and Wodicka, 1998)
- A massive biotite monzogranite is dated at 1830 ±3 Ma, which also constrains the minimum age of the regional, pervasive deformation episode.

Figure 7: Zircon images and concordia diagrams for Paleoproterozoic plutonic samples, Hall Peninsula, southern Baffin Island, Nunavut. Ellipses plotted and mean ages reported at the 2σ confidence level. Abbreviation: MSWD, mean square of weighted deviates: **a)** transmitted light image of zircon grains recovered from sample 13SUB-R001A; abbreviation: opx, orthopyroxene; **b**) backscattered electron (BSE) images of zircons from sample 13SUB-R001A; white scale bar is 20 µm, white grain numbers and black ellipses correspond to analyses in Rayner (2015); **c)** concordia diagram of U-Pb results from sample 13SUB-R001A; inset: detail of ca. 1850 Ma results, dashed line ellipses are excluded from the calculation of the weighted mean; **d)** transmitted light image of zircon grains recovered from sample 12MBC-Y48A; scale bar is 300 µm; **e**) BSE images of zircons from sample 12MBC-Y048A; white scale bar is 20 µm, white grain numbers and black ellipses correspond to analyses in Rayner (2015); **f)** concordia diagram of U-Pb results from sample 12MBC-Y048A; dashed line ellipses are excluded from the calculation of the weighted mean; **g)** transmitted light image of zircon grains recovered from sample 12MBC-Y103A; black scale bar is 300 µm; **h**) BSE images of zircons from sample 12MBC-Y103A; white scale bar is 20 µm, white grain numbers and black ellipses correspond to analyses in Rayner (2015); **i)** concordia diagram of U-Pb results from sample 12MBC-Y103; dashed line ellipses are excluded from the calculation of the weighted mean.

Acknowledgments

The field relationships and resultant geological interpretations presented in this report are based on engaging and fruitful collaboration with H. Steenkamp, M. St-Onge, M. Young and the CNGO bedrock mapping team both in the field and in the office. The author is grateful for the support and assistance of the staff of the Geochronology Laboratories of the Geological Survey of Canada. In particular R. Chung, R. Christie, J. Peressini and T. Pestaj are thanked for their careful efforts and excellent work. P. Hunt provided the necessary high-quality scanning electron microscope images. The manuscript benefited from a thorough review by V. McNicoll. The Canadian Northern Economic Development Agency's (CanNor) Strategic Investments in Northern Economic Development (SINED) program provided support for this work.

Natural Resources Canada, Earth Sciences Sector contribution 20140278

References

From, R.E., St-Onge, M.R. and Camacho, A.L. 2014: Preliminary characterization of the Archean orthogneiss complex of Hall Peninsula, Baffin Island, Nunavut; *in* Summary of Activities 2013, Canada-Nunavut Geoscience Office, p. 53–62.

Jackson, G.D., Hunt, P.A., Loveridge, W.D. and Parrish, R.R. 1990: Reconnaissance geochronology of Baffin Island, N.W.T.; *in* Radiogenic Age and Isotopic Studies: Report 3, Geological Survey of Canada, Paper 89-2, p. 123–148.

Machado, G., Bilodeau, C. and St-Onge, M.R. 2013a: Geology, southern part of Hall Peninsula, south Baffin Island, Nunavut; Geological Survey of Canada, Canadian Geoscience Map 135 (preliminary), Canada-Nunavut Geoscience Office, Open File Map 2013-1, scale 1:250 000, doi:10.4095/292443

Machado, G., Bilodeau, C., Takpanie, R., St-Onge, M.R., Rayner, N.M., Skipton, D.R., From, R.E., MacKay, C.B., Creason C.G. and Braden, Z.M. 2013b: Hall Peninsula regional bedrock mapping, Baffin Island, Nunavut: summary of fieldwork; *in* Summary of Activities 2012, Canada-Nunavut Geoscience Office, p. 13–22.

MacKay, C.B., Ansdell, K.M., St-Onge, M.R., Machado, G. and Bilodeau, C. 2013: Geological relationships in the Qaqqanittuaq area, southern Hall Peninsula, Baffin Island, Nunavut; *in* Summary of Activities 2012, Canada-Nunavut Geoscience Office, p. 55–64.

Ludwig, K.R. 2003: User's manual for Isoplot 3.00: a geochronological toolkit for Microsoft® Excel®; Berkeley Geochronology Center, Special Publication 4, 74 p.

Rayner, N.M. 2014a: New U-Pb geochronological results from Hall Peninsula, Baffin Island, Nunavut; *in* Summary of Activities 2013, Canada-Nunavut Geoscience Office, p. 39–52.

Rayner, N.M. 2014b: Data table accompanying "New U-Pb geochronological results from Hall Peninsula, Baffin Island, Nunavut"; Canada-Nunavut Geoscience Office, Geoscience Data Series GDS2014-001, Microsoft® Excel® file, URL <http://cngo.ca/summary-of-activities/2013/> [November 2013].

Rayner, N.M. 2015: Data table accompanying "New (2013-14) U-Pb geochronological results from northern Hall Peninsula, southern Baffin Island, Nunavut"; Canada-Nunavut Geoscience Office, Geoscience Data Series GDS2015-002, Microsoft® Excel® file, URL <http://cngo.ca/summary-of-activities/2014/> [January 2015]

Sanborn-Barrie, M., Thrane, K., Rayner, N., Wodicka, N. and Connelly, J. 2015: Correlation of geological events across Davis Strait: broadening implications of GEM geoscience through international collaboration (abstract A15), *from* Greenland and Nunavut Geoscience Workshop 2014, Nuuk, Greenland, K. Thorsøe, D.J. Mate and M.D. Poulsen (comp.); *in* Summary of Activities 2014, Canada-Nunavut Geoscience Office, p. 175–190.

Scott, D.J. 1999: U-Pb geochronology of the eastern Hall Peninsula, southern Baffin Island, Canada: a northern link between the Archean of West Greenland and the Paleoproterozoic Torngat Orogen of northern Labrador; Precambrian Research, v. 93, p. 5–26.

Scott, D.J. and Wodicka, N. 1998: A second report on the U-Pb geochronology of southern Baffin Island, Northwest Territories; *in* Radiogenic Age and Isotopic Studies: Report 11; Geological Survey of Canada, Current Research, 1998-F, p. 47–57.

Scott, D.J. and Gauthier, G. 1996: Comparison of TIMS (U-Pb) and laser ablation microprobe ICP-MS (Pb) techniques for age determination of detrital zircons from Paleoproterozoic metasedimentary rocks from northeastern Laurentia, Canada, with tectonic implications; Chemical Geology, v. 131, p. 127–142.

Sircombe, K.N. 2004: AGEDISPLAY: an Excel workbook to evaluate and display univariate geochronological data using binned frequency histograms and probability density distributions; Computers and Geosciences, v. 30, p. 21–31.

Skipton, D.R. and St-Onge, M.R. 2014: Paleoproterozoic deformation and metamorphism in metasedimentary rocks west of Okalik Bay: a field template for the evolution of eastern Hall Peninsula, Baffin Island, Nunavut; *in* Summary of Activities 2013, Canada-Nunavut Geoscience Office, p. 63–72.

Steenkamp, H.M. and St-Onge, M.R. 2014: Overview of the 2013 regional bedrock mapping program on northern Hall Peninsula, Baffin Island, Nunavut; *in* Summary of Activities 2013, Canada-Nunavut Geoscience Office, p. 27–38.

Stern, R.A. 1997: The GSC sensitive high resolution ion microprobe (SHRIMP): analytical techniques of zircon U-Th-Pb age determinations and performance evaluation; *in* Radiogenic Age and Isotopic Studies, Report 10, Geological Survey of Canada, Current Research 1997-F, p. 1–31.

Stern, R.A. and Amelin, Y. 2003: Assessment of errors in SIMS zircon U-Pb geochronology using a natural zircon standard and NIST SRM 610 glass; Chemical Geology, v. 197, p. 111–146.

Thrane, K. and Connelly, J.N. 2006: Zircon geochronology from the Kangaatsiaq–Qasigiannguit region, the northern part of the 1.9–1.8 Ga Nagssugtoqidian orogen, West Greenland; Geological Survey of Denmark and Greenland Bulletin, v. 11, p. 87–99.

Whalen, J.B., Wodicka, N., Taylor, B.E. and Jackson, G.D. 2010: Cumberland batholith, Trans-Hudson Orogen, Canada: petrogenesis and implications for Paleoproterozoic crustal and orogenic processes; Lithos, v. 117, p. 99–118, doi:10.1016/j.lithos.2010.02.008

Wodicka, N. and Scott, D.J. 1997: A preliminary report on the U-Pb geochronology of the Meta Incognita Peninsula, southern Baffin Island, Northwest Territories; *in* Geological Survey of Canada, Current Research 1997-C, p. 167–178.

Geology, geochemistry and geochronology of basement rocks around the Discovery camp, Chidliak diamond project, northern Hall Peninsula, southern Baffin Island, Nunavut

K. Ansdell[1], A. Hunchak[2,3] and J. Pell[4]

[1]*Department of Geological Sciences, University of Saskatchewan, Saskatoon, Saskatchewan, kevin.ansdell@usask.ca*

[2]*Department of Geological Sciences, University of Saskatchewan, Saskatoon, Saskatchewan*

[3]*De Beers Canada, Toronto, Ontario*

[4]*Peregrine Diamonds Ltd., Vancouver, British Columbia*

This work was part of a collaboration between the University of Saskatchewan and Peregrine Diamonds Ltd. It aimed to better understand the Archean gneissic basement and Paleoproterozoic supracrustal units that outcrop on eastern Hall Peninsula. It augments observations made during the Hall Peninsula Integrated Geoscience Program, led by the Canada-Nunavut Geoscience Office.

Ansdell, K., Hunchak, A. and Pell, J. 2015: Geology, geochemistry and geochronology of basement rocks around the Discovery camp, Chidliak diamond project, northern Hall Peninsula, southern Baffin Island, Nunavut; *in* Summary of Activities 2014, Canada-Nunavut Geoscience Office, p. 45–56.

Abstract

This paper provides an overview of field observations made in August 2011, and subsequent petrographic, geochemical and geochronological analyses of basement rocks around the Discovery camp in the Peregrine Diamonds Chidliak diamond project on northern Hall Peninsula, Baffin Island, Nunavut. The lithological units include Neoarchean orthogneiss, which occur within domal structures in the southern and northern part of the study area, and metasedimentary, ultramafic and mafic rocks in the intervening area. The former consist of interbedded pelitic and psammitic rocks with mineral assemblages indicative of upper-amphibolite–facies metamorphism attained during the Paleoproterozoic. The meta-ultramafic rocks include distinctive porphyroblastic komatiitic units that have a trace-element signature suggestive of partial melting of a mantle plume in the garnet stability field. Overall, the units observed are similar to those mapped elsewhere during the Hall Peninsula Integrated Geoscience Project, and are interpreted to form part of the Archean gneissic basement that outcrops in eastern Hall Peninsula and the predominantly Paleoproterozoic supracrustal units that occur in the central portions of Hall Peninsula.

Résumé

Cet article présente un aperçu des observations de terrain faites en août 2011, ainsi que des résultats d'analyses pétrographiques, géochimiques et géochronologiques ultérieures effectuées sur des roches du socle entourant le camp minier où a eu lieu la nouvelle découverte de la Peregrine Diamonds Limitée dans le cadre de son projet diamantifère Chidliak, au nord de la péninsule Hall, dans l'île de Baffin, au Nunavut. Les unités lithologiques comprennent de l'orthogneiss néoarchéen, qui se manifeste au sein de structures en forme de dôme situées dans les parties méridionale et septentrionale de la zone d'étude, ainsi que des roches métasédimentaires, ultramafiques et mafiques, qui se retrouvent dans la partie centrale de la péninsule. Les unités néoarchéennes se composent de roches pélitiques et psammitiques interstratifiées dont le profil minéralogique témoigne d'un métamorphisme du faciès des amphibolites supérieur atteint au cours du Paléoprotérozoïque. Les roches méta-ultramafiques se composent d'unités komatiitiques porphyroblastiques distinctives dont la signature en éléments traces révèle qu'elles pourraient être associées à la fusion partielle d'un panache mantellique correspondant au champ de stabilité du grenat. De façon générale, les unités ressemblent à celles qui ont été cartographiées ailleurs dans le cadre du Projet géoscientifique intégré de la péninsule Hall et que l'on estime qu'elles font partie du socle gneissique archéen, qui affleure dans la partie est de la péninsule Hall, et des unités supracrustales d'origine sutrtout paléoprotérozoïque, qui se manifestent dans la partie centrale de la péninsule.

This publication is also available, free of charge, as colour digital files in Adobe Acrobat® PDF format from the Canada-Nunavut Geoscience Office website: http://cngo.ca/summary-of-activities/2014/.

Introduction

Until recently, the Precambrian rocks underlying Hall Peninsula, southeastern Baffin Island, were very poorly understood because the region had only been mapped at reconnaissance scale (1:506 880; Blackadar, 1967). Detailed mapping and sampling along a narrow corridor extending about 100 km east from Iqaluit (Scott, 1996) resulted in the only geochronological background for the whole peninsula, which suggested that tonalitic gneisses in the eastern part of the peninsula were Archean, whereas metasedimentary and plutonic rocks that dominate the western part of the peninsula were Paleoproterozoic (Scott, 1999). These rocks are all interpreted to have been deformed and metamorphosed during the Trans-Hudson Orogen, a Paleoproterozoic collisional orogenic belt extending from southeastern Baffin Island to central United States (Hoffman, 1988; Corrigan et al., 2009). In 2012, the Canada-Nunavut Geoscience Office initiated a more comprehensive regional mapping program with associated thematic studies. This Hall Peninsula Integrated Geoscience Program (HPIGP) has led to the production of new geological maps of Hall Peninsula (Machado et al., 2013; Steenkamp and St-Onge, 2014) and an increase in geoscience knowledge for the area through new geochemical, geochronological and metamorphic pressure and temperature studies. Northern Hall Peninsula can be subdivided into three main regions (Figure 1). There are Paleoproterozoic metasedimentary rocks that host orthopyroxene-bearing granitoid rocks in the west, whereas the eastern part of the peninsula is dominated by Archean tonalitic and monzogranitic gneiss. The intervening area is underlain by psammitic to pelitic metasedimentary gneiss, with rarer calcsilicate rocks, iron formation and mafic to ultramafic rocks. Metamorphism varies from amphibolite grade in the east to granulite grade in the west, and the peak of metamorphism is considered to be coeval with the first main Paleoproterozoic deformation event related to the Trans-Hudson Orogen (Steenkamp and St-Onge, 2014). The rocks were then incorporated into thick-skinned thrusts and folds during two further deformation events.

Given the limited geoscience knowledge prior to the initiation of the HPIGP, the potential for diamond deposits on Hall Peninsula was unknown. Peregrine Diamonds Ltd., a Canadian-owned diamond exploration company based in Vancouver, British Columbia, initiated an exploration campaign on southern Baffin Island that has since resulted in the discovery of numerous kimberlites on their Chidliak property (Pell et al., 2013). These were emplaced between 156 and 138 Ma based on U-Pb analyses of perovskite (Heaman et al., 2012), and the presence of diamondiferous kimberlites provides compelling evidence that much of this part of Hall Peninsula is underlain by ancient lithospheric mantle. Understanding the distribution and evolution of the Archean rocks may be important to understanding the distribution of potentially economic kimberlites.

The geophysical signature of the kimberlites are complex, so a B.Sc. project was developed to understand the variability in rock types in the basement, which would potentially assist Peregrine Diamonds in their interpretation of airborne and ground geophysical data. A small 20 km^2 swath of basement rocks in the vicinity of the Peregrine Diamonds Discovery camp (Figure 1) was chosen because there was significant variability in magnetic signature, suggesting a range in basement rock types (Figure 2). The objective of this paper is to provide an overview of the geological units identified during four days of helicopter-supported mapping in August 2011. Thirty-two samples were collected, including ten for whole-rock geochemistry and three for U-Pb geochronology. Comments on the petrographic, geochemical and geochronological results are also provided.

Geological observations

According to Blackadar (1967), the area of study included rocks identified as biotite-quartz-feldspar gneiss and biotite granite. The airborne magnetic survey data (Figure 2) suggest that there is a greater variety of lithological units within the area. Outcrops are scarce and much of the area, which has low relief, is covered by till and felsenmeer (Figure 3a).

Orthogneiss

The ovoid areas with highly magnetic signatures in the south and north of the area (Figure 2) were interpreted as gneiss domes prior to field examination. The cores of these areas are well exposed, particularly in the south, albeit fractured and lichen covered. They are composed of white-weathering tonalite, with minor biotite and gneissic banding. The orientation of the banding defines the shape of the regional magnetic features, although the intensity of the gneissic banding varies. There are local concentrations of mafic xenoliths and areas of irregular leucosome suggesting partial melting. Toward the margins of the domes, tonalitic gneiss is interleaved with granodioritic gneiss (Figure 3a) containing minor biotite, and is less commonly interleaved with amphibolite, and dioritic and porphyritic granitic gneiss (Figure 3b). In the porphyritic granitic gneiss, K-feldspar phenocrysts are up to 3 cm in length (Figure 2b) and the rock contains minor hornblende and biotite. Rare garnet was observed in granodioritic gneiss near the margins of the domal features. The contact between the orthogneiss and adjacent rock types is not exposed.

Magnetic susceptibility measurements made at each outcrop of orthogneiss are variable: tonalite is typically just above 2 SI, K-feldspar porphyritic granite is about 3 SI, mafic xenoliths are more than 30 SI and the remainder of the gneissic complex yields measurements below 0.5 SI.

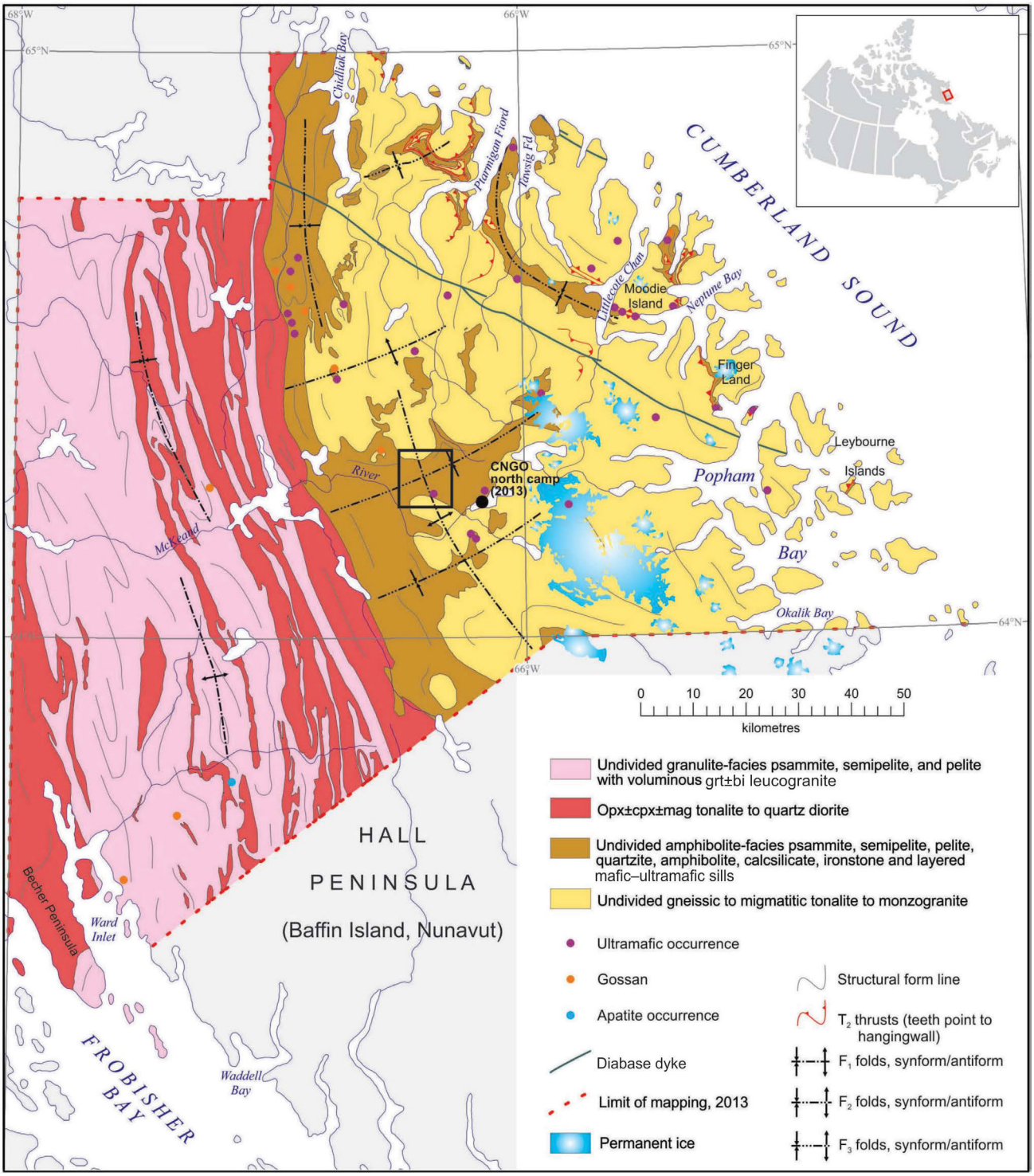

Figure 1: Geology of northern Hall Peninsula, Baffin Island, Nunavut (from Steenkamp and St-Onge, 2014). The box outlines the study area shown in Figure 2. Abbreviations: bi, biotite; Chan, channel; cpx, clinopyroxene; Fd, fjord; grt, garnet; mag, magnetite; opx, orthopyroxene.

Metasedimentary rocks

Outcrops in areas with an intermediate magnetic signature (green; Figure 2) are dominated by gneissic metasedimentary rocks. They typically consist of interbedded pelite to psammite (Figure 3c, d), with the former being richer in leucosome, indicating preferential partial melting. The pelitic gneiss contains quartz, feldspar, biotite with local garnet (up to 3 cm in size), sillimanite, hornblende and magnetite. White knots of intergrown fine-grained sillimanite, K-feldspar and quartz (faserkiesels) are common (Figure 3d), and in some places the faserkiesels are cored by garnet porphyroblasts. The psammitic layers locally contain pinhead-sized garnets and are commonly boudinaged. Within the metasedimentary rocks to the north of the camp were layers (10–20 cm thick) of silicate-facies iron formation. A quartz-rich layer was sampled for zircon geochronology but only yielded garnets as a heavy mineral when the samples were crushed and prepared for analysis. This could indicate that the quartz was derived through chemical precipitation, and that the protolith could have been a chert. This would be consistent with seafloor hydrothermal activity and the formation of thin silicate-facies iron formation units. The iron formation had a magnetic susceptibility measurement of about 70 SI, whereas the other metasedimentary rocks had measurements from 0 to 3 SI. It is unclear whether the contact between the orthogneiss and the metasedimentary gneiss is structural or stratigraphic as it is not exposed. No stratigraphic facing indicators were identified in the metasedimentary units.

Metamafic and meta-ultramafic rocks

The linear, broadly east-oriented, highly magnetic units between the northern and southern gneiss domes (red-purple stripes in magnetic data; Figure 2) are dominated by metamorphosed mafic and ultramafic rocks. Some of these occur in typically fine-grained layers, which are subparallel to the lithological variations in the metasedimentary gneiss. These are interpreted to be extrusive igneous rocks and could represent marker horizons in this area. The most distinctive units are ultramafic, highly magnetic (40–50 SI) and comprise layers with brown porphyroblasts in a greenish-brown fine-grained matrix (Figure 3e). The porphyroblasts are composed of olivine, with tremolite or magnesiohornblende dominating in the matrix. The elongate shape of the porphyroblasts defines the foliation. Locally, centimetre-wide layers of olivine have been serpentinized. In contrast, black-weathering and nonmagnetic fine-grained rocks containing hornblende and plagioclase are interpreted to be mafic (Figure 3f). Locally, the mafic rocks contain bands of calcsilicate minerals and, like the ultramafic units, the rocks are subparallel to lithological variations in the area.

Two isolated bodies (possibly boudins) of coarse-grained intrusive ultramafic rocks were observed in the metasedimentary strata. One outcrop, about 30 m across, is a brown-weathering peridotite containing magnesiohornblende crystals greater than 3 cm in length. The other outcrop is black-weathering, finer-grained metagabbro.

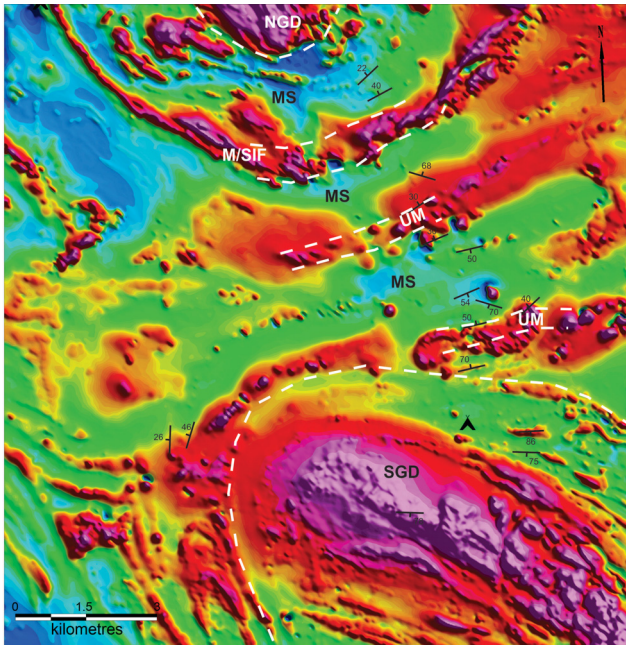

Figure 2: Airborne magnetic survey data from the study area, collected by Peregrine Diamonds Ltd. in 2008 and 2010. The tent symbol indicates the location of the Peregrine Diamonds Discovery camp. Strike and dip of dominant foliation are shown, which provides an indication of the locations of transects and outcrops. The dashed white lines provide approximate location of contacts between different rock units. Abbreviations: MS, metasedimentary rocks; M/SIF, metamafic rocks and silicate-facies iron formation; NGD, northern gneiss dome; SGD, southern gneiss dome; UM, meta-ultramafic rocks.

Deformation and metamorphism

The lithological units in the area appear to have been affected by at least two main deformational events and one high-grade regional metamorphic episode. The dominant foliation in the metasedimentary rocks between the northern and southern gneiss domes is gently to moderately north dipping and broadly parallel to lithological variations in the metasedimentary units (Figure 3c). In pelitic strata, this fabric is defined by the alignment of biotite and elongate faserkiesels (Figure 3d). The development of leucosome in the pelitic strata indicates that the rocks experienced metamorphic pressure and temperature conditions appropriate to generate partial melt. In the meta-ultramafic rocks, the olivine porphyroblasts also have a preferred orientation parallel to the dominant foliation (Figure 3e). Overall, the mineral assemblages in these rocks suggest that upper-amphibolite–facies metamorphism had been attained, which likely occurred during the first main deformation event. From field evidence, it is difficult to determine whether the compositional banding within the orthogneiss developed contemporaneously with the deformation

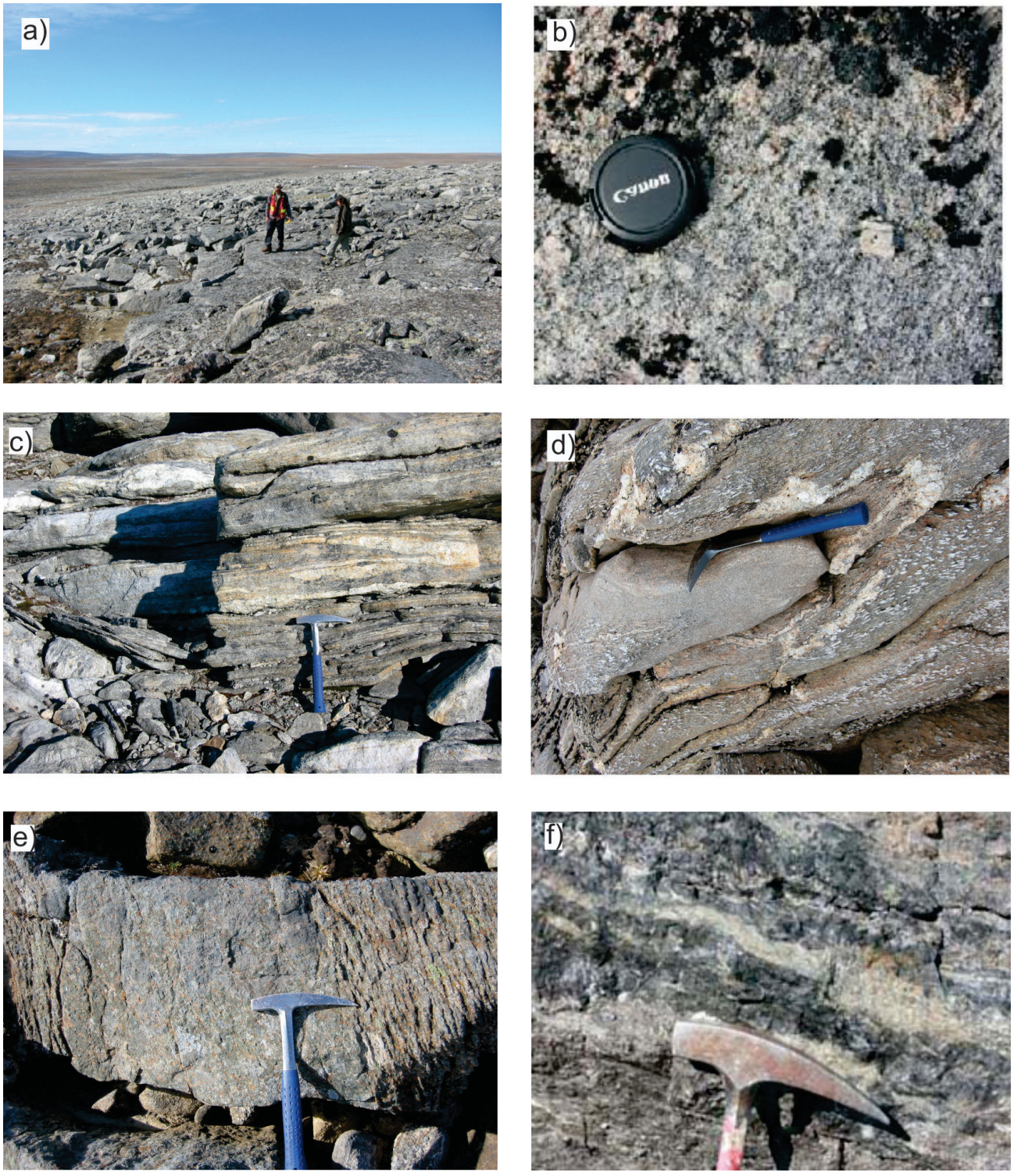

Figure 3: a) View looking west toward the Discovery camp, in the distance from an outcrop of granodioritic gneiss (sample AH-17) on the northern margin of the southern gneiss dome. The land surface is covered in felsenmeer; **b)** K-feldspar porphyritic granite (sample AH-18); **c)** biotite-bearing pelitic rock with tightly folded and boudinaged granitic vein; **d)** interbedded and folded grey psammitic, pelitic gneiss, bearing faserkiesel and garnet; **e)** interbedded brown-weathering porphyroblastic and nonporphyroblastic komatiite; **f)** fine-grained black-weathering mafic rock with irregular leucosome and calcsilicate bands.

observed in the metasedimentary rocks or during an earlier, potentially Archean, deformation event.

The later deformation event resulted in the folding of interbedded psammite and pelite, the fabrics described above (Figure 3d) and of leucosome in the pelite (Figure 3c). There are locations between the two gneiss domes where the dominant foliation dips to the south. Together these features are related to a postpeak metamorphic deformation event, linked potentially to north-south–oriented compression.

The orientation of banding on the western margin of the southern gneiss dome is to the west.

Geochemistry

Four representative samples from the orthogneiss complex, including an amphibolite from within the southern gneiss dome and six samples of the metamafic and ultramafic rocks, were analyzed for major and trace elements at the Saskatchewan Research Council Geoanalytical Laboratories in Saskatoon. They were crushed and ground in agate, and an aliquot fused with lithium metaborate prior to dissolution in dilute HNO_3. Major elements were measured using inductively coupled plasma–optical emission spectrometry (ICP-OES), whereas trace elements were measured by inductively coupled plasma–mass spectrometry (ICP-MS). The data are reported in Table 1.

Meta-mafic and meta-ultramafic rocks

The brown-weathering fine-grained rocks (Figure 2e; Table 1, samples AH-12, AH-21 and AH-30), interpreted as meta-ultramafic rocks in the field, can be classified as komatiite based on Mg:Al:Fe+Ti ratios (Figure 4a), using the classification of Jensen (1976). The rocks have MgO contents varying from 20.9 to 23.6 wt. %, and high Cr (1870–2280 ppm) and Ni (786–960 ppm) contents. The Al_2O_3/TiO_2 ratios (4.0–8.0), CaO/Al_2O_3 ratios (1.0–1.3) and $(Gd/Yb)_N$ ratios (>1) suggest that these rocks are Al-depleted komatiite (Nesbitt et al., 1979; Dostal, 2008); however, the TiO_2 content for two samples is greater than 1 wt. %, so they could be classified as meimechite. Keim (2012) suggested that compositionally similar rocks on Cumberland Peninsula could be enriched in Ti, and could be classified as Karasjok-type komatiite. One of the coarse-grained intrusive rocks (Table 1, sample AH-4) is also komatiitic in composition. A sample from the black-weathering, fine-grained rocks (Table 1, sample AH-7C), interpreted to be mafic in the field (Figure 3f), is compositionally a komatiitic basalt (Figure 4a). The patterns exhibited in mid-ocean ridge basalt (MORB)–normalized trace-element variation diagrams (Pearce, 1996) for these four rocks are similar (Figure 3b). Note that this diagram is constructed for basaltic rocks, whereas rocks analyzed in this study are more MgO rich, which suggests that they were derived by higher degrees of partial melting in the mantle. Figure 4b illustrates that the most incompatible elements (Th, Nb) are enriched relative to the less incompatible elements (Y), and that there is a negative Zr anomaly. This relationship between elements is most similar to the pattern exhibited by within-plate basalt most likely derived by melting of a mantle plume (Pearce, 1996).

Orthogneiss

The samples of granitoid gneiss that were analyzed contain concentrations of SiO_2 from 69.4 to 77.2 wt. % and K_2O from 3.74 to 4.98 wt. %, indicating that they are high-potassium granitoid rocks (LeMaitre, 1989). Based on the Al:Mg:Fe+Ti cation ratio, the amphibolite sample (sample AH-16) from the orthogneiss complex exposed in the southern gneiss dome can be classified as a high-Mg tholeiite (Figure 4a). However, all the orthogneiss samples preserve significant Nb, Ti and P negative anomalies (Figure 4c).

Geochronology

Unweathered representative samples of tonalitic gneiss (sample AH-14) and granodioritic gneiss (sample AH-17; Figure 3a) were taken from the core and margins of the southern gneiss dome, respectively. No crosscutting relationships between these rock units could be observed in the field, and the relationship with the metamorphosed supracrustal rocks in the study is also not known. Thus, the primary aim was to determine the age of formation of these rock units. The samples were crushed and zircons were separated using standard heavy-liquid and magnetic methods at the University of Alberta (Edmonton). Clear, nonmagnetic euhedral zircons were mounted in epoxy and polished to expose their interiors. The zircons were analyzed by laser-ablation multicollector inductively coupled plasma–mass spectrometry (LA-MC-ICP-MS) at the Radiogenic Isotope Facility at the University of Alberta, using procedures modified from Simonetti et al. (2005). Analyses of the core of 30 separate zircons from sample AH-14, and 67 separate zircons from AH-17 were acquired (Ansdell et al., 2015[5]).

All the zircons from sample AH-14 yielded concordant analyses, and the amount of ^{204}Pb is low, varying from 2 to 216 counts/second (Ansdell et al., 2015). The 20 youngest euhedral zircons yield $^{207}Pb/^{206}Pb$ ages that overlap within error and give an age of 2725 ±3 Ma (Figure 5a). The authors interpret this to represent the crystallization age of the tonalite. The older ages range from 2975 ±11 to 2814 ±11 Ma, and are interpreted to be grains inherited from the source of the tonalitic magma or from hostrocks.

[5] *CNGO Geoscience Data Series GDS2015-006, containing the data or other information sources used to compile this report, is available online to download free of charge at http://cngo.ca/summary-of-activities/2014/.*

Table 1: Major- and trace-element data from representative meta-ultramafic and metamafic rocks and orthogneiss from the southern gneiss dome. Abbreviation: bdl, below detection limit.

	Metamafic and meta-ultramafic rocks						Orthogneisses			
	Intrusive		Extrusive							
Sample #	**AH-004**	**AH-009**	**AH-007C**	**AH-012**	**AH-021**	**AH-030**	**AH-016**	**AH-017**	**AH-018**	**AH-019**
wt. %										
SiO_2	47.2	45.7	45.0	45.9	46.0	45.6	48.4	74.4	69.4	77.2
TiO_2	0.48	0.06	2.68	0.82	1.26	1.74	0.55	0.23	0.32	0.03
Al_2O_3	7.38	0.83	11.8	6.53	7.08	6.93	17.0	13.6	16.2	12.8
Fe_2O_3	12.2	38.9	12.5	13.2	13.4	13.9	10.5	1.92	1.92	0.49
MnO	0.19	3.92	0.25	0.16	0.18	0.18	0.16	0.03	0.04	0.05
MgO	19.3	4.75	11.4	23.6	22.2	20.9	8.95	0.43	0.74	0.06
CaO	8.95	4.97	12.2	6.49	8.34	9.31	12.1	1.33	2.59	0.78
Na_2O	1.29	0.06	0.83	0.19	0.92	0.31	1.59	3.29	4.59	3.35
K_2O	0.58	0.11	1.4	0.06	0.2	0.14	0.32	4.88	3.74	4.98
P_2O_5	0.07	0.46	0.51	0.08	0.12	0.16	0.05	0.03	0.08	<0.01
LOI	1.3	2.4	bdl	0.5	1.1	1.0	0.4	0.5	0.3	0.8
Total	99.54	99.76	99.87	99.43	100.5	100.27	100.62	100.54	100.12	100.04
ppm										
Sc	38	2	55	29	23	29	38	3	2	2
V	170	22	360	221	183	228	188	11	21	2
Cr	2190	18	1600	2280	2100	1870	385	12	13	7
Co	73.9	21.6	48.2	84.3	73.9	80.4	37.4	2.0	3.5	0.4
Cu	52.6	33.9	18.7	85.4	4.6	118	83.8	4.6	3.7	2.5
Ni	566	29	204	960	786	896	148	7	12	7
Zn	123	68	94	75	73	78	75	46	48	28
Ge	1.4	4.0	2.0	1.8	1.4	1.5	1.4	0.9	0.6	1.4
Sn	1	0.5	2.3	0.4	0.9	1.0	0.4	2.1	1.0	0.4
W	3	1	5	2	1	1	1	bdl	bdl	bdl
Cs	1.9	bdl	2.5	bdl	bdl	bdl	bdl	1.6	0.6	0.8
Rb	13.8	1.3	33.4	0.8	3.2	1.7	8.9	248	119	272
Sr	169	51	316	184	84	132	119	106	571	18
Ba	85	26	256	21	40	75	42	601	1280	42
Nb	1	1	58	2	8	19	1	12	4	4
Zr	35	16	160	25	59	87	26	233	223	52
Hf	1.3	0.4	5.1	1.2	2.3	3.2	1.0	9.6	6.9	4.2
Y	6.89	15.0	15.4	9.11	9.93	10.8	9.78	6.21	8.04	12.7
La	7	9	32	2	8	12	1	14	64	2
Ce	16	29	65	5	18	25	4	43	108	3
Pr	2.75	3.05	9.88	1.17	3.08	4.18	0.85	3.76	15.1	0.46
Nd	10.4	11.6	35.4	5.6	12.5	16.2	4.0	11.6	45.1	1.6
Sm	2.19	2.68	6.76	1.86	2.75	3.60	1.11	2.02	5.91	0.39
Eu	0.66	0.76	2.89	0.50	0.90	1.06	0.52	0.55	1.48	0.17
Gd	1.91	2.92	5.71	2.32	2.78	3.37	1.61	1.53	3.26	0.77
Tb	0.3	0.51	0.74	0.38	0.45	0.55	0.3	0.25	0.35	0.22
Dy	1.74	3.12	4.12	2.4	2.64	2.97	2.15	1.35	1.66	1.98
Ho	0.40	0.78	0.85	0.52	0.58	0.61	0.54	0.32	0.33	0.60
Er	0.81	1.72	1.60	1.00	1.12	1.21	1.24	0.70	0.64	1.69
Tm	0.14	0.30	0.26	0.16	0.19	0.21	0.23	0.13	0.12	0.36
Yb	0.8	1.86	1.58	1.07	1.12	1.23	1.45	0.84	0.65	2.65
Lu	0.1	0.3	0.2	0.2	0.2	0.2	0.2	0.1	0.1	0.4
Pb	5.28	5.20	9.14	1.91	1.90	2.42	2.17	34.3	29.0	52.1
Th	2.21	0.51	3.84	0.21	1.28	1.40	0.26	29.2	16.8	8.13
U	1.59	0.87	3.38	0.41	0.38	0.55	0.52	4.16	3.38	5.42
Be	0.7	3.0	4.0	0.2	0.6	0.9	0.2	2.3	1.9	1.4
Ga	9.7	5.5	20.5	11.2	11.1	12.0	13.4	17.8	19.4	19.2
As	1.0	1.9	0.2	1.4	1.4	2.6	0.3	2.4	0.2	1.6
Sb	1	1	bdl	bdl	1	1	1	1	1	bdl
Mo	0.6	0.7	0.7	0.2	0.3	0.3	0.2	0.3	0.4	0.5
Ag	0.4	0.3	1.5	0.4	0.3	0.8	0.5	0.4	0.3	0.2
Hg	bdl	bdl	0.2	0.1	bdl	bdl	0.1	bdl	bdl	bdl
Cd	bdl	bdl	0.1	bdl	bdl	bdl	bdl	0.1	0.1	bdl
Te	bdl	bdl	bdl	bdl	bdl	bdl	bdl	bdl	bdl	bdl
Se	1	3	1	bdl	bdl	bdl	bdl	bdl	bdl	bdl
Ta	0.22	0.10	5.79	0.25	1.24	2.50	0.18	2.90	0.99	0.36
Tl	0.10	0.02	0.12	0.01	0.02	0.04	0.07	0.95	0.44	0.80
Bi	0.3	bdl	bdl	bdl	0.2	bdl	bdl	bdl	bdl	bdl

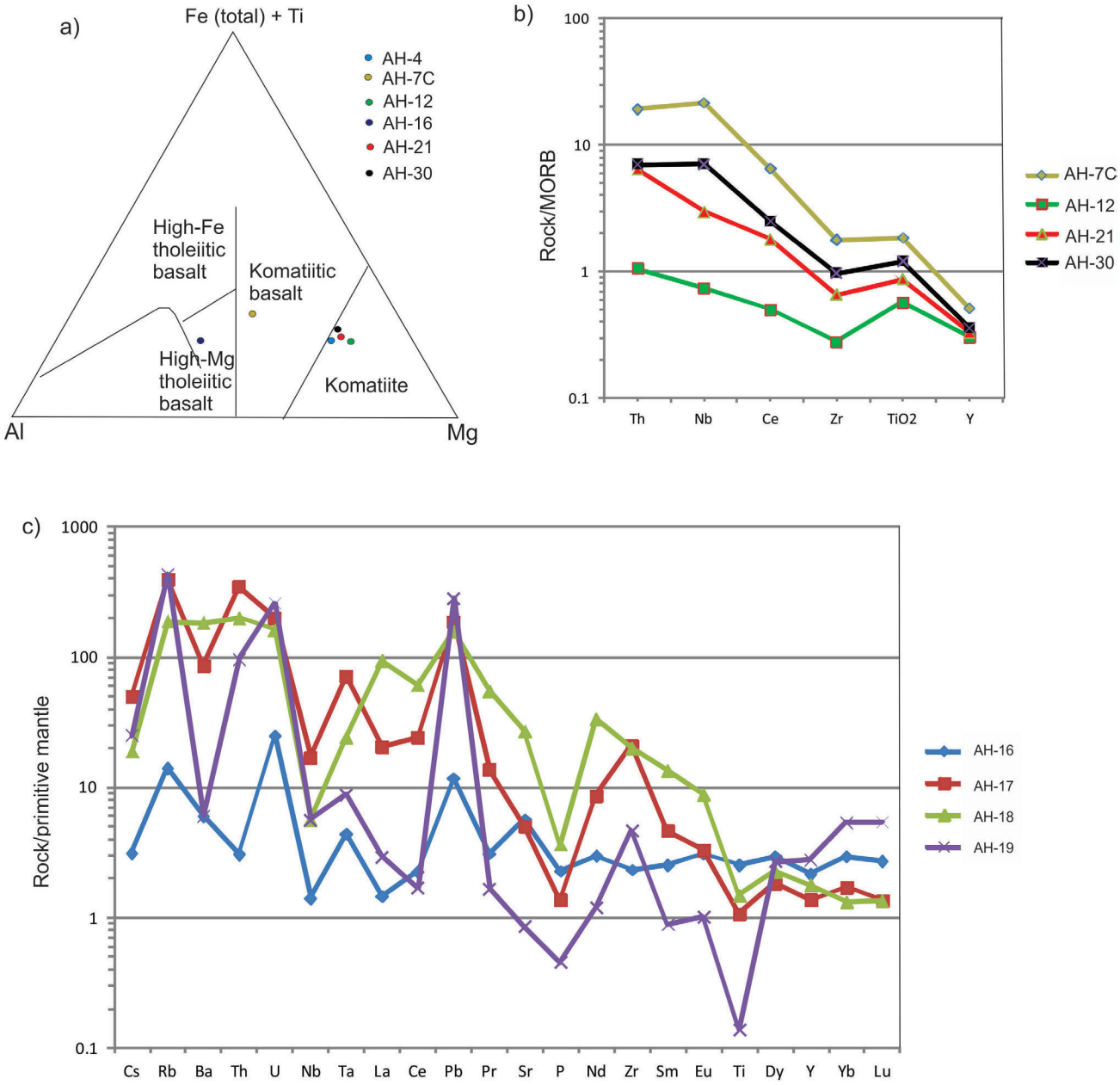

Figure 4: a) Jensen (1976) cation percentage plot showing the classification of the meta-ultramafic and metamafic rocks, Discovery camp; **b)** Pearce (1996) mid-ocean-ridge-basalt–normalized variation plot showing the patterns exhibited by the meta-ultramafic (samples AH-12, -21, -30) and metamafic (sample AH-7C) extrusive rocks; **c)** primitive-mantle–normalized extended variation plot for orthogneiss samples collected from the southern gneiss dome (samples AH-16, -17, -18, -19). Normalizing values are from Sun and McDonough (1989).

The analyses obtained from sample AH-17 zircons are more discordant than those from sample AH-14, and contain more common Pb, with ^{204}Pb varying from 121 to 746 counts/second (Ansdell et al., 2015). Twenty-one variably discordant grains (not including the oldest grain analyzed) yield ^{207}Pb/^{206}Pb ages that range from 2735 to 2685 Ma and yield an imprecise upper intercept age of 2702 ±47 Ma. A definitive age for this rock cannot be determined. No crosscutting relationships with sample AH-14 were observed in the field, although an interpretation is that the granodiorite forms part of the same suite of granitoid rocks as the tonalite. Inheritance appears to be insignificant in this rock, as one zircon yielded a ^{207}Pb/^{206}Pb age of 2792 ±18 Ma. Analyses that yield discordant ^{207}Pb/^{206}Pb ages down to 2103 ±20 Ma define a broad discordia zone with a lower concordia intercept in the Paleoproterozoic (Figure 5b). The interpretation is that this is a Neoarchean ca. 2700 Ma granodiorite in which the zircons were variably reset during high-grade metamorphism in the Paleoproterozoic.

Discussion

The focus of this project was to examine the variably magnetic basement rocks in the vicinity of the Discovery camp of the Peregrine Diamonds Chidliak diamond project, using a combination of field observations and petrographic analysis. In addition, whole-rock geochemical analyses and U-Pb geochronology were performed on metamorphosed igneous rocks discovered in the field in order to provide constraints on their origin and age.

This project highlights the usefulness of analyzing magnetic signatures to focus bedrock mapping as it clearly identifies variations in rock type and geometry of structures (Figure 2). This approach has also assisted in the delineation of bedrock map units on Hall Peninsula as part of the HPIGP, and overall, remote predictive mapping is an important first step when initiating mapping in many areas, particularly those that are difficult to access (Schetselaar et al., 2007; Machado et al., 2013; Steenkamp and St-Onge, 2014).

Geochronological constraints on the age of the tonalite (sample AH-14) and granodiorite (sample AH-17) in the southern gneiss dome suggest that these rocks crystallized between 2725 and 2700 Ma (Figure 5), and thus form part of the Archean orthogneiss basement in the eastern section of Hall Peninsula (Scott, 1999; From et al., 2014; Rayner, 2014). The age of the K-feldspar porphyritic granite was not determined, but could be part of the same suite as a deformed megacrystic granite in southern Hall Peninsula that yielded an age of 2701 ±2 Ma (Rayner, 2014). The age of older grains in the tonalite suggests inheritance and may provide an indication of the age range of intrusive rocks in eastern Hall Peninsula. In addition, the trace-element characteristics of the orthogneisses suggests that the intrusive rocks formed in a convergent margin setting as Nb and Ti are decoupled from the more fluid-compatible elements (Figure 4c).

Steenkamp and St-Onge (2014) show that local exposures of the Archean basement rocks are overlain by quartzite from the base of the metasedimentary sequence in the central part of Hall Peninsula; however, the nature of the contact between the orthogneiss and metasedimentary rocks in the Discovery camp area is not known, so could be either tectonic or an unconformity. Detrital zircons from quartzite (three samples) and psammite (one sample) on the eastern and western portions of southern Hall Peninsula yield maximum depositional ages between 2.1 and 1.9 Ga, while one sample of quartzite from the central part of southern Hall Peninsula yielded a maximum depositional age of 2.68 Ga (Rayner, 2014). The metasedimentary rocks and metaultramafic and metamafic rock around Discovery camp have not been dated and could be either Paleoproterozoic or Neoarchean in age.

The brown-weathering, variably porphyroblastic rocks are very distinctive in the field (Figure 3e), and are interpreted as extrusive rocks as they have a fine-grained groundmass and their outcrop patterns are subparallel to the interbedded pelite and psammite (Figure 2). They have a komatiitic composition (Figure 4a) but do not preserve the spinifex texture characteristic of komatiite. If a spinifex texture was present when the ultramafic rocks crystallized, it would have been recrystallized during high-grade Paleoproterozoic metamorphism. They are very similar in appearance, mineralogy and composition to 'spotty dykes' seen in a few places on Cumberland Peninsula (MacKay, 2012). The major- and trace-element characteristics of the ultramafic rocks are consistent with Al-depleted komatiite (Nesbitt et al., 1979), which may have been generated by high degrees of partial melting of a mantle plume (Figure 3b), at pres-

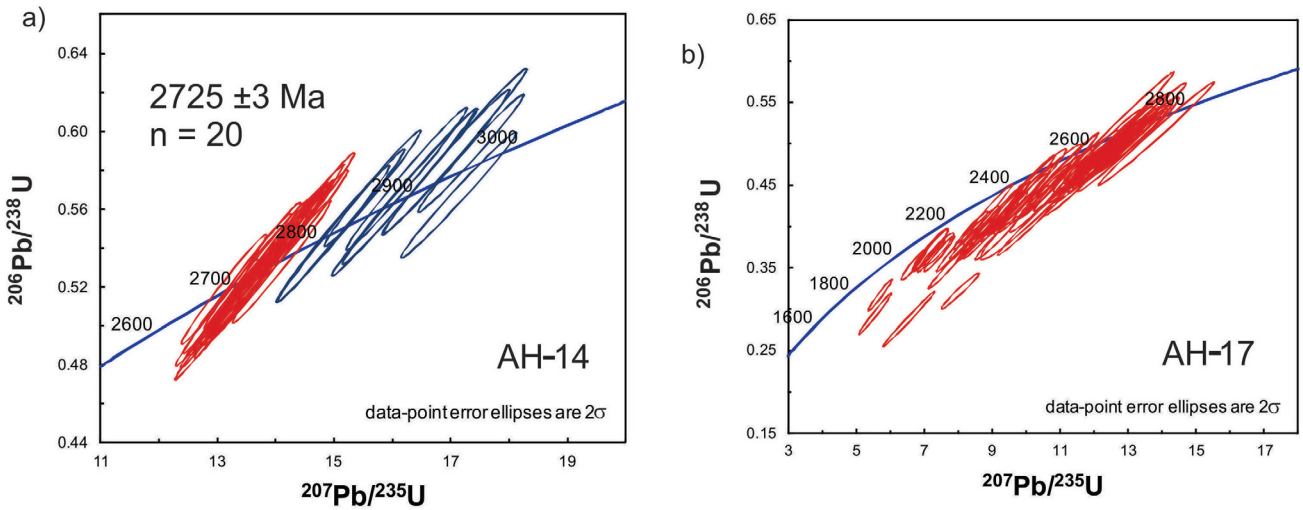

Figure 5: a) Concordia diagram for sample AH-14 tonalite from the core of the southern gneiss dome; the 20 analyses, shown with the red ellipses, were used to calculate the age of 2725 ±3 Ma; **b)** concordia diagram for sample AH-17 granodiorite from the northern margin of the southern gneiss dome. See Figure 3a for photograph of sample location.

sures at which garnet is stable and still present in the residuum. MacKay and Ansdell (2014) indicate that many of the Paleoproterozoic mafic rocks and some ultramafic rocks on Hall Peninsula have a similar within-plate trace-element signature, but that the mantle source may have been previously modified by subduction-related metasomatic processes. The komatiitic samples have elevated levels of Ti relative to normal komatiite, a characteristic that is similar to komatiite rocks on Cumberland Peninsula (Keim, 2012). More detailed comparisons between Paleoproterozoic mafic and ultramafic rocks on Hall and Cumberland peninsulas may help in determining whether they formed from the same mantle plume.

The metamorphic mineral assemblage observed in pelitic units of the metasedimentary sequence consists of biotite, garnet, sillimanite and melt leucosome, which indicates that upper-amphibolite–facies conditions were experienced. Flattened and elongate faserkiesel knots in the pelitic rocks define the dominant broadly east-west–oriented foliation in most of the study area (Figure 2), which is equivalent to the D_2 event reported in Skipton and St-Onge (2014). The outcrop-scale folding in the Discovery camp area (Figure 3c, d) postdates peak metamorphism, and is likely equivalent to the D_3 deformation event described by Steenkamp and St-Onge (2014) and Skipton and St-Onge (2014). The discordant analyses obtained from zircons in the granodioritic gneiss (sample AH-17; Figure 5b) strongly suggest that peak metamorphism occurred during Paleoproterozoic Trans-Hudson Orogen.

This project was initiated and an overview provided by Ansdell et al. (2012), prior to the initiation of the HPIGP; however, the observations, results and interpretations from this study contribute to understanding the geological history being developed by the HPIGP research team.

Economic considerations

Hall Peninsula is host to the Chidliak kimberlite province (Pell et al., 2013), and within the study area there are 11 known kimberlites, 3 of which crop out. The potential for discovery of other diamondiferous kimberlites is high, and relating basement rock types to their geophysical signature is important to potentially improve recognition of the smaller kimberlite targets.

The presence of ultramafic rocks in the study area suggests potential for concentrations of magmatic-related sulphide deposits of nickel, copper and platinum-group elements, similar to those in the Raglan area, Quebec (Lesher, 2007), although none were observed during mapping. The potential fertility of these rocks will need to be assessed, such as depletion of platinum-group elements, which might suggest that they have been extracted by immiscible sulphide melts (Lesher and Stone, 1996).

Acknowledgments

Peregrine Diamonds is thanked for generous in-kind support, including accommodation at the Discovery camp, helicopter support and sample shipping. The Natural Sciences and Engineering Research Council of Canada (NSERC) provided an Engage grant to K. Ansdell to support geochemical and geochronological analyses. B. Clements, A. O'Connor and C. Fitzgerald of Peregrine Diamonds provided support in the field and in Iqaluit. B. Novakovski (University of Saskatchewan) prepared polished thin sections and A. Dufrane (University of Alberta) performed the LA-MC-ICP-MS U-Pb analyses. Reviews by H. Steenkamp and D. Scott significantly improved the manuscript.

References

Ansdell, K., Hunchak, A. and Pell, J. 2012: Precambrian basement rocks in the vicinity of the Chidliak kimberlites: initial mapping on the Hall Peninsula, Baffin Island; GAC-MAC Annual Meeting, St. John's, Newfoundland, May 2012, abstract 320.

Ansdell, K., Hunchak, A. and Pell, J. 2015: Data table accompanying "Geology, geochemistry and geochronology of basement rocks around the Discovery camp, Chidliak diamond project, northern Hall Peninsula, southern Baffin Island, Nunavut"; Canada-Nunavut Geoscience Office, Geoscience Data Series GDS2015-006, Microsoft® Excel® file, URL <http://cngo.ca/summary-of-activities/2014/> [January 2015]

Blackadar, R.G. 1966: Geological reconnaissance, southern Baffin Island, district of Franklin; Geological Survey of Canada, Paper 66-47.

Corrigan, D., Pehrsson, S., Wodicka, N. and de Kemp, E. 2009: The Paleoproterozoic Trans-Hudson Orogen: a prototype of modern accretionary processes; *in* Ancient Orogens and Modern Analogues, J.B. Murphy, J.D. Keppie and A.J. Hynes (ed.), Geological Society, London, Special Publications, v. 327, p. 457–479.

Dostal, J. 2008: Igneous rock associations 10. Komatiites; Geoscience Canada, v. 35, p. 21–31.

From, R.E., St-Onge, M.R. and Camacho, A.L. 2014: Preliminary characterization of the Archean orthogneiss complex of Hall Peninsula, Baffin Island, Nunavut; *in* Summary of Activities 2013, Canada-Nunavut Geoscience Office, p. 53–62.

Heaman, L.M., Grutter, H.S., Pell, J., Holmes, P. and Grenon, H. 2012: U-Pb geochronology, Sr- and Nd-isotope compositions of groundmass perovskite from the Chidliak and Qilaq kimberlites, Baffin Island, Nunavut; 10th International Kimberlite Conference, Bangalore, Extended abstract 101KC-193.

Hoffman, P.F. 1988: United plates of America, the birth of a craton: early Proterozoic assembly and growth of Laurentia; Annual Review of Earth Planetary Science Letters, v. 16, p. 543–603.

Jensen, L.S. 1976: A new cation plot for classifying subalkalic volcanic rocks; Ontario Division of Mines, Miscellaneous Publication 66, 22 p.

Keim, R.D. 2012: Stratigraphy, petrology, and geochemistry of the North Touak-Cape Dyer volcanic belt, Baffin Island; University of Saskatchewan, M.Sc. thesis, 108 p.

LeMaitre, R.W. 1989: A Classification of Igneous Rocks and Glossary of Terms; Blackwell, Oxford, 193 p.

Lesher, C.M. 2007: Ni-Cu-(PGE) deposits in the Raglan area, Cape Smith Belt, New Quebec; *in* Mineral Deposits of Canada: A Synthesis of Major Deposit-Types, District Metallogeny, the Evolution of Geological Provinces, and Exploration Methods, W.D. Goodfellow (ed.), Special Publication 5, Mineral Deposits Division, Geological Association of Canada, p. 351–386.

Lesher, C.M. and Stone, W.E. 1996: Exploration geochemistry of komatiites; *in* D.A. Wyman (ed.), Trace element geochemistry of volcanic rocks: applications for massive sulphide exploration, Short Course Notes, Geological Association of Canada, v. 12, p. 153–204.

Machado, G., Bilodeau, C., Takpanie, R., St-Onge, M., Rayner, N., Young, M., Braden, Z., Creason, G., Skipton, D., From, R. and MacKay, C.B. 2013: Hall Peninsula regional bedrock mapping, Baffin Island, Nunavut: summary of fieldwork; *in* Summary of Activities 2012, Canada-Nunavut Geoscience Office, p. 13–22.

MacKay, C.B. 2012: Petrographic and geochemical study of the origin of "spotted" dykes and their relationship to the North Touak-Cape Dyer volcanic belt, Cumberland Peninsula, Baffin Island; University of Saskatchewan, B.Sc. thesis, 28 p.

MacKay, C.B. and Ansdell, K.M. 2014: Geochemical constraints on mafic and ultramafic rocks from the southern Hall Peninsula, Baffin Island, Nunavut; *in* Summary of Activities 2013, Canada-Nunavut Geoscience Office, p. 85–92.

Nesbitt, R.W., Sun, S.S. and Purvis, A.C. 1979: Komatiites: geochemistry and genesis; Canadian Mineralogist, v. 17, p. 165–186.

Pearce, J.A. 1996: A user's guide to basalt discrimination diagrams; *in* D.A. Wyman (ed.), Trace element geochemistry of volcanic rocks: applications for massive sulphide exploration, Short Course Notes, Geological Association of Canada, v. 12, p. 79–113.

Pell, J., Neilson, S., Dempsey, S., Grenon, H., Grutter, H. and Lockhart, G. 2013: Exploration and discovery of the Chidliak kimberlite province, Baffin Island, Nunavut: Canada's newest diamond district; *in* Proceedings of 10th International Kimberlite Conference, D.G. Pearson, H.S. Grutter, J.W. Harris, B.A. Kjarsgaard, H. O'Brien, N.V. Chalapathi Rao and S. Sparks (ed.), Special Issue of the Journal of the Geological Society of India, v. 2, p. 209–227.

Rayner, N.M. 2014: New U-Pb geochronological results from Hall Peninsula, Baffin Island, Nunavut; *in* Summary of Activities 2013, Canada-Nunavut Geoscience Office, p. 39–52.

Schetselaar, E.M., Harris, J.R., Lynds, T. and de Kemp, E.A. 2007: Remote predictive mapping I. remote predictive mapping (RPM): a strategy for geological mapping of Canada's North; Geoscience Canada, v. 34, no. 3–4, p. 93–111.

Scott, D.J. 1996: Geology of the Hall Peninsula east of Iqaluit, southern Baffin Island; *in* Geological Survey of Canada, Current Research 1996-C, p. 83–91.

Scott, D.J. 1999: U-Pb geochronology of the eastern Hall Peninsula, southern Baffin Island, Canada: a northern link between the Archean of West Greenland and the Paleoproterozoic Torngat Orogen of northern Labrador; Precambrian Research, v. 93, p. 5–26.

Simonetti, A., Heaman, L.M., Hartlaub, R.P., Creaser, R.A., McHattie, T.G. and Bohm, C. 2005: U-Pb zircon dating by laser ablation-MC-ICP-MS using a new multiple ion counting Faraday collector array; Journal of Analytical Atomic Spectroscopy, v. 20, p. 677–686.

Skipton, D. and St-Onge M.R. 2014: Paleoproterozoic deformation and metamorphism in metasedimentary rocks west of Okalik Bay: a field template for the evolution of, eastern Hall Peninsula, Baffin Island, Nunavut; *in* Summary of Activities 2013, Canada-Nunavut Geoscience Office, p. 63–72.

Steenkamp, H.M. and St-Onge, M.R. 2014: Overview of the 2013 regional bedrock mapping program on northern Hall Peninsula, Baffin Island, Nunavut; *in* Summary of Activities 2013, Canada-Nunavut Geoscience Office, p. 27–38.

Sun, S.-s. and McDonough, W.F. 1989: Chemical and isotopic systematics of oceanic basalts: implications for mantle composition and processes; Geological Society, London, Special Publications, v. 42, p. 313–345.

Geochemistry, mineralogy and sedimentology of surficial sediments, Hall Peninsula, southern Baffin Island, Nunavut

T. Tremblay[1], J. Leblanc-Dumas[2] and M. Allard[2]

[1]*Canada-Nunavut Geoscience Office, Iqaluit, Nunavut, tommy.tremblay@nrcan-rncan.gc.ca*

[2]*Centre d'études nordiques, Université Laval, Québec, Quebec*

This work was part of the 2012–2014 Hall Peninsula Integrated Geoscience Program (HPIGP), led by the Canada-Nunavut Geoscience Office (CNGO) in collaboration with the Government of Nunavut, Aboriginal Affairs and Northern Development Canada, and the Geological Survey of Canada. It involved strong contributions from the Universities of Alberta, Dalhousie, Laval, Manitoba, Ottawa, Saskatchewan and New Brunswick, and the Nunavut Arctic College. It has benefitted from support by local and Inuit-owned businesses and the Polar Continental Shelf Program. The focus is on bedrock and surficial geology mapping (1:100 000 scale). In addition, a range of thematic studies is being conducted, including Archean and Paleoproterozoic tectonics, geochronology, landscape uplift and exhumation, microdiamonds, sedimentary-rock xenoliths and permafrost. The goal is to increase the level of geological knowledge and better evaluate the natural-resource potential in this frontier area.

Tremblay, T., Leblanc-Dumas, J. and Allard, M. 2015: Geochemistry, mineralogy and sedimentology of surficial sediments, Hall Peninsula, southern Baffin Island, Nunavut; *in* Summary of Activities 2014, Canada-Nunavut Geoscience Office, p. 57–68.

Abstract

This paper and the accompanying digital database summarizes three years (2011–2013) of geochemistry, mineralogy (heavy minerals) and sedimentology data on surficial sediments from Hall Peninsula, Nunavut (NTS 25I, J, O, P, 26A, B). The maps and data provided in this paper are useful for estimating regional-scale mineral exploration potential on Hall Peninsula. Two hundred and sixty-four samples were analyzed for geochemical and/or heavy mineral content. Heavy mineral analysis on till and glaciofluvial sediments indicate good potential for diamond exploration. The kimberlite-indicator minerals of pyrope, forsterite (olivine) and chrome-diopside were found in significant numbers around the known Chidliak diamondiferous kimberlite field. The geochemical contents of some samples show relatively high polymetallic elemental concentrations, which include gold, silver, copper, zinc, nickel, platinum and palladium. Grains indicative of gemstone potential were found in the heavy mineral fraction of sediment samples, indicating some modest potential for rubies, sapphires and sapphirines. Both grain-size and geochemistry data is included in a sediment database for Hall Peninsula, which provides information useful for infrastructure development in the area.

Résumé

Le présent rapport et la base de données numériques qui l'accompagne résument trois années (2011–2013) de données d'analyses géochimiques, minéralogiques (minéraux lourds) et sédimentologiques des sédiments superficiels de la péninsule Hall, au Nunavut (SNRC 25I, J, O, P, 26A, B). Les cartes et les données présentées dans ce rapport servent à évaluer le potentiel de la péninsule Hall en matière d'exploration minérale à l'échelle régionale. On a procédé à l'analyse de 264 échantillons afin de déterminer soit leur contenu en minéraux lourds, soit leur composition géochimique, ou les deux. L'analyse des minéraux lourds des échantillons de till et de sédiments fluvioglaciaires révèle qu'il s'agit d'une région favorable à l'exploitation diamantifère. Les minéraux indicateurs de kimberlites, notamment le pyrope, la forstérite (olivine) et le diopside chromique, se retrouvent en grand nombre à de nombreux endroits autour du champ de kimberlites diamantifère connu de Chidliak. Le contenu géochimique de certains échantillons révèle la présence de concentrations élémentaires de nature polymétallique élevées, y compris de l'or, de l'argent, du cuivre, du zinc, du nickel, du platine et du palladium. Des grains, pouvant indiquer la présence de gemmes, trouvés dans la fraction des minéraux lourds des échantillons de sédiment témoignent du fait que la région peut receler des rubis, des saphirs et des saphirines en modeste quantité. Une base de données des sédiments échantillonnés dans la péninsule Hall contient toutes les données relatives à la granulométrie et à la géochimie susceptibles de fournir des renseignements utiles à la mise en place d'infrastructures dans cette région.

This publication is also available, free of charge, as colour digital files in Adobe Acrobat® PDF format from the Canada-Nunavut Geoscience Office website: http://cngo.ca/summary-of-activities/2014/.

Introduction

Between 2011 and 2013, a sediment (mostly till) sampling program was completed as part of surficial geology mapping on Hall Peninsula, Baffin Island, Nunavut (Figure 1). The study area covers approximately 38 000 km^2. This paper presents data and maps with geochemistry results for the northern half of the study area (NTS 26A, B). Results from the southern part of Hall Peninsula have been published previously (Tremblay and Leblanc-Dumas, 2014; Tremblay et al., 2014a, b). Both the original data files and the compilation data sheets (a streamlined, georeferenced version of the data) are provided in a Canada-Nunavut Geoscience Office Geoscience Data Series file (Tremblay and Leblanc-Dumas, 2015[3]). Sedimentological results for the entire peninsula have been compiled in this report (Figure 2).

The main physiographic features of Hall Peninsula are a flat plateau at around 600 m asl in the central part of the peninsula, eastern highlands covered with ice caps (up to 1200 m asl) and numerous steep fiords along the coastline. Hall Peninsula was entirely covered by ice during the last glaciation (Dyke et al., 2003), is located north of the treeline, and is underlain by continuous permafrost. The main bedrock geology units are Archean tonalite in the east, and Proterozoic paragneiss and granite in the west (Steenkamp and St-Onge, 2014). Kimberlite pipes and dykes were discovered south of Chidliak Bay, notably by using kimberlite-indicator minerals (KIMs; Clements et al., 2009; Pell, 2013; Tremblay et al., 2014b).

The simplified surficial map, shown in the background of all figures in this paper, is based upon data from four new 1:100 000 scale surficial geology maps currently in production by the authors. The thematic geological units selected for this map include moraine-associated sediment (till deposited in mostly ridged and hummocky moraine landforms), regolith-associated sediment (mostly till mixed with regolith but some areas are primarily regolith) and glaciolacustrine sediment (undivided). During glaciations, the regolith-associated sediment areas were mainly covered by cold-based glaciers, where erosive action was limited as the glacier was frozen at its base and there was limited or no sliding (Dyke, 1993; Leblanc-Dumas et al., 2013, 2015; Tremblay et al., 2013, 2014a). The 'white' areas are mostly composed of till and bedrock outcrops, which occur in areas dominantly influenced by the erosion and deposition of warm-based glaciers, with minor glaciofluvial, colluvial, alluvial and marine sediments. The area around the external borders of the regolith-associated sediment areas is the intermediate cold-based zone (Tremblay et al., 2013, 2014a). This zone shares characteristics of both cold-based and warm-based zones. The selected map units provide the reader with the general distribution of cold-based versus warm-based zones on Hall Peninsula. In plateau regions, zones are more complex due to discrete late, deglacial, warm-based glacier readvances that crosscut previous cold-based areas.

Geochemistry and sedimentology analytical techniques

Sediment descriptions and locations for this study are found in Tremblay and Leblanc-Dumas (2015, under the 'Samples' tab). Two hundred and sixty-four samples were analyzed for geochemical and/or heavy mineral content. Among those, a total of 238 sediment samples (2 kg each; 10 in 2011, 131 in 2012 and 97 in 2013) was analyzed for geochemistry. Within the samples analyzed for geochemistry, there are 203 till samples (or till mixed with regolith), 17 regolith samples, 7 glaciofluvial sediment samples, 10 glaciolacustrine sediment samples and 1 marine sediment samples. These sediments were also analyzed for grain size, Munsell colour and carbon content. A total of 192 heavy mineral samples (~10 kg bags; 87 in 2012 and 105 in 2013) was collected to provide information on the potential for kimberlites, massive sulphides, gold, gemstones and other commodities. Among the samples analyzed for heavy minerals, 162 are till (or till mixed with regolith), 5 are regolith sediments, 24 are glaciofluvial sediments and 1 is glaciolacustrine littoral sediments. The glaciofluvial samples were sieved in the field in order to bag about 10 kg of the <2.2 cm fraction.

Samples were processed at the Geological Survey of Canada (GSC) Sedimentology Laboratory (Ottawa, Ontario). A portion of the matrix (<2 mm) of each sample was wet-sieved to 63 µm for geochemical analysis. Another <2 mm portion was sent for grain-size analysis and inorganic carbon content analysis. Lastly, a portion was saved for archival purposes. The till sample grain size (sand, silt and clay; Figure 2 and 'Grain size' tab in Tremblay and Leblanc-Dumas, 2015) was determined by use of a laser particle size analyzer (Lecotrac LT100) in conjunction with sieving or digital image analysis instrumentation (Camsizer®) on the <63 µm fraction (see Girard et al., 2004, for details on laboratory protocols). The grain size of fractions between 63 µm and 2 mm was determined by wet sieving.

Inorganic carbon and loss-on-ignition (LOI) was measured with the LECO® CR412 carbon moisture analyzer ('CarbLOI' tab in Tremblay and Leblanc-Dumas, 2015). Munsell colour determination was done using an X-Rite SP64 portable sphere spectrophotometer.

A split of each 2 kg sample was dried and sieved to <0.063 mm fraction (till matrix) at the Acme Analytical

[3] *CNGO Geoscience Data Series GDS2015-003, containing the data or other information sources used to compile this paper, is available online to download free of charge at http://cngo.ca/summary-of-activities/2014/.*

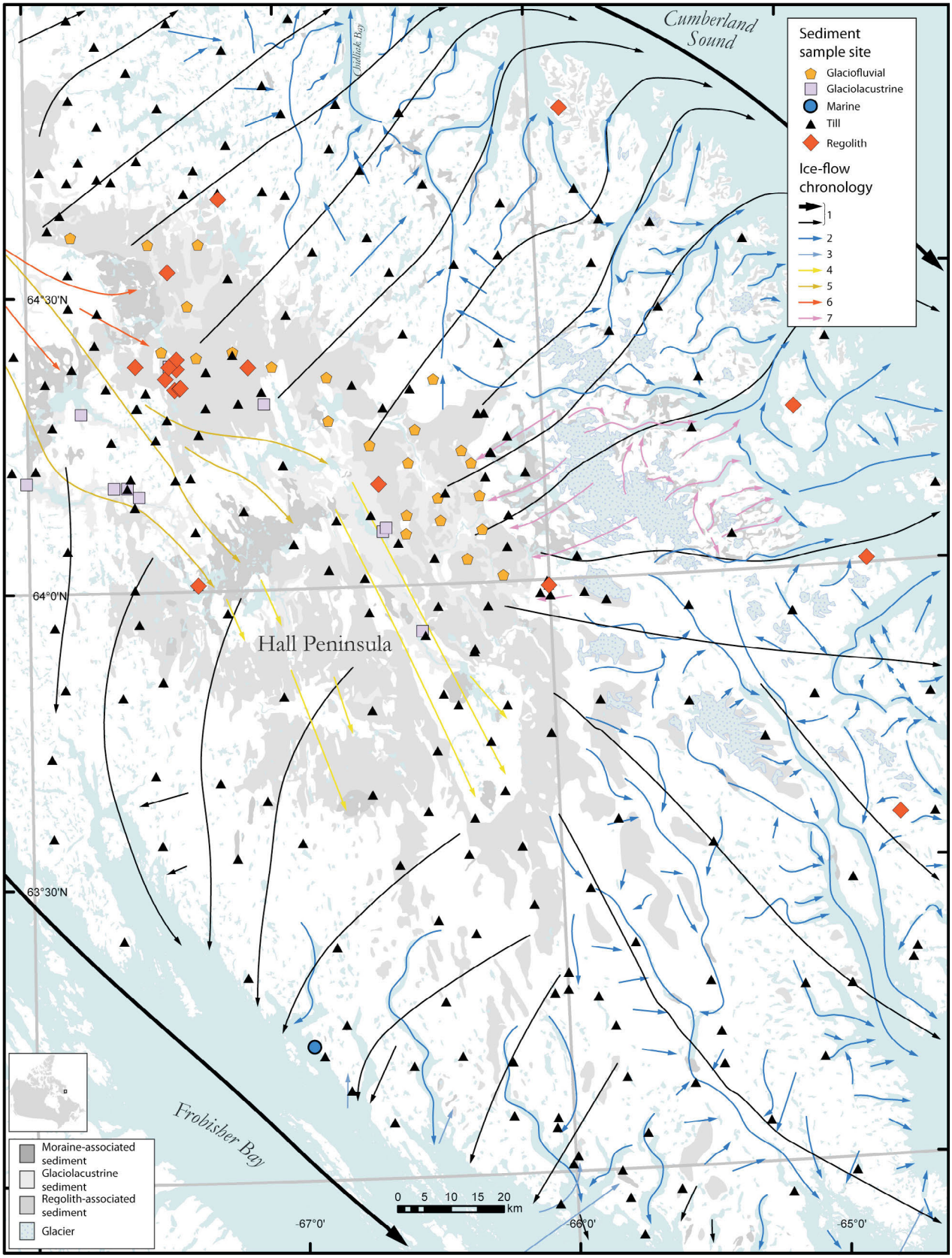

Figure 1: Sediment sample locations, simplified Quaternary map and ice-flow chronology (see text for thematic description of these two later items) for Hall Peninsula, Nunavut. The thick black arrow of phase 1 ice flow indicates ice streams in Frobisher Bay and Cumberland Sound.

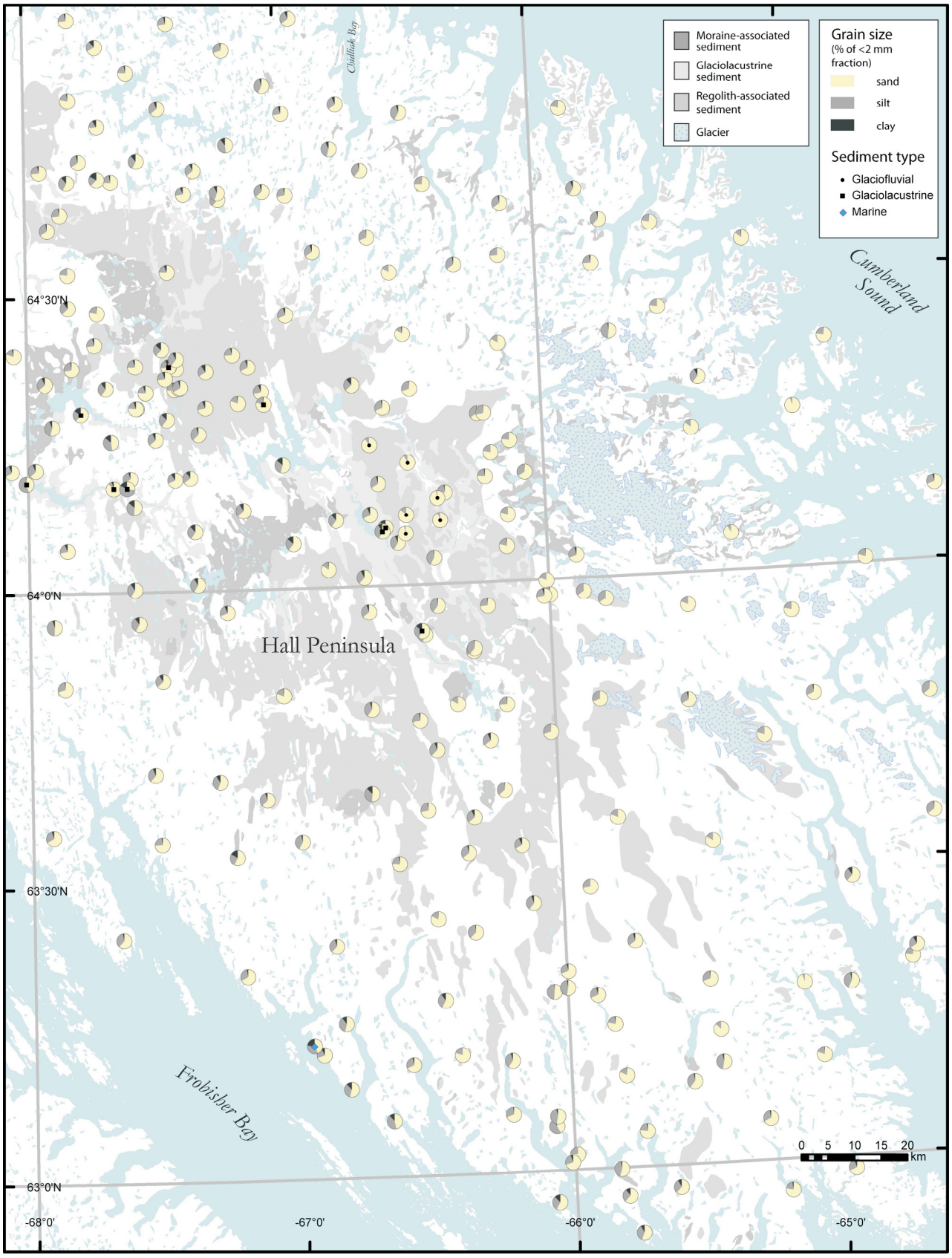

Figure 2: Grain size of till, regolith, glaciolacustrine, glaciofluvial and marine sediments across Hall Peninsula, Nunavut. The clay content is <4 µm.

Laboratories Ltd. (Vancouver, British Columbia) for analysis (see McClenaghan et al., 2013, for laboratory protocols). A 30 g split was digested by aqua regia and analyzed by inductively coupled plasma–mass spectrometry (ICP-MS) for 65 elements, including gold, base metals, platinum and rare-earth elements. Another 2 g split was digested with lithium metaborate/lithium tetraborate fusion and then analyzed by inductively coupled plasma–emission spectrometry (ICP-ES) for 11 major elements and 7 trace elements. Analytical accuracy and precision was monitored by including GSC blind CANMET standards (TILL-2 and TILL-4) in the analytical analysis. Laboratory duplicates of samples, Acme Analytical Laboratories Ltd. blanks, reference standards and analytical duplicates were also analyzed.

Samples were sent to Overburden Drilling Management Limited (Nepean, Ontario) for heavy mineral analysis (see Plouffe et al., 2013, for laboratory protocols). The standard pre-analysis treatment was applied to all samples, which first included sieving of pebbles (>2 mm; the 4–8 mm fraction were separated for lithological counting) and preconcentration of heavy minerals by shaking table. Field sample duplicates and GSC blanks from granite grus and till were inserted for quality control and quality assurance (Plouffe et al., 2013). The gold grains from a panning concentrate were counted, described and replaced in the same fraction. The heavy mineral preconcentrate was then submitted for heavy liquid separation (methylene iodide, specific gravity=3.2) and ferromagnetic separation. The >0.25 mm fraction of nonferromagnetic heavy mineral concentrate (NFHMC) was examined by binocular microscope for the identification of various distinctive mineral species, namely, kimberlite-indicator minerals (KIMs) and metamorphic massive-sulphide–indicator minerals (MMSIMs), which notably include gahnite, red rutile, pyrite, chalcopyrite and arsenopyrite (Averill, 2001). The mineralogical picking was performed on three different size fractions (0.25–0.5 mm, 0.5–1 mm, 1–2 mm) of NFHMC. Following further preparation, binocular identifications of MMSIMs and KIMs were undertaken and supported in some cases by scanning electron microscope (SEM) analysis.

Ice flow and glacial transport

Regional ice-flow studies on Hall Peninsula have been conducted by Tremblay et al. (2013, 2014a) and Johnson et al. (2013). The ice-flow history of the map area was influenced by the occurrence of diverging ice flow on the Hall Peninsula plateau during the last glacial maximum (phase 1), which was coalescent with the large ice streams of Frobisher Bay and Cumberland Sound (Miller, 1980). During deglaciation, ice flow was focused in the U-shaped glacial valleys and fiords (phase 2) located at the southern and eastern margins of the Hall Peninsula plateau (Johnson et al., 2013). A late ice-flow reversal is observed on the north coast of Frobisher Bay (phase 3; Stravers et al., 1992). Three distinct phases of glacial readvance are marked by the presence of moraines on the southern Hall Peninsula plateau (phase 4), toward Hall moraine (phase 5; Miller, 1980) and toward Frobisher Bay moraine (phase 6; Blake, 1966). The extent of phase 4's southerly deglacial ice flow may be slightly larger than indicated (Johnson et al., 2013), but ice-flow indicators for this event are weak and uncertain in regions marginal to cold-based zones. A last phase of westward ice flow is observed around the main present-day ice cap (phase 7; Miller, 1980), and marked by numerous hummocky moraines.

Because of the importance of glacial transport, the ice-flow chronology map (Figure 1) is useful for mineral exploration in the areas covered with till (warm-based zone) or till mixed with regolith (intermediate cold-based zone). Samples of till with/without regolith from the regolith-associated sediment areas display less glacial transport than till samples from warm-based glacier zones. In the case of the regolith samples, where the glacier was mostly cold-based, glacial transport evidence is weak and limited to a few erratic boulders. Other active geomorphological agents, such as colluvial, glaciofluvial and glaciolacustrine processes, are more likely to affect the transport of mineral-exploration indicators in the cold-based zone, and to a lesser extent in the intermediate cold-based zone. Glaciofluvial sediments were sampled in the cold-based zone for the specific purpose of estimating the mineral potential for kimberlite, as KIMs and most MMSIMs tend to be well preserved during small to moderate amounts of meltwater transport (McClenaghan et al., 1998). Most glaciofluvial sediment samples are from poorly sorted deposits, with angular to subangular clasts, and are linked with short glaciofluvial channels, indicating limited glaciofluvial transport (see 'Samples' tab in Tremblay and Leblanc-Dumas, 2015).

Economic considerations

Geochemical and heavy mineral contents of surficial sediment samples from Hall Peninsula are presented in Figures 3 to 9 and the raw data can be found under the 'Geochem' and 'Heavy mineral' tabs in Tremblay and Leblanc-Dumas (2015). These maps and data constitute a useful basis for estimating the regional-scale mineral exploration potential of Hall Peninsula.

Geochemistry results indicate that Ag and Au from the fine portion of till and regolith (Figure 3) show maximum values of 498 and 41 ppb, respectively. The Ag and Au anomalies are generally located in the western part of study area and are associated with Paleoproterozoic rocks rather than Archean tonalite rocks found to the east (see geological map in Steenkamp and St-Onge, 2014). As seen on Figure 4, Zn and Cu show maximum values of 178 and

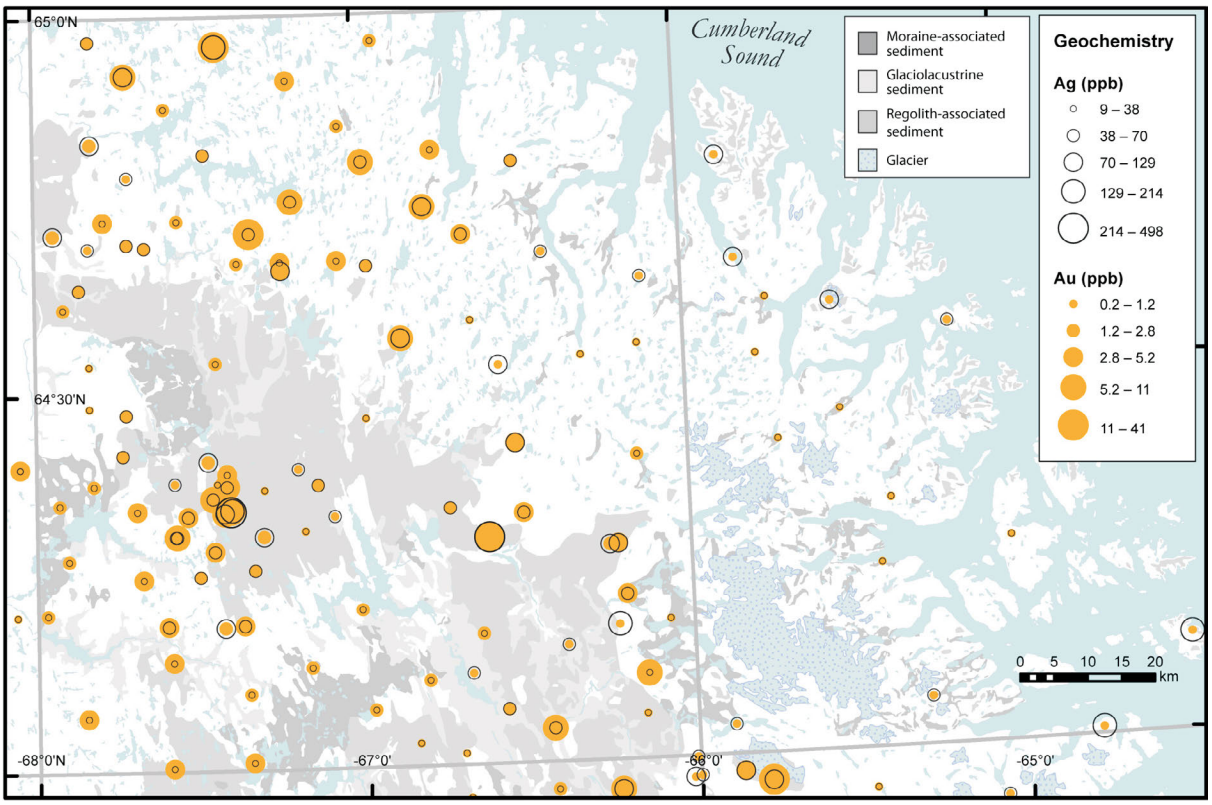

Figure 3: Distribution of Au and Ag, from till, till mixed with regolith and regolith samples, Hall Peninsula, Nunavut. Geochemical analysis by inductively coupled plasma–mass spectrometry with aqua regia dissolution on <63 µm fraction.

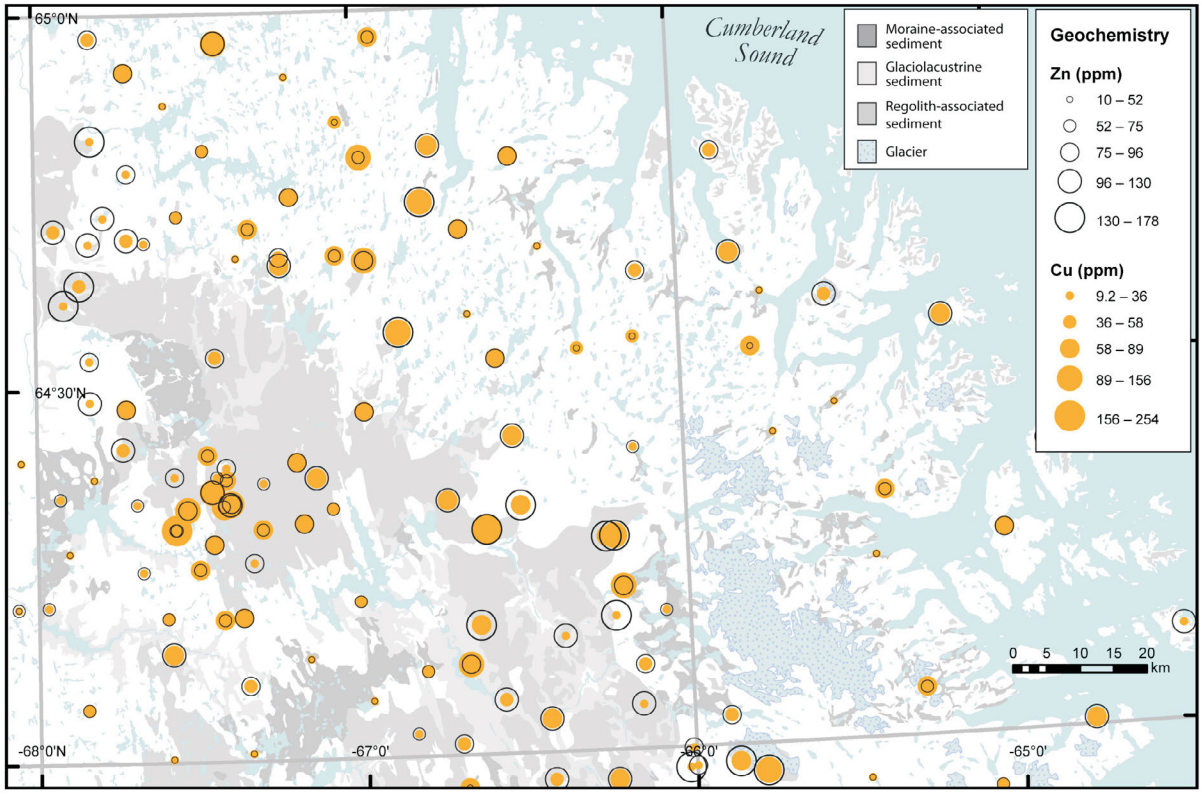

Figure 4: Distribution of Zn and Cu, from till, till mixed with regolith and regolith samples, Hall Peninsula, Nunavut. Geochemical analysis by inductively coupled plasma–mass spectrometry with aqua regia dissolution on <63 µm fraction.

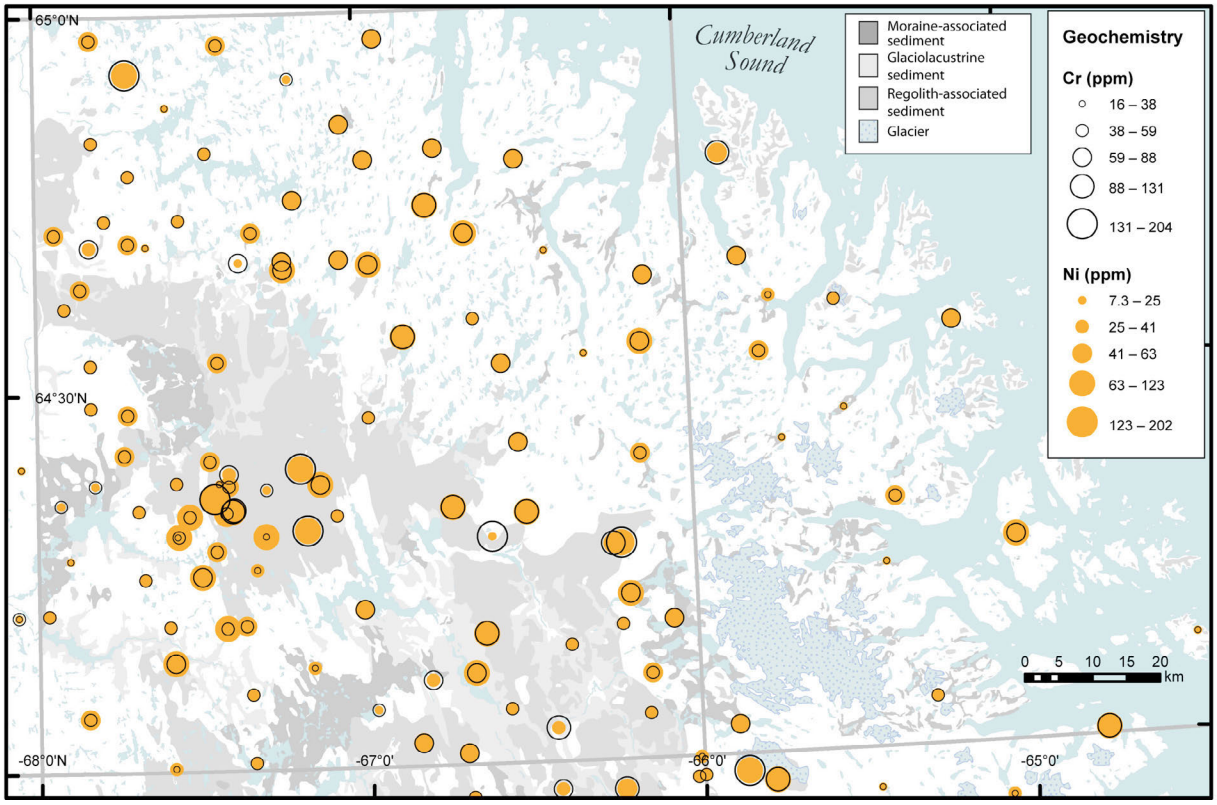

Figure 5: Distribution of Cr and Ni, from till, till mixed with regolith and regolith samples, Hall Peninsula, Nunavut. Geochemical analysis by inductively coupled plasma–mass spectrometry with aqua regia dissolution on <63 µm fraction.

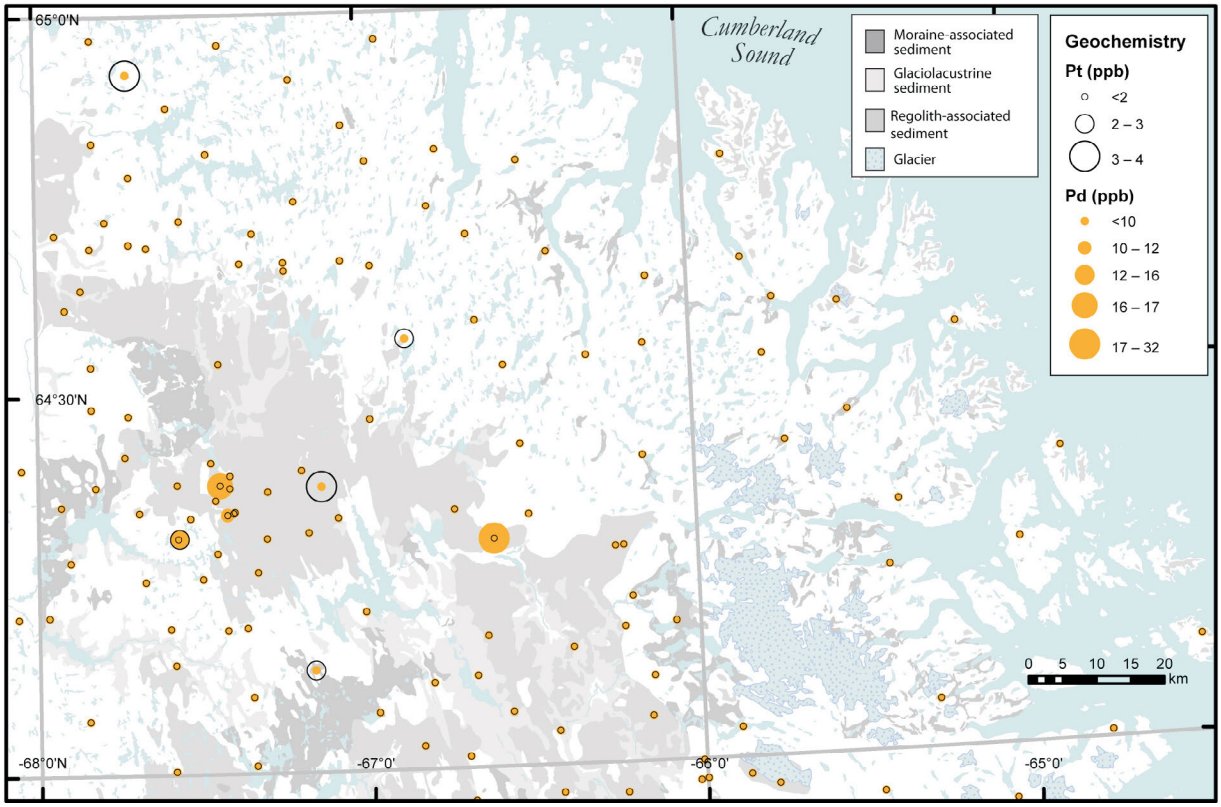

Figure 6: Distribution of Pt and Pd, from till, till mixed with regolith and regolith samples, Hall Peninsula, Nunavut. Geochemical analysis by inductively coupled plasma–mass spectrometry with aqua regia dissolution on <63 µm fraction.

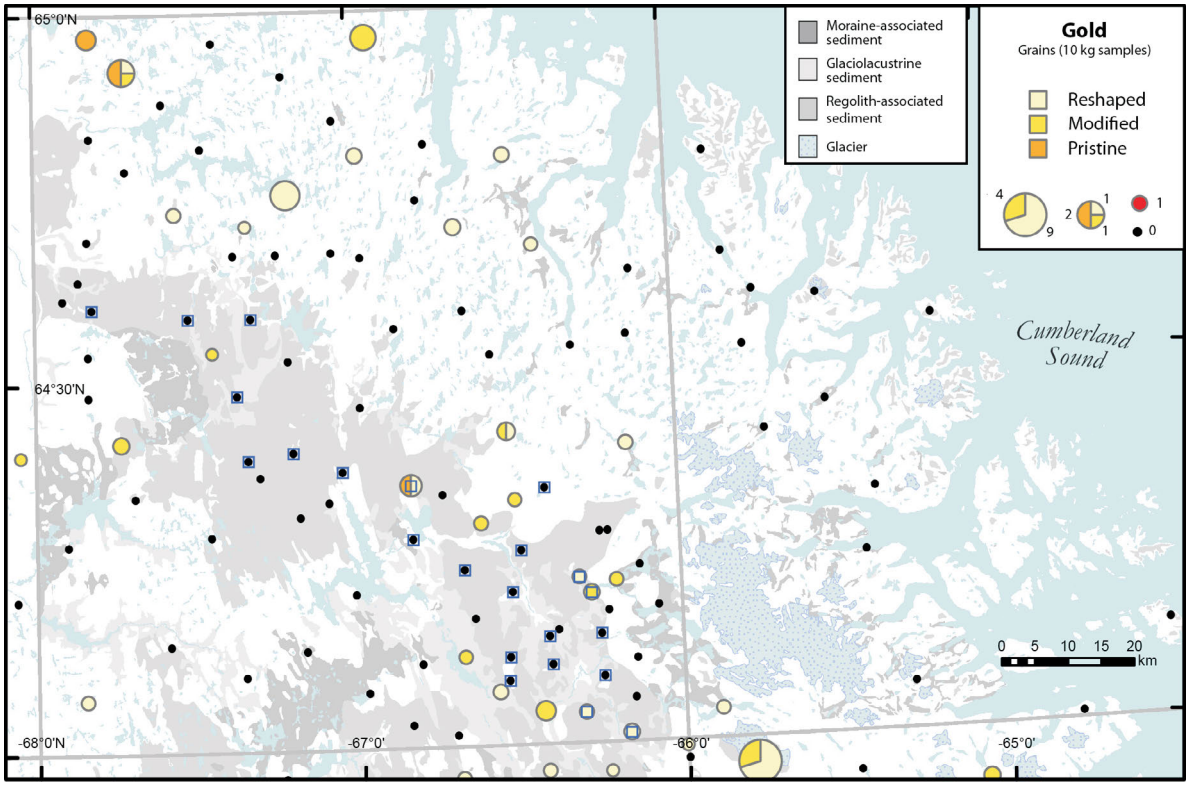

Figure 7: Distribution of gold grains, from the heavy mineral fraction (normalized to 10 kg table feed) of till, till mixed with regolith, regolith and glaciofluvial sediment samples, Hall Peninsula, Nunavut. Glaciofluvial sediment samples are indicated by blue squares.

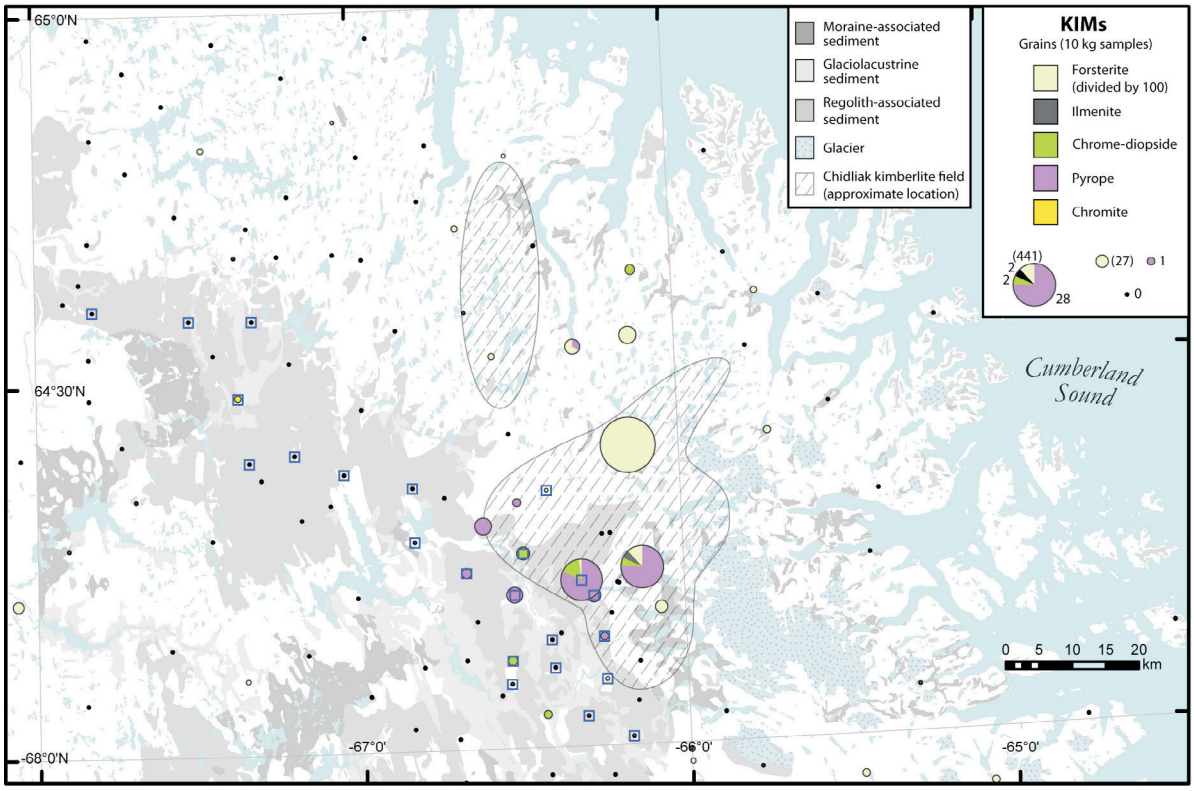

Figure 8: Distribution of kimberlite-indicator minerals (KIMs), from the heavy mineral fraction (normalized to 10 kg table feed) of till, till mixed with regolith, regolith and glaciofluvial sediment samples, Hall Peninsula, Nunavut. Glaciofluvial sediment samples are indicated by blue squares.

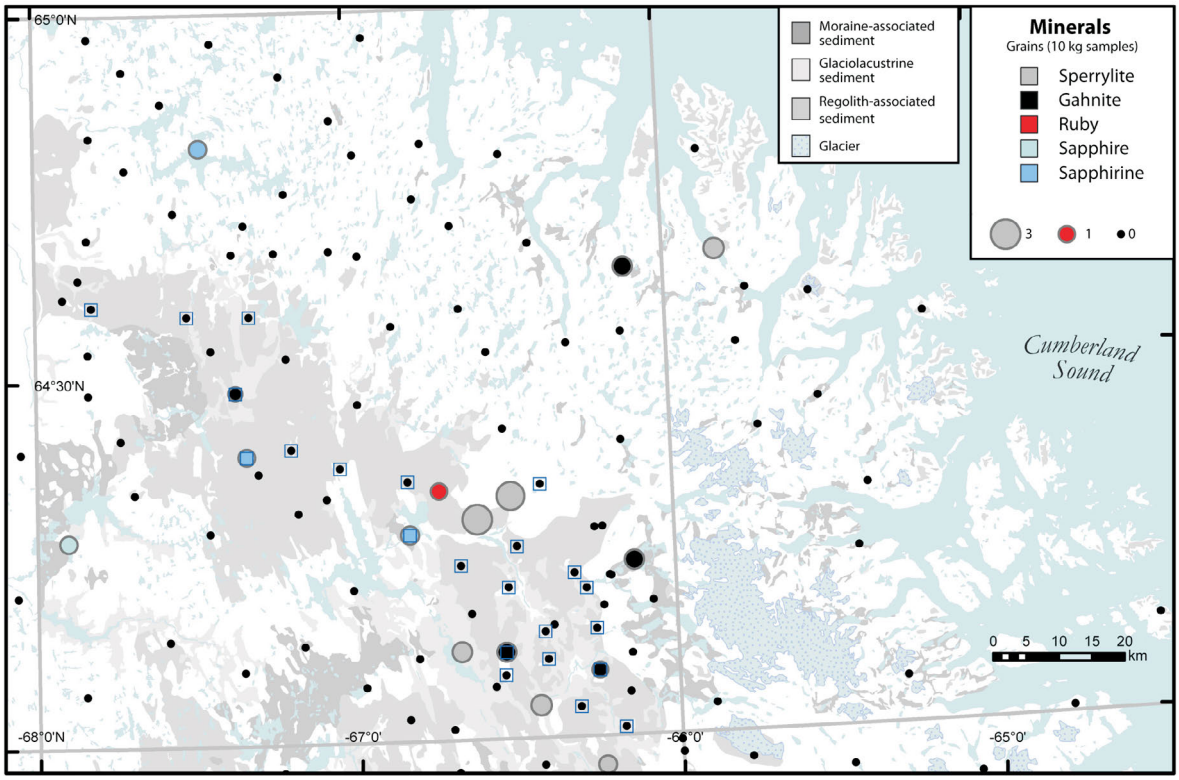

Figure 9: Distribution of various minerals grains, from the heavy mineral fraction (normalized to 10 kg table feed) of till, till mixed with regolith, regolith and glaciofluvial sediment samples, Hall Peninsula, Nunavut. Glaciofluvial sediment samples are indicated by blue squares

254 ppm, respectively, and are also located in the western part of the study area. Maximum values of Cr and Ni are 204 and 202 ppm (Figure 5), and their distributions are similar to Au, Ag, Zn and Cu as they concentrate in a few zones located in the western part of study area. These zones could be investigated for polymetallic deposits, possibly associated with layered mafic-ultramafic intrusive rocks (Steenkamp et al., 2014; St-Onge et al., 2015). On Figure 6, Pt and Pd display anomalous values reaching 4 and 32 ppb, respectively. The Pt and Pd could also be associated with layered mafic-ultramafic intrusions.

Figure 7 shows that 32 samples contain gold grains, with four of those samples containing four or more grains. The maximum number of gold grains per sample is 13 grains, with nine reshaped and four modified grains, indicating some glacial transport or being derived from older sediments. The average number of gold grains per sample is generally quite low, between zero and two grains. Glaciofluvial sediments display a lower background concentration of gold grains in the heavy mineral fraction (close to zero grains per sample), relative to the till samples.

Kimberlite-indicator minerals are found in relatively high concentrations in the south-central portion of study area. On Figure 8, the results are normalized to 10 kg samples, based on table feed. Ilmenite, pyrope and chrome-diopside grains are grouped around the Chidliak diamondiferous kimberlite field. The maximum number of forsterite (olivine) grains is estimated at 6000 grains (sample 13TIA-T009), 99.5% of them in the 0.25 to 0.5 mm size fraction, and 0.5% in the 0.5 to 2 mm size fraction. At nineteen stations, over one forsterite grains were observed (Figure 8). Forsterite may be derived from a local source other than kimberlite, as many older ultramafic bodies are documented in the area. Olivine might also indicate the location of layered mafic-ultramafic intrusive rocks (Steenkamp et al., 2014; St-Onge et al., 2015).

The maximum amount of pyrope garnets observed is 28 grains, of which 80% are in the 0.25 and 0.5 mm size fraction and 20% are in the 0.5 and 2 mm size fraction. At nine stations, more than one pyrope grain was observed, and at two stations over 20 pyrope grains were observed (Figure 8). Pyrope garnets were found in glaciofluvial sediments west of the Chidliak diamondiferous kimberlite field, possibly extending the area where kimberlite potential is previously known. Only a few chrome-diopsides were found, with five at one station and six stations with one or more grains (Figure 8). One sample contained one ilmenite grain and one sample contained one chromite grain (Figure 8). According to ice-flow data and known KIM data (Clements et al., 2009), most KIMs from the vicinity of the Chidliak diamondiferous kimberlite field area were probably transported toward the north or the northeast. In

areas of regolith and till mixed with regolith, the transport of KIMs was done by weak, elusive glacial processes, likely to be oriented in various different directions, including to the south (Johnson et al., 2013). However, as mentioned in the previous section, in the cold-based zone, colluvial, glaciofluvial and glaciolacustrine processes most likely account for an important part of the displacement of KIMs from their original kimberlite emplacement.

Grains indicative of gemstone potential, including ruby and sapphire, were found in two different heavy mineral samples, with one grain per sample. In addition, there were three samples with one sapphirine each (Figure 9). They indicate a modest potential for gemstone exploration on Hall Peninsula. Gahnite (up to one grain for five samples) and sperrylite (up to three grains for six samples) are found in the map area (Figure 9). The occurrence of sperrylite indicates some potential for platinum-group elements (PGE; McClenaghan and Cabri, 2011); however, it does not match exactly the location of Pt and Pd geochemical anomalies. The PGEs could potentially be associated with layered mafic-ultramafic intrusive rocks. The presence of gahnite might indicate the presence of metamorphosed massive sulphides (Averill, 2001), which could occur in the Paleoproterozoic supracrustal sequence. High concentrations of gahnite, sperrylite and gold grains in some surficial sediment samples on Hall Peninsula were reported by Peregrine Diamonds Ltd. (2010).

The sedimentology and geochemistry database provides a useful source of information for infrastructure development and environmental baseline studies on Hall Peninsula. Grain-size information on the surficial sediments will provide important information for assessing potential ground instability linked with permafrost. For example, fine-grained sediments are prone to having higher ice contents, the melting of which could potentially lead to ground disturbance once roads or buildings are installed. Grain-size analyses indicate that regolith, some tills and glaciolacustrine sediments tend to have higher clay content than the other types of sediments (Figure 2). Oppositely, glaciofluvial sediments and some tills have higher sand concentration compared with other tills or regolith. In addition, the 238 geochemistry samples provide a good regional background level for 66 elements applicable to environmental studies.

Acknowledgments

Universal Helicopters pilots provided safe field transport in 2011, 2012 and 2013. Preparation and interpretation of surficial mapping, glacial history and geomorphology was enhanced by discussions with D. Mate (formerly with Canada-Nunavut Geoscience Office now with Canadian Northern Economic Development Agency), P. Budkewitsch (Aboriginal Affairs and Northern Development Canada), H. Steenkamp (Canada-Nunavut Geoscience Office), M. Lamothe (Université du Québec à Montréal), D. Willis (Peregrine Diamonds Ltd.), B. Clements (Peregrine Diamonds Ltd.) and N. Januszczak (De Beers Canada). Surficial mapping was prepared using three-dimensional technology with the assistance of C. Gilbert (Canada-Nunavut Geoscience Office) and M. Boutin (Institut national de la recherche scientifique). The Canadian Northern Economic Development Agency's (CanNor) Strategic Investments in Northern Economic Development (SINED) program provided financial support for this work. R. Paulen (Geological Survey of Canada, Ottawa) has thoughtfully reviewed this paper.

Natural Resources Canada, Earth Sciences Sector contribution 20140286

References

Averill, S.A. 2001: The application of heavy indicator mineralogy in mineral exploration with emphasis on base metal indicators in glaciated metamorphic and plutonic terrains; Geological Society of London, Special Publication 185, p. 69–81.

Blake, W., Jr. 1966: End moraines and deglaciation chronology in northern Canada with special reference to southern Baffin Island; Geological Survey of Canada, Paper 66-26, 31 p.

Clements, B., Pell, J., Holmes, P. and Grenon, H. 2009: Following kimberlite indicator minerals to Chidliak, Baffin Island: Canada's newest diamond district; *in* Workshop B: Indicator Mineral Methods in Mineral Exploration, 24th International Applied Geochemistry Symposium, Fredericton, New Brunswick, May 31, 2009, p. 83–88.

Dyke, A.S. 1993: Landscapes of cold-centred Late Wisconsinan ice caps, Arctic Canada; Progress in Physical Geography, v. 17, no. 2, p. 223–247.

Dyke, A.S., Moore, A. and Robertson, L. 2003: Deglaciation of North America; Geological Survey of Canada, Open File 1574, 2 sheets, 1 CD-ROM.

Girard, I., Klassen, R.A. and Laframboise, R.R. 2004: Sedimentology laboratory manual, Terrain Sciences Division; Geological Survey of Canada, Open File 4823, 134 p.

Johnson, C., Ross, M. and Tremblay, T. 2013: Glacial geomorphology of north-central Hall Peninsula, southern Baffin Island; Geological Survey of Canada, Open File 7413, 57 p.

Leblanc-Dumas, J., Allard, M. and Tremblay, T. 2013: Quaternary geology and permafrost characteristics in central Hall Peninsula, Baffin Island, Nunavut; *in* Summary of Activities 2012, Canada-Nunavut Geoscience Office, p. 101–106.

Leblanc-Dumas, J., Allard, M. and Tremblay, T. 2015: Characteristics of a preglacial or interglacial regolith preserved under nonerosive ice during the last glacial maximum in central Hall Peninsula, southern Baffin Island, Nunavut; *in* Summary of Activities 2014, Canada-Nunavut Geoscience Office, p. 69–78.

McClenaghan, M.B. and Cabri, L.J. 2011: Review of gold and platinum group element (PGE) indicator minerals for surficial sediment sampling; Geochemistry: Exploration, Environment, Analysis, v. 11, p. 251–263, doi:10.1144/1467-7873/10-IM-026

McClenaghan, M.B., Kjarsgaard, I.M., Schulze, D.J., Berger, B., Stirling, J.A.R. and Pringle, G. 1998: Mineralogy and geochemistry of the Diamond Lake kimberlite and associated esker sediments, Kirkland Lake, Ontario; Geological Survey of Canada, Open File 3576, 200 p.

McClenaghan, M.B., Plouffe, A., McMartin, I., Campbell, J.E., Spirito, W.A., Paulen, R.C., Garrett, R.G. and Hall, G.E.M. 2013: Till sampling and geochemical analytical protocols for Geological Survey of Canada projects; Geochemistry: Exploration, Environment, Analysis, v. 13, p. 285–301, doi:10.1144/geochem.2011-083

Miller, G.H. 1980: Late Foxe glaciation of southern Baffin Island, N.W.T., Canada; Geological Society of America Bulletin, v. 91, no. 7, p. 399–405.

Pell, J., Clements, B., Grütter, H., Neilson, S. and Grenon, H. 2013: Following kimberlite indicator minerals to source in the Chidliak kimberlite province, Nunavut; *in* New Frontiers for Exploration in Glaciated Terrain, R.C. Paulen and M.B. McClenaghan (ed.), Geological Survey of Canada, Open File 7374, p. 47–52.

Peregrine Diamonds Ltd. 2010: Peregrine discovers kimberlite indicator and precious metal anomalies at Qilaq; Peregrine Diamonds Ltd., press release, February 4, 2010, URL <http://www.pdiam.com/i/pdf/2010-02-04_NR.pdf> [October 2014].

Plouffe, A., McClenaghan, M.B., Paulen, R.C., McMartin, I., Campbell, J.E. and Spirito, W.A. 2013: Processing of unconsolidated glacial sediments for the recovery of indicator minerals: protocols used at the Geological Survey of Canada; Geochemistry: Exploration, Environment, Analysis, v. 13, p. 303–316.

Steenkamp, H.M. and St-Onge, M.R. 2014: Overview of the 2013 regional bedrock mapping program on northern Hall Peninsula, Baffin Island, Nunavut; *in* Summary of Activities 2013, Canada-Nunavut Geoscience Office, p. 27–38.

Steenkamp, H.M., Bros, E.R. and St-Onge, M.R. 2014: Altered ultramafic and layered mafic-ultramafic intrusions: new economic and carving stone potential on northern Hall Peninsula, Baffin Island, Nunavut; *in* Summary of Activities 2013, Canada-Nunavut Geoscience Office, p. 11–19.

St-Onge, M.R., Rayner, N.M., Liikane, D. and Chadwick, T. 2015: Mafic, ultramafic and layered mafic-ultramafic sills, Meta Incognita Peninsula, southern Baffin Island, Nunavut; *in* Summary of Activities 2014, Canada-Nunavut Geoscience Office, p. 11–16.

Stravers, J.A., Miller, G.H. and Kaufman, D.S. 1992: Late glacial ice margins and deglacial chronology for southeastern Baffin Island and Hudson Strait, eastern Canadian Arctic; Canadian Journal of Earth Sciences, v. 29, p. 1000–1017.

Tremblay, T. and Leblanc-Dumas, J. 2014: Geochemical and mineralogical data for southern Hall Peninsula, Nunavut; Canada-Nunavut Geoscience Office, Geoscience Data Series GDS2014-003, Microsoft® Excel® files.

Tremblay, T. and Leblanc-Dumas, J. 2015: Geochemical, mineralogical and sedimentological data for Hall Peninsula, Nunavut; Canada-Nunavut Geoscience Office, Geoscience Data Series GDS2015-003, Microsoft® Excel® files.

Tremblay, T., Leblanc-Dumas, J., Allard, M., Gosse, J.C., Creason, C.G., Peyton, P., Budkewitsch, P. and LeBlanc, A.-M. 2013: Surficial geology of southern Hall Peninsula, Baffin Island, Nunavut: summary of the 2012 field season; *in* Summary of Activities 2012, Canada-Nunavut Geoscience Office, p. 93–100.

Tremblay, T., Leblanc-Dumas, J., Allard, M., Ross, M. and Johnson, C. 2014a: Surficial geology of central Hall Peninsula, Baffin Island, Nunavut: summary of the 2013 field season; *in* Summary of Activities 2013, Canada-Nunavut Geoscience Office, p. 109–120.

Tremblay, T., Leblanc-Dumas, J., Ross, M., Allard, M., McClenaghan, B., Johnson, C. and Mate, D. 2014b: Surficial geology and geomorphology of central Hall Peninsula, Baffin Island, Nunavut: summary of the 2013 field season; Nunavut Mining Symposium 2014, Iqaluit, Nunavut, presentation.

Characteristics of a preglacial or interglacial regolith preserved under nonerosive ice during the last glacial maximum in central Hall Peninsula, southern Baffin Island, Nunavut

J. Leblanc-Dumas[1], M. Allard[2] and T. Tremblay[3]

[1]*Centre d'études nordiques, Université Laval, Québec, Quebec, julie.leblanc-dumas.1@ulaval.ca*

[2]*Centre d'études nordiques, Université Laval, Québec, Quebec*

[3]*Canada-Nunavut Geoscience Office, Iqaluit, Nunavut*

This work was part of the 2012–2014 Hall Peninsula Integrated Geoscience Program (HPIGP), led by the Canada-Nunavut Geoscience Office (CNGO) in collaboration with the Government of Nunavut, Aboriginal Affairs and Northern Development Canada, and the Geological Survey of Canada. It involved strong contributions from the Universities of Alberta, Dalhousie, Laval, Manitoba, Ottawa, Saskatchewan and New Brunswick, and the Nunavut Arctic College. It has benefitted from support by local and Inuit-owned businesses and the Polar Continental Shelf Program. The focus is on bedrock and surficial geology mapping (1:100 000 scale). In addition, a range of thematic studies is being conducted, including Archean and Paleoproterozoic tectonics, geochronology, landscape uplift and exhumation, microdiamonds, sedimentary-rock xenoliths and permafrost. The goal is to increase the level of geological knowledge and better evaluate the natural-resource potential in this frontier area.

Leblanc-Dumas, J., Allard, M. and Tremblay, T. 2015: Characteristics of a preglacial or interglacial regolith preserved under nonerosive ice during the last glacial maximum in central Hall Peninsula, southern Baffin Island, Nunavut; *in* Summary of Activities 2014, Canada-Nunavut Geoscience Office, p. 69–78.

Abstract

This paper presents the results of laboratory analyses performed on a regolith that is presumed to be of Neogene or interglacial origin. The presence of a regolith area, as well as felsenmeers and weakly eroded bedrock outcrops, suggest that a cold-based glacier covered the central Hall Peninsula, protecting it from glacial erosion during the last glacial maximum. Field observations and laboratory analyses, such as geochemical extractions (iron, aluminum, silicon), silt-clay mineralogy and electronic scanning microscope imaging, on surficial deposit samples and on the regolith indicate that the regolith is a regional residue that could have effectively been protected from erosion. The regolith would be preglacial or interglacial in situ material originating from the weathering of the bedrock in a warm climate. The presence of illite as well as crystalline kaolinite, shown by X-ray analyses on the silt-clay fraction of regolith samples, supports this hypothesis. This glacial geology study supports the search for economic minerals in the region. The characterization of the permafrost in the area will be useful for land management related to future infrastructure development by mining companies.

Résumé

Le présent article fait état des résultats d'analyses en laboratoire effectuées sur du régolite que l'on présume d'origine néogène ou interglaciaire. La présence d'une région formée de régolite, et comportant également des champs de pierres et des affleurements rocheux peu érodés, semble indiquer qu'un glacier à base froide aurait recouvert la partie centrale de la péninsule Hall, la protégeant ainsi des effets de l'érosion glaciaire au cours du dernier maximum glaciaire. Les observations de terrain et les analyses en laboratoire, notamment les extractions géochimiques (fer, aluminium, silicium), la minéralogie des fractions limoneuse et argileuse, et l'imagerie réalisée à l'aide d'un microscope à balayage électronique, portant aussi bien sur des échantillons de dépôts de surface que sur le régolite, démontrent qu'il s'agit, dans le cas de ce dernier, d'un vestige régional qui aurait pu effectivement être protégé des effets de l'érosion. Il s'agirait donc de matériel en place d'origine préglaciaire ou interglaciaire provenant de l'altération météorique du substratum rocheux dans des conditions de climat chaud. La présence d'illite et de kaolinite cristalline, que révèlent les analyses aux rayons X des fractions limoneuse et argileuse des échantillons de régolite, est un autre point venant à l'appui de cette hypothèse. Cette étude de la géologie glaciaire de la région contribue aux travaux de recherche de minéraux économiques dans la péninsule Hall. La

This publication is also available, free of charge, as colour digital files in Adobe Acrobat® PDF format from the Canada-Nunavut Geoscience Office website: http://cngo.ca/summary-of-activities/2014/.

caractérisation du pergélisol dans cette région s'avérera également utile aux activités de gestion des terres liées à la mise en place éventuelle d'infrastructures par les sociétés minières.

Introduction

During the summer of 2011, exploratory fieldwork was conducted by the Canada-Nunavut Geoscience Office (CNGO) in an area 85 km northeast of Iqaluit (Figure 1). The work verified a wide, red and highly weathered regolith area, which could be related to a weakly eroding, possibly cold-based glacier or no ice cover on that part of the peninsula during the last glacial maximum. In July 2012 and 2013, a detailed study of a 60 by 35 km area within this relatively highly weathered plateau was completed by a Université Laval team in collaboration with the CNGO. The aim of the work was to better understand the glaciodynamic history of the region, determine the main ice-flow directions and identify the regional limits between cold- and warm-based regimes of the ice sheet to verify the hypothesis. The main field observations and detailed mapping of the surficial geology of the region have been presented in previous papers (Leblanc-Dumas et al., 2012; Tremblay et al., 2012, 2013). Laboratory analyses were performed on samples of surficial deposits and permafrost material to help determine the main climatic conditions that formed the regolith and provide insight into the time it took to form the regolith and how it was preserved. The analytical work included grain size, morphoscopy and exoscopy of quartz grains, X-ray mineralogy, Fe, Al and Si extractions and geochemistry. This article presents the main analytical results of this study.

Geomorphological context

The central part of the study region is covered by >3 m of regolith that forms a wide plateau with little vegetation and no emergent outcrop (Figure 2). The red colour and the absence of signs of transport indicate that the material comes from in situ geochemical alteration of the underlying bedrock, identified as a garnet granite and paragneiss (Tremblay et al., 2013). The lithological facies observed in permafrost cores collected from the regolith reveal the original mineralogy and structure of the bedrock. Below 1.5 m depth, the red material becomes blue and white, locally stratified with undisturbed orange and brown mineralogical facies (Figure 3), and the ice content is mainly pore ice with few ice lenses. Rock fragments collected deep in the cores have shown similar mineralogical assemblages to the material described above. No signs of glacial erosion are visible and only a few erratics indicate that the region was previously covered by ice. In some areas, the material has been eroded down to bedrock by glaciofluvial processes and highly weathered bedrock can be observed in sections,

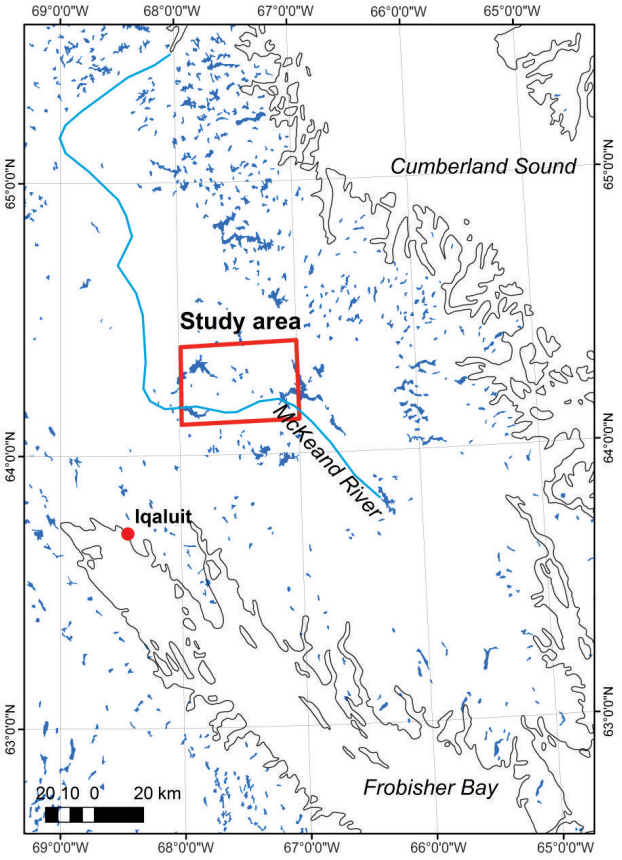

Figure 1: Location of the study area, central Hall Peninsula, Baffin Island, Nunavut.

Figure 2: Red regolith forms a wide plateau on central Hall Peninsula, Nunavut. Note the absence of vegetation and outcropping bedrock.

Figure 3: Regolith collected below 1.5 m shows the original bedrock structure and variable lithological mineralogy, Hall Peninsula, Nunavut. Scale in centimetres.

indicating that alteration of the material preceded the Wisconsinan glaciation.

The central region of Hall Peninsula (Figure 4) is surrounded by a mixture of glacially transported material and regolith soils (intermediate/transition zone) extending to the east of the study region where weakly glacially scoured bedrock is found. At the western and southern margin of the regolith, till is found in association with well-scoured bedrock showing south-southeast striations corresponding to the glacier readvance associated with the Hall moraine (Miller, 1980; Tremblay et al., 2013). On the west side of the study area, there is a moraine ridge that averages 15 m high and 150 m wide. It represents a part of the Frobisher Bay moraine, which extends 150 km from Frobisher Bay to the head of Cumberland Sound (Blake, 1966). This moraine was formed during a minor readvance of the Laurentide Ice Sheet around 8000–9000 years BP (Blake, 1966; Miller, 1980; Hodgson, 2005; Tremblay et al., 2013).

The central part of the study region, which is an area of regolith, has been mapped as a cold-based zone (covered by a glacier with a frozen base) whereas the region to the west and south, with the Frobisher moraine and till material, has been mapped as a warm-based zone (covered by a glacier with a melted base) and the eastern region was mapped as an intermediate cold-based zone (indicative of both warm- and cold-based conditions; Sugden, 1978; Tremblay et al., 2013). Glaciolacustrine deposits and shorelines are found next to the moraine and are associated with numerous glaciolacustrine deltas, which reach heights of 25 m.

Material characteristics

In total, four types of surficial deposits were collected for laboratory analyses and included 1) regolith (Figure 4), 2) intermediate material composed of a mixture of glacially transported material and regolith, 3) till and 4) glaciolacustrine sediments. In addition, five permafrost cores were collected: two in the regolith area (F1HP12 and F2HP12) and three in glaciolacustrine deposits (F1HP13, F2HP13, F3HP13; Figure 4). The samples were collected and analyzed for geochemical and sedimentological characteristics.

Grain-size analyses

The grain-size composition of the regolith at the surface is dominated by sand (2–0.063 mm diameter) with 43.97 to 67.82% of the total sample. The remnant composition is 10.31 to 39.05% gravel (>2 mm) and 12.07 to 26.76% pelite (>0.063 mm; Table 1). The dominant grain size in the matrix of the regolith surface samples corresponds to a fine to very fine sand and is very poorly sorted. With depth, the grain size of the regolith increases slightly, as it transitions to undisturbed saprolite but stays mainly composed of sand (70.93–83.51%) between a depth of 96 to 155 cm (Figure 5). Above 155 cm, the red material was affected by cryoturbation due to freeze-thaw processes in the permafrost, but below that level, the material is undisturbed and the original grey colour of the bedrock is preserved, indicating that it was probably preserved under permafrost conditions since the formation of the regolith (Figure 6). Therefore, the material found below 155 cm depth represents in situ weathered bedrock not affected by cryoturbation and is very friable. Grain-size analysis of this material was not completed as it would not be informative.

Regolith samples are characterized by colours ranging from dark brown to brown-yellow, pale brown–yellow and yellow-olive, according to the Munsell Soil Color Charts (Munsell Color–X-Rite, Incorporated, 2000).

Morphoscopy and exoscopy of quartz grains

Morphoscopy is used to observe transportation marks left on the surface of quartz grains in order to identify its environment of sedimentation. Approximately 100 to 120 grains of quartz were picked from regolith samples from surficial deposits and permafrost cores. They were observed with a scanning electron microscope (SEM) to identify those transportation marks and a proportion of each surface appearance was assessed using four characteristics (angular, subangular, blunt-shiny and round-mat) for each sample. The result shows that 60 to 94% of the grains have angular edges characteristic of a material that was not affected by any transport agent (Chamley, 1987). The crystalline structure of quartz (hexagonal) is perceptible on a few grains (Figure 7a) indicating that it comes from in situ alteration of the bedrock (Pomerol et al., 2005). For the remnant grains, 6 to 38% have subangular edges, 0 to 2% have a blunt-shiny appearance and 0 to 5% have a round-mat appearance.

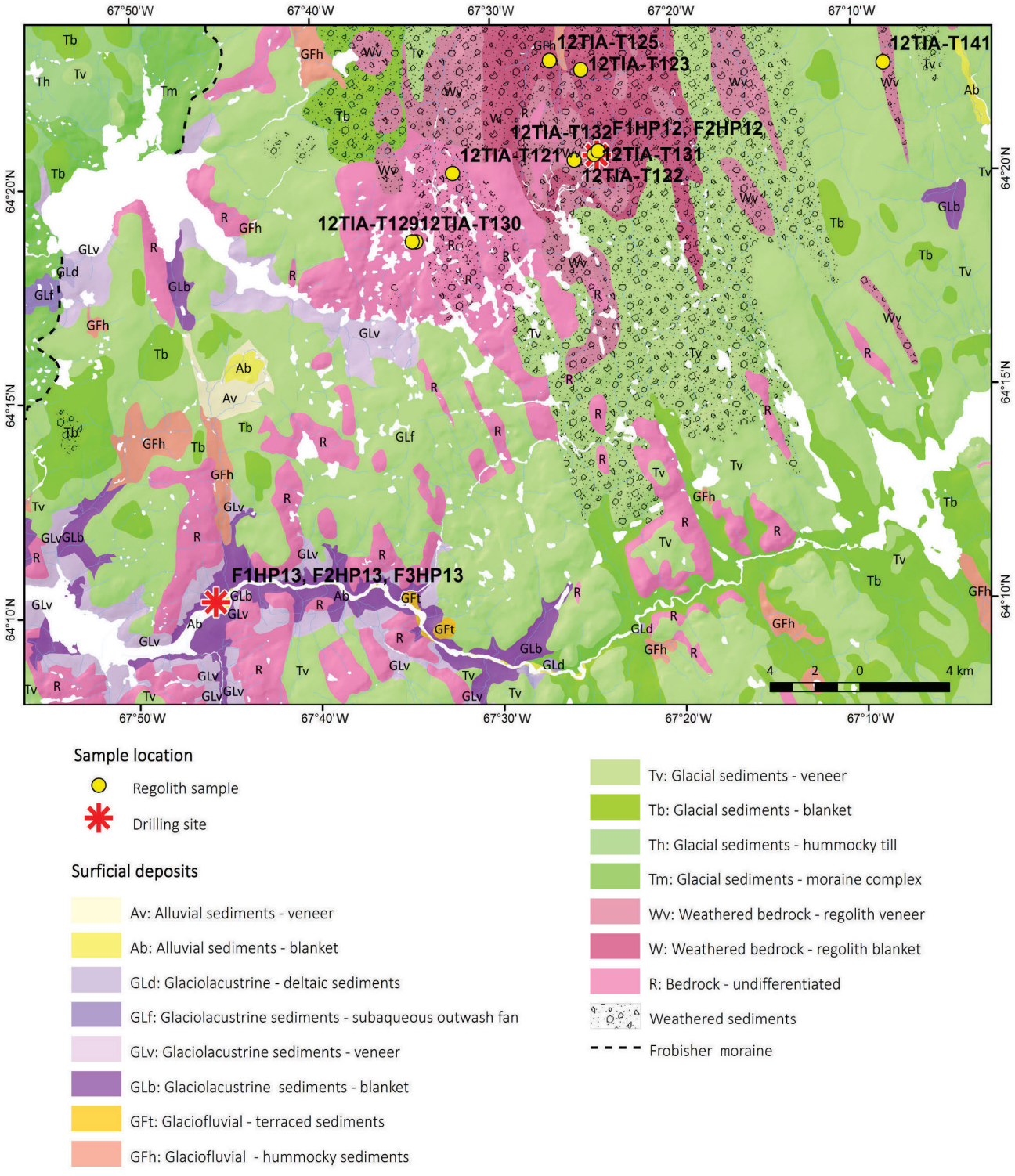

Figure 4: Surficial geology of the study area, central Hall Peninsula, Nunavut. Location of regolith sample sites and drilling sites indicated.

Table 1: Results of laboratory analyses of regolith obtained from surficial deposits, Hall Peninsula, Nunavut.

Sample	Colour[1]	Grain size			Clay minerals	Extractable iron			CIA-1	CIA-2
		Pebble (%)	Sand (%)	Pelite (%)		Fe_d (g/kg)	Fe_o (g/kg)	Fe_p (g/kg)	(Fe_a/Fe_c)	
12TIA-T121	light yellowish-brown	23.64	58.56	17.8	I, V, Cl?, K, VI	0.23	0.86	0.06	-1.27	76.18
12TIA-T122	yellowish-brown	34.36	48.93	16.71	-	0.31	1.09	0.06	-1.32	87.59
12TIA-T123	yellowish-brown	24.66	50.22	25.12	I, V, Cl?, K, VI	0.34	1.2	0.13	-1.24	79.94
12TIA-T125	olive-yellow	10.92	65.3	23.77	I, V Cl, K, VI	0.23	0.58	0.07	-1.45	73.18
12TIA-T129	yellowish-brown	10.31	67.82	21.87	-	0.35	0.91	0.09	-1.48	81.11
12TIA-T130	light yellowish-brown	12.73	66.68	20.59	I, V Cl, K, VI	0.14	0.36	0.05	-1.39	73.22
12TIA-T131	yellowish-brown	39.05	48.88	12.07	I, V, K, VI	0.26	1.3	0.09	-1.16	78.04
12TIA-T132	yellowish-brown	19.76	53.48	26.76	I, V, K, VI	0.21	1.7	0.1	-1.07	85.8
12TIA-T141	strong brown	35.48	43.97	20.54	I, V Cl, K, VI	0.23	0.67	0.05	-1.4	79.92

[1] Munsell Soil Color Charts (Munsell Color–X-Rite, Incorporated, 2000)

Abbreviations: a, amorphous; c, crystalline; CIA-1, chemical index of alteration; CIA-2, second chemical index of alteration; Cl, chlorite; d, dithionite-citrate-bicarbonate; I, illite/mica; K, kalonite; o, ammonium oxalate acid; p, pyrophosphate; V, vermiculite; VI, intermediate vermiculite-illite clay mineral

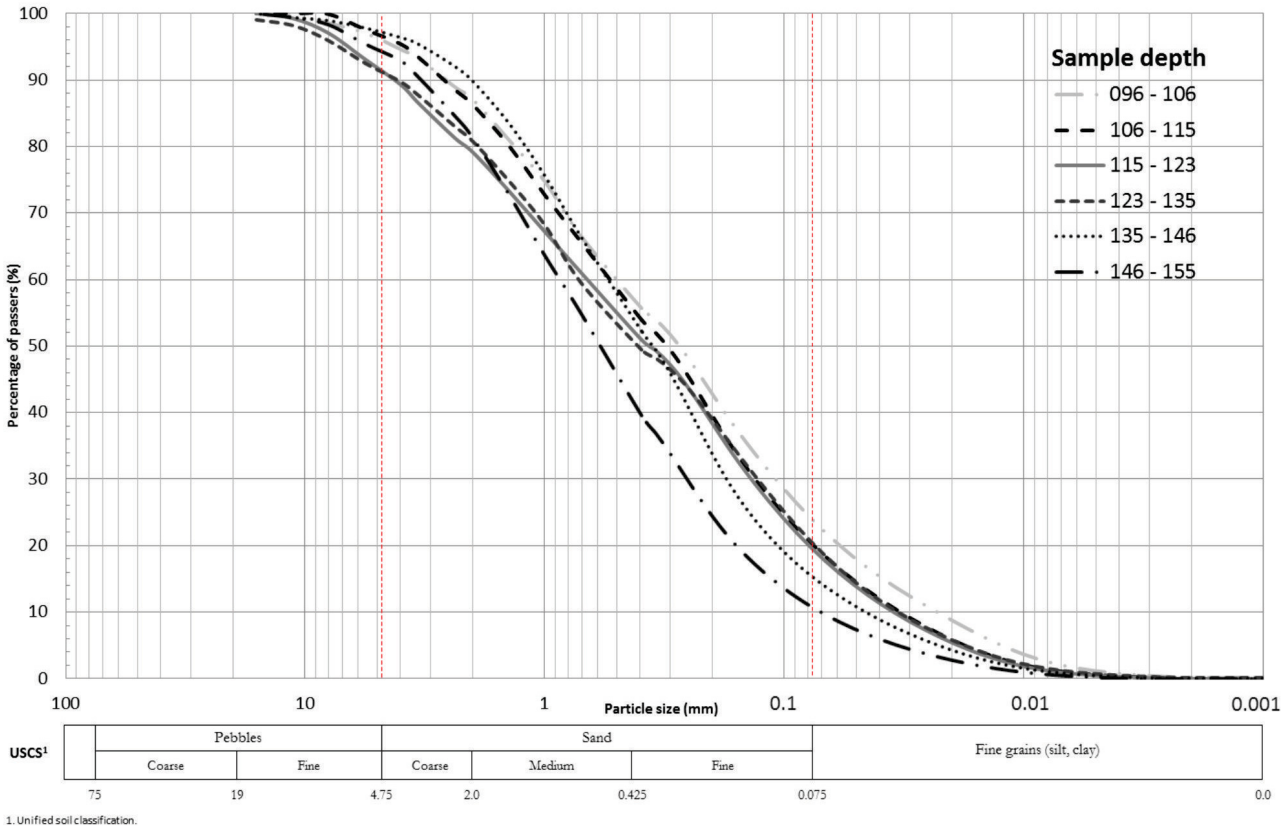

Figure 5: Percentage of grains passing through sieve stack as a function of grain size for regolith samples collected from permafrost corehole F2HP12, Hall Peninsula, Nunavut. Sample depth in centimetres.

Exoscopy performed on quartz grains shows important exfoliation on the surface of the quartz grains and geometric dissolution (Figure 7b, c). For all of the regolith samples observed, the surfaces of the grains were clean, showing no silica deposits. Iron and aluminum oxides were observed in the cavities of all grains (Figure 7a–d) and could be deposits from weathering products. Impact marks, such as v-shaped and crescent marks, were found on some of the quartz grains (Figure 7d) but no signs of glacial transport, such as striations or scour marks, were observed. The same observations were made on quartz grains collected from regolith from the F1HP12 and F2HP12 permafrost core samples.

Figure 6: Permafrost core sample from F2HP12, collected from saprolite, Hall Peninsula, Nunavut. Note the blue colour of the undisturbed material. Scale in centimetres.

X-ray mineralogy

Analyses by X-ray diffractometry were performed on rock fragments and saprolite material collected from permafrost core samples and regolith from surficial deposits. The results show a uniform mineral composition for the rock fragments, the saprolite material and the regolith. The primary minerals found in the rock fragment samples are quartz, anorthite, microcline and phlogopite (mica; e.g., Figure 8) and those found in the corresponding saprolite material are quartz, anorthite, orthoclase, as well as illite and kaolinite (e.g., Figure 9). The illite and kaolinite are clay minerals resulting from the chemical alteration of bedrock and commonly found in temperate and tropical re-

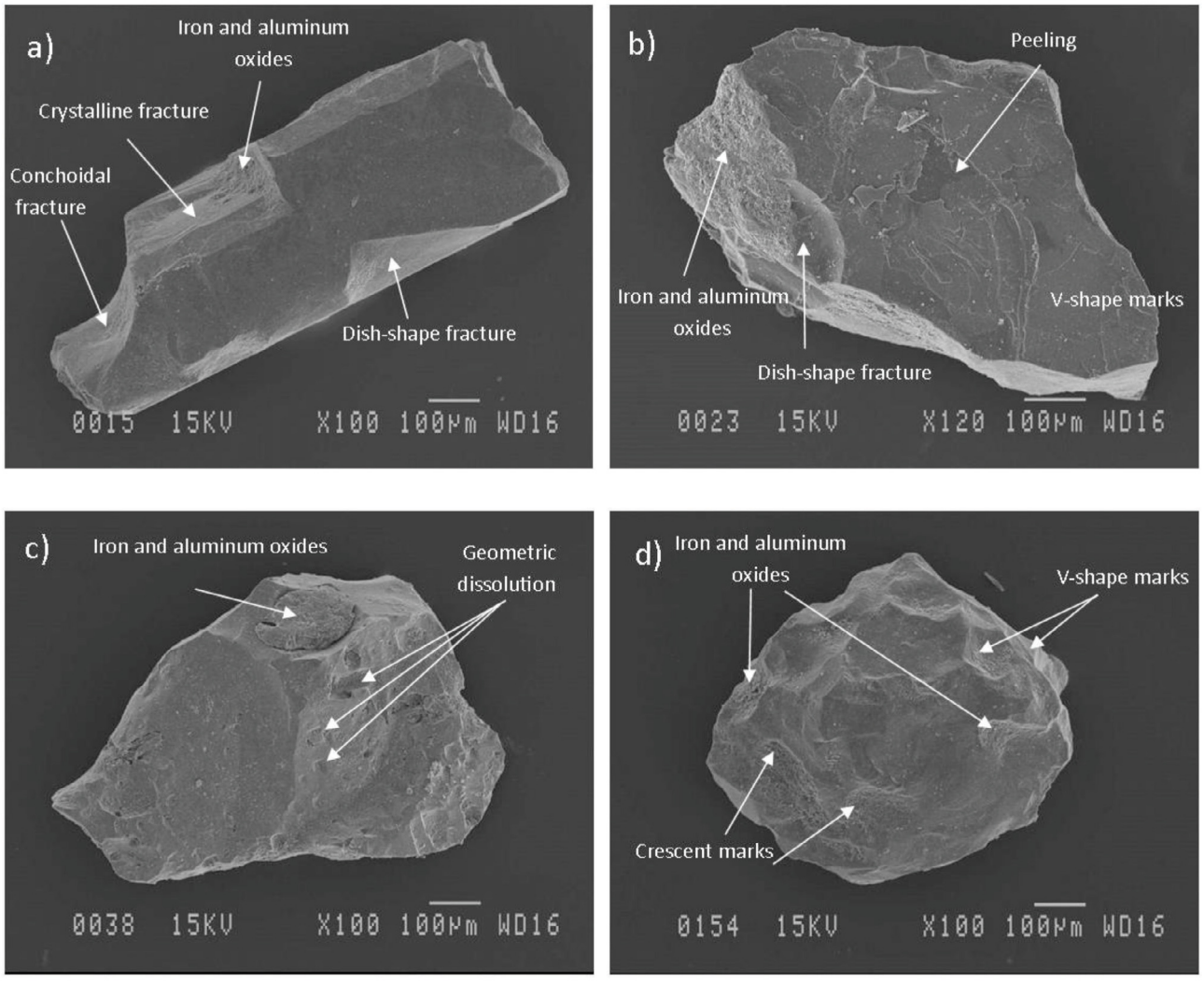

Figure 7: Quartz grains collected from regolith samples (Hall Peninsula, Nunavut) and observed with a scanning electron microscope (SEM). **a)** Grain presenting a hexagonal crystalline structure, found in sample 12TIA-T122. **b)** Grain showing peeling figures, found in sample 12TIA-T123. **c)** Grain with geometric dissolution figures, found in sample 12TIA-T125. **d)** Grains showing v-shaped and crescent marks, found in sample 12TIA-T131.

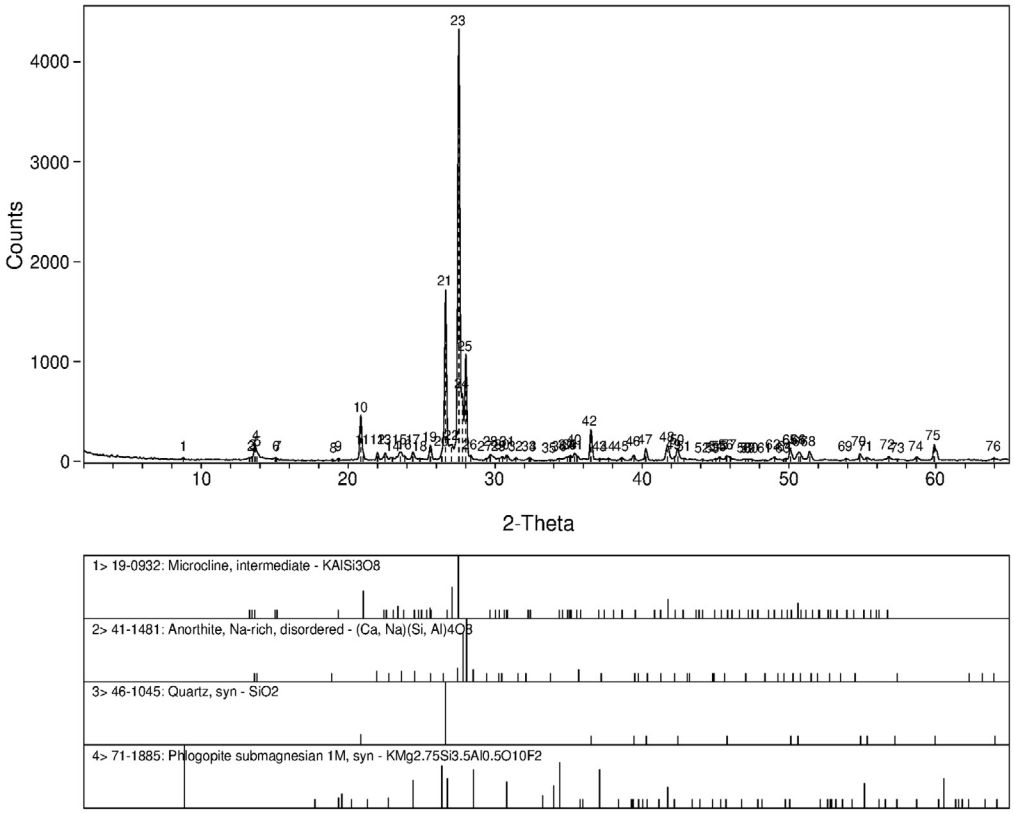

Figure 8: Results of X-ray diffractometry performed on a rock fragment collected from the regolith in permafrost corehole F1HP12, at a depth of 218 to 230 cm, Hall Peninsula, Nunavut.

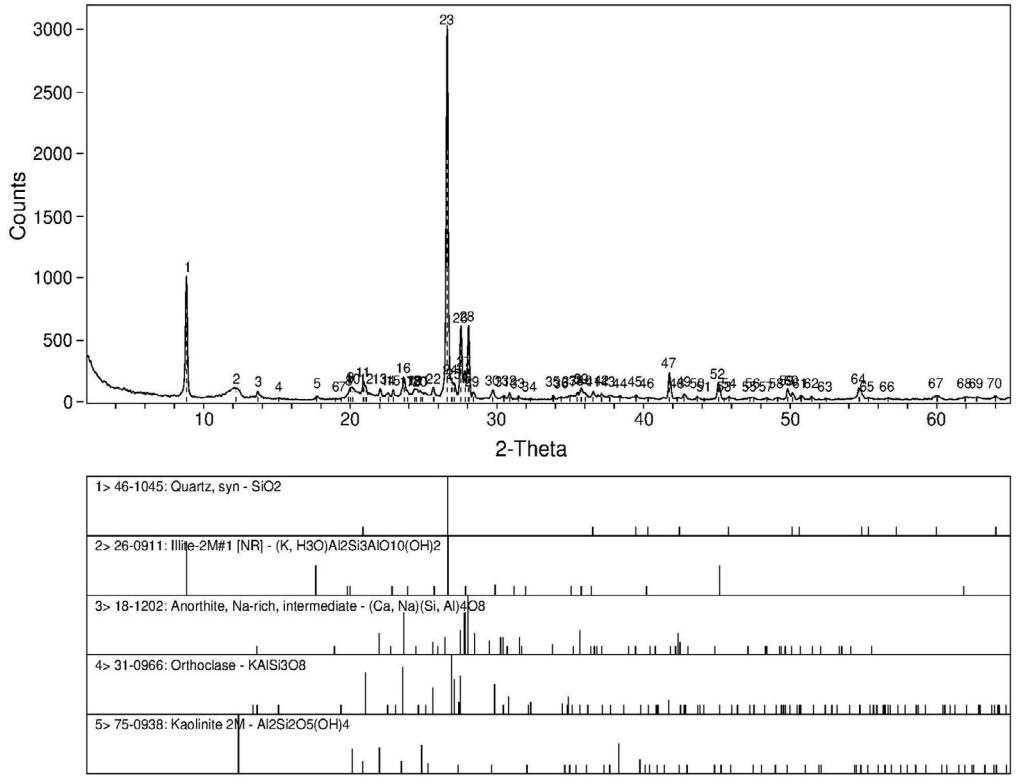

Figure 9: Results of X-ray diffractometry performed on saprolite material collected from permafrost corehole F2HP12, at a depth of 155 to 165 cm, Hall Peninsula, Nunavut.

gions (Miskovsky, 1987). It is interpreted that the presence of the clay minerals in an arctic environment implies that the material was inherited from a warmer period of geological history, which corresponded to tropical conditions. The same clay minerals are found in samples of regolith from the regolith areas (Table 1). However, some samples of regolith also contain minerals such as amphibole, pyroxene, vermiculite, chlorite, talc, goethite and/or heavy minerals. This can be explained by variations in bedrock geology across the study area.

Extractions of Fe, Al and Si

Higher concentrations of amorphous iron instead of crystalline forms of iron should occur in regolith and thus higher chemical index of alteration (CIA-1) values should occur in the regolith area compared to surrounding areas of till. Crystalline forms are found in fresh rock and are more common in grains that were not exposed to chemical alteration, such as recent till. Surficial deposits of regolith and till were submitted for Fe, Al and Si extractions. The extractable crystalline and amorphous forms of iron, as well as aluminum and silica, were extracted using dithionite-citrate-bicarbonate, ammonium oxalate acid and pyrophosphate to determine the CIA-1 (McKeague, 1978):

1) Fe_o–Fe_p = amorphous form of Fe (Fe_a)
2) Fe_d–Fe_o = crystalline form of Fe (Fe_c)
3) CIA-1 = Fe_a/Fe_c

where Fe_o is iron extracted with ammonium oxalate acid, Fe_p is iron extracted with pyrophosphate and Fe_d is iron extracted with dithionite-citrate-bicarbonate.

For all surficial regolith, intermediate and till samples, the content of iron extracted with oxalate surpasses iron extracted with dithionite (Table 1, Figure 10) resulting in a negative crystalline form content leading to a negative CIA-1. This kind of result has been observed in other studies where the samples contained magnetite (e.g., Baril and Bitton, 1969). In Baril and Bitton (1969), the magnetite was extracted by oxalate and the results were abnormally high for oxalate extractions. High Fe_o values were found both in the regolith, intermediate and till samples and in the permafrost core samples from this study and can't be explained by the occurrence of magnetite, due to the absence of this mineral in most of the collected samples. The Fe extraction method is therefore questionable without a better of understanding of the behaviour of extracting solutions. This is also the case for the Al and Si extractions; results cannot be interpreted with certainty.

Geochemistry and second chemical index of alteration

The second chemical index of alteration (CIA-2) used for this study is a weathering index that yields crucial insights into the contribution of chemical and physical weathering to the production of rock detritus. Considering that chemical and physical weathering is a function of climate, the CIA-2 can provide important information about the environmental conditions that existed for a weathered surface

$$\text{CIA} - 2 = \frac{Al_2O_3}{Al_2O_3 + CaO + Na_2O + K_2O} \times 100$$

(Nesbitt and Yong, 1982; Bahlburg and Dobrinski, 2011; Refsnider and Miller, 2013). Progressive chemical weathering of feldspar leads to the loss of cations and the transformation to more stable minerals, while aluminum oxides remain stable. This chemical index of alteration represents the ratio of aluminum oxides to the mobile cations as shown by the equation (Ebert et al., 2012):

The highest degree of weathering is represented by kaolinite, which has a CIA-2 value of 100%. Kaolinite is the ultimate result of chemical weathering of aluminum silicates,

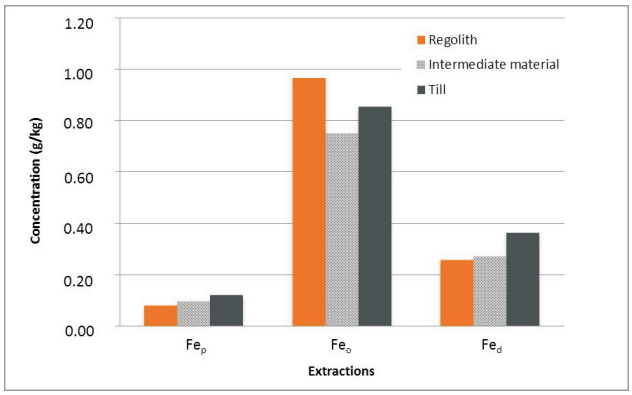

Figure 10: Mean concentrations of Fe extracted with dithionite-citrate-bicarbonate (Fe_d), ammonium oxalate acid (Fe_o) and pyrophosphate (Fe_p) from regolith, intermediate material (regolith mixed with till) and till, central Hall Peninsula, Nunavut.

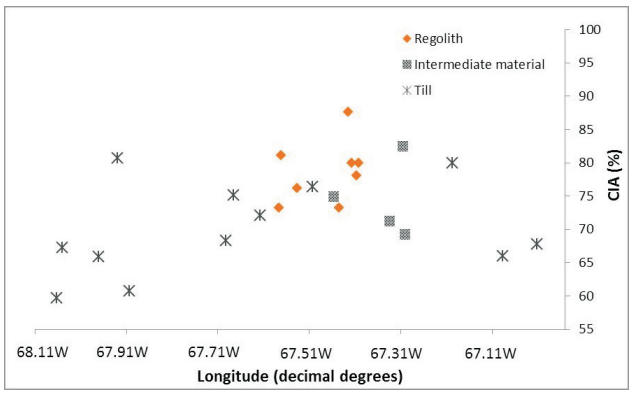

Figure 11: East-west distribution of second chemical index of alteration (CIA-2) results obtained for rock pulp from regolith, intermediate material (regolith mixed with till) and till samples, central Hall Peninsula, Nunavut.

for example feldspar, and is formed in hot and humid regions, such as tropical rainforests.

Three different types of samples were analyzed to obtain their CIA-2 values: rock pulp or rock chips collected from surficial deposit samples and rocks collected from bedrock outcrops or felsenmeers. The results obtained from rock pulp indicate an average CIA-2 of 79.44, 74.47 and 62.48% for the regolith, the intermediate material and the till, respectively (Figure 11). The east-west distribution of the CIA-2 results on rock pulp clearly shows a greater CIA-2 for the central regolith area. For the rock chips, CIA-2 values obtained for the intermediate material and the till areas are similar with a mean CIA-2 of 63.10 and 60.69% weathering, respectively. No rock chips were found in the regolith. Results obtained from rock samples collected from felsenmeers in the regolith area indicate 71.83% weathering. For the intermediate material and till areas, the results obtained from rock samples are at least 10% less than for samples from the regolith area.

Regolith origin and preservation

The higher CIA-2 results and the presence of secondary clay minerals, such as illite and kaolinite (Table 1), indicate that the regolith was formed during a warmer climatic period, which possibly preceded glaciation or even occurred during interglacial periods, when the climate was more temperate or even tropical. The mineral composition of the regolith and its rock fragments, shown by X-ray diffractometry, indicates that the centre of the study region is dominated by highly weathered granitic rocks. These rocks have been locally eroded to tor formations and in some cases original structural features have been preserved. The SEM imagery of the quartz grains showed important alteration features that are uncommon on glacially transported material. The lack of transportation marks on the quartz grains also suggests ice did not move the material.

Weathering and sedimentology results from permafrost core samples indicate that the regolith was not eroded during the last glaciation and was likely preserved in subglacial permafrost conditions for an extended period of time. For this material to have been preserved during the last glaciation underneath the Laurentide Ice Sheet, the thermal regime at the ice-bed interface had to be cold-based with a connection to the underlying permafrost.

As shown by the occurrence of weathered material and weakly scoured bedrock east and west of the regolith area, the cold-based zone on Hall Peninsula was probably more widespread than the former regolith area during the last glacial maximum and was only recently affected by warm-based ice. Most of the central plateau of Hall Peninsula was probably cold based for the first half of the Quaternary period. Successions of ice readvances occurred in the study region following the last glacial maximum, as shown by the presence of the Hall and Frobisher moraines. These glacial deposits indicate a primarily warm-based thermal regime of the ice for the second half of the Quaternary period on the central Hall Peninsula plateau. The occurrence of non-transported regolith in the central part of the study region indicates that local zones might have been protected from glacial erosion following the last glacial maximum. Two hypotheses could explain the conservation of this material: 1) conservation under local cold-based ice or 2) the absence of an ice cover. The thermal regime at ice-bed interface and the scouring rate of the ice varied through time and space leading to deposition and conservation of three types of surficial deposits material (regolith, intermediate material and till).

Economic considerations

This glacial geology study supports the search for economic minerals in the region. Drift prospecting in glaciated terrain is complicated due to difficulties in predicting erosion and transport distances of ore-bearing glacial drift. In these cold-based ice regions, the minerals found in till come from in situ alteration of the underlying bedrock rather than from a source up-ice. Knowing the exact limits of cold-based ice will facilitate drift prospecting. Furthermore, knowledge of the permafrost characteristics, such as sediment types and grain size of the regolith, will be useful for land management related to future infrastructure development by mining companies.

Acknowledgments

This project was funded and organized by the Canada-Nunavut Geoscience Office (CNGO) based in Iqaluit, with support from the Centre d'études nordiques (CEN), ArcticNet (Network of Centres of Excellence of Canada program) and the Geological Survey of Canada (GSC), Ottawa. The Canadian Northern Economic Development Agency's (CanNor) Strategic Investments in Northern Economic Development (SINED) program provided financial support for this work. E. L'Hérault (CEN), W. Sladen (GSC) and G. Oldenborger (GSC) are thanked for their technical contribution to the drilling and geophysical field operations. The surficial map was prepared using three-dimensional technology with the assistance of C. Gilbert (CNGO) and M. Boutin (GSC-Quebec). Universal Helicopters provided safe field transport during the summers of 2012 and 2013. D. Mate, formerly Chief Geologist of CNGO now with Canadian Northern Economic Development Agency, provided camp facilities and logistics. Methodology and interpretation of the results were improved by conversations with M. Caillier, A. Grenier and D. Marcotte. A.-M. LeBlanc and D. Mate helped with the revision of this paper.

Natural Resources Canada, Earth Sciences Sector contribution 20140329

References

Bahlburg, H. and Dobrzinski, N. 2011: A review of the Chemical Index of Alteration (CIA) and its application to the study of Neoproterozoic glacial deposits and climate transitions; Chapter 6 *in* The Geological Record of Neoproterozoic Glaciations, E. Arnaud, G.P. Halverson and G. Shields-Zhou (ed.), The Geological Society, Memoir no. 36, p. 81–92.

Blake, W., Jr. 1966: End moraines and deglaciation chronology in northern Canada with special reference to southern Baffin Island; Geological Survey of Canada, Paper 66-26, 31 p.

Chamley, H. 1987: Sédimentologie; Dunod, Paris, 175 p.

Ebert, K., Willendring, J., Norton, K.P., Hall, A. and Hättestrand, C. 2012: Meteoric ^{10}Be concentrations from saprolite and till in northern Sweden: implications for glacial erosion and age; Quaternary Geochronology, v. 12, p. 11–12.

Hodgson, D.A. 2005: Quaternary geology of western Meta Incognita Peninsula and Iqaluit area, Baffin Island, Nunavut; Geological Survey of Canada, Bulletin 582, 74 p., 1 CD-ROM.

Leblanc-Dumas, J., Allard, M. and Tremblay, T. 2013: Quaternary geology and permafrost characteristics in central Hall Peninsula, Baffin Island, Nunavut; *in* Summary of Activities 2012, Canada-Nunavut Geoscience Office, p. 101–106.

McKeague, J.A. 1978: Manuel de méthodes d'échantillonnage et d'analyse des sols (2^{e} édition); Société canadienne de la science du sol, p. 114–123.

Miller, G.H. 1980: Late Foxe glaciation of southern Baffin Island, N.W.T., Canada; Geological Society of America Bulletin, v. 91, no. 7, p. 399–405.

Miskovsky, J.C. 1987: Géologie de la Préhistoire: méthodes, techniques, applications; Association pour l'étude de l'environne7ment géologique de la préhistoire, Paris, 1297 p.

Munsell Color–X-Rite, Incorporated 2000: Munsell Soil Color Charts; X-Rite, Incorporated, 50 p.

Nesbitt, H.W. and Young, G.M. 1982: Early Proterozoic climate and plate motions inferred from major element chemistry of lutites; Nature, v. 299, p. 715–717.

Pomerol, C., Lagabrielle, Y. and Renard, M. 2005: Éléments de géologie (13^{e} edition); Dunod, Paris, 762 p.

Refsnider, K.A. and Miller, G.H. 2013: Ice-sheet erosion and the stripping of Tertiary regolith from Baffin Island, eastern Canadian Arctic; Quaternary Science Review, v. 67, p. 176–189.

Sugden, D. 1978: Glacial erosion by the Laurentide Ice Sheet; Journal of Glaciology, v. 20, no. 83, p. 367–391.

Tremblay, T., Leblanc-Dumas, J., Allard, M., Gosse, J.C., Creason, C.G., Peyton, P., Budkewitsch, P. and LeBlanc, A.-M. 2013: Surficial geology of southern Hall Peninsula, Baffin Island, Nunavut: summary of the 2012 field season; *in* Summary of Activities 2012, Canada-Nunavut Geoscience Office, p. 93–100.

Tremblay, T., Leblanc-Dumas, J., Allard, M., Ross, M. and Johnson, C. 2014: Surficial geology of central Hall Peninsula, Baffin Island, Nunavut: summary of the 2013 field season; *in* Summary of Activities 2013, Canada-Nunavut Geoscience Office, p. 109–120.

Geological reconnaissance for Ordovician stratigraphy and petroleum potential, Akpatok Island, Nunavut

S. Zhang[1] and D.J. Mate[2]

[1]*Canada-Nunavut Geoscience Office, Iqaluit, Nunavut, shunxin.zhang@nrcan-rncan.gc.ca*

[2]*Canadian Northern Economic Development Agency, Iqaluit, Nunavut (formerly Canada-Nunavut Geoscience Office, Iqaluit, Nunavut)*

This work was part of the Geo-mapping for Energy and Minerals (GEM) Program in Hudson Strait and Ungava Bay, and is being co-led by the Geological Survey of Canada (GSC) and the Canada-Nunavut Geoscience Office. The study area is focused on Akpatok Island, located in Ungava Bay. The objective of this work is to better evaluate the hydrocarbon potential in the Hudson Strait and Ungava Bay.

Zhang, S. and Mate, D.J. 2015: Geological reconnaissance for Ordovician stratigraphy and petroleum potential, Akpatok Island, Nunavut; *in* Summary of Activities 2014, Canada-Nunavut Geoscience Office, p. 79–88.

Abstract

The work presented here is part of the Geo-mapping for Energy and Minerals program (GEM) Hudson-Ungava Project. The aim of the project is to evaluate the hydrocarbon potential in Hudson Bay, Hudson Strait and Ungava Bay. A one-day geological reconnaissance on Akpatok Island, carried out by the Canada-Nunavut Geoscience Office on August 15, 2014, resulted in 1) identification of the elevation and possible stratigraphic position of the organic-rich interval; 2) recognition that the rock sequence of Ordovician age on Akpatok Island contains good to very good petroleum source rocks; and 3) identification of outcrops with workable sections at different elevations across the island. This work provided essential data for more detailed stratigraphic fieldwork in the future, and will help in a preliminary assessment of the hydrocarbon source-rock potential in Ungava Bay and the Hudson Strait.

Résumé

Le présent ouvrage s'inscrit dans le cadre du projet Hudson–Ungava du programme de Géocartographie de l'énergie et des minéraux, qui a pour but d'évaluer le potentiel en hydrocarbures de la baie d'Hudson, du détroit d'Hudson et de la baie d'Ungava. Le Bureau géoscientifique Canada-Nunavut a procédé à une excursion de reconnaissance géologique sur le terrain dans l'île Akpatok le 15 août 2014. Au cours de cette excursion, on a réussi à 1) identifier l'emplacement stratigraphique et l'élévation de l'intervalle riche en matières organiques, 2) établir que la séquence ordovicienne de l'île Akpatok renferme des roches mères pétrolières de très bonne qualité et 3) identifier les affleurements susceptibles de présenter des sections se prêtant à l'étude à différentes élévations dans l'ensemble de l'île. Ces tâches ont permis de recueillir des données essentielles à la poursuite éventuelle de travaux stratigraphiques sur le terrain plus détaillés, tout en contribuant aux efforts d'évaluation préliminaire du potentiel de la baie d'Ungava et du détroit d'Hudson de receler des roches mères sources d'hydrocarbures.

Introduction

Akpatok Island, 903 km^2 in area, is centred at 60°25'N, 68°08'W in Ungava Bay between northern Quebec and Nunavut (Figure 1a). It is one of many Ordovician outliers on the Canadian Shield, and it is the only location where Paleozoic rocks are exposed in the Hudson Strait–Ungava Bay area. Its important tectonic and geographic location makes it key for understanding the Paleozoic stratigraphy and petroleum potential in the region. To date, very little research has been conducted on the island.

The Ordovician and younger bedrock geology and hydrocarbon potential on Akpatok Island and surrounding marine area is known mainly from 1) geophysical investigations by the Geological Survey of Canada (Grant and Manchester, 1970; Sanford and Grant, 2000; Pinet et al., 2013); 2) a single drillhole, Premium-Homestead Akpatok F-26 at 60°25'40"N, 68°20'30"W (Figure 1b, c), drilled for hydrocarbon exploration by Premium Iron Ores Ltd. in 1969 (Kerkhoff, 1971); 3) three stratigraphic sections measured on the west coast of the island near the Premium-Homestead Akpatok F-26 wellsite and fossils collected

This publication is also available, free of charge, as colour digital files in Adobe Acrobat® PDF format from the Canada-Nunavut Geoscience Office website: http://cngo.ca/summary-of-activities/2014/.

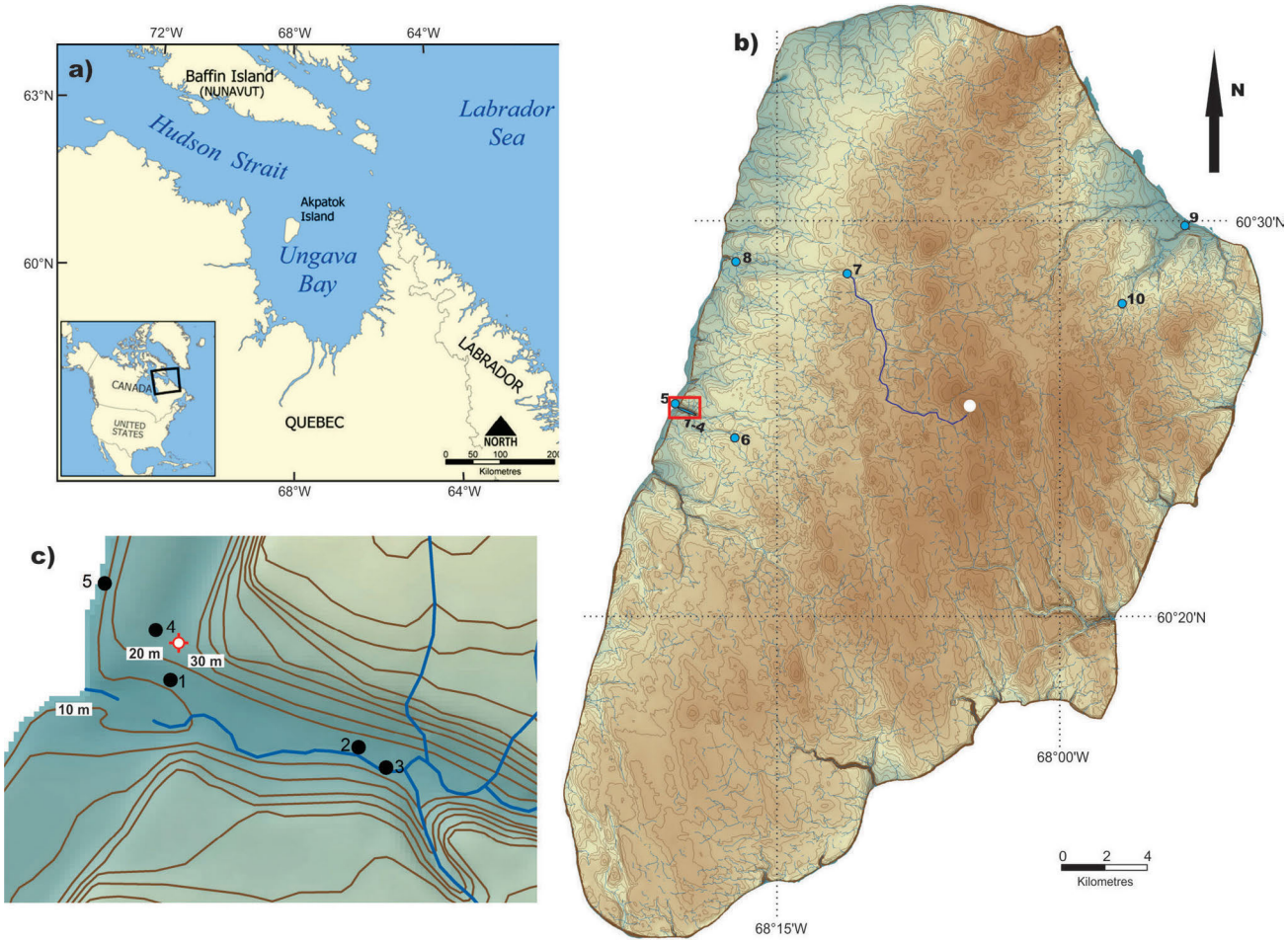

Figure 1: a) Location of Akpatok Island in Ungava Bay and Hudson Strait; **b)** elevation map of Akpatok Island, showing the field localities (blue dots) visited and the highest elevation on the island (white dot); **c)** enlargement of the area marked by the red rectangle in part b; red circle and cross represent Akpatok F-26 well. Black dots with numbers are station numbers referred to in the text.

from these sections (Workum et al., 1976); 4) Rock-Eval 2 data collected from three samples of the Ordovician sections on the island (Macauley, 1987) and 5) Rock-Eval 6 data collected from 41 samples of the core obtained at Premium-Homestead Akpatok F-26 (Zhang, 2014). All these studies were unable to fully answer the following scientific questions:

- Is the Paleozoic sequence in Ungava Bay the same as those in Hudson Bay and Foxe Basin?
- Are there any potential petroleum source rocks within the Paleozoic sequence in Ungava Bay?
- If yes, what are their stratigraphic positions? Are they at the same stratigraphic positions as those in Hudson Bay and the Foxe Basin?

With the increased interest in hydrocarbon exploration in the Canadian Arctic, new data are obviously needed to answer these questions and help reassess the petroleum potential of Ungava Bay and Hudson Strait. In order to meet this objective, the GEM Hudson-Ungava Project designed a two-week field study on the island; however, because of logistics issues, this study was reduced to a focused reconnaissance survey to assess the need and establish the objectives for a full-scale investigation in the years to come. This paper summarizes the fieldwork conducted during this one-day (August 15, 2014) reconnaissance and includes a discussion of the petroleum source-rock potential and the exposed Ordovician strata on the island.

Previous studies on the Ordovician stratigraphy and petroleum potential of Akpatok Island

Ship Point Formation equivalent

The Premium-Homestead Akpatok F-26 well (Kerkhoff, 1971) was terminated at 371 m and entirely cored from 285 m downward. Precambrian gneiss was penetrated between 362 and 371 m, and sandstone, siltstone, limestone and shale from 15 to 362 m. About 75 m of the sedimentary rocks immediately above the Precambrian are mainly sandstone, siltstone and shale, and the rest are basically limestone interbedded with shale. The conodont fauna collected from the interval 264–298 m show similarity to that of the upper part of the Ship Point Formation of Foxe Basin (Fig-

ure 2), with an age of early Middle Ordovician (Workum et al., 1976). This part of the succession was named the Ungava Bay Formation by Sanford and Grant (1990).

The source-rock evaluation for the Ship Point equivalent strata was done by Zhang (2014). Forty-one shale samples were collected from Akpatok F-26 core (285–328.5 m) for Rock-Eval 6 analysis. This core is stored at the Canada–Nova Scotia Offshore Petroleum Board Core Lab. Analysis of the Rock-Eval 6 data shows that the samples of Ship Point Formation correlative unit on Akpatok Island have minimum and maximum total organic carbon (TOC) values of 0.14 and 0.93%, respectively, with an average of 0.38%; and minimum and maximum T_{max} values (a parameter of thermal maturation for petroleum source rock), based on the 'valid' samples with a sharp and clean S2 peak on the pyrograms, of 422 and 435°C, with an average of 427.5°C. Therefore, the sedimentary rocks equivalent to the Ship Point Formation below sea level at Akpatok Island have poor to fair petroleum source-rock potential, and are largely thermally immature (Zhang, 2014).

Bad Cache Rapids–Churchill River groups equivalent

Three stratigraphic sections were measured and fossils collected in three valleys near the Akpatok F-26 wellsite (Workum et al., 1976). Workum et al. (1976) indicated that the Paleozoic sequence of Akpatok Island consists of ≥244 m of horizontally exposed limestone. The exposed carbonate rocks yield macrofossils and microfossil conodonts, which were correlated with the upper Bad Cache Rapids and Churchill River groups on Southampton Island, Hudson Bay (Workum et al., 1976; Figure 2). However, the name Akpatok Formation was proposed for the ≥244 m of exposed limestone, which was assumed to be of the same general age as the Churchill River Group of Hudson Bay (Sanford and Grant, 1990).

A preliminary appraisal of the hydrocarbon source-rock potential of the Bad Cache Rapids–Churchill equivalent strata (Macauley, 1987) was based on three samples collected from the valley immediately southeast of the Akpatok F-26 wellsite. One sample was collected from outcrop and the other two from rubble. The Rock-Eval 2 data show that these samples contain minimum and maximum TOC of 0.51 and 2.11%, with an average of 1.28%, and minimum and maximum T_{max} values of 424 and 433°C, with an average of 429°C (Macauley, 1987). These limited data indicate that the sedimentary-sequence equivalent to the Bad Cache Rapids–Churchill River groups exposed on Akpatok Island contains an interval with fair to good petroleum source rocks, but they are thermally immature for petroleum generation.

Workum et al. (1976) noted that there are probably less than 2000 feet (610 m) of Ordovician sedimentary section any-

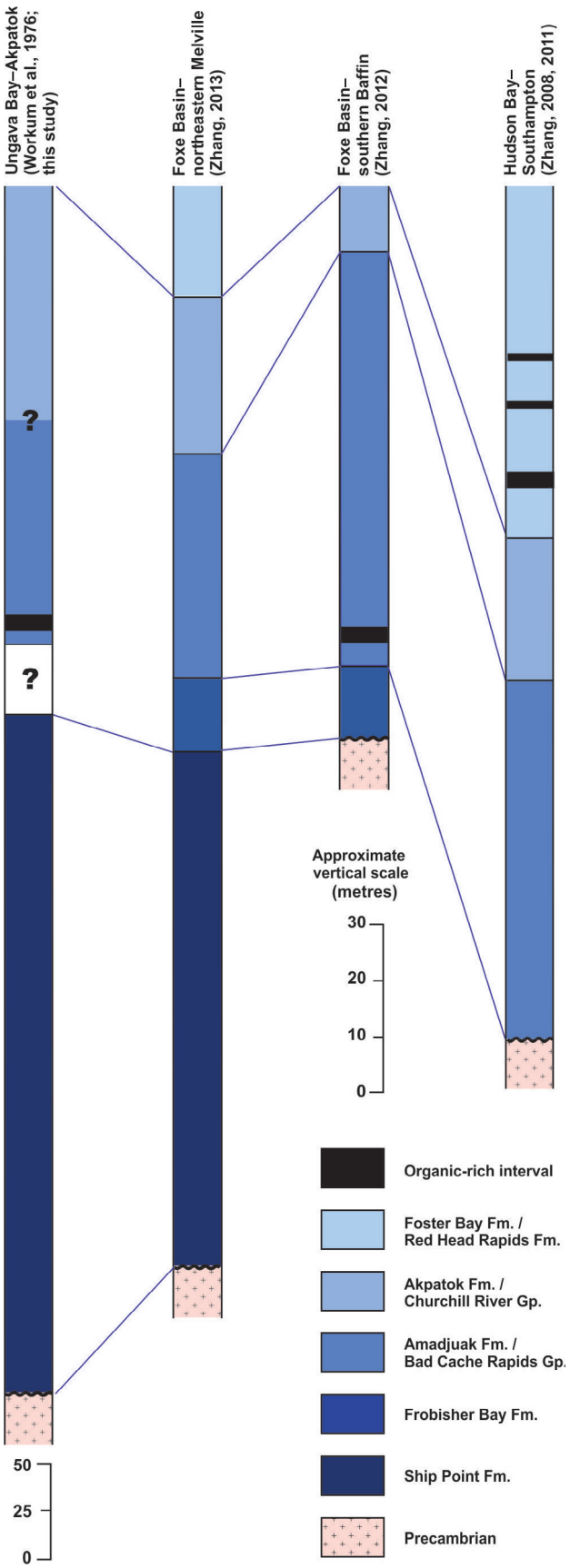

Figure 2: Regional Ordovician lithostratigraphy in the Ungava Bay–Foxe Basin–Hudson Bay area.

where within Ungava Bay, suggesting that there has probably never been sufficient overburden pressure to generate hydrocarbon in the area. The studies of both Macauley (1987) and Zhang (2014) support the low-maturity interpretation of Workum et al. (1976); however, about 2.6 km of sedimentary succession was recognized south of the Cape Hopes fault, about 20 km north of Akpatok Island, by a high-resolution seismic survey (Pinet et al., 2013).

Challenges in the study of Ordovician stratigraphy and petroleum potential on Akpatok Island

- In the Foxe Basin, the Frobisher Bay Formation has been established by Sanford and Grant (1990) between the Ship Point and Amadjuak formations (Figure 2). Sanford and Grant (1990) did not identify the Frobisher Bay Formation on Akpatok Island, although, in Sanford and Grant (2000), the Frobisher Bay Formation unconformably occurs between the Ship Point and Amadjuak formations, based on high-resolution marine seismic profiles.
- The exposed carbonate rocks on the island were correlated with the upper Bad Cache Rapids and Churchill River groups of Southampton Island, Hudson Bay (Workum et al., 1976). These formations are correlated with the Amadjuak and Akpatok formations in the Foxe Basin area (Figure 2). If the Amadjuak Formation has been recognized in the subsurface (Sanford and Grant, 2000), all the exposed carbonate rocks above the organic-rich interval were correlated with the Akpatok Formation in Foxe Basin and the Churchill River Group in Hudson Bay by Sanford and Grant (1990). This leaves open the question of the age of either the Amadjuak Formation or that of the outcrop organic-rich interval.
- Workum et al. (1976) measured three sections near the Akpatok F-26 wellsite that have a combined thickness of about 150 m. This covers approximately the lower half of the entire exposed stratigraphic sequence on the island, which is about 280 m thick based on the highest contour lines on the elevation map and horizontal distribution of the strata (the thickest location is marked by the white dot in the centre of the island in Figure 1b). There has been no study on the upper 130 m of the strata, although Sanford and Grant (1990) included this in their Akpatok Formation. If the lower 150 m of strata could be correlated with the Bad Cache Rapids and Churchill River groups (or Amadjuak and Akpatok formations), as suggested in Workum et al. (1976), then could the upper 130 m be correlated with the Foster Bay Formation in the Foxe Basin area or the Red Head Rapids Formation in the Hudson Bay area, or even to the Silurian?
- The samples tested by Macauley (1987) have low TOC values (between 0.51 and 2.11%, with an average of 1.28%), which is much lower than those from the Foxe Basin area (TOC in a 2 m thick black shale interval of Amadjuak Formation on southern Baffin Island ranging between 1.68 and 12.97%, with an average of 7.8%; Zhang, 2012), and Hudson Bay area (TOC in the lower black shale interval of the Red Head Rapids Formation on Southampton Island ranging between 0.43 and 17.3%, with an average of 9.8%; Zhang, 2008). The low TOC content of the organic-rich interval in the Ordovician sequence on Akpatok Island, as reported by Macauley (1987), could be naturally low or samples richer in TOC were simply not found and sampled at that time.

Reconnaissance survey on Akpatok Island

A one-day reconnaissance survey was carried out on the 15th of August 2014, during which ten localities were visited, and five and thirteen samples were collected for Rock-Eval 6 analysis and processing for conodont microfossils, respectively (Table 1), The authors tried to collect data to answer the following questions:

- Is there any petroleum source rock better than that reported by Macauley (1987), and what is its stratigraphic position?
- What is the total thickness of the Paleozoic strata exposed on the island?
- What needs to be done, if more detailed fieldwork is planned for 2015?

Data collection for petroleum source-rock potential

A deeply cut valley (Figure 1b, c) is located immediately southeast of the Akpatok F-26 wellsite. In the valley, the

Table 1: Summary of field localities and sample sites during a one-day reconnaissance survey in 2014.

Station	Co-ordinates		Sample	
			Conodonts (C)	Rock Eval (R)
1	60°25'31.1"	68°20'02.3"	No samples	
2	60°25'26.7"	68°19'38.2"	SZ14-02A-01C SZ14-02A-02C	SZ14-02A-02R
3	60°25'25.3"	68°19'34.6"		SZ14-03A-01R SZ14-03A-02R
4	60°25'34.3"	68°20'04.1"		SZ14-04A-01R
5	60°25'37.3"	68°20'10.6"	SZ14-05A-01C SZ14-05A-02C	
6	60°24'42.5"	68°17'07.5"	SZ14-06A-01C SZ14-06A-02C SZ14-06A-03C	
7	60°28'54.8"	68°11'09.8"	SZ14-07A-01C SZ14-07A-02C	
8	60°29'15.0"	68°16'57.7"	SZ14-08A-01C SZ14-08A-02C	
9	60°30'04.5" 60°29'57.2"	67°53'31.5" 67°53'32.6"	SZ14-09A-01C SZ14-09A-02C	
10	60°28'02.7"	67°56'53.7"	No samples	

rocks are very well exposed on the upper part of the escarpments, but deeply eroded and covered by the rubble for most of the lower part of the cliff. Only 2–3 m of strata are exposed at the bottom of the escarpments around station 2.

In this valley, a 21 m interval of argillaceous and bituminous limestone was described by Workum et al. (1976), but Macauley (1987) indicated that no exposures of good organic-rich limestone were found on Akpatok Island. During the one-day reconnaissance survey, a search for the outcrops of argillaceous and bituminous limestone in this valley was carried out on foot from 10:30 a.m. to 2:00 p.m., but no such outcrop was found. However, almost in-place rubble of argillaceous and bituminous limestone was found at three localities (Figure 1c, stations 2-4).

Station 2

Station 2 is near the mouth of the valley, about 450 m east-southeast of the Akpatok F-26 wellsite (Figure 1c). At this station, a large piece of local, brown, argillaceous and bituminous limestone rubble was found (Figure 3a); one sample (SZ14-02A-02R) was collected for Rock-Eval 6 analysis.

Station 3

Station 3 is about 80 m east-southeast of station 2 (Figure 1c). Two large pieces of local, brown, argillaceous and bituminous limestone rubble were found at this locality (Figure 3b–d), and three samples were collected for Rock-Eval 6 analysis. Sample SZ14-03A-03R was from a graptolite-rich fossiliferous layer on the top of the local, brown, argillaceous and bituminous limestone rubble (Figure 3d).

Station 4

Station 4 is adjacent to the Akpatok F-26 wellsite (Figure 1c); the area around the wellsite is flat and allows a Twin Otter plane to land and take off. The flat area is covered by deeply eroded limestone rubble, the colour of some pieces of rubble being lighter than the others (Figure 3e). When the light-coloured rubble is broken, it shows the true colour of the brown, argillaceous and bituminous limestone (Figure 3f). One sample (SZ-04A-01R), containing a number of small pieces of light-coloured rubble, was collected for Rock-Eval 6 analysis.

Estimate of the elevation of the brown argillaceous and bituminous limestone

The brown, argillaceous and bituminous limestone rubble, which was found at stations 2 and 3 between the 10 and 20 m contour lines, and at station 4 between 20 and 30 m (Figure 1c), is most likely somewhat displaced. Therefore, the interval of brown argillaceous and bituminous limestone almost certainly occurs between 10 and 40 m above mean sea level in the valley where the samples were collected; however, it is currently unknown if the entire 30 m thick succession is composed of the argillaceous and bituminous limestone.

Rock-Eval 6 data

Rock-Eval 6 data (Table 2) were generated from five samples collected from the three localities mentioned above. The Rock-Eval 6 experimental procedure, and its application to hydrocarbon exploration, are presented in Lafargue et al. (1998) and Behar et al. (2001). The guidelines developed by Peters (1986) for Rock-Eval 2 were used in interpreting the data herein.

1) **Total organic carbon (TOC) and free (S1) and residual (S2) hydrocarbons:** TOC >2%, S1 >2 mg HC/g rock and S2 >10 mg HC/g rock are considered to be very good potential source rocks (Peters, 1986). Five samples have average and maximum TOC, S1, and S2 values of 3.11 and 4.19%, 0.56 and 1.04 mg HC/g rock, and 18.5 and 26.38 mg HC/g rock, respectively (Table 2), indicating a good to very good petroleum source rock.

2) **Temperature at S2 peak (T_{max}) and production index (PI):** Petroleum generation requires T_{max} values of at least 435–445°C, depending upon the kerogen type. Samples with S2 <0.2 mg HC/g rock are considered to produce unreliable T_{max} values, whereas PI of 0.1 is the minimum value to indicate oil generation (Peters, 1986). The five samples have S2 between 8.71 and 26.38 mg HC/g rock, significantly >0.2. Their T_{max} and PI values range from 423 to 426°C (averaging 425°C), and from 0.02 to 0.04 (averaging 0.03), respectively (Table 2). Therefore, the brown argillaceous and bituminous limestone is thermally immature.

3) **Hydrogen index (HI), ratio of S2 to S3 (S2/S3) and kerogen type:** HI >600 with S_2/S_3 >15 and HI of 300–600 with an S2/S3 ratio of 10–15 are assigned to Type I and Type II kerogen, respectively (Peters, 1986). Five samples have HI between 494 and 666 with S2/S3 between 9.4 and 30.7, so it is difficult to determine if the brown argillaceous and bituminous limestone contains Type I or Type II kerogen, or a mixture of these two end members. The modified van Krevelen diagram (Figure 4) also does not provide a clear answer, although a decrease of HI coupled with an increase of OI could suggest some oxidation of organic matter in these immature samples.

Data collection for stratigraphy

Ordovician rocks are mostly exposed on vertical cliffs on Akpatok Island. In order to search for outcrops with workable sections and the highest elevation with exposed outcrop, a reconnaissance survey was carried out on foot and with helicopter support from 2:30 pm to 6:30 pm on August 15, 2014.

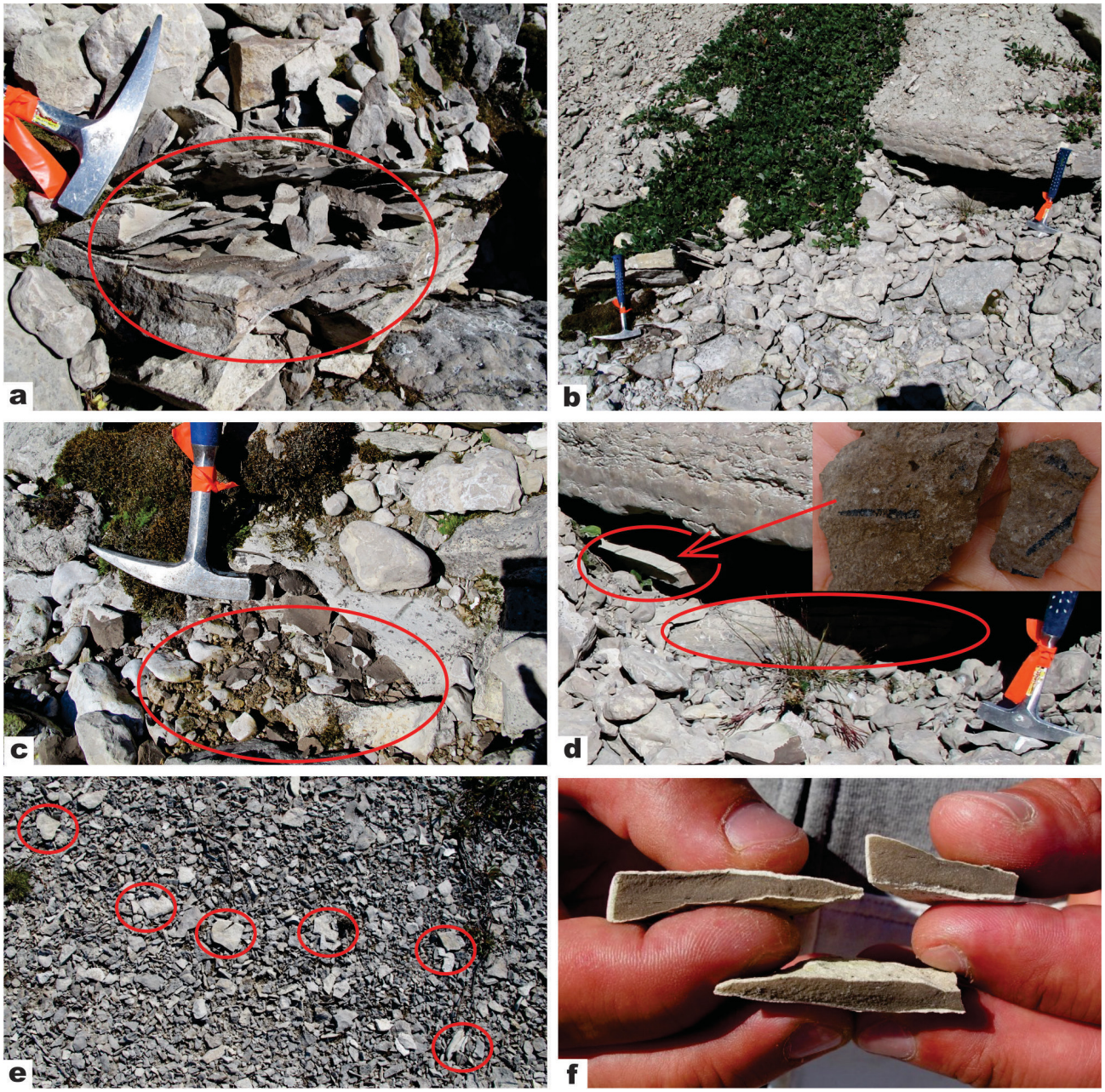

Figure 3: Brown argillaceous and bituminous limestone rubble at stations 2 **(a)**, 3 **(b–d)** and 4 **(e, f)**; c is an enlargement of the area marked by the hammer in the lower left corner of b; d is an enlargement of the area marked by the hammer on the right side of b, and is where the graptolites were found; f shows the internal colour of the light-coloured rubble in e. See Figure 1c for station locations.

Table 2: Rock-Eval 6 data for five samples of brown, argillaceous and bituminous limestone rubble from stations 2–4. Abbreviations: C-#, Geological Survey of Canada curatorial number; HI, hydrogen index (S2/TOC); MINC, mineral carbon; OI, oxygen index (S3/TOC); OICO, oxygen index specific to CO; PC, Pyrolyzable organic carbon; PI, production index; RC, residual organic carbon; S1, free hydrocarbons; S2, hydrocarbon potential; S3, CO_2 from organic source (mg CO_2/g TOC); S3CO, CO from organic source (mg CO/g TOC); T_{max}, temperature at S2 peak; T_{peak}, the maximal temperature reached during the S2; TOC, total organic carbon.

Sample	C-#	Qty.	S1	S2	PI	S3	T_{max}	T_{peak}	S3CO	PC (%)	TOC	RC (%)	HI	OICO	OI	MINC (%)
SZ14-02A-02R	C-475445	50.8	0.20	8.71	0.02	0.46	426	464	0.08	0.78	1.52	0.74	573	5	30	10.6
SZ14-03A-01R	C-475446	50.2	1.04	26.38	0.04	0.86	423	461	0.31	2.34	4.13	1.79	639	8	21	9.8
SZ14-03A-02R	C-475447	50.4	0.75	23.52	0.03	0.86	426	464	0.31	2.06	3.53	1.47	666	9	24	9.2
SZ14-03A-03R	C-475448	50.3	0.59	23.07	0.03	2.02	426	464	0.70	2.07	4.19	2.12	551	17	48	9.0
SZ14-04A-01R	C-475449	50.6	0.22	10.76	0.02	1.15	424	462	0.37	0.98	2.18	1.20	494	17	53	7.7

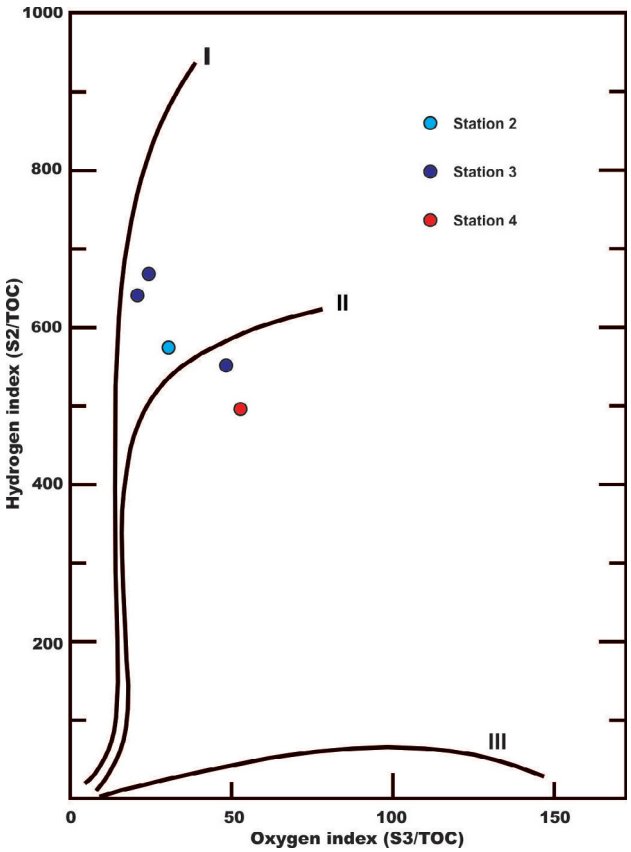

Figure 4: Modified van Krevelen diagram showing the relationship between hydrogen and oxygen indices of five samples of brown argillaceous and bituminous limestone rubble from stations 2–4.

Stations 5 and 6

Station 5 (Figures 1b, c, 5a) is about 200 m northwest of the Akpatok F-26 wellsite, and forms a cliff close to the shore. This cliff exposes the lowest identified Ordovician outcrop at high tide. Two samples were collected from this station for processing of conodont microfossils (Table 1); this hopefully will help in addressing the contentious assignment to either the Frobisher Bay Formation or the Amadjuak Formation.

Station 6 (Figures 1b, c, 5b) is in the upper reach of the southern branch of the valley where stations 1–4 are located. This is the outcrop with the highest elevation (130 m) in this valley, and the exposed rocks form a relatively flat-lying topography compared to its lower reach. No macrofossils were found. Three samples were collected at this station for processing of conodont microfossils (Table 1) in order to assign these beds to the Amadjuak Formation or Akpatok Formation.

Station 7

The highest elevation on Akpatok Island, 280 m, occurs in the central portion of the island; it is marked by a white dot in Figure 1b. The search for the highest elevation where Ordovician rocks are exposed started at this point and followed a dry creek marked by the blue line in Figure 1b. Unfortunately, this part of the creek is shallow, dry and covered by limestone rubble. There are no outcrops between the highest point of the island and station 7, at an elevation of 140 m (Figure 1b). The outcrop at station 7 is shown in Figure 5c, where the exposed rocks form gentle topography. A fossil cephalopod (Figure 6a) was found at station 7. Although this is a common macrofossil in the Amadjuak Formation (or Bad Cache Rapids Group), it cannot be used as an index fossil to determine stratigraphic position because of the poor preservation and the absence of other fossils. Two samples were collected for processing of conodont microfossils (Table 2).

Station 8

Station 8 is in the lower reach of the creek where station 7 is located (Figure 1b). This part of the creek is a deeply cut valley, and well exposed rocks form vertical cliffs (Figure 5d) at an elevation of 70 m. Fossil gastropods (Figures 6b, c) and cephalopods (Figure 6d) were found at station 8; in particular, the characteristic macluritid gastropod (Figure 6c) is present in most strata of the Amadjuak Formation in the Foxe Basin area and Bad Cache Rapids Group on Southampton Island (Bolton, 2000). Based on this, there is little doubt that the Amadjuak Formation occurs on Akpatok Island. Two samples were collected from station 8 for processing of conodont microfossils (Table 2).

Station 9

Station 9 is located within a valley on the northeast coast of the island, about 10–20 m above mean sea level (Figure 1b). The elevation of this location is slightly higher than station 5 on the west coast. The rocks are well exposed in the cliffs along the valley (Figure 5e), although no macrofossils were found at this station. Two samples were collected from station 9 for processing of conodont microfossils (Table 2), in order to test whether the Frobisher Bay Formation is present above sea level on the island.

Station 10

Station 10 is an observation station in the same valley as station 9. At an elevation of about 140 m, the outcrop disappears.

Estimate of the stratigraphic position of the brown argillaceous and bituminous limestone

The estimate of the stratigraphic position of the brown argillaceous and bituminous limestone is based on the following observations: 1) the macluritid gastropod (Figure 5e), the characteristic fossil of the Amadjuak Formation, was found at station 8 at an elevation of 70 m; and 2) the rubble of the brown argillaceous and bituminous limestone was found at elevations between 10 and 30 m. Therefore, it is most likely that the organic-rich interval occurs in the lower Amadjuak Formation on Akpatok Island.

Future work

Post-reconnaissance survey

Post-reconnaissance studies include 1) analysis of Rock-Eval 6 data collected from the samples of brown argillaceous and bituminous limestone, the results of which are presented and discussed herein, and 2) processing (currently underway) of the limestone samples for conodont microfossils, for subsequent lithostratigraphic and biostratigraphic interpretation.

Future fieldwork

In order to answer the scientific questions raised in the introduction, more detailed data than those collected during the one-day reconnaissance survey are definitely needed.

Figure 5: Outcrops at **a)** station 5 (indicated by red arrow), **b)** station 6, **c)** station 7, **d)** station 8, and **e)** station 9.

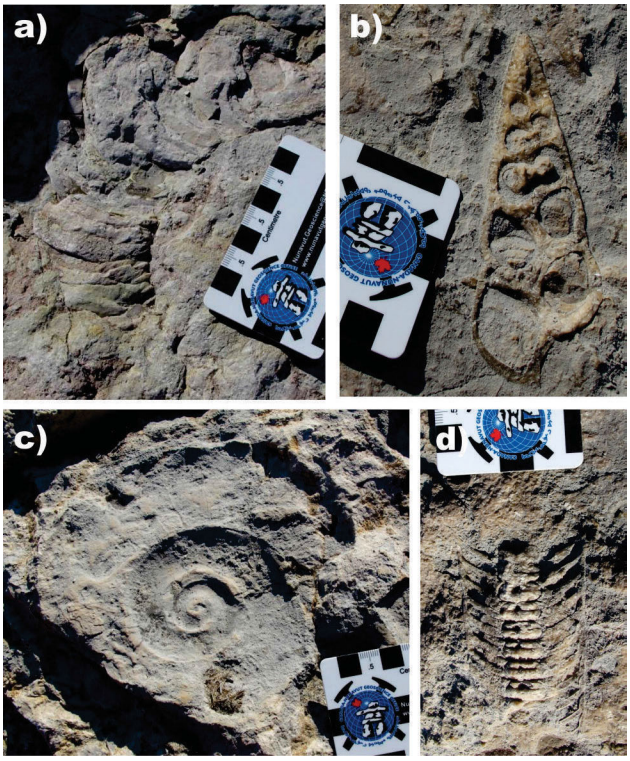

Figure 6: Selection of the fossils found during the one-day reconnaissance: **a)** cephalopod at station 7, **b)** and **c)** gastropods at station 8, and **d)** cephalopod at station 8.

Detailed study of the brown argillaceous and bituminous limestone

There is no doubt that an organic-rich interval occurs in the Ordovician sedimentary sequence on Akpatok Island. However, the outcrops that expose this interval have so far not been found. Therefore, the thickness and the true TOC content of this interval are unknown. Future fieldwork should focus on searching for outcrops with brown argillaceous and bituminous limestone at an elevation between 10 and 40 m in the valley where the rubble was found, as well as in other valleys on the island. If the outcrops are found, samples for Rock-Eval 6 analysis should be collected at regular intervals if the succession is monotonous.

Detailed sampling for biostratigraphic study

No outcrops above an elevation of 130–140 m were found during this reconnaissance survey; moreover, outcrops have not been reported by any previous studies. Therefore, any future fieldwork should focus on the search of outcrops between 140 and 280 m. In order to identify the different stratigraphic units and to eventually propose sound biostratigraphic correlation with other areas in Foxe Basin and Hudson Bay, samples for processing of conodont microfossils need to be collected at vertical intervals of 2 m or less and cover the three following parts of the strata: 1) the lowest accessible outcrops at low tide (dark colour of the foreground in Figure 5a); 2) the known outcrops 10–140 m above mean sea level; and 3) any newly discovered outcrops between 140 and 280 m.

Economic considerations

The aim of the project was to evaluate the presence of an organic-rich interval (i.e., the source rock of the petroleum system) in the Paleozoic stratigraphic framework of the Ungava Bay area. This one-day reconnaissance survey on Akpatok Island resulted in 1) identification of the elevation and possible stratigraphic position of the organic-rich interval, and 2) recognition that the Ordovician sedimentary succession on Akpatok Island contains good to very good petroleum source rock. As such, it has contributed new data and led to a better understanding of the petroleum potential in the region.

This preliminary work has increased the understating of the Ordovician stratigraphy and petroleum potential in the Ungava Bay area and could eventually assist in the evaluation of the petroleum system in the Hudson Strait, where the Ordovician source rocks might have been buried at sufficient depth for the generation of petroleum (Pinet et al., 2013). Future exploration activities might result in economic hydrocarbon discoveries that would benefit northern communities and economic development in Nunavut.

Acknowledgments

This project is part of the Geo-mapping for Energy and Minerals (GEM) program Hudson-Ungava project. Financial support from the GEM program and logistic support from the Polar Continental Shelf Project (PCSP) are greatly appreciated.

The authors thank the polar-bear monitors from Avataa Explorations and Logistics Inc. in Kuujjuaq, northern Quebec. Special thanks go to R. Stewart (Geological Survey of Canada–Calgary) for his help in collecting Rock-Eval 6 data, C. Gilbert (Canada-Nunavut Geoscience Office) for her compilation of the elevation map and D. Lavoie (Geological Survey of Canada–Quebec) for his review of the manuscript.

Natural Resources Canada, Earth Sciences Sector contribution 20140279

References

Behar, F., Beaumont, V. and De B. Penteado, H.L. 2001: Rock-Eval 6 technology: performances and developments; Oil and Gas Science and Technology – Rev. IFP, v. 56, no. 2, p. 111–134, doi:10.2516/ogst:2001013

Bolton, T.E. 2000. Ordovician megafauna, southern Baffin Island, Nunavut; *in* Geology and Paleontology of the Southeast Arctic Platform and Southern Baffin Island, Nunavut, A.D. McCracken and T.E. Bolton (ed.), Geological Survey of Canada, Bulletin 557, p. 39–158.

Grant, A.C. and Manchester, K.S. 1970: Geophysical investigation in the Ungava Bay–Hudson Strait region of northern Canada; Canadian Journal of Earth Sciences, v. 7, p. 1062–1076.

Kerkhoff, L.F. 1971: Well history report: Premium-Homestead Akpatok F-26; Canada Department of Energy, Mines and Resources, Resource Management and Conservation Branch, 34 p.

Lafargue, E., Marquis, F. and Pillot, D. 1998: Rock-Eval 6 applications in hydrocarbon exploration, production and soil contamination studies; Revue de l'Institut Français du Pétrole, v. 53, no. 4, p. 421–437.

Macauley, G. 1987: Geochemistry of organic-rich Ordovician sediments on Akpatok and Baffin islands, Northwest Territories; Geological Survey of Canada, Open File 1502, 27 p.

Peters, K.E. 1986: Guidelines for evaluating petroleum source rock using programmed pyrolysis; American Association of Petroleum Geologists Bulletin, v. 70, p. 318–329.

Pinet, N., Lavoie, D. and Keating, P. 2013: Did the Hudson Strait in Arctic Canada record the opening of the Labrador Sea? Marine and Petroleum Geology, v. 48, p. 354–365, doi:10.1016/j.marpetgeo.2013.08.002

Sanford, B.V. and Grant, A.C. 1990: New findings relating to the stratigraphy and structure of Hudson Platform; *in* Current Research, Part D, Geological Survey of Canada, Paper 90-1D, p. 17–30.

Sanford, B.V. and Grant, C. 2000: Geological framework of the Ordovician system in the southeast Arctic Platform, Nunavut; *in* Geology and paleontology of the southeast Arctic Platform and southern Baffin Island, Nunavut, A.D. McCracken and T.E. Bolton (ed.), Geological Survey of Canada, Bulletin 557, p. 13–38.

Workum, R.H., Bolton, T.E. and Barnes, C.R. 1976: Ordovician geology of Akpatok Island, Ungava Bay, District of Franklin; Canadian Journal of Earth Sciences, v. 13, p. 157–178.

Zhang, S. 2008: New insights into Ordovician oil shale in Hudson Bay Basin: their number, stratigraphic position, and petroleum potential; Bulletin of Canadian Petroleum Geology, v. 56, p. 329–352.

Zhang, S. 2012: Ordovician stratigraphy and oil shale, southern Baffin Island, Nunavut—preliminary field and post-field data; Geological Survey of Canada, Open File 7199, 26 p., doi:10.4095/291521

Zhang, S. 2014: Rock-Eval 6 data from the Premium-Homestead Akpatok F-26 well on Akpatok Island, Nunavut; Geological Survey of Canada, Open File 7627, 23 p., doi:10.4095/293963

Geological framework of the 1.9–1.6 Ga Elu Basin, western Nunavut: representative sedimentology, gamma-ray spectrometry and lithogeochemistry

A. Ielpi[1,2] and R.H. Rainbird[2]

[1]*Canada-Nunavut Geoscience Office, Iqaluit, Nunavut, alessandro.ielpi@nrcan.gc.ca*

[2]*Natural Resources Canada, Geological Survey of Canada, Ottawa, Ontario*

This work was part of the Geo-mapping for Energy and Minerals (GEM) Program in the Elu Basin area. It is being co-led by the Geological Survey of Canada (GSC) and the Canada-Nunavut Geoscience Office. The study area comprises National Topographic System map area 77A. The objective of this work is to improve the sedimentological framework within the Elu Basin and explore its economic potential.

Ielpi, A. and Rainbird, R.H. 2015: Geological framework of the 1.9–1.6 Ga Elu Basin, western Nunavut: representative sedimentology, gamma-ray spectrometry and lithogeochemistry; *in* Summary of Activities 2014, Canada-Nunavut Geoscience Office, p. 89–96.

Abstract

The Paleo- to Mesoproterozoic Elu Basin is located in the Kitikmeot Region of Nunavut, Canada, and consists of a 1.9–1.6 Ga belt of sandstone-dominated fluvial deposits and shallow-marine carbonate rocks resting unconformably on Archean metasedimentary, metaigneous and granitoid rocks of the Slave Province. During the summer of 2014, the first phase of the three year Elu Basin geoscience project focused on the stratigraphic and sedimentological analysis of fluvial sandstone-dominated deposits, as well as on an overall reconnaissance of the study area. Field observations were integrated with gamma-ray spectrometry and targeted lithogeochemical sampling. Study results have led to the development of an improved stratigraphic and sedimentological framework for the lower units of the Elu Basin, and an improvement of the exploration context for unconformity-related uranium deposits. Investigation of unconformity surfaces, the preferential targets, was carried out using gamma-ray spectrometry and bulk-rock sampling, especially where coarse-grained clastic rocks directly overlie metasedimentary and metaigneous rocks. Accessory mineralization was also recognized along stratigraphic unconformities within the basin fill. The results underline the exploration potential of both low-cost and time-efficient gamma-ray spectrometry for identifying concentrations of radioactive nuclides, and bulk geochemical analyses for determining concentrations of base metals and rare-earth elements such as zirconium, barium, lanthanum and cesium.

Résumé

Le bassin d'Elu, dont l'âge s'étend du Paléoprotérozoïque au Mésoprotérozoïque et qui se situe dans la région de Kitikmeot, au Nunavut (Canada), se compose d'une zone de dépôts fluviaux surtout constitués de grès et de roches carbonatées mis en place en milieu marin peu profond, et lesquels reposent à leur tour en discordance sur les roches métasédimentaires, métaignées et granitoïdes archéennes de la province des Esclaves. Au cours de l'été de 2014, la première phase du projet géoscientifique du bassin d'Elu, qui doit s'étendre sur trois ans, a porté sur l'analyse stratigraphique et sédimentologique des dépôts fluviaux à prédominance de grès et sur des activités de reconnaissance générale de la région à l'étude. Aux observations de terrain sont venus s'ajouter des travaux de spectrométrie gamma et d'échantillonnage lithogéochimique sélectif. Les résultats obtenus ont permis d'améliorer non seulement le cadre stratigraphique et sédimentologique s'appliquant aux unités inférieures du bassin d'Elu, mais aussi les conditions liées à l'exploration des gisements d'uranium associés à des discordances. Les travaux de spectrométrie gamma et d'échantillonnage massif se sont effectués surtout sur les surfaces de discordance, soit des zones qui constituent des cibles préférentielles, plus particulièrement aux endroits où les roches clastiques à grain grossier reposent directement sur les roches métasédimentaires et métaignées. Des traces de minéralisation dite « accessoire » ont également été remarquées le long de discordances stratigraphiques au sein du remplissage de bassin. Les résultats obtenus mettent en valeur les avantages potentiels que présentent aussi bien le recours à la spectrométrie gamma, qui s'avère une méthode rentable et rapide pour localiser les concentrations en nucléides radioactifs, que l'analyse géochimique, à l'aide de laquelle il est possible d'établir le potentiel d'une région en matière d'exploration en vue d'y déceler la présence de concentrations de métaux communs et d'éléments des terres rares, tels le zirconium, le baryum, le lanthane et le césium.

This publication is also available, free of charge, as colour digital files in Adobe Acrobat® PDF format from the Canada-Nunavut Geoscience Office website: http://cngo.ca/summary-of-activities/2014/.

Introduction

The Elu Basin geoscience project started in the summer of 2014 as a three year field-based study developed to evaluate the stratigraphy, sedimentology and economic potential of Paleo- to Mesoproterozoic rocks exposed in western Nunavut (Rainbird and Ielpi, in press). The Elu Basin is located in the Kitikmeot Region of Nunavut (Arctic Canada; Figure 1) and consists of one of several intracratonic depocentres within the Canadian Shield (Fraser et al., 1970). Geological mapping of the Elu Basin was last performed during the 1970s and the area has been relatively ignored since then. However, many Paleo- to Mesoproterozoic basins of Northern Canada have well-known economic potential for uranium, lead-zinc and, to a lesser degree, nickel, cobalt, copper, iron, manganese, arsenic, sulphur and selenium (Long and Turner, 2012). Filling an existing lack of knowledge on the Elu Basin and its economic potential represents the main goal of the present geoscience project.

In the first year of the Elu Basin geoscience project, reconnaissance geological mapping has been integrated with depositional architectural analysis of large exposures, as well as with targeted sampling and analysis using a hand-held gamma-ray mass spectrometer. Two stratigraphic units have been investigated to date, the Burnside River and Ellice formations. Detailed sedimentological and depositional-architecture observations were made on the Ellice Formation. A database of field gamma-ray spectrometry data and bulk-rock geochemical analyses has been collected on all the clastic sedimentary units and basement rocks to establish background values, test for possible anomalies and evaluate the mineral potential.

Geological setting

The Elu Basin is approximately centred on 68°18'N to 107°40'W, and comprises an irregular ~100 by 30 km, east-northeast-oriented tract of Paleo- to Mesoproterozoic siliciclastic and carbonate rocks, which are exposed along the shores of Tariyunnuaq (formerly Melville Sound) and Elu Inlet (Figure 1). Along the south-southeastern flank of the basin, these strata rest unconformably on Archean rocks of the Slave Province. A dominant north-trending greenstone belt is bounded to the east and west by granitoid and gneissic rocks, and intersects the Elu Basin at Hope Bay ('Hope Bay greenstone belt'; Sherlock et al., 2012).

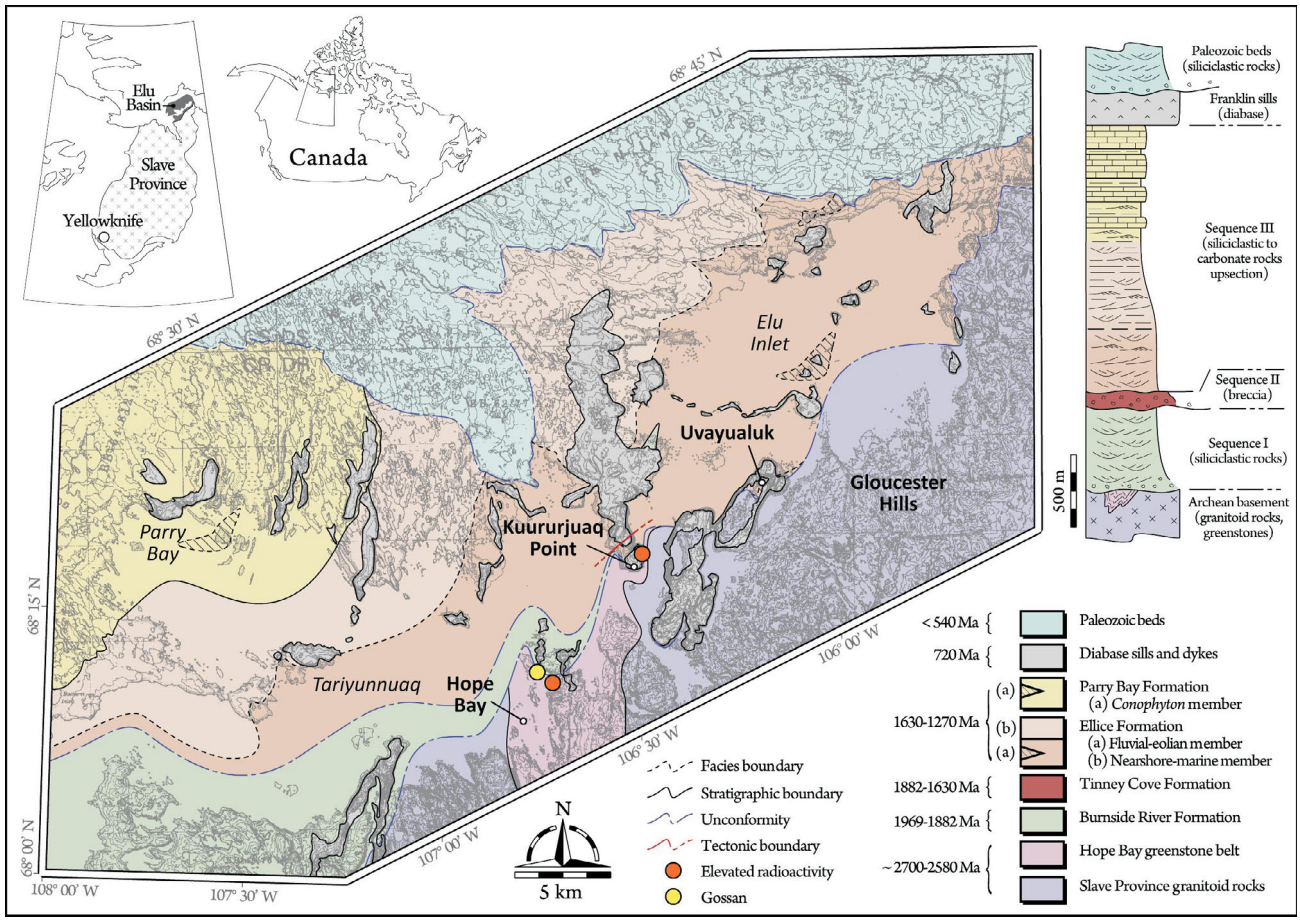

Figure 1: Preliminary geology of the Elu Basin, Kitikmeot Region, Nunavut, modified in part from Campbell (1979). Geochronology from Bowring and Grotzinger (1992) and Heaman et al. (1992). Place names with the generic in lower case are unofficial.

The Elu Basin fill consists of four lithostratigraphic units (from the oldest and lowermost): Burnside River, Tinney Cove, Ellice and Parry Bay formations (Campbell, 1979), which have been dated to 1.9–1.6 Ga (Bowring and Grotzinger, 1992; Heaman et al., 1992). The fluvial Burnside River Formation is composed of unsorted sandstone and conglomerate, and displays distinctive red staining due to iron-oxide cement and ubiquitous trough-crossbedding. The Tinney Cove Formation, recognized at only one locality in the Elu Basin, is a coarse, disorganized, conglomeratic unit interpreted as alluvial-fan to slope-scree deposits. The Ellice Formation is a continental to shallow-marine clastic unit, with overlying carbonate rocks. Carbonate rocks at the top of the Ellice Formation are gradational with the dolostone-dominated Parry Bay Formation, which accumulated in a shelf setting (Campbell, 1979). These deposits are grouped in three unconformity-bounded packages that are correlated with supra-regional sequences (Figure 1), the traceability of which extends across much of the Canadian Shield (Rainbird and Davis, 2007; Rainbird et al., 2007). The basin fill is cut by diabase sills and dykes attributed to the Franklin event at 720 Ma (Heaman et al. 1992) and is covered to the north-northeast by sedimentary deposits of suspected Cambrian to Ordovician age (O'Neill, 1924; Thorsteinsson and Tozer, 1962).

Methods

Helicopter-based studies were performed during the second half of July 2014, covering parts of NTS area 77A (Elu Inlet). The main objectives of this study were to investigate the sedimentology and fluvial architecture of the Burnside River and Ellice formations, as they comprise sandstone and conglomerate units deposited in mainly fluvial depositional settings. It was decided to focus on the Ellice Formation in 2014, with the Burnside River Formation in the western part of Tariyunnuaq to be studied in 2015. Detailed observations, including measurement of stratigraphic sections, were conducted along stepped, shore-platform and cliff exposures, up to 60 m high and laterally continuous for up to 400 m. The sedimentological features of the measured strata were observed along the same exposures. Facies and architectural analysis was aided by line-drawing on photographic panels derived from ground and oblique aerial imagery. Collection of ~1300 paleoflow measurements from crossbedding also supported paleogeographic reconstruction. Additional field activities included bulk sampling and collection of gamma-ray spectral signatures from all representative rock types, including basement rocks. Lithogeochemical analyses were performed by Activation Laboratories Ltd. (Ancaster, Ontario). Spectral signatures consist of a total radioactivity value expressed in nano-Sievert per hour (nSv/h), and bulk content of potassium (%), as well as uranium and thorium (ppm). The RS-125 model hand-held spectrometer manufactured by Radiation Solutions Inc. was used in the field. The full suite of results from bulk-rock geochemistry and gamma-ray spectrometry analyses is contained in CNGO Geoscience Data Series GDS2015-004[3].

Results

Basal contact relationships

In the study area, basal strata of the Elu Basin exhibit variable relationships with underlying rocks. In Tariyunnuaq and Elu Inlet, the Burnside River Formation overlies granitoid rocks, whereas in Hope Bay it overlies rocks of the Hope Bay greenstone belt, here consisting of folded metasedimentary, mafic metaigneous and mafic intrusive rocks (Sherlock et al., 2012). There is extensive hematitic alteration of the volcanic rocks, which are unconformably overlain by dark maroon sandstone and quartz-pebble–rich conglomerate that was deposited in depressions interpreted as paleovalleys. At Kuururjuaq Point (Figure 2a), to the northeast, a lenticular cliff-face exposure of angular sandstone-clast breccia and/or conglomerate up to 30 m thick belonging to the Tinney Cove Formation overlies ~10 m of maroon arkosic sandstone of the Burnside River Formation, from which the sandstone clasts were derived (Figure 2b). The Burnside River Formation overlies in turn foliated Archean volcanic rocks exposed along the shore, where the contact is partly obscured by large blocks of Franklin diabase derived from the cliff top. Further to the east, coarse micaceous sandstone of the basal Ellice Formation unconformably overlies hematite- and sericite-altered, red, granitic rocks of the Slave Province.

Sedimentology of the Ellice Formation

The Ellice Formation comprises an approximately fining-upward succession of quartz-rich sandstone 1 km thick, with minor conglomerate, shale and carbonate rocks. The sedimentology of the Ellice Formation is depicted in Figure 3. Detailed measured sections with paleoflow data are reported in Figure 4. Conglomerate is more abundant in the lower 200 m of the Formation, whereas the upper 500 m are dominated by interbedded fine-grained sandstone, shale and dolostone. Following this distinction, the Ellice Formation is here informally subdivided into a lower coarse-clastic member and an upper carbonate-clastic member.

In the coarse-clastic member, conglomerate and weakly sorted sandstone are ubiquitously trough-crossbedded in crosscutting, conglomerate-dominated lensoid units (Figure 3a), or large-scale sandstone-dominated inclined beds (Figure 3b). These units display a mildly dispersed paleoflow pattern lower in the section or in their coarser portions (Figure 4a). The upper sandstone-dominated por-

[3] *CNGO Geoscience Data Series GDS2015-004, containing the data or other information sources used to compile this paper, is available online to download free of charge at http://cngo.ca/summary-of-activities/2014 .*

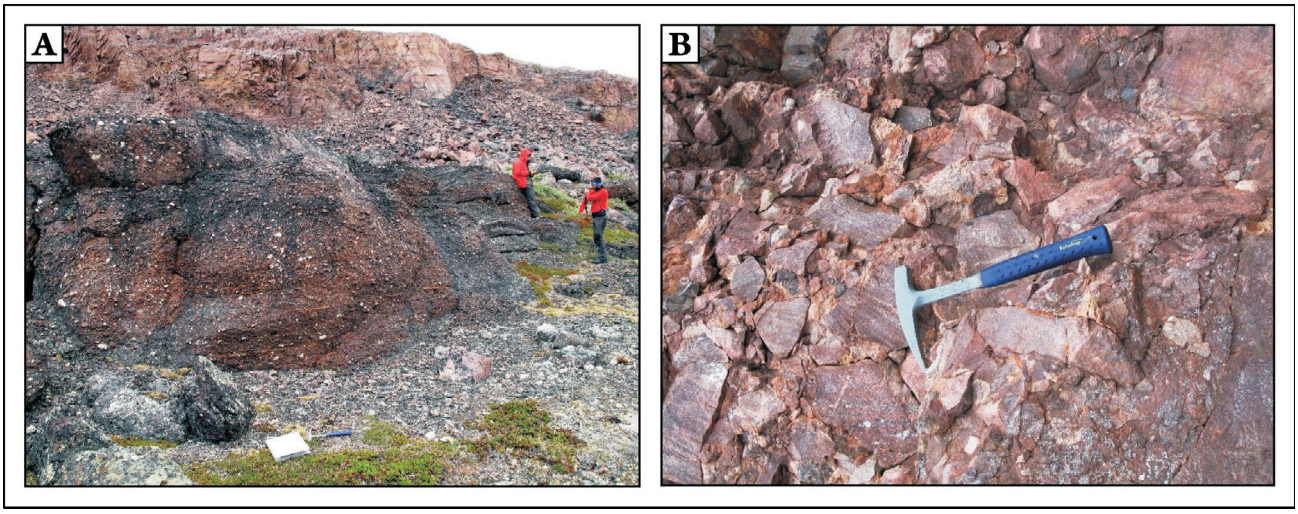

Figure 2: Basal conglomerate units in the Elu Basin, Kitikmeot Region, Nunavut: **a)** heterolithic, hematitic conglomerate of the Burnside River Formation overlying altered Archean metasedimentary rocks of the Hope Bay greenstone belt (left foreground); **b)** basal breccia of the Tinney Cove Formation composed exclusively of angular clasts from the underlying Burnside River Formation.

tions show less dispersion, with paleoflow consistently to the northwest (Figure 4b). Due to their weak sorting and abundance of unidirectional current indicators, these deposits are interpreted as representing a fluvial environment. Conglomeratic lensoid units possibly represent the fill of amalgamated channel belts and sandstone-dominated inclined beds are possibly the product of accretion and reworking of compound-channel bars (Bridge, 2006).

Isolated and large-scale planar crossbeds, composed of very well-sorted, fine- to medium-grained quartz sandstone, occur within the lower member fluvial deposits (Figure 3c, d). The deposits consist of tabular crossbed sets up to 4 m thick that display polymodal paleotransport. Due to their textural and compositional maturity, and distinctive large, tabular crossbedding, these deposits are interpreted as representing an eolian-dune environment (Hunter, 1977).

In the upper carbonate-clastic member, fine sandstone, siltstone and dolostone are organized in decimetre-thick strata that are planar and laterally extensive. The abundance of carbonate increases upsection toward the gradational contact with the overlying Parry Bay Formation. The clastic portion is compositionally mature but poorly sorted, ranging from fine-grained sand to silt. Typical lithology is parallel-laminated dark siltstone and wavy to parallel-laminated, tan-weathering dolomitic sandstone (Figure 3e). Wavy lenticular bedding is common. Thicker and coarser sandstone beds are lenticular with scoured bases and cross-stratified fill that displays unimodal northwest paleotransport. Further to the west, where it transitions into the Parry Bay Formation, crossbedded and wavy-bedded sandstone is interbedded within dome-topped dolostone strata composed of laterally linked stromatolites (Figure 3f). The close interbedding of these lithotypes points to a nearshore-marine to coastal plain environment, subject to deltaic progradation and shoreface aggradation during periods of enhanced clastic supply, and shallow-water carbonate shelves, which expanded during periods of clastic starvation (Ielpi, 2013). The overall upward increase in carbonate suggests an overall transgressive setting.

Gamma-ray spectrometry

Gamma-ray spectrometry of both basement and sedimentary rocks yielded background values of radioactive nuclides. Within the basement, analyses were performed on granitoid, greenstone (i.e., both extrusive and intrusive mafic metaigneous rocks) and metasedimentary rocks of the Archean Slave Province. Granitoid rocks yielded the highest dose rates, still to be considered as background, reaching 73.3 nSv/h on average and peaking at 118 nSv/h. These values result from concentrations of potassium, uranium and thorium of up to 6.8%, 2.7 ppm and 5.4 ppm, respectively. Mafic metaigneous and metagreywacke rocks have lower dose rates, with an average value of 30.2 nSv/h and peak of 55.6 nSv/h, attributed to concentrations of potassium, uranium and thorium of up to 1.7%, 3.6 ppm and 10.7 ppm, respectively.

Within the Elu Basin, dose rates vary from 7.8 to 216 nSv/h, averaging 68 nSv/h. Elevated dose rates in the lower stratigraphic units (i.e., Burnside River and Tinney Cove formations) occur in proximity to erosional unconformities. At Kuururjuaq Point, deposits of these two formations are characterized by dose rates of 92.8 and 97.5 nSv/h respectively, with peaks of 111.0 and 144.0 nSv/h. These results are attributed to values of potassium, uranium and thorium of up to 3.8%, 9.3 ppm and 26.6 ppm, respectively. Lower readings were recorded along the eastern shore of Hope Bay, where the lowermost deposits of the Burnside River

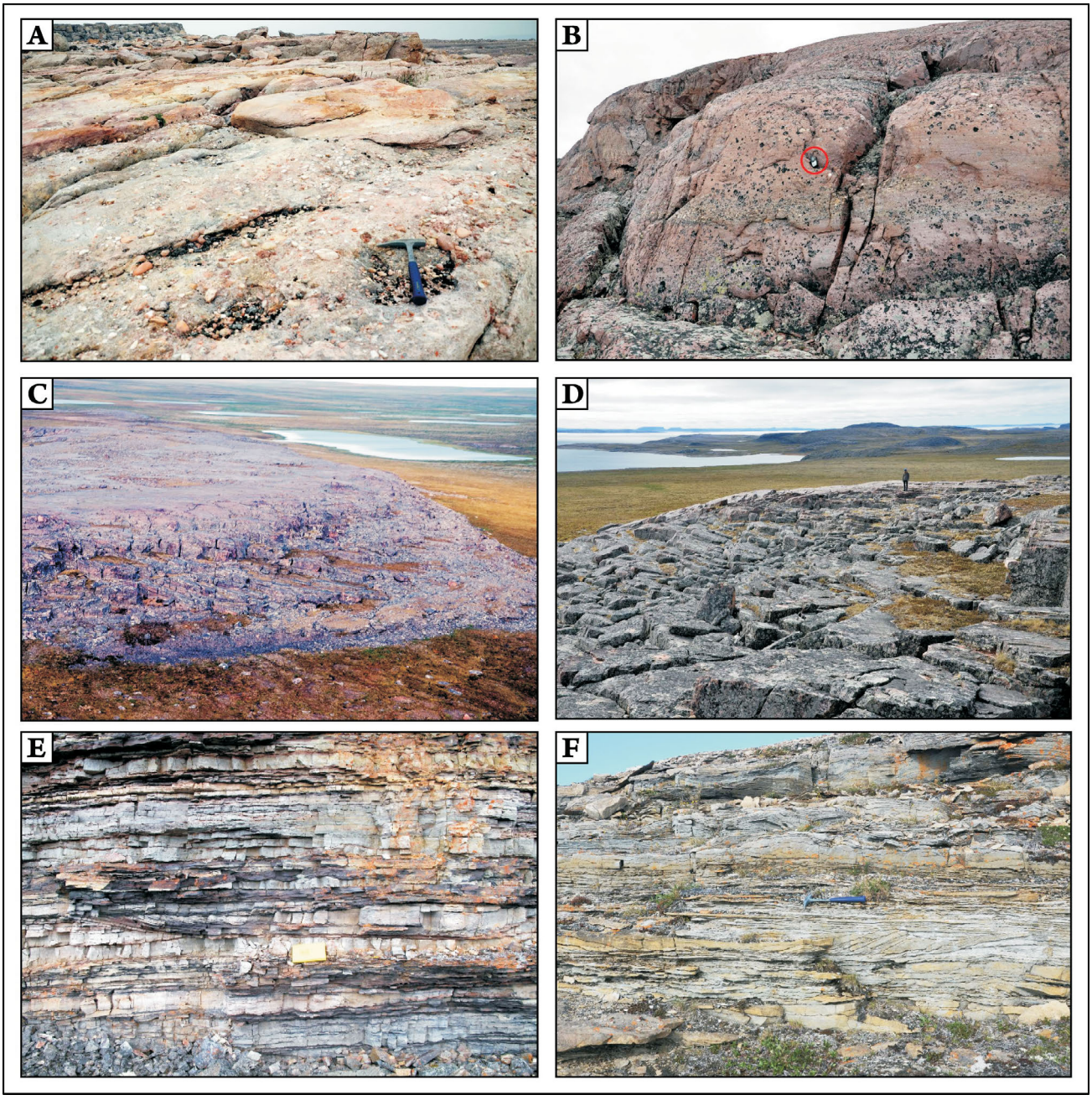

Figure 3: Sedimentological features of the Ellice Formation, Kitikmeot Region, Nunavut: **a)** lenses of pebble-cobble conglomerate are commonly preserved in the lower member (rock hammer for scale is 28 cm long); **b)** large-scale trough-crossbedding in pebbly sandstone of the lower member (hand-held radio circled for scale); **c)** oblique aerial view of large-scale, eolian crossbeds in the basal member (foresets are inclined to right; field of view approximately 50 m in foreground); **d)** outcrop-scale view of crossbedding shown in (a) with geologist in background for scale; **e)** heterolithic strata of the upper member (notebook for scale); **f)** stromatolitic dolostone layers (above rock hammer) in the uppermost part of the formation points to a gradational transition into the overlying Parry Bay Formation.

Formation yielded an average dose rate of 57.6 nSv/h, peaking at 93.1 nSv/h. In these deposits, radioactivity is linked to concentrations of potassium, uranium and thorium of up to 1.7%, 3.6 ppm and 22.7 ppm, respectively. A significant discrepancy between the natural radioactivity of basement rocks and that of their overlying deposits was noted at both these locations. Stratigraphically higher in the basin fill, the fluvial and eolian deposits of the Ellice Formation also yielded background values, with an average dose rate of 39.3 nSv/h and a peak of 164 nSv/h (from several locations). The nearshore-marine deposits of the Ellice Formation yielded slightly higher dose rates, with an average of 164.4 nSv/h and a peak of 216 nSv/h. These values are the product of concentrations of potassium, uranium and thorium of up to 9.5%, 4.9 ppm and 48.1 ppm, respectively.

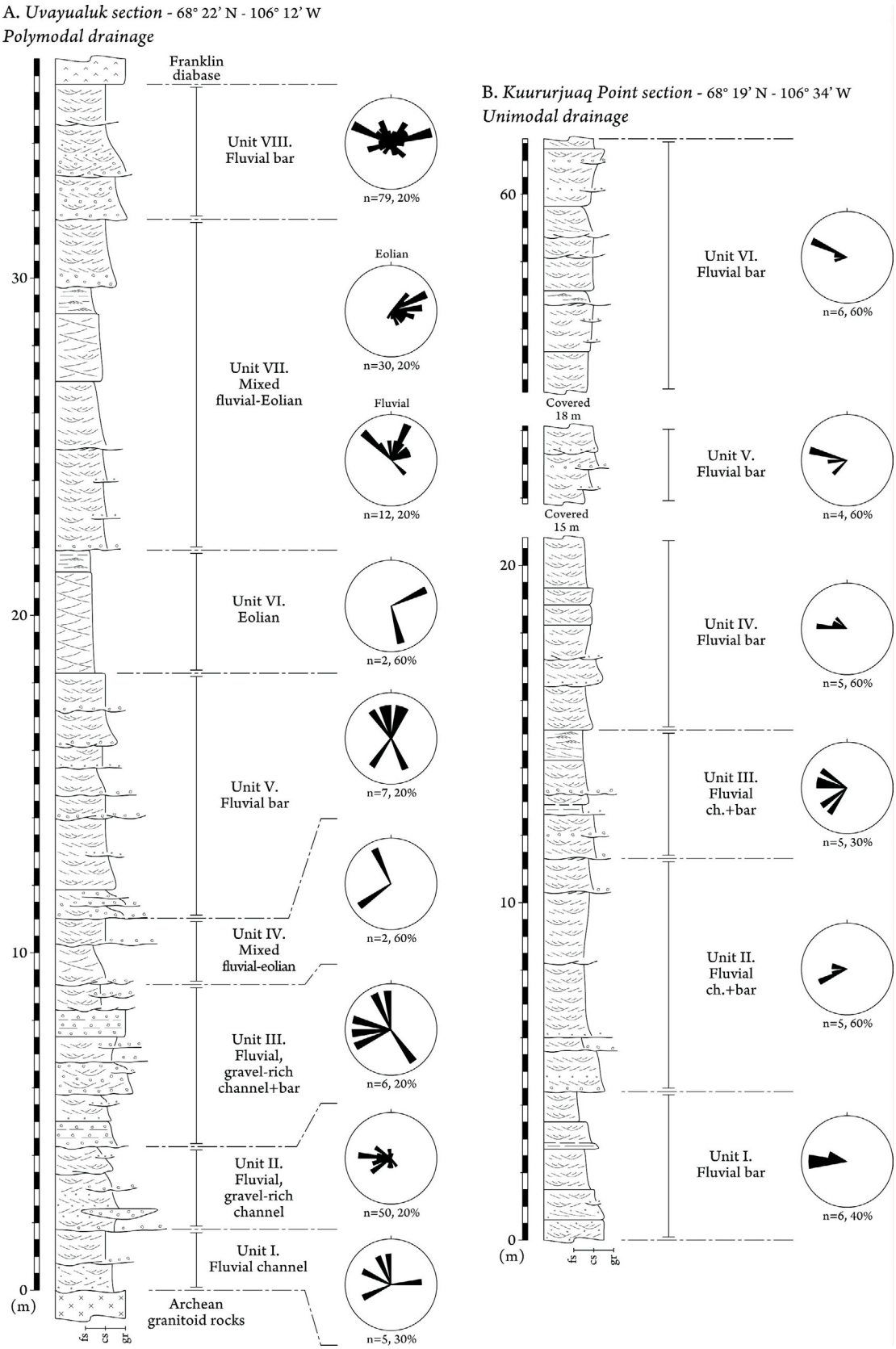

Figure 4: Sedimentary logs measured along two stepped-cliff exposures of the Ellice Formation, Kitikmeot Region, Nunavut, with paleoflow data showing mildly dispersed directions of transport in the lower stratigraphic portions measured at Uvayualuk, and more consistent northwest transport upsection at Kuururjuaq Point. Abbreviation: ch, channel.

Lithogeochemistry

Lithogeochemical analyses were conducted mostly on sedimentary rocks; however, a gossan contained within basement rocks was also sampled at one location. Two main localities were sampled: Hope Bay and Kuururjuaq Point (Figure 1). Along the eastern shore of Hope Bay, where pebble-conglomerate beds of the basal Burnside River Formation present slightly elevated radioactive-dose rates (see previous paragraph), 10 bulk samples were collected (14RAT010 A01 to A010). Analysis of this suite of samples generated homogeneous results, with concentrations of uranium and thorium varying between 1.47 and 6.53 ppm, and 3.4 and 19.1 ppm, respectively. By comparison, these values are slightly above background when compared to Athabasca Basin deposits (Jefferson et al., 2007). The suite of samples also yielded notable concentrations of zirconium (up to 371 ppm), likely related to the presence of heavy-mineral laminae. In a basement exposure within 200 m of this sampling site, a gossan is underlain by pyrite and chalcopyrite disseminated at the contact between gabbro and mafic metaigneous rocks of the Archean Hope Bay greenstone belt. A suite of five samples (14RAT027 A01 to A05) yielded negligible results on uranium and thorium, but anomalous values of gold (up to 8990 ppb), platinum (up to 87.9 ppb), copper (up to 1510 ppm) and arsenic (up to 802 ppm). By comparison, the highest gold concentrations in the nearby economic Doris site of the Hope Bay gold deposit reach 22 000 ppb (Carpenter et al., 2003). These results present evidence for gold-rich, volcanogenic massive-sulphide or precious-metal vein prospectivity.

At Kuururjuaq Point, the contact between the Burnside River and Tinney Cove formations presents slightly elevated radioactive-dose rates (see previous paragraph): here, a suite of 11 samples was collected, 5 from the Burnside River Formation (14RAT001 A02 to A06) and 6 from the Tinney Cove Formation (14RAT001 B03 to B08). Samples from the Burnside River Formation generated a homogeneous dataset, with background concentrations of uranium and thorium ranging between 2.02 and 3.24 ppm, and 5.12 and 11.4 ppm, respectively. The suite of samples also showed elevated values of zirconium (up to 171 ppm) and barium (up to 554 ppm), which suggests the presence of a detrital heavy-mineral source of thorium. Samples from the overlying Tinney Cove Formation showed more dispersed concentrations, ranging between 1.06 and 4.38 ppm for uranium, and 6.39 and 49.5 ppm for thorium. The latter suite of samples also generated notable concentrations of zirconium (up to 1073 ppm), barium (up to 394 ppm), lanthanum (up to 166 ppm) and cesium (up to 362 ppm), supporting yet again the likely presence of concentrations of detrital heavy minerals. No diagenetic phosphate minerals are suggested by these data.

Discussion and conclusions

Reconnaissance mapping was performed in the Elu Basin of Nunavut, Canada, as part of a three year multidisciplinary geoscience project. Field activities were aided by field gamma-ray spectrometry and lithogeochemical sampling with the aim of assessing possible mineral potential for an underexplored sector of Arctic Canada. Gamma-ray spectrometry and bulk-rock analyses yielded overall comparable results, underlining the efficiency of low-cost, field-based spectrometry for the exploration of sedimentary basins. Overall background levels of uranium characterize sandstone units and unconformable surfaces at the base of, or within, the basin fill. Field results confirm subdivision into four lithostratigraphic units that comprise three unconformity-bounded sequences, with supra-regional traceability. Lithogeochemical results show no correlation with stratigraphy, except for concentrations of detrital heavy minerals.

Detailed sedimentological studies of the Ellice Formation demonstrated a higher complexity in its internal architecture and stratigraphy than previously described. The Ellice Formation is here informally subdivided into a lower coarse-clastic member, deposited in fluvial and newly recognized eolian depositional environments, and an upper interbedded carbonate-clastic member, deposited in nearshore-marine to coastal plain environments. An upward increase in carbonate interlayers points to an overall transgressive setting. Sedimentological analyses were aided by the collection of paleoflow indicators. Fluvial paleoflow patterns display mild dispersion between west and north in lower or coarser portions of the Formation; the upper, sandstone-dominated portions exhibit less dispersed paleoflow toward the northwest. Eolian crossbedding exhibits polymodal paleotransport.

Economic considerations

Correlative sedimentary basins, such as the Thelon and Athabasca (Jefferson et al., 2007), contain the largest high-grade uranium deposits of the world, which are located in the proximity of their basal unconformity. Similar potential has been postulated for the unconformity between the Archean rocks of the Slave Province and the overlying Proterozoic terrestrial sandstone units (cf. Gall, 1994). The Ellice, Tinney Cove and Burnside River formations yielded overall background radiation, with slightly elevated readings reported at Kuururjuaq Point (Figure 1; Campbell, 1979). The field observations made this summer suggest that an accumulation of sediment on detrital heavy minerals contributed to these elevated dose rates. The analysis of a gossan overlying pyrite and chalcopyrite within basement rocks is consistent with the known gold, platinum and copper deposits in the Hope Bay greenstone belt (Sherlock et al., 2012). Other local concentrations of zirconium, barium,

lanthanum and cesium are consistent with detrital heavy minerals, and/or basement pegmatites.

Acknowledgments

The authors wish to thank W. Greenman for his valuable field assistance, and are grateful for the logistical support and comfortable base of operations provided by T-MAC Resources Inc. at their Doris Lake facility at Hope Bay. They warmly acknowledge the insightful review of the manuscript by C.W. Jefferson and D.J. Mate, who provided comments that significantly improved the text.

This project is part of the Geo-mapping for Energy and Minerals (GEM) program in the Elu Basin area. Financial support from the GEM program is greatly appreciated. The Canadian Northern Economic Development Agency's (CanNor) Strategic Investments in Northern Economic Development (SINED) program also provided financial support for this work. Logistical support and excellent piloting by D. Rusch and D. Bell from Great Slave Helicopters were provided through the assistance of the Polar Continental Shelf Project. Expediting services were ably provided by K. Vickers of Discovery Mining Services, Yellowknife.

Natural Resources Canada, Earth Sciences Sector contribution 20140304

References

Bowring, S.A. and Grotzinger, J.P. 1992: Implications of new chronostratigraphy for tectonic evolution of Wopmay Orogen, northwest Canadian Shield; American Journal of Science, v. 292, p. 1–20.

Bridge, J.S. 2006: Fluvial facies models: recent developments; *in* Facies Models Revisited, H.W. Posamentier and R.G. Walker (ed.), SEPM Special Publication, v. 84, p. 85–170.

Campbell, F.H.A. 1979: Stratigraphy and sedimentation in the Helikian Elu Basin and Hiukitak Platform, Bathurst Inlet–Melville Sound, Northwest Territories; Geological Survey of Canada, Paper 79-8, p. 19.

Carpenter, R.L., Sherlock, R.L., Quang, C., Kleespies, P. and McLeod, R. 2003: Geology of the Doris North gold deposit, northern Hope Bay volcanic belt, Slave Structural Province, Nunavut; Geological Survey of Canada, Current Research, 2003-C6, 10 pp.

Fraser, J.A., Donaldson, J.A., Fahrig, W.F. and Tremblay, L.P. 1970: Helikian basins and geosynclines of the northwestern Canadian Shield; *in* Symposium on Basins and Geosynclines of the Canadian Shield, A.J. Baer (ed.), Geological Survey of Canada, Paper 70-40, p. 213–238.

Gall, Q. 1994: The Proterozoic Thelon Paleosol, Northwest Territories, Canada; Precambrian Research, v. 68, p. 115–137.

Heaman, L.M., LeCheminant, A.N. and Rainbird, R.H. 1992: Nature and timing of Franklin igneous events, Canada: implications for a Neoproterozoic mantle plume and the break-up of Laurentia; Earth and Planetary Science Letters, v. 109, p. 117–131.

Hunter, R.E. 1977: Basic types of stratification in small eolian dunes; Sedimentology, v. 24, p. 361–387.

Jefferson, C.W., Thomas, D.J., Gandhi, S.S., Ramaekers, P., Delaney, G., Brisbin, D., Cutts, C., Portella, P. and Olson, R.A. 2007: Unconformity-associated uranium deposits of the Athabasca Basin, Saskatchewan and Alberta; *in* EXTECH IV: Geology and Uranium EXploration TECHnology of the Proterozoic Athabasca Basin, Saskatchewan and Alberta, C.W. Jefferson and G.D. Delaney (ed.), Geological Survey of Canada, Bulletin 588, p. 23–67.

Ielpi, A. 2013: Frequency-reliant correlative patterns of asymmetric lacustrine-paralic sequences: a genetic approach to the late Miocene Bithynia Marlstones of the southeastern Volterra Basin; Journal of Sedimentary Research, v. 83, p. 377–394.

Ielpi, A. and Rainbird, R.H., 2015: Data table accompanying "Geological framework of the 1.9-1.6 Ga Elu Basin, western Nunavut: representative sedimentology, gamma-ray spectrometry and litho-geochemistry"; Canada-Nunavut Geoscience Office, Geoscience Data Series GDS2015-004, Microsoft® Excel® file, URL <http://cngo.ca/summary-of-activities/2014/> [January 2015].

Long, D.F. G. and Turner, E.C. 2012: Tectonic, sedimentary and metallogenic re-evaluation of basal strata in the Mesoproterozoic Bylot basins, Nunavut, Canada: are unconformity-type uranium concentrations a realistic expectation?; Precambrian Research, v. 214–215, p. 192–209.

O'Neill, J.J. 1924: Geology of the Arctic coast of Canada, West of Kent Peninsula; *in* Report of the Canadian Arctic Expedition 1913-18, v. 11, Geology and Geography, Part A, 107 p.

Rainbird, R.H. and Davis, W.J. 2007: U-Pb detrital zircon geochronology and provenance of the late Paleoproterozoic Dubawnt Supergroup; linking sedimentation with tectonic reworking of the western Churchill Province, Canada; Geological Society of America Bulletin, v. 119, p. 314–328.

Rainbird, R.H. and Ielpi, A. in press: GEM 2 Rae Project: Reconnaissance mapping and thematic studies of the Elu Basin. Geological Survey of Canada, Open File.

Rainbird, R.H., Stern, R.A., Rayner, N.M. and Jefferson, C.W. 2007: Age, provenance, and regional correlation of the Athabasca Group, Alberta and Saskatchewan, constrained by igneous and detrital zircon geochronology; *in* EXTECH IV: Geology and Uranium EXploration TECHnology of the Proterozoic Athabasca Basin, Saskatchewan and Alberta, C. W. Jefferson and G. D. Delaney (ed.), Geological Survey of Canada, Bulletin 588, p. 193–209.

Sherlock, R.L., Shannon, A., Hebel, M., Lindsay, D., Madsen, J., Sandeman, H., Hrabi, B., Mortensen, J.K., Tosdal, R.M. and Friedman, R. 2012: Volcanic stratigraphy, geochronology, and gold deposits of the Archean Hope Bay greenstone belt, Nunavut Canada; Economic Geology, v. 107, p. 991–1042.

Thorsteinsson, R. and Tozer, E.T. 1962: Banks, Victoria and Stefansson Islands, Arctic Archipelago; Geological Survey of Canada, Memoir 330, 85 p.

Aeromagnetic survey of the McKeand River area, southern Baffin Island, Nunavut

W. Miles[1], D.J. Mate[2], M.R. St-Onge[3] and H.M. Steenkamp[4]

[1]*Natural Resources Canada, Geological Survey of Canada, Ottawa, Ontario, Warner.Miles@nrcan-rncan.gc.ca*

[2]*Canadian Northern Economic Development Agency, Iqaluit, Nunavut (formerly Canada-Nunavut Geoscience Office, Iqaluit, Nunavut)*

[3]*Natural Resources Canada, Geological Survey of Canada, Ottawa, Ontario*

[4]*Canada-Nunavut Geoscience Office, Iqaluit, Nunavut*

This work was part of the 2012–2014 Hall Peninsula Integrated Geoscience Program (HPIGP), led by the Canada-Nunavut Geoscience Office (CNGO) in collaboration with the Government of Nunavut, Aboriginal Affairs and Northern Development Canada, and the Geological Survey of Canada. It involved strong contributions from the Universities of Alberta, Dalhousie, Laval, Manitoba, Ottawa, Saskatchewan and New Brunswick, and the Nunavut Arctic College. It has benefitted from support by local and Inuit-owned businesses and the Polar Continental Shelf Program. The focus is on bedrock and surficial geology mapping (1:100 000 scale). In addition, a range of thematic studies is being conducted, including Archean and Paleoproterozoic tectonics, geochronology, landscape uplift and exhumation, microdiamonds, sedimentary-rock xenoliths and permafrost. The goal is to increase the level of geological knowledge and better evaluate the natural-resource potential in this frontier area.

Miles, W., Mate, D.J., St-Onge, M.R. and Steenkamp, H.M. 2015: Aeromagnetic survey of the McKeand River area, southern Baffin Island, Nunavut; *in* Summary of Activities 2014, Canada-Nunavut Geoscience Office, p. 97–104.

Abstract

An aeromagnetic survey of the McKeand River area on southern Baffin Island, Nunavut began in early August 2014. The survey will collect 74 818 line-km of data and is scheduled to be completed in November 2014. The new aeromagnetic data will help fill a gap in an area lacking any aeromagnetic coverage and having few published bedrock geological maps. Aeromagnetic surveys measure magnetic properties of underlying bedrock using a sensor in a fixed-wing aircraft or helicopter, and are one of the tools used in geological mapping. This new survey is designed to support new targeted geoscience projects and bedrock geology mapping to be undertaken by the Canada-Nunavut Geoscience Office (CNGO) and the Geological Survey of Canada (GSC) in the summer of 2015. These initiatives will be carried out as part of a two-year activity within the GEM-Baffin project area entitled 'Completing the regional bedrock mapping of the southern half of Baffin Island'.

Résumé

Un levé aéromagnétique de la région McKeand River dans la partie sud de la Terre de Baffin, au Nunavut, a commencé au début août, 2014. Le levé inclus 74 818 km linéaires et est prévu d'être achevé en novembre 2014. Le relevé fournira des données aéromagnétiques dans une zone sans couverture aéromagnétique existante et sans cartes géologiques de la roche en place publiées. Les levés aéromagnétiques mesurent les propriétés magnétiques de la roche en place et sont l'un des outils utilisés dans la cartographie géologique. Le levé a été conçu comme contribution aux nouveaux projets géoscientifiques ciblés et de cartographie géologie de la roche en place qui seront entrepris par le Bureau géoscientifique Canada-Nunavut (BGCN) et la Commission géologique du Canada (CGC) pendant l'été 2015 dans le cadre du projet GEM-Baffin, par l'intermédiaire de l'activité de deux ans intitulée « Fin de la cartographie régionale de la roche en place pour la moitié sud de la Terre de Baffin ».

Introduction

Geological mapping and thematic bedrock studies conducted by the Canada-Nunavut Geoscience Office (CNGO) on Hall Peninsula, Nunavut have significantly increased the level of geological knowledge in a frontier region. Accomplishments have included providing a better tectonic and metallogenic framework for the peninsula and identification of several new mineral-deposit types and showings. One of the more significant discoveries has been

This publication is also available, free of charge, as colour digital files in Adobe Acrobat® PDF format from the Canada-Nunavut Geoscience Office website: http://cngo.ca/summary-of-activities/2014/.

the occurrence of layered mafic–ultramafic intrusions, which may have Ni–Cu–platinum-group element (PGE) potential (Steenkamp et al., 2014). Steenkamp et al. (2015) have recently documented the occurrence of new, locally mineralized, layered mafic–ultramafic intrusions both north and south of Hall Peninsula, in the Irvine Inlet (NTS area 26G; Figure 1) and Meta Incognita Peninsula areas, respectively, indicating that this type of mineral occurrence can be expected across the broader region.

The McKeand River area, which encompasses the McKeand River, Irvine Inlet and Sylvia Grinnell Lake

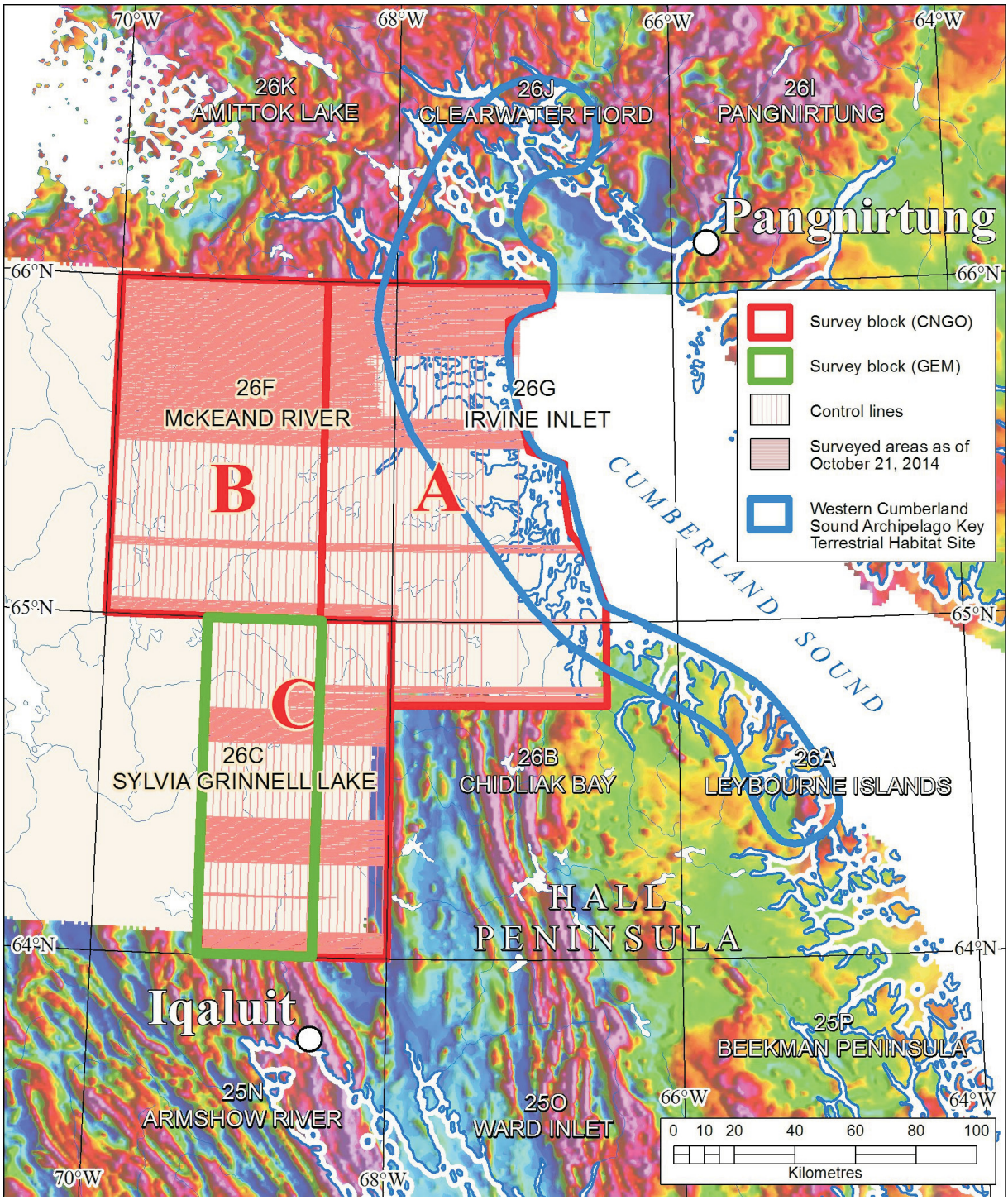

Figure 1: McKeand River area, showing aeromagnetic survey blocks, coverage supported variously by the CNGO and GSC Geomapping for Energy and Minerals (GEM) program, and the Western Cumberland Sound Archipelago Key Terrestrial Habitat Site (Latour et al., 2008).

1:250 000 NTS areas (NTS 26G, F and C, respectively; Figure 1), is devoid of modern baseline geoscience information (bedrock, surficial deposits and aeromagnetic data), thus making informed exploration and land-use decisions very difficult. Reconnaissance-scale geological mapping (1:506 880) conducted in the mid-1960s (Blackadar, 1967) currently provides the only ground-collected geoscience dataset for this area. Unfortunately, the data are too widely spaced to produce a regional geological map with the level of accuracy, confidence and scale required for modern-day applications. In order to address this knowledge gap and to build on the success of the Hall Peninsula Integrated Geoscience Program (Machado et al., 2013a, b; Steenkamp et al., 2014b), the CNGO is collaborating with the Geological Survey of Canada (GSC) Geo-mapping for Energy and Minerals (GEM) program to acquire new aeromagnetic data for the McKeand River area (Figure 1), located west and north of Hall Peninsula. This new dataset will be used to support future targeted CNGO geoscience projects, as well as a modern bedrock geology compilation by the GEM program for all of Baffin Island south of 70°N and east of 80°W.

Geological overview

Southern Baffin Island is underlain by Archean and middle Paleoproterozoic rocks that were metamorphosed and deformed during the accretionary and continental-collision phases of the Trans-Hudson orogeny. This major mountain-building event involved northwestward subduction of the Superior Plate craton beneath an amalgamated collage of smaller crustal blocks (Churchill Plate), with terminal collision occurring between 1.82 and 1.80 Ga (Hoffman 1988; Lewry and Collerson, 1990; St-Onge et al., 2007, 2009). The orogenic system extended from northeastern to south-central North America and has been physically and temporally compared to the Himalayas as a modern analogue (St-Onge et al., 2006).

The bedrock west of Cumberland Sound (NTS areas 26A through H) was previously mapped at 1:506 880 (Blackadar, 1967). This reconnaissance-scale mapping documented a dominance of variably deformed orthogneiss, orthopyroxene-bearing granite, and paragneiss comprising mostly pelite, psammite, quartzite and carbonate rock types. In general, foliation fabrics are west to southwest dipping and no major structural features, such as faults, have been reported.

Recently, the CNGO conducted fieldwork as part of the Hall Peninsula Integrated Geoscience Program (Machado et al., 2013a, b; Steenkamp et al., 2014a, b), which aimed to provide higher resolution bedrock (1:100 000) and surficial (1:125 000) coverage in NTS areas 26A and B. Field observations generally corroborate Blackadar's (1967) work but also document newly identified, large-scale isoclinal folds and thick-skinned thrusts oriented parallel to the dominant regional deformation fabric, and amphibolite- to granulite-facies metamorphic mineral assemblages (Braden, 2013; Skipton et al., 2014). The observed metamorphism and deformation have been attributed to Trans-Hudson orogenesis (Steenkamp and St-Onge, 2014). The northeastern portion of Hall Peninsula is underlain by Archean polymetamorphosed tonalite to granodiorite (From et al., 2014; Rayner, 2014). The northwestern portion of the peninsula is dominated by Paleoproterozoic, intrusive, orthopyroxene-bearing granite to monzogranite, and psammitic to pelitic metasedimentary units that locally include mafic volcanic and calcsilicate layers (MacKay and Ansdell, 2014; Rayner, 2014).

The Archean basement rocks host highly concentrated diamondiferous kimberlite deposits (Pell et al., 2013; Nichols, 2014; Nichols et al., 2014; Zhang and Pell, 2014). The surface extent of the basement units on eastern Hall Peninsula has been delimited, but these are believed to extend north into the aeromagnetic-survey area. Thus, the aeromagnetic survey will assist in constraining areas where Archean crust and potential kimberlite intrusions may or may not exist. Constraints on the spatial distribution of other rock types with mineralization potential, such as layered mafic–ultramafic intrusions and gossanous sulphide-bearing or mafic volcanic metasedimentary units, can also be expected.

Magnetic method

Aeromagnetic surveys provide geologists with information on the composition and structure of underlying bedrock. The bedrock contains varying amounts of magnetic minerals that act as bar magnets, or dipoles, with a north and south pole. In the absence of a magnetic field, these would be randomly oriented, but they become aligned parallel to Earth's magnetic field and together produce a local magnetic field, a phenomenon known as magnetic induction. Aeromagnetic surveys record Earth's total magnetic field, comprising a long-wavelength global magnetic field produced by the core and the induced magnetic field produced mainly by the crust, which provides insight into the nature of the underlying bedrock. This latter component of the magnetic field may be separated from the total measured magnetic field by subtracting a model of the long-wavelength global field. This process yields the geologically important residual magnetic field.

Aeromagnetic surveys are carried out by mounting a magnetometer on an aircraft, flying regularly spaced traverse lines perpendicular to the geological fabric over a target area and measuring the total intensity of the magnetic field. Earth's magnetic field varies over time, the periods of variation extending from a few seconds to millions of years. This is referred to as secular or geomagnetic variation. Spe-

cific variations that have no geological significance and are of high frequency are generally related to electric currents in Earth's ionosphere and magnetosphere. In aeromagnetic surveys, these are commonly referred to as diurnal variations, whose effects on acquired magnetic data must be minimized to improve data quality. This is achieved by restricting surveying during periods of rapid diurnal variation and by acquiring control-line data. Control lines are flown perpendicular to traverse lines. Control line values at intersections with traverse lines are used to correct traverse-line data for the effects of diurnal variation.

Survey area

The survey of the McKeand River area was proposed to cover all or parts of NTS areas 26B, C, F and G (Figure 1), between the communities of Pangnirtung and Iqaluit. The survey area was divided into blocks A, B and C to give maximum flexibility for contracting and data collection. Vintage data exist to the north of blocks A and B. These analogue surveys were acquired between 1968 and 1971 (Geological Survey of Canada, 1972) using 805–1200 m line spacing. The data were digitized from 1:63 360 contour maps by selecting values at the intersections of contour and flight lines. Modern, high-resolution, GPS-controlled aeromagnetic surveys (Dumont and Dostaler, 2010) were flown with 400 m line spacing to the east and south of block C on Hall Peninsula. Surveys farther south on Meta Incognita Peninsula (Geological Survey of Canada, 1998, 1999) were flown with 800 m line spacing.

Survey planning and design must accommodate migratory bird habitats. A portion of the Western Cumberland Sound Archipelago Key Terrestrial Habitat Site (Latour et al., 2008) overlaps block A.

Aeromagnetic survey design

Community engagement

Starting in the fall of 2011, the CNGO conducted four years of community engagement in both Pangnirtung and Iqaluit regarding geoscience mapping projects and the acquisition of new aeromagnetic data. Each community visit included engagement meetings with the Hamlet Council, Hunters and Trappers organizations, Qikiqtani Inuit Association (QIA) Community Lands and Resource committees, and the public. The purpose was to receive input on proposed geoscience-research activities and how to conduct research with as little impact as possible on people in the communities, wildlife and the environment. During this engagement, the CNGO developed close community relationships and gained valuable insights on how to respectfully conduct geoscience-research activities in the region. These insights included

- limiting low-level flights in March and April during caribou hunting season;
- working in coastal areas during spring break-up to minimize disturbances to people, as few camp on the land at this time;
- recognizing that Chidliak Bay and Ptarmigan Fiord are very important summer camping spots for families in Pangnirtung;
- learning that many people in Pangnirtung and Iqaluit are interested in finding new carving stone resources;
- conducting research in August, since caribou usually migrate away from the proposed study area before this time; and
- conducting an aeromagnetic survey in the fall, when it would cause the least overall disturbance.

Residents of Pangnirtung were not comfortable with the initial aeromagnetic survey proposal presented by the CNGO in 2012 for the McKeand River area. They were unsure about the effects the survey might have on caribou behaviour and the associated impacts on hunting. As a result, the CNGO decided to postpone its survey at that time and continued to discuss and develop plans with the community.

During engagement meetings in 2013, the Hamlet of Pangnirtung indicated that it was keen to develop local economic opportunities and wanted new geoscience mapping to be conducted in the Clearwater Fiord area (NTS areas 26J and K; Figure 1) with the hope of stimulating mineral exploration. Given the community priority, the CNGO resumed planning for an aeromagnetic survey in this area. In addition, the CNGO and GSC initiated plans for a new field-mapping campaign through the GEM program. During the planning phase, applications for all appropriate research and land-use licenses were made, including a Nunavut Scientific Research license(?) from the Nunavut Research Institute and a Land-Use Permit from the QIA.

Wildlife management

Significant emphasis was placed on minimizing the impact of the aeromagnetic survey on wildlife. The two main wildlife concerns in the survey area were impacts on migratory birds and caribou, specifically during rutting and calving seasons. A wildlife-impact mitigation and monitoring plan was established by the authors and incorporated as a requirement into the contractor's operating procedures. The overarching mitigation measure was for the contractor to cease surveying if concentrations of caribou or migratory bird colonies were encountered and only return once the wildlife had left the area. The contractors were also responsible for reporting all encounters with wildlife in the area and were to detail locations and dates of observation, animal behaviour during encounters and actions taken to avoid contact or disturbance.

To further minimize the impact of the survey on caribou populations, the average flight altitude for the survey was

set to a minimum of 150 m (492 feet), with significantly higher altitudes over valley areas (Figure 2). For a reference of scale, this altitude is equal to six times the height of the eight-storey wing of the Frobisher Inn located in Iqaluit. If large concentrations of wildlife were spotted, the flight level would be restricted to 610 m vertical distance and 1500 m horizontal distance. The timing of this aeromagnetic survey (August–November 2014) was planned specifically to avoid the caribou spring-migration period and the calving and post-calving seasons, thereby further minimizing impact on the animals during these critical periods.

The eastern edge of the survey area overlaps a portion of the Western Cumberland Sound Archipelago Key Terrestrial Habitat Site (Latour et al., 2008). In this area, several thousand Common Eiders concentrate along the coasts and fiords of Cumberland Sound during August and September, and significant populations of Common Eiders and Thick-billed Murres breed in Cumberland Sound. These nesting birds can be sensitive to disturbance, including low-level flights, from May to October.

To minimize impact, flights during periods when birds were predicted to be present were significantly reduced. The contractor was restricted to beginning the survey in the archipelago area after September 1, 2014 and was encouraged to further delay surveying there for as long as possible. It was estimated that the fixed-wing aircraft would require 54 hours to survey the Western Cumberland Sound Archipelago Key Terrestrial Habitat Site. After completing each survey line, the plane would return on an adjacent line offset by 400 m and would never fly over the same ground twice. Also, the aircraft would not hover, circle or touch down during surveying in the archipelago. Finally, flying to the seaward side of any observed seabird colonies was to be avoided at all times.

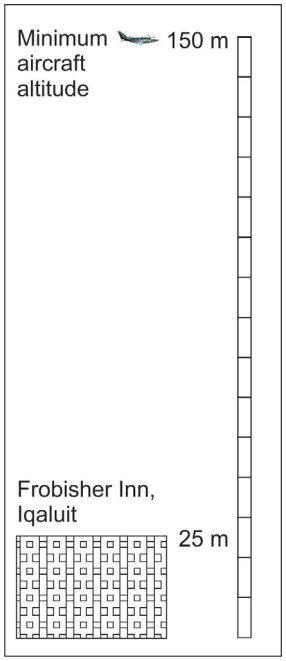

Figure 2: Comparison of minimum survey altitude to height of the Frobisher Inn, Iqaluit.

Logistics

Logistics for this survey were based out of Iqaluit, Nunavut. The southern boundary of block C was only 25 km from the Iqaluit Airport and therefore required minimal ferry time. The Iqaluit Airport's asphalt airstrip is more than 2440 m (8,000 feet) long and suitable for all aircraft used in this survey. Hangar facilities and fuel were also available in Iqaluit, making it an ideal base for operations.

Survey timing

The aeromagnetic survey began on August 5, 2014, and is scheduled to be finished by November 2014. The end of surveying will be dictated by safety considerations that prevent low-level flights from occurring in temperatures below –30°C and in low light. Climate-normal information for Iqaluit (Canadian Climate Normals, 2014) indicates that low daily averages for maximum temperature will preclude low-level surveying in December through February and curtail flying in March. In addition, in spite of precipitation and accompanying low-level cloud and possible fog conditions, production flights should be possible between about 50 and 90% of the time during the proposed August–November survey period. Furthermore, considering that low-level aeromagnetic surveying abides by Visual Flight Rules, airborne surveying based out of Iqaluit is limited by low light conditions in mid-November through mid-February.

Surveying during an August–November period ensures time for data processing and interpretation in advance of field mapping planned for the summer of 2015.

Flight altitude and line spacing

Aeromagnetic surveys are flown perpendicular to the strike of the regional geology fabrics to improve the delineation of geological contacts detected by the magnetometer, and to reduce power-aliasing effects (Reid, 1980). By extrapolating the strike of the geological fabric from existing GSC aeromagnetic survey data to the south and in consultation with GSC and CNGO geologists, a traverse-line orientation of 090° was chosen. GSC aeromagnetic surveys utilize a ratio of flight altitude to line spacing of 1:2.5, considered by Reid (1980) to be acceptable when flying perpendicular to the strike of geological fabric.

This aeromagnetic survey is regional in nature, and aims to aid new geological mapping and identify areas with high exploration potential. Considering this, a line spacing of 400 m and a flight altitude of 150 m was utilized. These specifications correspond to the survey parameters recommended by Reid (1980).

With the optimum survey-line spacing and flight altitude determined, the suitability of a multisensor aeromagnetic/gamma-ray spectrometric survey was considered. A spectrometric component could have been incorporated with only minimal incremental cost if 1) the survey could have been flown with an expected mean terrain clearance suitable for spectrometric surveys (125 m to a maximum of 300 m), 2) the region was free of snow and ice in the proposed time frame, and 3) the survey area was not under water. However, with the late start date of September 1, 2014 in very important survey areas and significant snow accumulations possible in October in the Iqaluit area, the acquisition of spectrometric data was considered too high risk and was not pursued further.

Tie-line spacing

The error related to geomagnetic activity increases with the flight time between control lines. A base-station magnetometer monitors diurnal activity and surveying is curtailed if the field varies more than 3.0 nT/minute. Tie-line spacing on the order of 2400 m, or about the distance flown in 30 seconds, improves the effectiveness of the levelling network and minimizes the influence of diurnal variations. This allows greater tolerance of the higher diurnal variation expected in the Arctic and minimizes survey downtime due to this variation.

Flight altitude and smooth drape surface

A smooth drape surface approximates the expected flight path and altitude that a survey aircraft can attain. All GSC aeromagnetic surveys are now flown using a preplanned smooth drape surface. This surface is calculated from digital terrain models and designed to conform to the maximum rate of climb and descent of the aircraft (Dumont, 2005), which is approximately 5% for a fixed-wing aircraft and 30% for a helicopter. The drape surface is followed using GPS navigation with a vertical tolerance of ±15 m. As a result, all tie-line intersections will be within 30 m of the preplanned drape surface position. Minimizing altitude differences between traverse and control lines helps in the levelling procedure in that the magnetic differences will also be minimized at these intersection points. Furthermore, smooth drape surfaces ensure that adjacent flight line altitudes are consistent, not varying based on topography and flight direction.

A smooth drape surface was generated for the survey of the McKeand River area using Canadian Digital Elevation Data (Geobase®, 2014) and a 5% climb and descent rate for fixed-wing aircraft. Subtracting the digital elevation model from the smooth drape surface gives a measure of the expected mean terrain clearance. The mean terrain clearance based on a smooth drape nominal flight altitude of 150 m is 178 m. Using a ratio of flight altitude to line spacing of 1:2.5, the optimum line spacing for this mean terrain clearance would be 445 m. Although higher than the optimum altitude, the mean terrain clearance is still within the range that is acceptable for a survey with 400 m line spacing and indicates that the choice of a fixed-wing platform was reasonable.

Contracting

A Request for Proposals for prequalified airborne geophysical contractors for the survey of the McKeand River area received six bids. A contract for block A and block B was awarded to Geo Data Solutions GDS Inc. (based in Laval, Quebec) on July 28, 2014. Following the acquisition of additional survey funding, the contract for surveying the eastern portion of block C was also awarded to Geo Data Solutions GDS Inc., on August 21, 2014.

Progress to date

The contractor began production flights on August 5, 2014, over block B. This area was flown using a Piper Navajo PA-31 (C-FVTL). On September 5, 2014, surveying began on block A using a Beechcraft King Air (C-FLRB) twin-engine aircraft. These aircraft were joined by another Piper Navajo PA-31 (C-FQQB) on September 21, 2014 (Figure 3). No surveying occurred in the Western Cumberland Sound Archipelago Key Terrestrial Habitat Site until after September 1, 2014. Surveying is scheduled for completion during November 2014. As of October 14, 2014, 36 309 line-km of data had been acquired. Acquisition has been limited by inclement weather and diurnal variation issues. In addition, a geomagnetic storm that occurred between September 11 and 14, 2014 prohibited any data acquisition. If further weather, diurnal variation or other issues limit data collection, requests may be submitted to extend licenses, screenings and permit exemptions until April 30, 2015. If the extensions are granted, the current contract may be amended to reflect the completion of flying in spring 2015.

Economic considerations

Recent fieldwork and published geological maps for the greater southern Baffin Island region have shown that it has a demonstrable potential for layered mafic–ultramafic magmatic Ni-Cu-PGE mineralization. This includes new occurrences associated with layered bodies on both Hall and Meta Incognita peninsulas (Steenkamp et al., 2014, 2015; St-Onge et al., 2015). Additionally, diamondiferous kimberlites are a known commodity on Hall Peninsula (Pell et al., 2013; Nichols, 2014; Nichols et al., 2014; Zhang and Pell, 2014). As the Irvine Inlet–McKeand River–Sylvia Grinnell Lake area is characterized by a paucity of modern high-resolution geological maps and publicly available aeromagnetic coverage, the results of the survey detailed in this report will be invaluable in evaluating the nature of the crustal architecture and establishing a geological context

Figure 3: Aircraft used on the aeromagnetic survey of the McKeand River area, southern Baffin Island, Nunavut. Photo courtesy of Geo Data Solutions GDS Inc.

for diamonds and sulphide mineralization in this area, and should stimulate exploration in the near future.

Conclusion

Preliminary versions of the aeromagnetic data will be used by CNGO and GSC geologists during fieldwork in summer 2015. Maps and profile and gridded data will be made available to the public approximately three to four months following completion of the survey. The maps will be published as PDF files and will be available for download through GeoGratis (http://geogratis.cgdi.gc.ca/) and from www.CNGO.ca. The digital profile and gridded data, along with metadata, will be available through the Geoscience Data Repository for Geophysical Data (http://gdr.agg.nrcan.gc.ca/ gdrdap/dap/search-eng.php).

Acknowledgments

The authors thank the aeromagnetic survey contractor, Geo Data Solutions GDS Inc., for their efforts in the face of inclement weather and geomagnetic storms, as well as their diligent reporting of wildlife encounters. The Canadian Northern Economic Development Agency's (CanNor) Strategic Investment in Northern Economic Development (SINED) and Natural Resources Canada's Geo-Mapping for Energy and Minerals (GEM) programs provided financial support for this work. This paper benefited from thorough and thoughtful reviews by M. Thomas and V. Tschirhart.

Natural Resources Canada, Earth Sciences Sector contribution 20140283

References

Blackadar, R.G. 1967: Geology, Cumberland Sound, District of Franklin; Geological Survey of Canada, Preliminary Map 17-1966, scale 1:506 880, doi:10.4095/108490

Braden, Z.M. 2013: Paleoproterozoic pressure-temperature-deformation path in the Newton Fiord region, eastern Baffin Island, Nunavut; B.Sc. thesis, Dalhousie University, Halifax, Nova Scotia.

Environment Canada 2014: Canadian climate normals, 1981–2010 station data; Environment Canada, URL <;;0;http://climate.weather.gc.ca/climate_normals/results_1981_2010_e.html?stnID=1758&lang=e&StationName=Iqaluit&SearchType=Contains&stnNameSubmit=go&dCode=5&dispBack=1> [October 2014].

Dumont, R. 2005: Drape DTM 1.0: software to calculate a smooth drape surface for an airborne geophysical survey; Geological Survey of Canada, Open File 4937, doi:10.4095/220500

Dumont, R. and Dostaler, F. 2010: Geophysical series, NTS 25-I/SE and part of 25-I/SW, aeromagnetic survey, Hall Peninsula, Nunavut; Geological Survey of Canada, Open File 6413, doi:10.4095/261656

From, R.E., St-Onge, M.R. and Camacho, A.L. 2014: Preliminary characterization of the Archean orthogneiss complex of Hall Peninsula, Baffin Island, Nunavut; *in* Summary of Activities 2013, Canada-Nunavut Geoscience Office, p. 53–62, URL <http://cngo.ca/summary-of-activities/2013/> [November 2014].

Geobase® 2014: Canadian digital elevation model; Natural Resources Canada, URL <http://www.geobase.ca/geobase/en/browse.do?produit=cded&decoupage=250k&map=026> [October 2014].

Geological Survey of Canada 1972: Baffin Island (sheet 26J/1 and 26J/2), District of Franklin; Geological Survey of Canada, Geophysical Series Map 5469G, scale 1:63 360, doi:10.4095/114502

Geological Survey of Canada 1998: Release of high resolution aeromagnetic total field survey of Baffin Island, Northwest Territories, Phase II; Geological Survey of Canada, Open File 3496, scale 1:100 000, doi:10.4095/209934

Geological Survey of Canada 1999: Release of high resolution aeromagnetic total field survey of Baffin Island, Northwest Territories, Phase I; Geological Survey of Canada, Open File 3413, scale 1:100 000, doi:10.4095/210116

Hoffman, P.F. 1988: United Plates of America, the birth of a craton: Paleoproterozoic assembly and growth of Laurentia: Annual Review of Earth and Planetary Sciences, v. 16, p. 543–603.

Latour, P.B., Leger J., Hines J.E., Mallory M.L., Mulders D.L., Gilchrist H.G., Smith P.A. and Dickson D.L. 2008: Key migratory bird terrestrial habitat sites in the Northwest Territories and Nunavut (3rd edition); Canadian Wildlife Service, Occasional Paper 114.

Lewry, J.F. and Collerson, K.D. 1990: The Trans-Hudson Orogen: extent, subdivision, and problems; *in* The Paleoproterozoic Trans-Hudson Orogen of North America, J.F. Lewry and M.R. Stauffer (ed.), Geological Association of Canada, Special Paper 37, p. 1–14.

Machado, G., Bilodeau, C., Takpanie, R., St-Onge, M.R., Rayner, N.M., Skipton, D.R., From, R.E., MacKay, C.B., Creason C.G. and Braden, Z.M. 2013a: Hall Peninsula regional bedrock mapping, Baffin Island, Nunavut: summary of fieldwork; *in* Summary of Activities 2012, Canada-Nunavut Geoscience Office, p. 13–22, URL <http://cngo.ca/summary-of-activities/2012/> [November 2014].

Machado, G., Bilodeau, C. and St-Onge, M.R. 2013b: Geology, southern part of Hall Peninsula, south Baffin Island, Nunavut; Geological Survey of Canada, Canadian Geoscience Map 135 (preliminary), Canada-Nunavut Geoscience Office, Open File Map 2013-1, scale 1:250 000, doi:10.4095/292443

MacKay, C.B. and Ansdell, K.M. 2014: Geochemical study of mafic and ultramafic rocks from southern Hall Peninsula, Baffin Island, Nunavut; *in* Summary of Activities 2013, Canada-Nunavut Geoscience Office, p. 85–92, URL <http://cngo.ca/summary-of-activities/2013/> [November 2014].

Nichols, K.M.A. 2014: Diamond sources beneath the Hall Peninsula; M.Sc. thesis, University of Alberta, Edmonton, Alberta.

Nichols, K.M.A., Stachel, T., Stern, R.A., Pell, J.A. and Mate D.J. 2014: Diamond sources beneath the Hall Peninsula, Baffin Island, Nunavut: an update of the preliminary assessment; *in* Summary of Activities 2013, Canada-Nunavut Geoscience Office, p. 20–26, URL <http://cngo.ca/summary-of-activities/2013/> [November 2014].

Pell, J., Grütter, H., Neilson, S., Lockhart, G., Dempsey, S. and Grenon, H. 2013: Exploration and discovery of the Chidliak kimberlite province, Baffin Island, Nunavut: Canada's newest diamond district; *in* Proceedings of 10th International Kimberlite Conference, Springer, India, p. 209–227.

Rayner, N.M. 2014: New uranium-lead geochronological results from Hall Peninsula, Baffin Island, Nunavut; *in* Summary of Activities 2013, Canada-Nunavut Geoscience Office, p. 39–52, URL <http://cngo.ca/summary-of-activities/ 2013/> [November 2014].

Reid, A.B. 1980: Aeromagnetic survey design; Geophysics, v. 45, p. 973–976.

Skipton, D.R. and St-Onge, M.R. 2014: Paleoproterozoic deformation and metamorphism in metasedimentary rocks west of Okalik Bay: a field template for the evolution of eastern Hall Peninsula, Baffin Island, Nunavut; *in* Summary of Activities 2013, Canada-Nunavut Geoscience Office, p. 63–72, URL <http://cngo.ca/summary-of-activities/2013/> [November 2014].

Steenkamp, H.M. and St-Onge, M.R. 2014: Overview of the 2013 regional bedrock mapping program on northern Hall Peninsula, Baffin Island, Nunavut; *in* Summary of Activities 2013, Canada-Nunavut Geoscience Office, p. 27–38, URL <http://cngo.ca/summary-of-activities/2013/> [November 2014].

Steenkamp, H.M., Beauregard, M.A. and Mate, D.J. 2015: Carving stone and mineral resource potential of the Opingivik deposit, southern Baffin Island, Nunavut; *in* Summary of Activities 2014, Canada-Nunavut Geoscience Office, p. 153–162, URL <http://cngo.ca/summary-of-activities/2014/> [January 2015].

Steenkamp, H.M., Bros, E.R. and St-Onge, M.R. 2014: Altered ultramafic and layered mafic-ultramafic intrusions: new economic and carving stone potential on northern Hall Peninsula, Baffin Island, Nunavut; *in* Summary of Activities 2013, Canada-Nunavut Geoscience Office, p. 11–20, URL <http://cngo.ca/summary-of-activities/2013/> [November 2014].

St-Onge, M.R., Searle, M.P. and Wodicka, N. 2006: Trans-Hudson Orogen of North America and Himalaya-Karakoram-Tibetan Orogen of Asia: structural and thermal characteristics of the lower and upper plates; Tectonics, v. 25, no. 4, doi:10.1029/2005TC001907

St-Onge, M.R., Van Goole, J.A.M., Garde, A.A. and Scott, D.J. 2009: Correlation of Archaean and Palaeoproterozoic units between northeastern Canada and western Greenland: constraining the pre-collisional upper plate accretionary history of the Trans-Hudson Orogen; *in* Earth Accretionary Systems in Space and Time, P.A. Cawood and A. Kröner (ed.), The Geological Society of London, Special Publications, v. 318, p. 193–235.

St-Onge, M.R., Wodicka, N. and Ijewliw, O. 2007: Polymetamorphic evolution of the Trans-Hudson Orogen, Baffin Island, Canada: integration of petrological, structural and geochronological data; Journal of Petrology, v. 48, p. 271–302, doi:10.1093/petrology/eg1060

Zhang, S. and Pell, J. 2014: Conodonts recovered from the carbonate xenoliths in the kimberlites confirm the Paleozoic cover on the Hall Peninsula, Nunavut; Canadian Journal of Earth Sciences, v. 51, no. 2, p. 142–155, doi:10.1139/cjes-2013-0171

Bedrock mapping of eastern Meta Incognita Peninsula, southern Baffin Island, Nunavut

M.R. St-Onge[1], N.M. Rayner[2], H.M. Steenkamp[3] and D.R. Skipton[4]

[1]*Natural Resources Canada, Geological Survey of Canada, Ottawa, Ontario, Marc.St-Onge@NRCan-RNCan.gc.ca*

[2]*Natural Resources Canada, Geological Survey of Canada, Ottawa, Ontario*

[3]*Canada-Nunavut Geoscience Office, Iqaluit, Nunavut*

[4]*Department of Earth Sciences, University of Ottawa, Ottawa, Ontario*

This work was part of the Geo-mapping for Energy and Minerals (GEM) Program on Baffin Island and is being led by the Geological Survey of Canada (GSC) in collaboration with the Canada-Nunavut Geoscience Office, Aboriginal Affairs and Northern Development Canada, Nunavut Arctic College, the University of Ottawa and Carleton University. The study area comprises all or parts of six 1:250 000 scale National Topographic System map areas south and east of Iqaluit (NTS 25G, I, J, K, N, O). The objective of this work is to complete the regional bedrock mapping for the southern half of Baffin Island and develop a new, modern, geoscience compilation for the region.

St-Onge, M.R., Rayner, N.M., Steenkamp, H.M. and Skipton, D.R. 2015: Bedrock mapping of eastern Meta Incognita Peninsula, southern Baffin Island, Nunavut; *in* Summary of Activities 2014, Canada-Nunavut Geoscience Office, p. 105–118.

Abstract

This paper summarizes the field observations and initial interpretations following five weeks of regional and targeted bedrock mapping on eastern Meta Incognita Peninsula, Baffin Island, Nunavut. Under the Geo-mapping for Energy and Minerals (GEM) Program, this area was targeted in 2014 to upgrade the geoscience knowledge and document the economic potential of the greater Iqaluit area south of Frobisher Bay. Field observations have constrained the distribution of metasedimentary units comprising quartzite, marble, psammite, pelite and semipelite, all of which can be correlated with the contiguous middle Paleoproterozoic Lake Harbour Group in the type area north of Kimmirut. The full range of siliciclastic and minor carbonate rock types can be traced to the easternmost tip of Meta Incognita Peninsula. The spatial distribution of a suite of layered mafic to ultramafic sills intrusive into the sedimentary strata was also documented and will be the focus of further study. Layering in the sills was observed on the centimetre to metre scale, with many bodies containing disseminated sulphide, some associated with ferricrete. The distribution and eastern limit of high-grade felsic and mafic plutonic rocks, tentatively interpreted as part of the middle Paleoproterozoic Cumberland Batholith, were delineated. Four distinct phases of deformation and two metamorphic episodes were recognized. The deformation and metamorphic events can be correlated with similar features and assemblages previously documented both on Baffin Island and on the Ungava Peninsula of northern Quebec, and will be utilized to compare, and improve upon, existing regional tectonic models.

Résumé

Cet article résume les observations de terrain et les interprétations préliminaires suivant cinq semaines de cartographie régionale et ciblée de la roche en place sur la péninsule Meta Incognita orientale, Terre de Baffin, Nunavut. Le programme Géo-cartographie pour l'énergie et les minéraux (GEM) a ciblé cette région en 2014 afin d'améliorer la connaissance géoscientifique et documenter le potentiel économique de la région d'Iqaluit au sud de la baie Frobisher. Les observations de terrain ont délimité la distribution d'unités métasédimentaires composées de quartzite, de marbre, de psammite, de pélite et de semipélite. Toutes ces unités peuvent être corrélées avec le Groupe de Lake Harbour contigu d'âge Paléoprotérozoïque moyen dans la région type au nord de Kimmirut. La pleine gamme de roches siliciclastiques, et de façon moins importante carbonatée, se retrouve jusqu'à l'extrémité est de la péninsule Meta Incognita. La distribution spatiale d'une série de filons-couches mafiques à ultramafiques intrusifs dans les strates métasédimentaires fut également documentée et fera l'objet d'une étude plus approfondie. La stratification fut observée à l'échelle centimétrique à métrique, avec de nombreux filons-couches contenant des sulfures disséminés, et parfois associés à des sédiments ferrugineux. La distribution et la limite est de roches plutoniques felsiques et mafiques de haut-grade interprétées de façon préliminaire comme faisant partie du batholite Cumberland d'âge Paléoprotérozoïque moyen furent délimitées. Quatre phases distinctes de déformation et deux épisodes

This publication is also available, free of charge, as colour digital files in Adobe Acrobat® PDF format from the Canada-Nunavut Geoscience Office website: http://cngo.ca/summary-of-activities/2014/.

métamorphiques ont été reconnus. Les événements de déformation et de métamorphisme peuvent être corrélés avec des éléments structuraux et des assemblages métamorphiques similaires précédemment documentés sur la Terre de Baffin et sur la péninsule d'Ungava, dans le nord du Québec. Ceux-ci seront utilisés pour comparer et améliorer les modèles tectoniques régionaux existants.

Introduction

The Geo-mapping for Energy and Minerals (GEM) program targeted eastern Meta Incognita Peninsula in 2014 (green outline in Figure 1) to help complete the regional bedrock-mapping coverage for the southern half of Baffin Island. Fieldwork on the peninsula (parts of NTS areas 25G, I, J, K, N, O) was led by the Geological Survey of Canada (GSC) in collaboration with the Canada-Nunavut Geoscience Office (CNGO). Regional and targeted bedrock mapping also involved participants from Aboriginal Affairs and Northern Development Canada, Nunavut Arctic College, University of Ottawa and Carleton University. This paper presents an overview of the regional geology, the principal tectonostratigraphic units mapped, and the main structural elements, dominant mineral assemblages and economic potential identified during five weeks of fieldwork in 2014.

History of bedrock mapping and geological framework

The reconnaissance geological investigations of Baffin Island south of latitude 66°N, initiated in 1949 by Y.O. Fortier and W.L. Davison, and which continued in 1950 and 1951 along the coastal areas of Meta Incognita Peninsula between Iqaluit and Kimmirut (Davison, 1959), were completed in 1965 in the course of 'Operation Amadjuak', a fixed-wing and helicopter-supported project (Blackadar, 1967). Bedrock mapping was carried out across eighteen 1:250 000 NTS map areas and the data so obtained, together with that derived from published and unpublished Geological Survey of Canada maps, were compiled and published by Blackadar (1967).

A three year project by the Geological Survey of Canada (1995–1997) to systematically map the bedrock geology of the western portion of Meta Incognita Peninsula between Markham Bay and longitude 68°W (Figure 1; NTS areas 25K, L, M, N) at a scale of 1:100 000 resulted in the publication of GSC maps 1979A–1985A (St-Onge et al., 1999a–g). A regional aeromagnetic survey of the southern Baffin and Hudson Strait region was also completed in 1997 (Geological Survey of Canada, 1998, 1999; Pilkington and Oneschuk, 2007).

The metasedimentary and metaplutonic units on Meta Incognita Peninsula are part of the northeastern (Quebec–Baffin) segment of the Trans-Hudson Orogen, a collisional orogenic belt that extends in a broad arcuate shape from northeastern to south-central North America (Hoffman 1988; Lewry and Collerson, 1990), and which comprises tectonostratigraphic assemblages accumulated on, or accreted to, the northern margin of the lower-plate Archean Superior Province during the middle Paleoproterozoic (St-Onge et al., 2006, 2009). Northern Quebec and southern Baffin Island are characterized by three orogen-scale stacked tectonic elements (Figure 2; St-Onge et al., 2002), which include the following tectonostratigraphic units (from lowest to highest structural level):

- level 1 – Archean tonalitic orthogneiss interpreted as the northern continuation of the Superior craton and middle Paleoproterozoic supracrustal cover correlated with the Povungnituk Group, Ungava Peninsula (St-Onge et al., 1996);
- level 2 – dominantly monzogranitic and granodioritic middle Paleoproterozoic gneiss interpreted as the northern extent of the Narsajuaq arc (Scott, 1997; St-Onge et al., 2009), or alternatively as Narsajuaq-age intrusions emplaced within level 3 (Corrigan et al., 2009);and
- level 3 – the tectonostratigraphic units of the Lake Harbour Group (Jackson and Taylor, 1972) and a number of metaplutonic gneissic units interpreted as the cover sequence and crystalline basement of a middle Paleoproterozoic accreted terrane termed the 'Meta Incognita microcontinent' by St-Onge et al. (2000).

Various phases of the Cumberland Batholith (Whalen et al., 2010) intrude all units in level 3. The supracrustal, gneissic and plutonic units on eastern Meta Incognita Peninsula were the main focus of fieldwork in 2014.

Tectonostratigraphic units

Monzogranite-granodiorite-tonalite gneiss and monzogranite gneiss

Several types of orthopyroxene-bearing, compositionally layered metaplutonic rocks (i.e., monzogranite-granodiorite-tonalite gneiss and monzogranite gneiss) occur at the lowest structural levels exposed along the western portion of the project area (Figure 3). The orthogneisses are in physical continuity with, and/or are lithologically similar to, plutonic rocks north and northeast of Kimmirut that have been correlated by Scott (1997), Wodicka and Scott (1997), Thériault et al. (2001) and St-Onge et al. (2002) with metaplutonic units of the middle Paleoproterozoic Narsajuaq arc in northern Quebec (Figure 2; St-Onge et al., 1992; Dunphy and Ludden, 1998). Targeted geochronological studies are planned to test this correlation.

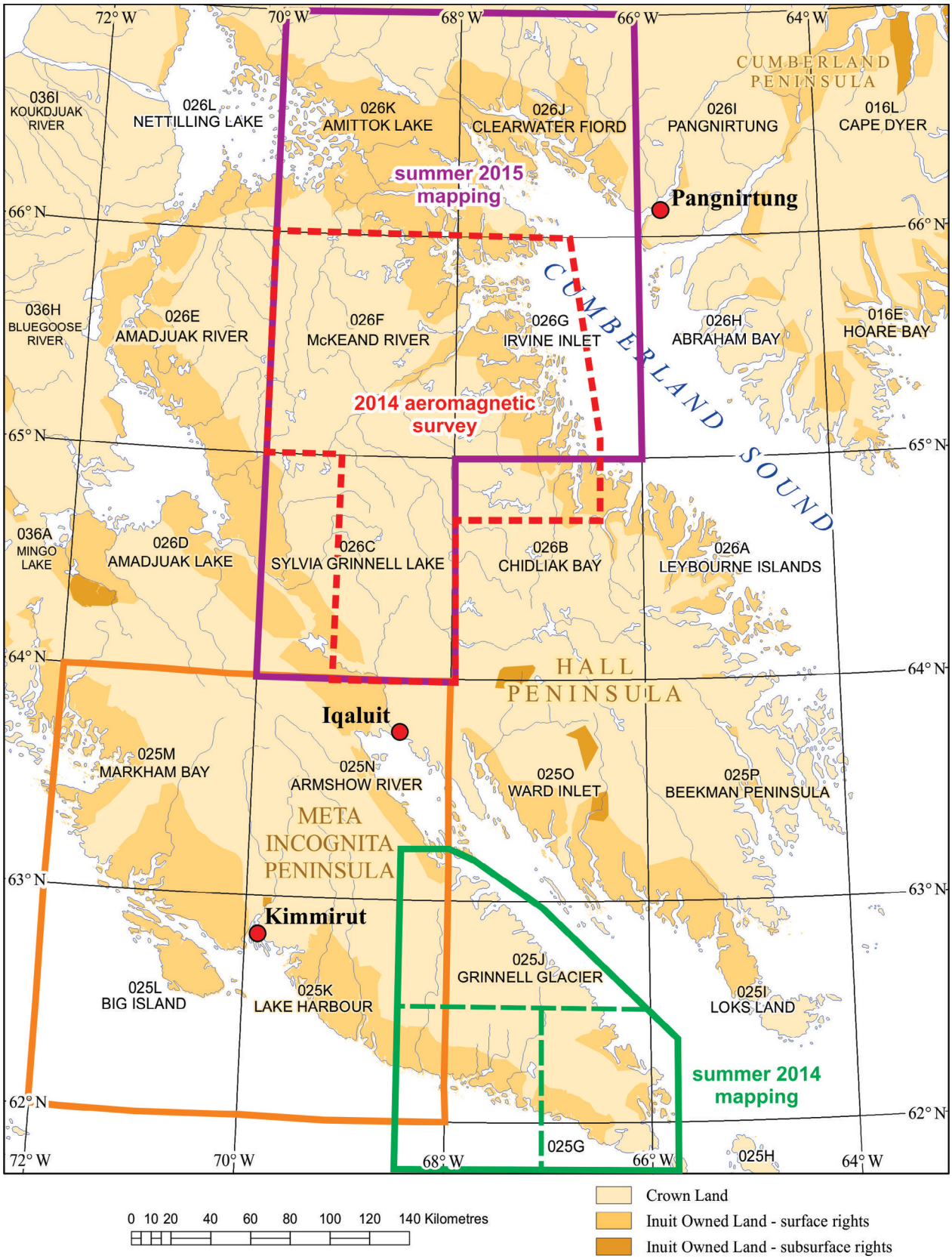

Figure 1: Location of the 2014 Meta Incognita Peninsula (green outline) and the 2015 Clearwater Fiord–McKeand River–Sylvia Grinnell Lake (purple outline) field areas, Baffin Island, Nunavut; the three planned 1:100 000 scale bedrock geological maps for eastern Meta Incognita Peninsula are separated with a green dashed line; the McKeand River aeromagnetic survey area is outlined in red (Miles et al., 2015) and the 1995–1997 western Meta Incognita Peninsula project area is outlined in orange.

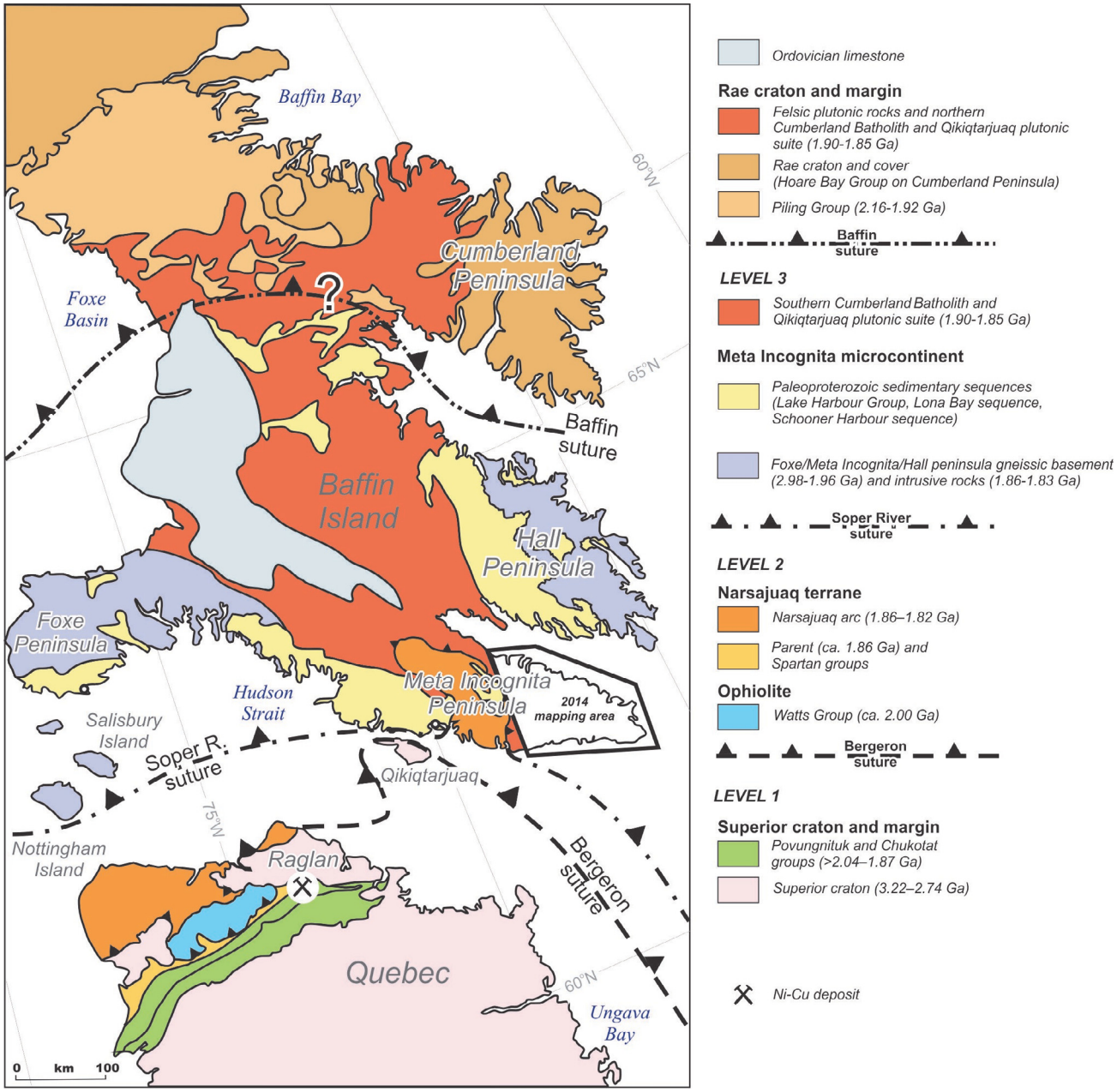

Figure 2: Simplified geological terrane map of the Quebec–Baffin segment of the Trans-Hudson Orogen (modified from St-Onge et al., 2007), providing a regional tectonic context for the eastern Meta Incognita field area (outlined with the black polygon and shown in greater detail in Figure 3), Baffin Island, Nunavut.

Monzogranite–diorite gneiss

Buff- to pink-weathering, well layered orthopyroxene-biotite±hornblende monzogranite gneiss underlies large areas within Pritzler Harbour, Newell Sound and York Sound (Figure 3). In most outcrops examined, the monzogranite gneiss is interlayered with subordinate, boudinaged and discontinuous layers of hornblende-orthopyroxene-clinopyroxene diorite to quartz diorite (Figure 4).

The distribution of the orthogneiss, its spatial association with the supracrustal rocks of the Lake Harbour Group, and the relative overall strain contrast between gneissic and supracrustal units might suggest the orthogneiss represents the stratigraphic basement to the Lake Harbour Group described below. However, this is difficult to determine in the field as all observed contacts between orthogneiss and supracrustal units are tectonic and characterized by coplanar metamorphic fabrics, indicating at the very least some degree of reworking. It is anticipated that strategic geochronological analyses will help address this issue.

All components of the gneiss are crosscut by veins of white to pink biotite monzogranite and syenogranite that range from well foliated to relatively massive, and from a few

centimetres to over a decametre in thickness (Figure 4). Similarities in rock type, mineral assemblage and amount of deformation suggest that the monzogranite and syenogranite veins are related to, and possibly comagmatic with, plutons of the Cumberland Batholith (see below) that intrude this unit in the study area.

Lake Harbour Group

The quartzite, marble, psammite and semipelite mapped on eastern Meta Incognita Peninsula are lithologically similar to the metasedimentary strata of the contiguous Lake Harbour Group in its type locality (St-Onge et al., 1996, 1998; Scott et al., 1997). Two lithologically and geographically distinct sequences have been recognized on the eastern peninsula. Over much of the study area (longitude 68°30'W) to west of York Sound (Figure 3), the Lake Harbour Group is composed of quartzite, garnetiferous psammite, minor semipelite and pelite, structurally overlain by laterally continuous to boudinaged bands of pale grey to white marble and calcsilicate rocks ('Kimmirut sequence' of Scott et al., 1997). To the east, and including extensive exposures of supracrustal rocks on the eastern islands and bluffs of Meta

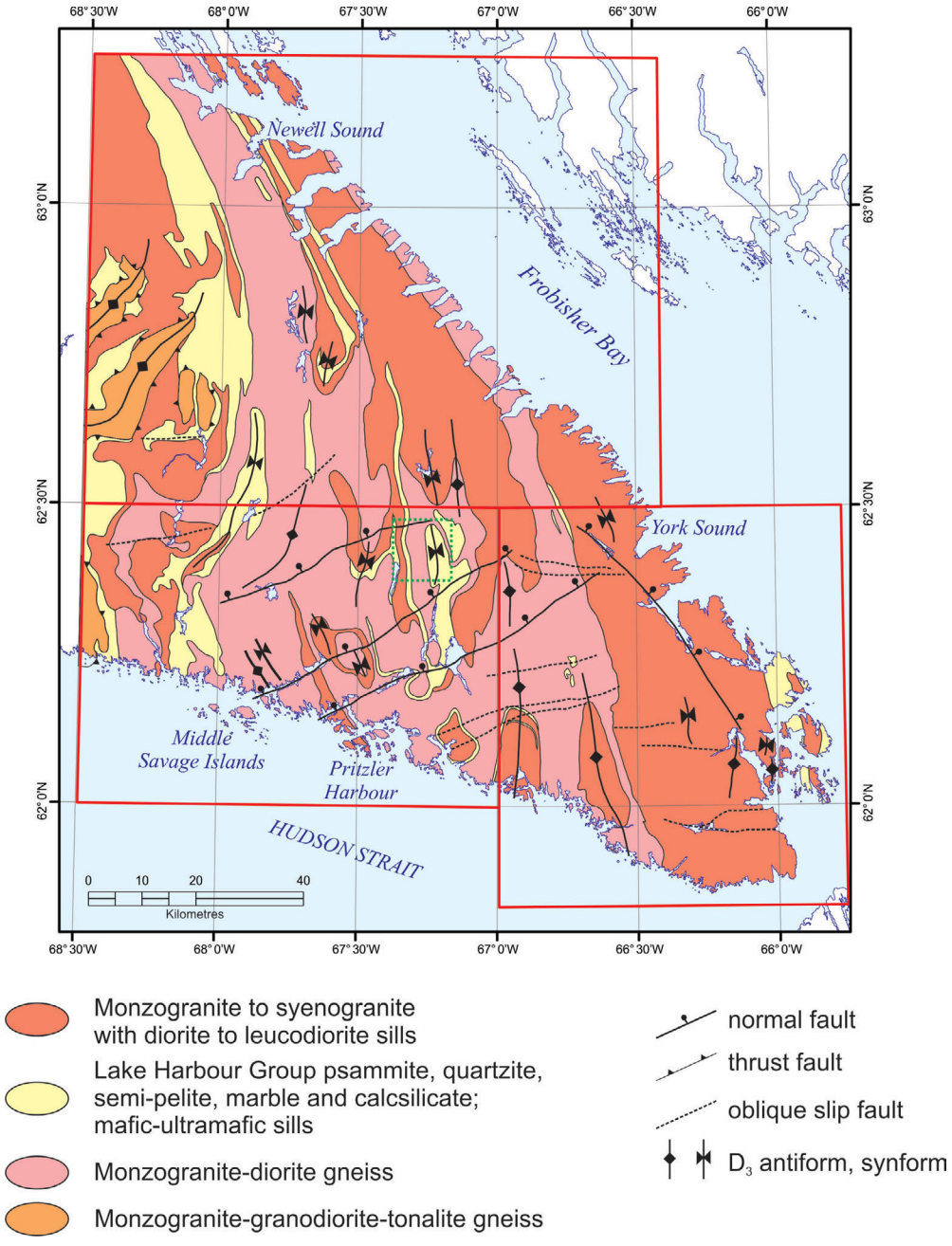

Figure 3: Simplified bedrock geology of eastern Meta Incognita Peninsula, Baffin Island, Nunavut, based on 2014 regional and targeted mapping; the bedrock geological maps planned for publication in early 2015 are outlined in red and the area corresponding to that of Figure 12 is outlined in green.

Figure 4: Layered monzogranite–diorite gneiss, crosscut by a vein of white monzogranite (in lower right corner of photograph), Meta Incognita Peninsula, Baffin Island, Nunavut; hammer is 35 cm long.

Figure 6: Shallowly-dipping, well-layered, garnet-bearing orthoquartzite, Lake Harbour Group, Meta Incognita Peninsula, Baffin Island, Nunavut; geologist for scale is 2 m tall.

Incognita Peninsula, the Lake Harbour Group is dominated by garnetiferous psammite interlayered with pelite and/or semipelite, and comprises less than 5% marble and calcsilicate rocks ('Markham Bay sequence' of Scott et al., 1997). Both sequences are nevertheless intruded by generally concordant sheets of mafic to ultramafic rocks.

Psammite, quartzite, semipelite and pelite

Compositional layers within the psammite range from centimetres to tens of centimetres in thickness and can be traced for up to tens of metres along strike. They are defined by variations in the modal abundance of quartz, plagioclase, biotite, lilac garnet, sillimanite, rare cordierite and granitic melt (Figure 5). Garnet-sillimanite pelite typically occurs as thin layers within garnet-biotite semipelite, the latter subordinate within the psammite. The psammite and semipelite are generally rusty weathering, and characterized by trace amounts of disseminated graphite, pyrite and chalcopyrite.

Figure 5: Garnet-sillimanite-biotite-melt psammite, Lake Harbour Group, Meta Incognita Peninsula, Baffin Island, Nunavut.

Quartzite occurs as discrete, well-layered panels (Figure 6) several metres to several hundred metres thick. It is notably abundant along a broad band crossing the peninsula at the longitude of Newell Sound and the Middle Savage Islands (Figure 3). Quartzite layers compositionally range from orthoquartzite to feldspathic quartzite, commonly contain graphite±garnet±sillimanite and are strongly recrystallized. Primary sedimentary features such as crossbedding or graded bedding were not observed. White leucogranite, rich in lilac garnet and sillimanite, is a ubiquitous constituent within the siliciclastic package, occurring as concordant layers or pods less than 0.5 m thick (Figure 7). Locally, the leucogranite outcrops as large discrete tabular bodies several tens of metres thick.

Marble and calcsilicate

Most of the calcareous rocks are medium to coarse grained and are locally characterized by compositional layering de-

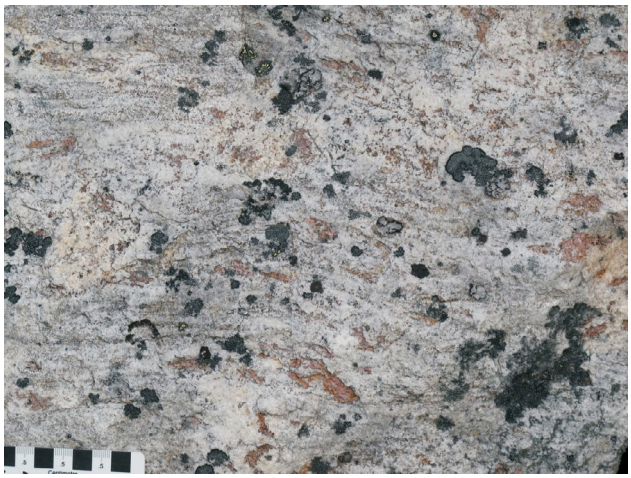

Figure 7: Close-up of a tabular body of garnet-sillimanite leucogranite emplaced in Lake Harbour Group psammite and feldspathic quartzite, eastern Meta Incognita Peninsula, Baffin Island, Nunavut.

fined by varied modal proportions of calcite, forsterite, humite, diopside, tremolite, phlogopite, spinel, apatite and rarely wollastonite. Individual layers range from centimetres to metres in thickness and can be traced for tens of metres along strike. Calcsilicate rocks are commonly interlayered with siliciclastic rocks and generally associated with marble. Locally, the calcareous strata include layers of calcareous grit characterized by abundant 1–2 mm detrital quartz grains (Figure 8). Thicknesses of individual calcareous rock sequences typically range from several decametres to less than 200 m. Individual marble units can be traced several kilometres along strike. No primary bedding structures were observed in the calcareous rocks.

Mafic and ultramafic rocks

Generally concordant sheets of medium- to coarse-grained mafic to ultramafic rocks occur within both sequences of the Lake Harbour Group. Individual bodies are typically 10–20 m thick, although some reach a few hundred metres in thickness and extend up to several kilometres along strike. Metagabbroic textures and compositional layering at the centimetre to metre scale defined by variations in modal abundance of clinopyroxene, orthopyroxene, hornblende and plagioclase are commonly preserved in the mafic bodies (Figure 9). The concordant nature, tabular shape and sharp contacts of these bodies suggest that they are sills. Several ultramafic bodies, either clinopyroxene-orthopyroxene±hornblende metapyroxenite or olivine-clinopyroxene-orthopyroxene metaperidotite, were observed. In numerous localities, the ultramafic rocks are compositionally layered with many bodies containing disseminated sulphide, some associated with a ferricrete, which consists of medium to coarse clastic sediment cemented by an iron oxy-hydroxide. A full field description of the mafic and ultramafic rocks on Meta Incognita Peninsula is given in St-Onge et al. (2015).

Figure 8: Diopside-phlogopite-spinel-apatite-quartz calcareous grit, Lake Harbour Group, Meta Incognita Peninsula, Baffin Island, Nunavut.

The layered mafic-ultramafic sills define a magmatic suite that characterizes the whole of southern Baffin Island. The size and distribution of these mantle-derived rocks suggest that they may form part of a major large igneous province event and warrant further study. A senior undergraduate field assistant is initiating a M.Sc. thesis on the petrology, geochemistry and geochronology of the layered mafic-ultramafic suite and associated mineralization. Whether this suite is correlative with, or of a different age than, the suite of similar layered intrusions in northern Quebec and associated Raglan Ni-Cu deposit will be one of the questions addressed in the thesis.

Monzogranite to syenogranite plutons

The principal plutonic rock types mapped on eastern Meta Incognita Peninsula include tan- to pink-weathering orthopyroxene-biotite±magnetite monzogranite, biotite±hornblende±magnetite monzogranite, biotite-garnet± orthopyroxene monzogranite and biotite monzogranite to syenogranite. A number of the plutonic bodies are distinctively K-feldspar megacrystic (Figure 10), whereas others contain abundant enclaves of siliciclastic and calcareous rock types, interpreted to be derived from the Lake Harbour Group. In a number of well-exposed localities, the granitic units truncate the monzogranite–diorite gneiss and associated Lake Harbour Group strata, suggesting that intrusion followed the early deformation of the orthogneiss and supracrustal units (see below).

These coarse- to medium-grained, massive to foliated metaplutonic rocks occur along strike from, and are continuous with, extensive regions underlain by the Cumberland Batholith on Meta Incognita and western Hall peninsulas (Figure 2; St-Onge et al., 1999a–g; Machado et al., 2013a, b; Steenkamp and St-Onge, 2014). The continuity of the plutonic rocks suggests that many of those in the 2014 map area are also part of the 1.86–1.85 Ga batholith (Jackson et al., 1990; Wodicka and Scott, 1997; Scott and Wodicka,

Figure 9: Layered metagabbro, Meta Incognita Peninsula, Baffin Island, Nunavut; hammer is 35 cm long.

Figure 10: Foliated K-feldspar megacrystic monzogranite, Meta Incognita Peninsula, Baffin Island, Nunavut.

1998; Scott, 1999; Whalen et al., 2010). Geochronological samples of all major plutonic rock types were acquired during the course of the fieldwork to test this correlation.

Diorite to leucodiorite

Sheets of hornblende-orthopyroxene-clinopyroxene diorite to leucodiorite, 10–200 m wide and up to several kilometres long (Figure 11), are broadly coplanar with the dominant foliation in the surrounding orthopyroxene-biotite±magnetite monzogranite or host Lake Harbour Group siliciclastic strata. Unlike the mafic sills described above, the dioritic sheets are not layered, nor are they associated with ultramafic rocks. The diorite bodies are locally extensive enough to usefully highlight fold interference geometries.

Deformation and metamorphism

The completion of targeted regional mapping on eastern Meta Incognita Peninsula and the re-examination of key outcrops in previously mapped areas in the western portion of the peninsula have facilitated the development of a comprehensive structural and metamorphic framework for southeastern Baffin Island. Deformation and metamorphism are polyphase, with at least four regional episodes of compression (D_1–D_4) and two thermal events (M_1-M_2) recognized.

D_1 deformation and M_1 metamorphism

The tectonostratigraphic units described above are generally characterized by the development of a pervasive millimetre- to centimetre-scale compositional foliation (S_1) that is shallow to steeply dipping, and invariably parallel to lithological contacts between supracrustal and plutonic units. In metasedimentary strata, S_1 is defined by layers of aligned M_1 biotite, sillimanite, garnet and locally cordierite, alternating with layers of dominantly plagioclase, K-feldspar and quartz. The garnet can be several millimetres in size and appear poikiloblastic. In the metasedimentary units, S_1 is interpreted as a metamorphic enhancement of primary bedding (S_0).

Figure 11: Folded diorite sheet in background emplaced in orthopyroxene-biotite±magnetite monzogranite, Meta Incognita Peninsula, Baffin Island, Nunavut; width of field of view is 600 m.

In foliated mafic and felsic plutonic units, S_1 is defined by the alternating distribution of dominantly ferromagnesian-rich layers comprising granoblastic, millimetre-scale M_1 orthopyroxene, biotite, magnetite, clinopyroxene, hornblende and/or garnet, and layers consisting of dominantly plagioclase and quartz±K-feldspar. The alignment of the orthopyroxene, biotite, clinopyroxene and hornblende highlights the S_1 foliation in metaplutonic units when present.

Prograde granulite-facies M_1 metamorphism of the Lake Harbour Group on western Meta Incognita Peninsula is constrained at ca. 1.84 Ga by St-Onge et al. (2007). Geochronological and petrological studies will be undertaken to test whether the same metamorphic event can be documented in the eastern portion of the peninsula.

D_2 deformation and M_2 metamorphism

On eastern Meta Incognita Peninsula, zones of subsequent deformation within psammitic and pelitic units of the Lake Harbour Group are marked by the pervasive growth of amphibolite-facies (M_2) biotite-sillimanite-quartz±garnet assemblages at the expense of the thermal peak (granulite facies) M_1 garnet±cordierite assemblages described above. The abundant, fine M_2 biotite and sillimanite laths define a distinct, penetrative, schistose (finely layered), retrograde S_2 foliation.

At a broader scale, the D_2 deformational event defined by St-Onge et al. (2002) is the oldest compressional deformation event that affects all three orogen-scale stacked tectonic levels of southern Baffin Island (Figure 2). It involves 1) accretion of the Lake Harbour Group supracrustal strata, monzogranite–diorite gneiss and Cumberland Batholith assemblage to the structurally underlying monzogranite-granodiorite-tonalite gneiss; 2) accretion of the Narsajuaq arc package (level 2) to the structurally underlying northern margin of the Superior craton (level 1); and 3) imbrication of Paleoproterozoic cover and Archean basement units in the lower structural level.

On western Meta Incognita Peninsula, the presence of repetitions and truncations of distinct tectonostratigraphic units and the overall ramp-flat fault geometry of the D_2 structures (Scott et al., 1997; St-Onge et al., 2001, 2002) suggest that juxtaposition of units occurred along a system of southwest-verging thrust faults. The D_2 faults are typically associated with the development of mylonitic fabrics in zones ranging in thickness from tens to locally hundreds of metres. The D_2 deformation was also accompanied by outcrop- to map-scale recumbent folding of the older D_1–M_1 fabric (St-Onge et al., 2002).

New growth and recrystallization of zircon and monazite in metasedimentary units from the western peninsula indicate that M_2 retrograde metamorphism occurred at ca. 1820±1 to 1813±2 Ma (Wodicka and Scott, 1997; Scott et al., 2002; St-Onge et al., 2007). Geochronological and petrological studies will help constrain the extent of D_2-M_2 reworking on eastern Meta Incognita Peninsula.

D_3 deformation

The D_1 and D_2 structures and fabrics are reoriented by a set of regional north- to northwest-trending D_3 folds. The D_3 folds range from metre scale to map scale (Figure 3) and display a consistent west- to southwest-verging asymmetry. The D_3 folding on eastern Meta Incognita Peninsula is readily evident both in the field and on airphotos (Figure 12) and involves all tectonostratigraphic units described above. No mesoscopic fabric development associated with D_3 has been documented.

In northern Quebec, crustal-scale D_3 folding of structural levels 1 and 2 is constrained at ca. 1.76 Ga (Lucas and St-Onge, 1992). Lucas and Byrne (1992) proposed that the orogen-parallel folds resulted from continued horizontal compression during postcollisional intracontinental shortening in the northeastern segment of the Trans-Hudson Orogen.

D_4 deformation

Upright refolding of all older structural elements about east- to northeast-trending D_4 fold axes has generated the fold interference, dome-and-basin map pattern most evident in the southern and eastern portions of the peninsula (Figures 3, 12). The interference of D_3 and D_4 folds generated sufficient structural relief to allow for the study of the crustal architecture of southern Baffin Island and Meta Incognita Peninsula, including the three principal structural levels exposed at the present-day erosion surface. The D_4 folding in northern Quebec is constrained between 1.76 and 1.74 Ga (Lucas and St-Onge, 1992).

Regional considerations

The regional structural grain observed on eastern Meta Incognita Peninsula is dominantly north- to northwest-striking, with west- to southwest-verging folds and thrusts (Figure 3) consistent with observations elsewhere along southern Baffin Island (extending west to Foxe Peninsula). These are in contrast to a distinct set of east-verging folds and thrust imbricates of Archean basement and middle Paleoproterozoic cover units immediately to the north on Hall Peninsula (Machado et al., 2013a, b; Steenkamp and St-Onge, 2014). Further to the north on Cumberland Peninsula and to the northwest in the central Baffin Island area (Figure 2), folds and thrusts are south-verging and north-verging respectively. These structural changes appear to be a reflection of the tectonic interaction of a number of crustal blocks during the middle Paleoproterozoic assembly of the Nuna supercontinent, including the Rae craton, Meta Incognita microcontinent, Narsajuaq arc, Superior craton and

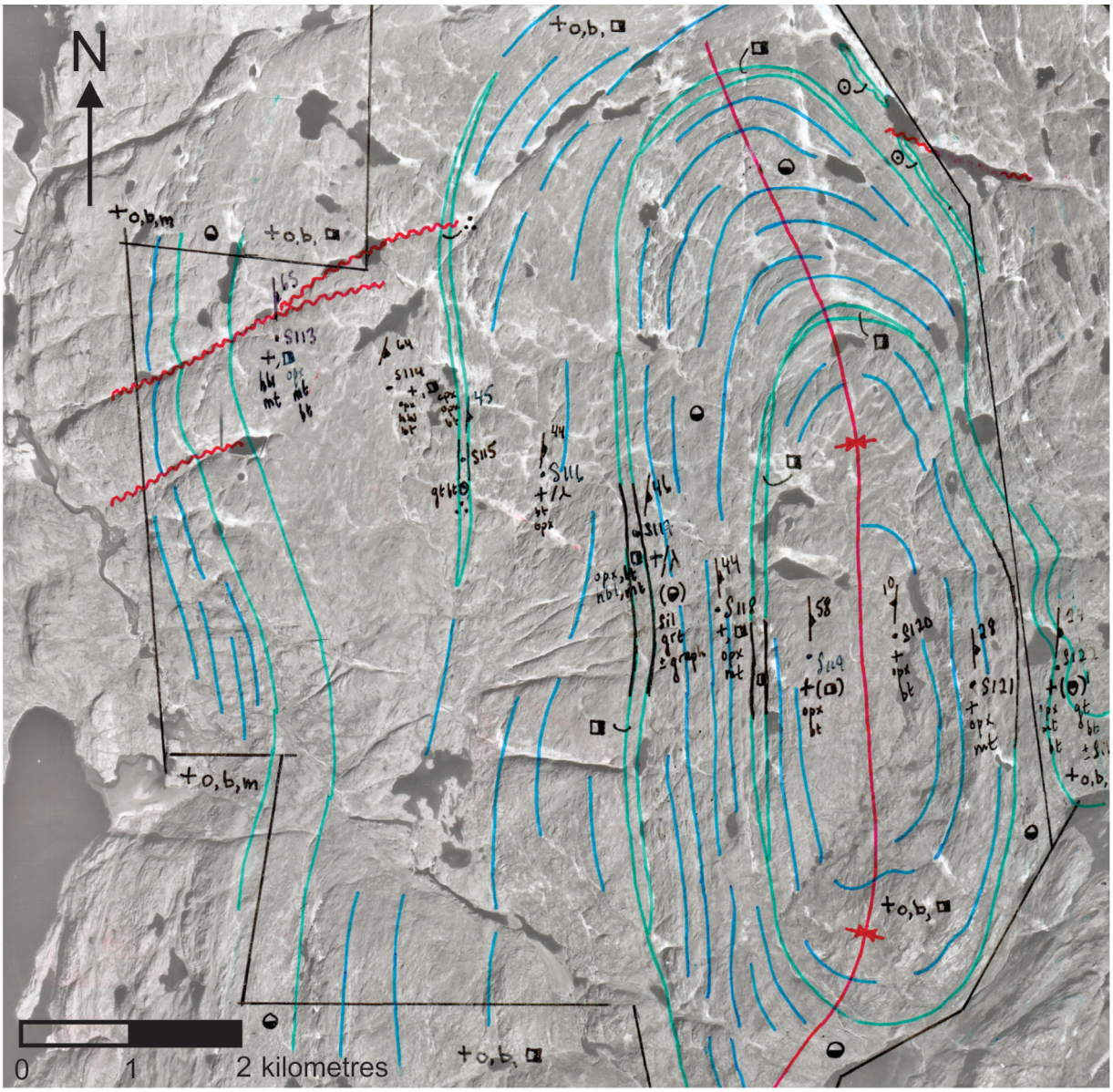

Figure 12: Airphoto-scale, north-trending and west-verging D_3 fold of monzogranite, diorite and Lake Harbour Group strata, Meta Incognita Peninsula, Baffin Island, Nunavut, that is refolded about an east-trending D_4 fold axis; symbols and coloured lines drawn on the airphoto are a graphical representation of the traverse data and geology; location of the airphoto is shown on Figure 3.

possibly the North Atlantic craton. An M.Sc. thesis using published tectonic and structural data, as well as the new observations from the 2014 and 2015 field seasons, will aim to integrate the various datasets into a regional 3-D tectonostructural model of the northeastern segment of the Trans-Hudson Orogen to compare, and improve upon, existing regional tectonic models, such as those in Corrigan et al. (2009), St-Onge et al. (2009) and Whalen et al. (2010).

Future work

Planned laboratory work in fall and winter 2014 includes bedrock geochronology of the eastern Meta Incognita and western Hall peninsula areas to establish the age of the major Archean and Paleoproterozoic rock packages. The primary focus, which bears on a representative suite of plutonic units and detrital samples, aims to contribute to the calibration of the legend for the new bedrock maps.

A visiting postdoctoral fellow, who will be joining the project in early 2015, will document the pressure and temperature conditions of samples collected from Meta Incognita Peninsula in 2014 (thermobarometry and quantitative phase diagram modelling), constraining mineral assemblages and growth history, as well as attendant geochronology.

With Meta Incognita Peninsula mapping successfully completed in 2014, the last unmapped region and likely tectonic keystone for the entire eastern Arctic segment of the Trans-Hudson Orogen is the Clearwater Fiord–McKeand River–Sylvia Grinnell Lake area. Engagement, planning and permitting activities are underway in preparation for an eight week mapping campaign between mid-June and mid-August 2015. Given the large aerial extent to be mapped in 2015 (covering all or part of five NTS 1:250 000 map areas outlined in purple on Figure 1), fieldwork will be targeted to the areas of greatest significance. To this end, a modern, high-resolution aeromagnetic survey (dashed red outline on Figure 1) is being conducted over the McKeand River area. Details of the survey are described in Miles et al. (2015).

Economic considerations

A number of lithological associations and occurrences with potential economic implications were identified during the 2014 systematic and targeted mapping campaign on eastern Meta Incognita Peninsula. The layered mafic-ultramafic sills emplaced in sulphidic siliciclastic strata have a lithological context similar to that hosting Ni–Cu–platinum-group element mineralization elsewhere in the Trans-Hudson Orogen (e.g., Raglan deposit in the eastern Cape Smith Belt of northern Quebec; St-Onge and Lucas, 1994; Lesher, 2007). The field characteristics of the sills are described in more detail in St-Onge et al. (2015). Serpentinized ultramafic rocks have been identified at a number of localities in the map area, some of which may provide material suitable as carving stone.

Abundant granitic pegmatite dykes and veins on the peninsula containing muscovite, biotite and locally tourmaline were sampled for further analysis into their rare-earth element mineralization potential.

Acknowledgments

Enthusiastic field assistance in the notably scenic, yet physically demanding terrain, of eastern Meta Incognita Peninsula was provided by A. Bigio, T. Chadwick, R. Hinanik, H. Iyerak, D. Liikane, A. Markey and D. Mate. In addition to contributions in the field, C. Gilbert's knowledge, care and organization of the project data management proved invaluable. D. Guilfoyle's prowess in the kitchen fuelled the many and varied participants of the team, who are grateful for her contributions and flexibility. Universal Helicopters, and in particular pilots G. Nuttall and G. Hartery, are thanked for safe and professional air support. Many thanks to the management and administrative support of S. Dehler, D. Mate, M. Francis, R. Khoun and T. Schroeder. The Polar Continental Shelf Program provided logistical support. Finally, A. Laviolette, G. Buller, R. Buenviaje and S. Eagles are acknowledged for invaluable help with capturing the archival and new data for Meta Incognita Peninsula. N. Wodicka and D. Matte are thanked for careful and insightful reviews of this paper.

Natural Resources Canada, Earth Sciences Sector contribution 20140276

References

Blackadar, R.G. 1967: Geological Reconnaissance, southern Baffin Island, District of Franklin; Geological Survey of Canada, Paper 66-47, 32 p., doi:10.4095/100926

Corrigan, D., Pehrsson, S., Wodicka, N. and de Kemp, E. 2009: the Palaeoproterozoic Trans-Hudson Orogen: a prototype of modern accretionary processes; *in* Ancient Orogens and Modern Analogues, J.B. Murphy, J.D. Keppie and A.J. Hynes (ed.), The Geological Society, London, Special Publications, v. 327, p. 457–479, doi:10.1144/SP327.19

Davison, W.L. 1959: Lake Harbour, Baffin Island, District of Franklin, Northwest Territories; Geological Survey of Canada, Preliminary Map 29-1958, 1:63 360 scale, doi:10.4095/108520

Dunphy, J.M. and Ludden, J.N. 1998: Petrological and geochemical characteristics of a Paleoproterozoic magmatic arc (Narsajuaq Terrane, Ungava Orogen, Canada) and comparisons to Superior Province granitoids; Precambrian Research, v. 91, p. 109–142.

Geological Survey of Canada 1998: Release of high resolution aeromagnetic total field survey of Baffin Island, Northwest Territories, Phase II; Geological Survey of Canada, Open File 3496, 1:100 000 scale, doi:10.4095/209934

Geological Survey of Canada 1999: Release of high resolution aeromagnetic total field survey of Baffin Island, Northwest

Territories, Phase I; Geological Survey of Canada, Open File 3413, 1:100 000 scale, doi:10.4095/210116

Hoffman, P.F. 1988: United Plates of America, the birth of a craton: Early Proterozoic assembly and growth of Laurentia; Annual Reviews of Earth and Planetary Sciences, v. 16, p. 543–603.

Jackson, G.D. and Taylor, F.C. 1972: Correlation of major Aphebian rock units in the northeastern Canadian Shield; Canadian Journal of Earth Sciences, v. 9, p. 1650–1669.

Jackson, G.D., Hunt, P.A., Loveridge, W.D. and Parrish, R.R. 1990: Reconnaissance geochronology of Baffin Island, N. W. T.; *in* Geological Survey of Canada, Current Research 89-2, p. 123–148.

Lesher, C.M. 2007: Ni-Cu-(PGE) deposits in the Raglan area, Cape Smith Belt, New Quebec; in Mineral Deposits of Canada: a Synthesis of Major Deposit Types, District Metallogeny, the Evolution of Geological Provinces and Exploration Methods, W.D. Goodfellow (ed.), Geological Association of Canada, Special Publication, v. 5, p. 351–386.

Lewry, J.F. and Collerson, K.D. 1990: The Trans-Hudson Orogen; extent, subdivisions, and problems; *in* The Early Proterozoic Trans-Hudson Orogen of North America, J.F. Lewry and M.R. Stauffer (ed.), Geological Association of Canada, Special Paper 37, p. 1–14.

Lucas, S.B. and Byrne, T. 1992: Footwall involvement during arc-continent collision, Ungava orogen, northern Canada; Journal of the Geological Society of London, v. 149, p. 237–248.

Lucas, S.B. and St-Onge, M.R. 1992: Terrane accretion in the internal zone of the Ungava orogen, northern Quebec. Part 2: Structural and metamorphic history; Canadian Journal of Earth Sciences, v. 29, p. 765–782.

Machado, G., Bilodeau, C. and St-Onge, M.R. 2013a: Geology, southern part of Hall Peninsula, south Baffin Island, Nunavut; Geological Survey of Canada, Canadian Geoscience Map 135 (preliminary); Canada-Nunavut Geoscience Office, Open File Map 2013-1, scale 1:250 000. doi:10.4095/292443

Machado, G., Bilodeau, C., Takpani, R., St-Onge, M.R., Rayner, N.M., Skipton, D.R., From, R.E., MacKay, C.B., Creason, C.G. and Braden, Z.M. 2013b: Hall Peninsula regional bedrock mapping, Baffin Island, Nunavut: summary of field work; in Summary of Activities 2012, Canada-Nunavut Geoscience Office, p. 13-22.

Miles, W., Mate, D.J., St-Onge, M.R. and Steenkamp, H.M. 2015: Aeromagnetic survey of the McKeand River area, southern Baffin Island, Nunavut; *in* Summary of Activities 2014, Canada-Nunavut Geoscience Office, p. 97–104.

Pilkington M. and Oneschuk, D. 2007: Aeromagnetic and gravity; *in* Digital Geoscience Atlas of Baffin Island (south of 70°N and east of 80°W), Nunavut, M.R. St-Onge, A. Ford and I. Henderson (ed.), Geological Survey of Canada, Open File 5116.

Scott, D.J. 1997: Geology, U-Pb, and Pb-Pb geochronology of the Lake Harbour area, southern Baffin Island: implications for the Paleoproterozoic tectonic evolution of north-eastern Laurentia; Canadian Journal of Earth Sciences, v. 34, p. 140–155.

Scott, D.J. 1999: U-Pb geochronology of the eastern Hall Peninsula, southern Baffin Island, Canada: A northern link between the Archean of West Greenland and the Paleoproterozoic Torngat orogen of northern Labrador; Precambrian Research, v. 93, p. 5–26.

Scott, D.J. and Wodicka, N. 1998: A second report on the U-Pb geochronology of southern Baffin Island; *in* Geological Survey of Canada, Current Research 1998-F, p. 47–57.

Scott, D.J., Stern, R.A., St-Onge, M.R. and McMullen, S.M. 2002: U-Pb geochronology of detrital zircons in metasedimentary rocks from southern Baffin Island: implications for the Paleoproterozoic tectonic evolution of Northeastern Laurentia; Canadian Journal of Earth Sciences, v. 39, p. 611–623.

Scott, D.J., St-Onge, M.R., Wodicka, N. and Hanmer, S. 1997: Geology of the Markham Bay–Crooks Inlet area, southern Baffin Island, Northwest Territories; *in* Geological Survey of Canada, Current Research 1997-C, p. 157–166.

Steenkamp, H.M. and St-Onge, M.R. 2014; Overview of the 2013 regional bedrock mapping program on northern Hall Peninsula, Baffin Island, Nunavut; in Summary of Activities 2013, Canada-Nunavut Geoscience Office, p. 27–38.

St-Onge, M.R. and Lucas, S.B. 1994: Controls on the regional distribution of iron-nickel-copper-platinum group element sulfide mineralization in the eastern Cape Smith Belt, Quebec; Canadian Journal of Earth Sciences, v. 31, p. 206–218.

St-Onge, M.R., Hanmer, S. and Scott, D.J. 1996: Geology of the Meta Incognita Peninsula, south Baffin Island: tectonostratigraphic units and regional correlations; *in* Geological Survey of Canada, Current Research 1996-C, p. 63–72.

St-Onge, M.R., Lucas, S.B. and Parrish, R.R. 1992: Terrane accretion in the internal zone of the Ungava orogen, northern Quebec. Part 1: Tectonostratigraphic assemblages and their tectonic implications; Canadian Journal of Earth Sciences, v. 29, p. 746–764.

St-Onge, M.R., Rayner, N.M., Liikane, D. and Chadwick, T. 2015: Mafic, ultramafic and layered mafic-ultramafic sills, Meta Incognita Peninsula, southern Baffin Island, Nunavut; *in* Summary of Activities 2014, Canada-Nunavut Geoscience Office, p. 11–16.

St-Onge, M.R., Scott, D.J. and Lucas, S.B. 2000: Early partitioning of Quebec: Microcontinent formation in the Paleoproterozoic; Geology, v. 28, p. 323–326.

St-Onge, M.R., Scott, D.J. and Wodicka, N. 1999a: Geology, Frobisher Bay, Nunavut; Geological Survey of Canada, Map 1979A, 1:100 000 scale, doi:10.4095/210833

St-Onge, M.R., Scott, D.J. and Wodicka, N. 1999b: Geology, Hidden Bay, Nunavut; Geological Survey of Canada, 1980A, 1:100 000 scale, doi:10.4095/210835

St-Onge, M.R., Scott, D.J. and Wodicka, N. 1999c: Geology, McKellar Bay, Nunavut; Geological Survey of Canada, Map 1981A, 1:100 000 scale, doi:10.4095/210836

St-Onge, M.R., Scott, D.J. and Wodicka, N. 1999d: Geology, Wright Inlet, Nunavut; Geological Survey of Canada, Map 1982A, 1:100 000 scale, doi:10.4095/210840

St-Onge, M.R., Scott, D.J. and Wodicka, N. 1999e: Geology, Blandford Bay, Nunavut; Geological Survey of Canada, Map 1983A, 1:100 000 scale, doi:10.4095/210837

St-Onge, M.R., Scott, D.J. and Wodicka, N. 1999f: Geology, Crooks Inlet, Nunavut; Geological Survey of Canada, Map 1984A, 1:100 000 scale, doi:10.4095/210838

St-Onge, M.R., Scott, D.J. and Wodicka, N. 1999g: Geology, White Strait, Nunavut; Geological Survey of Canada, Map 1985A, 1:100 000 scale, doi:10.4095/210839

St-Onge, M.R., Scott, D.J. and Wodicka, N. 2001: Terrane boundaries within Trans-Hudson Orogen (Quebec–Baffin segment), Canada: changing structural and metamorphic

character from foreland to hinterland; Precambrian Research, v. 107, p. 75–91.

St-Onge, M.R., Scott, D.J. and Wodicka, N. 2002: Review of crustal architecture and evolution in the Ungava Peninsula–Baffin Island area: connection to the Lithoprobe ECSOOT transect; Canadian Journal of Earth Sciences, v. 39, p. 589–610, doi:10.1139/E02-022

St-Onge, M.R., Scott, D.J., Wodicka, N. and Lucas, S.B. 1998: Geology of the McKellar Bay–Wight Inlet –Frobisher Bay area, southern Baffin Island, Northwest Territories; *in* Geological Survey of Canada, Current Research 1998-C, p. 43–53.

St-Onge, M.R., Searle, M.P. and Wodicka, N. 2006: Trans-Hudson Orogen of North America and Himalaya-Karakoram-Tibetan Orogen of Asia: Structural and thermal characteristics of the lower and upper plates; Tectonics, v. 25, TC4006, 22 p, doi:10.1029/2005TC001907

St-Onge, M.R., Van Gool, J.A.M., Garde, A.A. and Scott, D.J. 2009: Correlation of Archaean and Palaeoproterozoic units between northeastern Canada and western Greenland: constraining the pre-collisional upper plate accretionary history of the Trans-Hudson orogen; *in* Earth Accretionary Systems in Space and Time, P.A. Cawood and A. Kroner, The Geological Society, London, Special Publications, v. 318, p. 193–235, doi:10.1144/SP318.7

St-Onge, M.R., Wodicka, N. and Ijewliw, O. 2007: Polymetamorphic evolution of the Trans-Hudson Orogen, Baffin Island, Canada: Integration of petrological, structural and geochronological data; Journal of Petrology, v. 48, p. 271–302, doi:10.1093/petrology/eg1060.

Thériault, R.J., St-Onge, M.R. and Scott, D.J. 2001: Nd isotopic and geochemical signature of the Paleoproterozoic Trans-Hudson Orogen, southern Baffin Island, Canada: implications for the evolution of eastern Laurentia; Precambrian Research, v. 108, p. 113–138.

Whalen, J.B., Wodicka, N., Taylor, B.E. and Jackson, G.D. 2010: Cumberland batholith, Trans-Hudson Orogen, Canada: Petrogenesis and implications for Paleoproterozoic crustal and orogenic processes; Lithos, v. 117, p. 99–118, doi: 10.1016/j.lithos.2010.02.008

Wodicka, N. and Scott, D.J. 1997: A preliminary report on the U-Pb geochronology of the Meta Incognita Peninsula, southern Baffin Island, Northwest Territories; *in* Geological Survey of Canada, Current Research 1997-C, p. 167–178.

Infrastructure and climate warming impacts on ground thermal regime, Iqaluit International Airport, southern Baffin Island, Nunavut

A.-M. LeBlanc[1], G.A. Oldenborger[2], W.E. Sladen [2] and M. Allard[3]

[1]*Natural Resources Canada, Geological Survey of Canada, Ottawa, Ontario, Anne-Marie.LeBlanc@nrcan-rncan.gc.ca*

[2]*Natural Resources Canada, Geological Survey of Canada, Ottawa, Ontario*

[3]*Centre d'études nordiques, Université Laval, Québec, Quebec*

LeBlanc, A.-M., Oldenborger, G.A., Sladen, W.E. and Allard, M. 2015: Infrastructure and climate warming impacts on ground thermal regime, Iqaluit International Airport, southern Baffin Island, Nunavut; *in* Summary of Activities 2014, Canada-Nunavut Geoscience Office, p. 119–132.

Abstract

In the context of a changing climate, for planned or newly built infrastructure it is useful to differentiate between the effects of climate warming and anthropogenic factors on the permafrost thermal regime. In 2010, a study was initiated on permafrost sensitivity and terrain conditions for the Iqaluit International Airport, Nunavut. The airport has a history of terrain stability problems and is now entering a major improvement phase. The separate and combined impacts of climate warming, snow accumulation and the infrastructure itself on the ground thermal regime were simulated using numerical modelling. Results indicate that the thermal impact of a thick snow cover year after year outweighs the effect of a warming trend in air temperature of 1°C per decade over 30 years. Change in the ground thermal regime over time due only to new embankment material depends on ground surface and permafrost conditions prior to the embankment construction. Embankment insulation with polystyrene causes the permafrost table to initially move upward; however, over time, the relatively large increase in the active-layer thickness below the insulation might eventually affect the stability of the embankment and the permafrost. Following an increase in air temperature of 3°C over 30 years, the simulations indicate maximum increases in active-layer thickness and permafrost temperature of 0.9 m and 1.8°C at 15 m depth, with the warmest ground found under the toe of the old apron embankment as well as under the original paved surfaces.

Résumé

Dans un contexte où de nouvelles infrastructures sont planifiées ou construites au moment où le climat est en changement, il devient utile de différencier entre les effets du réchauffement climatique et des facteurs anthropiques sur le régime thermique du pergélisol. Une étude a été initiée en 2010 sur la sensibilité du pergélisol et les conditions de terrain à l'aéroport d'Iqaluit. Par le biais de la modélisation numérique, les impacts isolés et combinés du réchauffement climatique, de l'accumulation de neige et des nouvelles infrastructures sur le régime thermique du sol sont simulés. Les résultats montrent que l'impact thermique, année après année, d'un couvert nival épais sur le sol l'emporte sur le changement thermique induit par une tendance au réchauffement de la température de l'air de 1°C par décennie sur une période de 30 ans. La modification du régime thermique du pergélisol avec le temps due à la mise en place du nouveau remblai dépend des conditions de surface du sol et des conditions du pergélisol avant la construction du remblai. L'addition d'un isolant (polystyrène) dans le remblai permet au plafond du pergélisol de remonter dans le remblai. Cependant, avec le temps l'épaississement relativement important de la couche active sous l'isolant peut éventuellement affecter la stabilité du remblai et du pergélisol. Lorsqu'une augmentation de la température de l'air de 3°C sur 30 ans est utilisée, l'épaississement maximal de la couche active est de 0.9 m alors que la hausse de la température du pergélisol est de 1.8°C à 15 m de profondeur. Le pergélisol le plus chaud se trouve sous le pied de l'ancienne aire de trafic ainsi que sous les surfaces initialement pavées.

This publication is also available, free of charge, as colour digital files in Adobe Acrobat® PDF format from the Canada-Nunavut Geoscience Office website: http://cngo.ca/summary-of-activities/2014/.

Introduction

It is now common knowledge that climate change may threaten the integrity of northern infrastructure by altering the ground thermal regime and should therefore be considered in the design of infrastructure on permafrost (Instanes, 2005). Common methods used to aid in the reduction of permafrost degradation under transportation infrastructure include increasing embankment thickness and adding embankment insulation (Doré and Zubeck, 2009). However, the structure itself, snow accumulation and water ponding along embankments will also influence the ground thermal regime (Fortier et al., 2011; Allard and Lemay, 2012). In the context of a changing climate, for planned or newly built infrastructure it is useful to differentiate between the effects of climate warming and anthropogenic factors on the permafrost thermal regime to better understand the causes behind the thermal changes of permafrost.

In 2010, a joint study was initiated between the Canada-Nunavut Geoscience Office (CNGO), Natural Resources Canada (NRCan) and Université Laval Centre d'études nordiques (CEN) on permafrost sensitivity and terrain conditions within Iqaluit with an emphasis on the Iqaluit International Airport area. The airport has a history of terrain stability problems (Mathon-Dufour, 2014) and is now entering a major improvement phase (2014–2017), including the extension of paved areas. In order to support engineering design and management decisions, a multitechnique and multidisciplinary approach has been used (Allard et al., 2012; LeBlanc et al., 2012, 2013; Short et al., 2012, 2014; Mathon-Dufour, 2014; Oldenborger et al., 2014). In addition to previous work, ground surface temperature sensors were deployed to monitor the surface microclimate and support numerical modelling. This paper presents results of simulations for the separate and combined effects of anthropogenic factors, such as the infrastructure itself, snow accumulation and climate change on the ground thermal regime. A representative two-dimensional cross-section was created between the runway and what is now the main apron of the new terminal building.

Study site

Iqaluit is located on southeastern Baffin Island at the head of Frobisher Bay (63°45'N, 68°33'W) in a zone of continuous permafrost (Figure 1a). The airport is built on flat terrain surrounded by hills and rocky plateaus of the Precambrian Shield (St-Onge et al., 2006). The runway was originally constructed in 1942 (Figure 1b), followed by a runway extension at the northwest end and by the construction of additional aprons and taxiways in 1958 (Figure 1c). The 1942 portion of the runway and most of the undisturbed area between the runway and Apron I is built on glaciomarine delta deposits composed mainly of sand, silty sand, boulders and gravel. The runway extension is built on fill overlying glaciofluvial outwash and bedrock; alluvial channels and lacustrine deposits are also present under the embankments of taxiways, aprons and access roads (Figure 1c).

The study focuses on a two-dimensional cross-section (A–A') through the runway to Apron I (Figure 1d). Different ground surface conditions have been observed in the area east of the runway since 1942. Before the construction of Apron I, a main channel of Carney creek was flowing east of the runway (Figure 1b). During the construction of Apron I, this channel was filled and relocated toward the runway (Figure 1d). Most of the area between the runway and Apron I will be affected by planned construction by the end of 2014. This includes the extension of Apron I 40 m toward the runway, a new drainage channel, and a 3 m thick embankment to create a gentle slope toward the drainage channel close to the toe of the runway embankment.

The two-dimensional cross-section intercepts one air-rotary borehole drilled in 2010 in undeveloped terrain (DDH-02, Figure 1d). Visual observation of disturbed soil samples and approximate stratigraphic depths were recorded. Diamond drilling and extraction of permafrost cores was carried out in 2013 at various locations in the airport area (Mathon-Dufour, 2014). The stratigraphy of the glaciomarine delta deposits is generally defined by coarse sand underlain by fine sand. Depth to bedrock is unknown in the area between the runway and Apron I, but an electrical resistivity survey carried out in the vicinity of DDH-02 indicated that the bedrock surface should be at least 16 m deep. Embankment thickness is approximately 2.2 m, but can vary locally (Mathon-Dufour, 2014).

Climatic data

Environment Canada weather station data from Iqaluit are available from 1946; datasets between 1946 and 2011 are homogenized (Vincent et al., 2012) and recent climate data are available directly from the Government of Canada (Environment Canada, 2014). A cooling trend in the mean annual air temperature (MAAT) of about 0.3°C per decade occurred between 1946 and 1992, followed by a warming trend of about 1.1°C per decade between 1993 and 2013 (Figure 2). However, if the steplike increase in air temperature between 1993 and 2000 is excluded, the 14-year warming trend is approximately 0.5°C (Figure 2). For the normal period 1981–2010, the MAAT was –9.3°C with annual precipitation of 404 mm, of which 49% occurred as rain (Environment Canada, 2014). For the same period, the seasonal average surface wind speeds recorded in Iqaluit were 15.3, 16.1, 13.8 and 17.5 km/h for the winter, spring, summer and fall seasons, respectively (Environment Canada, 2014).

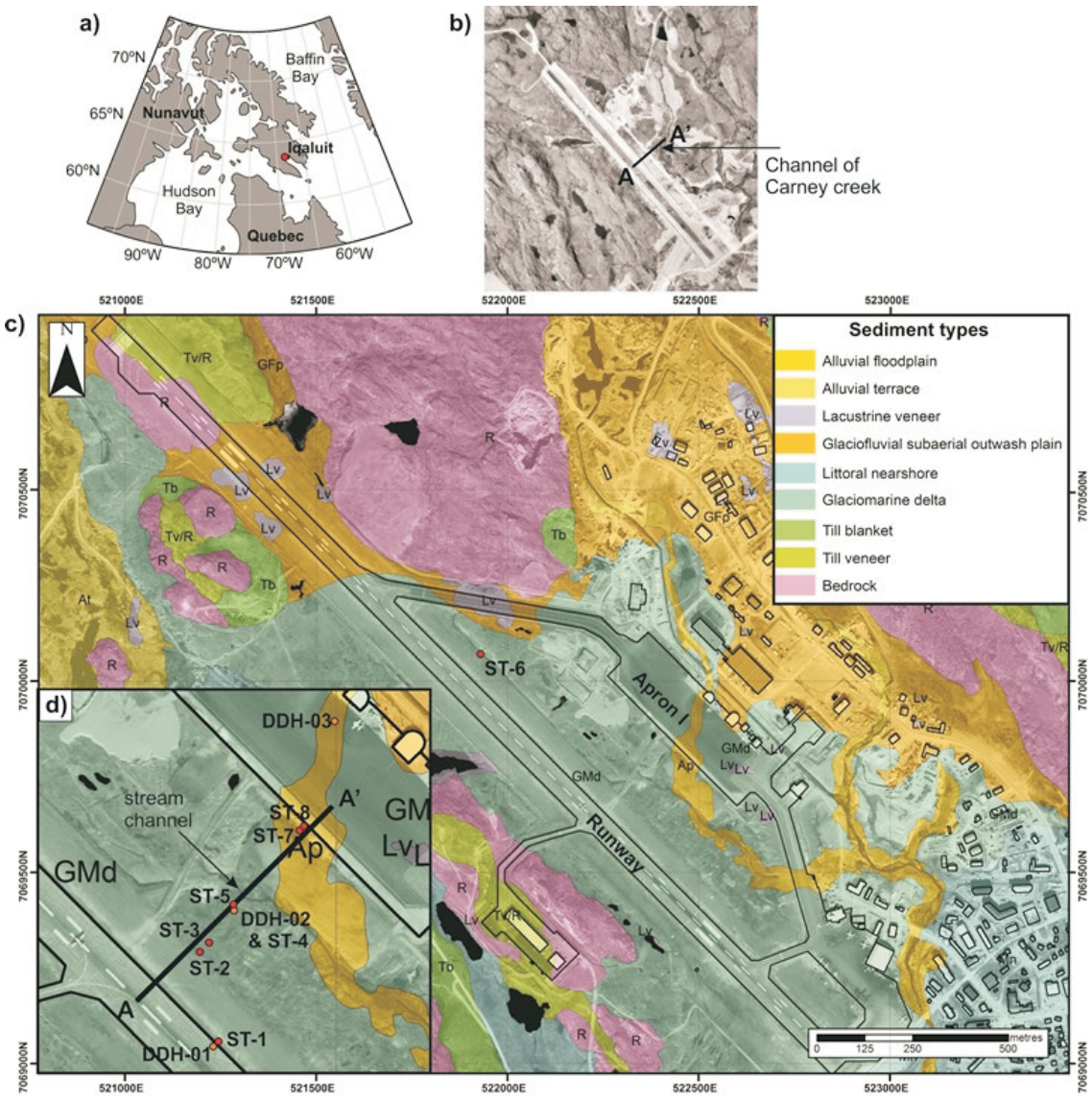

Figure 1: a) Location map of Iqaluit, Nunavut, at the head of Frobisher Bay, Baffin Island, Nunavut. **b)** Arial photograph of Iqaluit International Airport taken in 1948. **c)** Surficial geology of the Iqaluit International Airport area (Allard et al., 2012). **d)** Location of the two-dimensional cross-section (A–A'), thermistor cables (DDH) and ground surface temperature loggers (ST). Background image (WorldView-1 satellite image, August 19, 2008, DigitalGlobe, Inc., 2008) includes copyrighted material from DigitalGlobe, Inc., all rights reserved. UTM Zone 19.

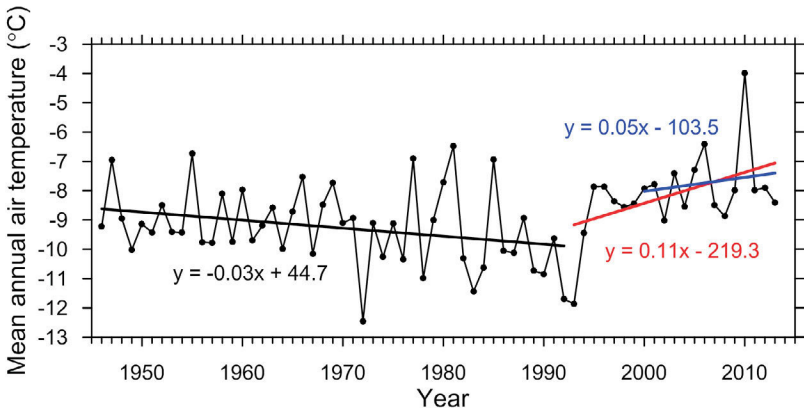

Figure 2: Mean annual air temperature for Iqaluit, Nunavut, between 1946 and 2013 (Vincent et al., 2012; Environment Canada, 2014).

Ground and near-surface temperatures

Borehole DDH-02 was instrumented with a thermistor cable to a depth of 15 m, while borehole DDH-01 and DDH-03 were installed and instrumented in 2011 under the paved surfaces of the runway and Apron I embankments (Figure 1d) to depths of 14.25 and 10 m. At DDH-02, annual mean permafrost temperatures recorded in 2012 in undisturbed terrain were –5.4 and –5.6°C at depths of 10 and 15 m with an active-layer thickness of approximately 1.4 m. In 2012, at sites DDH-01and DDH-03, permafrost temperatures under the paved embankment were –4.7 and –5.1°C (DDH-01) at depths of 10 and 15 m and –4.0°C (DDH-03) at a depth of 10 m with active-layer thicknesses of 2.5 and 2.6 m, respectively (Mathon-Dufour, 2014).

Ground temperature at depth can be simulated using air temperature, near-surface ground temperature and ground thermal properties. To establish the thermal boundary conditions for different ground surface conditions specific to the Iqaluit International Airport area, single-channel temperature loggers, HOBO Pro v2 data loggers manufactured by Onset®, were used to measure air temperature at one location (Environment Canada weather station, adjacent to airport facilities) and ground surface temperature at specific locations at one hour intervals. The loggers have a resolution of 0.03ºC and an accuracy of ±0.4ºC. Eight single-channel loggers, at sites ST-1 to ST-8, were buried 2 cm below the surface with seven close to the cross-section and one (ST-6) at the base of the runway drainage channel (Figure 1c, d). Snow-cover thickness at those sites was measured from a snow transect conducted in February 2012 along the cross-section. Monthly mean ground surface temperature is plotted as a function of monthly mean air temperature for each site in Figure 3. Averages of the monthly means (2010–2014) are also shown as solid black lines for each site in Figure 3. Daily mean ground surface temperature at ST-5 is plotted in Figure 3e to illustrate the daily relation and variability between air and ground surface temperatures. During the freezing season, the ground surface temperature is dominantly influenced by the snow cover and the soil water content via latent heat effect. For a dry and bare surface or a thin snow cover, the relation between air and ground surface temperature is close to 1:1 (e.g., ST-1 and ST-4). A thicker insulating snow cover results in ground surface temperature being shifted toward 0°C from fall to spring (e.g., ST-7). Soil with high moisture content will also maintain a ground surface temperature close to 0°C in the fall due to the dissipation of latent heat during phase change (e.g., ST-5). Once the ground surface has frozen, the near-surface temperatures will then decrease as air temperature falls. During the thawing season, near-surface temperatures are influenced by ground thermal properties, solar radiation, peat layer and vegetation cover (Karunaratne and Burn, 2004). No instrumentation was deployed to measure temperature of paved surfaces. For northern conditions, the range of freezing n-factors (ratio of the ground surface freezing index, or number of degree-days below 0°C, to the air freezing index) for asphalt pavement is 0.9 to 0.95 (Figure 3i; Lunardini, 1978). The thawing n-factor for asphalt pavement is a function of average wind speed during the thawing season (Joint Departments of the Army and Air Force USA, 1988). In Iqaluit, for an average wind speed of 13.8 km/h, the thawing n-factor for asphalt pavement is 1.9 (Figure 3i).

Ground thermal regime simulations

The two-dimensional conceptual model and its modifications over time (Figure 4) are based on geotechnical information collected onsite and historical data. The surface elevation of the two-dimensional cross-section has been extracted from a digital elevation model (DEM) generated at 1 m resolution, from 50 cm WorldView-1 stereo satellite images acquired August 19, 2008 (DigitalGlobe, Inc., 2008), using a proprietary stereo image matching process by PhotoSat Information Ltd. The model's subsurface profile is divided into four layers: bedrock, coarse sand, fine sand and embankment material. Stratigraphic information obtained in 2010 from borehole DDH-02 was validated using permafrost cores extracted in 2013 (Mathon-Dufour, 2014).

The properties of each unit of the thermal model are defined in Table 1. Except for the embankment material, soils were assumed to be saturated; therefore, the volumetric water content is equal to the soil porosity. The volumetric unfrozen water content depends on the temperature and was estimated using a power function (Nicolsky et al., 2009). The thermal conductivity for saturated soil was estimated from Côté and Konrad (2005) using a thermal conductivity of solid particles of k_s=2.9 W/(m·K). The volumetric heat capacity varies from unfrozen to frozen soil according to the water content and temperature. It was calculated as described in Andersland and Ladanyi (1994), except for bedrock where heat capacity remains constant.

A geothermal heat flux of 0.03 W/m^2 is applied at the bottom of the grid based on the thermal conductivity of bedrock (Table 1) and a temperature gradient of about 0.01 K/m (Chouinard et al., 2007). Zero heat flux boundaries are assigned on both sides of the model. The surface boundary of the thermal model is defined by the relations between the air and ground surface temperatures shown in Figure 3. The thermal effect of snow cover is implicitly included in surface temperature and is constant over time.

A modified version of the numerical code HydroGeoSphere (Therrien et al., 2010) was used to solve for the conductive two-dimensional transient heat transfer, taking into account the phase change problem. The groundwater flow modelling capability of HydroGeoSphere is applicable to the transient heat transfer problem in permafrost because

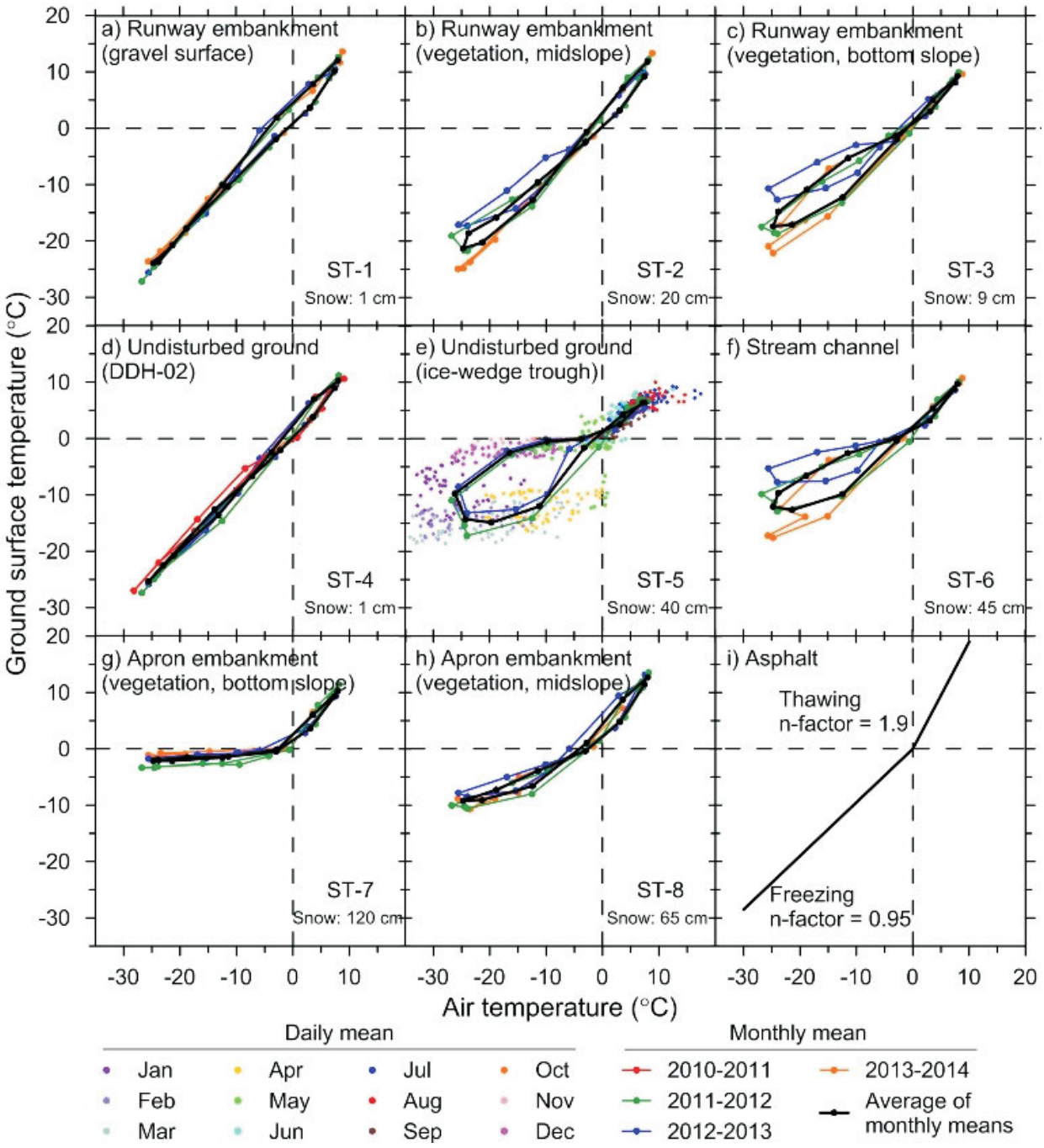

Figure 3: a–h) Monthly mean ground surface temperature as a function of monthly mean air temperature at sites ST-1 to ST-8, Iqaluit International Airport, Nunavut. Averages of monthly means for available years between 2010 and 2014 are shown for each site and daily mean temperatures are shown for site ST-5 (Figure 3e). Site locations shown on Figure 1. **i)** Thawing and freezing n-factors for asphalt, Iqaluit International Airport.

the governing differential equations of groundwater flow and heat transfer by conduction have similar forms (Fortier et al., 2011; LeBlanc, 2013).

The two-dimensional domain was divided into a set of finite elements. The mesh size coarsens with depth: 0.5 m in the top layers, including the embankment, the coarse sand and the fine sand down to an elevation of 10.7 m; 1 m in the fine sand between 10.7 and 0 m of elevation; 2 m in the top layers of the bedrock; and up to 6 m at the base of the model. The mesh size was refined to 0.15 m in the embankment to include the polystyrene insulation. Riseborough (2008) demonstrated that the estimated active-layer thickness error, while using linear interpolation on simulated ground thermal profiles, is <30% of the mesh size. Adaptive monthly time stepping was used to bring the simulation up

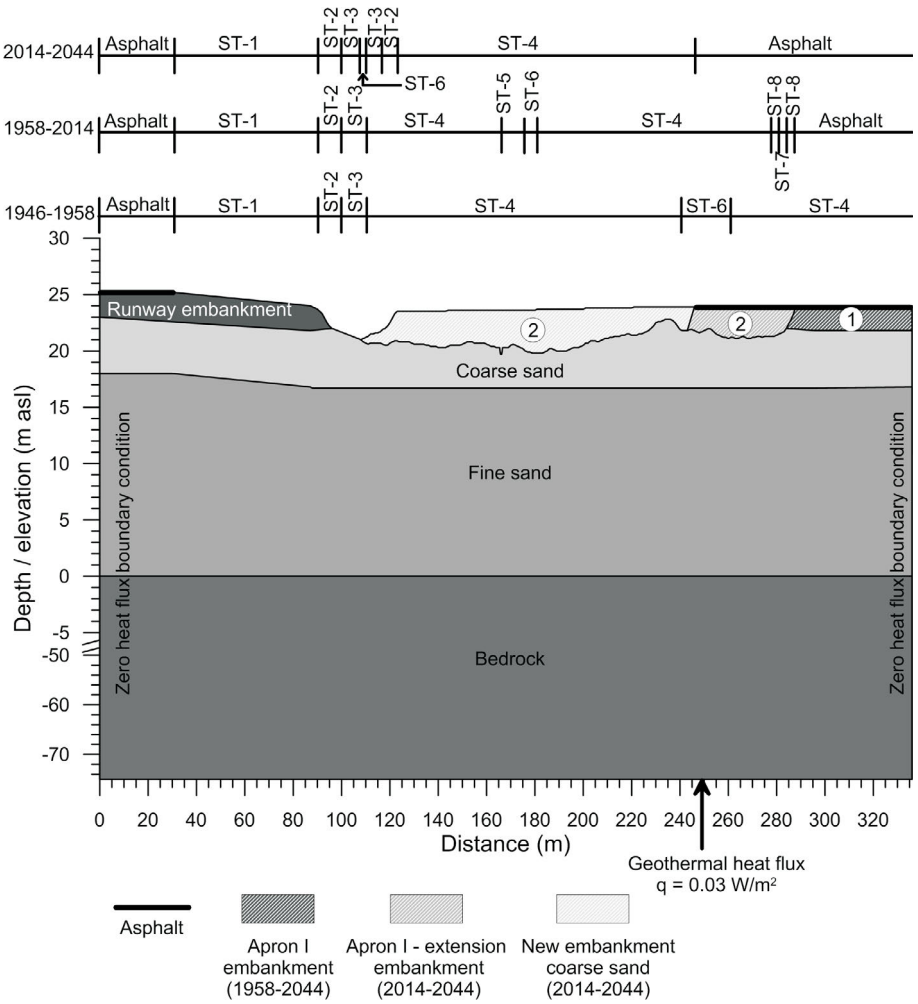

Figure 4: Two-dimensional subsurface conceptual model and three surface boundary conditions from 1946 to 2044 (see Figure 3 for specifics on surface boundary conditions), Iqaluit International Airport, Nunavut. Geometry ①: Apron I (1958–2044); geometry ②: Apron I extension and embankment toward the runway (2014–2044).

Table 1: Thermal and physical properties of the layers of the two-dimensional subsurface conceptual model, Iqaluit International Airport, Nunavut.

	Thermal conductivity[1]		Volumetric water content[2]	Saturation	Empirical constant[3]		Dry density[2]	Volumetric heat capacity[4]	
	k_u	k_f	θ_w	S_r	T_0	b	ρ	c_u	c_f
	(W/(m·K))	(W/(m·K))	(%)	(%)			(kg/m^3)	(MJ/(m^3·K))	(MJ/(m^3·K))
Embankment	2.11	2.12	7.5	50	0.01	0.7	2200	1.66	1.51
Coarse sand	1.96	2.71	25	100	0.01	0.7	2100	2.57	2.06
Fine sand	1.38	2.35	47	100	0.1	0.5	2000	3.50	2.66
Bedrock	3.00		0	-	-	-	-	2.08 [5]	
Polystyrene insulation	0.042 [4]		-	-	-	-	-	0.06 [4]	

[1]Côté and Konrad (2005): for unsaturated soil, parameters for well-graded gravel (crushed and natural) and gravel and coarse sand were used

[2]Values estimated from borehole information in Iqaluit

[3]Nicolsky et al. (2009)

[4]Andersland and Ladanyi (1994)

[5]Waple and Waple (2004); minerals composition from Laboratoire de construction 2000 Inc. (1988)

Abbreviations: f, frozen (at –5°C); u, unfrozen (at 5°C)

to 2011 and to simulate future ground temperature distributions, whereas adaptive daily time stepping was used between 2011 and 2014 in order to directly use the ground surface temperatures measured at different locations.

The simulation was initiated using an isothermal profile of –5.6°C, which corresponds to the mean monthly air temperature for October 1946. The model was then run with a nonvarying climate using air temperatures recorded in 1946–1947 until equilibrium was reached. From this point, ground temperatures were simulated following the air temperature record until September 2014. Nodes associated with the embankment geometries 1 and 2 (Figure 4) were kept inactive for the 1946–1958 period. In 1958, the nodes of the Apron I embankment were made active (geometry 1) until present day to simulate the current ground temperature distribution. In October 2014, the nodes of the embankment extension of Apron I and of the new 3 m thick embankment made of coarse sand were made active (geometry 2). Three cases over a 30-year period, starting in October 2014, were then simulated to assess the future ground temperature distributions under the infrastructure and its surroundings: 1) a constant sinusoidal function based on 2001 to 2013 air temperatures, 2) a climate-warming rate of 0.5°C per decade superposed on the annual fluctuation, and 3) a climate-warming rate of 1°C per decade superposed on the annual fluctuation. Both rates of warming are consistent with the trends observed in Iqaluit (Figure 2). Each case was duplicated to consider 1) the embankment alone and 2) the embankment with the polystyrene insulation.

Simulation results

Initially, the past and current ground temperature distributions were simulated using the cooling (1946–1992) and the warming (1993–2014) trends in the air temperature record as well as the change in surface conditions that have occurred since 1946. Results are shown in Figure 5 for 1958 (prior to the construction of the apron embankment), 1959 (after the construction of apron embankment), 1993 (onset of climate warming) and 2012. Thermal profiles extracted from the two-dimensional models are shown in Figure 6 for three locations: a) paved runway surface with underlying embankment, b) undisturbed terrain at the location of DDH-02, and c) toe of apron embankment. All results are shown for September, when the active layer is thick. In 1958, the thawing front under the paved runway surface was at 2.4 m depth, 0.2 m below the base of the runway embankment, and the permafrost temperature at 15 m depth was –5.2°C (Figure 6a). At the same depth in the undisturbed terrain, the permafrost temperature varies spatially between –5.9 and –4.4°C. The warmest permafrost is found beneath the stream channel at 250 m (Figure 5a). The active-layer thickness is approximately 1.5 m under undisturbed terrain with thin snow cover (Figure 6b). In 1959, the permafrost temperatures were in transition primarily as a result of infrastructure development, particularly between 175 and 336 m, as well as changes in MAAT (Figure 5b). The stream channel was relocated to 175 m, toward the runway, creating two cold permafrost cells at depth on each side, while the thermal effect of the previous channel is vanishing. The apron embankment forces the snow to be accumulated at its toe, as observed in winter, initiating an increase in ground temperatures at 280 m. The effect of the apron embankment results in a colder permafrost near the surface but slightly warmer permafrost below 6.5 m depth from the original surface. In 1993, at the end of a long cooling trend, the permafrost temperatures and active-layer thickness have decreased (Figure 5c). The thawing front is now within the runway embankment, 2.0 m below the paved surface (Figure 6a), whereas it is approximately 1 m below undisturbed terrain with thin snow cover (Figure 6b). The ground temperature at 15 m depth is –6.1°C under the paved runway surface and –7.1°C under undisturbed terrain with a thin snow cover. Ground temperature and active-layer thickness have generally decreased except at the apron embankment toe where a thick snow cover is present. At this location the ground temperature is –3.2°C at 15 m depth and the active-layer thickness is 1.7 m (Figure 6c). The thermal effect of the old channel has completely disappeared (Figure 5c). The recent climate warming trend, recorded after 1993, causes the permafrost temperatures to increase (Figure 5d). In September 2012, the ground temperatures at 15 m depth are –4.8, –5.6 and –2.7°C under the paved runway surface and the undisturbed terrain with a thin and a thick snow cover, respectively. Under the thick snow cover at the toe of the embankment, the increase in ground temperature between 1993 and 2012 is 0.5°C compared to ~1.4°C everywhere else but the active layer is still thicker: 2 m (Figure 6c) compared to 1.5 m in undisturbed terrain with thin snow cover (Figure 6b). Under the paved runway surface, the thawing front reaches the coarse sand layer underlying the embankment, 2.7 m below the paved surface (Figure 6a).

The adjustment of permafrost temperatures due to the new apron embankment and the paved and unpaved surfaces is shown in Figure 7a for September after 10 years of simulation with a constant MAAT. Results obtained after 20 and 30 years are equivocal to the 10-year simulation. Thermal profiles from the same three locations in Figure 6 are shown in Figure 8. The effect of the new embankment material on the ground thermal regime is similar to the effect of construction of Apron I in 1958. At locations where the permafrost was relatively cold due to a previously thin snow cover, the permafrost temperatures decrease by several degrees between the old surface and 6.4 m depth, below which there is a slight increase of 0.4 to 0.6°C. The permafrost table moves upward to 1.6 m from the new surface (Figure 8b). However, in areas of previously thick snow cover, where permafrost was relatively warm in 2012, the

addition of embankment material causes the temperatures at all depths to decrease by 1 to 4°C (Figure 8c). Adding polystyrene insulation within the embankment material at 1 m from the paved surface causes the permafrost table to move upward just under the insulation (Figures 7b, 8c). This effect leads to permafrost cooling in the first metres below the surface. However, below 4 m depth (from old surface), the temperatures are higher by a few tenths of a degree Celsius compared to the scenario without insulation.

The simultaneous effects of embankment, insulation and climate warming after a period of 30 years are shown in Figure 7c and d with associated thermal profiles in Figure 8.

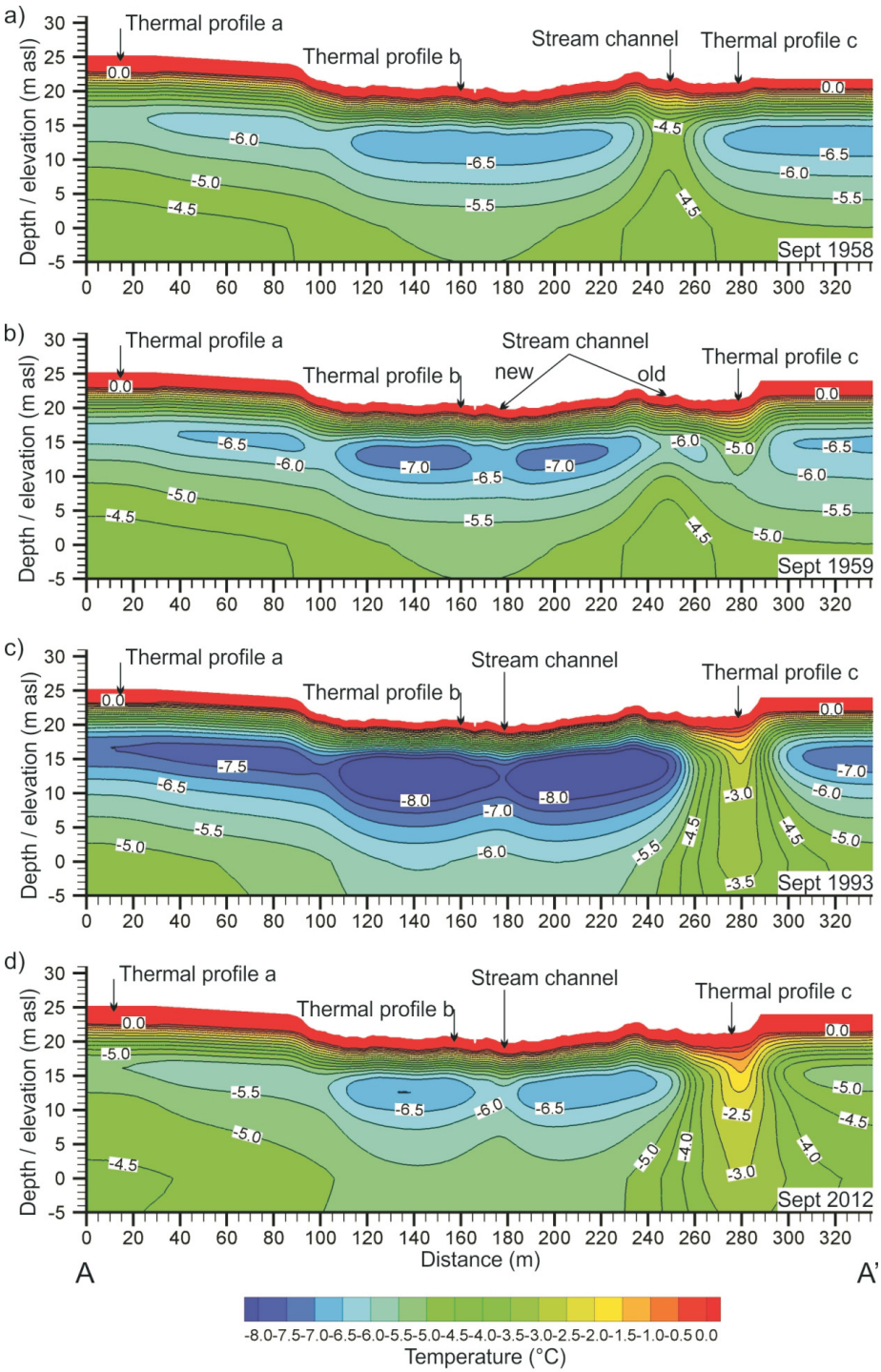

Figure 5: Permafrost temperature distribution for the month of September, Iqaluit International Airport, Nunavut: **a)** 1958, **b)** 1959, **c)** 1993 and **d)** 2012. See Figure 6 for the thermal profiles.

In general, the warming trends cause the permafrost to be warmer at depth while remaining colder close to the surface compared to the conditions prior to the apron extension and the placement of fill material toward the runway. At the toe of the old apron embankment, where a thick snow cover existed, the combined impact of new embankment material (with or without insulation) and the warming trend of 0.5°C per decade leads to modelled permafrost temperatures remaining below the preconstruction temperatures at 15 m depth (Figure 8c). A 1.0°C per decade warming trend is needed for temperatures at 15 m depth to warm to the same level as prior to the apron extension. The ground temperatures at 15 m depth (from the original ground surface) for previously undisturbed terrain for thin and thick snow covers are –4.9°C (Figure 8b) and –3.4°C (Figure 8c), respectively, for a warming trend of 0.5°C; and –4.3°C (Figure 8b) and –2.9°C (Figure 8c), respectively, for a warming trend of 1.0°C. Under the paved runway surface, for warming trends of 0.5 and 1.0°C per decade, ground temperatures at 15 m depth increase by1.2 and 1.8°C, respectively, leading to permafrost temperatures of –3.6 and –3.0°C for the two scenarios (Figure 8a). After 30 years, the simulations indicate an increase in active-layer thickness after it initially moved upward to within the new embankment or close to its base. With the warming trend of 0.5°C per decade, the active layer is about 0.3 m thicker than current conditions, regardless of paving or insulation. Differences in active layer thickening between various site conditions become more evident with the warming trend of 1°C per decade. The active layer increases by 0.6 m under the paved runway surface (Figure 8a) compared to an increase of 0.9 m under the unpaved embankment (Figure 8b), due to the lower thermal conductivity of the unsaturated runway embankment. Thickening of the active layer is greater in the scenario where polystyrene insulation is used (0.8 m compared to 0.5 m for the scenario without insulation) although the thawing front remains above the preconstruction surface (Figure 8c). Within the first 10 years of simulation (with or without warming trends), the thermal effect of the old channel at 175 m has almost or completely disappeared (Figure 7).

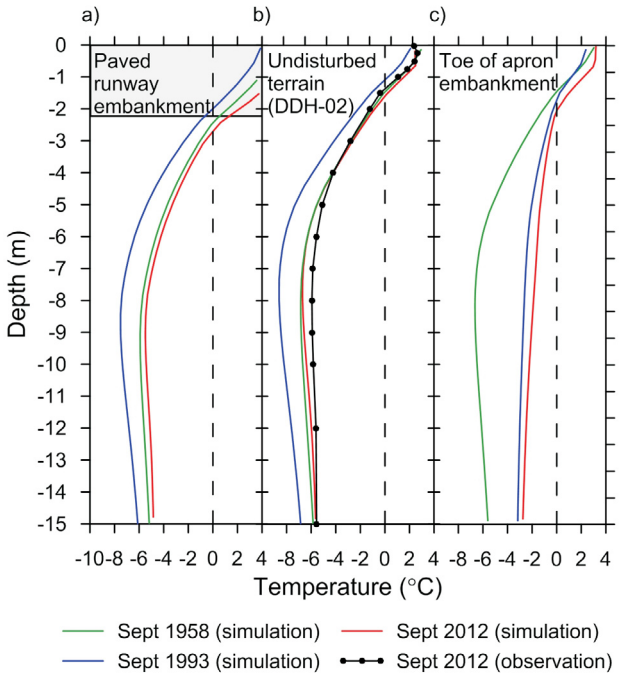

Figure 6: Simulated and observed thermal profiles for the month of September, Iqaluit International Airport, Nunavut, under: **a)** paved runway surface with underlying embankment, **b)** undisturbed terrain at DDH-02 and **c)** toe of apron embankment.

Discussion

Results of this study of simulated past and current ground temperatures and active-layer thicknesses at Iqaluit International Airport are in agreement with other studies in the Iqaluit area and in other northern communities (see below). Variability in the simulated permafrost temperature distribution reflects the differences in the observed ground thermal regime (Mathon-Dufour, 2014) under paved surfaces, unpaved embankment (or runway shoulders) and undisturbed terrain. For example, the temperature profile recorded at the thermistor cables DDH-02 for the month of September 2012 is consistent with modelled values (Figure 6b). Simulated temperatures under the paved runway surface are also in good agreement with the ground thermal regime recorded at the thermistor cable DDH-01. The simulated temperature increase of about 1.4°C at 15 m depth is also in good agreement with the mean increase of about 1.3°C at 20 m depth in different types of soil in northern Quebec between 1993 and 2008 (Smith et al., 2010). Throop et al. (2010) indicated an increase of 2.0°C per decade at 5 m depth in two shallow boreholes in Iqaluit between 1993 and 2003, which agrees well with the increase of 1.8 and the 2.0°C simulated at 5 m depth between 1993 and 2012 under undisturbed terrain and paved surfaces, respectively. Differences between the simulated and the observed results can be attributed to incorrect assignment of initial conditions, thermal and physical properties, three-dimensional heterogeneity, and other heat-transfer processes. Spatial variability is more complex than represented in the conceptual model, especially where alluvial sediments underlie the apron embankment. At this location, water could accumulate in the active layer resulting in warmer ground temperatures (Mathon-Dufour, 2014).

The simulated results indicate that the effect on the ground thermal regime of the modified stream channel vanishes completely within 10 years. Only conductive and latent heat transfers were simulated. However, if the increase in ground-ice content at the preconstruction stream channel location could have been simulated, the latent heat effect would have probably played a more important role. Furthermore, it is possible that the filled stream channel repre-

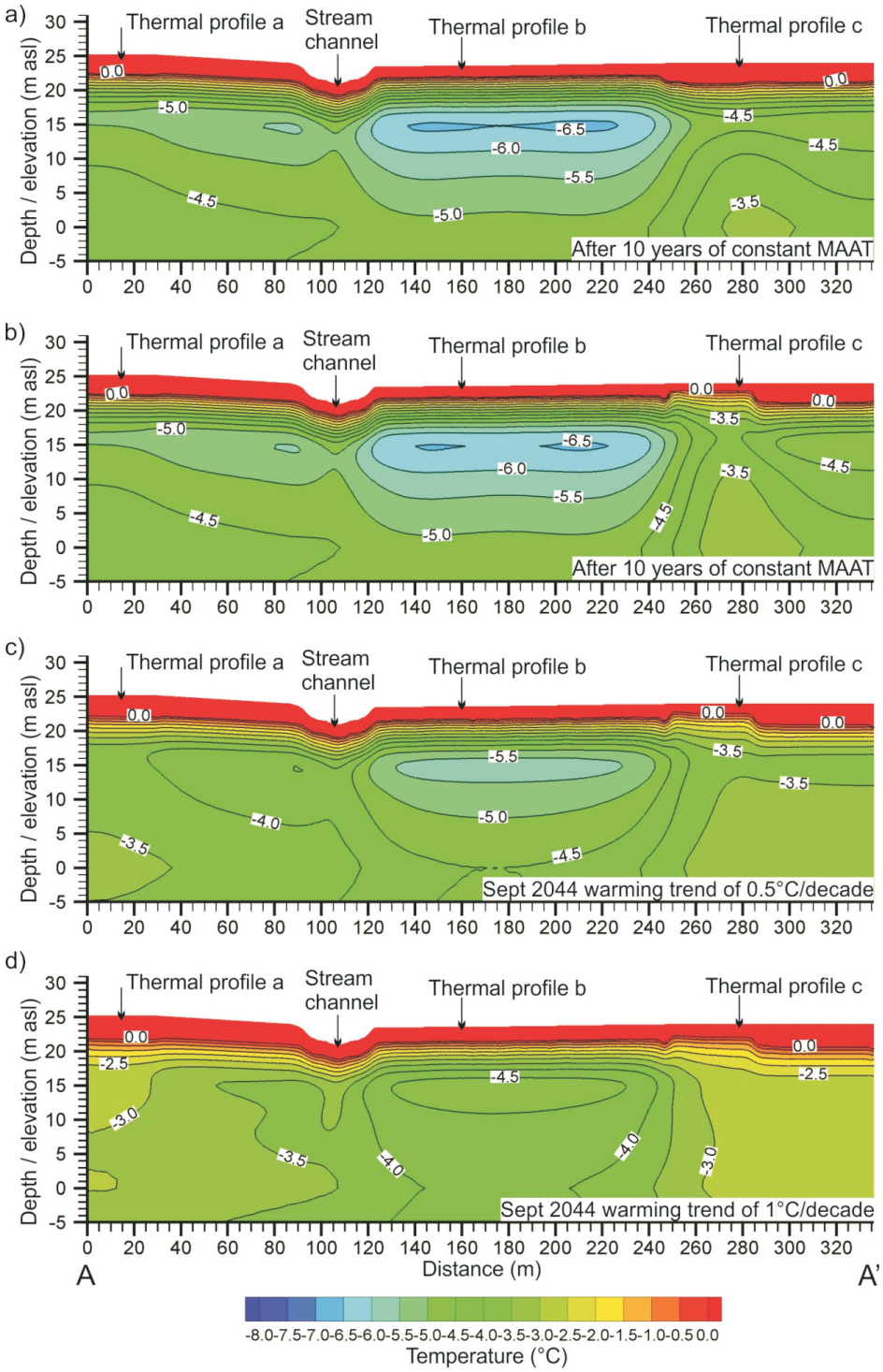

Figure 7: Simulated permafrost temperature distribution for the month of September for different scenarios, Iqaluit International Airport, Nunavut: **a)** embankment without warming trend, **b)** embankment and insulation without warming trend, **c)** embankment and insulation with warming trend of 0.5°C per decade, and **d)** embankment and insulation with warming trend of 1°C per decade. Abbreviation: MAAT, mean annual air temperature.

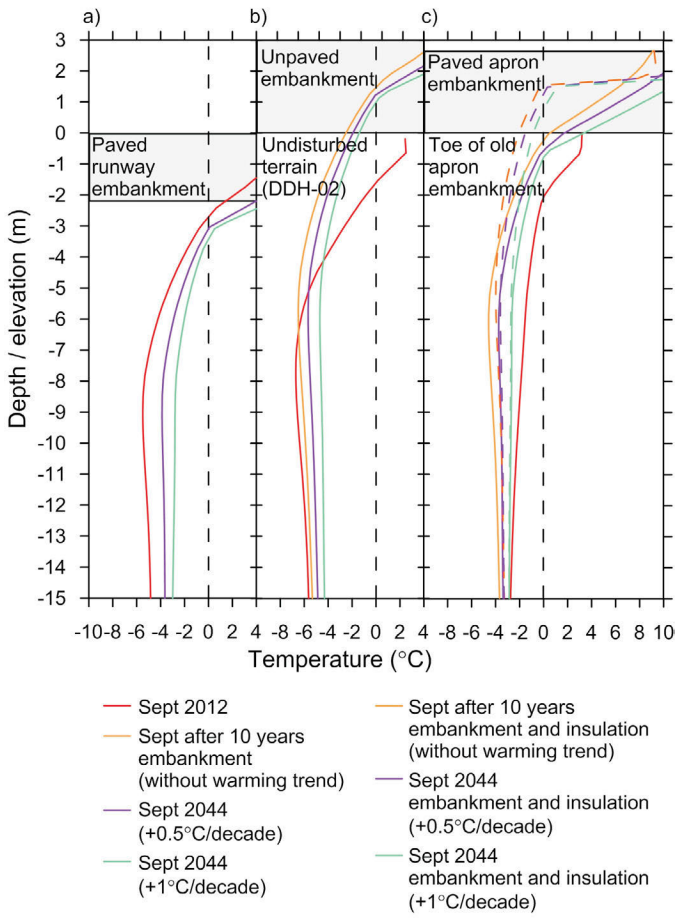

Figure 8: Simulated thermal profiles for the month of September, Iqaluit International Airport, Nunavut, under **a)** paved runway surface with underlying embankment, **b)** new unpaved surface with underlying embankment over undisturbed terrain at DDH-02, and **c)** new paved surface with underlying embankment over the toe of the old apron embankment.

sents a preferential groundwater flowpath, which would result in convective heat transfer. In this way, the pre-existing stream channel has the potential to modify the permafrost temperature long after it is filled. Cumulative impacts of convective and conductive heat transfer are beyond the scope of this paper.

The simulated thermal impact of a constant thick snow cover from year to year outweighs the thermal change induced by the warming trend of 1°C per decade over 30 years if the surface temperatures measured at ST-7 are considered. During the cooling trend from 1958 to 1993, the accumulation of snow at the toe of the old apron embankment caused the permafrost temperature at 15 m depth to increase by 2.3°C. In comparison, the increase in permafrost temperature is less under the paved runway surface (1.8°C at 15 m depth) following an increase in air temperature of 3°C over 30 years.

Because of the insulating effect of the snow in winter, in the case where a warming trend was applied (between 1993 and 2014) and thick snow cover was considered, the rate of increase in permafrost temperatures and thickening of the active layer was lower in an area of thick snow cover than in an area with thin snow cover. However, thickening of the active layer also depends on the thermal profile. For profiles closer to the melting point, thick snow will have a greater influence since small increases in temperature will induce a phase change (LeBlanc, 2013) but these conditions were not reached during the timeframe of the simulation. However, results indicate that the active-layer thickness for a given soil is thicker under a snowbank due to its thermal insulating effect, which prevents the soil from cooling back to lower temperatures in winter and then enhances the thaw penetration the following summer (Allard and Lemay, 2012). Because surface conditions are continually affected by wind drifting and clearing the snow from runways and aprons, spatial variation in snow accumulation is considered in the surface boundary condition but kept constant throughout the simulation period.

Modification of ground thermal regime over time due to new embankment material depends on the ground surface and the permafrost conditions prior to the embankment construction. For relatively cold permafrost, adding an embankment causes permafrost temperatures to decrease near the surface as the permafrost table moves upward, which is essential to preserve the permafrost integrity. However, the negative effect of this is the increase of permafrost temperatures by a few tenths of degree Celsius below 6.5 m depth from the original surface. A similar thermal effect at depth was shown by Fortier et al. (2011) for warm permafrost. At the Iqaluit airport, the local insulating effect of snow leads to areas of warmer permafrost surrounded by colder ground temperatures. At these locations, placement of fill material causes the temperatures at all depths to decrease by several degrees. However, the effect of the embankment does not prevent the warming of the ground at depth following an increase in air temperature. For the warming trend simulations, the warmest permafrost is found at the toe of the old apron embankment where the ground was relatively warm prior to construction, as well as under the original paved surfaces (runway and old apron). In reality, because observed ground temperatures are greater at 10 m depth under Apron I than under the runway, and because some thermal effects are not modelled, warmer permafrost than that simulated for the future should be expected under the old apron and at its toe.

The thermal effect of adding polystyrene insulation within the embankment is similar to the effect of adding a new embankment: permafrost temperatures near the surface decrease while permafrost at depth warms by a few tenths of a degree Celsius. The positive effect of insulation in summer time, which is to impede the heat flow toward the active layer, appears to be a disadvantage in winter time because the insulation does not allow heat loss from the surface, thereby preventing the permafrost from cooling (Doré and Zubeck, 2009). Even if the permafrost table is still within the embankment after the 30 years of warming, the relatively large increase in the active-layer thickness of 0.8 m below the insulation could no longer be considered to be protecting the stability of the embankment and eventually the permafrost, especially if water accumulates between the insulation and the thawing front.

Conclusions

In 2010 and 2011, ground surface temperature sensors were deployed to monitor the surface microclimate at the Iqaluit International Airport on embankment slopes, undisturbed terrain, stream channels, ditches, and areas with variable thicknesses of snow cover. Combined with historical data since the construction of the airport and other geotechnical information, the ground surface temperatures were used to support numerical modelling of ground thermal evolution. A two-dimensional cross-section between the runway and what is now the main apron was used to show the separate and combined impacts of climate warming, snow accumulation, and the infrastructure itself on the ground thermal regime. Results indicate that the thermal impact of a thick snow cover year after year outweighs the effect of a warming trend in air temperature of 1°C per decade over 30 years. Change in the ground thermal regime over time due only to new embankment material depends on the ground surface and permafrost conditions prior to the embankment construction. Embankment insulation with polystyrene causes the permafrost table to move upward; however, with a warming trend of 1°C per decade over 30 years, the results indicate a relatively large increase in the active-layer thickness below the insulation that might eventually affect the stability of the embankment and the permafrost. For 30-year warming trends of 0.5 and 1°C per decade, the simulations indicate a maximum increase in active-layer thickness of 0.3 and 0.9 m, respectively, and a maximum permafrost temperature increase of 1.2 and 1.8°C, respectively, at 15 m depth. The warmest ground is found under the toe of the old apron embankment as well as under the original paved surfaces. Spatial variability in surface conditions and terrain types is more complex than simulated and other heat transfer processes might play an important role in permafrost sustainability.

Economic considerations

Iqaluit International Airport is the largest business gateway to Nunavut and is a critical piece of infrastructure for maintaining and increasing economic opportunity in Iqaluit, the eastern Arctic and across Canada's North. It is the only year-round transportation link, making it a vital component of life in Nunavut. The airport has a history of terrain stability problems, of which many are related to permafrost and terrain conditions. To ensure the integrity of the Iqaluit International Airport, the Government of Nunavut (GN) in partnership with industry has moved forward with the Iqaluit International Airport Improvement Project, which is the biggest capital project undertaken by the GN at a cost of approximately $300 million over 30 years. This project involves runway resurfacing and repair, apron expansion and new facility construction. With the onset of climate warming and with newly built infrastructure, the underlying permafrost will continue to warm and possibly degrade causing additional maintenance and sustainability problems. The results from this study will help northern transportation infrastructure managers to better understand the causes behind the thermal changes of permafrost.

Acknowledgments

The authors thank J. Graham, J. Hawkins, K. Henderson and the management team at Iqaluit International Airport for site access and co-operation. The authors thank D. Mate (now with the Canadian Northern Economic Development

Agency) and the Canada-Nunavut Geoscience Office for in-kind contributions and the Canadian Northern Economic Development Agency's (CanNor) Strategic Investments in Northern Economic Development (SINED) for financial support. This project is part of the Natural Resources Canada Climate Change Geoscience Program. C. Duchesne provided helpful comments and thorough reviews, which greatly improved the clarity of this paper.

Natural Resources Canada, Earth Sciences Sector contribution 20140323

References

Allard, M. and Lemay, M. 2012: Nunavik and Nunatsiavut: from science to policy, an integrated regional impact study (IRIS) of climate change and modernization; ArcticNet Inc., Quebec City, 303 p.

Allard, M., Doyon, J., Mathon-Dufour, V., LeBlanc, A.-M., L'Hérault, E., Mate, D., Oldenborger, G.A. and Sladen, W.E. 2012: Surficial geology, Iqaluit, Nunavut; Geological Survey of Canada, Canadian Geoscience Map 64, scale 1:15 000.

Andersland, O.B. and Ladanyi, B. 1994: Physical and thermal properties; Chapter 2 *in* Frozen Ground Engineering, Chapman & Hall, New York, 352 p.

Chouinard, C., Fortier, R. and Mareschal, J.-C. 2007: Recent climate variations in the subarctic inferred from three borehole temperature profiles in northern Quebec, Canada; Earth and Planetary Science Letters, v. 263, p. 355–369.

Côté, J. and Konrad, J.-M. 2005: A generalized thermal conductivity model for soils and construction materials; Canadian Geotechnical Journal, v. 42, p. 443–458.

DigitalGlobe, Inc. 2008: WorldView-1 satellite image; DigitalGlobe, Inc., image, URL <https:// browse.digitalglobe.com/imagefinder/showBrowseMetadata?catalogId=10100100051A2800> [November 2012].

Doré, G and Zubeck, H.K. 2009: Cold regions pavement engineering; American Society of Civil Engineering Press, Reston, Virginia, 416 p.

Environment Canada 2014: Historic climate data; Government of Canada, URL <http://climate.weather.gc.ca> [September 2014].

Fortier, R., LeBlanc, A.-M. and Yu, W. 2011: Impacts of permafrost degradation on a road embankment at Umiujaq in Nunavik (Quebec), Canada; Canadian Geotechnical Journal, v. 48, p. 720–740.

Instanes, A. 2005: Infrastructure: buildings, support systems, and industrial facilities; *in* Arctic Climate Impact Assessment, C. Symon, L. Arris and B. Heal (ed.), Cambridge University Press, New York, p. 907–944.

Joint Departments of the Army and Air Force USA 1988: Arctic and subarctic construction: calculation methods for determination of depths of freeze and thaw in soils; United States Government Printing Office, Technical Manual TM 5-852-6/AFR 88-19, v. 6, 62 p.

Karunaratne, K.C. and Burn, C.R. 2004: Relations between air and surface temperature in discontinuous permafrost terrain near Mayo, Yukon Territory; Canadian Journal of Earth Sciences, v. 41, p. 1437–1451.

Laboratoire de construction 2000 Inc. 1988: Étude aéroport Iqaluit/Study Iqaluit Airport; Travaux Publics Canada, Dossier 88220, 45 p.

LeBlanc, A.-M. 2013: Modélisation tridimensionnelle du régime thermique du pergélisol de la vallée de Salluit au Québec nordique en fonction de différents scénarios de réchauffement climatique; Ph.D. thesis, Université Laval, Québec, Quebec, 409 p.

LeBlanc, A.-M., Mathon-Dufour, V., Allard, M., Oldenborger, G.A., Short, N., L'Hérault, E. and Sladen, W.E. 2013: Permafrost characterization at the Iqaluit International Airport, Nunavut, in support of decision-making and planning; *in* Summary of Activities 2012, Canada-Nunavut Geoscience Office, p. 131–142.

LeBlanc, A.-M., Short, N., Oldenborger, G.A., Mathon-Dufour, V. and Allard, M. 2012: Geophysical investigation and InSAR mapping of permafrost and ground movement at the Iqaluit airport; *in* Cold Regions Engineering 2012: Sustainable Infrastructure Development in a Changing Cold Environment, B. Morse and G. Doré (ed.), American Society of Civil Engineers, p. 644–654.

Lunardini, V.J. 1978: Theory of n-factors and correlation of data; *in* Proceedings of the Third International Conference on Permafrost, July 10–13, 1978, Edmonton, Alberta, The National Research Council of Canada, Ottawa, v. 1, p. 41–46.

Mathon-Dufour, V. 2014: Caractérisation du pergélisol en vue de la réfection et de l'adaptation aux changements climatiques de l'aéroport d'Iqaluit, Nunavut; M.Sc. thesis, Université Laval, Québec, Quebec, 259 p.

Nicolsky, D.J., Romanovsky, V.E. and Panteleev, G.G. 2009: Estimation of soil thermal properties using in-situ temperature measurements in the active layer and permafrost; Cold Regions Science and Technology, v. 55, p. 120–129.

Oldenborger, G.A., LeBlanc, A.-M. and Sladen, W.E. 2014: Geophysical monitoring of permafrost conditions at Iqaluit International Airport, Nunavut; *in* Summary of Activities 2013, Canada-Nunavut Geoscience Office, p. 129–138.

Riseborough, D. 2008. Estimating active layer and talik thickness from temperature data: implications from modeling results; *in* Proceedings of the Ninth International Conference on Permafrost, D.L. Kane and K.M. Hinkel (ed.), Institute of Northern Engineering, University of Alaska Fairbanks, June 29–July 3, 2008, Fairbanks, Alaska, p. 1487–1492.

Short, N., LeBlanc, A.-M., Sladen, W.E., Allard, M. and Mathon-Dufour, V. 2012: Seasonal surface displacement derived from InSAR, Iqaluit, Nunavut; Geological Survey of Canada, Canadian Geoscience Map 66, scale 1:15 000.

Short, N., LeBlanc, A.-M., Sladen, W., Oldenborger, G., Mathon-Dufour, V. and Brisco, B. 2014: RADARSAT-2 D-InSAR for ground displacement in permafrost terrain, validation from Iqaluit Airport, Baffin Island, Canada; Remote Sensing of Environment, v. 141, p. 40–51.

Smith, S.L., Romanovsky, V.E., Lewkowicz, A.G., Burn, C.R., Allard, M., Clow, G.D., Yoshikawa, K. and Throop, J. 2010: Thermal state of permafrost in North America - a contribution to the international polar year; Permafrost and Periglacial Processes, v. 21, p. 117–135.

St-Onge, M.R., Jackson, G.D. and Henderson, I. 2006: Geology, Baffin Island (south of 70°N and east of 80°W), Nunavut; Geological Survey of Canada, Open File 4931, scale 1:500 000.

Therrien, R., McLaren, R.G., Sudicky, E.A. and Panday, S.M. 2010: HydroGeoSphere - a three-dimensional numerical model describing fully-integrated subsurface and surface flow and solute transport; Université Laval and University of Waterloo, 443 p.

Throop, J., Smith, S.L. and Lewkowicz, A.G. 2010: Observed recent changes in climate and permafrost temperatures at four sites in northern Canada; *in* Geo2010, Proceedings of the 63rd Annual Canadian Geotechnical Conference and the 6th Canadian Permafrost Conference, September 12–16, 2010, Calgary, Alberta, p. 1265–1272.

Vincent, L.A., Wang, X.L., Milewska, E.J., Wan, H., Yang, F. and Swail, V. 2012: A second generation of homogenized Canadian monthly surface air temperature for climate trend analysis; Journal of Geophysical Research., v. 117, issue D18110, doi:10.1029/2012JD017859

Waple, D.W. and Waple, J.S. 2004: A review and evaluation of specific heat capacities of rocks, minerals, and subsurface fluids. Part 1: mineral and nonporous rocks; Natural Resources Research, v. 13, p. 97–122.

Reconnaissance seabed mapping around Hall and Cumberland peninsulas, Nunavut: opening up southeastern Baffin Island to nearshore geological investigations

J.E. Hughes Clarke[1], J. Muggah[2], W. Renoud[2], T. Bell[3], D.L. Forbes[3, 4], B. Cowan[3] and J. Kennedy[5]

[1]*Ocean Mapping Group, Department of Geodesy and Geomatics Engineering, University of New Brunswick, Fredericton, New Brunswick, jclarke@unb.ca*

[2]*Ocean Mapping Group, Department of Geodesy and Geomatics Engineering, University of New Brunswick, Fredericton, New Brunswick*

[3]*Department of Geography, Memorial University of Newfoundland, St. John's, Newfoundland and Labrador*

[4]*Natural Resources Canada, Geological Survey of Canada and Bedford Institute of Oceanography, Dartmouth, Nova Scotia*

[5]*Fisheries and Sealing Division, Department of Environment, Government of Nunavut, Iqaluit, Nunavut*

This work was part of the 2012–2014 Nuliajuk Seabed Mapping Program (NSMP). The program is being run by the Ocean Mapping Group at the University of New Brunswick (UNB) on behalf of the Fisheries and Sealing Division, Department of Environment, Government of Nunavut (GN). The funding for the additional mapping objectives is being generated jointly by the Government of Nunavut, the Canada-Nunavut Geoscience Office (CNGO), Natural Resources Canada (NRCan), the University of New Brunswick, Memorial University of Newfoundland (MUN), ArcticNet and the Canadian Hydrographic Service. The study area is currently focused on the coastal marine regions within the Nunavut Land Claims Agreement, extending from Iqaluit to Clyde River.

Hughes Clarke, J.E., Muggah, J., Renoud, W., Bell, T., Forbes, D.L., Cowan, B. and Kennedy, J. 2015: Reconnaissance seabed mapping around Hall and Cumberland peninsulas, Nunavut: opening up southeastern Baffin Island to nearshore geological investigations; *in* Summary of Activities 2014, Canada-Nunavut Geoscience Office, p. 133–144.

Abstract

The waters around southeastern Baffin Island are some of the least known areas of Canada's submerged lands. The existing knowledge of bedrock geology offshore of Hall and Cumberland peninsulas is constrained primarily by aeromagnetic signatures. The surficial geology is inferred mainly from regional bathymetry and ice-flow directions on the adjacent landmasses.

With the almost complete lack of bathymetric definition within 10–30 km of the coastline, the area is not even safely accessible to shipping. Any future development of land-based resources on Hall and Cumberland peninsulas will require safe shipping access to port facilities. With the macrotidal environment and numerous restricted channels, the area has significant unexplored potential for tidal-power generation within the waters included in the Nunavut Land Claim Agreement. For either of these opportunities, adequate environmental assessment of the area will be a necessary precursor to development. That assessment will require knowledge of the submarine-geohazard potential, including iceberg scouring, active sediment-transport processes and submarine mass-wasting. To address these deficiencies in geoscience knowledge, a reconnaissance seabed-mapping program has been underway for the past three years.

The project activities of the Nuliajuk Seabed Mapping Program (NSMP) include 1) definition of safe access routes into the coastal waters of the Nunavut Land Claims Agreement; 2) delineation of seabed morphology along those access routes as an aid in understanding potential marine geohazards; and 3) acquisition of shallow sub-bottom profiling along those routes to define the distribution of surficial sediment.

Résumé

Les eaux circulant autour de la partie sud-est de l'île de Baffin recouvrent les terres submergées les plus méconnues du Canada. L'état de connaissances actuelles au sujet de la géologie du substratum rocheux au large des côtes des péninsules Hall et Cumberland provient surtout de l'étude des signatures aéromagnétiques. La géologie de surface de la région est déduite

This publication is also available, free of charge, as colour digital files in Adobe Acrobat® PDF format from the Canada-Nunavut Geoscience Office website: http://cngo.ca/summary-of-activities/2014/.

surtout à partir de la bathymétrie régionale et des indications des directions de l'écoulement glaciaire qui ont été relevées dans des masses terrestres contiguës.

En raison du fait qu'il n'existe pratiquement aucunes données bathymétriques des 10 à 30 km s'étendant au large des côtes, il est impossible de naviguer de façon sécuritaire dans cette région. Tout projet de mise en valeur des ressources de la terre des péninsules Hall et Cumberland exigera que les navires puissent accéder sans danger à des installations portuaires. En raison du milieu microtidal et de la présence de nombreux chenaux à accès restreint, cette région présente de grandes possibilités, jusqu'à date inexplorées, de production d'énergie marémotrice à l'intérieur des eaux couvertes en vertu de l'accord de revendications territoriales du Nunavut. Peu importe sa nature, toute mise en valeur éventuelle exigera auparavant que l'on procède à une évaluation environnementale appropriée. Une telle évaluation n'est possible que si l'on dispose de connaissances au sujet des géorisques sous-marins possibles que peuvent présenter des phénomènes, tels l'affouillement causé par les glaciers, les processus actifs de transport des sédiments et les épisodes de mouvement de masse sous-marins. Un programme de reconnaissance aux fins de cartographie du fond marin a été mis sur pied il y a trois ans afin de pallier à cette lacune au niveau de l'état actuel des connaissances géoscientifiques.

Parmi les travaux entrepris dans le cadre du programme de cartographie du fond marin de Nuliajuk, on note 1) la détermination de voies d'accès sécuritaires dans les eaux couvertes en vertu de l'accord de revendications territoriales du Nunavut; 2) la délimitation de la morphologie du fond marin le long de ces voies d'accès dans le but de mieux comprendre les géorisques marins qui peuvent de présenter; et 3) l'acquisition de sondages à faible profondeur des sédiments sous-jacents le long de ces mêmes voies d'accès, en vue de cerner le mode de répartition des sédiments de surface.

Introduction

Although accelerated terrestrial geological mapping of southeastern Baffin Island has been undertaken during the past six years through the Geo-Mapping for Energy and Minerals (GEM) program and on an ongoing basis by the Canada-Nunavut Geoscience Office (CNGO), the adjacent coastal waters remain almost completely unmapped due primarily to a lack of safe shipping access. As a result, baseline geoscience knowledge, knowledge of potential marine geohazards and the resource potential of the marine portion of the Nunavut Lands Claims Area remain almost entirely unknown.

This paper presents a summary of a reconnaissance seabed-mapping program that has now been operational from the RV *Nuliajuk* for three field seasons and is focused on the nearshore and shallow (<300 m) coastal waters around Hall and Cumberland peninsulas.

Methods

New multibeam-sonar and sub-bottom–profiling data are being collected from the RV *Nuliajuk*, a 19 m long fisheries research and training vessel owned and operated by the Government of Nunavut. Its primary mandate is to conduct exploratory fishery investigations to stimulate new living-resource industries in Nunavut. This activity fully occupies the optimal sea-ice and weather window in August to September of each year.

As a secondary and opportunistic program, in partnership with the University of New Brunswick (UNB) and Memorial University of Newfoundland (MUN), the vessel has been outfitted with a hull-mounted multibeam-sonar and sub-bottom–profiling system (Brucker et al., 2013). Using transit windows and time outside the optimal weather window, an additional six to eight weeks of marine-geoscience mapping can be undertaken annually.

Unlike single-beam bathymetric mapping operations that provide only two-dimensional (2-D) profiles, multibeam coverage can delineate seabed morphology at wavelengths as short as ~5% of the water depth. As a result, geomorphological studies analogous to those on land can, for the first time, be carried out on the seabed. The first multibeam coverage of this region was obtained starting in 2003 through the ArcticNet program of the CCGS *Amundsen*, which has now been running for more than a decade (Bartlett et al., 2006). The *Amundsen* multibeam data have been collected annually along widely spaced routes as the vessel transits offshore. Notably, however, the *Amundsen* almost never operates in depths less than 200 m unless there is pre-existing bathymetric information. As a result, the *Amundsen*-generated bathymetry (red lines in Figure 1) almost never extends inshore.

The model for *Nuliajuk* mapping operations is similarly to acquire underway data during all transit periods. With her shoal draft, high manoeuvrability and forward-looking scanning sonar, she is capable of working independently in uncharted shoal waters. The region under investigation by the *Nuliajuk* has been mostly avoided by surface shipping due to an almost complete lack of nautical charting surveys. Using partnerships with government geoscience organizations, including the CNGO and the Public Safety Geoscience Program of NRCan, as well as ship-time support for ArcticNet science projects and from the Fisheries and Sealing Division of the Government of Nunavut, additional

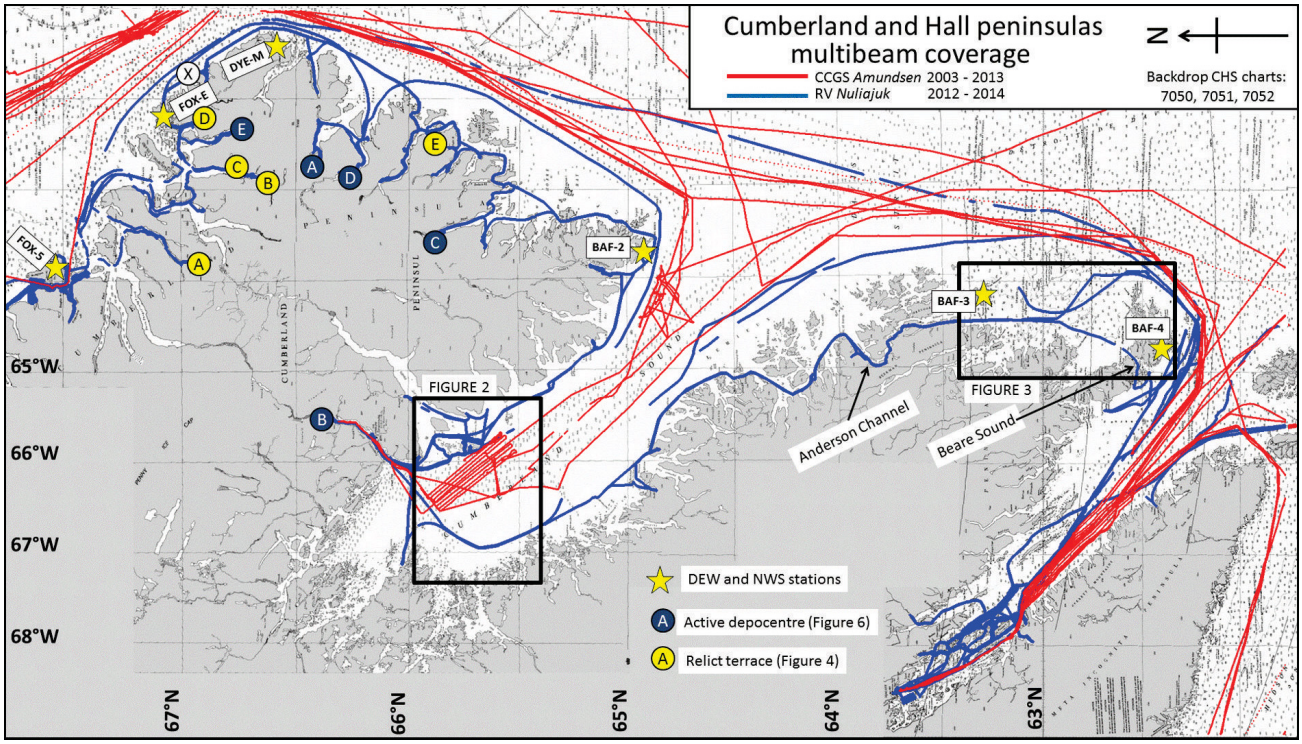

Figure 1: Available multibeam bathymetric coverage, southeastern Baffin Island. Red lines represent the tracks of CCGS *Amundsen* between 2003 and 2013. Blue tracks indicate the 2012–2014 activity of the RV *Nuliajuk* Seabed Mapping Program. The background is a composite of Canadian Hydrographic Service (CHS) Charts 7050, 7051 and 7052 at 1:500 000. On those areas of the charts where soundings are absent, no bathymetric data are available. Stars indicate restricted corridors of bathymetric sounding carried out to provide safe vessel access to Distant Early Warning (DEW) line and North Warning System (NWS) sites.

dedicated mapping time has been added to the program to expand the coverage into areas of interest to those clients. The end result is an opportunistic set of new corridors of marine-geoscience mapping information in previously unknown waters (blue lines in Figure 1).

Area of operations

For the past three years, the focus of the fisheries research has been on the nascent inshore Greenland halibut fishery off southern and eastern Baffin Island. As a result, the vessel starts and ends its operations each season in Iqaluit with transits around Hall Peninsula to Pangnirtung and onward around Cumberland Peninsula to Qikiqtarjuaq (Figure 1). Finally, two transits are conducted annually along the east-central coast of Baffin Island to Clyde River.

Relationship to adjacent terrestrial mapping

With the recent acceleration of terrestrial mapping through the GEM program and the CNGO, the pre-existing reconnaissance and regional framework mapping (Blackadar, 1967; Dyke et al., 1982) has been vastly expanded. Two programs, the Cumberland Peninsula program running from 2008 to 2010 and the Hall Peninsula Integrated Geoscience Program from 2011 to 2013 (Machado et al., 2013; Steenkamp and St-Onge, 2014), have resulted in a new series of terrestrial maps for both bedrock and surficial geology. These maps, however, stop at the coastline. Inferences on ice flow directions offshore are made almost entirely on the basis of extrapolation of onshore trends. Inferences about submerged bedrock and surficial geology rely on an extremely sparse set of historical observations (e.g., Maclean et al., 1986).

Regional bathymetry, defined from very sparse observations, has been the primary tool to reconstruct offshore glacial activity. Cross-shelf grounded ice-stream activity has been inferred from the presence of deep troughs, such as the Broughton trough (Gilbert, 1982) and Cumberland Sound (Maclean et al., 1986; Jennings, 1992).

With the paucity of available ground-truthing and dating, surficial sediments on land are classified and mapped, to a large extent, on the basis of surface character and landforms, which can be observed in aerial photographs (Dyke et al., 1982). Multibeam-sounding data and resulting shaded-relief bathymetry provide a near-equivalent (and in some ways superior) capability underwater.

Previous work on marine geology

The first bathymetric surveys of inshore regions of Hall and Cumberland peninsulas started with the 1955 Distant Early Warning (DEW) line surveys. These were site-specific corridors that only served the minimum requirement of access

to the infrastructure, with no intent to examine any of the surrounding relief. The additional late 1980s inshore surveys to support the expanded North Warning System (NWS) were also undertaken only to support narrow corridors to the sites. In all cases, only single-beam echo sounders were used, thus precluding any short-wavelength morphological analysis.

Regional bathymetric-framework studies of the eastern Baffin Shelf were undertaken in the 1960s (Løken and Hodgson, 1971) but did not extend south of Qikiqtarjuaq and neither did the subsequent 1980s programs, with the exception of Sunneshine Fiord, (1982–1983 SAFE surveys; Syvitski and Schafer, 1985). Similarly, shelf geological investigations (Praeg et al., 2007) were entirely north of Clyde River. Limited geophysical investigation of the crustal structure was attempted off the mouth of Cumberland Sound using a rock drill (Maclean et al., 1986) and there has been only one body of work on the Quaternary history of the deepest part of Cumberland Sound (Maclean et al., 1986; Jennings, 1992). Closer inshore studies were precluded by the lack of nautical charting to allow access.

Thus, outside of the restricted DEW/NWS corridors (marked by stars in Figure 1), the relief and geology of most of the coastal waters and shelf around these two peninsulas remain completely unknown. Rare small-boat targeted mapping has investigated drowned shorelines (see below and Miller 1975). The complete lack of charting information has discouraged any vessel-based access.

Results from 2012, 2013 and 2014 programs

Bedrock outcrop delineation

With 100% seafloor coverage, the revealed morphology can be used to identify regions where bedrock outcrop is at the seafloor (or only slight buried by drift). Even without dredging, the nature of the faulting/jointing patterns can provide a potential indication of the likely formations involved. Combined with the offshore extensions of the aeromagnetic surveys, this could aid in offshore bedrock delineation.

The most extensive bedrock mapping to date has been in central Cumberland Sound (Figure 2). As the central area is

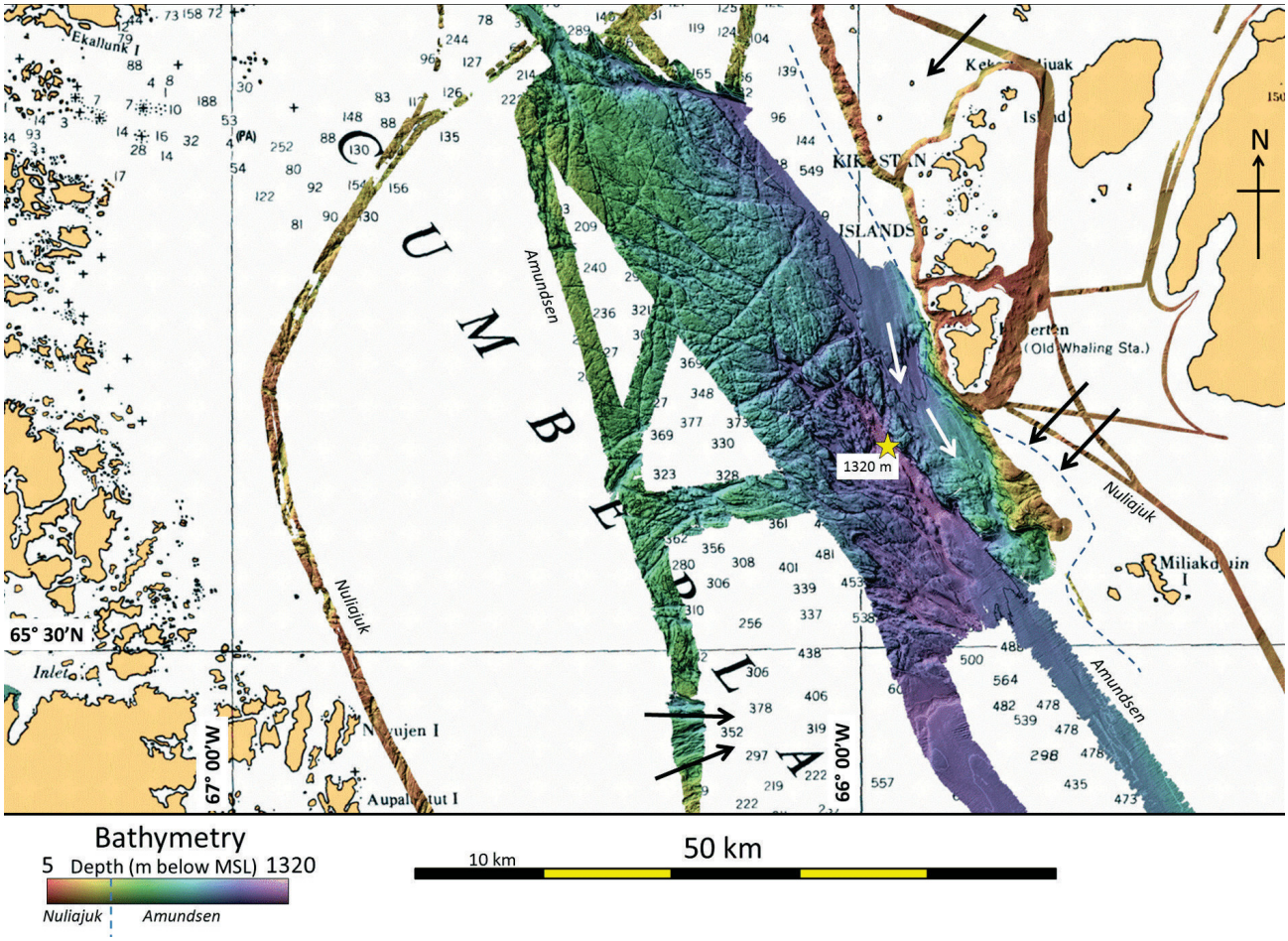

Figure 2: Delineated bedrock outcrop from available multibeam coverage in central Cumberland Sound. Backdrop is CHS chart 7051. Lack of soundings indicates no previous data. All data >400 m were collected by the CCGS *Amundsen*. All data in water of ~400 m depth or shallower have been provided by the Nuliajuk Seabed Mapping Program (NSMP). Arrows indicate direction of apparent grounded ice-stream flow lineations.

deep (>1 km), the *Amundsen* has been able to operate with its low frequency (30 kHz) multibeam system, obtaining swaths up to 3 km wide. As a result, the area covered has been the most extensive to date. Notably, however, that coverage is almost entirely within the pre-existing transit-track bathymetry dating from the 1960s. Expansion of that bedrock mapping into the shallower waters on the flanks of the sound is only possible with a vessel like the *Nuliajuk*. The 200 kHz EM2040 multibeam echo-sounder system of this vessel, however, is limited to depths less than about 350 m. Figure 2 illustrates the new nearshore corridors established during the first three years. All the new contributions have been outside the previously charted regions. The west side of the trough is predominantly bedrock outcrop. In contrast, the shallower terrace east of the Kikastan Islands reveals extensive till drapes over bedrock. Many of these drapes are clearly ice moulded, indicating ice streams coming out of Kingnait Fiord off Cumberland Peninsula (Figure 2, arrows).

From the fault and joint pattern visible in the bedrock morphology imaged to date, there is very little discernible evidence of overprinting of ice-flow directions. Only where there are overlying sediments is there evidence of grounded ice-flow activity (Figure 2).

Evidence for moraines and submarine grounded ice-stream activity

Previous inferences about the extrapolation of grounded ice streams beyond the coastline have been based primarily on the extrapolation of onshore flow vectors (Tremblay et al., 2013, 2014). Even on land, the flow axes are picked primarily from long-wavelength relief, such as regional valley trends. In the absence of any constraint on submerged bathymetry, such inferences are of little value offshore. Other than the extremely elongate relief of the central deep section of Cumberland Sound, there is little available evidence for submerged flow patterns coming off either Hall Peninsula or Cumberland Peninsula.

Ultimately, the best evidence is the revelation of seabed morphology from multibeam coverage that indicates grounded ice streams (Figure 2) or moraine structures (Figure 3b). This will indicate flow or retreat directions, depth of touchdown and potentially whether the glaciodynamic setting was cold or warm based. Knowledge of the submarine glacial history provides predictive capability for interpreting the marine surficial geology.

The NSMP multibeam coverage provides the first insights into the ice-flow directions on the inner shelf (Figures 2, 3b). On a regional basis, the lack of penetration in sub-bottom data provides evidence that there is only very minor sedimentation on either till or bedrock surfaces. Rare sub-bottom penetration, primarily in localized basins (e.g., Figure 3a, d), can be used to infer glaciomarine or Holocene sedimentation. These newly identified basins can be the focus of future coring programs to ground-truth the acoustic mapping, as initiated in 2014 with both RV *Nuliajuk* and CCGS *Amundsen*.

Iceberg-scour evidence

A major impediment to seabed installations (such as pipelines, power cables, fibre-optic communication cables and tidal-power infrastructure) is the hazard of modern iceberg scouring. Evidence for this can be derived from multibeam relief (Figure 3c), which indicates the maximum depth and penetration of this scouring. Despite the ubiquitous present-day presence of icebergs, only a small subset of the currently mapped seafloor shows evidence of iceberg scouring, even when clearly covered with till rather than bedrock. This suggests that the wander paths of the icebergs are constrained by offshore bathymetric variations. Many of the inlets of these two peninsulas have constraining sill depths, which will act to limit the landward penetration of icebergs. However, evidence for iceberg activity can clearly be seen from the multibeam relief well inside some of the inlets (stars indicated on Figures 4, 5). Where the impacts are seen overprinting modern sedimentary activity (delta-front channel relief and active tidal bedforms), they can be confirmed to be modern.

Submerged shore terraces

Just as emergent terraces on land are dated to constrain rate of uplift, submerged terraces (if datable) can be used to constrain subsidence rates (e.g., Shaw and Forbes, 1995). These are critical inputs to projections of future relative sea-level change in Nunavut communities (James et al., 2011).

Miller and Dyke (1974) presented evidence of drowned delta terraces in Merchants Bay. Dyke et al. (1982) hypothesized a hinge line, with the eastern part of Cumberland Peninsula subsiding. Their model suggested progressively shallower and later low stands westward.

To test this hypothesis, the NSMP undertook a search for drowned delta terraces throughout eastern Cumberland Peninsula beginning in 2012 (Cowan et al., 2014). Several relict delta terraces have been discovered and mapped, revealing a pattern of progressively greater depths eastward (Figure 4). A gravity- and piston-coring program was undertaken in 2014 from, respectively, RV *Nuliajuk* and CCGS *Amundsen* in an effort to date some of these features to test the model of Dyke et al. (1982). The NSMP has also revealed a drowned boulder barricade (a shore-zone landform with a modern analogue at Pangnirtung) in 17 m present water depth near Qikiqtarjuaq (Cowan et al., 2014).

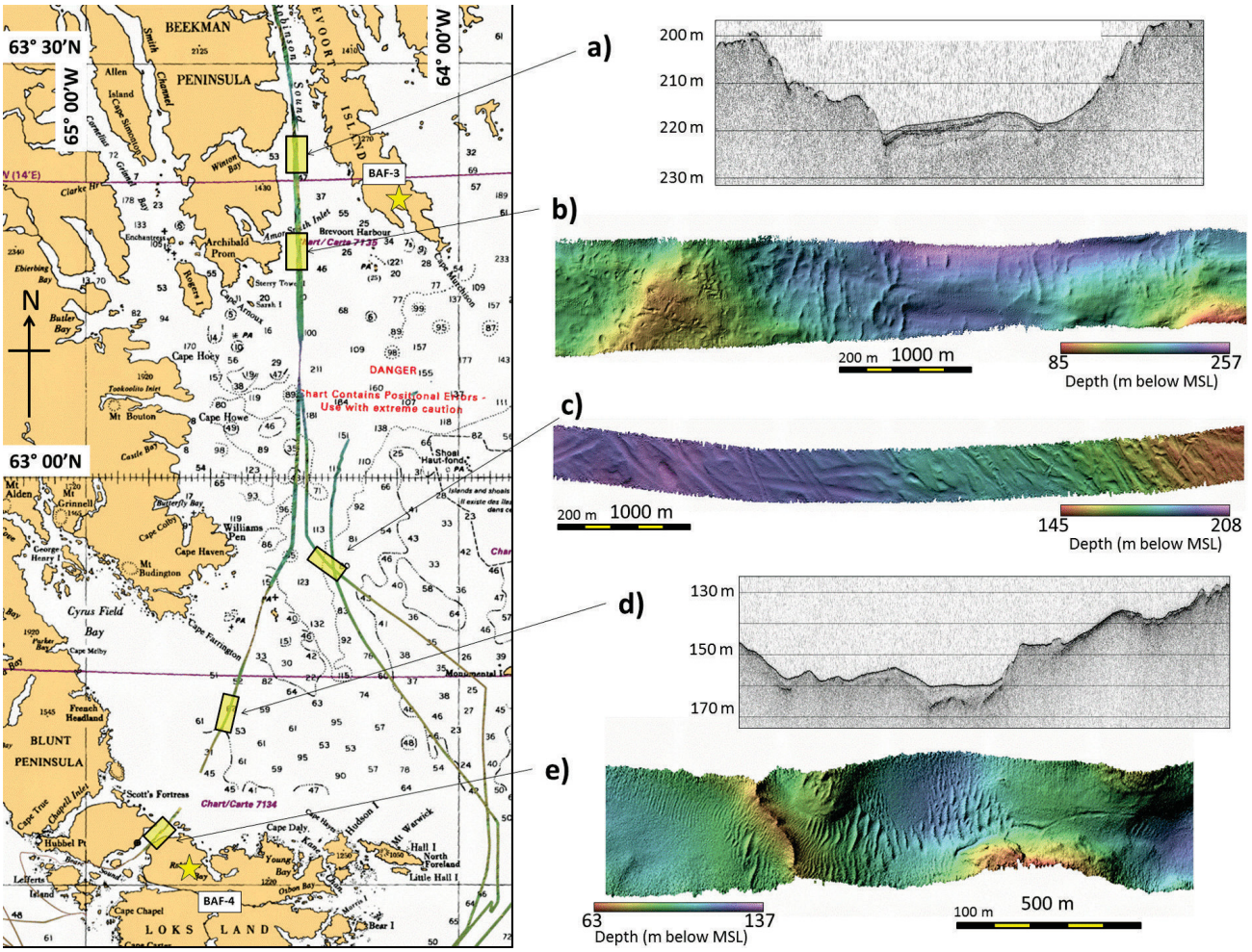

Figure 3: Transit corridor from Beare Sound to Anderson Channel, southeastern tip of Hall Peninsula, showing evidence for **a)** stratified and draped glaciomarine sediments with a thin transparent postglacial mud cover, **b)** De Geer moraines, **c)** iceberg scouring, **d)** acoustically transparent late Holocene sediments, and **e)** active tidal bedforms.

Initial assessment of tidal-power potential

Frobisher Bay and Cumberland Sound are macrotidal environments with peak tidal ranges of 13 and 5 m, respectively. Extensive investigations of tidal-power potential have been undertaken in more southerly latitudes (Bedard et al., 2006). One of the strongest indicators of tidal-power potential has been the presence of bathymetric constrictions in regions of large tides with rapidly varying tidal phase. Because there are so many bedrock-restricted coastal channels within the island archipelagos along Cumberland and Hall peninsulas, there is a high potential for the development of tidal power.

At the present time, the bathymetric framework underlying the available regional hydrodynamic tidal models (e.g., Fisheries and Oceans Canada's Webtide; Collins et al., 2011) is insufficient to adequately delineate potential sites of enhanced tidal streams. With improved bathymetric definition in narrow constrictions, it would be possible to begin quantitative assessment of the potential for sustained tidal streams.

Although the coastline is known to be heavily indented with narrow channels between islands and between islands and the mainland, the relief within these channels has previously been almost entirely unknown. A deliberate objective of this program is to establish safe navigable channels within the coastal archipelago. Specific examples are the identification of a new navigable channel inside Loks Land (Beare Sound, Figure 1) and the first mapped corridor through the Anderson Channel (Figure 1). These surveys serve as the first reconnaissance for tidal-power potential. The multibeam data define the relief and the presence of active tidal bedforms (Figures 3e, 5). Unlike more southerly latitudes, the added danger of iceberg and sea-ice keel impacts has to be taken into account. The multibeam data can also provide direct evidence of ice-scour activity (e.g., Figure 3c).

Complementary information about the likely locations of intensified tidal-current activity may also be inferred from the presence of polynas open during the winter months (e.g., between the islands closing off inner Frobisher Bay).

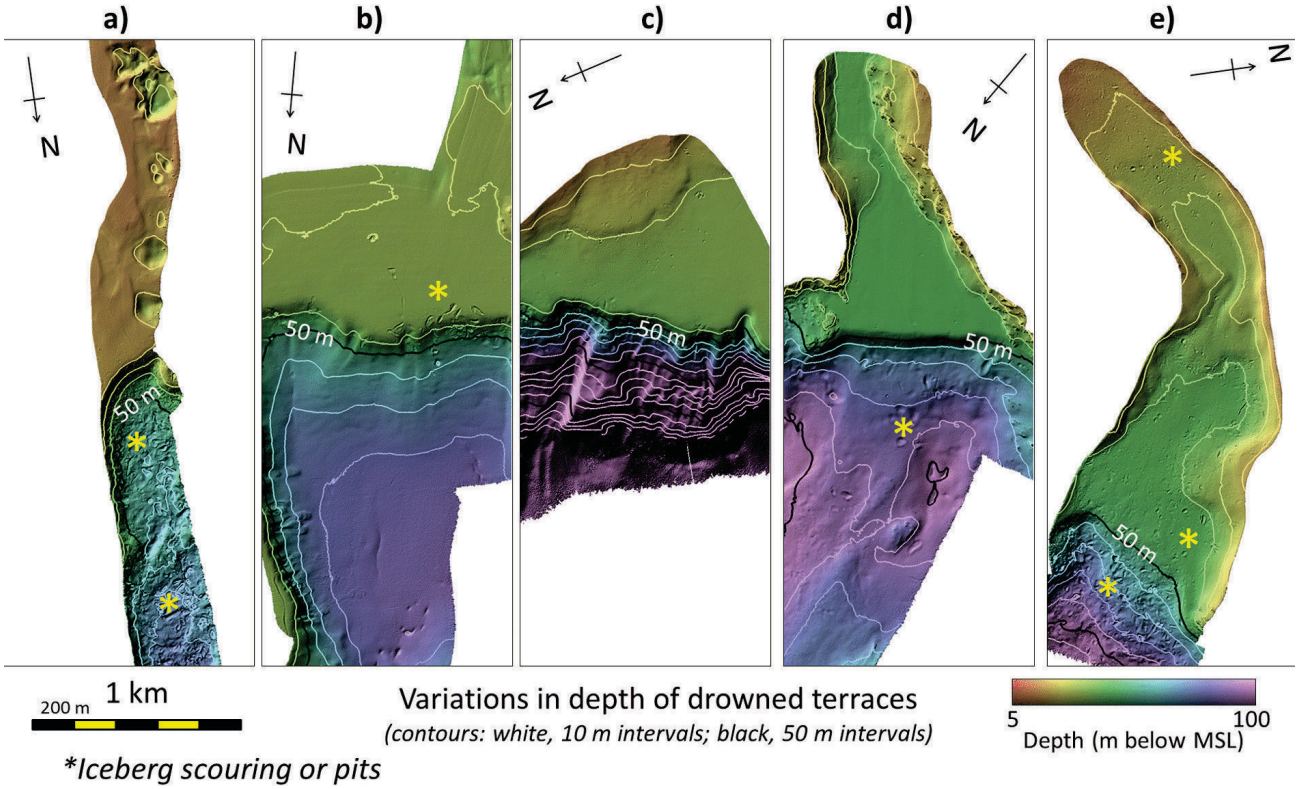

Figure 4: Drowned delta terraces in **a)** Kangiqtugaapiruluk (formerly Kangert Fiord), **b)** and **c)** upper and central Boas Fiord, **d)** Itturjuanga, and **e)** Pause bay (unofficial name). Stars indicate iceberg impact morphology. See Figure 1 for location.

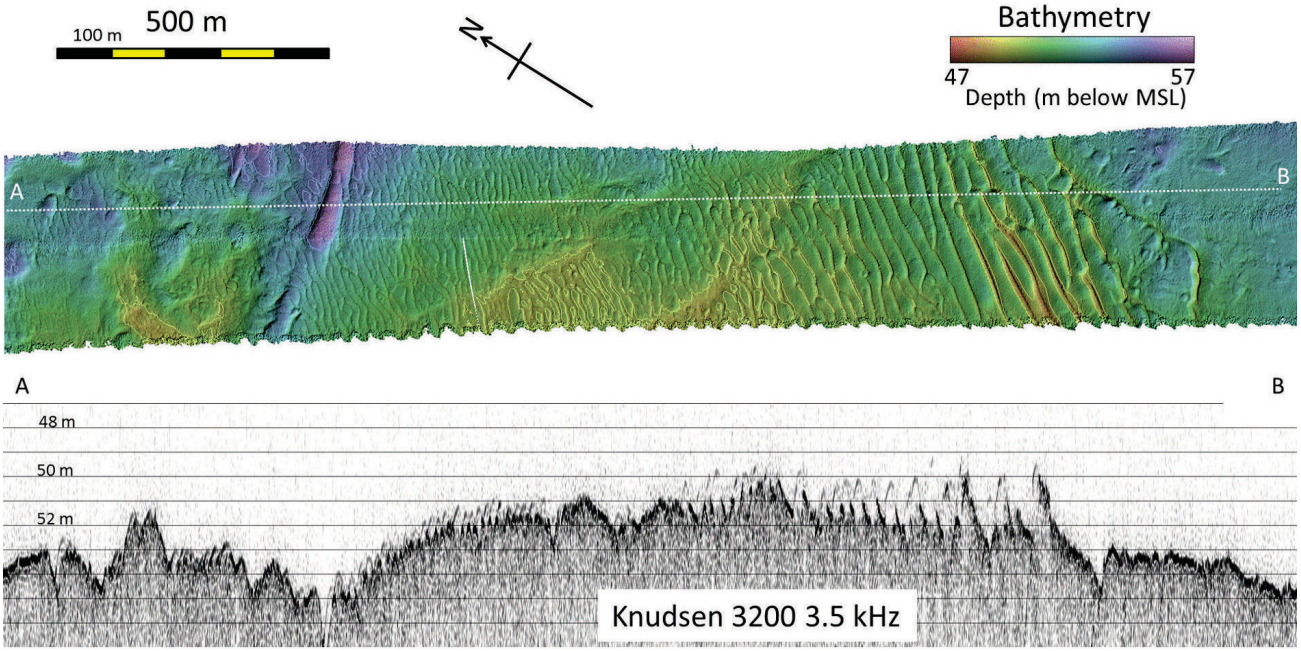

Figure 5: Active tidal bedforms developed in a thin layer over a deflated surface, off the mouth of Akpait Fiord (location 'X' in Figure 1).

Parallel studies of tidal-power potential and the stability of the seabed at suitable locations has been a major focus of the Geological Survey of Canada in more southern latitudes. Examples in the Bay of Fundy (Todd et al., 2014) and Georgia Basin (Barrie and Conway, 2014) clearly indicate that, in areas of significant tidal streams, glacial deposits have been extensively reworked into sand-wave fields. These are both a potential resource of well-sorted sand for aggregate and a potential hazard for future seabed infrastructure. Surprisingly few tidal bedform fields have been identified from the NSMP data to date, perhaps a result of the much shorter time since ice retreat.

Active fiord-head depocentres

Submerged delta terraces are found in fiord-head or side-entry settings that were exposed early in the deglaciation of Cumberland Peninsula. Nevertheless, a large number of small ice caps and valley glaciers persist in the region, and tidewater ice fronts were still active until recently in some valleys (Gilbert, 1985). In other cases, such as Mermaid Fiord, active sandur (outwash-plain) deposition is continuing, fed by meltwater discharge from glaciers in a large drainage basin.

Such depocentres can serve as potential sites for paleoclimate and paleoseismic investigations. Figure 6 provides examples of five active fiord-head depocentres that illustrate the varying maturity of the prodelta morphology.

Over time following the retreat of the tidewater glacier, the deltaic deposition will gradually bury the fiord-floor relief associated with either glacially striated bedrock outcrop (Figure 6a) or subglacial discharge (Figure 6b). The most mature deltaic depocentres will exhibit the development of major channel systems (Figure 6e) comparable to those seen at other more northerly Baffin Island fiords (e.g., Syvitski and Hein, 1991).

Evidence of landslides

With the concern about the level of seismicity in the Baffin Bay region (Campbell and Bennett, 2014), identification and dating of submerged landslide deposits can be used to constrain the periodicity of previous seismic triggers. In the adjacent Frobisher Bay, this program (Mate et al., 2015) has clearly demonstrated the presence of submarine-landslide deposits. To date, working in the Hall Peninsula and Cumberland Peninsula regions, comparable levels of submarine mass wasting have not yet been identified. Some prodelta failures in this region may be seismically triggered. In addition, a postdepositional landslide scar has been mapped on the relict prodelta slope of a side-entry submerged delta terrace in Mermaid Fiord.

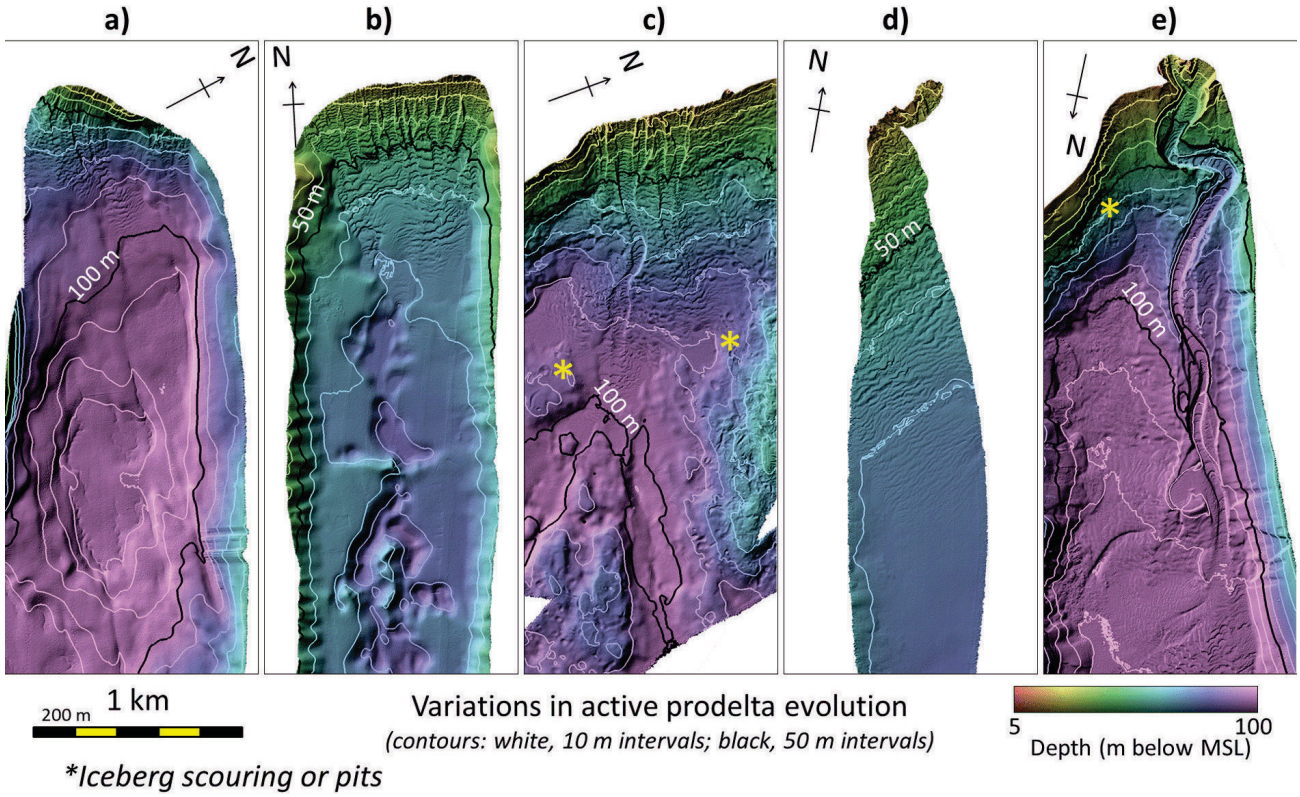

Figure 6: Variations in the development of bedform morphology on the prodelta of fiord-head depocentres, showing increasing maturity (from left to right): **a)** Bear cove (unofficial name), **b)** Pangnirtung Fiord, **c)** Touak Fiord, **d)** Mermaid Fiord, and **e)** Southwind Fiord. Stars indicate iceberg impact morphology. See Figure 1 for location.

Safe-access routes

As an essential prerequisite to all coastal marine investigations, a safe-passage corridor needs to be established so that survey and research vessels can approach the coastline. For the majority of the coastline investigated, there are no prior approach routes. This program has opened up both access and coastal corridors.

All data collected have been provided to the Canadian Hydrographic Service (CHS) for chart updating. Once accepted by the CHS and incorporated into charting products, the same data can then serve to allow the Canadian Coast Guard access to these regions to undertake search-and-rescue operations in support of commercial and tourism shipping and community activities.

Prior to the release of formal nautical charting products, preliminary versions of these data are already being provided to research vessels to facilitate safe access. The CCGS *Hudson* had access to the data in 2013 and the CCGS *Amundsen* used these data for coring operations in 2014.

Data distribution

There are presently no marine geological (or bathymetric) products for this region at scales larger than 1:500 000. With the exception of the DEW and NWS sites, there are also no chart products at scales larger than 1:500 000.

Because the data are collected from sequential annual transits, there is no systematic regional coverage around these peninsulas with the exception of the focused NSMP work by Mate et al. (2015) in inner Frobisher Bay. Beginning in 2003 with the CCGS *Amundsen* multibeam program, the Ocean Mapping Group (OMG) at UNB has been maintaining a public portal for this new and annually expanding coverage (Muggah et al., 2010). Since 2012, this has been expanded to include the RV *Nuliajuk* data. At this time, the CCGS *Amundsen* and the RV *Nuliajuk* multibeam data are available for download via an interactive Google Maps® interface from http://www.omg.unb.ca/Projects/Arctic/google/.

From this site, gridded data at 10 m resolution are available as a series of tiled map sheets. The 2014 *Nuliajuk* data from the NSMP will be added to this compilation. These data are provided directly to the Canadian Hydrographic Service on an annual basis for the purpose of generating and updating nautical charting products according to their prioritization scheme.

Future intentions

Specific directed mapping using the RV *Nuliajuk* in 2014 is currently underway and planned for Frobisher Bay at time of submission (October 2014). At this time, there are no plans to undertake systematic mapping away from the population centres. The required transits to support fisheries science will continue, however, so there is still the opportunity to build on this reconnaissance work on an annual basis. The 2015 program will remain focused on the inshore Greenland halibut fishery, so Hall and Cumberland peninsulas project will be expanded through at least the collection of transit data. Specific targeted objectives that are planned are a continuation of the drowned-terrace study and expanded investigations of depocentres to look for evidence of seismic activity.

Economic considerations

In order to exploit economically viable orebodies identified on southeastern Baffin Island, the first requirement will be to access those localities. Given the extreme relief, the ideal access will be from the closest protected coastline. Prior to this program, there was a 10–30 km wide zone around almost all the region that was completely uncharted. In the third year of this program, there is now a guaranteed inshore coastal route around the entire perimeter of both peninsulas. Along this route, multiple safe-access corridors have been established into most of the major inlets. These routes have already been used for 2014 CCGS *Amundsen* operations.

The same data are freely available through the OMG web portal to provide users—whether government, commercial or community—full access to the seabed morphology revealed as a byproduct of these surveys. The geomorphic data serve to identify potential hazards to responsible development of Nunavut's coastal natural resources. These include the identification of areas of extensive seabed iceberg and ice-keel scouring, the presence of active tidal bedforms and regions of potential submarine-landslide susceptibility.

A particular opportunity arises from the identification of narrow straits in which there are enhanced tidal currents and suitable substrates for tidal-power infrastructure. With the increasing maturity of tidal power development in more southerly waters, suitable sites in Nunavut may provide a future source of power for natural-resource development and/or communities to reduce their reliance on imported hydrocarbons.

Conclusions

New marine geological mapping of nearshore waters is now being undertaken in previously unsurveyed areas around Hall and Cumberland peninsulas on Baffin Island in eastern Nunavut. This program is an extension of the more focused studies in the vicinity of Iqaluit (Mate et al., 2015) and Qikiqtarjuaq. The mapping utilizes additional time windows available within an existing Government of Nunavut field program and takes advantage of a small but suitably equipped vessel with just the incremental cost of survey staff. As a result, the NSMP is able to acquire low-

cost and high-impact data at a fraction of the expense of a conventional, dedicated, icebreaker-based, hydrographic-survey program.

As these data are compiled over the multiyear program, they can be incorporated into surficial geological maps and geomorphological studies. These maps and studies will help to minimize risk associated with the required shipping activity that would be part of natural-resource development and would help optimize the design of infrastructure projects.

Acknowledgments

Funding for ship time and associated logistics was provided by the Government of Nunavut, the Canada-Nunavut Geoscience Office, Natural Resources Canada, ArcticNet, the Canadian Hydrographic Service, UNB and MUN. The success of the field program would not have been possible without the support and professionalism of the captain and crew of the RV *Nuliajuk*.

References

Barrie, J.V. and Conway, K.W. 2014: Seabed characterization for the development of marine renewable energy on the Pacific margin of Canada; Continental Shelf Research, v. 83, p. 45–52.

Bartlett, J., Beaudoin, J., Hughes Clarke, J.E. and Brucker, S. 2006: ArcticNet: the current and future vision of its seabed mapping program; *in* Proceedings of the Canadian Hydrographic Conference, 2006, CD-ROM.

Bedard, R., Previsic, M., Polagye, B., Hagerman, G. and Casavant, A. 2006: Tidal In Stream Energy Conversion (TISEC) Project; Electric Power Research Institute, EPRI TP-008-NA, URL <http://oceanenergy.epri.com/streamenergy.html> [November 2014].

Blackadar, G., 1967: Geological reconnaissance, southern Baffin Island, District of Franklin; Geological Survey of Canada, Paper 66-47, 32 p.

Brucker S., Muggah, J. Church, I. Hughes Clarke, J.E. Hamilton, T. Hiroji, A. and Renoud, W. 2013: Hydrographic efficiencies of operating a 19 m research platform in the eastern Canadian Arctic; *in* Proceedings of the United States Hydrographic Conference, 2013, p. 1–21.

Campbell, D.C. and Bennett, J.R. 2014: Preliminary results from recent investigations of marine geological hazards in Baffin Bay, Nunavut and Greenland; *in* Summary of Activities 2013, Canada-Nunavut Geoscience Office, p. 121–128, URL <http://cngo.ca/summary-of-activities/2013/> [November 2014].

Cowan, B., Bell, T. and Forbes, D.L. 2013: Coastal dynamics of an Arctic shoreline below sea level, Broughton Channel, Nunavut; *in* ArcticNet Annual Scientific Meeting, Program with Abstracts, p. 132.

Cowan, B., Bell, T., Forbes, D.L., Hughes Clarke, J.E. and Muggah, J. 2014: Report of 2012 and 2013 seabed surveys with RV *Nuliajuk*, Cumberland Peninsula, Baffin Island, Nunavut; Memorial University of Newfoundland, Department of Geography, unpublished cruise report.

Dyke, A S., Andrews, J T. and Miller, G H. 1982: Quaternary geology of Cumberland Peninsula, Baffin Island, District of Franklin; Geological Survey of Canada, Memoir 403, 32 p. (2 sheets), <http://geoscan.nrcan.gc.ca/starweb/geoscan/servlet.starweb?path=geoscan/downloade.web&search1=R=116169> [November 2014].

Gilbert, R. 1982: The Broughton Trough on the continental shelf of eastern Baffin Island, Northwest Territories; Canadian Journal of Earth Sciences, v. 19, p. 1599–1607.

Gilbert, R. 1985: Quaternary glaciomarine sedimentation interpreted from seismic surveys of fiords on Baffin Island, NWT; Arctic, v. 38. no. p. 271–280.

James, T.S., Simon, K.M., Forbes, D.L., Dyke, A.S. and Mate, D.J. 2011: Sea-level projections for five pilot communities of the Nunavut Climate Change Partnership; Geological Survey of Canada, Open File 6715, 23 p., URL <http://ftp2.cits.rncan.gc.ca/pub/geott/ess_pubs/288/288019/of_6715.pdf> [November 2014].

Jennings, A.E. 1992: The Quaternary history of Cumberland Sound, southeastern Baffin Island: the marine evidence; Géographie physique et Quaternaire, v. 47, no. 1, p. 21–42.

Løken, O.H. and Hodgson, D.A. 1971: On the submarine geomorphology along the east coast of Baffin Island; Canadian Journal of Earth Sciences, v. 8, p. 185–195, doi:10.1139/e71-020

Machado, G., Bilodeau, C., Takpanie, R., St-Onge, M.R., Rayner, N.M., Skipton, D.R., From, R.E., MacKay, C.B., Creason C.G. and Braden, Z.M. 2013: Hall Peninsula regional bedrock mapping, Baffin Island, Nunavut: summary of fieldwork; *in* Summary of Activities 2012, Canada-Nunavut Geoscience Office, p. 13–22, URL <http://cngo.ca/summary-of-activities/2012/> [November 2014].

Maclean, B., Williams, G.L., Jennings, A. and Blakeney, C. 1986: Bedrock and surficial geology of Cumberland Sound, Northwest Territories; *in* Current Research, Part B, Geological Survey of Canada, Paper 86-1B, p. 605–615, URL <http://geoscan.nrcan.gc.ca/starweb/geoscan/servlet.starweb?path=geoscan/downloade.web&search1=R=120672> [November 2014].

Mate, D.J., Campbell, D.C, Barrie, J.V., Hughes Clarke, J.E., Muggah, J., Bell, T. and Forbes, D.L. 2015: Integrated seabed mapping of Frobisher Bay, southern Baffin Island, Nunavut, to support infrastructure development, exploration and natural-hazard assessment; *in* Summary of Activities 2014, Canada-Nunavut Geoscience Office, p. 145–152, URL <http://cngo.ca/summary-of-activities/2014/> [January 2015].

Miller, G.H. 1975: Glacial and climatic history of northern Cumberland Peninsula, Baffin Island, Canada, during the last 10,000 years; Ph.D. thesis, Department of Geological Sciences, University of Colorado, Boulder Colorado.

Miller, G.H. and Dyke, A.S. 1974: Proposed extent of late Wisconsin Laurentide ice on Baffin Island; Geology, v. 2, p. 125–130.

Muggah, J., Church, I., Beaudoin, J. and Hughes Clarke, J.E. 2010: Seamless online distribution of Amundsen multibeam data; Proceedings of the Canadian Hydrographic Conference, Paper S7.2.

Praeg, D, Maclean, B. and Sonnichsen, G. 2007: Quaternary geology of the northeast Baffin Island continental shelf, Cape Aston to Buchan Gulf (70° to 72°N); Geological Survey of Canada, Open File 5409, 98 p., URL <http://

geoscan.nrcan.gc.ca/starweb/geoscan/servlet.starweb?path=geoscan/downloade.web&search1=R=223452> [November 2014].

Shaw, J. and Forbes, D.L. 1995: The postglacial relative sea-level lowstand in Newfoundland; Canadian Journal of Earth Sciences, v. 32, p. 1308–1330.

Steenkamp, H.M. and St-Onge, M.R. 2014: Overview of the 2013 regional bedrock mapping program on northern Hall Peninsula, Baffin Island, Nunavut; *in* Summary of Activities 2013, Canada-Nunavut Geoscience Office, p. 27–38, URL <http://cngo.ca/summary-of-activities/2013/> [November 2014].

Syvitski, J.P.M. and Hein, F.J. 1991: Sedimentology of an Arctic basin: Itirbilung Fiord, Baffin Island, Northwest Territories; Geological Survey of Canada, Paper 91-11, 66 p., URL <http://geoscan.nrcan.gc.ca/starweb/geoscan/servlet.starweb?path=geoscan/downloade.web&search1=R=132684> [November 2014].

Syvitski, J.P.M. and Schafer, C.T. 1985: Sedimentology of Arctic Fjords Experiment (SAFE): 1, project introduction; Arctic, v. 38, p. 264–270.

Todd, B.J., Shaw, J., Li, M.Z., Kostylev, V.E. and Wu, Y. 2014: Distribution of subtidal sedimentary bedforms in a macrotidal setting: the Bay of Fundy, Atlantic Canada; Continental Shelf Research, v. 83, p. 64–85.

Tremblay, T., Leblanc-Dumas, J., Allard, M., Gosse, J.C., Creason, C.G., Peyton, P., Budkewitsch, P. and LeBlanc, A.-M. 2013: Surficial geology of southern Hall Peninsula, Baffin Island, Nunavut: summary of the 2012 field season; *in* Summary of Activities 2012, Canada-Nunavut Geoscience Office, p. 93–100, URL <http://cngo.ca/summary-of-activities/2012/> [November 2014].

Tremblay, T., Leblanc-Dumas, J., Allard, M., Ross, M. and Johnson, C. 2014: Surficial geology of central Hall Peninsula, Baffin Island, Nunavut: summary of the 2013 field season; *in* Summary of Activities 2013, Canada-Nunavut Geoscience Office, p. 109–120, URL <http://cngo.ca/summary-of-activities/2013/> [November 2014].

Integrated seabed mapping of Frobisher Bay, southern Baffin Island, Nunavut to support infrastructure development, exploration and natural-hazard assessment

D.J. Mate[1], D.C. Campbell[2], J.V. Barrie[3], J.E. Hughes Clarke[4], J. Muggah[4], T. Bell[5] and D.L. Forbes[2, 5]

[1]*Canadian Northern Economic Development Agency, Iqaluit, Nunavut (formerly Canada-Nunavut Geoscience Office, Iqaluit, Nunavut)*

[2]*Natural Resources Canada, Geological Survey of Canada–Atlantic, Dartmouth, Nova Scotia, Calvin.Campbell@NRCan-RNCan.gc.ca*

[3]*Natural Resources Canada, Geological Survey of Canada–Pacific, Sidney, British Columbia*

[4]*Department of Geodesy and Geomatics Engineering, University of New Brunswick, Fredericton, New Brunswick*

[5]*Department of Geography, Memorial University, St. John's, Newfoundland and Labrador*

Mate, D.J., Campbell, D.C, Barrie, J.V., Hughes Clarke, J.E., Muggah, J., Bell, T. and Forbes, D.L. 2015: Integrated seabed mapping of Frobisher Bay, southern Baffin Island, Nunavut to support infrastructure development, exploration and natural-hazard assessment; *in* Summary of Activities 2014, Canada-Nunavut Geoscience Office, p. 145–152.

Abstract

Integrated seabed mapping is an important prerequisite for effective management of offshore areas. With the rapidly expanding City of Iqaluit on its shores and mineral resources on nearby Hall Peninsula, Frobisher Bay will undoubtedly see new infrastructure development over the next several years. The 2014 field season marked the first of a two-year, collaborative, seabed-mapping project in the region. The purpose of the project is to improve understanding of the geology of Frobisher Bay and, ultimately, to support decision-making with respect to its seabed use. Using both legacy and newly acquired high-resolution seabed-morphology and geology data, the project will generate a suite of bathymetric and geological maps for the floor of Frobisher Bay. Initial results reveal three zones (outer, middle and inner) with distinctive seabed morphology and surficial geology, and extensive evidence of seabed-slope instability in the inner zone.

Résumé

La cartographie intégrée des fonds océaniques s'avère une étape préliminaire essentielle à la gestion efficace des zones extracôtières. En raison de l'expansion rapide le long de ses berges de la ville d'Iqaluit et de la présence de ressources minérales dans la péninsule de Hall avoisinante, la baie Frobisher peut s'attendre à voir la mise en place de nouvelles infrastructures au cours des prochaines années. La saison de terrain de 2014 a marqué la première année d'un projet collaboratif de cartographie de deux ans du fond marin de la région. Le but du projet est d'améliorer le niveau de connaissance au sujet de la géologie de la baie Frobisher et, en dernier ressort, d'appuyer la prise de décisions en matière d'utilisation des fonds marins de la baie. À l'aide aussi bien de données historiques que de données à haute résolution nouvellement acquises de la morphologie et de la géologie du fond marin, il sera possible de dresser une série de cartes bathymétriques et géologiques du fond de la baie Frobisher dans le cadre de ce projet. Les résultats préliminaires mettent en évidence trois zones (extérieure, centrale et intérieure) présentant une morphologie du fond marin et une géologie de surface à caractère distinctif, ainsi que de nombreuses indices attestant de l'instabilité des pentes sous-marines dans la zone intérieure.

Introduction

It is widely recognized that effective management of offshore regions requires the integration of multiple spatial datasets from the marine environment (e.g., Pickrill and Todd, 2003; Todd and Shaw, 2009; Brown et al., 2012). Probably the most fundamental of these datasets is high-resolution bathymetric information, which is analogous to high-resolution topographic information on land. Collection of high-resolution bathymetry using multibeam echosounder systems (MBES), with coincident acquisition of acoustic-backscatter intensity data, provides detailed infor-

This publication is also available, free of charge, as colour digital files in Adobe Acrobat® PDF format from the Canada-Nunavut Geoscience Office website: http://cngo.ca/summary-of-activities/2014/.

mation on the morphology and texture of the seabed. Combining these datasets with other coregistered data, such as sub-bottom profiles, potential fields (gravimeter/magnetometer), water-column imagery and ground-truth information from seabed samples and photography, provides fundamental marine-geoscience information for answering a wide range of management questions related to infrastructure development, navigation, fisheries, and mineral and energy resources (Pickrill and Todd, 2003).

Frobisher Bay is a large inlet with Nunavut's capital city, Iqaluit, located near its innermost end (Figure 1). This makes the bay an important seaway for the transportation of commodities to and from the area. Frobisher Bay is a focus area for a number of infrastructure developments to support the growing population of Iqaluit, along with natural-resource development in the region. These initiatives include a possible new mine at the Chidliak diamond property, potential hydroelectric development at Jaynes Inlet and Armshow South, the proposed installation of a fibre-optic cable on the seabed and the construction of a new deep-water port. New marine-geoscience information is required to assess the feasibility of these projects and to determine potential constraints, such as nearshore ice, tidal currents, iceberg scour, submarine landslides, active faults, natural petroleum seeps, wave exposure, coastal instability and related hazards. The purpose of this paper is to provide details about a new seabed-mapping project in Frobisher Bay, planned for 2014 and 2015.

Project description and objectives

The Canada-Nunavut Geoscience Office, Natural Resources Canada, the Nunavut Department of Environment and partners from Canadian universities are collaborating to map the seabed of Frobisher Bay. The project will use previously collected bathymetric and geological data, supplemented by newly acquired multibeam, sub-bottom and core data, to characterize the seabed in the bay. The main objective of this work is to provide stakeholders and decision-makers with the critical marine-geoscience knowledge needed to manage development in the area. Specifically, the project will result in

- seabed mapping of potential approaches and areas suitable for port and submarine cable (fibre-optic and hydroelectric) development within Frobisher Bay;
- evaluation of potential marine geological hazards, including seabed sediment dynamics and slope stability, which may impact Arctic port development;
- assessment of the distribution of submarine landslides in Frobisher Bay and the regional risk of such natural hazards as earthquakes and tsunamis;
- confirmation and/or identification of natural petroleum seeps at the mouth of Frobisher Bay; and
- correlation of bedrock exposures at the seabed to the terrestrial bedrock geology between Hall Peninsula (Machado et al., 2013b; Steenkamp and St-Onge, 2014) and Meta Incognita Peninsula (St-Onge et al., 2015), in order to further define the tectonic assemblage of southern Baffin Island and models for its metallogenic potential.

Methods

This study relies mainly on multibeam bathymetry, sub-bottom profiler and sample data collected by CCGS *Amundsen* and RV *Nuliajuk*. The *Amundsen* is equipped with a Kongsberg Simrad EM302 multibeam system consisting of 400 beams with a nominal frequency of 30 kHz. The sub-bottom profiler system on the *Amundsen* is a Knudsen 320BR 16-element echo sounder with a nominal frequency of 3.5 kHz. On the *Nuliajuk*, the multibeam system is a Kongsberg Simrad EM2040C consisting of 400 beams with a nominal frequency of 200 kHz. The sub-bottom profiler on the *Nuliajuk* is a Knudsen 3200 two-element echo sounder operating at 3.5 kHz.

Some multibeam and coincident sub-bottom profiler data already exist for Frobisher Bay. These were collected with the support of ArcticNet (http://www.arcticnet.ulaval.ca/) as part of the underway acquisition program on the *Amundsen* (Bartlett et al., 2006) and in the course of reconnaissance and opportunity-based data acquisition on the *Nuliajuk* (Hughes Clarke et al., 2015; Figure 1). In addition, the Geological Survey of Canada collected high- and ultra high resolution seismic-reflection profiles and seafloor samples in outer Frobisher Bay during six marine geological-survey expeditions to the area between 1968 and 1990 (Figure 1b). The seismic-reflection systems were typically a single small-volume air gun (0.16 L) and the Huntec Deep-Towed Seismic System (DTS) using a boomer plate source. The samples consist of piston cores and grabs. The geophysical and geological data collected during these early campaigns are valuable for understanding the subsurface stratigraphy in Frobisher Bay, despite the relatively sparse coverage.

Several map products will be produced as part of this project. The maps will be developed using methods applied to numerous other marine-mapping projects on Canada's east and west coasts (e.g., Shaw and Todd, 2006; Pinet et al., 2011). The first map product generally consists of sun-illuminated seafloor topography accompanied by a description of the main geomorphological features of the seabed. The second map product is the geology sheet and is analogous to a surficial-geology map on land. This second sheet is a synthesis of all available geomorphological and geological data. In general, a genetic approach is used in mapping the sedimentary units, rather than the formational approach traditionally used in bedrock mapping (Shaw and Todd, 2006). Beyond these two sheets, additional geospatial in-

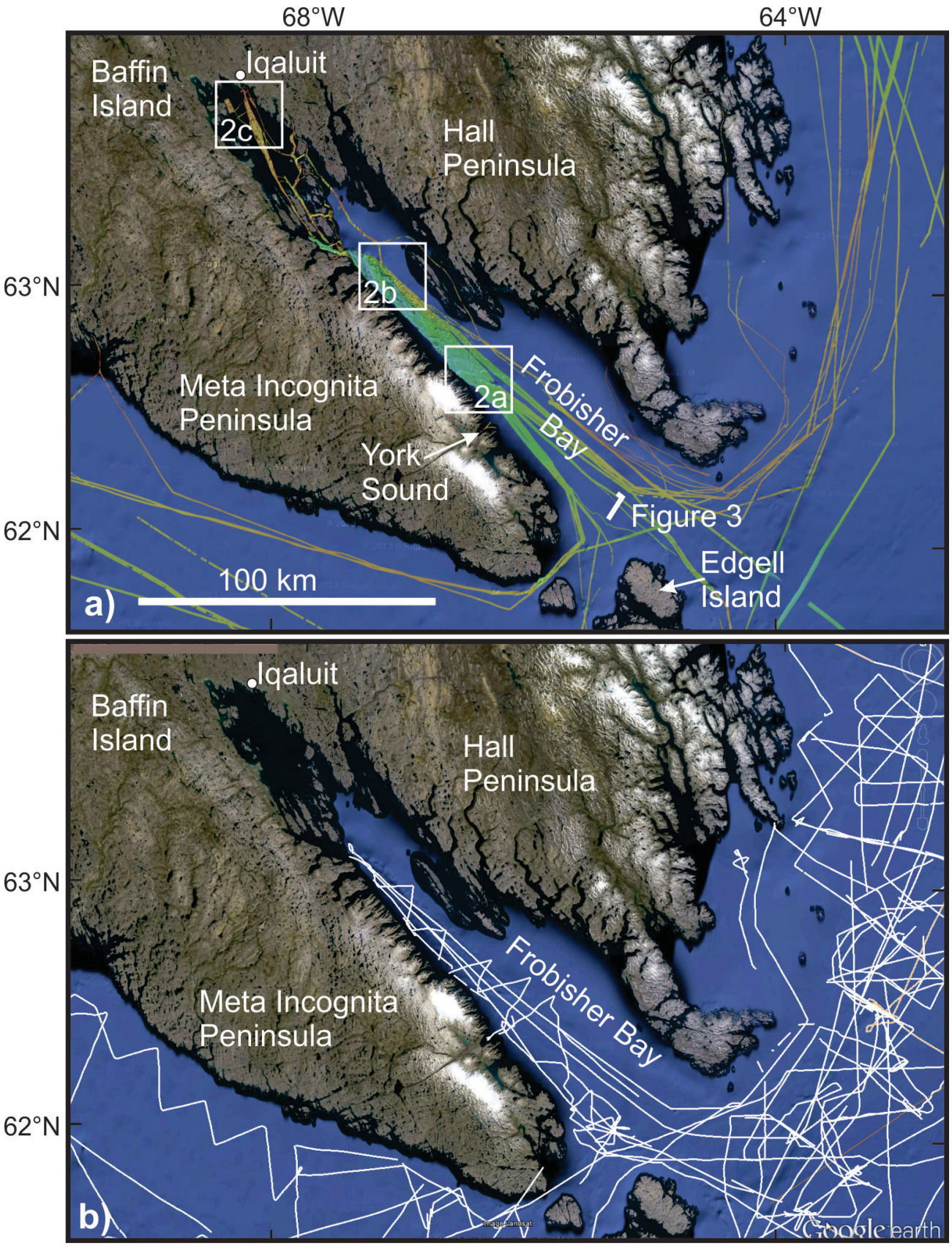

Figure 1: a) Frobisher Bay and vicinity, showing the coverage of multibeam bathymetry data prior to the start of the 2014 project; labelled squares indicate the locations of Figures 2a–c. **b)** Survey lines of high- and ultra high resolution seismic-reflection profiles collected by the Geological Survey of Canada between 1968 and 1990. Figure base map is from Google Earth™ (Google, 2014).

formation to be generated includes the seafloor-sediment texture (inferred from backscatter and sediment grain-size data), the distribution of such geological hazards as submarine landslides, locations of sediment transport and structural elements revealed in bedrock outcrops.

Preliminary observations

The existing multibeam data from Frobisher Bay reveal a range of geomorphologies preserved on the seabed that represents evidence of the region's underlying bedrock, glacial and postglacial history and seabed processes.

The seabed of Frobisher Bay can be broadly divided into three morphological zones. Zone 1 is relatively smooth and extends from outer Frobisher Bay north of Edgell Island to off York Sound on Meta Incognita Peninsula (Figures 1, 2a). High-resolution seismic-reflection data collected in 1990 show that the seabed is underlain by an interval of well-stratified glaciomarine and postglacial sediments of varying thickness, overlying stacked till deposits that are typically in erosional contact with underlying bedrock (Figure 3). The transition between zones 1 and 2 is marked by a series of smooth bathymetric steps. Based on high-resolution seismic-reflection data (Figure 4), these steps may be the expression of underlying eroded bedrock draped by approximately 10 m of glaciomarine and postglacial sediment.

Zone 2 extends from York Sound to the mid-bay islands; here the seabed is characterized by an extensive zone of exposed bedrock with sediment infilling small basins and troughs (Figures 2b, 4). The bedrock shows similar lineaments to the bedrock on western Hall Peninsula and is possibly the submerged continuation of the granitic and metasedimentary rocks of the Western Lithological Domain of Machado et al. (2013a).

Zone 3 extends from the mid-bay islands to the head of Frobisher Bay (Figure 2). In this zone, the seabed consists of a mix of small areas of exposed bedrock, glacial moraines and drumlinoid features. Most of the seabed in zone 3 appears to be draped by several metres of glaciomarine and postglacial sediments that, in some locations, show evidence of mass wasting (Figure 5). The draped sediments give the seabed morphology in zone 3 a somewhat subdued appearance.

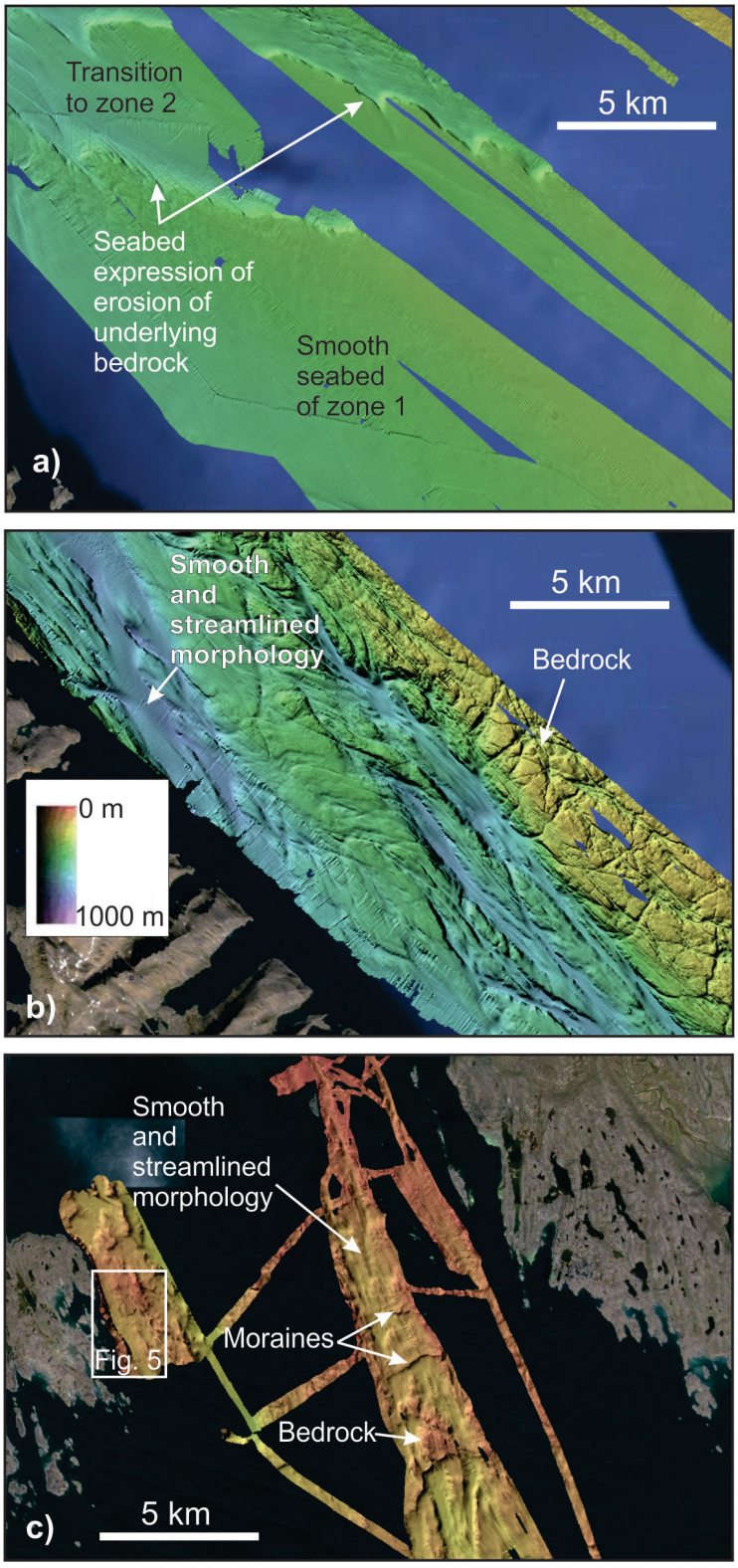

Figure 2: Multibeam bathymetry data from Frobisher Bay showing the three broad morphological zones: **a)** the seabed of the outer part of the bay is smooth with some seafloor expression of underlying buried bedrock (zone 1); **b)** the middle part of the bay, seaward of the mid-bay islands, shows the seabed expression of bedrock and glacial erosion and deposition (zone 2); **c)** inside the mid-bay islands, there is evidence of glacial and postglacial processes (zone 3). Figure location is shown on Figure 1. Figure base map is from Google Earth™ (Google, 2014).

Discussion

Early work on the marine geology of Frobisher Bay focused on the glacial and deglacial history of the region, based largely on sediment cores (e.g., Osterman and Andrews, 1983). Since these early research activities, there has been relatively little published on the marine geology of the area. The new mapping project will provide important insights into the seabed and sub-seabed geology of the region. This project is one of the first seabed-mapping projects for the Baffin region that is undertaking systematic and continuous data collection over a large area, rather than opportunity-based or targeted surveying of specific features. As a result, the 'whole picture' of the seabed geology of Frobisher Bay will be revealed.

It is apparent from the existing data in Frobisher Bay that the seabed geology is highly variable, ranging from fine-grained, unconsolidated marine sediments to intrusive and metamorphosed bedrock. The genetic mapping approach that will be applied in this project will provide information on the lithology of the mapped units. The glacial landforms preserved on the floor of Frobisher Bay, especially in the inner part of the bay, will help provide new information about the glacial history of this part of Baffin Island and can be compared to terrestrial and earlier marine-based published studies. Imaging of sedimentary bedforms will provide important insights into the circulation and tidal patterns. Interpretation of the existing data suggests evidence for seabed instability and geological hazards in the bay as well. This project will address these issues, first by mapping the distribution of the features and then by attempting to determine the cause and recurrence of hazard events, thus improving knowledge of tsunami risk and threats to coastal and seabed infrastructure.

Economic considerations

Besides helping to augment understanding of the geology of Frobisher Bay, the mapping results from this project will be a useful tool for a number of end-users. Similar studies from other Canadian marine areas have demonstrated the high utility of integrated seabed mapping (Todd and Shaw, 2009). This approach has been effectively used to plan in-stream tidal-power projects, manage offshore fisheries, reduce the impact of offshore development, establish marine protected areas and resolve seabed-use conflicts. This project will ensure that future management and potential infrastructure planning for Frobisher Bay are guided by the best available scientific information.

Conclusions

Frobisher Bay is an important waterway that will likely see infrastructure development in the near future to support

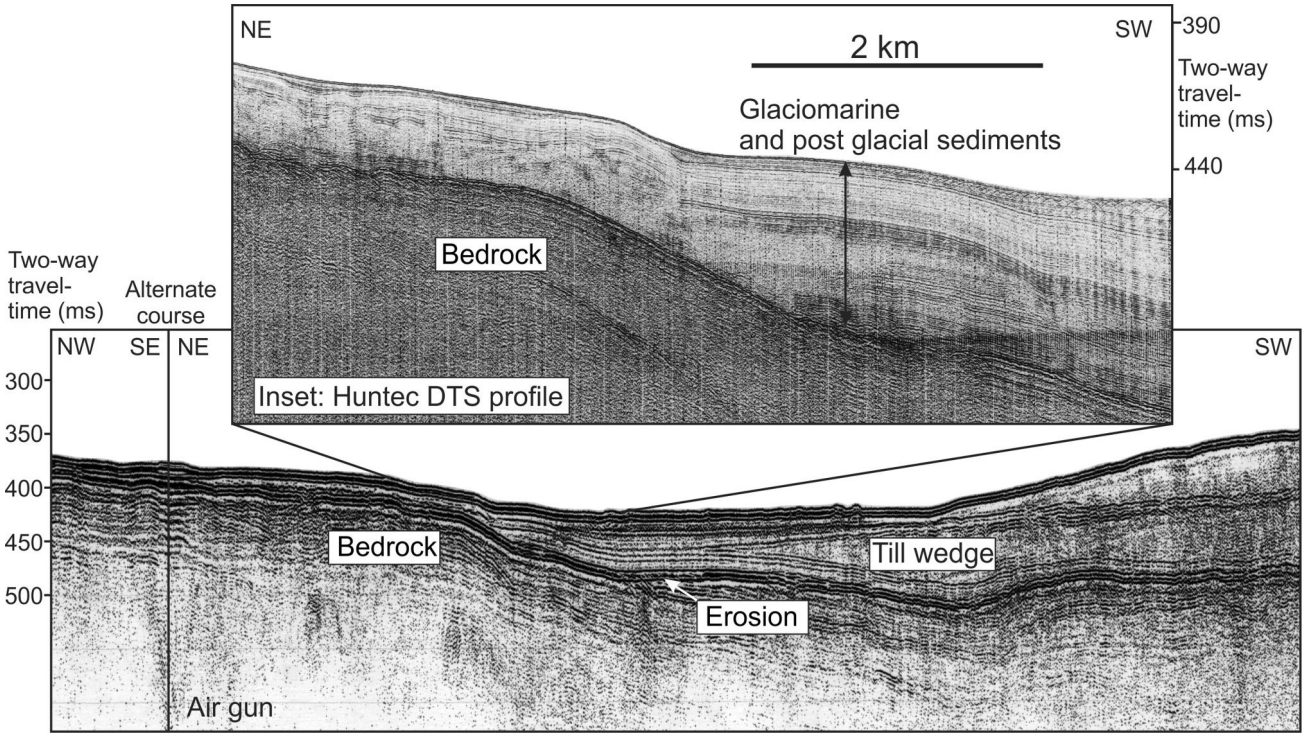

Figure 3: High-resolution seismic-reflection profiles collected in 1990 from outer Frobisher Bay. The air-gun profile is interpreted to show ~75 m of glacial, glaciomarine and postglacial sediments overlying eroded bedrock. Inset shows a portion of coincident ultra high resolution data from the Huntec Deep-Towed Seismic System (DTS). Note the well-stratified glaciomarine and postglacial sediments that overlie till and bedrock. Figure location is shown on Figure 1. The vertical scale is in milliseconds two-way traveltime; sediment-thickness estimates are based on an assumed sound velocity of 1500 m/s.

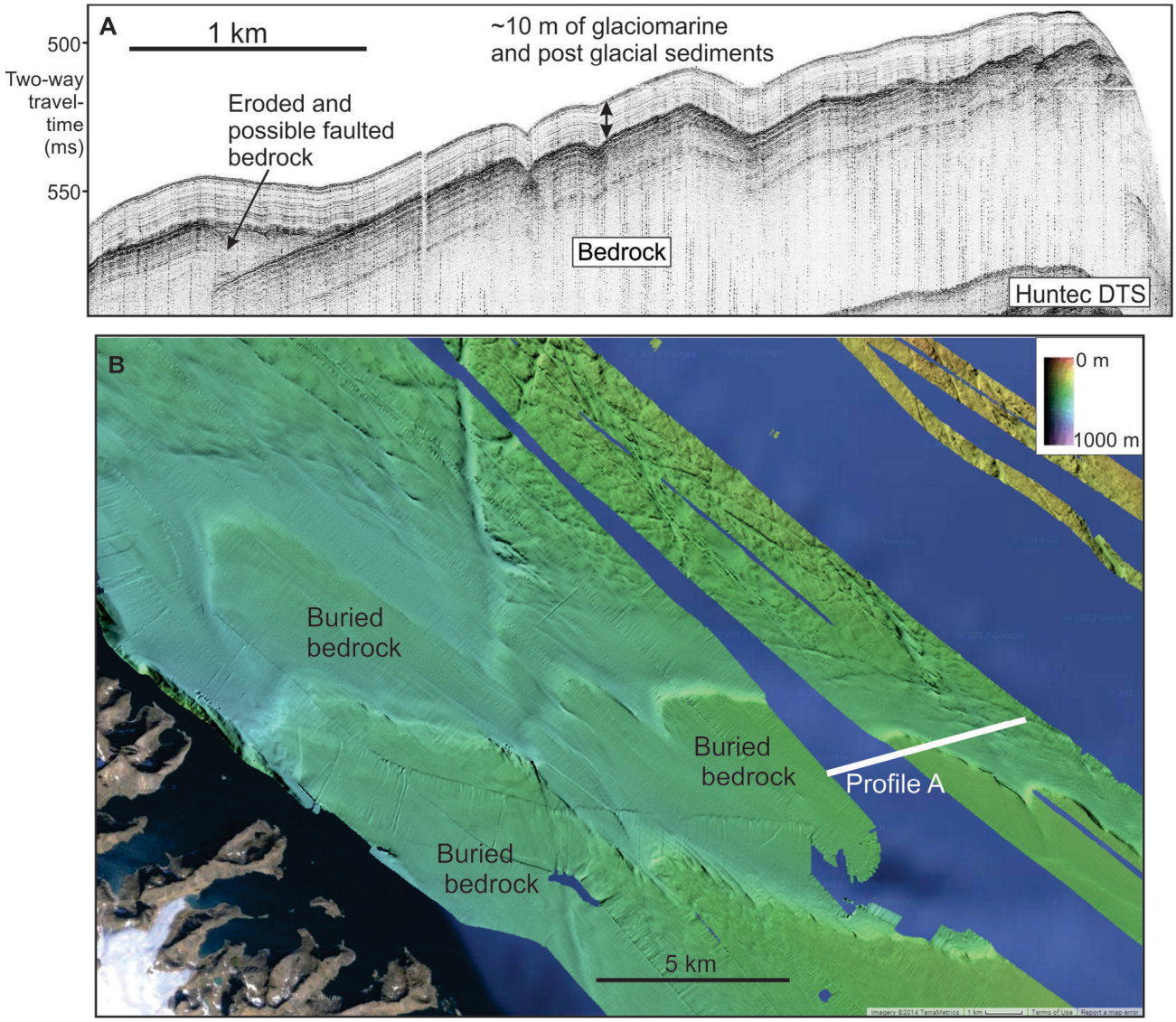

Figure 4: a) Ultra high resolution seismic-reflection data over the stepped morphology at the transition between morphological zones 2 and 3. The data show glaciomarine sediments draped over probable underlying eroded bedrock. The vertical scale is in milliseconds two-way traveltime; sediment-thickness estimates are based on an assumed sound velocity of 1500 m/s. **b)** Bathymetric map showing the location of the profile in part A. Figure base map is from Google Earth™ (Google, 2014).

rapid population growth in Iqaluit and natural-resource developments in the region. An integrated seabed-mapping project is underway in the bay that will provide key geoscience knowledge needed to manage this large offshore area. The regionally continuous mapping of the bay will provide valuable insights into the seabed geology, processes and hazards that would not be revealed in site-specific surveys.

Acknowledgments

The authors thank the captains, crews and scientific staff on board the RV *Nuliajuk*, CCGS *Amundsen*, and CCGS *Hudson* during surveys of the region. J. Kennedy is thanked for co-ordinating data collection on the *Nuliajuk*. ArcticNet, the University of New Brunswick and the Geological Survey of Canada provided data collected prior to the start of this project. Financial support for this study was provided by the Canadian Northern Economic Development Agency's (CanNor) Strategic Investments in Northern Economic Development (SINED) program and the Program of Energy Research and Development (PERD).

Natural Resources Canada, Earth Sciences Sector contribution 20140337

References

Bartlett, J., Beaudoin, J., Hughes Clarke, J.E. and Brucker, S. 2006: ArcticNet: the current and future vision of its seabed mapping program; *in* Proceedings, Canadian Hydrographic Conference 2006, CD-ROM.

Brown, C.J., Sameoto, J.A. and Smith, S.J. 2012: Multiple methods, maps, and management applications: purpose made

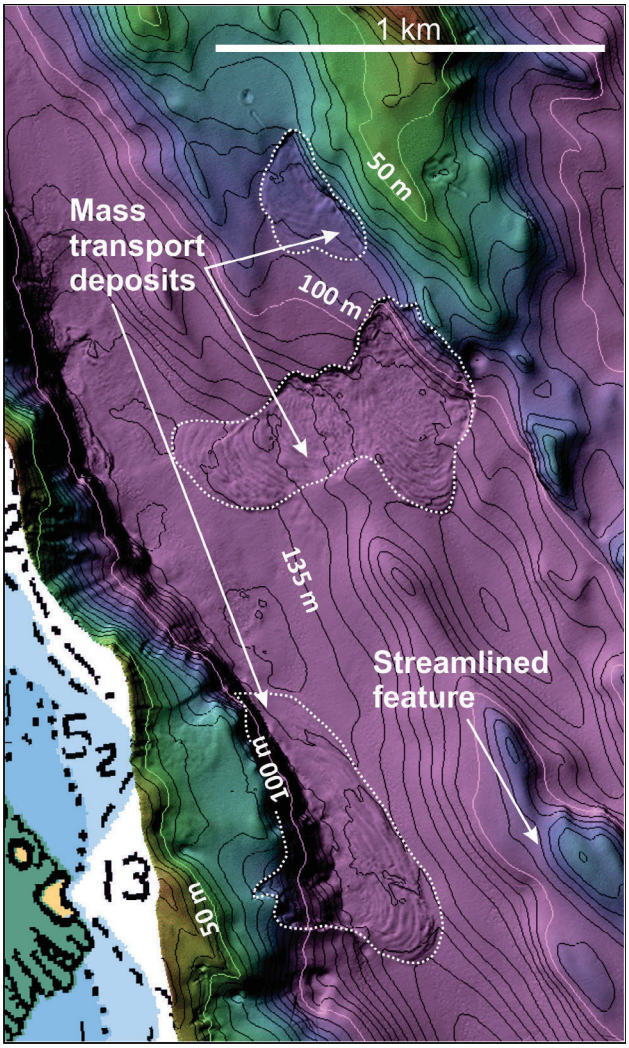

Figure 5: Multibeam bathymetry showing some mass-transport deposits (outlined by dotted white lines) and streamlined features near Iqaluit. Location is shown on Figure 2c.

seafloor maps in support of ocean management; Journal of Sea Research, v. 72, p. 1–13, doi:10.1016/j.seares.2012.04.009

Google 2014: Google Earth™ satellite image of southeastern Baffin Island, Nunavut; Google, image, URL <http://earth.google.com> [©2014 Google - Imagery, ©2013 IBCAO, Landsat; November 2014].

Hughes Clarke, J.E., Muggah, J., Renoud, W., Bell, T., Forbes, D.L., Cowan, B. and Kennedy, J. 2015: Reconnaissance seabed mapping around Hall and Cumberland peninsulas, Nunavut: opening up southeastern Baffin Island to nearshore geological investigations; *in* Summary of Activities 2014, Canada-Nunavut Geoscience Office, p. 133–144, URL <http://cngo.ca/summary-of-activities/2014/> [January 2015].

Machado, G., Bilodeau, C. and St-Onge, M.R. 2013a: Geology, southern part of Hall Peninsula, south Baffin Island, Nunavut; Geological Survey of Canada, Canadian Geoscience Map 135 (preliminary); Canada-Nunavut Geoscience Office, Open File Map 2013-1, scale 1:250 000, doi:10.4095/292443

Machado, G., Bilodeau, C., Takpanie, R., St-Onge, M.R., Rayner, N.M., Skipton, D., Young, M.D., From, R., MacKay, C., Creason C.G. and Braden, Z. 2013b: Hall Peninsula regional bedrock mapping, Baffin Island, Nunavut: summary of fieldwork; *in* Summary of Activities 2012, Canada-Nunavut Geoscience Office, p. 13–22, URL <http://cngo.ca/summary-of-activities/2012/> [January 2015].

Osterman, L.E. and Andrews, J.T. 1983: Changes in glacial-marine sedimentation in core HU77-159, Frobisher Bay, Baffin Island, N.W.T.: a record of proximal, distal, and ice-rafting glacial-marine environments; *in* Glacial-Marine Sedimentation, B.F. Molnia (ed.), Plenum Press, New York, p. 451–493.

Pickrill, R.A. and Todd, B.J. 2003: The multiple roles of acoustic mapping in integrated ocean management, Canadian Atlantic continental margin; Ocean and Coastal Management, v. 46, p. 601–614.

Pinet, N., Brake, V., Campbell, D.C. and Duchesne, M. 2011: Seafloor and shallow subsurface of the St. Lawrence River estuary; Geoscience Canada, v. 38, p. 31–40.

Shaw, J. and Todd, B.J. 2006: The new marine map series: underpinning ocean management in Canada; Bedford Institute of Oceanography Science Review 2005, Department of Fisheries and Oceans, Maritime Region, Dartmouth, Nova Scotia, p. 26–29, URL <http://www.bio.gc.ca/info/documents/267211-05.pdf> [October 2014].

St-Onge, M.R., Rayner, N.M., Steenkamp, H.M. and Skipton, D.R. 2015: Bedrock mapping of eastern Meta Incognita Peninsula, southern Baffin Island, Nunavut; *in* Summary of Activities 2014, Canada-Nunavut Geoscience Office, p. 105–118, URL <http://cngo.ca/summary-of-activities/2014/> [January 2015].

Steenkamp, H.M. and St-Onge, M.R. 2014: Overview of the 2013 regional bedrock mapping program on northern Hall Peninsula, Baffin Island, Nunavut; *in* Summary of Activities 2013, Canada-Nunavut Geoscience Office, p. 27–38, URL <http://cngo.ca/summary-of-activities/2013/> [November 2014].

Todd, B.J. and Shaw, J. 2009: International Year of Planet Earth 5: applications of seafloor mapping on the Canadian Atlantic Continental Shelf; Geoscience Canada, v. 36, no. 2, p. 81–94, URL <http://journals.hil.unb.ca/index.php/GC/article/view/12583/13454> [October 2014].

Carving stone and mineral resource potential of the Opingivik deposit, southern Baffin Island, Nunavut

H.M. Steenkamp[1], M.A. Beauregard[2] and D.J. Mate[3]

[1]*Canada-Nunavut Geoscience Office, Iqaluit, Nunavut, holly.steenkamp@nrcan-rncan.gc.ca*

[2]*Minerals and Petroleum Resources, Department of Economic Development and Transportation, Government of Nunavut, Arviat, Nunavut*

[3]*Canadian Northern Economic Development Agency, Iqaluit, Nunavut (formerly Canada-Nunavut Geoscience Office, Iqaluit, Nunavut)*

Steenkamp, H.M., Beauregard, M.A. and Mate, D.J. 2015: Carving stone and mineral resource potential of the Opingivik deposit, southern Baffin Island, Nunavut; *in* Summary of Activities 2014, Canada-Nunavut Geoscience Office, p. 153–162.

Abstract

The Opingivik carving stone quarry, located in southwestern Cumberland Sound, Baffin Island, Nunavut, provides serpentinite carving stone to Inuit carvers in the Hamlet of Pangnirtung. In the 2014 field season, the Canada-Nunavut Geoscience Office and the Government of Nunavut Department of Economic Development and Transportation partnered to make a detailed study of the Opingivik site. Given the size of the carving stone deposit, and stone quality and characteristics, Opingivik has the potential to expand and supply carving stone to a broader community of carvers beyond Pangnirtung. Work in the study area also revealed two layered mafic–ultramafic intrusions and several sulphide mineral occurrences. These new discoveries indicate the potential for economic mineral resources and highlight the need for modern geological mapping in this area. Representative rock samples were collected from each lithology for geochemical analysis and assay, and for carving suitability where appropriate. The geological field relationships and observations, assessment of the carving stone deposit and a subset of the analytical data are provided in this summary paper.

Résumé

La carrière de pierre à sculpter Opingivik située au sud-ouest du détroit de Cumberland, dans l'île de Baffin, au Nunavut, fournit aux sculpteurs inuits du hameau de Pangnirtung la serpentinite qui leur sert de pierre à sculpter. Au cours de la saison de terrain de 2014, le Bureau géoscientifique Canada-Nunavut et le ministère du Développement économique et des Transport du gouvernement du Nunavut ont travaillé ensemble dans le but d'étudier en détail le site d'Opingivik. Étant donné la taille du gisement de pierre à sculpter, ainsi que la qualité et les caractéristiques propres à cette pierre, il en ressort que le site d'Opingivik est en mesure de prendre de l'expansion et de fournir de la pierre à sculpter à un plus grand nombre de sculpteurs résidant au-delà de la région de Pangnirtung. Les travaux entrepris dans la région à l'étude ont également permis de relever la présence de deux intrusions mafiques-ultramafiques stratifiées et de plusieurs venues de minéraux sulfurés. Ces nouvelles découvertes mettent en valeur le potentiel en ressources minérales d'intérêt économique de la région et soulignent l'importance d'y procéder à des travaux de cartographie géologique. Des échantillons de chaque unité lithologique ont été recueillis aux fins d'essais et d'analyse géochimique, ainsi qu'en vue de déterminer, le cas échéant, leur aptitude à servir de roche à sculpter. Le présent rapport sommaire fait état des observations faites sur le terrain, de l'évaluation du gisement de roche à sculpter et d'un sous-ensemble de résultats d'analyses.

Introduction

Artisan carving stone is a valuable natural resource in Nunavut. The stone is traditionally gathered by hand from dozens of quarries and sites throughout the territory (Beauregard and Ell, 2013; Beauregard et al., 2013). The commodity supplies a growing Inuit population whose carvers have developed artistic styles unique to the Canadian Arctic and, in many cases, have gained global recognition and acclaim. Over time, some active carving stone deposits will become exhausted, requiring that new carving stone deposits be identified, the stone assessed for artisan suitability and new sites developed and managed to ensure productivity and the safety of those who use them.

This publication is also available, free of charge, as colour digital files in Adobe Acrobat® PDF format from the Canada-Nunavut Geoscience Office website: http://cngo.ca/summary-of-activities/2014/.

Since 2010, the Government of Nunavut Department of Economic Development and Transportation (EDT) has been conducting the Nunavut Carving Stone Deposit Evaluation Program (NCSDEP; Beauregard et al., 2013; Steenkamp et al., 2014; Beauregard et al., 2015). The program focuses on establishing grade, tonnage and artisan suitability for carving stone gathered from known deposits for soft-stone sculpture, the leading sector of Nunavut's arts industry. In August 2014, the Canada-Nunavut Geoscience Office (CNGO) and EDT collaborated on geological mapping and a resource assessment of the excellent-quality Opingivik (a derivative from its traditional name *Upirngivik*) carving stone deposit. The site is located approximately 112 km southwest of Pangnirtung, near the Opingivik outpost camp on the southwestern shore of Cumberland Sound, Baffin Island (Figure 1; 65°15'01.6"N, 67°04'25.2"W). Several other carving stone sites along the south shore of Cumberland Sound have also been brought forward by Pangnirtung residents to the NCSDEP and CNGO through community engagement meetings and subsequent quarry site visits between 2011 and 2014 (Figure 1). The Opingivik quarry is within Inuit Owned Lands parcel PA-24. Land-surface rights for this parcel are managed by the Qikiqtani Inuit Association.

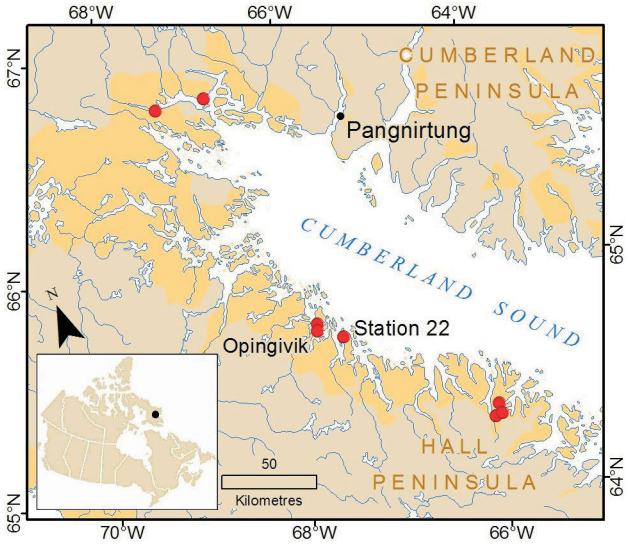

Figure 1: Locations of the Opingivik quarry and other carving stone occurrences on western Cumberland Sound, Baffin Island, Nunavut, brought forward to the Nunavut Carving Stone Deposit Evaluation Program and the Canada-Nunavut Geoscience Office by Pangnirtung residents between 2011 and 2014; station 22 lies outside of the study area but was visited and sampled, and a subset of analytical results from this carving stone location is included in Table 1; Inuit Owned Lands are shown in orange.

The aims of this project were multifaceted: establish the surface extent of carving stone resources around the deposit; characterize and assess the quality of the stone; investigate the geological relationships between all rock types and structural features in the study area; and explore for other nearby potential resources. Field station observa-

Table 1: Subset of analytical data from the full raw geochemical dataset found in Steenkamp (2015); selected metal concentrations highlight the economic potential of the serpentinite, layered mafic–ultramafic intrusion, and sulphide-bearing metasedimentary units and orthopyroxene monzogranite; station locations are referenced on the geological map in Figure 2; Abbreviations: LM-UI, layered mafic–ultramafic intrusion; Grt, garnet; Bt, biotite; Opx, orthopyroxene; BDL, below detection limit.

			Cr (ppm)	Co (ppm)	Ni (ppm)	Cu (ppm)	Pd (ppb)	Pt (ppb)	Au (ppb)
	Detection limit:		20	1	20	10	0.5	0.5	1
	Station	Sample							
Serpentinite	5	A1	3110	123	2290	10	BDL	0.5	4
	6	A1	1200	108	2390	BDL	BDL	BDL	10
	6	A2	1180	115	2590	BDL	BDL	BDL	10
	6	A3	930	99	2360	BDL	BDL	BDL	2
	6	A4	790	106	2730	BDL	BDL	BDL	2
	6	A5	1150	101	2460	BDL	BDL	BDL	2
	7	B1	1380	104	2560	BDL	BDL	BDL	2
	14	A1	1180	108	2500	BDL	BDL	BDL	1
	22	B1	6330	124	2140	40	BDL	BDL	3
LM-UI	24	A1	2470	81	990	50	6.9	8.9	BDL
	24	A2	3020	109	1760	30	3.7	5.1	2
	24	A3	140	38	110	50	3.9	4.1	2
Gt-Bt Psammite	2	B1	70	84	300	660	3.1	2	31
	18	A1	130	45	230	360	12.3	1.3	24
	18	A2	60	89	530	330	78.1	13.2	34
	21	A1	160	23	90	410	4.8	1.9	5
Opx Monzogranite	16	A1	130	49	170	350	7.3	3.5	8
	17	B1	220	45	120	60	16.1	10.8	4
	24	B1	1120	68	440	170	5.1	5.1	4
	25	B1	60	15	80	320	4.9	2.1	4
	25	B2	120	43	70	50	0.7	BDL	2

tions, photographs, ArcGIS map project and layers, and the full geochemical dataset that accompanies this summary paper are available in Steenkamp (2015)[4].

Geological setting

Southern Baffin Island is underlain by Archean and middle Paleoproterozoic rocks that experienced metamorphism and deformation associated with the accretionary and continental-collision phases of the Trans-Hudson Orogen. This major mountain-building event involved northwestward subduction of the Superior Plate craton below an amalgamated collage of smaller crustal blocks (Churchill Plate), with terminal collision occurring between 1.82 and 1.80 Ga (Hoffman, 1988; Lewry and Collerson, 1990; St-Onge et al., 2007, 2009). The orogenic system extended from northeastern to south-central North America and has been physically and temporally compared to the Himalayas as a modern analogue (St-Onge et al., 2006).

The bedrock west of Cumberland Sound (NTS map areas 26A though 26H), including the Opingivik area, was mapped at a scale of 1:506 880 by Blackadar (1967). This reconnaissance-scale mapping documents a dominance of variably deformed orthogneiss, orthopyroxene-bearing granite and paragneiss, the latter comprising mostly pelite, psammite, quartzite and carbonate rocks. Recent mapping conducted south of Opingivik (Machado et al., 2013a, b; Steenkamp and St-Onge, 2014) generally corroborates Blackadar's (1967) work but also documents newly identified regional-scale isoclinal folds and thick-skinned thrusts oriented parallel to the dominant regional-deformation fabric, and amphibolite- to granulite-facies metamorphic mineral assemblages (Braden, 2013; Skipton and St-Onge, 2014). The observed metamorphism and deformation are interpreted to reflect the Trans-Hudson Orogen in this area (Steenkamp and St-Onge, 2014).

The northeastern portion of Hall Peninsula is underlain by Archean, polymetamorphosed tonalite to granodiorite (From et al., 2014; Rayner, 2014a, b). The northwestern portion of the peninsula is dominated by Paleoproterozoic intrusive orthopyroxene-bearing granite to monzogranite and psammitic to pelitic metasedimentary units that are locally interlayered with mafic volcanic and calcsilicate layers (MacKay and Ansdell, 2014; Rayner, 2014a, b).

Methods

Geological mapping at Opingivik involved five days of fieldwork (August 16–21, 2014) based from a campsite located 500 m southeast of the active Opingivik quarry. The mapping team was accompanied by NCSDEP carver Jerry Ell and two families from the Hamlet of Pangnirtung, who assisted with boat transportation, logistics, camp management and wildlife monitoring. Geological mapping was first conducted around the Opingivik serpentinite deposit to define its boundaries, and then around the local peninsula to determine whether more serpentinite or other potentially economic mineral occurrences exist. Samples were collected for geochemical analysis, as lithological representatives for the study area, and for artisan suitability and characterization where applicable. The carving stone deposit was surveyed with a base station established at the edge of the small lake called Iqalugalik, and survey stakes were positioned on a north bearing every 25 m up the hill to a distance of 350 m.

Geological observations and field relationships

Bedrock in the north, east, and south parts of the study area (Figure 2) is exposed in steep hills and cliffs between terraces of thick, low-lying vegetation. In contrast, bedrock is poorly exposed in the western part of the study area, which is dominated by marshland and a few highly weathered, low-relief hills.

Metasedimentary rocks

The valley on the west side of the study area is underlain by metasedimentary rocks. Stratigraphic layering of the metasedimentary rocks is oriented parallel to the regional west-dipping foliation observed to the south on Hall Peninsula (Machado et al., 2013b; Steenkamp and St-Onge, 2014). The metasedimentary strata are interpreted to have been intruded by orthopyroxene-bearing monzogranite (described below), which is found at both east and west contacts of the metasedimentary package. The metasedimentary rocks consist mainly of garnet+biotite±sillimanite semipelite with minor, intercalated layers of garnet+biotite psammite and clinopyroxene±orthopyroxene diorite. A 30 m long enclave of garnet+biotite psammite, similar to that found in the valley, was observed in monzogranite at station 2 (Figure 2). The garnet+biotite psammite was sampled for geochemical analysis from three locations in the study area; the analyzed samples contain 10–30 cm wide layers with local concentrations of disseminated, fine-grained pyrite, pyrrhotite and minor chalcopyrite (Figure 3a, b; Table 1, stations 2, 18, 21). The metasedimentary rocks in the study area are provisionally correlated with the Paleoproterozoic Lake Harbour Group (Jackson and Taylor, 1972), based on the similarity of rock types.

Layered mafic–ultramafic intrusions

Two layered mafic–ultramafic intrusions (LM-UI) outcrop along strike from each other within the study area (Figure 2) and are presumed to represent the same unit. The oc-

[4]*CNGO Geoscience Data Series GDS2015-005, containing the data or other information sources used to compile this paper, is available online to download free of charge at http://cngo.ca/summary-of-activities/2014/.*

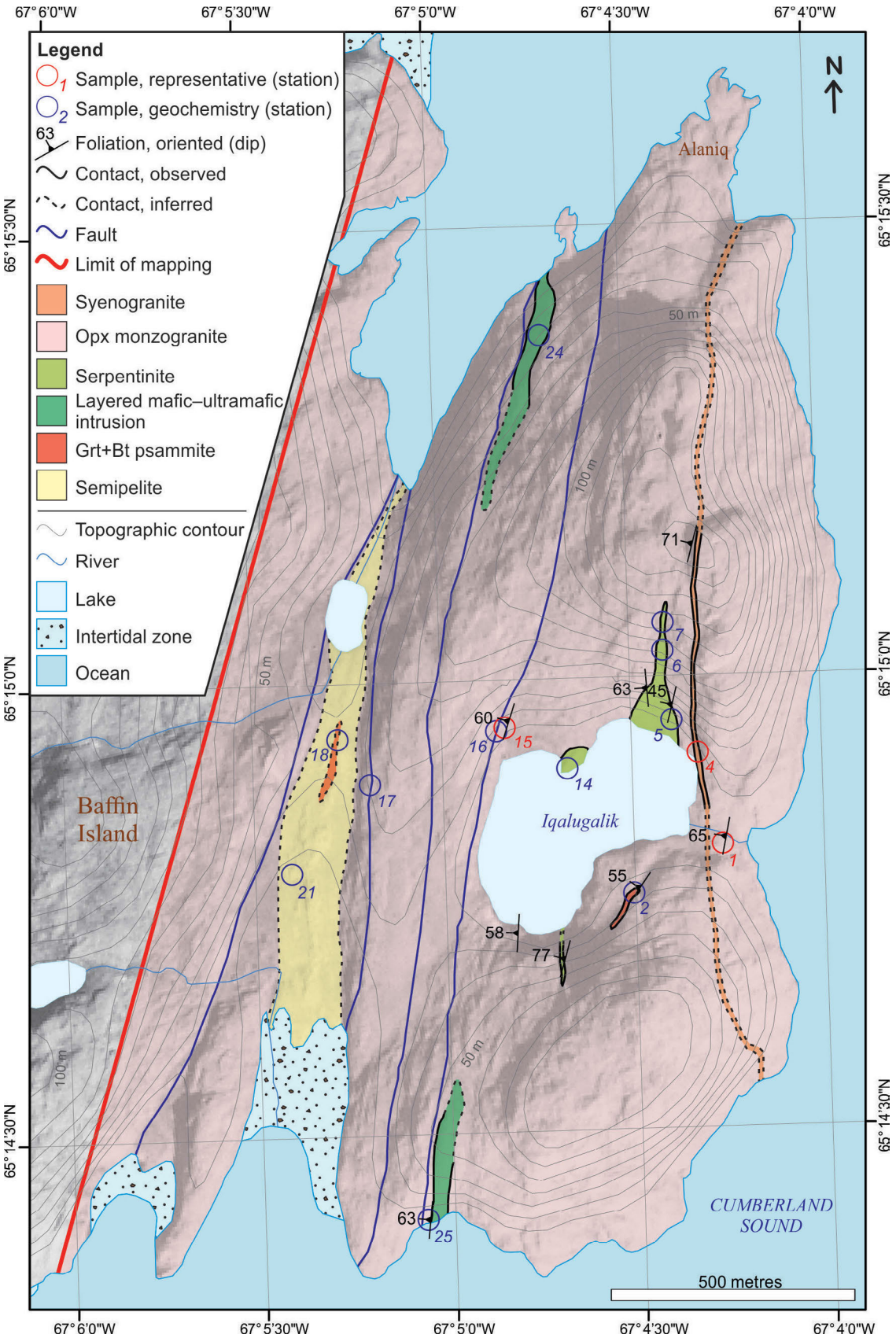

Figure 2: Geology in the vicinity of the Opingivik carving stone deposit, Baffin Island, Nunavut; station numbers correspond to the sample data subset presented in Table 1 and the full geochemical dataset contained in Steenkamp (2015); Abbreviations: Grt, garnet; Bt, biotite; Opx, orthopyroxene.

Figure 3: Occurrences having mineral exploration potential near the Opingivik carving stone deposit, Baffin Island, Nunavut: **a)** sample of metasedimentary garnet-biotite psammite unit containing abundant disseminated sulphides (Table 1, station 18, sample A1); **b)** shallow pit dug to expose metasedimentary garnet-biotite psammite bedrock with abundant disseminated sulphides; **c)** the northern layered mafic–ultramafic intrusion (LM-UI; Table 1, station 24, samples A1, A2, A3) is approximately 40 m thick, structurally overturned and hosted in orthopyroxene±biotite monzogranite (Table 1, station 24, sample B1), which contains sulphide mineralization below the LM-UI; **d)** brittle faulting of sulphide-bearing orthopyroxene±biotite monzogranite (Table 1, station 25, samples B1, B2) directly below the stratigraphic bottom of the southern LM-UI; Abbreviations: LM-UI, layered mafic–ultramafic intrusion; Py, pyrite; Po, pyrrhotite; Ccp, chalcopyrite.

currences are oriented parallel to the regional foliation, dip to the west and are interpreted to be overturned based on inverted magmatic compositional layering. The bodies are varied in composition from clinopyroxenite at the base (west side of each body), through internally layered magnetite peridotite for about 35 m, to gabbro at the top (east side).

The northern LM-UI is approximately 40 m thick (Figure 3c) and cut by orthopyroxene-bearing monzogranite. Samples were collected for geochemical analysis from each compositional member (Table 1, station 24, samples A1, A2, A3), as well as from the altered, pyrite- and chalcopyrite-bearing orthopyroxene monzogranite underlying the intrusion (Table 1, station 24, sample B1).

The southern LM-UI is comparable in size and character to the northern one, but the base of the southern body is adjacent to a 10 m wide brittle fault zone (Figure 3d), which marks the contact with the intrusive monzogranite. Samples of the sheared monzogranite, which directly underlie the southern LM-UI, also contain disseminated pyrite, pyrrhotite and minor chalcopyrite (Table 1, station 25, samples B1, B2).

Serpentinite

The serpentinite deposit occurs as a boudin within the intrusive orthopyroxene-bearing monzogranite (described below) that is widest along the shore of Iqalugalik (approximately 100 m; Figure 4a) and pinches out to the north on the hillside at about 120 m elevation. Orange-weathering boulders (Figure 4b; Table 1, station 7) mark the pinch-out point on the hill. The east (Figure 4c; Table 1, station 5) and west contacts of the serpentinite deposit are exposed, and appear to conform to the regional west-dipping foliation. Most of

Figure 4: Observations from around the Opingivik carving stone deposit: **a)** view to the south from above the active quarry; the serpentinite deposit is defined by white dashed lines, and five white canvas tents in the background provide scale; **b)** orange-weathering, dark green serpentinite boulder containing fine-grained magnetite ribbons, found where the Opingivik deposit pinches out on the hillside above the active quarry (Table 1, station 7); **c)** subcrop and outcrop along the eastern serpentinite contact with the host orthopyroxene monzogranite; **d)** view to the southwest from above the active quarry; carvers are removing slumped overburden to access the medium green serpentinite found in the centre of the deposit; **e)** polished slabs of serpentinite from the west (1) and centre (2) of the deposit, and the west (3) and east (4) walls of the active quarry (Table 1, station 6, samples A2, A3, A4, A5, respectively); **f)** well-foliated, medium-grained orthopyroxene monzogranite that underlies most of the study area; hammer for scale is 40 cm long and view is to the south. Abbreviations: Bt, biotite; Opx, orthopyroxene.

the deposit between these contacts is covered by grassy overburden and soil. The active quarry (Figure 4d) measures approximately 3 m by 4 m, and is located at about 75 m elevation on the eastern side of the serpentinite deposit (at station 6 on Figure 2).

Serpentinite samples collected across the deposit are extremely variable in character (Figure 4e; Table 1, station 6) and have hardnesses ranging between 2.5 and 3. Stone extracted from within the active quarry (east side of the serpentinite deposit) is dark green to black, relatively soft and homogeneous, and composed of fine- to very fine grained antigorite with minor disseminated chrysotile and magnetite. In the centre of the deposit above the active quarry is an outcrop of medium green serpentinite containing 1–2 cm long ribbons of very fine grained magnetite, and antigorite pseudomorphs after a spherical mineral presumed to have been olivine. Serpentinite from the western contact of the deposit is light to medium green and fine grained, and also contains 1–2 cm long magnetite ribbons. Here, pale green haloes around the magnetite ribbons may indicate iron depletion from the serpentine as it was concentrated in the magnetite. Recrystallized light brown chrysotile is visible in coarser grained sections of the matrix and in randomly oriented, thin (<8 mm) veins in the serpentinite from the western contact of the deposit.

Serpentinite also underlies a small peninsula in Iqalugalik (Figure 2) and was sampled for geochemical analysis (Table 1, station 14). The outcrop at station 14 is highly altered, having amphibolite-facies tremolite and actinolite replacement. In addition, fractures 1–10 cm wide are healed with tremolite and actinolite, and locally with quartz. The stone at station 14 is not suitable for carving due to its heterogeneity, increased hardness and brittle character.

Orthopyroxene±biotite monzogranite

The study area is underlain mainly by well-foliated, medium-grained orthopyroxene±biotite monzogranite (Figure 4f). In the study area, the unit contains a steeply west-dipping foliation, which is defined by aligned orthopyroxene and/or biotite grains, stretched and recrystallized quartz and feldspar, and locally by centimetre- to metre-thick enclaves and layers of fine- to medium-grained clinopyroxene±orthopyroxene diorite. The foliation orientation is consistent with the regional west-dipping foliation established to the south on Hall Peninsula (Machado et al., 2013a, b; Steenkamp and St-Onge, 2014). Locally, sulphide mineralization is associated with brittle fault zones that cut the monzogranite. Mineralized samples from the fault zones were collected for geochemical analysis (Table 1, stations 16 and 17). This unit is provisionally correlated with the ca. 1.89 Ga intrusive orthopyroxene-bearing monzogranite from southern Hall Peninsula dated by Rayner (2014a, b), based on the similarities of the rock types, metamorphic grade and field relationships.

Syenogranite

A 2–5 m wide syenogranite dyke obliquely crosscuts the foliation in the orthopyroxene±biotite monzogranite about 40 m east of the serpentinite deposit and active quarry. The dyke is compositionally homogeneous, medium to coarse grained and laterally continuous across the study area. Small-scale syenogranite occurrences were found associated with the brittle faults that run generally north-south through the region.

Results

Evaluation of the Opingivik carving stone deposit

The Opingivik deposit is an important resource on southern Baffin Island that has the potential to serve carvers across the southern Baffin region (Beauregard and Ell, 2013). The quarry has produced an estimated 200 tonnes of good- to excellent-quality carving stone since the early 2000s. Soft to medium-soft carving stone is available in blocks measuring up to 1 m by 0.5 m and can be selected by carvers for their specific use. The dimensions of frost-fractured blocks increase with depth in the quarry.

Based on the size of the wasterock pile (25 m by 25 m by 4 m; Figure 4d) and an average proportion of wastage of 60%, an estimated 500 tonnes of overburden, frost-fractured outcrop and carver-selected artisan serpentinite have been removed by shovel, grub hoe, pickaxe and pry bar from the active quarry. The quarry bottom has not yet reached depths where water drainage becomes an issue, but the quarry walls are prone to slow collapse when they become water saturated.

Two outcrops of medium to medium-hard serpentinite at the western contact across from station 5 (Figure 2) have the potential to produce large blocks. At that location, competent rock will need to be broken and extracted using the plugger-and-feather method, and shaping and polishing of carvings will require carbide power tools. At least 200 tonnes of surface-accessible fair- to good-quality carving stone is available here. Subcropping frost-fractured carving stone occurs at the base of the dirt-covered hillside about 125 m south of the quarry. This site has yet to be dug out and rated for its artisan suitability.

From the active quarry, small drag sleds and skiffs are used to haul carver-selected stone blocks 150 m down the hill to Iqalugalik. Stone is then transferred into a small boat, paddled to an adjacent shore, transferred back onto sleds and finally dragged about 110 m to tidewater. Here, the stone is loaded into powerboats for transport to Pangnirtung. The tidal range is about 8–10 m in the small, rocky harbour. Recent unsafe sea-ice conditions have limited snowmobile access to the quarry, forcing carvers to gather stone during open-water months by boat. Despite this, some users con-

tinue to collect loads weighing up to 3000 kg from Opingivik.

Geochemical data

Twenty-five samples were collected and representative portions sent to Activation Laboratories Ltd. (Ancaster, Ontario) for geochemical analysis (Table 1; Steenkamp, 2015). Samples with weathered, rusted or vegetated surfaces were first trimmed using a rock saw in preparation for analysis. Activation Laboratories crushed each sample and then pulverized the crushed rock using a soft-steel mill. Aliquots of the powdered samples were analyzed by lithium metaborate/tetraborate fusion, inductively coupled plasma–emission spectrometry (ICP-ES) and inductively coupled plasma–mass spectrometry (ICP-MS) for major-element oxides and trace elements, respectively. Platinum-group elements (palladium, platinum and gold) were analyzed by the fire-assay ICP-MS method.

The serpentinite samples have consistent nickel and cobalt concentrations, regardless of sample location within the Opingivik deposit. Serpentinite from station 22 has significantly different geochemistry because the body is not related to the Opingivik site, and has a considerably higher chromium concentration. It is located 75 m from tidewater on an island approximately 10 km east of Opingivik and was investigated as a new potential carving stone resource. This serpentinite body, however, is relatively small (15 m by 10 m) and the stone is harder, coarser grained and heterogeneous in comparison with Opingivik stone.

Samples analyzed from the northern LM-UI (station 24) include the basal clinopyroxenite (A1), the layered peridotite (A2), and gabbro (A3) at the top of the intrusion. The peridotite has the highest chromium, cobalt and nickel concentrations, and the basal clinopyroxenite the highest platinum-group element concentrations, of the three samples.

From the metasedimentary samples collected, the garnet-biotite psammite from station 2 yielded the highest copper concentration. The sulphide-rich sample (A2) from station 18 has the highest concentrations of palladium, platinum and gold in the dataset.

The sampled orthopyroxene monzogranite is associated with brittle fault zones (stations 16, 17, 25) and/or the LM-UIs (stations 24, 25). The sulphide-bearing sample collected from below the northern LM-UI (station 24) has the highest chromium, cobalt and nickel concentrations for this rock type.

Economic considerations

Many carvings made from Opingivik stone have been sold to national and international buyers. The Opingivik serpentinite deposit requires further assessment of its potential before it is capable of supplying raw material beyond Pangnirtung to other southern Baffin Island communities.

The extent of subsurface carving stone around the Opingivik deposit, specifically in areas covered by overburden and vegetation downslope from the active quarry, remains unknown. This could quickly and inexpensively be determined by conducting a walking magnetic geophysical survey over the deposit area. Serpentinite typically contains more magnetite than the host orthopyroxene±biotite monzogranite, and would therefore have a distinct geophysical signature. In areas where subsurface serpentinite is indicated to exist, hand-pitting through the overburden to the bedrock would then be required, and the artisan suitability of newly exposed stone would need to be assessed and incorporated into the deposit evaluation.

The Opingivik area also has exploration potential for mineral deposits based on the sulphide mineral occurrences and layered mafic–ultramafic intrusions observed and analyzed in this study. Sulphide mineralization found in fault zones of orogenic systems can sometimes be associated with hydrothermal gold or other precious and base metals (Taylor, 2007). In addition, a variety of economic deposits containing nickel, copper and platinum-group elements is associated with a range of mafic and ultramafic magmatic rocks (e.g., Eckstrand et al., 2004; Naldrett, 2004; Eckstrand and Hulbert, 2007). Analytical results from the new discoveries in the study area suggest that further investigation of the exploration potential in the region around Opingivik is warranted. These occurrences of mineralized rocks underscore the need for modern, higher resolution geological mapping on the western side of Cumberland Sound. As of October 2014, there were no active mineral claims in the Opingivik area.

Acknowledgments

The authors thank the following contributors: Pangnirtung carver and Opingivik quarry advocate, Jaco Ishulutaq, and his wife, Oleepa, for helping to organize and support this project; Lootie, Rosie and Patrick Nauyuk, and Annie Angnakak of Pangnirtung for their guidance, wildlife monitoring and prospecting skills; NCSDEP carver Jerry Ell for his Inuktitut translation, logistics planning and carving stone expertise; and Natural Resources Canada's Polar Continental Shelf Program and Universal Helicopters for their logistics assistance and safe air travel. Financial support for this study was provided by the Canadian Northern Economic Development Agency's (CanNor) Strategic Investments in Northern Economic Development (SINED) program. This paper benefited from a thorough and thoughtful review by D. James.

Natural Resources Canada, Earth Sciences Sector contribution 20140295.

References

Beauregard, M. and Ell, J. 2015: Nunavut Carving Stone Deposit Evaluation Program: 2013 and 2014 fieldwork in the Kitikmeot Region, Belcher Islands, Hall Peninsula and Repulse Bay, Nunavut; *in* Summary of Activities 2014, Canada-Nunavut Geoscience Office, p. 163–174.

Beauregard, M.A. and Ell, J. 2013: Defining the commodity of Nunavut's soapstone on behalf of carvers, communities and art industry; presentation at Nunavut Mining Symposium 2013, Mineral and Petroleum Resources, Department of Economic Development and Transportation, Government of Nunavut, Iqaluit, Nunavut, 27 slides.

Beauregard, M.A., Ell, J., Pikor, R.K. and Ham, L.J., 2013: Nunavut Carving Stone Deposit Evaluation Program (2010–2013): third year results; *in* Summary of Activities 2012, Canada-Nunavut Geoscience Office, p. 151–162.

Blackadar, R.G. 1967: Geology, Cumberland Sound, District of Franklin; Geological Survey of Canada, Preliminary Map 17-1966, scale 1:506 880, doi:10.4095/108490

Braden, Z.M. 2013: Paleoproterozoic pressure-temperature-deformation path in the Newton Fiord region, eastern Baffin Island, Nunavut; B.Sc. thesis, Dalhousie University, Halifax, Nova Scotia.

Eckstrand, O.R. and Hulbert, L.J. 2007: Magmatic nickel-copper-platinum group element deposits; *in* Mineral Deposits of Canada: a Synthesis of Major Deposit Types, District Metallogeny, the Evolution of Geological Provinces, and Exploration Methods, W.D. Goodfellow, (ed.), Geological Association of Canada, Mineral Deposits Division, Special Publication 5, p. 205–222.

Eckstrand, O.R., Good, D.J., Yakubchuk, A. and Gall, Q. 2004: World distribution of Ni, Cu, PGE and Cr deposits and camps; Geological Survey of Canada, unpublished update of Open File 3791a.

From, R.E., St-Onge, M.R. and Camacho, A.L. 2014: Preliminary characterization of the Archean orthogneiss complex of Hall Peninsula, Baffin Island, Nunavut; *in* Summary of Activities 2013, Canada-Nunavut Geoscience Office, p. 53–62.

Hoffman, P.F. 1988: United Plates of America, the birth of a craton: Early Proterozoic assembly and growth of Laurentia; Annual Review of Earth and Planetary Sciences, v. 16, p. 543–603.

Jackson, G.D. and Taylor, F.C. 1972: Correlation of major Aphebian rock units in the northeastern Canadian Shield; Canadian Journal of Earth Sciences, v. 9, p. 1650–1669.

Lewry, J.F. and Collerson, K.D. 1990: The Trans-Hudson Orogen: extent, subdivision, and problems; *in* The Early Proterozoic Trans-Hudson Orogen of North America, J.F. Lewry and M.R. Stauffer (ed.), Geological Association of Canada, Special Paper 37, p. 1–14.

Machado, G., Bilodeau, C. and St-Onge, M.R., 2013a: Geology, southern part of Hall Peninsula, south Baffin Island, Nunavut; Geological Survey of Canada, Canadian Geoscience Map 135, scale 1:250 000, doi:10.4095/292443

Machado, G., Bilodeau, C., Takpanie, R., St-Onge, M.R., Rayner, N.M., Skipton, D.R., From, R.E., MacKay, C.B., Creason C.G. and Braden, Z.M. 2013b: Hall Peninsula regional bedrock mapping, Baffin Island, Nunavut: summary of fieldwork; *in* Summary of Activities 2013, Canada-Nunavut Geoscience Office, p. 13–22.

MacKay, C.B. and Ansdell, K.M. 2014: Geochemical study of mafic and ultramafic rocks from southern Hall Peninsula, Baffin Island, Nunavut; *in* Summary of Activities 2013, Canada-Nunavut Geoscience Office, p. 85–92.

Naldrett, A.J. 2004: Magmatic Sulfide Deposits: Geology, Geochemistry and Exploration; Springer Verlag, Heidelberg, Germany, 727 p.

Rayner, N.M. 2014a: New uranium-lead geochronological results from Hall Peninsula, Baffin Island, Nunavut; *in* Summary of Activities 2013, Canada-Nunavut Geoscience Office, p. 39–52.

Rayner, N.M. 2014b: Data table accompanying "New U-Pb geochronological results from Hall Peninsula, Baffin Island, Nunavut"; Canada-Nunavut Geoscience Office, Geoscience Data Series GDS2014-001, Microsoft® Excel® file.

Skipton, D.R. and St-Onge, M.R. 2014: Paleoproterozoic deformation and metamorphism in metasedimentary rocks west of Okalik Bay: a field template for the evolution of eastern Hall Peninsula, Baffin Island, Nunavut; *in* Summary of Activities 2013, Canada-Nunavut Geoscience Office, p. 63–72.

St-Onge, M.R., Searle, M.P. and Wodicka, N. 2006: Trans-Hudson Orogen of North America and Himalaya-Karakoram-Tibetan Orogen of Asia: structural and thermal characteristics of the lower and upper plates; Tectonics, v. 25, no. 4, doi:10.1029/2005TC001907

St-Onge, M.R., Van Goole, J.A.M., Garde, A.A. and Scott, D.J. 2009: Correlation of Archaean and Palaeoproterozoic units between northeastern Canada and western Greenland: constraining the pre-collisional upper plate accretionary history of the Trans-Hudson Orogen; *in* Earth Accretionary Systems in Space and Time, P.A. Cawood and A. Kröner (ed.), The Geological Society of London, Special Publications, v. 318, p. 193–235.

St-Onge, M.R., Wodicka, N. and Ijewliw, O. 2007: Polymetamorphic evolution of the Trans-Hudson Orogen, Baffin Island, Canada: integration of petrological, structural and geochronological data; Journal of Petrology, v. 48, p. 271–302, doi:10.1093/petrology/eg1060

Steenkamp, H.M. 2015: Data files accompanying "Carving stone and mineral resource potential of the Opingivik deposit, Baffin Island, Nunavut"; Canada-Nunavut Geoscience Office, Geoscience Data Series GDS2015-005, Microsoft® Excel® file and Esri ArcGIS project, URL <http://cngo.ca/summary-of-activities/2014/> [January 2015].

Steenkamp, H.M. and St-Onge, M.R. 2014: Overview of the 2013 regional bedrock mapping program on northern Hall Peninsula, Baffin Island, Nunavut; *in* Summary of Activities 2013, Canada-Nunavut Geoscience Office, p. 27–37.

Steenkamp, H.M., Pizzo-Lyall, M., Wallace, C.J., Beauregard, M.A. and Dyck, B.J. 2014: Geology, history and site-management planning of the Kangiqsukutaaq carving stone quarry, southern Baffin Island, Nunavut; *in* Summary of Activities 2013, Canada-Nunavut Geoscience Office, p. 193–200.

Taylor, B.E. 2007: Epithermal gold deposits; *in* Mineral Deposits of Canada: A Synthesis of Major Deposit-Types, District Metallogeny, the Evolution of Geological Provinces, and Exploration Methods, W.D. Goodfellow (ed.), Geological Association of Canada, Mineral Deposits Division, Special Publication 5, p. 113–139.

Nunavut Carving Stone Deposit Evaluation Program: 2013 and 2014 fieldwork in the Kitikmeot Region, Belcher Islands, Hall Peninsula and Repulse Bay, Nunavut

M.A. Beauregard[1] and J. Ell[2]

[1]*Minerals and Petroleum Resources, Department of Economic Development and Transportation, Government of Nunavut, Arviat, Nunavut, mbeauregard@gov.nu.ca*

[2]*Marchand, Manitoba*

Beauregard, M.A. and Ell, J. 2015: Nunavut Carving Stone Deposit Evaluation Program: 2013 and 2014 fieldwork in the Kitikmeot Region, Belcher Islands, Hall Peninsula and Repulse Bay, Nunavut; *in* Summary of Activities 2014, Canada-Nunavut Geoscience Office, p. 163–174.

Abstract

The Nunavut Carving Stone Deposit Evaluation Program is a collaborative project led by the Government of Nunavut Department of Economic Development and Transportation and involving the Canada-Nunavut Geoscience Office. This paper summarizes field observations and deposit evaluations of 31 carving stone sites in the Kitikmeot region, on the Belcher Islands, on Hall Peninsula and near Repulse Bay carried out in 2013 and 2014. Highlights include documentation of the eastern Kitikmeot Region's shared Aqituqtaqvik (Murchison River) quarry; newly documented reserves of 30 000 tonnes of artisan marble at Sanikiluaq's community quarry; several small-scale serpentinite deposits in the immediate vicinity of Repulse Bay; and a new tidewater deposit in the Leybourne Islands of Cumberland Sound that contains an estimated 25 000 tonnes of artisan serpentinite.

Including 2013 and 2014 results reported herein, a total of 94 carving stone sites have been documented in the vicinity of 23 communities across Nunavut since 2010. The Nunavut Carving Stone Deposit Evaluation Program has confirmed 15 substantial new deposits and determined grade, tonnage and composition of 9 active community quarries and 1 regional producer. The supply inventory of territorial carving stone shows that 17 of Nunavut's 25 communities have access to local carving stone resources adequate for their long-term needs.

Résumé

Le programme d'évaluation des gisements de pierre à sculpter du Nunavut est un projet de nature collaborative dirigé par le ministère du Développement économique et des Transport du gouvernement du Nunavut, et impliquant le Bureau géoscientifique Canada-Nunavut. Le présent rapport fait état des observations de terrain et des évaluations de gisements de pierre à sculpter réalisées en 2013 et 2014 à 31 sites de pierre à sculpter dans la région de Kitikmeot, les îles Belcher, la péninsule Hall et près de la baie Repulse. Parmi les points saillants de l'étude, on remarque la documentation de la carrière partagée d'Aqituqtaqvik (Murchison River, dans la région de Kitikmeot; la découverte de nouvelles réserves de 30 000 t de marbre évalué par les artisans dans la carrière communautaire de Sanikiluaq; la découverte de quelques petits gisements de serpentinite dans la région à proximité de la baie Repulse; et l'établissement de la présence de ressources estimées de 25 000 t de serpentinite évaluée par les artisans dans un gisement mis en place par les courants de marées récemment découvert dans les îles Leybourne, situées dans le détroit de Cumberland.

Depuis 2010, la présence de 94 sites de pierre à sculpter, y compris les sites relevés en 2013 et 2014 dont fait état le présent rapport, a été relevée à proximité de 23 collectivités dans l'ensemble du Nunavut. Dans le cadre du programme d'évaluation des gisements de pierre à sculpter du Nunavut, on a pu confirmer l'existence de 15 nouveaux gisements de taille et déterminer la teneur, le tonnage et la composition de la pierre de 9 carrières communautaires exploitées activement et chez un exploitant régional. L'inventaire territorial de l'approvisionnement en pierre à sculpter démontre que 17 des 25 collectivités du Nunavut ont accès à des ressources locales de pierre à sculpter en quantité suffisante pour satisfaire leurs besoins à long terme.

This publication is also available, free of charge, as colour digital files in Adobe Acrobat® PDF format from the Canada-Nunavut Geoscience Office website: http://cngo.ca/summary-of-activities/2014/.

Introduction

The Nunavut Carving Stone Deposit Evaluation Program (NCSDEP) is a collaborative project led by the Government of Nunavut Department of Economic Development and Transportation (GN-EDT) and involving the Canada-Nunavut Geoscience Office (CNGO). Assistance provided by local carvers from every community in Nunavut is also an integral part of the program.

The primary goals of the NCSDEP are to evaluate traditional carving stone sites and identify new deposits in Nunavut, based upon Inuit rights to carving stone set out in Article 19, Part 9 of the Nunavut Land Claims Act and carving stone documents prepared by the Government of Nunavut (Government of Canada, 1993; Nunavut Department of Economic Development and Transportation, 2007a, b). For more detailed descriptions of the program, and sizes and grade classifications of carving stone deposit, see Beauregard et al. (2013). All gathering sites and quarries brought forward to the NCSDEP through community consultation, and several new deposits derived from recent regional bedrock mapping programs, have been classified based on stone quality, composition and deposit tonnage. The NCSDEP intends to conduct geochemical analysis and petrographic assessment of carving stone from all of the visited sites in the coming year.

In 2013 and 2014, the NCSDEP evaluated carving stone resources in the Kitikmeot Region, Repulse Bay locale and the Belcher Islands. Additionally, multi-agency examinations were performed at Cape Dorset's Kangiqsukutaaq quarry (Qikiqtani Inuit Association, CNGO, GN-EDT and De Beers Canada Exploration Inc.), on Hall Peninsula (CNGO and GN-EDT) and at Pangnirtung's Opingivik quarry (CNGO and GN-EDT). This paper reports field observations, carving stone characteristics and deposit parameters from 34 sites visited in 2013 and 2014 (Figure 1, Table 1), including a 2011 site visit to Repulse Bay's Nau-

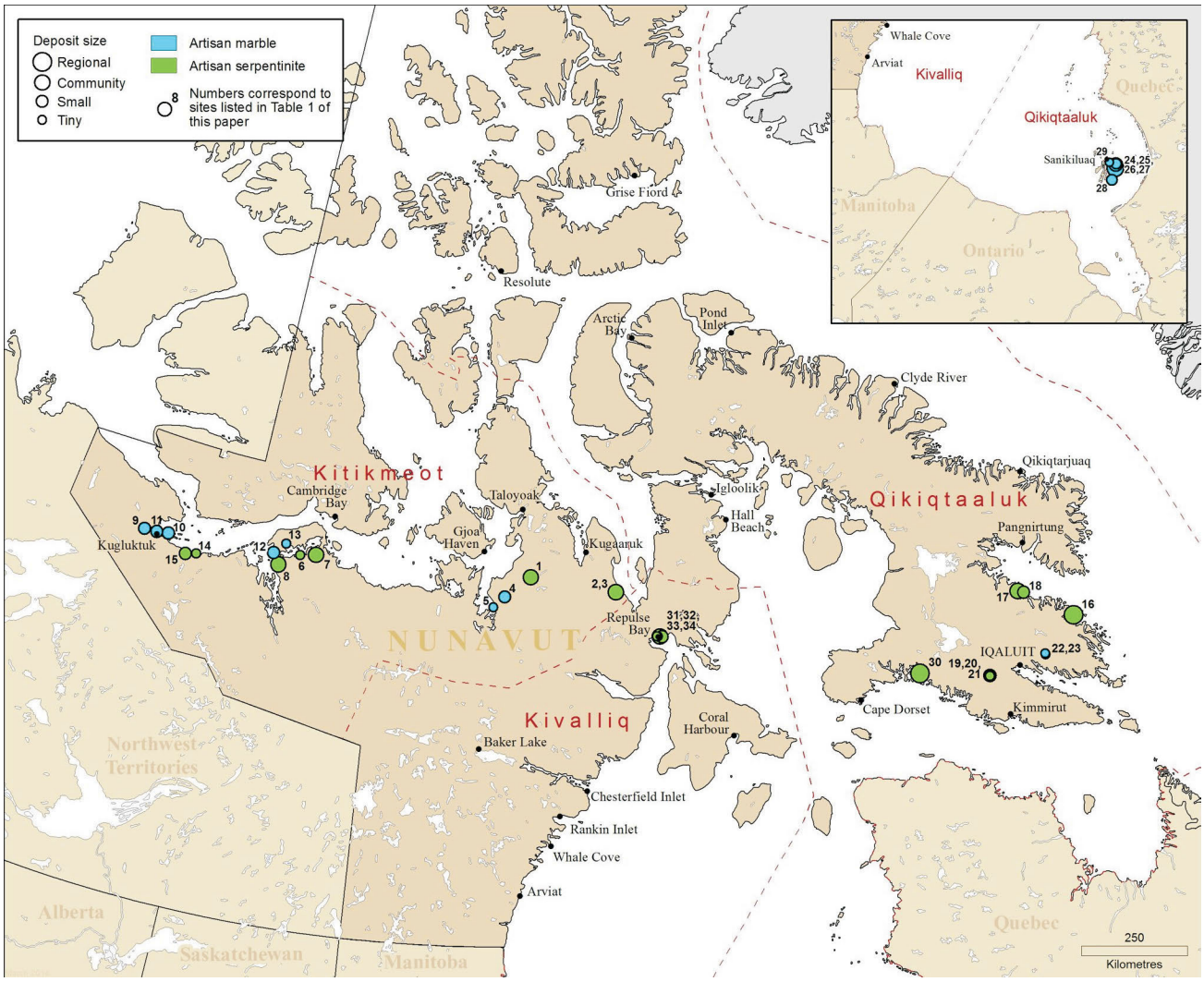

Figure 1: Carving stone sites, quarries and deposits visited by the Nunavut Carving Stone Deposit Evaluation Program in 2013 and 2014; numbers correspond to site numbers listed in Table 1.

Table 1: Nunavut Carving Stone Deposit Evaluation Program carving stone sites, quarries and deposits visited in 2013 and 2014. Abbreviation: GSC, Geological Survey of Canada.

Region	No.	Community	Site	Latitude (N)	Longitude (W)	Size	Quality
Kitikmeot	1	Gjoa Haven	Aqituqtaqvik quarry, Murchison River	68° 03' 32.4"	93° 09' 18.0"	Community	High
Kitikmeot	2	Kugaaruk	Kitingujaaq, hillside, green	67° 36' 53.9"	88° 20' 08.5"	Community	Lesser
Kitikmeot	3	Kugaaruk	Kitingujaaq, valley, black	67° 36' 59.9"	88° 19' 45.0"	Community	Lesser
Kitikmeot	4	Gjoa Haven	Marble, 34 km inland from site 5	67° 38' 46.5"	94° 41' 28.0"	Small	Lesser
Kitikmeot	5	Gjoa Haven	Marble, Victoria Headland	67° 25' 10.6"	95° 20' 16.9"	Tiny	Lesser
Kitikmeot	6	Cambridge Bay	Faulted peridotite, Hope Bay	68° 09' 33.8"	106° 44' 07.8"	Tiny	High
Kitikmeot	7	Cambridge Bay	Peridotite sill, Amitturyuap Kuugaa	68° 13' 21.7"	105° 49' 00.1"	Community	Lesser
Kitikmeot	8	Cambridge Bay	Granite-intruded peridotite, Kiluhiqtuq	67° 51' 54.3"	107° 52' 13.7"	Community	Lesser
Kitikmeot	9	Kugluktuk	Palliq marble quarry, Rae River	67° 54' 22.5"	115° 52' 50.8"	Small	High
Kitikmeot	10	Kugluktuk	Marble, Couper Islands	67° 55' 29.8"	114° 29' 53.3"	Small	Lesser
Kitikmeot	11	Kugluktuk	Kakoktalik quarry (Blaze Island)	67° 52' 38.9"	115° 10' 26.9"	Small	High
Kitikmeot	11	Kugluktuk	Marble, Couper Islands	67° 55' 29.8"	114° 29' 53.3"	Small	Lesser
Kitikmeot	12	Cambridge Bay	Ekehayoak marble, Kiluhiqtuq	68° 05' 57.3"	108° 17' 37.8"	Tiny	High
Kitikmeot	13	Cambridge Bay	Nauyak marble, Tariyunnuaq	68° 20' 45.0"	107° 39' 57.0"	Tiny	Lesser
Kitikmeot	14	Kugluktuk	Peridotite xenoliths, mainland	67° 40' 18.8"	112° 38' 14.4"	Tiny	Lesser
Kitikmeot	15	Kugluktuk	Kugakyuak quarry, Hanerok River	67° 36' 41.9"	113° 12' 50.2"	Small	Lesser
Qikiqtaaluk	16	Iqaluit	Leybourne Islands deposit	64° 14' 46.8"	65° 02' 59.0"	Regional	High
Qikiqtaaluk	17	Pangnirtung	Opingivik quarry	65° 15' 01.6"	67° 04' 25.2"	Community	High
Qikiqtaaluk	18	Pangnirtung	Looty's site	65° 10' 12.3"	66° 49' 34.6"	Small	Lesser
Qikiqtaaluk	19	Iqaluit	GSC ultramafic body, northwest gully	63° 48' 21.3"	70° 06' 39.8"	Small	High
Qikiqtaaluk	20	Iqaluit	GSC utramafic body, north	63° 48' 12.8"	70° 06' 12.2"	Tiny	Lesser
Qikiqtaaluk	21	Iqaluit	GSC ultramafic body, west	63° 48' 04.3"	70° 06' 33.8"	Tiny	Lesser
Qikiqtaaluk	22	Iqaluit	Hall Peninsula marble, south	63° 44' 19.1"	67° 08' 52.5"	Tiny	Lesser
Qikiqtaaluk	23	Iqaluit	Hall Peninsula marble, F001	63° 45' 31.5"	67° 09' 13.1"	Tiny	Lesser
Qikiqtaaluk	24	Sanikiluaq	Qullisajaniavvik quarry, Tukarak Island	56° 10' 37.3"	78° 53' 43.0"	Regional	High
Qikiqtaaluk	25	Sanikiluaq	Aqituniavvik quarry, Tukarak Island	56° 16' 49.1"	78° 48' 27.2"	Community	High
Qikiqtaaluk	26	Sanikiluaq	Ippak marble, Salty Bill Hill	56° 17' 45.5"	78° 45' 08.2"	Small	High
Qikiqtaaluk	27	Sanikiluaq	Iqaluk marble, Salty Bill Hill	56° 17' 50.6"	78° 46' 11.3"	Small	High
Qikiqtaaluk	28	Sanikiluaq	Marble, Kipula Inlet	55° 49' 10.2"	79° 17' 02.4"	Small	High
Qikiqtaaluk	29	Sanikiluaq	Marble, Kasegalik Lake	56° 25' 08.9"	79° 10' 12.8"	Tiny	Lesser
Qikiqtaaluk	30	Cape Dorset	Kangiqsukutaaq quarry, Korok Inlet	64° 23' 50"	73° 19' 10"	Regional	High
Kivalliq	31	Repulse Bay	Innuqsulik, ATV trail	66° 31' 41.7"	86° 04' 14.7"	Small	Lesser
Kivalliq	32	Repulse Bay	Peridotite, road	66° 33' 03.4"	86° 16' 10.7"	Tiny	Lesser
Kivalliq	33	Repulse Bay	Merosarq, road	66° 33' 24.5"	86° 19' 34.8"	Tiny	Lesser
Kivalliq	34	Repulse Bay	Naujaat (Back Harbour)	66° 32' 03.0"	86° 11' 24.6"	Community	Lesser

jaat deposit. Results from 3 sites visited in collaboration with project partners are reported elsewhere (Steenkamp et al., 2014a, 2015; Figure 1 and Table 1, sites 17, 18 and 30).

Kitikmeot Region carving stone resources

In 2012, Kitikmeot Region community consultations brought forward 39 traditional carving stone sites (Beauregard, 2013b) and 2 additional sites were identified through literature review (Lahti, 1968; Gebert, 1990). The inland Aqituqtaqvik quarry near the Murchison River was identified as the sole long-term supplier of artisan serpentinite to carvers in the communities of Gjoa Haven, Kugaaruk and Taloyoak.

In 2013, 15 carving stone deposits were evaluated in the Kitikmeot Region (Beauregard, 2013a; Figure 1, Table 1). Also, new carving stone resources were confirmed in the vicinities of Cambridge Bay, Gjoa Haven, Kugaaruk and Kugluktuk. Taloyoak artists utilize carving stone from the Aqituqtaqvik quarry because a more local resource has not yet been identified. Assessed carving stone resources include relatively larger, lesser quality, artisan serpentinite deposits in the central and eastern Kitikmeot Region and smaller, generally higher quality, artisan marble deposits in the central and western Kitikmeot Region.

Gjoa Haven

The mainland area south of Gjoa Haven consists of Proterozoic supracrustal rocks and Archean supracrustal and plutonic rocks of the Rae Province (Hoffman and Hall, 1993). Strata of the Proterozoic Chantrey Group marble are preserved in a synform that extends from the west side of Chantrey Inlet to Darby Lake (Frisch, 1992). On the north limb of the synform, poorly exposed basal strata host white marble in a 2 m by 15 m inland site and light grey artisan marble

in a 0.5 m by 5 m site at Victoria Headland (Figure 1 and Table 1, sites 4 and 5, respectively). Both sites contain lesser quality, medium-hard to hard, fine-grained marble.

The Aqituqtaqvik artisan serpentinite quarry (Figure 1 and Table 1, site 1) lies within a discontinuous Archean amphibolite unit of the Rae Province that locally contains ultramafic schist and serpentinite (Ryan et al., 2008). Based on reported annual community requirements of 10 tons, 8 tons and 5 tons for Taloyoak, Gjoa Haven and Kugaaruk, respectively (Caine, 1977), an estimated total of 750 tonnes of carving stone has been supplied by the quarry since the 1970s.

The Aqituqtaqvik quarry occurs in a low-lying area and is not immediately obvious from the host peridotite that surrounds it. Artisan serpentinite is gathered from outcrop, subcrop and frost-heaved boulders in the quarry. The host peridotite is variably foliated, and locally contains 5 cm wide patches of white asbestiform tremolite in outcrop to the west and in frost-heaved boulders and subcrop to the east. Within 100 m to the north and east of the quarry are a number of small pits created by blasting during mineral exploration in the 1970s (Gebert, 1993) and shallow hand-dug pits from four decades of carving stone gathering.

High-quality carving stone is constrained to a 20 m by 10 m area with only three small outcrops exposed (Figure 2a). The outcrops are all about 2 m tall, aligned to the northwest and well worked. Stone is broken from these outcrops using the plugger-and-feather method (Figure 2b). The carving stone deposit can be divided into two sections based on artisan quality. A 20 m by 6 m zone of good- to excellent-quality, medium-soft black serpentinite is available in blocks up to 1 m^3 from outcrop, subcrop and frost-heaved boulders. A narrow northwest-trending fault separates this serpentinite from poor-quality peridotite to the southwest. The serpentinite grades into a less competent, fair-quality, medium to medium-hard black serpentinite with minor flakes and ro-

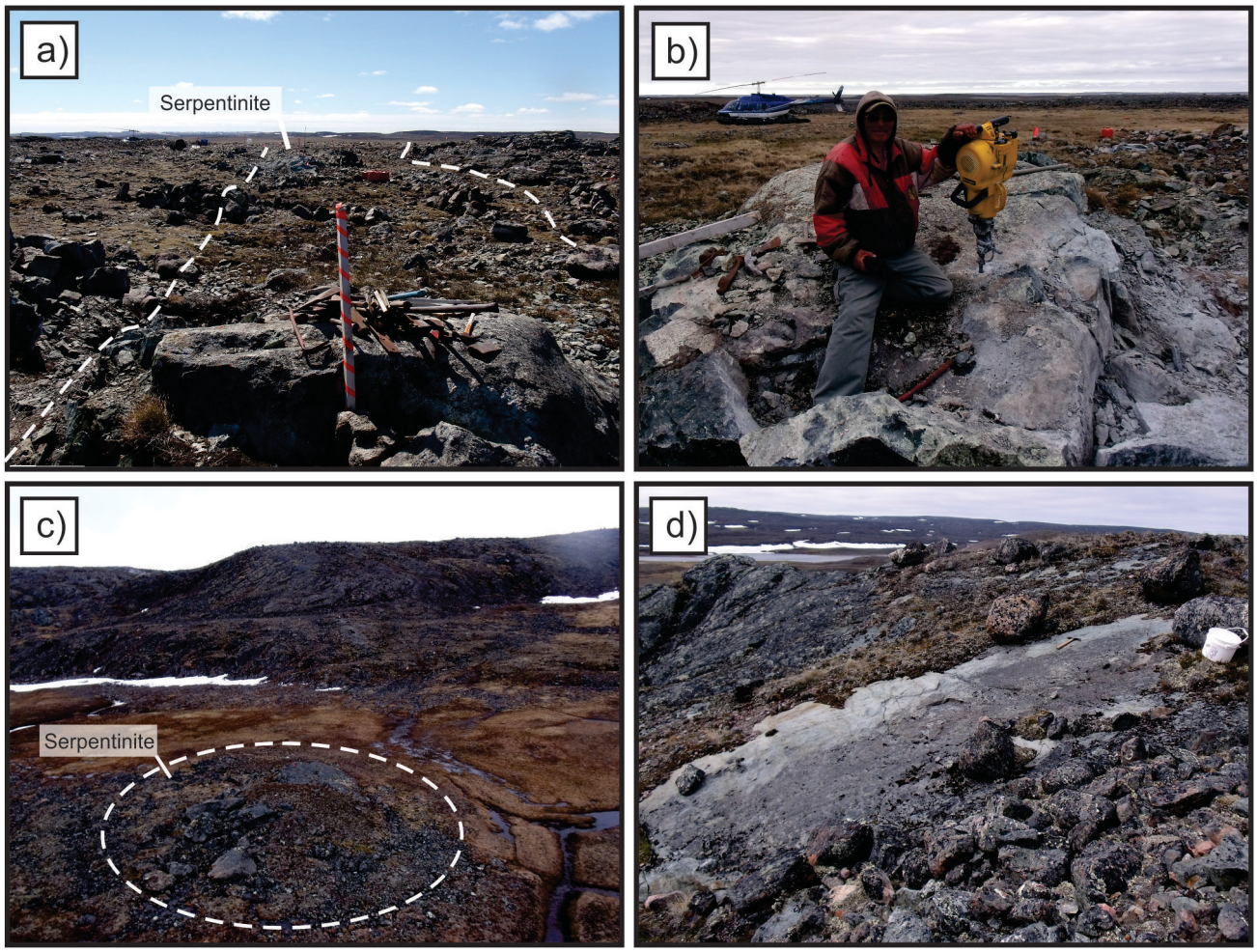

Figure 2: Eastern Kitikmeot Region carving stone sites: **a)** northwest-trending artisan serpentinite deposit at the Aqituqtaqvik quarry, defined by dashed white lines; flagged picket is 1.25 m high for scale; **b)** plugger-and-feather method of excavation used to extract blocks of stone (i.e., without blasting) from a well-worked carving stone outcrop at the Aqituqtaqvik quarry; **c)** aerial west-facing view of Kugaaruk's Kitingujaaq valley outcrop of black artisan serpentinite near Committee Bay; dashed white oval is 40 m across; **d)** Kugaaruk's Kitingujaaq hillside outcrop of green artisan serpentinite located approximately 400 m north of (c); east-facing view with 35 cm long hammer for scale.

settes of light green tremolite. This lower quality serpentinite occurs in a 20 m by 4 m zone as frost-heaved boulders and occasional subcrop along the northeastern portion of the deposit, and can be extracted in blocks up to 40 cm wide.

Kugaaruk

Kugaaruk's Kitingujaaq deposits (Figure 1 and Table 1, sites 2 and 3) occur within a serpentinized, 2 km long peridotite sill in tonalite, part of the Archean plutonic suite on the southwest coast of Committee Bay (Sandeman et al., 2004). Two separate outcrops, one of black serpentinite in the flat valley floor (site 3; Figure 2c) and the other of green serpentinite on a nearby hillside (site 2; Figure 2d), each contain ≥200 tonnes of medium-hard to hard, fair-quality stone. The serpentinite at both sites is fine grained, homogeneous and available in large blocks. Peridotite adjacent to carving stone outcrops is less altered to unaltered, and therefore non-artisan rock.

Taloyoak

The Taloyoak carving stone consultation brought forward eight traditional sites, half of which were poorly located or lacking guides. In 2013, the two nearest sites were visited but both were set aside as they do not host suitable material. Taloyoak remains impoverished for local carving stone.

Cambridge Bay

The mainland area south of Cambridge Bay consists of Proterozoic sedimentary rocks, and Archean supracrustal and plutonic rocks of the Slave Province (Hoffman and Hall, 1993). Five artisan serpentinite sites on the mainland were brought forward during consultations. Two of three sites visited were previously documented by regional and mineral-industry mapping campaigns in Archean mafic volcanic belts (Lahti, 1968; Gebert, 1990).

Six artisan marble sites in Kiluhiqtuq (formerly Bathurst Inlet) and Tariyunnuaq (formerly Melville Sound) were also brought forward during consultation. Two tiny artisan marble deposits (Figure 1 and Table 1, sites 12 and 13) have been identified in association with contact metamorphism between the Coronation diabase sills and dykes, part of the 723 Ma Franklin Magmatic Event (Shellnutt et al., 2004), and Helikian carbonate rocks (Campbell, 1978).

An artisan serpentinite deposit (Figure 1 and Table 1, site 7) occurs within a foliated peridotite sill found within the Hope Bay greenstone belt on a hilltop south of Amitturyuap Kuugaa (formerly the Kuugaarjuk River; Gebert, 1990; Sherlock et al., 2012). This inland deposit is exposed in a 20 m long by 8 m wide by 3 m high section near the eastern end of the peridotite sill (Figure 3a). The stone is dark green to black, medium-hard to hard, fair-quality artisan serpentinite. Blocks up to 1 m in length can be extracted using the plugger-and-feather method. A weak foliation may add inconsistency to the width of the material extracted.

A granite-intruded peridotite body (Figure 1 and Table 1, site 8) occurs on a small point in Kiluhiqtuq (formerly Bathurst Inlet; Figure 3b, c). Most of the medium-hard to hard serpentinized peridotite at this site is dark grey, coarse grained and equigranular. There is ≥200 tonnes of this fair-quality, competent stone that can be extracted in blocks up to 2 m^3 using the plugger-and-feather method. The softer, less competent, fine-grained serpentinite in the contact aureole adjacent to the granite intrusion is only used to create artifacts of simple form.

A peridotite sill (Figure 1 and Table 1, site 6) in the Hope Bay greenstone belt (Lahti, 1968) is exposed at tidewater and easily accessible by boat. Here, approximately 25 tonnes of high-quality artisan serpentinite occurs inside a brittle fault (Figure 3d). Despite high wastage due to the fractured nature of the rock, the site yields stone blocks up to 30 cm in length. Serpentinized peridotite adjacent to the fault is soft to medium soft, dark green and good quality.

Kugluktuk

The distinctive geomorphology of the mainland and islands in the Kugluktuk area is due to a series of Neoproterozoic Coronation sills intruding Proterozoic Rae Group sedimentary rocks from the upper Rae River, east to the Couper Islands and into the Coronation Gulf (Baragar and Donaldson, 1973a, b; Shellnutt et al., 2004). Archean supracrustal and plutonic rocks on the mainland between Kugluktuk and Kiluhiqtuq (formerly Bathurst Inlet) host two ultramafic deposits of lesser quality and several traditional carving stone sites yet to be visited.

A tidewater site (Figure 1 and Table 1, site 14) hosts a 75 m long band of ultramafic xenoliths in granodiorite. The peridotite xenoliths contain 200 kg to several tonnes of carving stone each, and are exposed in flat horizontal outcrops and vertical scarps. Evidence of minor drilling and blasting of some of the smaller, good-quality, medium-soft artisan serpentinite xenoliths was observed. The larger xenoliths are of fair quality and medium hardness. Extraction by the plugger-and-feather method is required at this site.

The inland Kugakyuak site (Figure 1 and Table 1, site 15) is a small peridotite intrusion that is hosted in orthogneiss and poorly exposed at the base of a Coronation sill scarp. This small quarry south of the Hanerok River was once utilized to gather fair-quality carving stone of medium hardness, in blocks up to 60 cm long. However, carvers have reported minor asbestiform tremolite in Kugakyuak stone.

Coronation diabase sills formed a number of small artisan marble sites where they intrude Proterozoic Rae Group carbonate rocks in the Kugluktuk area. Three artisan marble sites were visited in 2013.

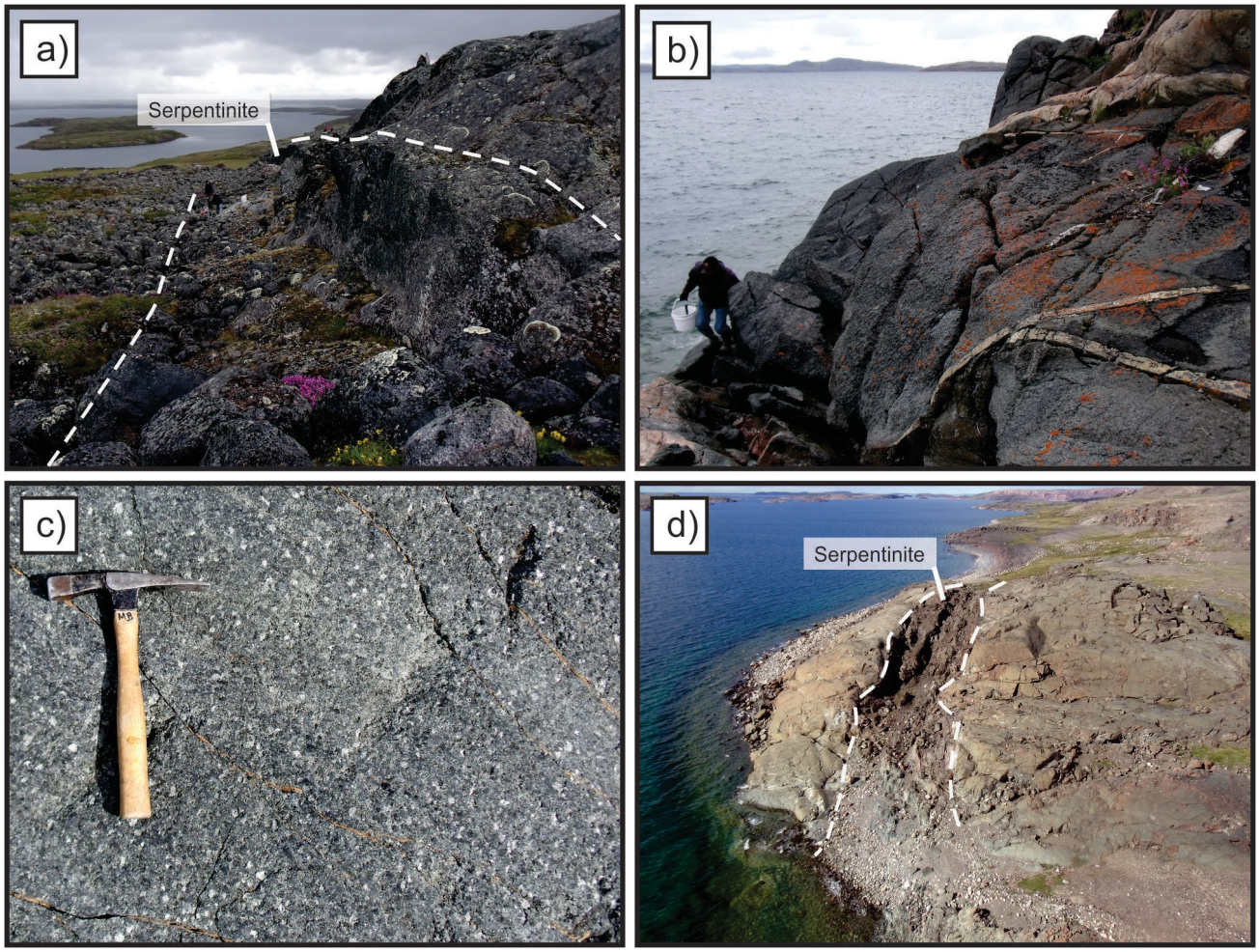

Figure 3: Central Kitikmeot Region carving stone sites near Cambridge Bay: **a)** east-trending artisan serpentinite at the Kuugaarjuk deposit (outlined by dashed white lines); **b)** granite-intruded peridotite on tidewater in Kiluhiqtuq (formerly Bathurst Inlet); **c)** detail of coarse-grained, equigranular peridotite shown in (b); 35 cm long hammer for scale; **d)** small site of high-quality artisan serpentinite site in faulted peridotite sill at which high wastage can be expected; 15 m wide fault zone is outlined by dashed white lines in north-facing aerial view.

The Palliq site (Figure 1 and Table 1, site 9) lies below a waterfall on the Rae River and is the preferred long-term quarry for Kugluktuk's carvers (Willoughby, 2002). A north-dipping Coronation sill overlies dolostone on the north bank of the river. On the south bank of the river, a 25 m long by 5 m wide by 2 m deep excavation of river sediments and flaggy dolostone allows for extraction of good-quality and variably coloured artisan dolostone layers (Figure 4a). An estimated 1500 tonnes of river bank sediment and waste rock have been excavated for the gathering of 250 tonnes of carving stone. Hand-excavated debris from the river-bank quarry is carried away by annual spring flooding (Figure 4b).

Fractured carbonate rocks appear to have increased competency and are lighter in colour, likely due to hydrothermal-fluid alteration in this region. This more competent, medium-hard to hard artisan marble is also gathered by carvers from Kugluktuk (Figure 1 and Table 1, sites 10 and 11). The Kakotalik quarry is the nearest deposit of such artisan marble to Kugluktuk (site 11; Figure 4c).

Belcher Islands carving stone resources

The Belcher Islands in southern Hudson Bay are a set of long, narrow islands underlain by a sequence of Proterozoic metasedimentary rocks framed between upper and lower flood basalt units (Jackson, 1960). A Proterozoic diabase sill formed artisan marble deposits by mafic-ultramafic contact alteration of the Proterozoic Belcher Group dolomite unit (Beauregard and Ell, 2013). Five excellent-quality carving stone deposits are found at the contact between diabase and dolomite on the east side of the Belcher Islands.

The Belcher Islands host Nunavut's second and fourth largest carving stone producers, the active Qullisajaniavvik quarry and the abandoned Aqituniavvik quarry, respec-

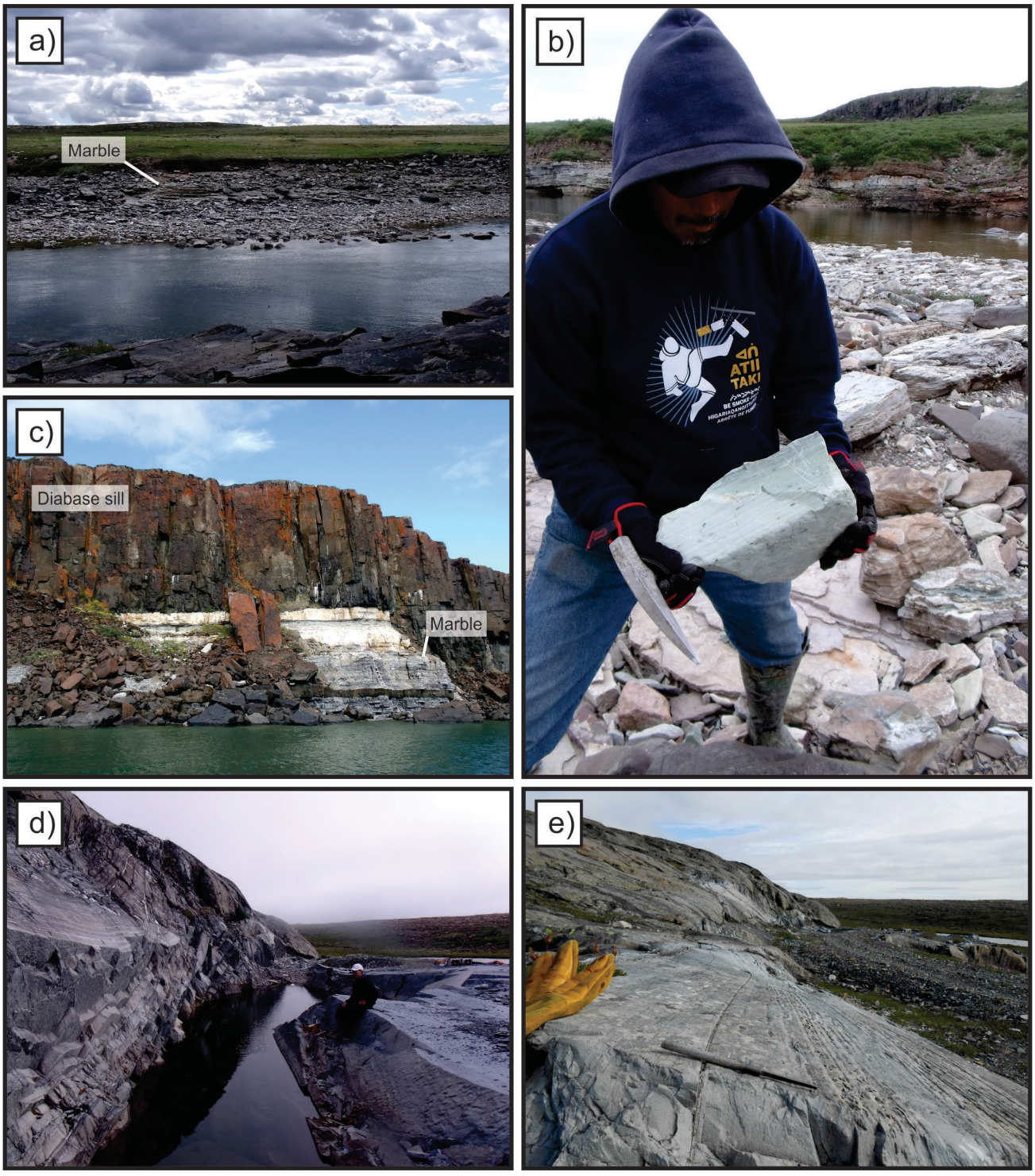

Figure 4: Western Kitikmeot Region and Belcher Islands carving stone sites: **a)** Kugluktuk's traditional Palliq artisan marble site on the south bank of the Rae River; field of view at water level is ~75 m; **b)** carver holding block of serpentinized artisan marble amongst debris from the Palliq quarry; Coronation sill extends from the top half of the north river bank to the ridge top in this north-facing view; **c)** Kugluktuk's Kakotalik white artisan marble quarry in a faulted section of altered dolomite beneath a Coronation sill is visible from the community; fallen basalt columns are ~12 m high in this north-facing view; **d)** Sanikiluaq's Qullisajaniavvik quarry in the Belcher Islands, in an open-folded structure of stratiform diabase sill above a wide zone of altered dolomite; steeply dipping beds to the left plus excavation plus flat black outcrop to the right constitute Nunavut's softest artisan marble in this north-facing view; **e)** 100+ m long and 10+ m wide extension of competent, soft artisan marble to the south of Sanikiluaq's community quarry, north-facing view.

tively (Figure 1 and Table 1, sites 24 and 25, respectively). In 2013, two quarries, two small deposits and one tiny deposit in the Belcher Islands were evaluated (Beauregard and Ell, 2013). In 2014, artisan suitability and reserves at the active community quarry were assessed, and an additional small deposit was identified.

The Qullisajaniavvik quarry has been in continuous use since the 1970s (Figure 4d). Excellent-quality artisan marble, locally referred to as 'argillite', is a competent, soft to medium-soft rock that Sanikiluaq carvers can shape and polish by hand. The deposit is well exposed, with only minor amounts of debris generated because most stone is suitable for carving. The quarry excavation is 83 m long, including a 23 m long water-filled section that is up to 8 m deep. Water is pumped out of the pit in order to access beds of the softer, light green to grey, banded artisan marble preferred by most carvers. Excavation must be initiated using the plugger-and-feather method and then followed up with hammer, chisel and pry bar. Carving stone is excavated during the summer from the steeply dipping beds that are typically less than 1 m thick. Stone is stockpiled at the quarry, or at a small harbour 1 km away, and transported the 65 km from Tukarak Island to Sanikiluaq by small boat during summer or by snowmobile during winter.

Sanikiluaq's Qullisajaniavvik quarry has reserves of at least 30 000 tonnes of artisan marble, which is double the total lifetime production of Cape Dorset's Kangiqsukutaaq quarry (Figure 1 and Table 1, site 30; Steenkamp et al., 2014a). Artisan marble extends for 100 m south of the quarry, so the reserve figure is based on deposit dimensions of 200 m long, 10 m wide and 10 m deep (Figure 4e).

Two small inland deposits at Salty Bill Hill on Tukarak Island (Figure 1 and Table 1, sites 26 and 27) contain at least 100 tonnes each of good-quality, medium-soft artisan marble. Another small tidewater deposit in the southern Belcher Islands (Figure 1 and Table 1, site 28) is of similar size and grade to those at Salty Bill Hill. A tiny site (Figure 1 and Table 1, site 29) with 0.2 m by 1 m blocks of medium-hard artisan marble occurs on the all-terrain vehicle (ATV) trail at Kasegalik Lake.

Repulse Bay carving stone resources

The Repulse Bay area is underlain by Archean gneiss and migmatite of the Rae Province (Heywood, 1967). Three lesser quality artisan serpentinite quarries (Figure 1 and Table 1, sites 31–33) are accessible by gravel road and ATV trail. The deposits consist of small, deformed, tabular peridotite bodies hosted in gneiss, each of which is approximately 10 m long by 2 m wide. The peridotite bodies have a 50 cm rim comprising mostly tremolite, and cores containing fair-quality artisan serpentinite with local trace amounts of asbestiform tremolite.

Repulse Bay's tidewater Naujaat deposit (Figure 1 and Table 1, site 34), located 2 km east of the community airport, was visited in 2011 (Beauregard and Ell, 2012). At this site, an east-trending serpentinized mafic-ultramafic dyke, which is 15 m wide and exposed for 60 m, constitutes fair-quality carving stone (see Figure 5a). The homogeneous, fine-grained serpentinized peridotite is medium grey and has a hardness of 3.0–3.5, thus requiring diamond tools for shaping.

Hall Peninsula carving stone resources

In 2014, three sites with potential carving stone, identified during regional bedrock-geology mapping outside of Iqaluit, were visited by the NCSDEP (Steenkamp et al, 2014b). The Leybourne Islands site (Figure 1 and Table 1, site 16) contains at least 25 000 tonnes of high-quality, medium-hard, dark green artisan serpentinite. It occurs as an altered ultramafic sill in Archean orthogneiss that was subsequently metamorphosed and deformed during the Trans-Hudson orogeny (Steenkamp and St-Onge, 2014). The carving stone outcrop measures 100 m long by 25 m wide by 8 m high, and is situated approximately 100 m up a steep hillside from tidewater (Figure 5b, c). The plugger-and-feather method could be applied here to extract very large blocks, as the stone is generally competent and homogeneous.

An altered ultramafic body (Figure 1 and Table 1, sites 19–21) associated with Paleoproterozoic Lake Harbour Group metasedimentary rocks was visited approximately 80 km west of Iqaluit (St-Onge et al., 1997). An outcrop on the west side of an eroded gully (Figure 5d) contains approximately 50 tonnes of excellent-quality, dark green artisan serpentinite, where blocks up to 30 cm wide could be accessed. Further work is warranted on the kilometre-wide ultramafic intrusion.

A 200 m wide river valley approximately 50 km east of Iqaluit exposes a 100 m thick marble unit that is part of a Paleoproterozoic metasedimentary rock package correlative with the Lake Harbour Group on southern Baffin Island (St-Onge et al., 2006). The marble is typically impure, containing medium-grained accessory minerals. Artisan marble is uncommon and restricted to tiny pods and seams at this site (Figure 1 and Table 1, sites 22 and 23).

Economic considerations

Carving stone in Nunavut is a long-term commodity with an estimated 500–800 tonnes of artisan serpentinite and marble gathered annually from an abundance of surface-accessible deposits. Seventeen of Nunavut's twenty-five communities have access to local carving stone resources adequate for their long-term needs.

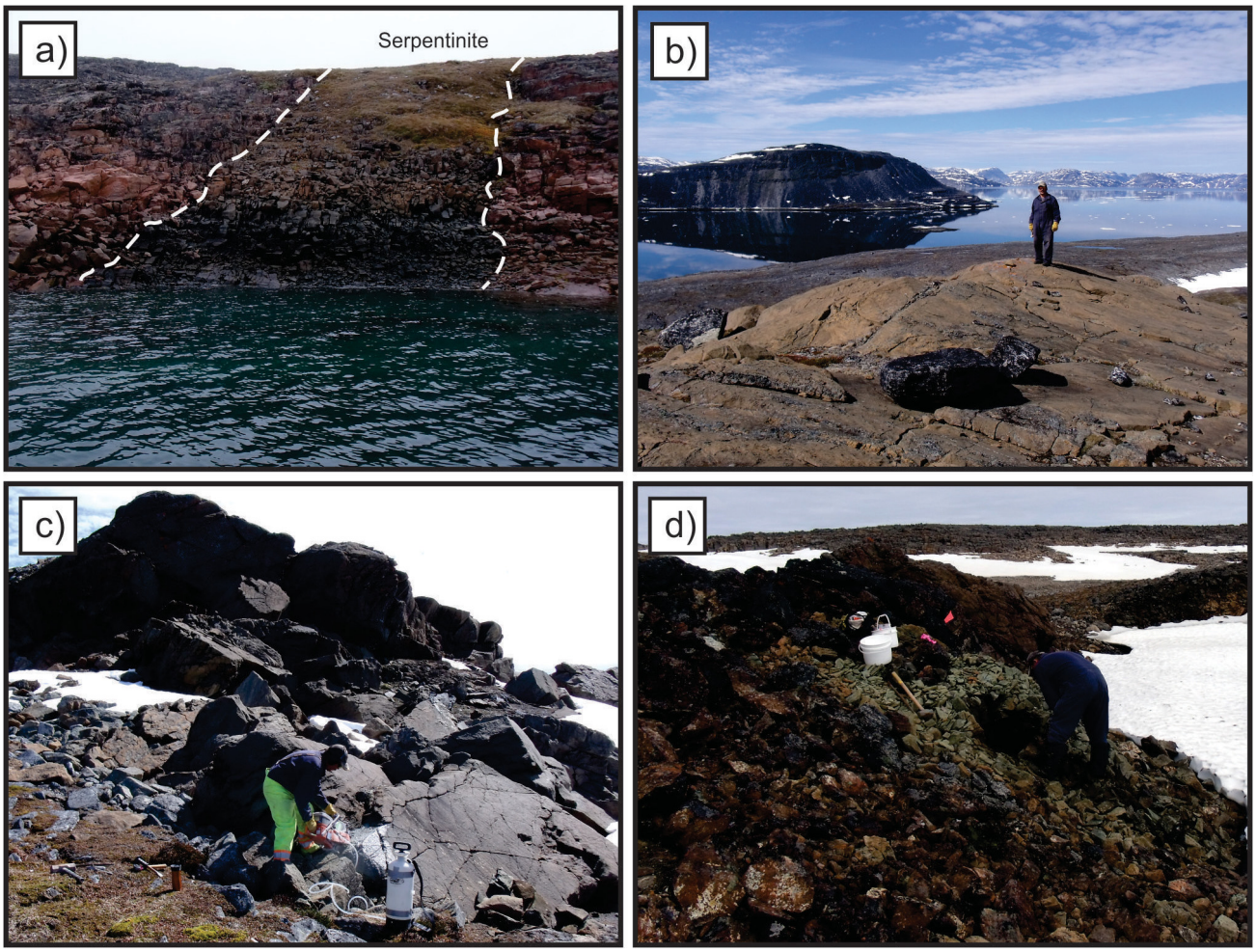

Figure 5: Repulse Bay and Hall Peninsula carving stone sites: **a)** Naujaat deposit is a fine-grained serpentinized mafic-ultramafic dyke directly across the bay east of Repulse Bay; 15 m wide dyke is outlined by dashed white lines in east-facing view; **b)** west-facing view atop the 25 000 tonne resource of artisan serpentinite in the Leybourne Islands, southern Baffin Island, **c)** east-facing view of high-quality artisan serpentinite deposit in the Leybourne Islands; **d)** 50 tonne deposit of high-quality artisan serpentinite in the northwest corner of a 1 km wide ultramafic intrusion located 80 km west of Iqaluit.

The NCSDEP completed evaluations at 31 traditional and new carving stone sites (with 3 sites reported elsewhere) in 2013 and 2014 across the Kitikmeot Region, in the Belcher Islands, and near Repulse Bay and Iqaluit. The Aqituqtaqvik quarry near Murchison River has provided the eastern Kitikmeot Region with up to 750 tonnes of artisan serpentinite since the 1970s and has an estimated 500 tonnes of remaining reserves. The Qullisajaniavvik quarry near Sanikiluaq has also been producing since the 1970s and contains reserves of at least 30 000 tonnes of excellent-quality artisan marble. Repulse Bay carvers have access to several small artisan serpentinite sites near the hamlet. The tidewater Naujaat deposit is still in need of further assessment. A new carving stone deposit with enough reserves to serve a region is confirmed in the Leybourne Islands on the southern shore of Cumberland Sound, with Pangnirtung and Iqaluit being the nearest communities.

Conclusions

The field observations, deposit descriptions and carving stone evaluations in this report document the final sites from a four-year territorial survey conducted by the NCSDEP. At this juncture, the program has visited and documented a total of 94 carving stone sites in the vicinity of 23 communities across Nunavut. Nunavut's carving stone supply currently stands at ten communities with access to substantial resources sufficient for at least four decades of production, seven communities with access to historical or newly augmented carving stone resources sufficient for at least one decade of production, and eight communities with insufficient local resources.

The NCSDEP may conduct follow-up visits at some sites that require further evaluation or comprehensive bedrock mapping, and continue exploration and literature review on

behalf of carving stone–impoverished communities. In the coming year, the program will also focus on geochemical analysis and petrographic characterization of collected samples.

Acknowledgments

The authors thank project carvers Uriash Puqiqnak of Gjoa Haven and Bobby Anavilok of Kugluktuk for carving stone expertise, translation services and logistics during the summer of 2013. Thanks also go to full-time carvers Jaco Ishulutaq of Pangnirtung, Jimmy Iqaluq Senior of Sanikiluaq and Paul Malliki of Repulse Bay for guidance, carving stone expertise, camping, country food, and boat and ATV use. The authors gratefully acknowledge the services provided by Alex Buchan, Joseph Kiyok and Clarence Klengenberg of Cambridge Bay; elder Paul Eliheetooq, Simon Hiqiniq, Paul Kammalik, Ben Putuguk and former Community Economic Development Officer (CEDO) Joseph Aglukkaq of Gjoa Haven; Levi Illuitok, Bartholomew Nirlungayuk, Emiliano Qirnqua, Alina Tungilik and CEDO Beatrix Apsaktaun of Kugaaruk; Robert Anablak, Roger Hilolok, Charlie Klengenberg and elder Joseph Niptanatiak of Kugluktuk; Jack Iqaluq, Ippak Iqaluk and former CEDO Daryl Dibblee of Sanikiluaq; and elder Simon Oleekatalik and CEDO Rosie Tucktoo of Taloyoak. Finally, thanks go to the Polar Continental Shelf Program and Universal Helicopters for safe and efficient air transportation. Financial support for this study was provided by the Canadian Northern Economic Development Agency's (CanNor) Strategic Investments in Northern Economic Development (SINED) program. A review by H. Steenkamp improved the clarity and content of this manuscript and is greatly appreciated.

References

Baragar, W.R.A. and Donaldson, J.A. 1973a: Geology, Coppermine, District of Mackenzie; Geological Survey of Canada, Map 1337A, scale 1:250 000, URL <http://geoscan.nrcan.gc.ca/starweb/geoscan/servlet.starweb?path=geoscan/downloade.web&search1=R=108895> [October 2014].

Baragar, W.R.A. and Donaldson, J.A. 1973b: Geology, Dismal Lakes, District of Mackenzie; Geological Survey of Canada, Map 1338A, scale 1:250 000, URL <http://geoscan.nrcan.gc.ca/starweb/geoscan/servlet.starweb?path=geoscan/downloade.web&search1=R=108896> [October 2014].

Beauregard, M. and Ell, J. 2012: 2010–2012 carving stone results in Kivalliq Region, Nunavut; Mineral and Petroleum Resources, Economic Development and Transportation, Government of Nunavut, unpublished report prepared for hamlets, regional Inuit associations and government agencies, 55 p.

Beauregard, M. 2013a: Artisan carving stone results – new results for Nunavut's arts industry from 2010–2013 Nunavut Carving Stone Deposit Evaluation Program; presentation at 2013 Nunavut Mining Symposium, 36 p, URL <http://2013.nunavutminingsymposium.ca/wp-content/uploads/2013/04/9-Beauregard-GNEDT.pdf> [November 2014].

Beauregard, M. 2013b: Cambridge Bay, Gjoa Haven, Kugaaruk, Kugluktuk and Taloyoak community carving stone consultations integrated with fieldwork results, Kitikmeot Region, Nunavut; Mineral and Petroleum Resources, Economic Development and Transportation, Government of Nunavut, unpublished report prepared for hamlets, regional Inuit associations and government agencies, 25 p.

Beauregard, M. and Ell, J. 2013: 2013 Carving stone results in Qikitaaluk (Baffin) Region, Nunavut; Mineral and Petroleum Resources, Economic Development and Transportation, Government of Nunavut, unpublished report prepared for hamlets, regional Inuit associations and government agencies, 43 p.

Beauregard, M., Ell, J., Pikor, R.K. and Ham, L.J. 2013: Nunavut Carving Stone Evaluation Program (2010–2013): third year results; *in* Canada-Nunavut Geoscience Office Summary of Activities 2012; Canada Nunavut Geoscience Office, p. 151–162.

Caine, T.W. 1977: Carving stone communities of the Northwest Territories: 1977 requirements, sources of supply and problems; unpublished report prepared by Indian and Northern Affairs Canada, Mining Section, 39 p.

Campbell, F.H.A. 1978: Geology of the Helikian rocks of the Bathurst Inlet area, Coronation Gulf, Northwest Territories; *in* Current Research, Part A, Geological Survey of Canada, Paper 78-1A, p. 97–106.

Frisch, T. 1992: Geology, Cape Barclay and part of Darby Lake, Nunavut; Geological Survey of Canada, Map 1779A, scale 1:250 000, URL <http://geoscan.nrcan.gc.ca/starweb/geoscan/servlet.starweb?path=geoscan/downloade.web&search1=R=183919> [October 2014].

Gebert, J. 1990: Preliminary geology of the Elu Inlet metavolcanic belt, north, central, and southern sheets, parts of NTS 77A/2, 7, 10; *in* Economic Geology Series (EGS) 1990-20, Indian and Northern Affairs Canada, Northwest Territories Geology Division, Yellowknife, scale 1:50 000.

Gebert, J. 1993: Lapidary and soapstone east of Chantry Inlet, Northwest Territories; *in* Economic Geology Series (EGS) 1993-02, Indian and Northern Affairs Canada, Northwest Territories Geology Division, Yellowknife, 20 p.

Government of Canada 1993 (amendments up to and including 2009): Agreement between the Inuit of the Nunavut Settlement Area and Her Majesty the Queen in right of Canada (Nunavut Land Claims Act); Indian and Northern Affairs Canada, Article 19 (Title to Inuit Owned Lands), Part 9 (Rights to Carving Stone), p. 149–150.

Heywood, W.W. 1967: Geology, northeastern District of Keewatin and southern Melville Province; Geological Survey of Canada, Preliminary Map 14-1966, scale 1:506 880, URL <http://geoscan.nrcan.gc.ca/starweb/geoscan/servlet.starweb?path=geoscan/downloade.web&search1=R=108488> [October 2014].

Hoffman, P. and Hall, L. 1993: Geology, Slave craton and environs, District of Mackenzie, Northwest Territories; Geological Survey of Canada, Open File 2559, scale 1:1 000 000, URL <http://geoscan.nrcan.gc.ca/starweb/geoscan/servlet.starweb?path=geoscan/downloade.web&search1=R=183951> [October 2014].

Jackson, G.D. 1960: Belcher Islands, Northwest Territories, 33M, 34D, E (report and Map 28-1960); Geological Survey of Canada, Paper 60-20, 13 p., and 1 map at 1:126 720 scale,

URL <http://geoscan.nrcan.gc.ca/starweb/geoscan/servlet.starweb?path=geoscan/downloade.web&search1=R=101205> [November 2014].

Lahti, W.I. 1968: Melville Bay prospecting report; Indian and Northern Affairs Canada, Northwest Territories Mining Recorder's Office, Yellowknife, Assessment Report 015317, scale 1:63 360.

Nunavut Department of Economic Development and Transportation 2007a: Ukkusiksaqtarvik – *The Place Where We Find Stone*: carving stone supply action plan; Nunavut Department of Economic Development and Transportation, URL <http://www.gov.nu.ca/sites/default/files/carving_stone_action_plan_english.pdf> [October 2014].

Nunavut Department of Economic Development and Transportation, 2007b: Sanujgait: a strategy for growth in Nunavut's arts and crafts sector; Nunavut Department of Economic Development and Transportation, URL <http://www.gov.nu.ca/sites/default/files/Sanaugait_arts_strategy.pdf> [October 2014].

Ryan, J.J., Nadeau, L., Hinchey, A.M., James, D.T., Young, M.D., Williams, S.P. and Schetselaar, E.M. 2008: Geology, southern Boothia mainland area, Pelly Bay–Rae Strait–Harrison Island map area, Nunavut; Geological Survey of Canada, Open File 5808, scale 1:250 000, URL <http://geoscan.nrcan.gc.ca/starweb/geoscan/servlet.starweb?path=geoscan/downloade.web&search1=R=225401> [October 2014].

Sandeman, H., Skulski, T. and Sanborn-Barrie, M. 2004: Geology, Ellice Hills, Nunavut; Geological Survey of Canada, Open File 1794, sheet 2 of 2, scale 1:100 000, URL <http://geoscan.nrcan.gc.ca/starweb/geoscan/servlet.starweb?path=geoscan/downloade.web&search1=R=215703> [October 2014].

Shellnutt, J.G., Dostal, J. and Keppie, J.D. 2004: Petrogenesis of the 723 Ma Coronation sills, Amundsen Basin, Arctic Canada; Precambrian Research, v. 129, no. 3–4, p. 309–324.

Sherlock, R.L., Shannon, A., Hebel, M., Lindsay, D., Madsen, J., Sandeman, H., Hrabi, B., Mortensen, J.K., Tosdal, R.M. and Freidman, R. 2012: Volcanic stratigraphy, geochronology, and gold deposits of the Archean Hope Bay Greenstone Belt, Nunavut, Canada; Economic Geology, v. 107, p. 991–1042, doi:10.2113/econgeo.107.5.991

Steenkamp, H.M. and St-Onge, M.R. 2014; Overview of the 2013 regional bedrock mapping program on northern Hall Peninsula, Baffin Island, Nunavut; *in* Summary of Activities 2013, Canada-Nunavut Geoscience Office, p. 27–38.

Steenkamp, H.M., Pizzo-Lyall, M., Wallace, C.J., Beauregard, M.A. and Dyck, B.J. 2014a; Geology, history and site-management planning of the Kangiqsukutaaq carving stone quarry, southern Baffin Island, Nunavut; *in* Summary of Activities 2013, Canada-Nunavut Geoscience Office, p. 193–200.

Steenkamp, H.M., Bros, E.R. and St-Onge, M.R. 2014b; Altered ultramafic and layered mafic-ultramafic intrusions: new economic and carving stone potential on northern Hall Peninsula, Baffin Island, Nunavut; *in* Summary of Activities 2013, Canada-Nunavut Geoscience Office, p. 11–20.

Steenkamp, H.M., Beauregard, M.A. and Mate, D.J. 2015: Carving stone and mineral resource potential of the Opingivik deposit, southern Baffin Island, Nunavut; *in* Summary of Activities 2014, Canada-Nunavut Geoscience Office, p. 153–162.

St-Onge, M.R., Hamner, S., Scott, D.J. and Wodicka, N. 1997: Geology, Blandford Bay, Nunavut; Geological Survey of Canada, Open File 3398, scale 1:100 000, URL <http://geoscan.nrcan.gc.ca/starweb/geoscan/servlet.starweb?path=geoscan/downloade.web&search1=R=210838> [October 2014].

St-Onge, M.R., Jackson, J.D. and Henderson, L. 2006: Geology, Baffin Island (south of 70°N and east of 80°W), Nunavut; Geological Survey of Canada, Open File 4931, scale 1:500 000, URL <http://geoscan.nrcan.gc.ca/starweb/geoscan/servlet.starweb?path=geoscan/downloade.web&search1=R=222520> [October 2014].

Willoughby, N. 2002: Visit to Palliq soapstone site, Rae River at White Falls; unpublished report prepared for Hamlet of Kugluktuk by Nunavut Department of Sustainable Development, 4 p.

Greenland and Nunavut Geoscience Workshop 2014, Nuuk, Greenland

K. Thorsøe[1], D.J. Mate[2] and M.D. Poulsen[3]

[1]*Geological Survey of Denmark and Greenland, Nuuk Office, Greenland, kit@geus.dk*

[2]*Canadian Northern Economic Development Agency, Iqaluit, Nunavut (formerly Canada-Nunavut Geoscience Office, Iqaluit, Nunavut)*

[3]*Geological Survey of Denmark and Greenland, Nuuk Office, Greenland*

Thorsøe, K., Mate, D.J. and Poulsen, M.D. 2015: Greenland and Nunavut Geoscience Workshop 2014, Nuuk, Greenland; *in* Summary of Activities 2014, Canada-Nunavut Geoscience Office, p. 175–190.

Hanghøj, J. and Kolb, J. 2015: Metallogeny of Greenland (abstract A16), *from* Greenland and Nunavut Geoscience Workshop 2014, Nuuk, Greenland, K. Thorsøe, D.J. Mate and M.D, Poulsen (comp.); *in* Summary of Activities 2014, Canada-Nunavut Geoscience Office, p. 184.

Abstract

The Geological Survey of Denmark and Greenland (GEUS) and the Canada-Nunavut Geoscience Office (CNGO) recently held a workshop in Nuuk, Greenland focused on exchanging information about mineral and petroleum resources and discussing geoscience questions common to both jurisdictions. This workshop included participants from the CNGO, Government of Nunavut Department of Economic Development and Transportation, Aboriginal Affairs and Northern Development Canada, the Geological Survey of Canada, Government of Greenland Ministry of Industry and Mineral Resources, and GEUS. Valuable perspectives were also shared by both Greenland and Nunavut on the value of geological surveys as important institutions for managing natural resources. The workshop consisted of 23 presentations and a field trip in Godthåbsfjord.

Discussions during the workshop confirmed that increased collaboration between Greenland and Nunavut could help solve a range of geoscience-related questions and help build competencies on both sides of Baffin Bay. Important scientific outcomes of increased collaboration would include better understanding of the oil and gas resource potential, tectonics and mineral occurrences in the area. Specific outcomes linked to this goal include: 1) having staff exchanges between the two jurisdictions; 2) exchanging information regarding the establishment and operation of geological survey offices and local capacity building; 3) meeting annually during the Prospectors and Developers Association of Canada (PDAC) conference in Toronto; and 4) co-ordinating another similar workshop in Nunavut in 2 to 3 years.

Résumé

Le Service géologique du Danemark et du Groenland (GEUS) et le Bureau géoscientifique Canada-Nunavut ont récemment tenu un atelier à Nuuk, au Groenland, dans le cadre duquel l'accent a été mis sur des échanges d'information au sujet des ressources minérales et pétrolières et sur des discussions relatives à des questions d'ordre géoscientifique touchant les deux compétences. Des représentants du ministère du Développement économique et des Transport du gouvernement du Nunavut, d'Affaires autochtones et Développement du Nord Canada, de la Commission géologique du Canada, du ministère de l'Industrie et des Ressources minérales du gouvernement du Groenland et de la GEUS ont aussi pris part à cet atelier. Il s'est également agi pour le Groenland et le Nunavut d'une occasion de faire valoir leurs points de vue respectifs au sujet de la pertinence d'organismes tels les levés scientifiques en tant qu'institutions qui jouent un rôle important dans la gestion des ressources naturelles. Vingt-trois présentations ont été faites à cet atelier auquel est venu s'ajouter une excursion à Godthåbsfjord.

Les discussions qui ont eu lieu au cours de l'atelier ont permis d'établir que des efforts de collaboration accrue entre le Groenland et le Nunavut pourraient contribuer à résoudre toute une gamme de questions de nature géoscientifique et pourrait également contribuer à renforcer les compétences des deux côtés de la baie de Baffin. D'importantes réalisations scientifiques pourraient découler de cette collaboration, y compris une meilleure compréhension du potentiel en ressources

This publication is also available, free of charge, as colour digital files in Adobe Acrobat® PDF format from the Canada-Nunavut Geoscience Office website: http://cngo.ca/summary-of-activities/2014/.

pétrolières et gazières, de la tectonique et des venues minérales de la région. Parmi les réalisations spécifiques susceptibles d'aider à atteindre cet objectif, on note 1) l'échange de personnel entre les deux compétences; 2) l'échange d'information au sujet de l'établissement et du fonctionnement de bureaux relevant des services géologiques et le renforcement des capacités locales; 3) la tenue d'une rencontre annuelle prévue à l'occasion du congrès de la *Prospectors and Developers Association of Canada* à Toronto; et 4) la tenue d'un atelier semblable à Nunavut dans 2 à 3 ans.

Introduction

This paper provides a summary of a recent workshop for geoscience staff from Greenland and Nunavut that focused on exchanging information about geology and mineral resources and also on discussing geoscience questions affecting both sides of Baffin Bay. Topics related to petroleum resources were discussed more briefly, and a more thorough discussion could be a suitable topic for a future workshop. The workshop was a valuable professional development opportunity for geoscience staff from both jurisdictions and helped develop a collaborative dialogue between Nunavut, Greenland, Denmark and Canada. Natural resource management in the Arctic, and geoscience training and capacity building activities were also discussed. In addition, valuable perspectives were shared on how both Greenland and Nunavut view geological surveys as institutions that support natural resource management. The workshop was co-organized by the Canada-Nunavut Geoscience Office (CNGO) in Iqaluit and the Geological Survey of Denmark and Greenland (GEUS) branch office in Nuuk.

Geology of Greenland

Greenland is the largest island on Earth, comprising a total area of 2 166 000 km^2 of which 410 000 km^2 are ice-free. The geological history of Greenland spans more than 3800 m.y. and represents a large variety of geological environments. The oldest areas constitute a basement shield composed mainly of deformed gneissic rocks representing root zones of Archean and Proterozoic orogenic belts. These belts are welded together to form a stable coherent block of which the North Atlantic craton and the Rae craton constitute two main components. Two prominent Proterozoic orogens, the Ellesmere–Inglefield mobile belt in North Greenland and the Makkovik–Ketilidian Orogen in South Greenland can be correlated to eastern Canada. Sedimentary basins developed adjacent to the basement shield during the following three time periods: 1) from the Meso- to Neoproterozoic, 2) from the Cambrian to Silurian, and 3) from the Devonian to Neogene. In the early Paleozoic, two distinct coast-parallel mountain belts formed: the Caledonian Orogen in North-East Greenland, and the Ellesmerian Orogen in North Greenland. Paleogene volcanic rocks related to the opening of the North Atlantic are represented as a flood basalt province in West and East Greenland. A geological map of Greenland is presented in Figure 1.

Geology of Nunavut

Nunavut is a vast territory, comprising almost a quarter of Canada, and its geology and natural resource potential are diverse. Geological provinces within Nunavut include the Churchill, Slave and Bear along with the Arctic Platform and Hudson Bay Lowlands. Several major tectonic events occurred in the past and include the Wopmay, Thelon, Trans-Hudson and Innuitian orogenies. Archean rocks are exposed throughout Nunavut and are characterized by granite-greenstone terranes. Siliciclastic rocks are common throughout, and Proterozoic and Phanerozoic rocks cover approximately one-third of Nunavut. A simplified geological map of Nunavut can be seen in Figure 2.

The landscape of Nunavut has been modified by past glaciations. During the last glaciation (Wisconsinan) the Laurentide Ice Sheet covered most of Nunavut with the thickest accumulation of ice centred over western Hudson Bay. The resulting erosion and deposition of glacial sediments has resulted in numerous aggregate deposits as well as the burial of mineral deposits and dispersal of their indicator minerals. Therefore, drift prospecting has now become an important exploration tool for large regions of the territory. Knowledge of permafrost, coastal sensitivity and marine geology are also becoming critical for infrastructure, resource and community development.

Workshop program and participants

This workshop was held in Nuuk, the capital of Greenland, from September 9 to September 11, 2014. It was hosted by GEUS at the Greenland Institute of Natural Resources. The program included two full days of presentations (Table 1). In total, 23 different presentations were given on a diverse range of topics including mineral exploration overviews of both jurisdictions; ruby discoveries in Greenland; Paleozoic xenoliths from kimberlite pipes on southern Hall Peninsula and implications for the petroleum potential in Baffin Bay; and the national mineral hunt in Greenland. On September 11 a geological field trip was taken in Godthåbsfjord.

Ten participants from Canada including eight from Nunavut, seven from Greenland and four from Denmark attended the workshop (Figure 3). Canadian participants represented the CNGO, Government of Nunavut Department of Economic Development and Transportation (GN), Aboriginal Affairs and Northern Development Canada

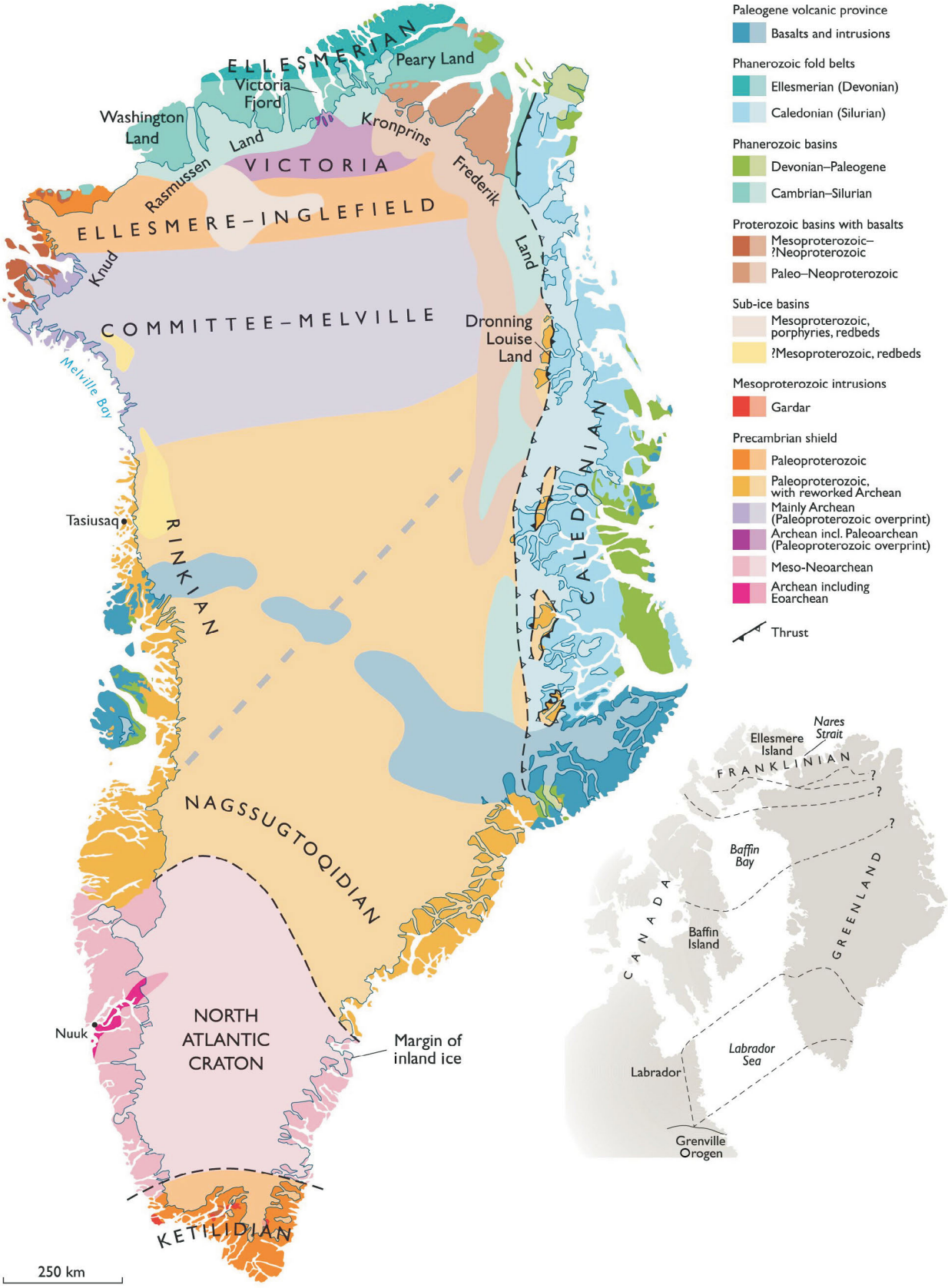

Figure 1: Geological map of Greenland with interpretation of sub-ice bedrock in terms of major provinces. Insert shows Canadian-Greenland correlations in the Precambrian shield (from Henriksen, 2008).

Figure 2: Geological map of Nunavut simplified from Harrison et al. (2011). Only areas in Nunavut north of 60°N are shown on this map.

(AANDC), and the Geological Survey of Canada (GSC). Four participants from Denmark represented GEUS, while seven participants from Greenland represented the Government of Greenland Ministry of Industry and Mineral Resources (MIM) and the GEUS branch office in Nuuk.

Program Abstracts

Abstract summaries for all presentations are provided below in chronological order. Please refer to Table 1 for the presenters name, title and organization.

GEUS in Greenland (A1)

The overall mission of GEUS is to provide, use and disseminate geoscience knowledge that is important for the use and protection of geological resources in Denmark and Greenland. Part of this mission is to support the governments of Denmark and Greenland, by providing state-of-the-art geoscientific knowledge of international standard. The activities of the geological survey are organized into five main program areas:

- data banks, information technology, and information for the general public
- water resources
- energy resources
- mineral resources and Greenland mapping
- nature and climate

Some of the core activities for GEUS are to assist Greenland in developing a sustainable mineral industry by collecting and providing basic geological data for Greenland, as well as to provide specific advice to government institutions and to the mineral and oil exploration industry about the geology of Greenland. To make GEUS activities more available to the people of Greenland and to help facilitate

Table 1: Titles of presentations and the names of presenters at the Greenland-Nunavut workshop.

Abstract	Presentation (September 9, 2014)[1]	Presenter
A1	GEUS in Greenland	K. Hanghøj, Head of Department, GEUS Copenhagen
A2	Canada-Nunavut Geoscience Office: an evolving Arctic geological survey	D. Mate, Chief Geologist, CNGO
A3	Nunavut mining and resource potential: 2014–2015 status update	L. Ham, Director, GN
A4	Status on mineral exploration in Greenland	A. Juul-Nielsen, Senior Geologist, MIM
A5	Mineral exploration in Nunavut	K. Costello, Director, AANDC
A6	Uranium exploration in Greenland	J. Petersen, Mineral Geologist, MIM
A7	The mid-Proterozoic Gardar Province, South Greenland: geology and rare-earth element potential	A. Bartels, Economic Geologist, GEUS Copenhagen
A8	A geomorphological transect across eastern Nunavut	T. Tremblay, Research Scientist, CNGO
A9	**S**outh-**E**ast **G**reenland **M**ineral **EN**dowment **T**ask (SEGMENT)	M.D. Poulsen, GEUS Nuuk Co-author: B.M. Stensgaard, GEUS Copenhagen
A10	Nunavut's soapstone: defining the supply for the community commodity of Arctic Canada	M. Beauregard, Resident Geologist, GN
A11	Greenlandic rubies	M.D. Poulsen, Mineral Geologist, GEUS Nuuk Co-author: N.T. Keulen, GEUS Copenhagen
A12	Ujarassiorit: the national mineral hunt	J. Petersen, Mineral Geologist, MIM
A13	Nunavut community outreach and engagement	R. Suluk, Manager, GN
Abstract	**Presentation (September 10, 2014)[1]**	**Presenter**
A14	Geology of Greenland	T.F. Kokfelt, Senior Researcher, GEUS Copenhagen
A15	Correlation of geological events across Davis Strait: broadening implications of GEM geoscience through international collaboration	M. Sanborn-Barrie, Research Scientist, GSC Ottawa Co-authors: K. Thrane, GEUS Copenhagen; N. Rayner, GSC Ottawa; N. Wodicka, GSC Ottawa; and J. Connelly, Natural History Museum of Denmark
A16	Metallogeny of Greenland	K. Hanghøj, Head of Department, GEUS Copenhagen Co-author: J. Kolb, GEUS Copenhagen
A17	Metallogeny of the Rae Province and its link to Nuna supercontinent assembly: implications for Nunavut and western Greenland	S. Pehrsson, Bedrock Geologist, GSC Ottawa Co-authors: C. Jefferson, R. Berman and E. Potter, GSC Ottawa
A18	Nickel potential of Greenland	T.F. Kokfelt, Senior Researcher, GEUS Copenhagen Co-authors: B.M. Stensgaard, L.L. Sørensen and D. Rosa, GEUS Copenhagen
A19	Bedrock geology and economic potential of Hall and Meta Incognita peninsulas on southern Baffin Island, Nunavut	H. Steenkamp, Regional Bedrock Scientist, CNGO
A20	Mississippi Valley–type Zn-Pb mineralization of North Greenland	K. Hanghøj, Head of Department, GEUS Copenhagen Co-authors: D. Rosa, GEUS Copenhagen; J.A. Rasmussen, Natural History Museum of Denmark; E.W. Sørensen, P. Kalvig and K. Hanghøj, GEUS Copenhagen
A21	Onshore oil and gas exploration in Greenland: a review	K. Grube Jakobsen, Petroleum Geologist, MIM; J.S. Adolfssen, Petroleum Geologist, MIM
A22	Sediment source fingerprint and basement characteristics	C. Knudsen, Chief Consultant, GEUS Copenhagen
A23	The discovery of an organic-rich black shale xenolith from kimberlite on Hall Peninsula, Nunavut: implications for petroleum potential in Cumberland Sound	S. Zhang, Research Scientist, CNGO

[1]Workshop participants not giving presentations: H. Heide-Jørgensen, Mineral Geologist, MIM; K. Thorsøe, Chief Consultant, GEUS Nuuk.
Abbreviations: AANDC, Aboriginal Affairs and Northern Development Canada; CNGO, Canada-Nunavut Geoscience Office; GEUS, Geological Survey of Denmark and Greenland; GN, Government of Nunavut, Department of Economic Development and Transportation; GSC, Geological Survey of Canada; MIM, Government of Greenland, Ministry of Industry and Mineral Resources.

capacity building and public outreach in Greenland, a GEUS branch office was opened in Nuuk in 2013. The office assists the Greenlandic administration, public and companies with geological advice and scientific knowledge about mineral resources, energy resources and climate.

Canada-Nunavut Geoscience Office: an evolving Arctic geological survey (A2)

The Canada-Nunavut Geoscience Office (CNGO) is formally co-managed by the Government of Nunavut (GN), Natural Resources Canada (NRCan), and Aboriginal Af-

Figure 3: Participants at the workshop held at the Greenland Institute of Natural Resources. Bottom from left: D.J. Mate, M. Sanborn-Barrie, M.D. Poulsen, L. Ham, S. Pehrsson. In the middle from left: K. Costello, H. Steenkamp, K. Thorsøe, A. Juul-Nielsen, K. Hanghøj, T. Tremblay, J. Petersen. In the rear from left: R. Suluk, M. Beauregard, S. Zhang, A. Bartels, C. Knudsen and T.F. Kokfelt.

fairs and Northern Development Canada (AANDC). Nunavut Tunngavik Inc., which represents the Inuit of Nunavut, also sits on the management board as a nonvoting member. The mandate of the office is to provide Nunavut with accessible geoscience information and expertise to support 1) responsible resource exploration and development, 2) responsible infrastructure development, and 3) geoscience capacity building and outreach. The office delivers a diverse suite of activities in collaboration with universities, industry and other government organizations, including NRCan's Geo-mapping for Energy and Minerals (GEM) program.

Sustainable development in Nunavut will likely involve the responsible development of natural resources in order to invest in the territory and develop human capital with the aim to evolve beyond a reliance on resource development. In this context, the CNGO has recently begun delivering a new two-year (2014–16) geoscience program. It intends to deliver applied geoscience projects that support responsible natural resource development, protect investments in infrastructure and disseminate geoscience data to users and decision-makers. The intent of this presentation is to provide an overview of the CNGO and its activities.

Nunavut mining and resource potential: 2014–2015 status update (A3)

Nunavut may potentially hold a quarter of Canada's natural resources, however, the geoscience knowledge-base for much of its land-mass is insufficient to support mineral exploration. The Government of Nunavut remains committed to public geoscience, and works collaboratively with the CNGO to deliver and carry out geoscience research.

Nunavut is geologically diverse, and a wide range of commodities including gold, zinc, copper, iron, uranium and diamonds, are current exploration targets. Nunavut has one settled land claim that makes Inuit beneficiaries the major recipients of any resource development. It also clearly defines the environmental regulations and processes for resource development. Additionally, the potential for petroleum prospects within Nunavut remains high.

Status of mineral exploration in Greenland (A4)

In Greenland, the number of exploration licences granted has been steadily increasing since 2002. In addition to the traditional licences (exploration, prospecting and exploitation licences), a new type of licence has recently been introduced: the small-scale mining licence.

A persistent marketing of the Greenlandic mineral potential in several countries has led to the positive development of several mineral projects. As a result of this, the Government of Greenland's objective is to license the opening of three to five mines on an environmentally and socially sustainable basis over the next five years. These mining projects may include the following:

- Isukasia (Isua) iron project, northeast of Nuuk, West Greenland
- Aappaluttoq ruby-sapphire project, south of Nuuk, West Greenland
- Killavaat Alannguat/Kringlerne rare-earth element (REE) project, South Greenland
- Kvanefjeldet REE project at Narsaq, South Greenland
- Citronen Fjord zinc-lead project, North Greenland
- White Mountain anorthosite project, West Greenland

In the future, the Government of Greenland will focus on the potential for occurrences of new major deposits of iron and base metals, rare-earth elements, gold and gemstones. Furthermore, the analysis of the zinc potential of North Greenland is an area that will receive special attention.

Mineral exploration in Nunavut (A5)

The territory of Nunavut was created on April 1, 1999 through the Nunavut Land Claims Agreement, along with a co-managed regulatory regime involving the governments of Canada and of Nunavut, Inuit organizations and the Institutions of Public Government. Exploration and deposit appraisal expenditures for 2014 are anticipated to be $166 million, placing Nunavut fifth in Canada. Diverse commodities are being explored for across the territory, including gold, diamonds, iron and uranium. There is also a mix of advanced, established and early stage projects that suggests Nunavut remains an attractive destination for explorers.

Nunavut has one producing mine, the Meadowbank gold mine. The mine entered commercial production in 2010 and currently has sufficient reserves to operate into 2018. Two other operations in the territory hold project certificates that permit mining: the high-grade Mary River iron project, located on northern Baffin Island, and the Doris North gold project, within the Hope Bay greenstone belt in western Nunavut.

Other advanced projects that are actively progressing through the regulatory process include Agnico-Eagle Mines Ltd.'s advanced stage Meliadine gold project, Sabina Gold and Silver Corp.'s Back River gold project and AREVA Resources Canada Inc.'s Kiggavik uranium project.

Uranium exploration in Greenland (A6)

Uranium exploration in Greenland was initiated in the 1950s by GEUS at the Kvanefjeld in South Greenland. Regional airborne radiometric surveys have been conducted in West and East Greenland, resulting in the identification of several areas with uranium mineralization (i.e., the Sarfartoq carbonatite in West Greenland).

Since 2007, Kvanefjeld has been investigated in detail by an Australian company, Greenland Minerals and Energy Ltd. (GME), who is conducting exploration on rare-earth elements and uranium deposits at the northern part of the Ilìmaussaq complex. The Ilìmaussaq complex is a Mesoproterozoic alkaline intrusive complex that hosts several multi-element deposits. The upper parts of the intrusive complex are represented in the northern part of the complex at the localities Kvanefjeld, Sørensen and Zone 3, which host REE-U-Zn-F deposits. Overall total resources of the northern part of the Ilìmaussaq complex, as reported by GME, are 956 Mt containing 575 Mlbs. U_3O_8, 10.33 Mt total rare-earth elements (TREO, includes 0.37 Mt heavy rare-earth oxide), 2.25 Mt zinc and 0.84 Mt yttrium oxide.

Kvanefjeld is the largest of the known uranium occurrences in Greenland. It is a unique type of uranium deposit where the majority of the uranium is hosted by the mineral steenstrupine, containing 0.2–0.5% UO_2. The hostrock, lujavrite, contains 200–400 ppm U and 600–800 ppm Th, the typical Th/U ratio lies between 2 and 3. The enrichment of uranium (and thorium) is thought to have occurred during crystallization and differentiation of the agpaitic rocks.

The mid-Proterozoic Gardar Province, South Greenland: geology and rare-earth element potential (A7)

The mid-Proterozoic Gardar Province in South-West Greenland developed in a continental-rift–related environment. Several alkaline intrusions and associated dyke swarms were emplaced in Archean and Proterozoic basement rocks during two main magmatic periods (1300–1250 Ma and 1180–1140 Ma).

Geochemical investigations of mafic dykes indicate a time dependent compositional change within the Gardar magmatism, providing evidence for the involvement of two geochemically distinct mantle components. A first depleted source, re-enriched by fluid metasomatism and a second more enriched source possibly intermixed with phlogopite and apatite components. The geochemical fingerprint of dykes, associated with the older Gardar magmatic period, shows remarkable similarities to penecontemporaneous dykes in South-East Greenland and North America indicat-

ing a much more widespread magmatism. Recent plate reconstructions (Evans and Mitchell, 2011) give rise to the assumption that these dyke swarms were formed behind a long-lived orogenic belt in response to back-arc basin formation.

Current REE exploration studies within the province are focused on highly evolved agpaitic nepheline syenite within the Ilímaussaq intrusion. In addition, significant REE enrichment is described for the Motzfeldt, Ivigtut and Paatusoq intrusions, but no detailed exploration studies have been conducted.

A geomorphological transect across eastern Nunavut (A8)

The effect of Quaternary glacial erosion on the landscape of central and eastern Nunavut is variable in its spatial distribution and intensity. Vast regions affected by glacial erosion are characterized by exposed fresh bedrock, till cover and evidence of glacial scouring, indicated by the presence of lakes over crystalline bedrock. Undulating terrain covered with a mantle of regolith preserves original Neogene landscapes on the plateaus of Boothia, Melville and Hall Peninsulas. These Neogene landscapes are preserved in cold-based glacier zones, where glacial erosion was minimal because the glacier was frozen to its base. The composition of the Neogene regolith depends on hostrock, ranging from boulder fields with little sandy matrix over tonalite rocks, to kaolinite-bearing orange clayey sands with minor boulder content over weathered garnet- and plagioclase-rich metasedimentary rocks. Satellite images and field studies illustrate the difference between the dendritic, organized fluvial landscape dating from the Neogene and the deranged fluvial landscape dating from the Quaternary. The increasing intensity of glacial erosion and transport is transitional from Neogene regolith (cold-based glacial terrain) to areas of till cover (warm-based glacial terrain). The surface material composition (geochemistry, sedimentology and heavy mineral content) informs us about the type of glacial transport and weathering processes that occurred across the transition zone from cold-based to warm-based glaciation.

South-East Greenland Mineral ENdowment Task, SEGMENT (A9)

The SEGMENT project is financed jointly by GEUS and the Ministry of Industry and Mineral Resources (MIM), Government of Greenland. The aim of SEGMENT is to provide better and more precise evaluations of the mineral endowment of the North Atlantic craton, the Ammassalik mobile belt and the Paleogene magmatic suite of South-East Greenland, between 62 and 67°N.

The project started in 2009 and 2010 with a regional fine-fraction stream sediment, fresh water and till sampling program. At the same time regional geological reconnaissance work was carried out. These datasets were used to plan more targeted geological research in the following years. Furthermore, regional aeromagnetic surveys were conducted in 2012 and 2013.

The focus region in 2011 and 2012 was the North Atlantic craton of South-East Greenland (62–64°N), centred on the Skjoldungen area. The work involved detailed mapping, tectonometamorphic and petrological studies, geochronology and isotopic mapping.

In 2014, the focus area for SEGMENT was the Tasiilaq region (64–67°N). Extensive petrological investigations were conducted on different intrusive complexes in the area and work on establishing a tectonometamorphic model and the lithostratigraphy of mafic and supracrustal rock units was undertaken.

Nunavut's soapstone: defining the supply for the community commodity of Arctic Canada (A10)

The Government of Nunavut has been evaluating carving stone sites since 2010 through the Nunavut Carving Stone Deposit Evaluation Program. The primary goals of the program are to verify the quality and size of traditional carving stone sites and identify new resources. The program relies on guidance from carvers and local community members to identify and assess traditional carving stone sites.

A total of 77 carving stone sites have been categorized for artisan suitability, tonnage and composition. A talc-rich rock type rarely found in Nunavut, 'soapstone', is a generic misnomer used in place of 'carving stone' by many Inuit carvers. Artisan serpentinite and artisan marble that can be shaped by carbide tools are Nunavut carvers' preferred choice of carving stone.

Nunavut's carving stone deposits range in size from tiny occurrences up to deposits containing 1 000 000 tonnes. The larger the resource, the more it is shared by carvers. A community-sized quarry or undeveloped deposit contains up to 1000 tonnes or more of material, while a regional-sized quarry or undeveloped deposit is 10 000 tonnes or larger in size. Deposits containing up to 1000 tonnes of material can supply average community use, while deposits containing up to 10 000 tonnes of material can provide carving stone to a much broader region. The Kangiqsukutaaq quarry on southern Baffin Island is Nunavut's only regional producer. This 1970s tidewater discovery has yielded a lifespan-averaged 450 tonnes per year, supplying one-third of Nunavut's carvers with excellent-quality carving stone.

The territory is now known to have 15 undeveloped carving stone deposits and 11 quarries able to provide several decades worth of carving stone to nearby communities. Of Nunavut's 25 communities, 17 have access to local carving

stone resources adequate for their long-term needs. Substantial high-quality resources await further study and future development.

Greenlandic rubies (A11)

During the past 15 years there has been considerable international and local interest in exploiting the Greenlandic occurrences of gemstone variants of corundum (sapphire and ruby). This has resulted in MIM issuing a number of exploration and small-scale licences and one full-scale exploitation licence for these commodities.

Rubies are found in several places in Greenland; within West Greenland this includes: the Maniitsoq area, the Nuuk area and the Fiskenæsset area. In South-East Greenland corundum occurs in the Tasiilaq area. The corundum localities in Greenland are found mainly near anorthosite, amphibolite and ultramafic bodies and are often related to intruding felsic sheets. Most ruby occurrences are found within the Fiskenæsset area. The Fiskenæsset anorthosite complex is extensive and measures 30 by 70 km and contains occurrences of gem-quality corundum, especially at the Aappaluttoq locality.

Collaborative research between MIM and GEUS focuses on geochemical fingerprinting of the Fiskenæsset rubies in order to compare them to other Greenlandic and international occurrences. The Aappaluttoq samples are distinguishable from other Greenlandic and international occurrences based on oxygen isotopes and trace element ratios for Fe, Ti and Cr. The samples from Aappaluttoq have very high Cr content and lower Ti and Fe. Other Fiskenæsset occurrences share similarities in geochemical signatures with the Aappaluttoq rubies to a greater extent than to other Greenlandic and international ruby occurrences.

Ujarassiorit: the national mineral hunt (A12)

Ujarassiorit is an annual public mineral hunt competition that began in 1989. It is a grassroots competition that aims to contribute to knowledge of mineral occurrences in Greenland. The aim is to make use of the Greenlandic people's traditional knowledge and connection with the land as they often visit places that are seldom visited by geologists. In this manner they can help find new areas of interest for geologists and through this create a greater interest in the geology of Greenland.

In this program any citizen in Greenland may submit samples of rocks they find on land for examination by MIM. The rock samples can be submitted by collectors at any post office in Greenland. A petrological description of and information about the rock type is made and returned to the submitter. Any mineralized samples are chemically analyzed and the results also returned to the submitter. Annually 700–1000 samples are submitted to Ujarassiorit. On average, 20–30% of the rock samples submitted are chemically analyzed. Submitted rock samples are judged based on observations and analytical results by geologists from MIM and GEUS. First place prize is C$10 000, second place is C$5000, there are two third place prizes of C$1900 and four fourth place prizes valued at C$1000 each.

Nunavut community outreach and engagement (A13)

One of the goals as stated in 'Sivumut Abluqta' (*Stepping Forward Together*) is for Nunavut to be self-reliant and develop its resources responsibly for the benefit of Nunavut. Recent surveys identify and forecast labour market requirements for Nunavut's minerals industry to include up to 1800 direct mining jobs in the territory over the next decade. The Government of Nunavut's plan is to ensure that Nunavummiut take advantage and benefit from these employment opportunities.

The strategy to achieve this is to tackle the challenges in an organized and structured way. This includes promoting awareness of careers in mining through outreach activities, creating necessary governing bodies to guide stakeholders in delivering education programs and providing effective training activities.

The shortage of skilled and/or experienced mine workers in Nunavut forces companies to bring in workers from outside the territory. Providing local skilled workers will reduce operating costs for mines and meet or exceed obligations from Inuit Impact and Benefits Agreements. Both of these outcomes will be beneficial to the industry and Nunavut.

Geology of Greenland (A14)

The content of this abstract is presented in the 'Geology of Greenland' section above.

Correlation of geological events across Davis Strait: broadening implications of GEM geoscience through international collaboration (A15)

Canada's Geomapping for Energy and Minerals (GEM) program targeted eastern Baffin Island for updated geoscience to advance tectonic models in support of resource assessment and exploration. Integrated GEM geoscience on Cumberland Peninsula established

- significant polydeformed Mesoarchean basement;
- discrete, foliated Neoarchean plutons;
- a central belt of Paleoproterozoic cover rocks (Hoare Bay), which include komatiite and clastic rocks, with minor marble;
- a 200 km long 1.89 Ga Opx–Grt±Bt granodiorite batholith (Qikiqtarjuaq suite); and
- cryptic Archean tectonometamorphism, penetratively overprinted by folding, tectonic imbrication and upper-amphibolite–facies metamorphism from 1.86 to 1.84 Ga.

Cumberland Peninsula's basement/cover relationships point to Rae craton affinity, however, there are differences in lithology, age, detrital provenance and/or tectonometamorphic events that are distinct from, or not yet recognized within, the Rae craton. Main tectonometamorphism is consistent with the ca. 1.86 Ga central Nagssugtoqidian Orogen, implicating collision of North Atlantic craton as a driving force.

The GEM project is continuing its mandate of geomapping for energy and minerals across the Davis Strait through the acquisition of U-Pb age data from the Paleoproterozoic Karrat Group and Prøven Igneous Complex of western Greenland. These new data elucidate the provenance and timing of deposition of cover rocks, document the extent of plutonism (1.90–1.87 Ga), and provide new insight into tectonometamorphic models for northeastern Laurentia.

Metallogeny of Greenland (A16)

In Greenland the North Atlantic craton is bounded by two later Proterozoic orogenies, the Nagssugtoqidian to the north and the Ketilidian to the south. Subsequent subsidence created large sedimentary basins in North and East Greenland, and rifting and volcanism created igneous provinces including the Gardar Province, and the North Atlantic large igneous province. Limited kimberlitic volcanism and carbonatite intrusions are found locally in several regions.

The diverse geological record in Greenland provides good potential for a wide variety of minerals. These include

- iron, gold, chromium and diamonds, especially in the Archean basement(e.g., Isua banded iron formation and Nalunaq gold deposit);
- base metals in sediments and metamorphosed sedimentary rocks (e.g., the zinc-lead deposits of Black Angel and Citronen Fjord);
- platinum-group elements and nickel in igneous Proterozoic and Paleogene rocks (e.g., the Skaergaard precious-metal deposit); and
- rare-earth elements, niobium, tantalum and other specialty metals in alkaline and peralkaline intrusions and in carbonatite intrusions (e.g., the Ilìmaussaq, Sarfartoq and Qeqertaasaq rare-earth multi-element deposits).

Since 2009, GEUS and the Government of Greenland have conducted annual assessment workshops on selected commodities. The Cu, REE, Zn, Ni and W potential have been assessed so far, and in 2014 a Au potential assessment will occur.

Metallogeny of the Rae Province and its links to Nuna supercontinent assembly: implications for Nunavut and western Greenland (A17)

The Rae Province's complex and protracted tectonic history, spanning several supercraton/supercontinent cycles, has endowed it with a diversity and abundance of mineral deposits linked to continental assembly. Its supracrustal belts formed (ca. 2.9–2.65 Ga) on older Paleo-Mesoarchean basement and were assembled by 2.6 Ga. Iron ore deposits (Mary River, Roche Bay) and Ni-PGE prospects (Prince Albert Hills) are restricted to Mesoarchean sequences (Mary River and Prince Albert), whereas iron-formation–hosted mesothermal gold deposits (Meadowbank, Three Bluffs) are found in the Neoarchean belts (Committee Bay and Woodburn). Bimodal magmatism at 2.6 Ga, possibly related to slab breakoff, hosts Cu-Au epithermal occurrences and Ni-Cu-PGE deposits (Ferguson, Axis Lake).

Between 2.3 and 1.7 Ga, orogenic events related to Nuna supercontinent amalgamation (Thelon, Snowbird, Hudsonian) punctuated epicratonic basin formation and magmatism. Magmatic-hosted Ni-Cu deposits (ca. 1.8–1.9 Ga, Thye Lake) are associated with the Rae-Hearne suture zone. Broken Hill–type Pb-Zn and polymetallic-U prospects formed in the marginal marine basins. Major Au deposits (Meadowbank, Meliadine) were reworked or localized by ca. 1.85 Ga Hudsonian structures. Subaerial, syncollisional basins, which accumulated during brittle-ductile phases of this reworking (1.84–1.75 Ga), host Cu, Cu-U-Ag and Cu-Au prospects. Unconformity-associated uranium deposits of the Thelon Basin (Boomerang, Kiggavik) formed around 1.6 Ga as a response to far-field stresses during accretion of Australia to western Laurentia.

Nickel potential of Greenland (A18)

Since 2009, GEUS has, in collaboration with the Government of Greenland, conducted annual workshops focused on assessing the mineral potential in Greenland for specific commodities. In 2012 the focus was on assessing the extent of undiscovered magmatic nickel deposits in the upper 1 km of the crust. Nineteen geologists with knowledge of Greenland geology, and international experts on magmatic nickel, formed a panel to conduct the assessment using the procedures and guidelines of the 'Global Mineral Resource Assessment Project' of the United States Geological Survey (USGS). Within 32 tracts (predefined areas) three magmatic nickel deposit types, and respective grade/tonnage models, were considered: 1) komatiite-hosted deposits, 2) contact-type deposits, and 3) deposits related to picritic and/or tholeiitic basalt dyke/sill complexes (also known as conduit-type deposits).

The statistical mean estimated number of undiscovered komatiite-hosted and conduit-type deposits were assessed to be four for each type, with no deposits of the contact-type, and at a 50% confidence level these were estimated to contain a total of 1.9 Mt of nickel. Of this estimate, 1.6 Mt of undiscovered resources were expected for conduit-type deposits (mainly the norite belt at the Mesoarchean Maniitsoq structure and the Paleogene flood basalt prov-

ince in West Greenland), 0.2 Mt for komatiite-hosted deposits (Ikertoq area in West Greenland), and less than 0.1 Mt related to contact-type deposits.

Bedrock geology and economic potential of Hall and Meta Incognita peninsulas on southern Baffin Island, Nunavut (A19)

The CNGO and GSC partnered to complete geological mapping on Hall and Meta Incognita peninsulas. These areas are underlain by Archean orthogneiss and Paleoproterozoic para- and orthogneiss that appear to correlate with rock units previously mapped to the east and west.

On both peninsulas, new areas with economic mineral potential have been identified and include layered mafic-ultramafic intrusions with Ni-Cu-PGE mineralization potential, gossanous graphite- and sulphide-bearing metasedimentary rocks, semiprecious spinel and apatite gemstones associated with marble and calcsilicate units, granitic pegmatite with REE potential and marble and serpentinite carving stone deposits. The Archean orthogneiss on Hall Peninsula also hosts a diamondiferous kimberlite district with significant economic potential.

Following a final field season of mapping in 2015, southern Baffin Island's bedrock geology will have been mapped at 1:100 000 scale. This will allow metamorphic and tectonic processes, as well as timing of events associated with the Trans-Hudson Orogen in this part of the Arctic, to be better understood. It will also provide a framework for understanding the petrogenesis of potentially economic deposits in the area.

Mississippi Valley–type Zn-Pb mineralization of North Greenland (A20)

The results of a zinc resource assessment indicate that the Franklinian Basin, North Greenland, is highly prospective for sedimentary exhalative (SEDEX) and Mississippi Valley–type (MVT) deposits. The Franklinian Basin is characterized by a distinct facies transition from shallow-water platform carbonate sediments in the south, to deep-water siliciclastic trough sediments to the north. While the platform carbonate sediments can host MVT deposits, the trough can host SEDEX deposits, so the whole basin is considered of interest for zinc-lead mineralization. The location of the northern margin to the Franklinian Basin in North Greenland is not established with certainty.

Deposition in the trough was ended by the mid-Paleozoic Ellesmerian orogeny, which formed the North Greenland fold belt and caused compression from north to south during the late Devonian to early Carboniferous.

Fieldwork in 2012 and 2013 revealed several new MVT showings, with sphalerite veinlets and pockets intermittently distributed within dolostone in the Turesø Formation (Upper Ordovician to Lower Silurian), of the Franklinian Basin carbonate platform. The fact that these showings are up to 200 km apart, demonstrates that a large-scale hydrothermal system, transporting zinc, operated in the eastern part of the Franklinian carbonate platform.

Onshore oil and gas exploration in Greenland: a review (A21)

Most of the oil and gas exploration in Greenland to date has been focused offshore. However, there are two areas of specific interest for hydrocarbons onshore, which have previously drawn attention from oil and gas companies. These two areas, the Disko/Nuussuaq area in West Greenland and Jameson Land in East Greenland, are briefly described below in terms of their hydrocarbon exploration potential.

The first discovery of onshore oil in Greenland was made on the Nuussuaq peninsula in 1992. Oil stains were evident in basalts, and in the following years, many oil seeps and stains were discovered in volcanic rocks and in the fluviodeltaic sandstone of the Nuussuaq Basin, in the Disko/Nuussuaq region. The Nuussuaq Basin formed during Early Cretaceous rifting between Greenland and Canada and is the only onshore basin analogue in West Greenland. Results from organic geochemical analyses indicate that five oil types may exist in the area.

The other onshore area of interest is Jameson Land, which forms part of a thick sedimentary basin deposited during the Upper Paleozoic to Mesozoic between eastern Greenland and western Norway. Many of the oil and gas fields offshore western Norway are producing from similar sedimentary sections as the ones found onshore Jameson Land. The subsurface of Jameson Land may prove to contain commercial hydrocarbon resources and new geological models are important in order to understand the petroleum system.

In the next phase of Greenland's Oil and Mineral Strategy (2014–2018) both of these onshore areas are expected to be open for licence applications (Jameson Land as an Open Door policy and the Disko/Nuussuaq area as a licensing round in 2016). In terms of application policy, Open Door policy basically means that pre-defined Open Door areas can be applied for all year around (from the opening date and until the area will be closed again), whereas an ordinary licensing round generally is held every two years in different predefined areas of Greenland and holds a fixed and limited application period in the relevant year only, in this case 2016.

Sediment source fingerprint and basement characteristics (A22)

Analysis of age distribution patterns of detrital zircon from recent stream sediments and their comparison with Mesozoic sandstones has proven to be a powerful tool in under-

standing sandstone provenance. Fingerprints from samples representing present day drainage also yield valuable information about the basement geology in areas with scarce geological information.

In central West Greenland detrital zircons with Archean ages constitute approximately 95% of all zircons in the Nagssugtoqidian (Paleoproterozoic) Orogen. In contrast to this, the fingerprint of detrital zircons from the Karrat Group contains approximately 50% Paleoproterozoic zircons. The Melville Bay area is characterized by no detrital Paleoproterozoic zircons in recent sediment samples and a very narrow Archean age distribution pattern with a peak around 2700 Ma in the south and a broader distribution pattern with a peak around 2700 Ma in the north. In Inglefield Land two detrital zircon ages are approximately equally common, namely ca. 1750 and 1950 Ma, whereas Archean zircons are rare.

A total of 134 recent stream sediment samples and 39 Cretaceous and Paleogene sandstone samples were collected on eastern parts of Ellesmere Island, Devon Island and Baffin Island during the summers of 2012 and 2013 by GEUS as part of a collaborative project together with the CNGO.

The discovery of an organic-rich black shale xenolith from a kimberlite on Hall Peninsula, Nunavut: implications for petroleum potential in Cumberland Sound (A23)

Presently, Hall Peninsula lacks Phanerozoic sedimentary cover, except for unconsolidated glacial deposits. However, a great number of carbonate and a few black shale xenoliths have been recovered from the Late Jurassic–Early Cretaceous kimberlites that occur in the area. The conodont microfossils discovered from the carbonate xenoliths proved that Upper Ordovician and Lower Silurian strata were present on Hall Peninsula at least before and during kimberlite emplacement. These strata, which have a total thickness of ~300 m elsewhere on southern Baffin Island, have since been eroded off Hall Peninsula sometime between the Early Cretaceous and today (Zhang and Pell, 2013, 2014). Their conodont colour alteration index (CAI) values range from 1.5 to 8, making them an excellent geothermometer for understanding kimberlite emplacement temperatures.

The black shale xenoliths represent an excellent oil-prone source rock, with average and maximum total organic carbon (TOC) values of 8.04 and 8.96%, and a possible depositional age of Early Silurian. Given the geological and geographic position of the peninsula, and the identified suspect natural petroleum seeps from uncertain source rocks in the Baffin Shelf area, especially in Cumberland Sound (Budkewitsch et al., 2013), these unique black shale xenoliths provide valuable physical evidence for inferring that the oil seeps in the region may have originated from Paleozoic source rocks overlain by Cretaceous strata thick enough to generate oil (Zhang, 2013).

Godthåbsfjord field trip

Nuuk is situated in the North Atlantic craton, which constitutes the oldest part of Greenland. During this workshop a field trip by boat was organized in Godthåbsfjord (Figure 4). The first stop was the Ivinnguit fault (locality 1; Figure 5a), which is a long fault zone cutting through the entire fjord and continuing toward the inland ice farther north of the map area. The structure was formed during continental collision between two (or possibly more) Archean terranes at 2.7 Ga, dividing the old Amîtsoq gneiss of 3.7 Ga age (Færingehavn terrane) and the Nûk gneiss of 3.2 Ga (Akia terrane). The Ivinnguit fault was visible several times along the field trip route.

Amphibolite was seen at locality 2 and pillow lava at locality 3 (Figure 5b). The interpretation of the large amphibolitic bodies in the area is that they were formed in island-arc environments. The amphibolite has been wedged between gneiss during continental collision that occurred 2.7 Ga. The deformed, but distinct Ameralik dykes were observed in the oldest gneisses in the area at Storø (Figure 5c).

An anorthosite and the gold-bearing shear zone at Storø (locality 5) were observed from distance, as they outcrop high on the almost vertical walls of Storø. The Storø gold-bearing shear zone is about 2.5 Ga old and parallel to the Ivinnguit Fault. The fault crosscuts rocks at localities 5 and 7. Along the route several undeformed Paleoproterozoic dykes were observed crosscutting the gneisses in the area (Figure 5d). A small glacier and moraines was observed at locality 6 along the Storø Shear Zone. The Qôrqut granite complex (locality 10 and 11; Figure 5e) is approximately 2.5 Ga. old and has three distinct units: 1) a lower more uniform and light coloured unit, 2) a middle zone of more mixed character, and 3) an upper zone with increasing amounts of pegmatite. Three soapstone occurrences were visited: one at Storø (locality 4) and on two small islands northeast of Storø; the second at Uummannaq (locality 8); and the third at Qeqertaq (locality 9; Figure 5f).

Workshop outcomes

The discussion and information exchange that were part of this workshop resulted in several outcomes that are expected to leave a legacy. First, it became obvious that collaboration between Greenland and Nunavut could help solve a range of geoscience-related questions on both sides of Baffin Bay, leading to a better understanding of the oil and gas resource potential, tectonics and mineral occurrences in the area. Scientific collaboration can be facilitated through staff exchanges as well as direct office to office collaboration. Second, Nunavut and Greenland together

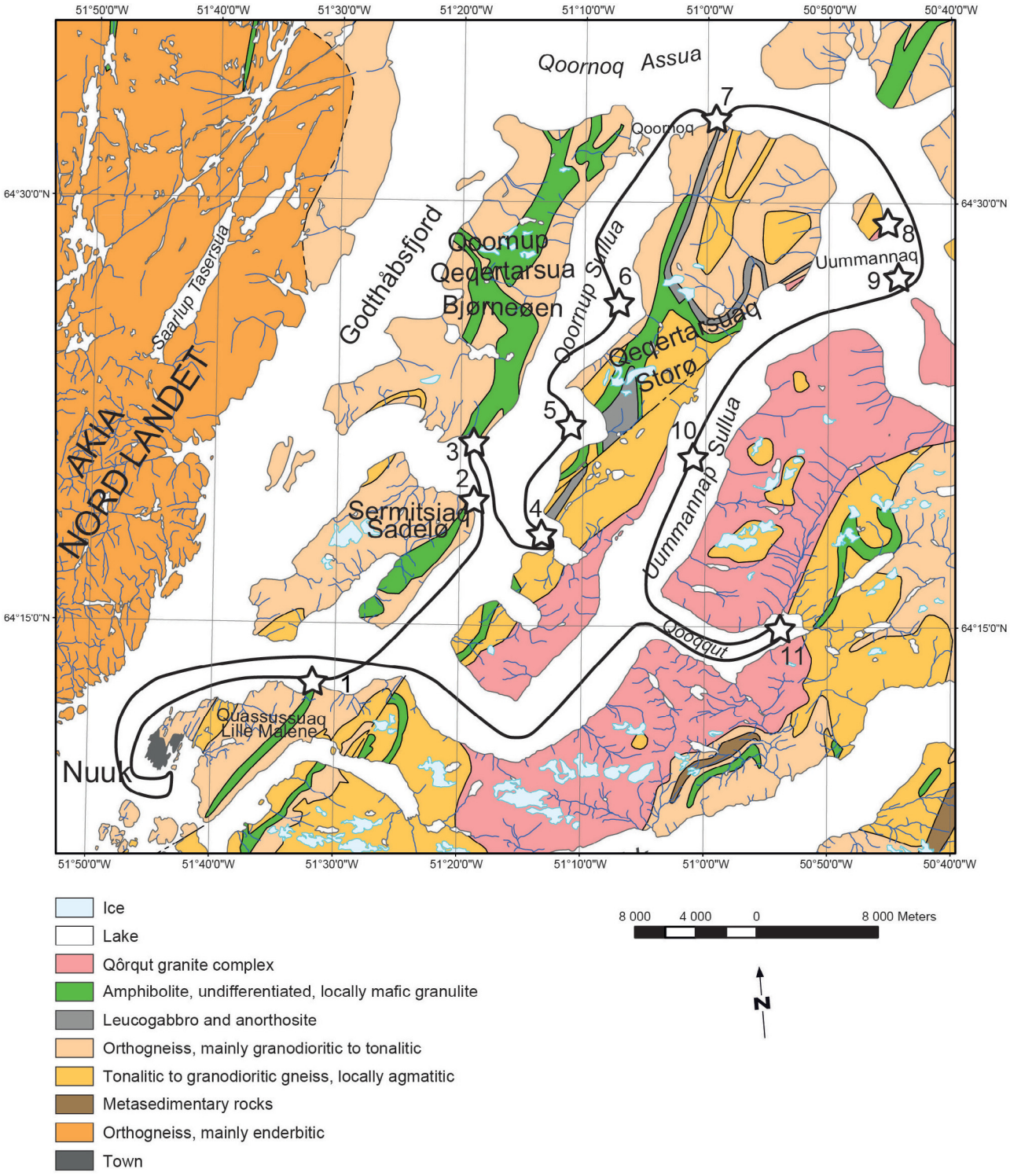

Figure 4: Map showing field trip route in Godthåbsfjord, Greenland. Stops on land occurred at localities 3, 4, 8 and 9. Stars indicate special areas of interest.

with Canada and Denmark should exchange information regarding the establishment and operation of geological survey offices and local capacity building. Third, the two jurisdictions decided to meet annually during the PDAC in Toronto, Canada in order to continue to share information and discuss issues of mutual interest. Fourth and finally, a similar geoscience workshop will be proposed in Nunavut in 2 to 3 years and ideally biannual scientific workshops at different locations hereafter. Workshops should be fairly broad in scope and strive to have participation of relevant scientists and government officials from Greenland and Nunavut as well as Canada and Denmark. Opportunities to

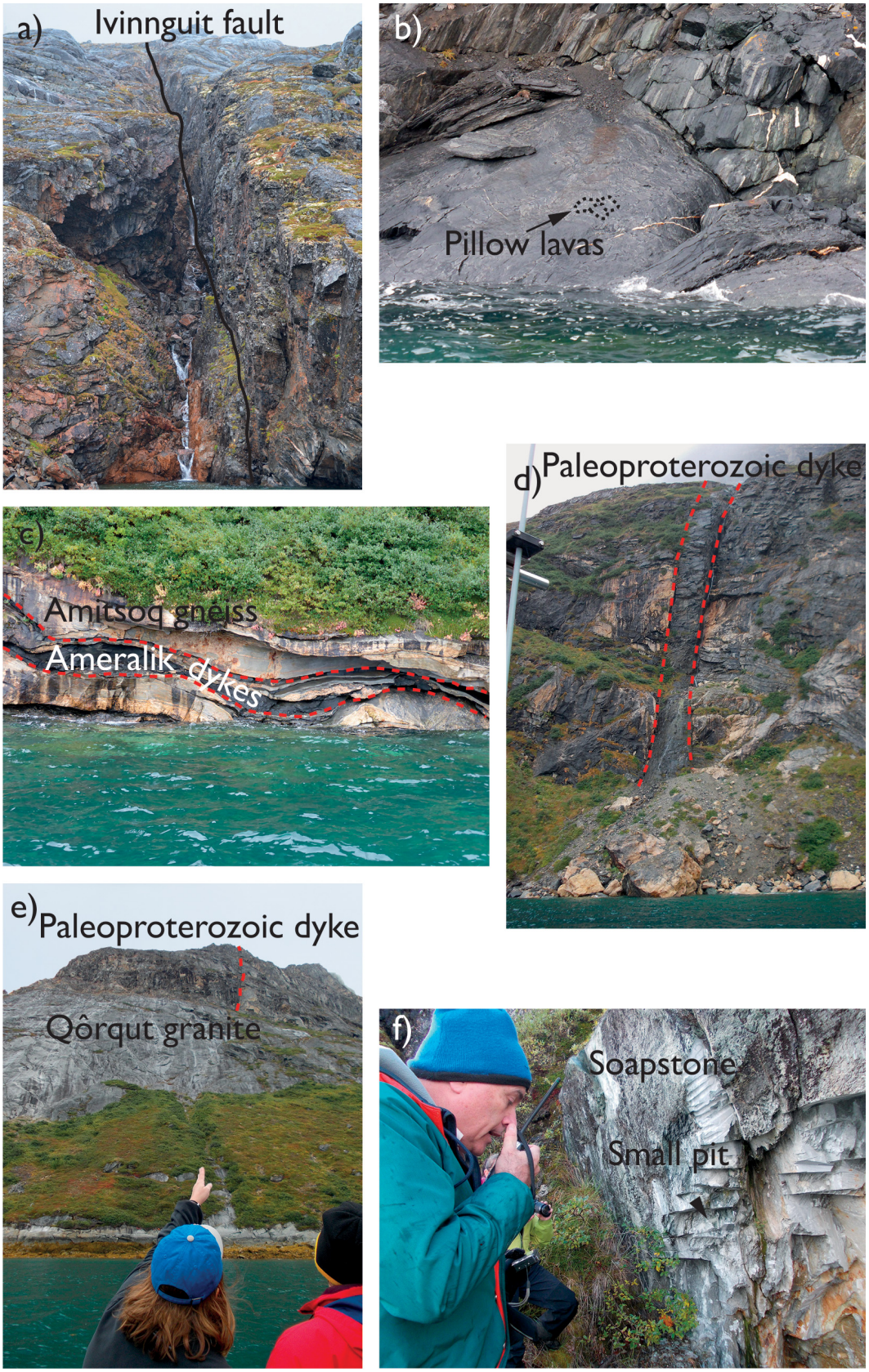

Figure 5: Photographs from the field trip to Godthåbsfjord, Greenland: **a)** The Ivinnguit fault at locality 1; **b)** pillow lavas at locality 2; **c)** the Ameralik dyke near locality 5; **d)** an undeformed Paleoproterozoic dyke crosscutting the gneiss; **e)** the Qôrqut granite and a Paleoproterozoic dyke as viewed from the boat; **f)** soapstone at locality 8, Uummannaq Island.

conduct joint science projects between the two jurisdictions were also discussed and could lead to new collaborative research opportunities.

Economic considerations

Geological surveys collect and maintain public geoscience information in order to support economic development, land-use planning and community development. Public geoscience information decreases discovery risk for industry by enabling them to focus exploration programs on areas with the greatest potential. Geological surveys are best positioned to conduct regional mapping programs and integrate diverse datasets into geological frameworks. They are also key stewards of geoscience information both digitally as well as within the expert knowledge of their government geologists. Effective geological surveys with well-maintained and publicly available geoscience data make jurisdictions more attractive to investment from the mineral, and oil and gas sectors.

The role and development of geological surveys in both Nunavut and Greenland is evolving. The CNGO represents the seed of a geological survey for Nunavut. This office was created at the same time as the territory was formed in 1999. It is formally co-managed by the governments of Canada (including the Geological Survey of Canada) and Nunavut with input from Nunavut Tunngavik Inc., which represents the Inuit of Nunavut. It strives to provide accessible geoscience information to support responsible natural resource and infrastructure development and has six permanent staff with expertise in Precambrian, Sedimentary and Quaternary geology along with GIS/cartography and data dissemination. One day the management of public lands and natural resources will be devolved by the Government of Canada to the Government of Nunavut. This devolution of responsibility has not occurred yet but when it does, it will include the transfer of the CNGO to Nunavut where it is expected to continue its growth into a full-fledged territorial geological survey.

In Greenland, the Ministry of Industry and Mineral Resources of the Government of Greenland (Naalakkersuisut) has the authority to undertake all administration in relation to mineral, and oil and gas activities. The role as a geological survey for Greenland is provided by GEUS, which was formed when the previous Geological Survey of Denmark (DGU) and Geological Survey of Greenland (GGU) merged in 1995. The Geological Survey of Denmark and Greenland (GEUS) support Naalakkersuisut by conducting basic geological investigations and research, and maintaining public geoscience data and information. However, the possibility of developing a GeoSurvey Greenland (GSG) in addition to GEUS is currently being discussed in Greenland, and a proposal on how such a survey could be structured was put forward by the previous Naalakkersuisut. Similar to the CNGO and GEUS, GSG would probably be managed by a board and be capable of providing geological advice to Naalakkersuisut related to natural resource development and regulation. If the GSG were to develop, it most likely would be in a formalized collaboration with GEUS, whose role would eventually change to that of a collaborative research partner.

Conclusion

The first ever geoscience workshop between Greenland and Nunavut was held from September 9 to 11, 2014 in Nuuk, Greenland. The intent of the workshop was to exchange information about the mineral and petroleum resources on both sides of Baffin Bay. The role of, and process for establishing, geological survey offices in the Arctic was also discussed using the CNGO and the vision for the GSG as examples. Following this workshop it is expected that collaboration between both jurisdictions on geoscience, and mineral- and petroleum-related issues will grow.

Acknowledgments

The authors would like to thank the Greenland Institute for Natural Resources for being able to accommodate the workshop. Also, thanks to the boatmen on M/S Sterna and Aage V. Jensen II for providing transportation services for the geological field trip. The authors also thank the GEUS, Nuuk Office for all the logistics help and co-ordination during the workshop. This was a key to its success. Last but not least, the authors want to thank all participants for their contributions to this workshop and article. It has been a very constructive experience.

Natural Resources Canada, Earth Sciences Sector contribution 20140296

References

Budkewitsch, P., Pavlic, G., Oakey, G., Jauer, C. and Decker, V. 2013: Reconnaissance mapping of suspect oil seep occurrences in Baffin Bay and Davis Strait using satellite radar: preliminary results; Geological Survey of Canada, Open File 7068, doi:10.4095/292280.

Evans, D.A.D. and Mitchell, R.N. 2011: Assembly and breakup of the core of Paleo-Mesoproterozoic supercontinent Nuna; Geology, v. 39, p. 443–446.

Harrison, J.C., St-Onge, M.R., Petrov, O.V., Strelnikov, S.I., Lopatin, B.G., Wilson, F.H., Tella, S., Paul, D., Lynds, T., Shokalsky, S.P., Hults, C.K., Bergman, S., Jepsen, H.F. and Solli, A. 2011: Geological map of the Arctic; Geological Survey of Canada, Map 2159A, scale 1:5 000 000.

Henriksen, N. 2008: Geological History of Greenland; Geological Survey of Denmark and Greenland, 272 p.

Kokfelt, T.F., Keulen, N.T., Weng, W.L. and Pedersen, M. 2013: Geological map of Greenland; Geological Survey of Denmark and Greenland, scale 1:500 000.

Zhang, S. 2013: Rock Eval 6 and vitrinite reflectance data from Baffin Island Shelf and Hudson Strait; Geological Survey of Canada, Open File 7341, 32 p., doi:10.4095/292376.

Zhang, S. and Pell, J. 2013: Study of sedimentary rock xenoliths from kimberlites on Hall Peninsula, Baffin Island, Nunavut; *in* Summary of Activities 2012, Canada-Nunavut Geoscience Office, p. 107–112.

Zhang, S. and Pell, J. 2014: Conodonts recovered from the carbonate xenoliths in the kimberlites confirm the Paleozoic cover on the Hall Peninsula, Nunavut; Canadian Journal of Earth Sciences, v. 51, p. 142–155.

The **Canada-Nunavut Geoscience Office** conducts new geoscience mapping and research, supports geoscience-capacity building, disseminates geoscience information and develops collaborative geoscience partnerships for Nunavut.

www.cngo.ca